PIERS 2006

Progress In Electromagnetics Research Symposium

Abstracts

March 26–29, 2006

Cambridge, USA

www.emacademy.org
www.piers.org

PIERS 2006 Cambridge Abstracts

Published by

The Electromagnetics Academy
777 Concord Avenue, Suite 207
Cambridge, MA 02138
www.emacademy.org

Printed in Cambridge, USA

ISBN: 1-933077-09-3

Progress in Electromagnetics Research Symposium
March 26–29, 2006
Cambridge, USA

PIERS 2006 CAMBRIDGE ORGANIZATION

PIERS Chair

J. A. Kong, MIT, USA

PIERS 2006 Cambridge General Chair

R. T. Shin, MIT Lincoln Laboratory, USA

PIERS 2006 Cambridge International Advisory Committee

M. Abouzahra	D. Briggs	W. Chew	S. T. Chun
A. K. Fung	T. M. Habashy	Y. Hara	H. C. Huang
A. Ishimaru	K. F. Lee	I. V. Lindell	S. G. Liu
K. M. Luk	S. Mano	Y. Miyazaki	P. Pampaloni
M. Pollack	A. Priou	M. Raugi	K. Senne
M. Silevitch	T. Tateiba	L. Tsang	K. A. Zaki
J. Zehentner	W. X. Zhang		

PIERS 2006 Cambridge Technical Program Committee

R. Atkins	A. Baghai-Wadji	G. Berginc	W. Boerner
L. C. Botten	H. Braunisch	C. H. Chen	K. S. Chen
T. J. Cui	T. Endo	D. Entekhabi	T. M. Grzegorczyk
M. Hallikainen	S. He	P. Hoff	W. Hong
K. Kobayashi	J. Lu	G. McNeal	E. Miller
M. Moghaddam	A. Moreira	G. Mrozynski	C. Myers
Z. P. Nie	K. O'Neill	J. Pacheco	J. Pribetich
C. Rappaport	X. Q. Sheng	J. van Zyl	J. Vrba
B. I. Wu	T. X. Wu		

PIERS 2006 Cambridge Administrative Committee

H. Chen	J. Chen	X. X. Cheng	T. M. Grzegorczyk
W. Herrington	Q. Jiang	B. Kemp	M. Lai
S. Lee	J. Lu	K. Suwa	D. X. Wang
B. I. Wu	Z. Wu	B. Zhang	Y. Zhang

PIERS 2006 CAMBRIDGE SESSION ORGANIZERS

A. Abubakar
Y. Barabanenkov
G. Berginc
E. Binaghi
H. Braunisch
S. Caorsi
L. Capineri
C. H. Chen
M. Cheney
G. F. Crosta
F. Del Frate
O. Dorn
N. Engheta
Y. A. Eremin
P. Ferrazzoli
J.-M. Fournier
V. Freilikher
J. Gomez-Rivas
T. M. Grzegorczyk
T. M. Habashy
M. Hallikainen
H. Kikuchi
K. Kobayashi
A. B. Kouki
S. Lang
J.-F. Lee
J. Li
V. A. Markel
A. Massa
E. L. Miller
H. Mosallaei
S. Mudaliar
M. Oristaglio
K. E. Oughstun
W. J. Padilla
M. Pastorino
M. Piana
C. Pichot
K. Radhakrishnan
R. Ramer
J. A. Sanchez-Gil
P. Sewell
K. Sheng
Y. Shestopalov
A. H. Sihvola
L. Solymar
D. D. Stancil
S. A. Tretyakov
D. P. Tsai
O. G. Vendik
C. G. Windsor
R. Wu
G. Xie
M. S. Zhdanov

PIERS 2006 CAMBRIDGE SPONSORSHIP

- The Electromagnetics Academy
- IEEE Geoscience and Remote Sensing Society
- MIT Lincoln Laboratory
- Office of Naval Research
- Mitsubishi Electric Corporation
- Cold Regions Research and Engineering Laboratory
- The Electromagnetics Academy at Zhejiang University
- MIT Center for Electromagnetic Theory and Applications, Research Laboratory of Electronics

PIERS 2006 SESSIONS

Session 0A1a
New Results and Prospective Co-operative Research Directions on Metamaterials: the Metamorphose Network

Modeling Isotropic DNG Media for Microwave Applications

I. Vendik, **O. Vendik**, **M. S. Gashinova**, **I. Kolmakov**, **and M. Odit**
St. Petersburg Electrotechnical University, Russia

L. Jylhä, **S. Maslovski**, **and S. Tretyakov**
Helsinki University of Technology, Finland

O. Ouchetto and S. Zouhdi
Laboratoire de Génie Electrique de Paris LGEP-Supélec, France

In this review presentation we will discuss various possibilities to realize isotropic artificial backward-wave materials. Different structures and models are suggested and discussed.

1) A composite medium consisting of two sublattices of dielectric spherical particles of high permittivity and different radii embedded in a dielectric matrix of smaller permittivity are considered. It has been shown [1] that such a composite medium reveals properties of an isotropic double negative media (DNG) in the frequency range where resonance oscillations of H_{111} mode in smaller spheres and E_{111} mode in larger spheres are excited simultaneously. The E_{111} resonance and the H_{111} resonance give rise to the magnetic dipole momentum and the electric dipole momentum, correspondingly. Averaging the magnetic momentum and the electric momentum over the cells belonging to the appropriate spherical particles reveals the negative permeability and the permittivity.

2) An improved mixing rule [2] for the effective permittivity and permeability of a composite material consisting of two sets of resonant dielectric spheres in a homogeneous background is presented. The equations are validated using the Mie theory and numerical simulations. The effect of a statistical distribution of sphere sizes on the increasing of losses in the operating frequency band is discussed and some examples are shown.

3) A new technique [3] is presented for the accurate computation of the effective constitutive parameters of lattices containing particles with complicated shape. This technique is based on the periodic unfolding method. The method is based on the decomposition of the fields in a main part without micro-oscillations, and a remainder part taking them into account. The idea of this decomposition is inspired by the method of Finite Element approximations. Verification data is presented for lattices of dielectric cubes obtained with the Maxwell-Garnett method. Corrector results are also studied as a function of frequency.

REFERENCES

1. Vendik, O. G. and M. S. Gashinova, "Artificial double negative (DNG) media composed by two different dielectric sphere lattices embedded in a dielectric matrix," *Proc. EuMC'4*, 1209, Amsterdam, October 2004.
2. Jylhä, L., I. Kolmakov, and S. Tretyakov, "Isotropic double negative material composed of dielectric spheres: improved mixing theory," EPFL Latsis Symposium 2005, *Negative Refraction: Revisiting Electromagnetics from Microwave to Optics*, 91, Lausanne, Switzerland, February 28-March 2, 2005.
3. Ouchetto, O., S. Zouhdi, A. Bossavit, G. Griso, and B. Miara, "Effective constitutive parameters of periodic composites," *Proc. EuMC'5*, 4–6, Paris, France, October 2005.

Optical Properties of Nanostructured Metamaterials

I. Romero[1], **S. Riikonen**[1], **and F. J. G. de Abajo**[1,2]

[1]Donostia International Physics Center, Spain
[2]Centro Mixto CSIC-UPV/EHU, Spain

The optical properties of different metamaterials composed of metallic nanoparticles are investigated from a theoretical point of view. We consider materials composed of layers of periodically disposed particles and analyze the anisotropic dielectric function of these systems as a function of frequency and layer spacing. The dielectric function is obtained by solving Maxwell's equations using a layer-KKR method and by comparing the reflectance of planar surfaces of such materials with Frenel's equations for different angles of incidence and polarizations of the incoming light. We will also discuss the role that the shape of the particles have in the dielectric function, comparing materialas composed of spherical and ellipsoidal particles.

Losses in the PEMC Boundary

I. V. Lindell and A. H. Sihvola
Helsinki University of Technology, Finland

PEMC (Perfect Electromagnetic Conductor) was recently introduced as an ideal boundary material [1]. It is characterized by one real parameter, the PEMC admittance M, whose special values $M = 0$ and $1/M = 0$ correspond to the respective PMC and PEC cases. Realization of a PEMC boundary in terms of a lossless gyrotropic slab has also been recently suggested [2]. For real M, PEMC boundary is lossless while the realization would always have some loss.

In the present study extension of ideal PEMC boundary to one with small losses is given. It is shown that it is not enough to give the admittance parameter M a complex value $M_r + jM_i$ but an additional conductance parameter G must be introduced as well so that a lossy version of PEMC must involve three real parameters satisfying the inequality $G > |M_i|$.

As a simple example, reflection of a linearly polarized plane wave from a slightly lossy PEMC surface is studied showing how the pure polarization rotation caused by the ideal PEMC is added by a (small) decrease of the amplitude and a (small) change to elliptic polarization. Also, an analysis of a Fabry-Perot type of resonator made of two PEMC planes with losses is described.

REFERENCES

1. Lindell, I. V. and A. H. Sihvola, "Perfect electromagnetic conductor," *J. Electromag. Waves Appl.*, Vol. 19, No. 7, 861–869, 2005.
2. Lindell, I. V. and A. H. Sihvola, "Realization of the PEMC boundary," *IEEE Trans. Antennas Propag.*, Vol. 53, No. 9, 3012–3018, 2005.

Microwave Applications of Left/Right-handed Transmission Lines

I. Vendik[1], O. Vendik[1], D. Kholodnyak[1], S. Zubko[1], I. Kolmakov[1]
I. Kolmakova[1], E. Serebryakova[1], I. Nefedov[2], S. Tretyakov[2]
F. Martín[3], J. Bonache[3], J. García-García[3], and I. Gil[3]

[1]St.-Petersburg Electrotechnical University, Russia
[2]Helsinki University of Technology, Finland
[3]Universitat Autònoma de Barcelona, Spain

Numerous investigations have been undertaken in the area of metamaterials exhibiting negative refractive index. Such artificial materials are also known as Veselago media or left-handed materials. Recently a transmission line (TL) approach to realization of metamaterials was introduced [1–3]. Concept of right-handed (RH) and its dual left-handed (LH) transmission lines was used for a description of artificial transmission lines. In this review paper we will present some recent developments in this field.

A possibility to design a phase shifter with reduced frequency dispersion using combined sections of LH TL and RH TL was analyzed [4]. It was shown that there is no improvement in the phase shifter bandwidth due to combining positive and negative transmission line sections, except replacing devices with large positive phase shifts by devices with an equivalent small negative phase shift. Reduction of frequency dispersion can be attained using artificial transmission-line sections with positive anomalous dispersion.

An attractive feature of LH and RH lines is that the dispersion characteristics of both lines have a negative-going slope and the frequency dependencies of the slope for these lines are in a close agreement over a wide frequency range. That makes possible a design of a wide-band digital phase shifter based on switchable LH and RH TL channels. A theoretical approach was suggested and applied to i) digital phase shifters based on switchable LH and RH TL channels using p-i-n diodes and ii) digital phase shifters based on tuneable composite RLH-TL using ferroelectric varactors [5]. Results of simulation and experimental investigations of one-bit and multi-bit phase shifters are presented.

Another interesting application of CRLH-TL concerns microwave filters. Specifically, by alternating LH and RH TL sections implemented by means of split rings resonators (SRR) or complementary split rings resonators (CSRR), it is possible to synthesise narrow band pass filters [6] and diplexers [7] with high frequency selectivity and small dimensions. This is achieved thanks to the resonant nature of the artificial TL sections employed, to the small electrical size of the resonators, and to the presence of transmission zeros, which can be tailored to achieve the required characteristics.

REFERENCES

1. Eleftheriades, G. V., O. Siddiqui, and A. K. Iyer, *IEEE Microwave and Wireless Component Letters*, Vol. 13, 51–53, 2003.
2. Caloz, C. and T. Itoh, *IMS 2003 Digest*, 195–198, 2003.
3. Antoniades, M. A. and G. V. Eleftheriades, *IEEE Antennas and Wireless Propagation Letters*, Vol. 2, 103–106, 2003.
4. Nefedov, I. S. and S. A. Tretyakov, *Microwave and Optical Technology Letters*, Vol. 45, 98–102, 2005.
5. Vendik, O. G., I. B. Vendik, D. V. Kholodnyak, S. P. Zubko, and E. V. Serebryakova, *Proc. EuMC35*, 909–912, Paris, 2005.
6. Bonache, J., F. Martín, F. Falcone, J. García-García, I. Gil, T. Lopetegi, M. A. G. Laso, R. Marqués, F. Medina, and M. Sorolla, *Microwave Opt. Technology Letters*, Vol. 46, 33–35, July 2005.
7. Bonache, J., I. Gil, J. García-García, and F. Martín, *Electronics Letters*, Vol. 41, 810–811, July 2005.

Mode Coupling at the Periodic Boundary of Metamaterial

G. Granet[1], **A. Poyedinchuk**[2], **and N. Yashina**[2]

[1]Universite Blaise Pascal, France
[2]IRE NAS of Ukraine, Ukraine

Mathematical modeling of electromagnetic waves interaction with periodic boundary of metamaterial is based, as a rule, on the traditional approach, that is the solution to boundary value problems of diffraction theory. The solution to relevant spectral problems for eigen oscillations (eigen frequency is a spectral parameter) or/and eigen waves (propagating constant is a spectral parameter) presents the essential complementation to this approach. The successful association of these two ways of consideration of boundary value problem provides the possibility to treat the physical regularities and peculiarities of the resonant wave scattering by metamaterial on qualitatively new level and to get deeper understanding of complicated phenomena.

In this presentation the spectral problems for eigen waves and mode (natural oscillations) of the wavy periodic boundaries of the media with negative permittivity or/and permeability are considered. The C-method serves as efficient tool for the solution of boundary value and spectral problems of electromagnetic wave diffraction by periodic boundary of metamaterials.

The numerical algorithms and corresponding codes have been constructed and implemented for computation of complex frequencies of eigen modes (oscillations) and propagation constants of surface waves.

The study of regularities and peculiarities in the spectral characteristics (eigen complex frequencies, propagation constants of eigen modes and waves, corresponding electromagnetic field patterns, etc.) behavior with geometrical and electromagnetic parameters of periodic boundary varying have been carried out within rather wide range of parameters.

Special attention has been focused on the study of the phenomenon of eigen modes (oscillations) and eigen waves coupling.

On the base of the theory of critical points (Morse's critical points) of analytical functions of several variables the mathematical model of the inter mode coupling phenomenon, arising on the wavy periodic boundary of material with single or/and double negative parameters has been developed.

Session 0A1b
Metamaterials with Negative Index and Related Phenomena

THz Metamaterials

W. J. Padilla and R. Averitt
Los Alamos National Laboratory, USA

THz time domain spectroscopy (TDS) is used to characterize the frequency dependent electromagnetic behavior of both electric and magnetic metamaterials. Time dependent response and dynamical tunable electromagnetic behavior is studied throughout the terahertz frequency regime.

The Positive and Negative Goos-Hänchen Shifts with Left-handed Slabs

J. B. J. Chen, **T. M. Grzegorczyk**, **B.-I. Wu**, **and J. A. Kong**
Massachusetts Institute of Technology, USA

A generalized analytic formulation for analyzing the Goos-Hänchen (GH) lateral shift direction is provided, from which we show that the phenomenon of both positive and negative GH shifts at different incident angles can be observed with left-handed material (LHM) slabs. The formulation also reveals that this unique phenomenon is related to the relative amplitudes of the evanescent waves inside the LHM slabs, which is confirmed by the study of energy flux patterns.

By introducing the analytical equation for the GH shift direction

$$sign\{S\} = sign\left\{-\frac{\mu_{1r}}{\mu_{2r}}\,[C-C_1][C-C_2]\right\} \tag{1}$$

where C is ratio of the growing and decaying evanescent wave amplitudes inside the slab, while C_1 and C_2 are functions of slabs parameters and the beam's incident angle, we are able to analyze the GH shift direction change and its dependence on the incident angles and the slab's thickness. Although the well-known equation $S = -\,\partial\Phi(k_x)/\partial k_x|_{k_x=k_{ix}}$ can also be used for the parametric study of GH shifts, Eq. 1 has the advantage of directly relating GH shift directions to the slab's parameters and the electromagnetic waves in the system. More importantly, the physical meaning of the value of C is the ratio of the growing and decaying evanescent wave amplitudes inside the slab. Hence Eq. 1 reveals the connections between the GH lateral shift direction change and the variations of the ratio of the evanescent wave amplitudes inside the slab.

It can be shown that the existence of a *simultaneous* positive and negative GH shift at different angles is due to the fact that the GH shifts can change directions as the LHM slab thickness becomes smaller. The changes of GH shift directions at different slab thicknesses can be understood intuitively. For a very thin LHM slab (relative to the wavelength), the presence of the slab has little effect on the waves and the total internal reflections are mainly due to the third medium resulting in positive GH shifts. For an electrically thick LHM slab, however, the total internal reflections are mainly due to the LHM slab, yielding a negative GH shift. In between these two extremes, there exist a certain slab thickness in which *simultaneous* positive and negative shifts occur. In addition, a unique property of the LHM slab is that depending on the constitutive parameters, a slab can be electrically thick but still yield a positive GH shift as if the slab were electrically thin. As an extreme example, when the LHM slab is exactly matched to the third medium, the GH shift is always positive regardless of the slab thickness. The physical reason for this effect is related to the energy flux pattern inside the slab, which is also addressed.

Sensitivity Analysis of the Full Wave Solution of a Near-Perfect Lens with $n = -1$

O. E. French, K. I. Hopcraft, and E. Jakeman
University of Nottingham, UK

Smith et al., in their 2003 paper [1], consider the resolution achievable by a single evanescent mode in the case of a nearly perfect lens for which $\epsilon = -1$ but for which $\mu = -1 + \delta_\mu$, and note that there is a deviation from perfect resolution in the case of such material parameters.

We generalise this result by presenting the full wave solution for a dipole source above a slab of left-handed medium (LHM) of refractive index $n = -1$, but with ϵ and μ differing from those ideal values that create the perfect lens through taking

$$\epsilon = -\frac{1}{1+\delta}, \tag{1}$$

$$\mu = -(1+\delta), \tag{2}$$

where δ is real, as in the 2004 paper by Lu et al [2]. It should be noted that depite their deviations from the ideal case, the permittivity and permeability of the slab remain real and so any modifications in resolution are not due to loss effects within the lens. Solutions for the form of the fields throughout all space are obtained using the method of Hertz potentials. The imperfection modelled by the presence of a non-zero value of δ creates a single resonance, rather than the infinity of resonances that is the defining characteristic of the ideal LHM lens, with the effect that the perfect lensing properties are compromised (see in addition Chew [3]).

Using an appropriately defined resolution criterion, we examine the sensitivity of the lens as a function of the material imperfection δ.

REFERENCES

1. Smith, D. R., D. Schurig, M. Rosenbluth, S. Schultz, S. A. Ramakrishna, and J. B. Pendry, *Appl. Phys. Letts.*, Vol. 82, No. 10, 1506, 2003.
2. Lu, J., T. M. Grzegorczyk, B.-I. Wu, J. Pacheco, M. Chen, and J. A. Kong, *Opt. Tech. Letts.*, Vol. 45, No. 1, 49, 2005.
3. Chew, W. C., *Opt. Tech. Letts.*, Vol. 42, No. 5, 49, 2004.

Existence of Negative Refraction Index in Periodic Semiconductor-ferrite Composite in Microwave Frequencies

R. X. Wu
Nanjing University, China

J. Q. Xiao
University of Delaware, USA

Taking the advantage of negative permeability of certain ferrites, a new type of negative index materials (NIMs) with only-mu-negative (MNG) materials based on semiconductor-ferrite multi-layers has been proposed. We have studied the effective refraction of index of the film composite in microwave frequencies using transfer matrix method. We have found negative index of refraction could be realized in this kind of composite. For the given ferrite with negative permeability, the effects of material parameters of n-type silicon on negative index have been studied. We have found that the effective negative index and power loss depend on the layer thickness ratio between semiconductor and ferrite, and the impurity concentration in semiconductor. In comparison with other existing NIMs in microwave frequencies, the composite has advantages of low power loss and small in size.

Electric Metamaterials

D. Schurig, D. R. Smith, and J. J. Mock
Duke University, USA

J. B. Pendry
Imperial College, England

T. F. Starr
Sensor Metrix, USA

Since the arrival of negative index, an array of wires has been the standard metamaterial design for achieving negative permittivity. Recently a number of issues have arisen demonstrating that this media is more complex than initially assumed, for example, the behavior of wires terminating on an interface, the importance of continuity between orthogonal wires in multidimensional media, and the transmission of longitudinal modes. Some of these issues point to the desirability of an alternative to wire media. We will discuss some of the recent findings for wire media as well as present an alternative design for achieving electric responding metamaterials.

Session 0A4
Electromagnetic Near Field Effects in Problems of Wave Radiation from and Scattering by Ordered and Disordered Media

A Doppler Method to Measure Forward Scattering of Radiowaves at Near Grazing Angles

G. Koh and S. A. Arcone
U. S. Army ERDC-CRREL, USA

We are developing a Doppler method to measure bistatic forward and backscatter from rough surfaces on a rotating table. The method avoids interference between the forward scatter and the direct signal between antennas. We use a 90-GHz FMCW system converted for Doppler use. We use horn lens antennas to produce a 1.4 degree beamwidth that illuminates a small area of the rotating table within which the translational velocity is fairly uniform; a more exact calculation of velocity variations within the area has not yet been worked out. The table rotates at about 0.05 Hz, which provides a translational velocity of about 0.3 m/s within the illuminated area and a Doppler shift of about 75 Hz. We rectify our measured signal and form our scattering probability density functions from the peak amplitudes, of which about 1500 occur during one table rotation. Our minimum grazing angle is still a relatively large 10 degrees. However, this limitation is imposed only by blockage of the antenna aperture by the edge of the one-meter radius table; smaller angles could be achieved with a larger table. Preliminary results for very rough scattering by crushed rock of 0.5–2 cm size show Rayleigh distributions for backscatter with a greater concentration of higher amplitudes at the smaller incidence angles of 60–70 degrees. The forward scatter shows more Gaussian distributions with greater amplitudes occurring at 75–80 degrees. These general results are expected. Rms heights and autocorrelation functions of the surfaces were measured on a separate, stationary surface with a laser profilometer, but this instrument could easily be adapted to a stationary mode over the rotating table. Calibration of absolute reflectivity will require a flat plate and precise beam alignments, and a more careful description of the illumination pattern is needed because the table is not in the far field.

Extended Unitarity for S-matrix and Electromagnetic Radiation Transfer in Dielectric Random Media with Effects of Near Fields and Opposite Wave Streams' Interference

Y. N. Barabanenkov and M. Y. Barabanenkov
Russian Academy of Sciences, Russia

The phenomenological radiative transfer theory is derived from the theory of wave multiple scattering in random media at neglecting the repeated scattering of a monochromatic wave by just the same inhomogeneity—so-called single-group approximation, together with the far-field approximation for fields scattered by inhomogeneities [1]. The best-known effect of the multi-group scattering events is the coherent backscattering enhancement (weak localization) caused by the contribution of so-called cyclical (maximally crossed) diagrams [2]. This effect gives a correction to the transfer equation for backward scattering cone, with cone width being of the order of the wavelength over the extinction length [3]. Despite the achivements of the weak localization theory, there is a problem to conform the contribution of the maximally crossed diagrams into multiple scattering of waves to the energy conservation law.

In this report we present an original and perhaps unexpected resolution to the stated problem using a physical idea that the weak localization phenomenon should be coupled with the evanescent waves in a random medium. Technically our approach is based on the modern development of the wave multiple scattering theory in terms of Sommerfeld-Weyl angular-spectrum decomposition of wave amplitudes, transfer relations [4], extended unitarity for 2×2 block S-scattering matrix and effect of energy emission from an evanescent wave [5]. In result we derive a transfer equation for 2×2 block coherence matrix of angular-spectrum amplitudes of waves inside a 3D random medium slab. The diagonal blocks of the coherence matrix describe the autocoherence peculiarities of waves going forward or backward with respect to an embedding parameter into the medium slab but the off-dioganal blocks present the cross-coherence of the opposite going waves. The derived transfer equation possesses a specific energy invariant (pseudo-trace of the coherence matrix), in respect of the embedding parameter, that conforms its solution to the energy coservation law, the energy transformation between propagating and evanescent waves being taken into account. We evaluate with the aid of this transfer equation a relative contribution of evanescent waves into the coherent backscattering of waves; the influence of evanescent waves on coherent backscattering cone width and on reducing of the random medium depth where the coherent backscattering is actually formed; a specific dependence of the evanescent waves' effect on the shape of a random medium inhomogeneity.

REFERENCES

1. Barabanenkov, Y. N. and V. M. Finkelberg, *Sov. Phys. JETP*, Vol. 26, 587–591, 1968.
2. Barabanenkov, Y. N., Y. A. Kravtsov, V. D. Ozrin, and A. I. Saichev, "Enhanced backscattering in optics," *Progress in Optics*, ed. Wolf, E., Elsevier, Amsterdam, Vol. 29, 65–197, 1991.
3. Barabanenkov, Y. N., "Wave corrections to the transport equation for backscattering," *Izv. Vyssch. Uchebn. Zaved. Radiofiz.*, Vol. 16, 88–96, 1973.
4. Barabanenkov, Y. N., V. L. Kouznetsov, and M. Y. Barabanenkov, *Progress in Electromagnetic Research, PIER*, ed. Kong, J. A., EMW, Cambridge, England, Vol. 24, 39–75, 1999.
5. Gulyaev, Y. V., Y. N. Barabanenkov, M. Y. Barabanenkov, and S. A. Nikitov, *Phys. Lett. A*, Vol. 335, 471–472, 2005; *Phys. Rev. E*, Vol. 72, 026602-1-026602-12, 2005.

Energy Invariants of Composition Rules for Scattering and Transfer Matrices of Propagating and Evanescent Electromagnetic Waves in Dielectric Structures

Y. N. Barabanenkov and M. Y. Barabanenkov
Russian Academy of Sciences, Russia

Elaborated in the middle of the past century theory of wave multiple scattering by inhomogeneous media was based on composition rule [1] for scattering operator (T-matrix). This theory was successfully applied to microscopic deriving the phenomenological radiative transfer theory [2] and led to prediction of weak wave localization in random media. During the last one and a half decade the wave multiple scattering theory mentioned was reformulated in terms of subdividing the volume or surface inhomogeneous dielectric structure into a system of elementary layers (slices) perpendicular to an embedding parameter and being separated by splits, which can be vanishingly small. In result using the Sommerfeld-Weyl angular-spectrum decomposition of wave amplitudes, a system of exact equations (transfer relations) [3] was obtained for the operator wave reflection and transmission coefficients of the structure and the operator wave amplitudes of waves in splits between slices (local fields). The transfer relations have already enabled to get, in particular, more insight into the origin of opacity of dielectric 2D photonic crystals [4].

In this report we show that the transfer relations lead to a specific composition rule for 2×2 block S-scattering matrix of electromagnetic wave field. This composition rule describes the incremental change of the scattering matrix of subsystem of slices upon attachment an additional subsystem of slices. In the case of infinitesimally thin attached slice, one obtains a system of four nonlinear differential equations for blocks of the S-matrix, with the Riccati equation being a basic one. We verify that this Riccati — system of equations has an energy invariant, with respect to the embedding parameter, in the form of the extended unitarity for S-matrix [5], which in different from the familiar unitarity includes some additional terms governing the energy transformation between propagating and evanescent waves. The transfer matrix relates to the S-matrix by a known way and satisfies a system of linear equations, which possesses an energy invariant in the form of extended pseuduunitarity, which in different from the known pseudo-unitarity also includes additional terms caused by existence of evanescent waves. We illustrate the possibilities of the Riccati — system of equations in example of 1D grating with linelike rulings, showing that an emitted energy flux upon evanescent wave scattering can travel through a dielectric structure even if the structure has a forbidden gap in the transmission spectrum of incident propagating waves.

REFERENCES

1. Goldberger, M. L. and K. M. Watson, *Collision Theory*, Wiley, New York, 1964.
2. Barabanenkov, Y. N., *Sov. Phys. Uspekhi*, Vol. 18, 673–689, 1976.
3. Barabanenkov, Y. N., V. L. Kouznetsov, and M. Y. Barabanenkov, *Progress in Electromagnetic Research, PIER*, ed. Kong, J. A., EMW, Cambridge, England, Vol. 24, 39–75, 1999.
4. Barabanenkov, M. Y. and Y. N. Barabanenkov, *JOSA* (in press).
5. Gulyaev, Y. V., Y. N. Barabanenkov, M. Y. Barabanenkov, and S. A. Nikitov, *Phys. Rev. E*, Vol. 72, 026602-1-026602-12, 2005.

Near Fields in Electromagnetic Wave Multiple Scattering in Random Media

Y. N. Barabanenkov and M. Y. Barabanenkov
Russian Academy of Sciences, Russia

Usually the near fields are not taken into account in study the electromagnetic wave multiple scattering in random media. Nevertheless their effects may be substantial, as it is shown in this report, even in such coherent phenomena as weak localization of waves in random media. Besides a contribution of near fields may be strong dependent on the shape of random medium inhomogeneity. One should note that consistent consideration the near fields effects became possible after a modern development of the wave multiple scattering theory in terms of Sommerfeld-Weyl angular-spectrum decomposition of wave amplitudes, transfer relations [1] and extended unitarity for 2×2 block S-scattering matrix [2], with accounting for energy transformation between propagating and evanescent waves at scattering by dielectric structures.

We start with a system of equations for angular spectral amplitudes of local monochromatic field waves going forward and backward with respect to an embedding parameter into the 3D random medium slab with given boundary conditions on the slab boundaries. We write also the Liouville type equation for 2×2 block density matrix of angular spectral amplitudes. This Liouvile equation possesses a specific energy invariant (pseudo-trace of density matrix), with respect to the embedding parameter. Applying the Furutsu-Dosker-Novikov formalism [3], we obtain the Dyson type equation in Bourret approximation for ensemble averaged angular spectral amplitudes and the transfer equation for 2×2 block coherence matrix. The Dyson equation is simple resolved, with result showing a strong dependence of evanescent wave contribution into coherent reflectance from slab on shape of dielectric permittivity correlation function. The transfer equation is transformed to integral form which can be resolved by iteration procedure. Every term of this procedure includes, in particular, products of opposite going waves' spectral amplitudes which may be propagating or evanescent, that gives a possibility to evaluate a relative contribution of evanescent waves into the coherent backscattering of waves and the influence of evanescent waves on coherent backscattering cone width and on reducing of the random medium depth where the coherent backscattering is actually formed.

REFERENCES

1. Barabanenkov, Y. N., V. L. Kouznetsov, and M. Y. Barabanenkov, *Progress in Electromagnetic Research, PIER*, ed. Kong, J. A., EMW, Cambridge, England, Vol. 24, 39–75, 1999.
2. Gulyaev, Y. V., Y. N. Barabanenkov, M. Y. Barabanenkov, and S. A. Nikitov, *Phys. Rev. E*, Vol. 72, 026602-1-026602-12, 2005.
3. Rytov, S. M., Y. A. Kravtsov, and V. I. Tatarskii, *Principles of Statistical Radiophisics*, Vol. 3, *Wave Propagation through Random Media*, Springer, Berlin, 1989.

Local Dielectric Measurement by Waveguide-type Microscopic Aperture Probe

T. Suzuki, **K. Sugimoto**, **Y. Yamagami**, **T. Negishi**, **and Y. Watanabe**
Nippon Institute of Technology, Japan

One of the dielectric measurement methods in millimeter and submillimeter wave bands is the freespace transmission method using two horns [1]. That is sufficient for large objects. For the measurement of microscopic regional dielectric distribution of some heterogeneous dielectric materials and cellular tissues, the aperture must be down-sized so as the spatial resolution to be smaller than the wavelength.

As the embodiment of small aperture, waveguide-type probes are employed in this research. The probes are made of WR-15 waveguide with one end shielded with metal plate of 0.3 mm, on which a 0.5 mm-dia or a 0.1 mm-dia hole is made. The probe replaces one of two horns in the free-space transmission measurement.

In order to evaluate the system, the dielectric constant of teflon has been measured both by the proposed system and the free-space transmission method with two horns. Dielectric constants are derived by comparing the change in the slope of phase differences between the case of free-space transmission and with the dielectrics. The frequency is swept over 50–70 GHz. Each phase slope is shown in Figure 1. Solid lines show the measured phase differences, and dotted lines show the least square. The two horns system gives $\varepsilon_r = 1.985$ and the proposed system gives $\varepsilon_r = 1.891$ with 0.5 mm aperture and $\varepsilon_r = 1.932$ with 0.1 mm aperture. They show good agreement. Next step is to improve the accuracy and the measurement by scanning.

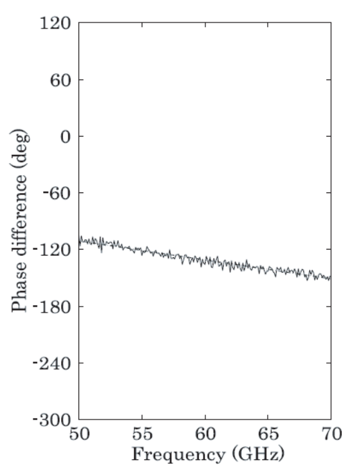

(a) Two horns.

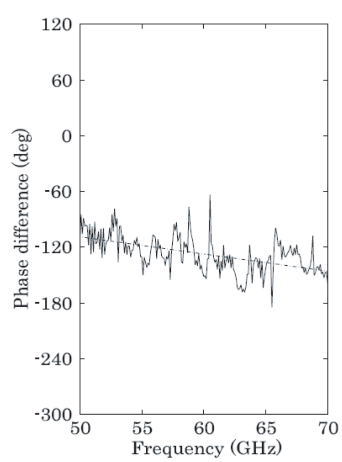

(b) Probe of 0.5 mm-dia aperture.

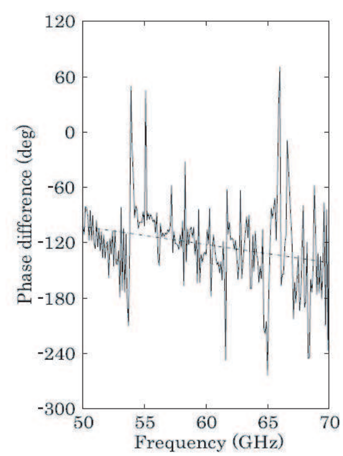

(c) Probe of 0.1 mm-dia aperture.

Figure 1: Phase differences and slopes.

REFERENCES

1. Goy, P. and M. Gross, "Free-space vector transmission-reflection from 18 to 760 GHz," *24th European Microwave Conference*, Communication C10.5, France, September 1994.

Power Absorption of Near Field of Elementary Radiators in Proximity of a Composite Layer

M. Y. Koledintseva, **P. C. Ravva**, **and J. L. Drewniak**
University of Missouri-Rolla, USA

M. Sabirov, **V. V. Bodrov**, **I. V. Sourkova**, **and V. I. Sourkov**
Moscow Power Engineering Institute (Technical University), Russia

Interest for the development, research, and applications of artificial dielectric and magnetodielectric composite materials, including conducting polymers, metamaterials, presently has increased. There are many effective-medium theories for homogenization of electromagnetic parameters of composites [1]. The problem is that exact parameters of composite phases are unknown a priori, or statistically distributed, and the necessary information on a composite contents and morphology can be obtained only experimentally. As soon as the effective parameters of composites are determined, they can be used for rigorous and approximate analytical and numerical electromagnetic analysis of structures containing such media.

It is practically interesting to study electromagnetic interaction of different radiators with composite layered structures both in far- and near-field zones. In particular, these problems arise at the development of shielding enclosures of different electronic devices. Typically, shielding is assured by reflection and absorption in the given frequency bands for all directions and polarizations of electromagnetic waves. In [2], the concept of engineering composites with the desired frequency response based on Maxwell Garnett formalism [1] and a genetic algorithm is presented, and an engineered infinitely large composite layer of finite thickness at normal and oblique plane wave incidence is considered. However, concepts of reflection and transmission coefficients, as well as of angles of incidence and polarization, are applicable only to the far-field region. In the near field zone, it is better to consider field intensity attenuation due to excitation of evanescent waves, scattering, different mechanisms of ohmic loss and energy transformation. In [3], the notions of absorption and radiation efficiencies in terms of power are introduced. The corresponding power fluxes in [3] are calculated rigorously and explicitly via the spectra of the fields using the known solutions of boundary problems for parallel-plane, cylindrical, and spherical cases.

Herein, the near-field behavior of elementary electric (or magnetic) dipoles close to a plane layer of engineered composites is analyzed using the approach [3]. The effect of conductivity of inclusions, their geometry, and concentration on the absorption and radiation efficiency of a radiator near composite layers is studied. The obtained results are compared with the full-wave FDTD simulations. The analysis may be useful for the design of electromagnetic shields, and for taking into account parasitic electromagnetic coupling inside an electronic module, where there are many chips and other active elements as sources of radiation. The represented approach can be also generalized for the case of a two-dimensional array of radiators, which will be useful for the design of frequency-selective surfaces.

REFERENCES

1. Sihvola, A., "Effective permittivity of dielectric mixtures," *IEEE Trans. Geosc. Remote Sens.*, Vol. 26, No. 4, 420–429, 1988.
2. Koledintseva, M. Y., et al., "Engineering of composite media for shields at microwave frequencies," *Proc. IEEE EMC Symposium*, Chicago, IL, Vol. 1, 169–174, Aug. 2005.
3. Sabirov, M., et al., "Power characteristics of radiators in multilayered dielectric structures," *Progress In Electromagnetic Research Symposium PIERS-04*, Pisa, Italy, 409–412, March 28–31, 2004.

The Imbedding Method in the Theory of Horn Array Antennas. Hypershort Impulses and the Near Fields

V. L. Kouznetsov
Moscow State Technical University of Civil Aviation, Russia

The usage of nanotechnologies in radiolocation has met some problems with distortion of hypershort impulses being radiated by horn array antennas. Qualitative explanation of this effect is connected with arising of reactive fields formed near the antenna's system. But quantitative description based on the traditional methods meets serious difficulties.

The method in which the reactive fields are considered as the superposition of inhomogeneous modes of radiation in horn array antennas is discussed in this work. But unlike classic aperture theory this method takes into account collective effects connected with mutually irradiation of horns. These effects are correctly described using the imbedding method. In general the ideology of this method approaches the ideology of [1].

The horn array antenna is considered as some transitional layer coordinating waveguide with free space. With all this the angular emission spectrum of the horn array antennas is defined as multiplication of the layer's matrix coefficient of transparency to "vector" of wave field in conveying waveguides. Components of this vector are components of angular emission spectrum of field in conveying waveguides.

Unlike [1] we use the model of superconductor for horn's walls. So deduction of the imbedding equations is based on the usage of the MMM method. Horn array antenna's model is described by a couple of mutually connected matrix equations for coefficients of reflection and conduction of transitional layer.

When the hypershot impulse has wide frequency spectrum, some group of frequencies inevitably falls into the space of Wood anomaly. Because of intermode interaction, playing the central role in the developing method, these anomalies become apparent in matrix coefficient of transparency. This leads to misphasing of frequency components of radiating field and divergence of impulse.

Let's note in conclusion that because of famous connection of diagrams of receiving and transmission antennas the results of the work can be useful in description of registration of near fields.

REFERENCES

1. Barabanenkov, Y. N., V. L. Kouznetsov, and M. Y. Barabanenkov, "Transfer relations for electromagnetic wave scattering from periodic dielectric one-dimension interface: TE polarization," *Progress in Electromagnetic Research: PIRS*, Vol. 24, 39–75, 1999.

Near-field Response in Lossy Media with Exponential Conductivity Inhomogeneity

R. J. Riddolls
Defence R&D Canada, Canada

This paper examines the near-field response to point source currents in lossy media with exponential conductivity inhomogeneity. The motivation for this work is to understand the modification of the lower ionosphere by powerful high frequency transmitters. The transmitted waves heat the lower ionospheric plasma, causing a localized conductivity perturbation. In the presence of the DC electric field of the polar electrojet, the conductivity perturbation produces a source current that can drive the production of extremely low frequency radiation. The major feature of inhomogeneous lossy media is the presence of distributed space charge. Significant simplification of the space charge description can be made by considering the ordering of the temporal and spatial time scales of the problem, and thus the importance of various terms in Maxwell's equations, such as conduction current versus displacement current, and static scalar potential versus dynamic vector potential. The analysis of the problem begins by using the charge continuity equation to find the scalar potential response to the source current in a medium with exponential conductivity inhomogeneity. This scalar potential is sufficient to determine the electric field response in the static or electroquasistatic limits. In the magnetoquasistatic limit, the scalar potential, along with the source current, act as driving terms for a vector potential. The role of feedback between the scalar and vector potentials in inhomogeneous lossy media is noted. The resulting vector potential equation is shown to have Kelvin function solutions with exponential arguments. Comparisons of the theory with measurements from ionospheric modification experiments are presented.

Surface and Volume Scattering from Rough Heterogeneous Media in the Optical Domain

H. Chanal, J. P. Segaud, and P. Borderies
ONERA Centre de Toulouse, France

M. Saillard
Université de Toulon et du Var, France

Scattering from rough heterogeneous media involves both surface and volume effects. This issue has many applications in geophysics, remote sensing (from the microwave domain to the optical one) and biomedicine, for instance. In optics, the total diffraction problem must be addressed accurately to understand the scattering properties of coatings. But volume and surface scatterings are both difficult issues that are usually studied separately. There is a need for rigorous methods that are able to handle in the same way both phenomena without any coupling hypothesis. We choose to use the Finite Difference Time Domain (FDTD) method as such a reference one. A Monte Carlo process is built to access to the statistical properties of rough heterogeneous media. It is composed of two steps:

- the generation of one deterministic medium realization;
- the FDTD computation over this realization to derive the electromagnetic near and far fields.

This process is repeated and the successive results are averaged to give the statistical response of the inhomogeneous medium. This work is restricted to the bidimensional geometry with the aim of investigating fine surface-volume coupling effects.

In a first part, we study the scattering of rough surfaces (homogeneous medium). Random profiles with gaussian height distributions and gaussian or exponential autocorrelation functions (ACF) are considered. Our method is compared with the Method of Moments (MoM) on a unique deterministic realization and on the average scattering patterns. The agreement proves to be always excellent for gaussian ACF and to decrease when the roughness increases for exponential ones due to the representations of the fine structures in the surface profiles which are different in both methods.

Then, we investigate the volume effects with randomly distributed cylindrical scatterers embedded in a semi-infinite homogeneous binder with flat interface. Effective propagation parameters are derived from the evolution of the near field with depth. These numerical results are compared to the Maxwell-Garnett and Bruggeman mixing laws and the Foldy-Twersky and Keller perturbative models for both polarization modes, validating the process implementation and allowing to precise the validity domain of approximate approaches.

Finally, we tackle the general case of rough heterogeneous media. Several interface types (the previous gaussian and exponential ACF surfaces and a new type of surfaces with profile correlated to the scatterers distribution in volume) are considered on top of heterogeneous media over a large range of volume fractions, particle sizes and optical constants. The hypothesis of surface and volume scattering splitting is systematically tested and surface -volume coupling effects are analyzed.

Optical Properties of Metal Nanoclusters on a Substrate

S. V. Sukhov
Institute of Radio Engineering and Electronics of RAS, Ulyanovsk Branch, Russia

S. G. Moiseev
Military Communications University, Ulyanovsk Branch, Russia

The past few years demonstated extended use of metallic nanoclusters as sensing elements in various biosensor systems. Most of these systems exploit the unique optical properties of gold nanoparticles determined by the localized surface plasmon resonance. The operation of such devices is based on the dependence of the plasmon resonance on either the local dielectric environment of an individual nanoparticle or the mean distance between the approaching particles. Reports are now available on the biospecific interactions taking place on gold particles in systems where nanoparticles are represented as ordered structures, either as selfassembled monolayers or as part of polymer assemblies. Urgency of study of properties of plane arrays of nanoparticles is related also with creation of covers with tunable optical properties. Varying the mutual arrangement of nanoparticles, one can change the reflective properties of surface and its resonant properties in wide spectral range.

We present a detailed discussion of optical properties of aggregated conjugate-based structures such as bispheres, linear chains, plane arrays. The interaction of electromagnetic wave with a cluster of nanoparticles situated on a substrate is considered. Our attention is focused on dependence of extinction and scattering spectra on the optical coupling of conjugates, effects of interparticle spacing and cluster structure. The reflection of light from nanoclusters is analyzed with structure factor taken into account for different mutual arrangement of nanoparticles. Both Coulomb (near-field) and retarded parts of optical fields acting between nanoparticles and from substrate side were considered in details.

Session 0A9
Advances in Integral Equation Techniques for Planar Circuits

Conformal Meshing in FFT Based EM Analysis

J. C. Rautio
Sonnet Software, Inc., USA

Shielded planar EM analysis is based on the FFT. This means it has extremely high accuracy and dynamic range (due to the complete absence of numerical integration), but it also analyzes a circuit based on a fine underlying FFT mesh. While the FFT mesh can be even finer than the pixels on a typical computer screen, it does result in more difficulty in analyzing non-Manhattan geometries. Conformal mesh eliminates this problem for a broad class of non-Manhattan geometries including curved transmission lines, like circular spiral inductors. The nature of this conformal meshing is described and examples are given. Complicated circuits with curving transmission lines can now be analyzed quickly even if they can not be analyzed at all (to the same degree of error) on any other EM tool of any kind.

An Analysis of Coaxial Line Slot Antenna for Hyperthermia Treatment by Spectral Domain Approach

T. Nakata, **H. Yoshitake**, **K. Wakino**, **Y. D. Lin**, **and T. Kitazawa**
Ritsumeikan University, Japan

An efficient extended spectral domain approach (ESDA) is applied to evaluate the scattering parameter of laterally slotted coaxial antenna for hyperthermia treatment (Figure 1), and then the results calculated by ESDA are compared with that by FEM simulation. In ESDA process, first total analyzing space is divided into four regions; region I, ($a \leq \rho \leq b$, $-\infty \leq z \leq 0$) region II, ($b \leq \rho \leq b+t$, $-c - \frac{w}{2} \leq z \leq -c + \frac{w}{2}$); region III, ($b+t \leq \rho \leq r$, $-\infty \leq z < d+g$); region IV, ($0 \leq \rho \leq b+t$, $d \leq z \leq d+g$), as shown in Figure 1. Then the aperture electric fields are introduced; ea and eb at the slot in the outer conductor; ec between region III and IV. After dividing the analyzing space, each region can be treated independently with equivalence theorem. The electromagnetic fields in each region are expressed in terms of the appropriate eigen functions which satisfy the boundary conditions. In the regions I and III, the fields are expressed by Fourier integral in the z-direction, while in the regions II and IV the fields are expanded by Fourier series. In transformed (spectral) domain, the Greens functions (which represent electromagnetic field in each region) are formulated and then the electromagnetic fields in each region are related to the aperture fields. The remaining boundary conditions, the continuity of the magnetic field at the interfaces between adjacent region, are applied to obtain a set of the integral equations in terms of the aperture fields. The aperture fields can be determined by applying the Galerkins procedure to these coupled integral equations. The scattering parameters, in turn, are obtained by taking inner products of the aperture fields with the eigen functions in each region.

Figure 2 shows the comparison of the reflection coefficients $|S_{11}|$ simulated by ESDA and FEM with changing the position of slot $c-\frac{w}{2}$ on the coaxial slot antenna. The antenna probe is embedded in a liver ($\varepsilon_{r2} = 43 - j12.38$). It is confirmed that the both results are in good agreement. Computational labor of the present method is far lighter than that of FEM, and is suitable for the iterative computation that is required for the optimization of antenna design. More over, the present method can afford to consider the effect of the metallization thickness in the outer conductor.

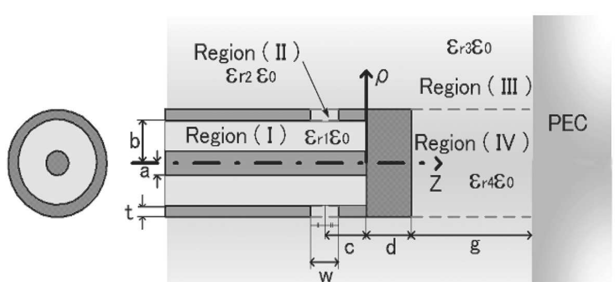

Figure 1: Schematic structure of slotted coaxial line antenna. $t = 0.10\,\text{mm}$, $a = 0.24\,\text{mm}$, $b = 0.80\,\text{mm}$, $d = 5.00\,\text{mm}$, $w = 2.00\,\text{mm}$, $g = 40.00\,\text{mm}$, $\varepsilon r1 = 2.1$, $\varepsilon r2 = \varepsilon r3 = \varepsilon r4 = 43 - j12.38$.

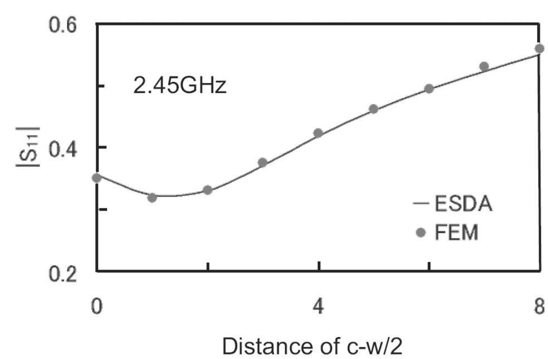

Figure 2: Comparison of reflection coefficients between ESDA and FEM with changing the position of slot.

Spectral Domain Analysis of Coupled Microstrip Using Spheroidal Wave Functions with Edge Conditions

C. A. Carter
Stevens Institute of Technology, USA

An analysis of coupled microstrip transmission lines using spheroidal wave functions and the spectral domain method will be presented. In the spectral domain method, the electromagnetic field equations and boundary conditions are formulated in the spectral, or Fourier transform, domain. This formulation is used to derive an equation that expresses the Fourier transform of the electric field in terms of the current distribution on the microstrip. Galerkin's moment method is then applied to yield a system of equations that can be used to solve for unknown propagation constants as a function of frequency.

The current distribution on microstrip is modeled as an expansion of known basis functions with unknown coefficients. Walsh functions, sinusoidal functions, sinusoidal functions with edge conditions and Chebyshev polynomials with edge conditions have been utilized as basis functions in prior research. Functions that incorporate the microstrip edge conditions more effectively model the current on the microstrip and require fewer terms in the current expansion. Previous research at Stevens Institute of Technology has utilized spheroidal wave functions to model the current distribution on single microstrip transmission lines. These functions were shown to model the current over a broad frequency range and required fewer expansion terms than other previously used basis functions.

For this presentation, the work carried out utilizing spheroidal wave functions in the analysis of single microstrip lines is extended to coupled microstrip. A brief overview of the theory of spheroidal wave functions will be included but the primary focus will be on practical issues of computation related to their use in the analysis of both single and coupled microstrip. Chebyshev polynomials with edge conditions have previously been used to model the current on coupled microstrip over a large frequency range. Preliminary results demonstrate that fewer spheroidal wave functions than Chebyshev polynomials are needed to compute the propagation constant as a function of frequency. Propagation constants computed for a range of frequencies and strip separation values are investigated.

Application of the Space Domain MoM Technique to the Analysis of Planar Guiding Structures

M. B. Ben Salah, **M. Souden**, **A. B. Kouki**, and **A. Samet**
Ecole Polytechnique de Tunisie, Tunisia

Integral equation methods are widely recognized as efficient techniques for studying the propagation characteristics of planar structures. In these techniques, the Method of Moments in the spectral domain is typically used since the Green's functions can be obtained in closed form. This approach has been shown to be quite effective for the modeling of planar guiding structures and is behind several empirical models used today in many commercial microwave CAD tools. Nevertheless, this approach requires the evaluation of infinite integrals with oscillating and slowly decaying integrands, for open structures, and infinite series for shielded ones. To circumvent this problem, a space domain formulation of the Method of Moments, widely used to characterize arbitrary planar structures and discontinuities, is proposed for the analysis of guiding structures. The closed form expressions of the Green's functions for the vector and scalar potentials in the space domain are found through the application of the Generalized Pencil of Functions (GPOF) method to the one dimensional case. In such a case, we show that the passage from the spectral to the space domain results in a simplified closed form expression in terms of Bessel functions of the second kind. This new formulation is applied to a microstrip line and the results are compared to other models.

On the Limitations of the Space Domain Formulation of the MoM Method for Planar Circuits

K. Kochlef, A. B. Kouki, and A. Samet
Ecole Polytechnique de Tunisie, Tunisie

The Method of Moments (MoM) is arguably the most well suited technique for the analysis of planar circuits. This technique has been traditionally formulated in the spectral domain, since it is only in this domain that the Green's functions can be determined exactly. However, the spectral domain formulation suffers from several limitations, particularly for open structures, that make its implementation and use difficult and the required computational resources high. In light of this, substantial research effort has been invested in developing a space domain alternative whereby an approximate space domain Green's function is derived from its spectral domain counterpart and used in space domain formulation of the MoM technique. Therefore, the accuracy of this technique depends on that of the space domain Green's function.

In this paper, we present a systematic investigation of the accuracy of the space domain MoM technique applied to single layer planar circuits with the aim of establishing its limitations and determining its zones of applicability. The study covers a wide range of parameters, including frequency, cell spacing, dielectric constant values and substrate height. We also examine the impact of varying the parameters of the generalized pencil of function (GPOF) technique, used to determine the space domain Green's function, on the precision of the technique and its zones of applicability. Finally we discuss potential remedies to overcome the limitation of the space domain techniques.

REFERENCES

1. Aksun, M. I., "A robust approach for the derivation of closed-form Green's function for a general microstrip geometry," *IEEE Trans. Microwave Theory Tech.*, Vol. 44, 651–658, May 1996.
2. Shuley, N. V., R. R. Boix, F. Medina, and M. Horno, "On the fast approximation of Green's functions in MPIE formulations for planar layered media," *IEEE Transactions on Microwave Theory and Techniques*, Vol. 50, No. 9, 2185–2112, September 2002.
3. Sarkar, T. K. and O. Pereira, "Using the matrix pencil method to estimate the parameters of a sum of complex exponentials," *IEEE Trans. Antennas and Propagation Magazine*, Vol. 37, 48–55, February 1995.
4. Alatan, L., M. I. Aksun, K. Mahadevan, and M. T. Birand, "Analytical evaluation of the MOM matrix elements," *IEEE Transactions on Microwave Theory and Techniques*, Vol. 44, No. 4, April 1996.

Critical Study of DCIM, and Development of Efficient Simulation Tool for 3D Printed Structures in Multilayer Media

M. I. Aksun and T. Onal
Koc University, Turkey

Since the discrete complex image method (DCIM) has been widely used to get closedform Green's functions for vector and scalar potentials, its formulation is first reviewed to clarify some issues related to the derivation and to its use with the method of moments (MoM). Then, an efficient and rigorous electromagnetic simulation algorithm, based on the combination of MoM and DCIM for the solution of mixed-potential integral equation (MPIE), is developed for 3D printed structures in multilayer media. As this approach, MoMDCIM, has already proved to be very efficient to analyze printed structures with only horizontal conductors in multilayer environment, and with horizontal and vertical conductors in single-layer media, it is extended to more general geometries with horizontal conductors and vertical conductors spanning more than one layer. Moreover, the algorithm proposed is possibly the most efficient approach to handle printed circuits with multiple vertical conductors, spanning one or more layers. It should be stressed that efficiency in this context refers to handling multiple vertical conductors with almost no additional fill-in cost of the MoM matrix. Some printed circuits and planar antennas are analyzed, and results are compared to those presented in the literature and obtained from the commercial software em by SONNET to validate the algorithm.

Thick Metal Models

J. C. Rautio
Sonnet Software, Inc., USA

Both the fine detail of fields at the edge of thick metal and the large scale fields over an entire circuit must be accurately represented in an EM analysis in order to correctly analyze thick metal in a planar circuit. This is a very difficult EM problem that has seen substantial research over the last decade. As a result, all serious commercial EM tools now include specialized thick metal models. The different models are briefly described and their relative advantages and disadvantages pointed out. Techniques for quantifying thick metal modeling error, as well as determining if a thick metal model is even needed, are detailed.

Analysis of Cylindrical Microstrip Line with Finite Thickness of Conductor

H. Miyagawa, T. Nishikawa, K. Wakino, Y. D. Lin, and T. Kitazawa
Ritsumeikan University, Japan

A hybrid-mode analysis of cylindrical microstrip line (Figure 1) based on Extended Spectral Domain Approach (ESDA) [1] is presented. Two formulation procedures are performed for the microstrip with zero-thickness conductor, that is, the procedures based on the current on the strip or the electric field at the aperture surface (the aperture field) as source quantities. When the aperture fields are taken as the sources, the procedure is easily applicable to the case with finite-thickness conductor [2]. By introducing the aperture fields and utilizing the equivalence theorem the whole region is divided into sub-regions. After dividing the region, each sub-region can be treated separately, and then the electromagnetic fields in each sub-region are expressed in terms of the appropriate eigen functions, which satisfy the boundary conditions in -direction. In transformed (spectral) domain, the Greens functions are derived easily, and then the electromagnetic fields in each sub-region are related to the aperture fields ea(f) and eb(f). The remaining boundary conditions, the continuity of the magnetic field at the interfaces of the aperture sub-region, are applied to obtain a set of the integral equations on the aperture fields. Applying the Galerkins procedure to the integral equations, we get the determinantal equation for the phase constant b. The characteristic impedance is evaluated based on the voltage-current definition. The numerical procedure with ESDA incorporates the effects of the edge singularities properly and can afford the efficient and accurate calculation method for the characteristic impedances in addition to the phase constants of cylindrical microstrip line. The numerical results for zero-thickness conductor by both procedures, based on current and aperture field, are in good agreement and also they agree well with the published data. The numerical results obtained by the procedure based on the aperture field have revealed for the first time the effects of conductor thickness and curvature of substrate on the characteristics of cylindrical microstrip.

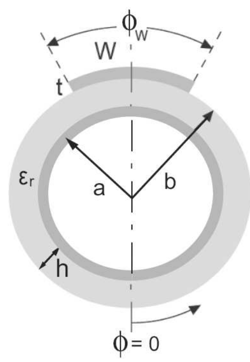

Figure 1: Cylindrical microstrip line.

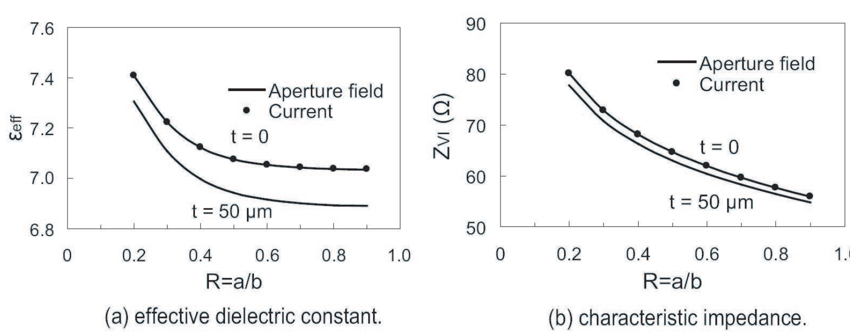

Figure 2: Curvature and thickness effects on propagation characteristics, $\varepsilon r = 9.6\,, \mathrm{h} = 1\,\mathrm{mm}, \mathrm{W} = 1\,\mathrm{mm}, \mathrm{f} = 10\,\mathrm{GHz}$.

REFERENCES

1. Kitazawa, T., "Nonreciprocity of phase constants, characteristic impedances and conductor losses in planar transmission lines with layered anisotropic media," *IEEE Trans. Microwave Theory Tech.*, Vol. 43, No. 2, 445–451, Feb. 1995.
2. Yamamoto, H., H. Miyagawa, T. Nishikawa, K. Wakino, and T. Kitazawa, "Full wave analysis for propagation characteristics of cylindrical coplanar waveguides with finite thickness of conductor," *IEEE Trans. Microwave Theory Tech.*, Vol. 53, No. 6, 2187–2195, June 2005.

Session 0P1
Inverse Problems

Microlocal Analysis of RADAR

C. Nolan
University of Limerick, Ireland

Microlocal analysis is a powerful mathematical tool that has developed as a refinement of geometrical optics. We will introduce it and show how to use it to analyze the scattering of radio waves (RADAR) from the earth's terrain, and how it can be used to efficiently image the earth remotely.

Detection of Small Tumors in Microwave Medical Imaging Using Level Sets and Music

N. Irishina, **M. Moscoso**, **and O. Dorn**
Universidad Carlos III de Madrid, Spain

In this work we focus on the application of microwaves for the early detection of breast cancer. We compare two different strategies for inverting TM data for small objects embedded in soft tissue. One is based on the more traditional formulation using a pixel representation, while the other uses shapes for modeling the tumors. Since the inverse problem is very ill-posed pixel-based reconstruction techniques require strong regularization in order to achieve a stable inversion. Regularization usually leads to a severe smoothing of tumor boundaries. This limits resolution. Moreover, typical tumors in this application have a high contrast in the dielectric parameters which is difficult to retrieve with pixel-based techniques. An inversion using a shape-based model offers the advantage of well defined boundaries and, at the same time, it incorporates an intrinsic regularization due to the reduced dimensionality of the inverse problem. Advantages and disadvantages of both approaches will be discussed for several numerically simulated situations.

The Mie Solution for Improving the Evolution Strategy in Breast Cancer Imaging

S. Pandalraju, P. Rashidi, and M. El-Shenawee
University of Arkansas, USA

D. Macias
Université de Technologie de Troyes, France

In a previous work in microwave imaging, we have successfully characterized threedimensional malignant breast cancer tumors employing evolution strategies. Particularly, we determined the form (with a number of unknowns dependent on the irregularity of the shape) and the location (three unknowns) of non-spherical tumors from scattering data. However, notwithstanding the encouraging results obtained, the iterative nature of the imaging method required several CPU hours on a Hewlett-Packard AlphaServer DS25. In this work we propose a strategy to speed up the imaging process through an improvement of the initialization of the evolutionary search.

An evolution strategy is a heuristic population-based optimization technique, inspired on the Darwinian principles of variation and selection, which searches the best fit solution through the exploration of a search space with the assistance of a forward solver and a fitness functional. The variation stage includes the recombination and mutation operations and is responsible for the increase in the variety of the search space. The selection process retains those elements of the population leading to more promising regions of the search space. The evolutionary loop continues until a convergence criterion has been fulfilled.

Instead of generating the initial population employing uniformly distributed random numbers, we initialize the evolution strategy with a population estimated by means of Mie's scattering theory. This approach is valid in the sense that tumors can be considered, at least in principle, as lossy spheres immersed in a homogeneous lossy medium. Thus, a decrease in the computing time required by the evolution strategy and method of moments imaging method could be expected since the search space has been reduced to a region in the neighborhood of the optimum.

Our preliminary results obtained employing the approach described above show potential in achieving convergence at a faster rate. Some issues related to the error sensitivity are also discussed in this work.

Radiative Transport Theory for Optical Molecular Imaging

A. D. Kimn
University of California, USA

We study the inverse fluorescent source problem for optical molecular imaging in tissues. We use the radiative transport equation to model light propagation in tissues. In particular, we make use of analytical results for a point source and a voxel source to compute estimates for the location and size of a general fluorescent source in a halfspace composed of a uniform absorbing and scattering medium. We present numerical results demonstrating this theory.

Reconstructing Absorption and Diffusion Shape Profiles in Optical Tomography Using a Level Set Technique

M. Schweiger[1], **O. Dorn**[2], **V. Kolehmainen**[3], **A. Zacharopoulos**[1], **and S. Arridge**[1]

[1]University College London, England
[2]Universidad Carlos III de Madrid, Spain
[3]University of Kuopio, Finland

A novel shape reconstruction algorithm for optical tomography is presented which is based on a level-set formulation for the shapes. The goal is to recover contrast and shapes of inclusions in the absorption as well as in the scattering/diffusion parameter simultaneously from boundary data. Evolution laws based on descent directions for a cost functional are derived for two different level-set functions, one describing the absorption and one the diffusion parameter, as well as for the parameter values inside these shapes. Numerical experiments are presented in 2-D which show that the new method is able to simultaneously recover shapes and contrast values of absorbing and scattering objects embedded in a slightly heterogeneous background medium from simulated noisy data. These results are compared with more traditional pixel-based reconstructions, of which the regularization parameter is determined by an L-curve method. It is shown that, using this regularization parameter, the pixelbased reconstructions are severely smeared-out over a relatively large domain, such that contrast values and sizes of the objects are not well recovered. Compared to these pixel-based reconstructions, the shape-based inversions deliver a very good guess for the shapes, and the contrast values are recovered with higher accuracy.

3D Shape Based Reconstruction for Optical Tomography Using Spherical Harmonics and BEM

A. Zacharopoulos and S. Arridge
University College London, UK

O. Dorn
Universidad Carlos III de Madrid, Spain

V. Kolehmainen
University of Kuopio, Finland

J. Sikora
Warsaw University of Technology, Poland

We consider the recovery of smooth 3 D region boundaries with piecewise constant coefficients in Optical Tomography (OT). The method is based on a parametrisation of the closed boundaries of the regions by spherical harmonics coefficients, and a Newton type optimisation process. A boundary integral formulation is used for the forward modelling. We show reconstructions for 3 D situations. An advantage of the proposed method is the implicit regularisation effect arising from the reduced dimensionality of the inverse problem. There are several physiologically interesting observations which can be derived from the knowledge of the absorption μ_a and diffusion, D, of light in tissue. This includes tissue oxygenation, blood volume and blood oxygenation.

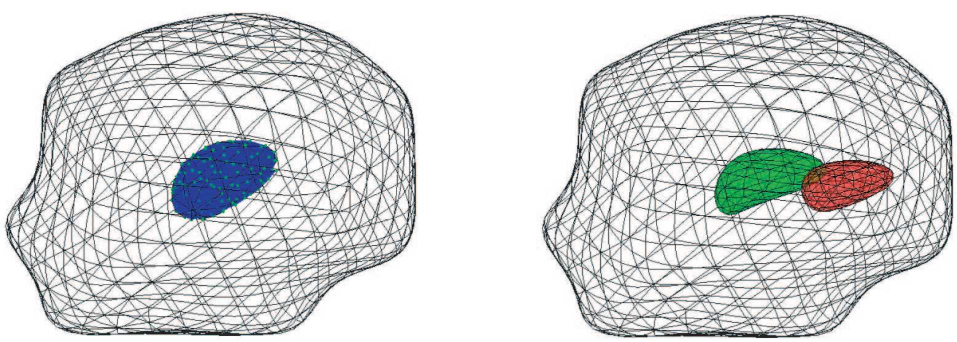

Figure 1: Recovery of the inhomogeneity shape from OT measurements on the surface using an initial guess for the optical parameters. (left) the target; (right) red: the initial guess, green: the reconstructed shape.

Detection of Inclusions in the Radiative Transfer Regime

G. Bal
Columbia University, USA

Inclusions can be modeled as variations in the constitutive parameters of radiative transfer equations for the energy density of waves propagating in highly heterogeneous media. In the practically useful regime where the inclusions have a small volume compared to the overall size of the system, we present asymptotic expansions that characterize the influence of the inclusions on available measurements and show how these formulas may be used towards detection and imaging. These asymptotic formulas are also compared with numerical simulations of the wave equation, where the inclusions are modeled as either void areas (where fluctuations are suppressed) or perfectly reflecting objects. Careful numerical simulations of wave equations in two space dimensions over domains of size comparable to 500 wavelengths allow us to assess the volume of the inclusions that can be detected and imaged from the available measurements. This is joint work with Olivier Pinaud.

A Parametric Level-set Approach to Tomographic Reconstruction

A. B. Tarokh
Brigham and Women's Hospital, USA

E. L. Miller
Northeastern University, USA

We consider an approach to the tomographic reconstruction problem based on a parametric form of the level-set method to describe the geometry of a 3D object. Inspired by the flexibility and simplicity of linear expansion methods that are commonplace in the signal processing and applied mathematics literatures, our method makes use of such expansions in the description of the level-set function. Given a fixed set of basis functions, the level-set function is described using a linear combination of these basis functions, with the expansion coefficients treated as unknowns. Our formulation admits the use of a wide range of basis functions, and we provide several specific examples of bases to demonstrate the method's flexibility (polynomial, sinusoidal, and Gaussian). A non-linear optimization method is developed for determining the optimal values of the unknowns. In addition to the level-set function expansion coefficients, we also estimate the space-varying textures of the anomaly and background. Modelling these features using linear expansions (similarly to the level-set function), we include the corresponding expansion coefficients in the non-linear optimization routine. Hence, our algorithm simultaneously optimizes the structure of the anomaly as well as the space-varying textures of the anomaly and background. Finally, to enforce an overall smoothness of the reconstructed target, we include in our optimization process a regularization term that penalizes the surface area of the target.

Our geometric approach to the tomographic imaging problem is an efficient, parametric technique that sequentially "evolves" the two-dimensional surface that bounds the modelled anomalous region of interest. The tomographic flow, or surface evolution, is affected through iterative cost-decreasing steps using a gradient-based evolution of the parameters that define the surface as well as the textures. The cost functional is defined as a typical log likelihood functional arising from the assumed Gaussian nature of the noise corrupting the observed data. The key attractive features of our approach are as follows: 1) Our model admits the presence of multiple spatially-separate anomalous regions in the medium. 2) We employ an appropriate regularization penalty to improve the robustness of the algorithm in the presence of noise. This penalty has the effect of encouraging a smooth reconstructed shape. 3) The simple characterization of the object in terms of a low number of parameters lends itself to efficient computational implementation.

The flexibility afforded by the use of basis expansion functions requires a method for determining those that should in fact be used in the reconstruction given a large dictionary of potions. This would imply that we simultaneously optimize over a vector of coefficients equal in cardinality to the dictionary of basis function, which is computationally intractable even for modestly-sized dictionaries. Hence, we seek to retain the advantages of having a large dictionary of basis functions for representing the level-set function corresponding to our anomalous region, while maintaining an overall tractable optimization. To this end, we introduce a greedy algorithm for selecting a small set of basis functions that yield improved cost, where the cost functional is retained from the non-adaptive case above.

We validate our approach through extensive numerical studies on simulated noisy data generated using X-ray and diffuse optical tomographic (DOT) models.

Shape Reconstruction in Diffuse Optical Tomography Using the Radiative Transfer Equation and Level Sets

O. Dorn and M. Moscoso
Universidad Carlos III de Madrid, Spain

We consider Diffuse Optical Tomography as an inverse problem for the radiative transfer equation in 2D. The goal is to find and characterize small objects embedded in a heterogeneous medium. We assume that we know certain characteristics of the background medium, as for example average values of the absorption and scattering coefficient, but small fluctuations of a reasonable amount are assumed to be unknown. The optical parameters inside the embedded objects (e.g., tumors or other anomalies) are assumed to be significantly different from the background values and constant, but their values (as well as the shapes of the objects) are unknown. The region of interest is surrounded by a band of clear fluid (e.g., CFL), which is assumed to be non-scattering or very low-scattering. The data consist then of the time-dependent outgoing photon flux at discrete receivers located at the boundary of the domain. A level set strategy is employed in order to find the topology, the shapes as well as the contrast of the unknown inclusions. Several numerical examples are presented which demonstrate the performance of the method in various situations.

Time-reversal and Signal Subspace Methods for Imaging and Inverse Scattering of Multiply Scattering Targets

E. A. Marengo and F. K. Gruber
Northeastern University, USA

In this work the inverse scattering problem of estimating the locations and scattering strengths of a number of multiply scattering point targets in the near or far field from single-snapshot active antenna array data is investigated with the aid of two signal subspace approaches: Time-reversal-based methods with an emphasis on time-reversal multiple signal classification (MUSIC) and a new signal subspace method developed in this work that is based on parameter search in high-dimensional parameter space. The second approach corresponds under additive white Gaussian noise to the maximum likelihood (ML) estimator for the target positions in the (distorted wave) Born approximated case. The approach also corresponds to the ML estimator for the multiple scattering case so long as the associated forward and inverse problems are treated in terms of an equivalent two-point scattering potential matrix or tensor instead of the one-point scattering potential function or the target reflectivities.

The methods are comparatively investigated, and it is found that for weakly interacting targets whose collective scattering is describable by the Born approximation the ML method outperforms the time-reversal approach in number of localizable targets, being it possible, e.g., to locate up to $N(N+1)/2-1$ or N^2-1 targets using coincident or non-coincident arrays of N transmitters and receivers, respectively, instead of the time-reversal limit of only up to $N-1$ targets. The number of targets that are in principle localizable using the time-reversal MUSIC approach remains unchanged under Born-approximable versus non-Born-approximable (exact, multiple scattering) conditions. On the other hand, if multiple scattering is significant then the high-dimensional search method yields a less dramatic advantage over the time-reversal approach in number of localizable targets. The high-dimensional signal subspace method is also found to yield better resolution performance at the expense of higher computational demand.

A new explicit formula (a non-iterative algorithm) to calculate the scattering strengths once the target locations have been determined is also developed which holds even in the nonlinear regime of multiply scattering targets. The approach is valid so long as the conditions for applicability of the time-reversal approach for generally non-coincident arrays are met, in particular, $M \leq \min(N_t, N_r)$ and $M < \max(N_t, N_r)$ where N_t and N_r are the number of transmitters and receivers, respectively, and M is the number of point targets.

The final part of the presentation includes extensions of the previous algorithms for the case of extended targets where instead of a single Green function vector or propagator per target there is an effectively finite-dimensional subspace of such propagators. The paper includes computer-simulated validations of the theory which comparatively address the performance of the methods.

The work reported in this presentation expands previous work co-authored by the present authors on time-reversal imaging and inverse scattering of multiply scattering point targets, with the main contributions of the present work residing in the development of a non-iterative formula for the full nonlinear inverse scattering reconstruction and in the comparative investigation of time-reversal in the context of alternative signal subspace approaches (the ML approach included) for the associated target localization problem with active arrays. This work also goes a step beyond in considering the generalization of these developments to extended targets.

REFERENCES

1. Gruber, et al., *J. Acoust. Soc. Am.*, Vol. 115, No. 6, 3042–3047, June 2004.
2. Devaney, et al., *J. Acoust. Soc. Am.*, Vol. 118, No. 5, November 2005.

Approximation of the Scattering Coefficients for a Non-RAYLEIGH Obstacle

G. F. Crosta
Università degli Studi Milano - Bicocca, Italy

Let $\Omega \subset \Re^2$ be a star shaped obstacle with smooth boundary, $\mathit{\Gamma}$. Let u denote the incident scalar plane wave and v the scattered wave complying with $(u+v)|_{\mathit{\Gamma}} = 0$ and the SOMMERFELD radiation condition. Let λ denote a pair of indices and $\{u_\lambda\}$ be the family of real wave functions, which is linearly independent and complete in $L^2(\mathit{\Gamma})$, provided $k^2 \notin \sigma[-\Delta_D]$ (the wavenumber squared is not an eigenvalue of the interior DIRICHLET LAPLACE operator). The scattering coefficients are defined by $f_\lambda = -(i/4)\langle u_\lambda | \partial_N(u+v)\rangle$, where $\partial_N(.)$ is the outward normal derivative on $\mathit{\Gamma}$ and $\langle .|\ .\rangle$ denotes the inner product in $L^2(\mathit{\Gamma})$.

If L denotes the approximation order and $\Lambda[L]$ the related set of indices, approximate scattering coefficients $\{p_\lambda^{(L)}\}$ can be introduced

$$p_\lambda^{(L)} = -(i/4)\langle u_\lambda | \partial_N u + (\partial_N v)_2^{(L)}\rangle \tag{1}$$

with

$$(\partial_N v)_2^{(L)} = \sum_{\mu\in\Lambda[L]} c_\mu^{(L)} \partial_N v_\mu. \tag{2}$$

Here $F_2 = \{\partial_N v_\mu\}$ is the family of normal derivatives of outgoing waves $\{v_\mu\}$, which is unconditionally complete, and $\{c_\mu^{(L)}\}$, $\mu \in \Lambda[L]$, are suitable expansion coefficients. Let $W \equiv \{w_\mu\}$ denote a family of functions such that

$$w_\mu = (1/2)\partial_{N[\mathbf{r}]} v_\mu + (i/4)\int_\Gamma \partial_{N[\mathbf{r}]} H_0^{(1)}[kR]\partial_{N[\rho]} v_\mu d\Gamma[\rho], \tag{3}$$

where $R = |\mathbf{r} - \rho|$.

The following results can be shown to hold.

1) The family W is linearly independent and complete in $L^2(\Gamma)$ provided $k^2 \notin (\sigma[-\Delta_D] \cup \sigma[-\Delta_N])$ i.e., k^2 is neither an eigenvalue of the interior DIRICHLET nor of the interior NEUMANN LAPLACE operators.

2) The coefficients $\{c_\mu^{(L)}\}$, which form the vector $\mathbf{c}^{(L)}$ of card $[\Lambda[L]]$ components, solve the well-posed algebraic system

$$\mathbf{W}^{(L)} \cdot \mathbf{c}^{(L)} = \mathbf{g}^{(L)}, \tag{4}$$

where $\mathbf{W}^{(L)} = [\langle w_\lambda | w_\mu \rangle]$ is the GRAMian of $\{w_\mu\}$ and $\mathbf{g}^{(L)} = [\langle g | w_\mu\rangle]$ is a vector of known terms obtained from

$$g = (1/2)\partial_{N[\mathbf{r}]} u - (i/4)\int_\Gamma \partial_{N[\rho]} u \partial_{N[\mathbf{r}]} H_0^{(1)}[kR] d\Gamma[\rho]. \tag{5}$$

3) Finally, an error estimate for $\| \partial_N v - (\partial_N v)_2^{(L)} \|_{L^2(\Gamma)}^2$ can be provided in terms of the smallest eigenvalue of a double layer acoustic potential.

RAYLEIGH's hypothesis is nowhere required i.e., both F_2 and W only have to be linearly independent and complete.

Three Satellite Geolocation from TDOA and FDOA Measurements

B. A. Kemp, **T. M. Grzegorczyk**, **B.-I. Wu**, **and J. A. Kong**
Massachusetts Institute of Technology, USA

Geolocation refers to the localization of an emitter from measurements by passive receivers (satellites) at known locations. We consider the problem of three satellites used for determining the location of an electromagnetic source that is known to be on or near the surface of the Earth. Typically, the multilateration solution is obtained from time-difference-of-arrival (TDOA) measurements. In this configuration, one of the three satellites is designated as the reference such that two TDOA equations are obtained by subtracting the time-of-arrival (TOA) measurements of the reference satellite from the TOA measurement of the non-reference satellites. Therefore, the three satellite case is underdetermined for the three dimensional (3D) localization problem (i.e., there are two equations and three unknowns $u = [x, y, z]^T$). The introduction of an altitude constraint, for example restricting the source location to the surface of the Earth, yields one additional equation such that the problem is critically determined. However, the true altitude of the source may not be known exactly due to variations of the Earth's surface from sea level. When there is relative motion between the source and receivers, the Doppler shift gives two frequency-difference-of-arrival (FDOA) equations. Thus, there are four (two TDOA and two FDOA) equations that can be used to determine the three source location coordinates. The three satellite geolocation problem is then overdetermined. We present a solution to the three satellite geolocation problem based on iterative linearization of the TDOA and FDOA equations. We show that the resulting iterative maximum likelihood estimator (ML) achieves the Cramer-Rao Lower Bound (CRLB) in low measurement noise, but the likelihood of nonconvergence increases with measurement noise. Furthermore, we demonstrate that introduction of a source altitude constraint decreases the estimator variance below the unconstrained CRLB and increases the numerical robustness for higher measurement noise. However, it is shown that error in the altitude constraint projects bias onto the estimated source location vector.

Inversion of Partial Information from the Polarisation Scattering Matrix in the Presence of Noise

S. Anderson
Defence Science and Technology Organisation, Australia

Consider the following scattering scenario. An unidentified scatterer Q_i from a known class Q is moving on a trajectory $\Gamma_{Q_i}(t)$ in R^3 and illuminated in the Fraunhofer zone by a class of sources T moving on trajectories $\Gamma_{T_k}(t)$. The sources radiate distinct rest-frame signals $\Phi_{T_k}(t).\hat{\pi}_{T_k}(\theta,\phi)$ which are scattered by Q_i according to the scattering matrix $\widetilde{S}_{Q_i}(\vec{k}_{sc},\vec{k}_{inc})$ in Q_i's rest-frame. Here $\hat{\pi}_{T_k}(\theta,\phi)$ represents the polarisation state of the signal radiated by T_k in its local rest-frame direction (θ,ϕ).

A class of (noisy) receivers R moving on trajectories $\Gamma_{R_j}(t)$ sample the scattered signals

$$\vec{Z}^{sc} \equiv \widetilde{G}_0(R_j,Q_i)\widetilde{S}_{Q_i}\widetilde{G}_0(Q_i,T_k)\Phi_{T_k}\hat{\pi}_{T_k}$$

and the direct signals

$$\vec{Z}^{dir} \equiv \widetilde{G}_0(R_j,T_k)\Phi_{T_k}\hat{\pi}_{T_k}$$

where $\widetilde{G}_0$ is the free space vector Green's function, in an obvious shorthand notation. The objective is to identify Q_i and $\Gamma_{Q_i}(t)$ from the receiver outputs.

In the general case, the receivers R measure $\widetilde{Z}^{sc}$ and $\widetilde{Z}^{dir}$, from which the required parameters are to be estimated. But suppose each R_j is able to sample only a single polarisation of the fields incident upon it,

$$Z^{sc}_{proj} \equiv \vec{Z}^{sc}\cdot\hat{\pi}_{R_j} \quad and \quad Z^{dir}_{proj} \equiv \vec{Z}^{dir}\cdot\hat{\pi}_{R_j}$$

The question arises, to what extent are class identification and parameter estimation compromised? In this paper we address the question in the context of passive radars operating in the HF and VHF bands and derive quantitative measures of the value of polarimetric information for several geometries of interest.

Session 0P4
Coherent Effects in Random Media

Validity of Kinetic Models for Waves in Random Media

G. Bal
Columbia University, USA

We consider the derivation of kinetic equations to model the correlation of two wavefields such as e.g., acoustic or electromagnetic wavefields propagating in possibly different highly heterogeneous media. The main mathematical tool in the derivation is the Wigner transform. The validity of the kinetic models is then assessed by comparing the spatial distribution of the energy density they predict with simulations of wave equations in highly heterogeneous media. The simulations are performed in two space dimensions on domains of size comparable to 500 wavelengths. This is joint work with Olivier Pinaud.

On the Intermittency of the Light Propagation in Disordered Optical Materials

Y. A. Godin and S. Molchanov
University of North Carolina at Charlotte, USA

We consider an ensemble of $N \gg 1$ statistically independent optical fibers of length L. If $H_j = -\frac{d^2}{dx^2} + V_j(x), x \in [0, L], j = 1, 2, \cdots, N$, is the random Hamil- tonian associated with the individual fiber j, then one can introduce the reflection and transmission coefficients $r_j(\omega, L)$, $t_j(\omega, L)$ depending on the frequency ω of the incident electromagnetic wave. These coefficients are independent random variables for different j–s with the same distribution depending on ω. Also we have $|r_j(\omega)|^2 + |t_j(\omega)|^2 = 1$, so that $|t_j(\omega)|^2$ ($|r_j(\omega)|^2$) represent the ratio of the transmitted (reflected) energy to the energy of the incident wave. For the transmission coefficient $t_j(\omega, L)$ we prove the following

Theorem 1 *Given fixed fiber* j , $\lim\limits_{L\to\infty} \frac{\ln |t_j(\omega)|^2}{L} = -2\gamma(\omega)$ *with probability one, where* $\gamma(\omega) \geq 0$ *is the classical Lyapunov exponent for the problem* $H_j\psi - \omega^2\psi = 0$. In other words, $|t.(\omega, L)|^2 \sim e^{-2\gamma(\omega)L}$ as $L \to \infty$ (so-called quenched asymptotics).

The mean energy transmission coefficient is equal to

$$\frac{1}{N} \sum_{j=1}^{N} |t_j(\omega)|^2 = \tau_N^2(\omega, L)$$

and for fixed L and $N \to \infty$ $\tau_N^2(\omega, L) \to \langle |t.(\omega, L)|^2 \rangle$ with probability one.

Theorem 2 *Consider the generalized transmission coefficient* $\langle |t.(\omega, L)|^p \rangle$. *Then there exists the following limit*

$$\lim_{L\to\infty} \frac{\ln\langle |t.(\omega, L)|^p \rangle}{L} = 2\mu_p(\omega).$$

The function $\mu_p(\omega)$ *is a convex decreasing function of* p *for fixed* ω, $\mu_p(\omega) \to \infty$ *as* $p \to -\infty$, *and* $\mu_p(\omega) = \mu_1(\omega)$ *for* $p \geq 1$. *In particular,* $\mu_2(\omega) = \mu_1(\omega)$, *i.e.,*

$$\langle |t.(\omega, L)|^2 \rangle \sim e^{2\mu_1(\omega)L} \quad \textit{(so-called annealed asymptotics).}$$

We associate $\mu_p(\omega)$ with the principal eigenvalue of the appropriate spectral problem that allows to perform the asymptotic analysis.

Theorem 3 *Let* $\sigma = \sqrt{\mathrm{Var}V(x)}$ *be the parameter of the disorder and* $\sigma \ll 1$ *(weak disorder). Then*

$$\gamma(\omega) \sim c(\omega)\sigma^2 \quad \textit{and} \quad \mu_p(\omega) \sim \frac{1}{2}\gamma(\omega)p(p-2) \quad \textit{for} \quad p \in [0, 1].$$

Therefore, $|t^2.(\omega, L)| \sim e^{-2c(\omega)\sigma^2 L}$ and $\langle |t(\omega, L)|^2 \rangle \sim e^{-c(\omega)\sigma^2 L}$, i.e.,

$$\langle |t(\omega, L)|^2 \rangle \gg t^2.(\omega, L), \quad L \to \infty.$$

The above result implies that the Lyapunov exponent of the energy transmission coefficient of a typical fiber differs by a factor of two from that for the ensemble of fibers.

Model of the Electromagnetic Contribution to Wurface Enhanced Raman Scattering (SERS)

V. Giannini, J. A. Sánchez-Gil, and J. V. García-Ramos
Consejo Superior de Investigaciones Científicas, Spain

E. R. Méndez
División de Física Aplicada, México

In this work, we present a theoretical model of the electromagnetic contribution to surface enhanced Raman scattering (SERS). The SERS effect is characterized by the enormous intensification of the Raman emission of molecules, when these are adsorbed on a metallic surface (with nanometric roughness). This intensification is several orders of magnitude higher than the Raman emission of isolated molecules. In recent years, SERS spectroscopy has improved in sensitivity so as to make possible the detection of a single molecule on a nanostructured substrate [1]. The SERS effect is due to the combined action of chemical and electromagnetic enhancement mechanisms. Leaving aside the contribution of the chemical mechanism, this is possible provided that there is a huge concentration of electromagnetic field on certain points of the substrate, due to the excitation and localization of surface plasmons [2–4].

We thus investigate the electromagnetic mechanism that is responsible for such surface-plasmoninduced, electromagnetic field enhancements. Our theoretical model incorporates the Raman response of a metallic surface covered with a dipole layer. The calculation of the scattered electromagnetic field is based on the exact Green's theorem integral equation formulation. With this model we are able to calculate the surface field, near field, and far field at the Raman-shifted frequency, separately of the electromagnetic field at pump frequency. A rigorous calculation of the scattered electromagnetic field has been carried out for random metal surfaces with similar properties to those exhibited by nanostructured metal substrates used in SERS. Numerical results are presented for single realizations, along with mean values of the SERS enhancement factor averaged over an ensemble of realizations [1].

REFERENCES

1. Nie, S. and S. R. Emory, "Probing single molecules and single nanoparticles by surface-enhanced raman scattering," *Science*, Vol. 275, 1102, 1997, and K. Kneipp, Y. Wang, H. Kneipp, L. T. Perlman, I. Itzkan, R. R. Dasari, and M. S. Feld, "Single molecule detection using surface-enhanced Raman scattering (SERS)," *Phys. Rev. Lett.*, Vol. 78, 1667, 1997.
2. Barnes, W., A. Dereux, and T. Ebbesen, "Surface plasmon subwavelength optics," *Nature*, Vol. 424, 824 2003.
3. Sánchez-Gil, J. A., J. V. García-Ramos, and E. M éndez, "Near-field electromagnetic wave scattering from random self-affine fractal metal surfaces: Spectral dependence of local field enhancements and their statistics in connection with surface-enhanced raman scattering," *Phys. Rev. B*, Vol. 62, 10515, 2000.
4. Sánchez-Gil, J. A., "Localized surface-plasmon polaritons in disordered nanostructured metal surfaces: Shape versus Anderson-localized resonances," *Phys. Rev. B*, Vol. 68, 113410, 2003.
5. Giannini, V., J. A. Sánchez-Gil, J. V. García-Ramos, and E. Médez, "Theoretical model of the electromagnetic contribution to surface enhanced Raman scattering (SERS)," *preprint*.

The Local Density of States in Finite Size Photonic Structures, Small Particles Approach

V. Prosentsov
University of Twente, The Netherlands

A. Lagendijk
FOM-Institute for Atomic and Molecular Physics, The Netherlands

We study the local density of states in finite size photonic structures by considering them as made of small particles. Dividing the structure into segments with a size small compared to the incident wavelength, one can apply methods suitable for the wave scattering by small particles. This local perturbation method correctly reproduces the lowest frequency resonance of the small particles and it fulfills the optical theorem (energy conservation). The small particles can be given prescribed positions in space: for instance random, or periodic as in a photonic crystal. By using the local perturbation method, we have calculated the local density of states for one, two, and three dimensional finite size photonic structures.

Spatial Wave Intensity and Field Correlations in Quasi-one-dimensional Wires

G. Cwilich
Yeshiva University, USA

Spatial intensity correlations between waves transmitted through random media are analyzed within the framework of the random matrix theory of transport. Assuming that the statistical distribution of transfer matrices is isotropic, we found that the spatial correlation function of the normalized intensity can be expressed as the sum of three terms, with distinctive spatial dependences. This result coincides with the one obtained in the diffusive regime from perturbative calculations, (Patrick Sebbah et al. in Phys. Rev. Lett. 88, 123901, 2002), but holds all the way from quasi-ballistic transport to localization. It is only the specific value of the coefficients which depends on the specific transport regime. Their values obtained from the Monte Carlo solution of the Dorokhov, Mello, Pereyra, and Kumar (DMPK) scaling equation are in full agreement with microscopic numerical calculations of bulk disordered wires. The experimental and numerical results are recovered inh the large-N (number of propagating channels) limit in Random Matrix theory. While correlations are positive in the diffusive regime, we predict a transition to negative correlations as the length of the system decreases.

Near-field Intensity Correlations in Semicontinuous Metal-dielectric Films

H. Cao[1], **K. Seal**[1], **A. K. Sarychev**[2], **D. A. Genov**[3]
V. M. Shalaev[3], **A. Yamilov**[1], **H. Noh**[1], **and Z. C. Ying**[4]

[1]Northwestern University, USA
[2]Ethertronics Inc., USA
[3]Purdue University, USA
[4]National Institute of Standards and Technology, USA

Spatial correlations of field and intensity are indicative of the nature of wave transport in random media and have been widely investigated in the context of electromagnetic wave propagation in disordered dielectric systems However, less is known of near-field intensity correlations in metallic random systems, which can exhibit rich phenomena due the involvement of intrinsic resonance effects-surface plasmons. Neither is clear the difference between correlation functions in metallic and dielectric systems.

This paper presents the first experimental study of near-field intensity correlations in metal-dielectric systems in regimes where localization and delocalization are expected. Significant differences are observed between the spatial intensity correlations functions in metal-dielectric systems and those of purely dielectric random media.

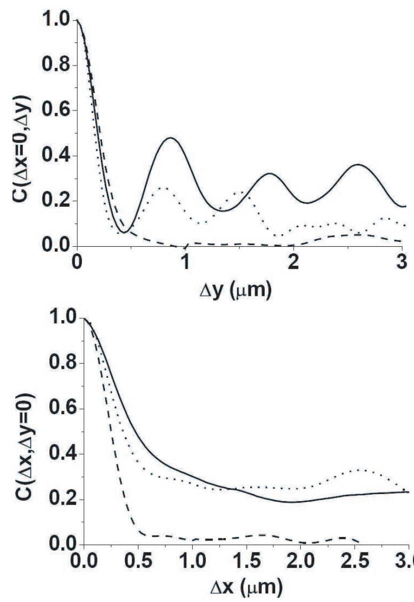

Figure 1: $C(0, \Delta y)$ and $C(\Delta x, 0)$ at $p = 0.36$ solid line), 0.65 (dashed line) and 0.83 (dotted line). For comparison, all curves are normalized to a value of unity.

In disordered metallic nanostructures, surface plasmon modes are governed by the structural properties of the system and may be strongly localized. Recent theoretical studies of metallic nanoparticle aggregates suggest that the eigenmodes of such systems may have properties of both localized and delocalized states. However, it is not clear how such eigenmodes impact the propagation or localization of surface plasmon polaritons excited by impinging light, an issue addressed in this study. In the current experiment, the concentration of metal particles on a dielectric surface p was varied over a wide range to control the amount of scattering. Spatial intensity correlations obtained from near-field optical microscopy (NSOM) images show a transition from propagation to localization and back to propagation of optical excitations in planar random metal-dielectric systems with increase in metal filling fraction.

Semicontinuous silver films on glass substrates were synthesized by pulsed laser deposition. Samples were illuminated by the evanescent field (in the total internal reflection geometry) of He-Ne lasers, and the local optical signal was collected by a fiber tip. From the near-field images, we computed the 2D correlation functions for near-field intensities. Fig. 1 shows the intensity correlation functions in the directions parallel and perpendicular to the incident wave vector $k_{\|}$, i. e., $C(0, \Delta y)$ and $C(\Delta x, 0)$. Along $k_{\|}$, $C(0, \Delta y)$ exhibits oscillatory behavior at $p = 0.36$ with a period of 870 nm. This oscillation is replaced by a monotonic decay at $p = 0.65$. At $p = 0.83$, the oscillations reappear with a smaller period of 690 nm. The presence of oscillations in $C(0, \Delta y)$ is an indication of wave propagation along the y-axis. This propagation is suppressed at $p = 0.65$, suggesting localization of near-field energy. Therefore, the existence, suppression and reappearance of the oscillations in the near-field intensity correlation function with increasing p correspond to a gradual transition from propagation to localization and back to propagation of optical excitations in the samples. Note that the oscillation periods observed above are always larger than λ, in contrast with purely dielectric media, which exhibit damped oscillations with a period of $\lambda/2$.

Cones, Spirals, and Möbius Strips in Multiply Scattered Light

I. Freund
Bar-Ilan University, Israel

Laser light scattered by a multiple scatterer invariably emerges elliptically polarized. In general, the orientations of the ellipses in elliptically polarized light vary throughout space. In three dimensions the orientation of an ellipse may be described by a 3-frame in which one frame axis is along the major axis of the ellipse, a second frame axis is along the minor axis of the ellipse, and the third frame axis is along the normal to the ellipse. These three axes are shown to generate cones, spirals, and Möius strips, characterized by a total of 27 different topological indices.

For ordinary ellipses (the vast majority) that are not on singular lines of circular or linear polarization, the Möbius strips have one full twist, and there are a total of 21 indices that are non zero. These indices, if independent, could collectively divide the field into $2^{21} = 2,097,152$ structurally different grains separated by grain boundaries on which an index becomes undefined. Selection rules, however, reduce the number of independent configurations to 140,608, while within a linear approximation for the local field surrounding an ellipse there exist degeneracies that further reduce the number of distinguishable configurations to 17,360. Of these, 1,728 are of first order, and should be readily accessible to experiments using recently developed optical near field methods.

Analytical expressions have been obtained for all indices in terms of the 20 parameters needed to define a general field of ellipses within the linear approximation, and more than 10,000 different configurations have been harvested in a simulated multiply scattered random field (speckle pattern), demonstrating that large numbers of configurations can be expected appear in practice.

This previously unsuspected, indeed unprecedented, structural proliferation is intrinsic to spatially varying elliptically polarized light, and in addition to random fields, is found in the fields of wave guides that support a small number of modes (2–3), as well as in the highly ordered fields of optical lattices. Other systems described locally by spatially varying 3-frames, such as liquid crystals, or the dielectric constants of continuous random media, can be expected to show a similar degree of structural proliferation.

Absorption Induced Confinement of Lasing Modes in Diffusive Random Medium

A. Yamilov[1], **A. L. Burin**[2], **X. H. Wu**[1], **and H. Cao**[1]

[1]Northwestern Unversity, USA
[2]Tulane University, USA

Tight focusing of pump light on a weakly scatting (diffusive) random medium can lead to lasing with coherent feedback [1]. Imaging of laser light on the sample surface revealed that the lasing modes were not extended over the entire random medium, instead they were located inside the pumped region with an exponential tail outside of it [2]. Since the quasimodes of a random system far from the onset of localization are usually extended states, the origin of the localized lasing modes is not clear.

We use FDTD method to simulate lasing in TM modes of 2D random media. The disordered system is a collection of dielectric cylinders placed at random in vacuum. The lateral dimension of 2D random system is $9.2\,\mu$m. Transport mean free path $l \simeq 1.3\,\mu\text{m} \ll L$, so that the system is in the diffusive regime. By assigning negative conductance (inside cylinders) to the pumped region and positive conductance to unpumped region, we are able to include both light amplification and reabsorption of the emitted light.

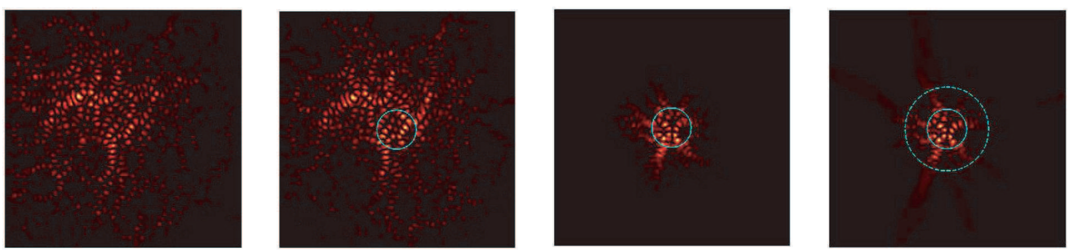

(a) (b) (c) (d)

Figure 1: Mode modification in the presence of reabsorption (see text).

Fig. 1(a) shows spatial intensity distribution of the (extended) quasimode with the longest lifetime in a passive diffusive system. in Fig. 1(b) we show the (first) lasing mode with gain inside the circular region near the center and no absorption outside. Although optical gain is local, the lasing mode is extended throughout the entire sample-the lasing mode profile remains the same as in Fig. 1(a). The lasing mode in the presence of reabsorption outside the circle, Fig. 1(c), is a new mode, completely different from the quasimode of the passive system. It is confined inside the pumped region, and shows an exponential decay outside. The reabsorption suppresses the feedback from absorbing part of the sample, effectively reducing the system size to V_{eff}. Indeed, Fig. 1(d) depicts the lasing mode when we remove all the random medium beyond one diffusive absorption length from the pump area (dashed circle). The frequency and spatial profile of the lasing mode remain the same as in Fig. 1(c).

This reduction of the effective system volume leads to a decrease of the Thouless number $\delta \equiv \delta\nu/\Delta\nu$, where $\delta\nu$ and $\Delta\nu$ are the average mode linewidth and spacing respectively. In a 3D diffusive system $\delta\nu \propto V_{eff}^{-2/3}$ and $\delta\nu \propto V_{eff}^{-1}$, therefore, $\delta \propto V_{eff}^{1/3}$. The smaller the value of δ, the larger the fluctuation of the decay rates γ of the quasimodes. We believe the broadening of the decay rate distribution along with the decrease of the total number of quasimodes (within V_{eff}) is responsible for the observation of discrete lasing peaks in the regime of tight focusing of pump beam [1].

REFERENCES

1. Cao, H., *Wave Random Media*, Vol. 13, R1, 2003.
2. Cao, H., Y. Ling, J. Y. Xu, and A. L. Burin, *Phys. Rev. E*, Vol. 66, R05601, 2002.

Exploiting Multiple Scattering of Waves in Random Media

J. A. Scales and K. van Wijk
Colorado School of Mines, USA

In this talk we describe our experimental work in the measurment of phase-coherent multiple scattering of waves in random media. We use a wide variety of non-contacting optical, millimeter wave and ultrasonic techniques to probe natural random media (such as rocks) as well as artificial systems. By using non-contacting methods we can record dense, high-fidelity data sets which sample the random fluctuations of the media. By carefully measuring the phase of these waves as well as their amplitude, we can exploit mesoscale fluctuations to achieve resolution beyond diffusion and radiative transfer, which neglect this phase information.

Coherent-potential-approximation Multiple-scattering Scheme for the Study of Photonic Crystals with Substitutional Disorder

V. Yannopapas
University of Patras, Greece

Photonic crystals of spherical scatterers have been theoretically studied using the the layer Korringa-Kohn-Rostoker (LKKR) method [1, 2] which is ideally suited for the calculation of the transmission, reflection and absorption coefficients of an electromagnetic (EM) wave incident on a composite slab consisting of a number of planes of non-overlapping particles with the same two-dimensional (2D) periodicity. For each plane of particles, LKKR calculates the full multipole expansion of the total multiply scattered wave field and deduces the corresponding transmission and reflection matrices in the plane-wave basis. The transmission and reflection matrices of the composite slab are evaluated from those of the constituent layers. In this study we present a photonic version of the coherent-potential approximation (CPA) [3, 4] for the study of photonic crystals with substitutional disorder (photonic alloys) within the LKKR context. The CPA method has been extensively used in the study of the electronic properties of disordered atomic alloys [5, 6] and is expected to give reasonably good results at least in the case of moderate disorder. It is the best approach for studying the properties of a disordered photonic crystal by means of substituting it with an effective periodic one whose properties correspond, on the average, to those of the actual disordered photonic crystal. The CPA-LKKR method is applied to case of dielectric photonic crystals of both cermet, i.e., opals, and network topology, i.e., inverted opals, as well as to the case of metallo-dielectric photonic crystals in order to determine an effective permittivity in the long-wavelength limit. The method is also used for the calculation of the transmission/ reflection and absorption coefficients of light incident on finite slabs of disordered photonic crystals.

REFERENCES

1. Stefanou, N., V. Yannopapas, and A. Modinos, "Heterostructures of photonic crystals: frequency bands and transmission coefficients," *Comput. Phys. Commun.*, Vol. 113, No. 1, 49–77, 1998.
2. Stefanou, N., V. Yannopapas, and A. Modinos, "MULTEM 2: A new version of the program for transmission and band-structure calculations of photonic crystals," *Comput. Phys. Commun.*, Vol. 132, No. 1–2, 189–196, 2000.
3. Stefanou, N. and A. Modinos, "Scattering of electromagnetic waves by a disordered two-dimensional array of spheres," *J. Phys. Condens. Matter*, Vol. 5, No. 47, 8859–8868, 1993.
4. Modinos, A., V. Yannopapas, and N. Stefanou, "Scattering of electromagnetic waves by nearly periodic structures," *Phys. Rev. B*, Vol. 61, No. 12, 8099–8107, 2000.
5. Phariseau, P., B. L. Györffy, and L. Scheire (editors), *Electrons in Disordered Metals and at Metallic Surfaces*, Plenum, New York, 1979.
6. Gonis, A., *Green Functions for Ordered and Disordered Systems*, North-Holland, Amsterdam, 1992.

Two-dimensional Randomly Rough Surfaces that Act as Gaussian Schell-model Sources

E. R. Méndez
División de Física Aplicada, Mexico

T. A. Leskova and A. A. Maradudin
University of California, USA

We consider the scattering of a scalar Gaussian beam of frequency ω incident normally on a twodimensional randomly rough surface defined by $x_3 = \zeta(\mathrm{x}_\parallel)$, where $\mathrm{x}_\parallel = (x_1, x_2, 0)$. The region $x_3 > \zeta(\mathrm{x}_\parallel)$ is vacuum while the region $x_3 < \zeta(\mathrm{x}_\parallel)$ is the scattering medium. We assume that the Dirichlet boundary condition is satisfied on the surface $x_3 = \zeta(\mathrm{x}_\parallel)$. We denote the scattered field in the vacuum region by $\Phi(\mathrm{x}|\omega)_{sc}$, and its value on the plane $x_3 = 0$, by $\Phi(\mathrm{x}_\parallel|\omega)_{sc}$. We seek the surface profile function $\zeta(\mathrm{x}_\parallel)$ for which $\Phi(\mathrm{x}_\parallel|\omega)_{sc}$ satisfies the condition $\langle\Phi(\mathrm{x}_\parallel|\omega)_{sc})\Phi^*(\mathrm{x}_\parallel|\omega)_{sc}\rangle = A^2\exp(-\mathrm{x}_\parallel^2/4\sigma^2)\exp[-(\mathrm{x}_\parallel - \mathrm{x}_\parallel^{\prime})^2/2\sigma_\mathrm{g}^2]\exp(-\mathrm{x}_\parallel^{\prime 2}/4\sigma_\mathrm{s}^2)$, where the angle brackets denote an average over the ensemble of realizations of $\zeta(\mathrm{x}_\parallel)$. Such a surface is a Gaussian Schell-model source of radiation. The field scattered from the resulting surface, although it is only partically coherent, has the intensity distribution of a fully coherent laser beam whose intensity in the plane $x_3 = 0$ has the form $A_L^2\exp(-2\mathrm{x}_\parallel^2/\delta_\mathrm{L}^2)$, where $\delta_L = 2\sigma_s\sigma_g/(\sigma_g^2 + \sigma_s^2)^{1/2}$ and $A_L\delta_L = 2A\sigma_s$.

Two approaches are used to determine the surface profile function that acts as a Gaussian Schellmodel source. Both are based on the geometrical optics limit of the phase perturbation theory expression for the scattered field. In the first approach the surface profile function $\zeta(\mathrm{x}_\parallel)$ is represented as a continuous array of triangular facets. The joint probability density function of two orthogonal slopes of each facet is determined from the condition that the field scattered from the resulting surface has the desired correlation property in the plane $x_3 = 0$. In the second approach it is shown that a surface profile function $\zeta(\mathrm{x}_\parallel)$ that is a stationary, zero-mean, isotropic, Gaussian random process, can also act as a Gaussian Schell-model source, when the rms height and transverse correlation length of the surface roughness are suitably chosen. Each of these two approaches is validated by the results of numerical simulation calculations of the intensity distribution of the scattered field, which show that it indeed has the form of a laser beam.

The Design of Two-dimensional Randomly Rough Surfaces with Specified Scattering Properties: Non-normal Incidence

A. A. Maradudin and T. A. Leskova
University of California, USA

In a recent paper [1] a method was proposed for designing a two-dimensional randomly rough surface on which the Dirichlet boundary condition is satisfied that, when illuminated at normal incidence by a scalar plane wave, produces a scattered field whose mean differential reflection coefficient has a specified dependence on the scattering angles. The method was based on the geometrical optics limit of the Kirchhoff approximation. The mean plane of the surface, the x_1x_2 plane, was tessellated by equilateral triangles. For x_1 and x_2 within a given triangle the surface profile function $\zeta(x_1x_2)$ was assumed to be a linear function of x_1 and x_2 of the form $b^{(0)} + a^{(1)}x_1 + a^{(2)}x_2$. The pair of slopes $a^{(1)}$ and $a^{(2)}$ for a given triangle were assumed to be random deviates that were independent of the pair of slopes for any other triangle, and all pairs of $a^{(1)}$ and $a^{(2)}$ had the same joint probability density function. The amplitude $b^{(0)}$ was determined by making the surface continuous. The mean differential reflection coefficient was found to be given in terms of this joint probability density function. This relation could be inverted to yield the joint probability density function in terms of the mean differential reflection coefficient that the surface was intended to produce. From the joint probability density function for $a^{(1)}$ and $a^{(2)}$ the marginal probability density functions were obtained, as well as the conditional probability for $a^{(2)}$ given $a^{(1)}$, and vice versa. The rejection method [2] was then used with these marginal and conditional probability density functions to construct an ensemble of realizations of the random surface. In the present work we extend the approach proposed in [1] to the case of non-normal incidence, and illustrate it by applying it to the design of a surface that scatters a plane wave in such a way as to produce a mean scattered intensity that is constant within a rectangular region of scattering angles, and produces no scattering outside this region. It is validated by the results of numerical simulation calculations.

REFERENCES

1. Méndez, E. R., T. A. Leskova, A. A. Maradudin, M. Leyva-Lucero, and J. Muñoz-Lopez, *J. Opt.*, A7, S141, 2005.
2. Press, W. H., S. A. Teukolsky, W. T. Vetterling, and B. P. Flannery, *Numerical Recipes in Fortran, 2nd Edition*, 281–282, Cambridge University Press, New York, 1992.

Session 1A1
Poster Session 1

An Improved Electrical Model of a Biological Cell Taking Electroporation into Account

N. Citro, **V. Tucci**, **B. de Vivo**, **and P. Lamberti**
University of Salerno, Italy

Electro-permeabilization of biological cells has been proposed as a very efficient pasteurization method in food technology, in biotechnology for gene transfer, in medicine for gene therapy, cancer chemotherapy, and drug delivery. Although the molecular processes involved in the permeabilization mechanisms are very complex, the formation of "pores" in the plasma membrane, under the influence of an electric field, is deemed responsible of the cellular responses. Electric field intensity and duration are the fundamental parameters in the modulation of the occurring phenomena. The effects of the application of an electric field can be evaluated by adopting either a lumped parameters circuital model or a continuous field based description of the cell structure. In both cases one of the main parameters affecting the cell response is the voltage across the membrane (trans-membrane voltage-TMV). If trans-membrane voltage is greater than a critical value, structural changes in the surface membrane occur that cause pore formation and, in turn, increased permeability. Recently, it has been shown that for pulses in the ns range, intracellular structures may be affected without appreciable modifications in the plasma membrane. However, in modelling the electro-permeabilization process, several physical constants need to be approximated in order to obtain realistic results from the numerical scheme approximating the theoretical model (circuital or field based).

In this work we have developed an electric model for living cells in order to predict an increasing probability for electric field interactions with intracellular substructures of cells when the electric pulse duration is reduced to the nanosecond range. Our model consist of a modified Hodgkin-HuxleyCtype non linear equivalent circuit for the outer cell membrane, pore formation and the effect of pores on the conductivity of the outer cellular membrane are taken into consideration. Moreover, the accumulation or depletion of ions in a restricted space surrounding the outer cell membrane (variable concentration), coupled with a linear R_C equivalent circuit for the nuclear membrane is considered.

The pore formation is governed by the so called Smoluchowski equation, which determines, together with the modified nonlinear equivalent circuit, a non linear behaviour of the conductivity of the outer cell membrane with the applied field. In order to take into account the parameters variations and/or uncertainties, in value or dislocation inside the system, an accurate range analysis is carried out. This approach, representing a peculiar aspect of this work, gives the possibility of evaluating the range of electrical pulses values (amplitude, rise time, duration) to be applied, in order to obtain reversible or irreversible effects on the cellular membrane.

A Novel Multiband and Broadband Fractal Patch Antenna

J. J. Huang, F. Q. Shan, and J. Z. She
Tsinghua University, China

Microstrip patch antenna (MPA) has attracted wide interest due to its important characteristics, such as light weight, mechanically robust, etc. However, the impedance bandwidth of a typical patch antenna may be just 1–2%. Much intensive research has been done in recent years to develop bandwidth-enhancement techniques: using a thick air or foam substrate results in a maximum bandwidth of less than 10%; using stacked or co-planar parasitic patches obtains a bandwidth of 10%–20%; using a gap-coupled probe feed achieves a bandwidth of 16%; more recently, the addition of a U-shaped slot and the use of an L-shaped probe have both been shown to provide bandwidth in excess of 30%. However, these techniques increase antenna volume, complicate the design and fabrication of the antennas.

Fractal geometries have recently been introducing in the design of antennas. One property associated with fractal geometry that is used in the design of antennas is self-similarity. A fractal antenna can be designed to receive and transmit over a wide range of frequencies using the self-similarity properties associated with fractal geometry structures.

In this paper, a novel multi-band and broadband fractal patch antenna is designed, measured and analyzed. The patch is printed on a microwave substrate FR4 of the thickness $H = 1\,\mathrm{mm}$ and the relative permittivity $\varepsilon_r = 4.4$. The antenna is fed through a 50 ohm microstrip line of the width $W = 2\,\mathrm{mm}$. As the FR4 substrate is not suitable to be used at frequencies above 4 GHz, $R0$ should not be too small. For the present design $R0 = 40\,\mathrm{mm}$. The radiation elements are composed of ten similar orthogonal bars. Both the length and width of the orthogonal bar are magnified by the factor of $Ra * Ra$. Four antennas with different Ra (1.01, 1.02, 1.03 and 1.05) are simulated, fabricated and measured. A tuning stub with the width T and the length L is added to the feed-line of the antenna of $Ra = 1.01$ to get a wider bandwidth of 18%. As the scale Ra increases, multi-band characteristics are observed. All results are proved by simulation and experiment.

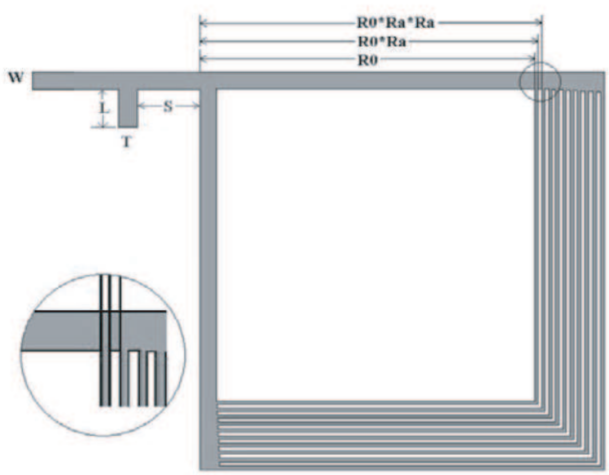

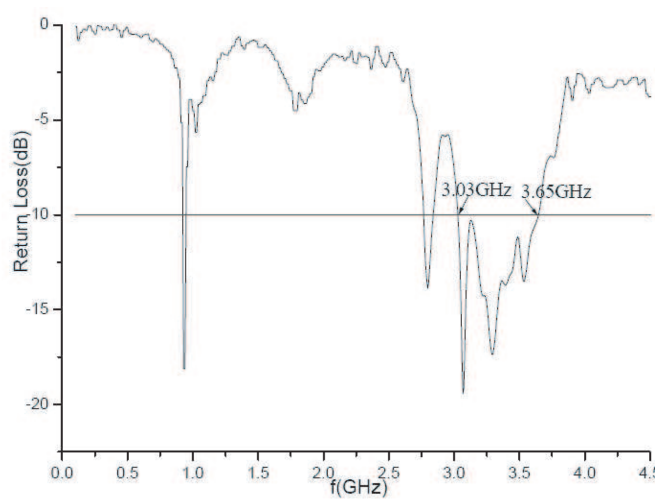

Improvement of Reflectarray Performances at Millimeter Waves by Reduction of the Cell Size

J. Lanteri, **C. Migliaccio**, **J. Y. Dauvignac**, **and C. Pichot**
Université de Nice Sophia-antipolis, France

Printed reflectarrays have been developed at millimetre wave since over 10 years in regards to their low profile and low cost. They consist of printed elements, typically patches or dipoles representing the elementary cell of the array. They are designed to scatter the incident field, coming from a feed antenna, with the proper phase required to form a planar phase surface and to scan the beam in a given direction.

In this paper we present beam scanning and gain improvements obtained by reducing the cell size. Generally, most of reflectarrays use cell size of half wavelength. Efforts have been made for finding appropriated patch shapes for increasing the variation of the reflected phase, the bandwidth or the fabrication simplicity. As the patch shape is not the aim of this work, the elementary cell used is a rectangular patch printed on a thin duroïd substrate of 2.2 dielectric permittivity. It has been chosen in order to be simple to design regarding to the cell size variation. Reflectarrays are designed using ray tracing theory. The equivalent aperture surface is divided into elementary cells loaded with printed elements (rectangular patches) optimized for obtaining the desired reflected phase. Small reflectarrays (diameter of 15 mm in order to simulate entire structure on HFSS software) with cell size of ($\lambda/2$) and ($\lambda/4$) respectively were designed at 94 GHz. Simulations were then conducted in order to characterize the effect of cell reduction on the array performances. In order to be compatible with further fabrication, the dimension of the patch is limited to a minimum value of $120\,\mu m$, so it reduces the phase compensation range. Despite the loss in phase, reduced size cells still improves performances. Nevertheless, the cell size investigation has shown that below the limit of ($\lambda/6$) the improvement is not significant. Indeed, the simulated gain of the ($\lambda/2$) reflectarray is 15 dB whereas the ($\lambda/4$) reflectarray's gain is 17.9 dB as for a ($\lambda/6$) reflectarray (gain is 18 dB).

For measurements, the primary source used is a standard open ended WR-10 waveguide. Measurements have shown that the ($\lambda/4$) reflectarray achieves a beam scanning angle of $\pm 60°$ with a loss of gain of 1 dB, whereas the ($\lambda/2$) has a loss of 3 dB in comparison with the gain obtained in axial direction. The measured gains are of 15.5 and 13.2 dBi respectively. These results were expected due to the increase of phase accuracy. They are 2 dB smaller than simulated ones because of the high blockage of the primary source with respect to the reflectarray surface.

Optical Near-field Study of Dielectric Nanostructures

M. Y. Mahmoud[1], **G. Bassou**[1,2], **L. Salomon**[2], **Z. Chekroun**[1], **and N. A. Djamai**[1]

[1]Université Djilali Liabès de Sidi Bel-Abbes, Algérie
[2]Université de Bourgogne, France

The photon scanning tunneling microscope is based on the frustration of a total internal reflection beam by the end of an optical fiber. This microscope has been used to obtain topographic information generally on smooth samples. We study the influence on image formation of several parameters in scanning near-field microscopy. The numerical calculations have been carried out using the differential method. We consider the case of three-dimensional system including a translational symmetry in one direction. Various oscillations patterns are observed from both sides of the nanostructure, which we interpret as interference between the diffracted waves scattered by the nanostructure (with the components of the wave vector parallel to the surface) and the evanescent incident wave above the surface. The period of oscillations depends on several parameters. The numerically obtained period corresponds well to the expected theoretical value. Using an optical near-field analysis and by calculating the electric field intensity distribution, we investigate the probe-sample distance effect. It is found that the distribution of the intensity related to the electric field is depending on sample-probe distance. We noticed the loss of details in the image and the presence of strong oscillations. Also, both of the polarization state of the illuminating light effect and the angle of incidence are investigated. We show how the depth of penetration has an effect on the field intensity distribution. After that we pay more attention to the depth of penetration. The analytical values of the penetration depth of the incident electromagnetic field of the system are in good agreement with the numerical values obtained with a differential method. We conclude that a differential method provides physical insight into the main features of the different images.

Array Patterns Synthesizing Using Genetic Algorithm

J. Jin, H. L. Wang, W. M. Zhu, and Y. Z. Liu
Institute of Communications Engineering, PLAUST, China

A planar array antenna with arbitrary geometry synthesis technique based on genetic algorithm is discussed. This approach avoids coding/decoding and directly works with complex numbers to simplify computing programming and to speed up computation. This approach uses two crossover operators that can overcome premature convergence and the dependence of convergence on initial population.

An example of satellite-born 61 elements antenna array with hexagonal (or equilateral triangular) grid was used and 23 beams are shaped.

The 3 dB contour of each beam is shown in Figure 1. Notice the shape of beams, for example beams in ring 2, for perfection shaping the footprints shape should wedge-shaped. Of course, it is achievable only by an infinitely large array. Due to restriction of elements number, the footprint shapes are kidney-shaped. However, it can satisfy the requirements.

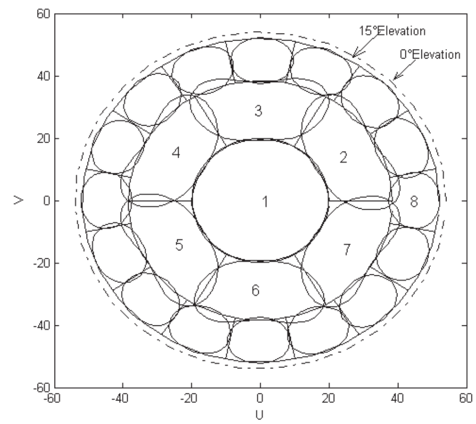

Figure 1: Cells arranged in rings.

Figure 2 and 3 are the patterns of beam 1 and 2. It is observed that the main lobe satisfy the requirement, and side lobe level suppress reach 30 dB which is outstanding the results of [7, 8].

For beam 1 shown as figure 2, $|I_{\max}/I_{\min}| = 20$. For beams in ring 2 a side lobe level of -30 , an $|I_{\max}/I_{\min}| < 40$ can be reached.

Simulation results show that this method is capable of synthesizing quite complex shapes and can realize good sidelobe suppression at the same time.

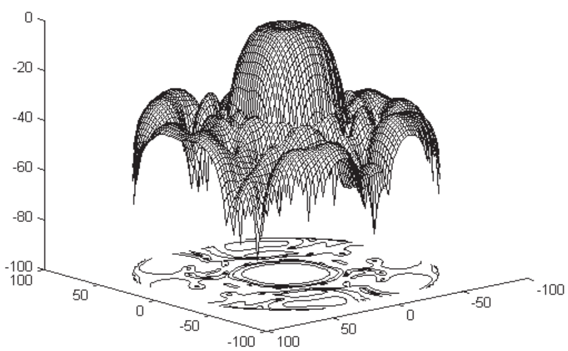

Figure 2: Pattern of beam 1.

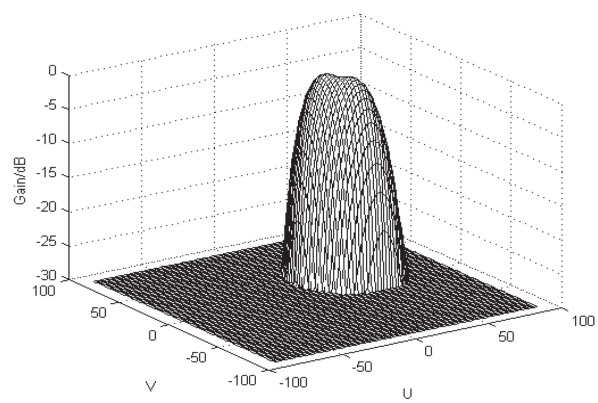

Figure 3: Pattern of beam 2.

Space-filling Patch Antennas with CPW Feed

M. R. Haji-Hashemi, H. Mir-Mohammad Sadeghi, and V. M. Moghtadai
Isfahan University of Technology, Iran

In this paper some types of space-filling patch antennas with coplanar waveguide feed, have been investigated. Space-filling curves map the multi-dimensional space into the one-dimensional space. A space-filling curve acts like a thread that passes through every cell element (or pixel) in the n-dimensional space so that every cell is visited only once. Therefore, the space-filling curve does not self-intersect. A space-filling curve imposes a linear order of the cells in the n-dimensional space. These geometries have the following properties: Self-Avoidance (as the line segments do not intersect each other), Simplicity (since the curve can be drawn with a single stroke of a pen) and self-similarity.

There are many types of space-filling curves (SFCs), e.g., the Peano, Hilbert, and Gosper curves, to name a few. They differ from each other in the way they visit and cover the points in space.

Some types of these curves have been studied previously in monopole, dipole and patch antenna configurations in the comprehensive category of fractal antennas.

In other point of view, coplanar waveguide feed is a well-known technique for increasing the bandwidth of patch antennas.

In this paper this technique has been imposed on some types of fractal space-filling patch antennas such as Hilbert curve patch antenna and Gosper curve patch antenna.

The effect of fractal iteration levels have been studied also their performances have been investigated numerically with conventional CPW patch antennas.

Simulation results have been obtained using IE3D-MOM code.

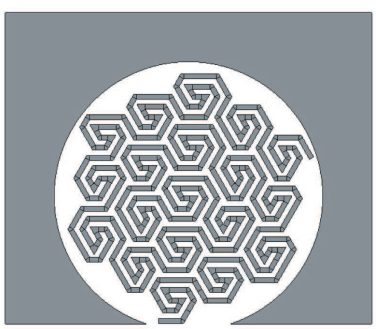

Figure 1: CPW-fed Gosper curve patch antenna.

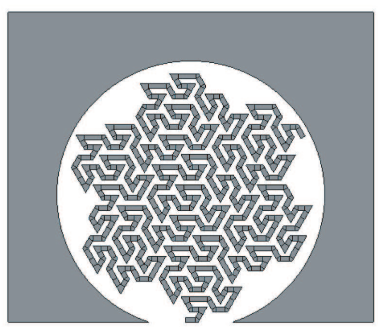

Figure 2: Another version of CPW-fed Gosper patch antenna.

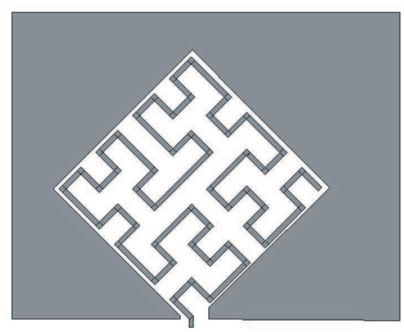

Figure 3: CPW-fed Hilbert curve patch antenna.

The Power Line Transmission Characteristics for an OFDM Signal

A. Mori[1], **Y. Watanabe**[1], **M. Tokuda**[1], **and K. Kawamoto**[2]

[1]Musashi Institute of Technology, Japan
[2]Sumitomo Electric Industries, Ltd., Japan

In this report, we measured what influence the characteristics of the electric power line with various forms gave to the transmission characteristic of OFDM (Orthogonal Frequency Division Multiplexing) signal through PLC (power line communication system) modem based on the OFDM method.

We classified the electric power line transmission line with various forms in a real environment into basic elements as shown in Fig. 1, which are important elements influencing the power line transmission characteristics. In Fig. 1, (a) is no branch, (b) an outlet type branch and (c) a switch type branch that is used in a power line for lamp. Next, differential permeation characteristics and group delays for the basic elements were measured. When the outlet was short in case (b), the differential permeation attenuation increased extremely in low-frequency band. Moreover, in case (c) attenuation like the resonance appeared in the low-frequency band at the branch length of 160 cm.

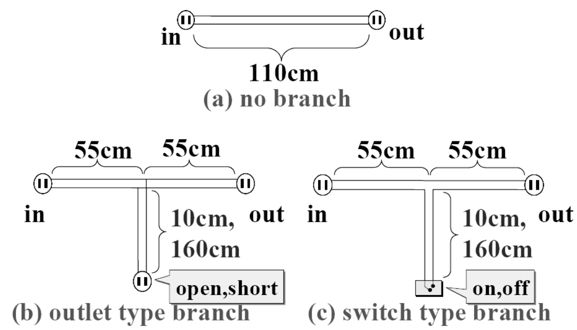

Figure 1: Basic elements of power line transmission model.

We measured PHY rate (Physical rate) for each basic element as shown in Fig. 1, which is connected with the PLC modem. The measurement system of PHY rate set in G-TEM (Giga-Hertz Transverse Electromagnetic) cell in order to suppress power supply coupling between sending and receiving modems. Normally, PLC modem is connected to AC power line, but in this case, the measurement system connected to DC power line is used to suppress the power supply coupling. The communication link between sending and receiving PCs through the modem was established and measured PHY rate. The frequency band of the modem is from 4 MHz to 34 MHz.

Table 1: Measured and calculated result.

	PHY rate[Mbps]	
basic element and termination condition	meas.	calc.
(a) no branch	183	186
(b) outlet type branch 10cm open	181	186
(b) outlet type branch 10cm short	166	170
(b) outlet type branch 160cm open	178	180
(b) outlet type branch 160cm short	181	186
(c) switch type branch 10cm off	180	185
(c) switch type branch 10cm on	181	186
(c) switch type branch 160cm off	183	186
(c) switch type branch 160cm on	168	171

At this time, the transmission characteristics of the electric power line are simulated from measured data. We composed the OFDM sending and receiving system on the computer, and simulated the PHY rate. The OFDM system consists of general FFT-base. The composition of the measured transmission characteristics for the electric power line is simulated as follows. First, wideband and uniform signal attenuation is imitated in the ATT (attenuator) block. Next, we imitated the attenuation and the group delay characteristics according to each basic element by a digital filter block. In addition, the thermal noise of the equipment is imitated by AWGN (Additive White Gaussian Noise) block.

Table 1 shows the results of PHY rate corresponding to each basic element as well as their termination conditions, and the calculated values agree well with the measured values. It is cleared that basic element (b) with termination condition of "10 cm short" influences most for the PHY rate and basic element (c) with termination condition of "160 cm on" influences next. In conclusion, it is revealed that the PHY rate of PLC modem based on OFDM signal can be calculated accurately by imitating the transmission characteristics of the power line used.

Relation between Balance-unbalance Conversion Factor and Leaked Electric Field in Power Line with Branch for PLC

Y. Watanabe and M. Tokuda
Musashi Institute of Technology, Japan

In this report, we focused attention on a Power Line Communication (PLC) system used the MHz band, and calculated balance-unbalance conversion factor and leaked electric field in the power line with branch in high frequency, such as 2 MHz–30 MHz. In order to understand the characteristics of an actual electric power line, first, we studied most simplified model without the branch, and next, we studied more simplified model with the branch.

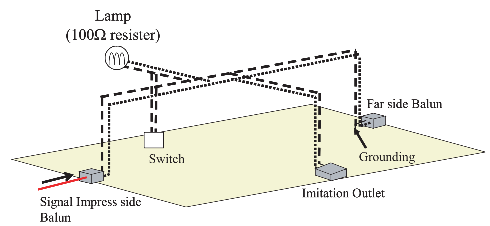

Figure 1: Appearance of power line with two branch model.

The power line model without the branch is gate form arranged on ground plane, and one of pair line in the model is grounded at far end side of signal impression. In case of the power line with branch, we studied two typical branch models, such as outlet branch model, in which both two lines of the pair line diverge in the same length, and switch branch model, in which only one line of the pair line become long so as to set on a lamp switch. And we calculated two cases with one branch model, in which only outlet branch line diverges from main line, and two branch model including both outlet branch line and switch branch line, as shown in Figure 1.

In calculation, we used the method of moments, and calculated the balance-unbalance conversion factor and the leaked electric field. In order to confirm the validity of the calculation, we measured balance-unbalance conversion factor and leaked electric field of the same model, and compared the measurement value with the calculation value.

Figure 2 is measured and calculated results of Longitudinal Conversion Loss (LCL). LCL is one of the balance-unbalance conversion factor. And Figure 3 is measured and calculated values of leaked electric field. As a result of the comparison with the measured and calculated values, they are approximated well in both balance-unbalance conversion factor and leaked electric field. Therefore, it was confirmed that the calculation model using the method of moment was effective to calculate LCL and leaked electric field in the power line.

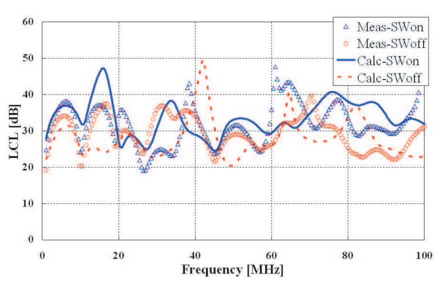

Figure 2: Measurement and calculation value of LCL.

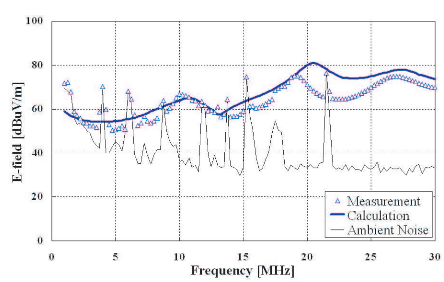

Figure 3: Measured and calculated values of leaked electric field.

REFERENCES

1. Watanabe, Y., M. Shigenaga, and M. Tokuda, "Electromagnetic field near power line for a power line communication system," *2004 International Symposium on Electromagnetic Conpatibility*, Sendai, 4C3-3, 845–848, Jun. 2004.

Ground Wave Propagation over Complex Topography

L. B. Liu[1,2], S. A. Arcone[1], and E. Rohrbach[2]

[1]U.S. Army ERDC-CRREL, USA
[2]University of Connecticut, USA

Surface-based non LOS communication in rural areas depends strongly on the wavelength, magnitude of the relief and ground electrical properties. We are investigating the seasonal non LOS propagation of 1- GHz signals over hilly terrain with tens of meters of relief using both field observations and 3-D numerical modeling. Our objectives are to compare the modeling and measured results of relative field intensity and wavefront direction to understand the dynamics of propagation over hills and onto plateaus. The surveyed conductivity and permittivity of our site appear fairly uniform. The vegetation is mainly grass, and the surface appears fairly smooth with limited, small-scale relief superimposed on the rolling hills we mapped with GPS. We located an omnidirectional transmitter antenna in a hidden valley, and used a directional receiver antenna to measure radiation directivity at several locations, both in summer and in winter with a heavy snow cover. For computational efficiency in our model volume ($\sim 10^6\,\mathrm{m}^3$), we have temporarily lowered the frequency to 100 MHz, lowered the relative permittivity (from 16 to 9), and simplified the topography. Our field results show that waves mostly arrive in the direction of the transmitter. 2-D slices in our 3-D modeling show that the waves creep rather than diffract over the smooth hill crests. The model valleys generate multiple events, and subsurface waves are also revealed. We are presently developing propagation over the full scale topography, the temporary results of which show large scale cylindrical spreading over the relief. However, it is the details within this general picture that we will compare with the field results.

A Design of a Quadplexer Consisting of BPFs Using Different Tapped Resonators

T. Ohno
Aoyama Gakuin University, Japan

K. Wada
The University of Electro-Communications, Japan

O. Hashimoto
Aoyama Gakuin University, Japan

In the planar passive circuits, a resonator, a filter and a multiplexer are the essential key circuits in recent technical trends. In general, various studies have been conducted on out-of-band rejection and downsizing of microwave filters. It is, however, difficult to accomplish the two demands mentioned above simultaneously because of the trade-off among the number of parts, cost and simplification of the structure. If control of the number of attenuation poles is possible by a simple approach, then, it is more effective to locate the attenuation poles near the passband used for duplexers and multiplexers. To achieve the requirements above, we use a bandpass filter (BPF) based on different tapped resonators. The advantage of the proposed BPF includes the compactness, and the control of the location and number of attenuation poles.

In this paper, a planar quadplexer consisting of BPFs using different tapped resonators are proposed, designed and calculated. Fig. 1 illustrates a schematic circuit of a quadplexer consisting of BPFs using different tapped resonators. In addition, Figs. 2 and 3 show the reflection, transmission and isolation characteristics of the quadplexer shown in Fig. 1. Referring to Figs. 1–3, it has been confirmed that the proposal enables the realization of the high-performance planar quadplexer theoretically.

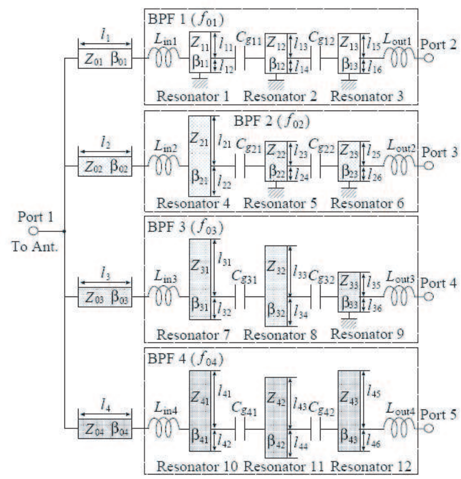

Figure 1: Schematic circuit of quadlexer consisting BPFs using different tapped resonators.

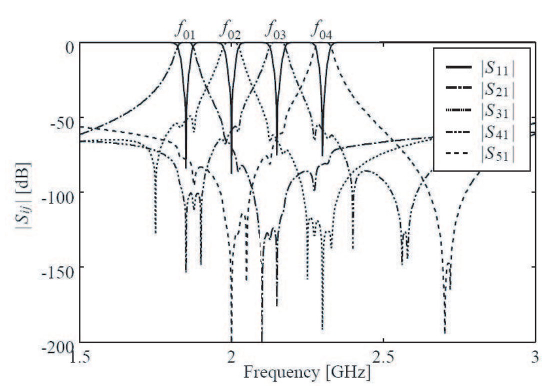

Figure 2: Theoretical results of the quadplexer shown in Fig. 1.

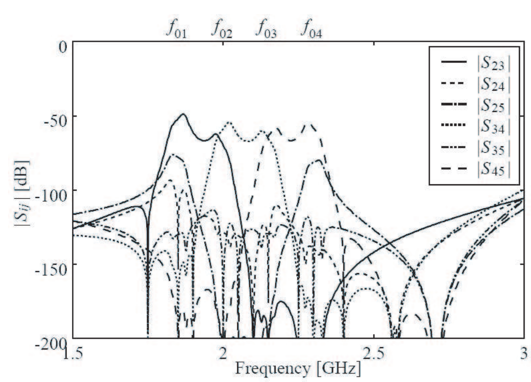

Figure 3: Isolation characteristics of the quadplexer shown in Fig. 1.

Basic Study on Relaxation of Uneven Heating in an Industrial Microwave Oven

R. Suga[1], O. Hashimoto[1], T. Takatomi[2], T. Ijuin[2], and S. Watanabe[1]

[1]Aoyama Gakuin University, Japan
[2]Daiwa Can Company, Japan

While foods are sterilized by being heated in a industrial microwave oven, uneven heating occurs inside the heated foods. This becomes a problem as the unheated part gets no sterilization and the overheated part causes deterioration of foods.

In this paper, a microwave oven was modeled based on an industrial one and model solution (starchy solution and salted starchy solution) simulated food as heated materials. Distribution of absorption power inside the heated materials in the industrial microwave oven was analyzed using parallel FDTD method, and the absorption power is substituted for heat transfer equation to analyze temperature distribution inside the heated materials. Figs. 1 and 2 show the analytical model of the industrial microwave oven used in parallel FDTD method. Figs. 3 and 1 show analysis results of temperature distribution. Refering to Figs. 3 and 1, it is confirm that parts of cup's edge is heated by the addition of sodium chloride. The tendency of the temperature distribution of the model solution was obtained and the fundamental data of the uniform appertization was provided.

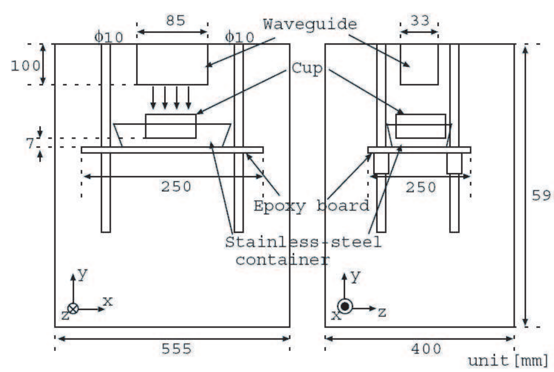

Figure 1: Analytical model.

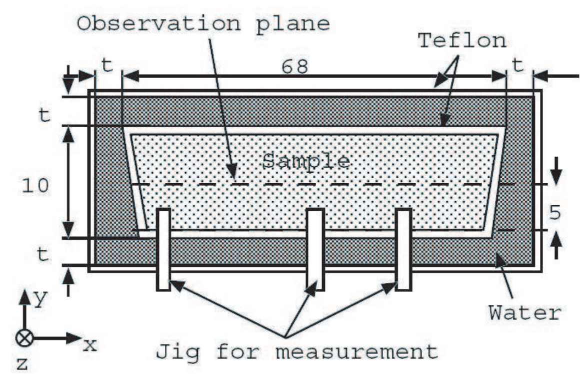

Figure 2: Cup for samples.

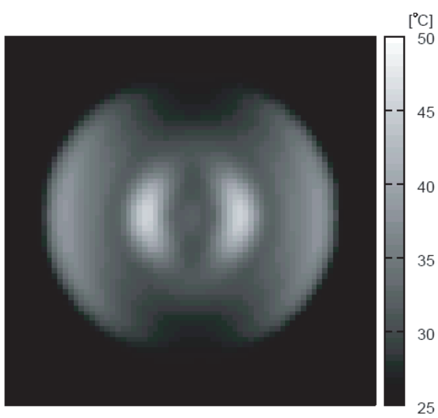

Figure 3: Temperature distribution of starchy solution (water film: 0 mm).

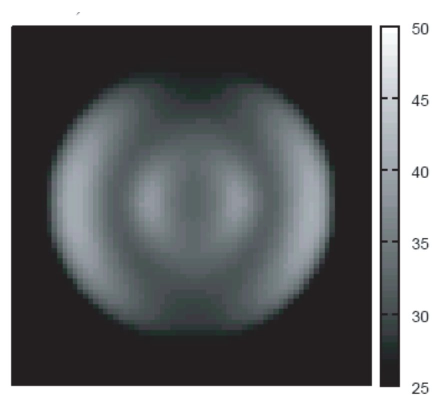

Figure 4: Temperature distribution of salted starchy solution (water film: 0 mm).

Measurement for Complex Permittivity Tensor Based on Free-space Transmission Method in Millimeter-wave Band

T. Sakai and O. Hashimoto
Aoyama Gakuin University, Japan

Rubber sheets mixed with carbon particles can be applied to wave absorbers. However, these materials usually have anisotropy which comes from the rolling method of manufacturing, because the carbon tends to be aligned along the rolling direction. So, it needs to measure complex relative permittivity tensor for the design of wave absorber in consideration of anisotropy. In this study, a measurement method which rotats sample to calculate complex relative permittivity tensor based on free-space reflection method using focusing lens and vector network analyzer is proposed.

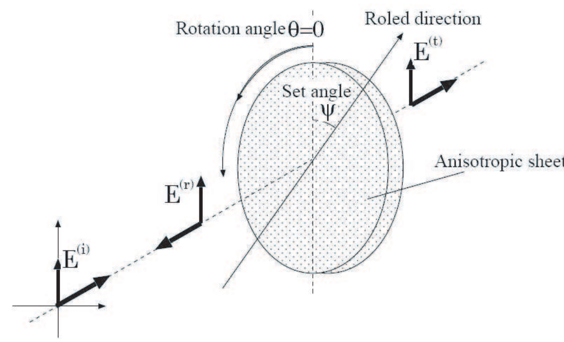

Figure 1: Analytical model.

In order to obtain the permittivity tensor of an anisotropic sheet, the transmission coefficients from these sheets must be analyzed. And the vector value of the transmission coefficients must be measured at each angle,from 0° to 180° as shown in Fig. 1. Then the permittivity tensor can be calculated by comparing the analyzed transmission coefficients with the measured values. For measurement, an anisotropic rubber sheet containing carbon particles was prepared. It was set at sample holder with rotating device and we measured the transmission coefficients in the range of 26.5 GHz to 40 GHz at only three points for each frequency.

Using above method, the values of the tensors are obtained as shown Fig. 2 and Fig. 3. It shows relativity of number of measurement points and permitivitty tensor. Then we calculate error of permittivity tensor and principal direction of tensor assuming the measurement sample theoretically. As the result, we verified that the proposed method can be used to measure permittivity tensor and principal direction of tensor.

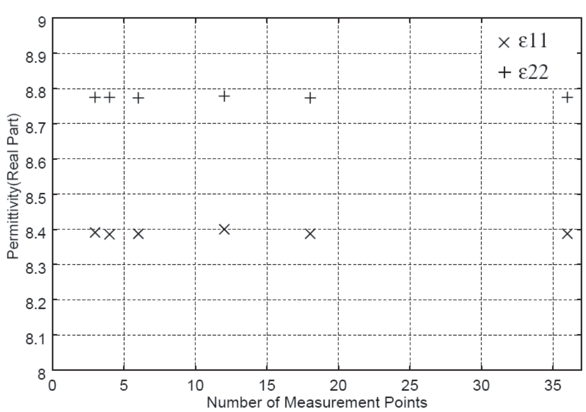

Figure 2: Real part of permittivity tensor.

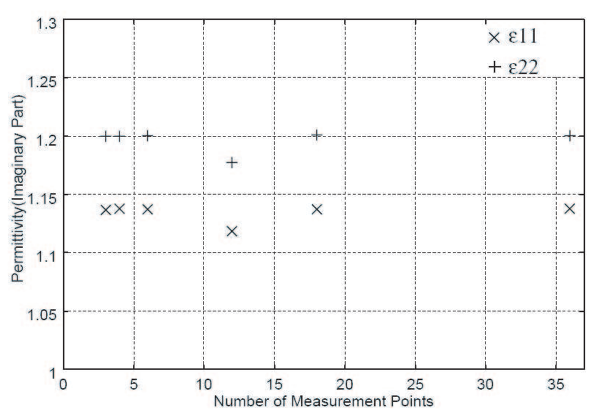

Figure 3: Imaginary part of permittivity tensor.

Analysis of Ultra-wideband Antennas for GPR Prospecting

G. Leone[1], **F. Soldovieri**[2], **R. Persico**[2], **and G. Prisco**[3]

[1]Università "Mediterranea" di Reggio Calabria, Italy
[2]Istituto per il Rilevamento Elettromagnetico dell'ambiente (IREA-CNR), Italy
[3]Seconda Università di Napoli, Italy

In recent applications in telecommunications and remote sensing at radiowaves, microwaves and terahertz frequencies, the exploitation of ultra-wideband (UWB) antennas is constantly growing up [1]. In particular, UWB antennas can provide higher imaging resolution and better target characterization in subsurface prospecting.

Design and analysis of such high-performance antennas exhibit significant challenges. In particular, in the case of GPR systems of our concern, typical requirements include not only a wide work bandwidth in order to provide short either "real" or "synthetic" pulse radiation, but also negligible interferences from undesired directions. All these features, moreover, have to be implemented in a portable systems. Still, we have to consider that, since the antennas work at close proximity or in contact with the investigated structure, their input impedance and radiated field are affected by it, so that the properties of the background medium must be taken into account in designing and analysing the antenna performance. Finally, mutual interactions between transmitting and receiving antenna must be also considered.

To directly measure the antenna properties in the operative GPR conditions, within an inhomogeneous variable scenario, is very difficult. This arises the need of a full-wave analysis of the antenna for the evaluation of its properties such as impedance, radiated field coupling, etc.

In addition, an accurate modelling of the antenna is crucial for the exploitation of inverse scattering approaches to GPR data, since the accurate knowledge of the incident field (i.e., the field impinging on the investigated zone in absence of scattering objects) is a key point to make the result of the inversion algorithm reliable.

In this contribution we present the modelling and characterization of different kind of antennas exploited in GPR applications such as bow-tie and ridged horn antennas.

The antennas are numerically analysed in different operative situations by means of the FEM-based software High Frequency Structure Simulator (HFSS), by Ansoft, which allows to model both the feeding and the radiating element of the antennas accurately.

REFERENCES

1. Hoorfar, A. and V. Jamnejad, "Electromagnetic modelling and analysis of wireless communication antennas," *IEEE Microwave Magazine*, 51–67, March 2003.
2. Soldovieri, F., R. Persico, and G. Leone, "Effect of source and receiver radiation characteristics in subsurface prospecting within the distorted born approximation," *Radio Science*, Vol. 40, No. RS3006, May 2005.

Session 1A2
Effective Parameters of Metamaterials: Difficulties in Definition, Characterization, and Interpretation of Measurements

On Effective Parameters of Periodical Metamaterials

S. Tretyakov
Helsinki University of Technology, Finland

Various metamaterials, very actively studied in recent years, usually consist of metal inclusions of complex shapes periodically arranged in space. If the period of the lattice and the dimensions of the inclusions are small compared with the wavelength, the material is usually considered as an effectively homogeneous material characterized by effective material parameters (permittivity and permeability). The shape and dimensions of inclusions define the electromagnetic response, which may be rather exotic (negative material parameters, for example).

It is well known that the effective medium description looses its physical meaning when any of the material dimensions (period, inclusion size) becomes comparable with the wavelength. Retrieved effective parameters cannot be anymore used as effective parameters, as they depend on the sample shape and size, as well as on the wave vector of the incident field. Moreover, in this regime these effective parameters are not response function, so that they do not obey causality, for example. There is another complication in modeling metamaterials — the resonant nature of the inclusions. Due to complex inclusion shape, inclusion resonance takes place at frequencies, where the overall inclusion dimension is still much smaller than the wavelength.

Formal retrieval of material parameters from computed or measured reflection and transmission coefficients of metamaterial slabs often leads to results that clearly violate causality and energy conservation laws, indicating that these parameters do not have the usual physical meaning. This can happen in the frequency regions quite far from the lattice resonance, where usually the effective medium description is meaningful. A typical example can be seen in Fig. 2 (left) of paper [1]. Even at low frequencies, quite far from the resonance, where the losses are small, the retrieved permittivity has a negative derivative with respect to the frequency (violating the reactance theorem), and in the resonance region the energy conservation law does not hold. In the literature, these problems have been attributed to the effect of the periodicity of the medium, and it has been suggested that although the meaning of the effective parameters is quite limited, they may be still useful in understanding the material response (e.g., [2]). This shows that the problem of effective parameter description and parameter retrieval calls for further study.

In this presentation we will discuss this problem using the approach of equivalent periodically loaded transmission lines [3](152–154). Extending this method to resonant inclusions, we will study how the impedance calculated from reflection-transmission data relates with the impedance defined as the ratio of averaged electric and magnetic fields. Limitations for the effective medium description coming from material periodicity and from resonant nature of the inclusions will be discussed.

REFERENCES

1. Koschny, T., L. Zhang, and C.M. Soukoulis, *Phys. Rev. B*, Vol. 71, 121103(R), 2005.
2. Koschny, T., P. Markos, E. N. Economou, D. R. Smith, D. C. Vier, and C. M. Soukoulis, *Phys. Rev. B*, Vol. 71, 245105, 2005.
3. Tretyakov, S., *Analytical Modeling in Applied Electromagnetics*, MA: Artech House, Norwood, 2003.

Characterization of Metamaterials as General Bianisotropic Effective Media

X. D. Chen, T. M. Grzegorczyk, and J. A. Kong
Massachusetts Institute of Technology, USA

Left-handed metamaterials are currently realized as a succession of unit cells within which metallic inclusions are printed. Because of the small size of these unit cells compared to the operating wavelength, the characterization of left-handed metamaterials as effective media has been a major research topic for the last few years. At first, uniaxial parameters were sought [1, 2], independently of the inclusions used within the unit cell. Later, it was was shown that a uniaxial representation is not accurate for some designs of inclusions, and non-zero bianisotropic terms were identified in the constitutive relation tensors [3]. Those terms were first estimated based on equivalent capacitances and inductances generated within the unit cell, thus providing a qualitative representation of their behavior with frequency.

The purpose of this presentation is two-folded. First, we provide a rigorous mathematical scheme for the retrieval of the uniaxial and bianisotropic parameters predicted in [3]. The formulation is based on the measurements of the complex reflection and transmission coefficients of a plane wave impinging onto the metamaterial at three incidences with two polarizations each [4]. In each case, the reflection and transmission coecients are expressed analytically, upon which the index of refraction and impedance are redefined to match a unique relation. This relation is then inverted using the same method as the one used for a uniaxial only retrieval [2] and yields the unknown consitutive tensors as function of frequency.

The second purpose of this presentation is to lift all assumptions on the constitutive tensors of the metamaterial. The starting point is therefore very general, where all nine complex parameters of the four constitutive matrices are unknown. Through the multiple measurements of complex reflection and transmission coefficients and the application of optimization algorithms, we show how to retrieve 72 frequency dependent unknown consitutive parameters.

REFERENCES

1. Smith, D. R., S. Shultz, P. Markoš, and C. M. Soukoulis, "Determination of effective permittivity and permeability of metamaterials from reflection and transmission coefficients," *Phys. Rev. B*, Vol. 65, 195104-1-5, 2002.
2. Chen, X., T. M. Grzegorczyk, B.-I. Wu, J. P. Jr., and J. A. Kong, "Robust method to retrieve the constitutive effective parameters of metamaterials," *Phys. Rev. E*, Vol. 70, 016608, 2004.
3. Marqués, R., F. Medina, and R. Rafii-El-Idrissi, "Role of bianisotropy in negative permeability and left-handed metamaterials," *Phys. Rev. B*, Vol. 65, 144440, 2002.
4. Chen, X., B.-I. Wu, J. A. Kong, and T. M. Grzegorczyk, "Retrieval of the effective constitutive parameters of bianisotropic metamaterials," *Phys. Rev. E*, Vol. 71, 046610, 2005.

Negative-definite Media

I. V. Lindell and A. H. Sihvola
Helsinki University of Technology, Finland

The class of negative definite (ND) media is a subclass of lossless bi-anisotropic media with negative definite medium six-dyadic. Thus, it generalizes the class of media which has recently come under great interest, variably labeled as that of double-negative media, negative-index media, backward-wave media, Veselago media or left-handed media. Among examples the class of uniaxially chiral ND media is specially considered. It is shown that the eigenfields are generalizations of TE and TM polarized fields and the Poynting vector of each eigenfield makes an obtuse angle with the propagation vector. When propagating along or transverse to the axis, the eigenwaves are pure backward waves.

Effective Metamaterial Representation by Parameter-fitting of Dispersion Models

G. Lubkowski, R. Schuhman, and T. Weiland
Technische Universität Darmstadt, Germany

In this paper, a straightforward approach to the extraction of effective electric permittivity and effective magnetic permeability for double negative (DNG) metamaterial structures from 3D field simulation data is presented. Effective parameters are obtained by fitting transmission and reflection of a homogeneous material (Fig. 1(a)) parameterized by frequency dependent Drude model (ϵ_{eff}) and Lorentz model (μ_{eff}) with the transmission and reflection of the simulated metamaterial cell (Fig. 1(b)).

Main difference between the proposed method and the known approaches based on invertion of reflection/transmission results, is that with the presented method one does not need to solve direct equations relating μ_{eff} and ϵ_{eff} with the simulated/measured scattering parameters. In this way one avoids numerical problems connected with the computation of these equations.

Proposed approach is applied to the extraction of effective material parameters for DNG metamaterial cells. Optimization results for $\mid s11 \mid$ parameter and extracted effective permittivity obtained with CST Microwave Studio are given in the Fig. 2.

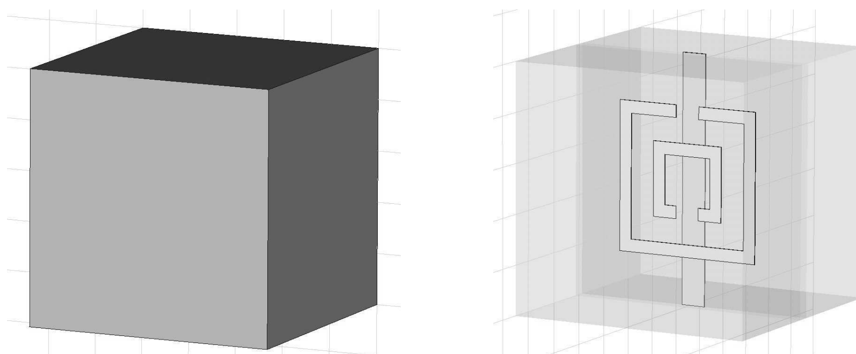

(a) (b)

Figure 1: (a) Effective representation of the SRR/wire structure; (b) SRR/wire reference structure.

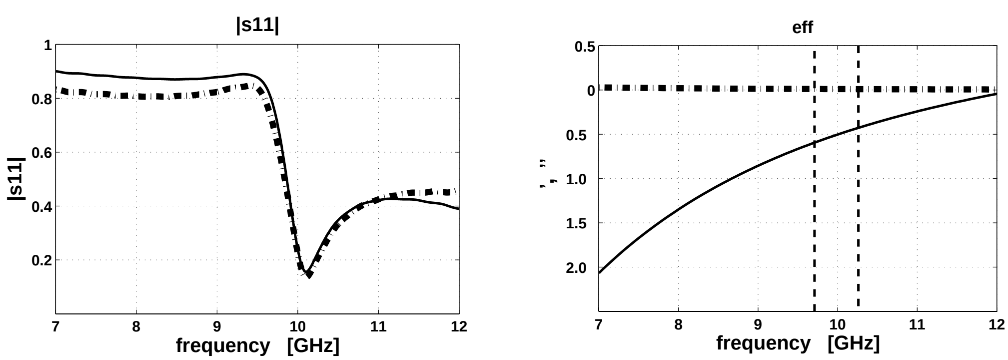

Figure 2: (LHS) Magnitude of the scattering parameter s11 for SRR/wire reference structure from Fig. 2P7 .1(b) (solid line) and for the optimized effective structure from Fig. 2P7 .1(a) (dash-dot line); (RHS) Effective electric permittivity $\epsilon_{eff} = \epsilon' - j\epsilon''$ extracted for the optimized structure in Fig. 2P7 .1(a): ϵ' solid line, ϵ'' dash-dot line.

Homogenisation Theory for Resonant Nonlinear Optical Metamaterials

J. M. Arnold
University of Glasgow, UK

Metamaterials for nonlinear optics are constructed from embeddings of resonant particulate or stratified planar materials within a matrix of homogeneous other material, which may itself be electromagnetically linear or nonlinear. Examples of such materials that have been successfully constructed in this way include semiconductor-doped glass (SDG), rare-earth doped silica fibre, similarly doped glass or silica planar waveguides, quantum-well superlattices and quantum-dot media. In all these materials, the nonlinearities may be passive or even active with suitable coupling to an external energy pump. The resonance in the embedded materials (between the carrier frequency of the electromagnetic radiation and transition energies between quantum electronic states of the embedded atoms) results in saturation effects which are intrinsic sources of electromagnetic nonlinearity.

Here the problem of homogenising such materials into effective medium parameters is examined in detail, using quantum-electronic models to describe the embedded resonances in the background medium. It is very well known that, when the optical carrier frequency Ω is far from all resonant frequencies, a nonlinear inhomogeneous medium can be homogenised to an effective homogeneous medium through the use of nonlinear susceptibility tensors $\chi^{(n)}_{k_1 k_2 \ldots k_n}$ for order-n nonlinearities. The situation when resonant interactions occur is much less clear, because the nonresonant nonlinear susceptibilities have no real meaning due to singularities in their description at the resonant frequencies. In particular, proximity effects and local fields play a significant role in the resonant nonlinear regime, making the homogenisation problem considerably more difficult. It turns out that in the fully resonant case a simplified Maxwell-Bloch model is the appropriate homogenised model, with averaged parameters for dipole moments etc. of the averaged effective medium. The averaged medium parameters are obtained from a full quantum-electronic model of the medium by an averaged Lagrangian method.

This theory permits the definition of, for example, the optical gain g of a pumped electronic medium as if g were an effective single parameter of the medium, along with a homogenised model of snonlinear saturation effects.

The Study of Effective Permittivity and Permeability of Curved Meta-materials

F. Yu[1], **J. Wu**[2], **and J.-P. Song**[1]

[1]Xi'an Jiaotong University, China
[2]China Research Institute of Radiowave Propagation, China

A new structure of metamaterials which is charactered by curved wires and SRRS, calculate permeability and magnetic permeability of artificial media using Perturbation Theory, simulated effective permittivity and permeability of curved Meta-materials, find which radius of curvature the negative effective permittivity and permeability could appearimple.

Restrictions and Limitations of Parameters in the Description of Complex Media

A. H. Sihvola and I. V. Lindell
Helsinki University of Technology, Finland

The electromagnetic characterization of metamaterials is not very easily incorporated into the traditional machinery to analyze fields and waves in ordinary media. Especially the existence of backward waves and the fact that a wave can be refracted to the "wrong" direction requires that the material parameter values have to be reconsidered. Permittivity and permeability have to be negative. But this is counter-intuitive because we are used to thinking of permittivity (and permeability) as measures of electric (magnetic) energy density. Of course, one can respond to this and defend the possibility of such a behavior by observing that resonating elements can cause it in a limited frequency band through the plasma-type characteristics. This is a high-frequency phenomenon. And then, if the elements to resonate can be made sufficiently complex-shaped so that a resonance can be made to take place within small space, one can bring down the negative band into "low" frequencies.

If we have liberated our minds from the taboo of positivity of the permittivity and permeability, concerning its real part, one may ask are there any restrictions left that it should obey. And another natural question is what kind of limitations can be posed on the imaginary parts. Obviously the sign of the imaginary part of the refractive index is fixed for dissipative materials in order to avoid amplification in the energy. But does this lead to separate restrictions for the imaginary parts of permittivity and permeability? In the presentation, these questions will be discussed concerning both isotropic materials and also more complicated ones that may display anisotropy and/or magnetoelectric coupling.

Experimental Extraction of the Effective Properties of Metamaterials from Measured S-parameters

V. V. Varadan
University of Arkansas, USA

This talk overviews experimental work related to metamaterials and chiral materials at microwave frequencies and address some of the controversies surrounding effective property extraction for metamaterials. A focused plane wave beam is used to illuminate planar samples in a free space set-up. TRL calibration in conjunction with a vector network analyzer leads to the establishment of two phase and amplitude reference planes for homogenization and effective medium modeling and subsequent extraction of complex permittivity, permeability and magneto-electric coupling if any from S-parameter measurements [1, 2]. Experimental results showing negative permittivity, permeability and refractive index are presented for ordered and random metamaterials that exhibit plasmonic resonances at the frequency range of interest. Several different types of scattering elements were used to make the samples, such as C left, right and racemic mixtures of small metallic springs, metallic Omega shaped elements, combinations of split ring resonators and wire elements. It is shown that it is possible for all such scatterers to exhibit negative refraction. Good agreement is obtained with numerically simulated data for effective properties. It is shown that disordered structures can also lead to NIM behavior thus periodicity is not required. There is current controversy regarding the allowed sign of the imaginary parts of the permittivity and permeability. Experimental data confirming loss in such materials from plots of power absorption, resistive part of the complex impedance and attenuation constant is shown for those cases where one of the material properties exhibits a negative imaginary part. Homogenization methods are used by experimentalists and theorists alike to derive effective medium properties and this is discussed with reference to the experimental study. A new method for extracting the effective properties of Omega media is presented in order to obtain a third material property, the magneto-electric coupling coefficient. Omega media are non-symmetric ($S11 \neq S22$). This however does not resolve the question of negative imaginary parts of the complex properties as had been suggested by some researchers.

REFERENCES

1. *IEEE I&M*, Vol. 39, 387, 1990.
2. *Radio Science*, Vol. 29, 9, 1994.

Metamaterials: Mechanisms of Subwavelength Imaging

E. Shamonina[1] and L. Solymar[2]
[1]University of Osnabrück, Germany
[2]Imperial College, UK

Metamaterials are artificial structures comprising of arrays of small resonant elements in which both the size and the distance between the elements are much smaller than the wavelength. A number of metamaterial devices have been designed to manipulate and control the near field following the idea of the perfect lens proposed by Pendy [1]. His idea was to image an object of subwavelength dimensions a distance away from the source plane by a plane parallel slab having a refractive index ?. A silver slab [1] or a multilayered silver metamaterial [2] can serve as a near-perfect lens, with the limit of resolution determined by surface plasmon resonances and by a high-frequency cut-off of the transfer function. There have been imaging experiments with silver slabs (see e. g., [3, 4]), with a single layer of a 2D array of Swiss Rolls [5, 6], and with two or more layers of 2D arrays of split ring resonators [7–10].

The purpose of the present work is to review the mechanisms of subwavelength imaging and discuss the relationship between imaging and focussing. The mechanisms discussed will be the excitation of (i) surface plasmons, (ii) magnetoinductive surface waves and (iii) phase conjugate waves at the outer boundary of the lens. In addition we shall consider microchannelling [11] based on the eigenmodes of the periodic medium and also on a set of magnetoinductive waves evanescent in the transverse direction and propagating in the longitudinal direction. Imaging and focussing will also be described in terms of coupled resonators [7] and finally the general topic of Poynting vector optics [12] will be discussed with indefinite media [8] as one of the examples.

REFERENCES

1. Pendry, J. B., "Negative refraction makes a perfect lens," *Phys. Rev. Lett.*, Vol. 85, 3966–3969, 2000.
2. Shamonina, E., V. A. Kalinin, K. H. Ringhofer, and L. Solymar, "Imaging, compression and Poynting vector streamlines with negative permittivity materials," *Electron. Lett.*, Vol. 37, 1243–1244, 2001.
3. Melville, D. O. S. and R. J. Blaikie, "Super-resolution imaging through a planar silver layer," *Opt. Express*, Vol. 13, 2127–2134, 2005.
4. Fang, N., H. Lee, C. Sun, and X. Zhang, "Sub-diffraction-limited optical imaging with a silver superlens," *Science*, Vol. 308, 534–537, 2005.
5. Wiltshire, M. C. K., J. B. Pendry, I. R. Young, D. J. Larkman, D. J. Gilderdale, and J. V. Hajnal, "Microstructured magnetic materials for radio frequency operation in magnetic resonance imaging (MRI)," *Science*, Vol. 291, 849–851, 2001.
6. Wiltshire, M. C. K., J. V. Hajnal, J. B. Pendry, D. J. Edwards, and C. J. Stevens, "Metamaterial endoscope for magnetic field transfer: near field imaging with magnetic wires," *Opt. Express*, Vol. 11, 709–715, 2003.
7. Maslovski, S., S. Tretyakov, and P. Alitalo, "Near-field enhancement and imaging in double planar polariton-resonant structures," *J. Appl. Phys.*, Vol. 96, 1293–1300, 2004.
8. Smith, D. R., D. Schurig, J. J. Mock, P. Kolinko, and P. Rye, "Partial focusing of radiation by a slab of indefinite media," *Appl. Phys. Lett.*, Vol. 84, 2244–2246, 2004.
9. Freire, M. J. and R. Marques, "A planar magnetoinductive lens for 3D subwavelength imaging," *Appl. Phys. Lett.*, Vol. 86, 182505, 2005.
10. Lin, I.-H., C. Caloz, and T. Itoh, "Near-field focusing by a nonuniform leaky-wave interface," *Microw. Opt. Techn. Lett.*, Vol. 44, 416–418, 2005.
11. Belov, P. A., C. R. Simovski, and P. Ikonen, "Canalization of subwavelength images by electromagnetc crystals," *Phys. Rev. B*, Vol. 71, 193105-1-4, 2005.
12. Russell, P. St. J., "Novel thick grating beam-squeezing device in ta2O5 corrugated planar waveguide," *Electron. Lett.*, Vol. 20, 72–73, 1984.

FDTD Simulation of Perfect Lens Imaging System

J. B. J. Chen, **T. M. Grzegorczyk**, **B.-I. Wu**, **and J. A. Kong**
Massachusetts Institute of Technology, USA

The ability of the Finite-Difference Time-Domain (FDTD) method to model a perfect lens made of a slab of homogeneous left-handed material (LHM) is investigated. It is shown that because of the frequency dispersive nature of the medium and the time discretization, an inherent mismatch in the constitutive parameters exists between the slab and its surrounding medium. This mismatch in the real part of the permittivity and permeability is found to have the same order of magnitude as the losses typically used in numerical simulations. Hence, when the LHM slab is lossless, this mismatch is shown to be the main factor contributing to the image resolution loss of the slab.

Using the Auxiliary Differential Equation (ADE) method to implement the frequency dispersive permittivity and permeability for Drude model, we show that after the FDTD discretization, the numerical permittivity (so as permeability) can be described as

$$\epsilon_r = 1 - \frac{\omega_{pe}^2}{4\sin(\omega_o \Delta t/2)/(\Delta t)^2} \tag{1}$$

It is clear that Eq. 1 approaches the Drude model $\epsilon_r = 1 - \omega_{pe}^2/\omega_o^2$ in the limit of $\Delta t \to 0$, which gives a value of -1 when $\omega_{pe} = \sqrt{2}\omega_o$. However, for a finite Δt used in an actual simulation, ϵ_r presents a slight deviation from exactly -1 at the same ω_{pe}. As an example, the value of ϵ_r from Eq. 1 is about -1.000297 for a typical grid size of $\lambda/100$, which is also the value of the refractive index since we choose here a magnetic plasma frequency identical to the electric one. This small perturbation does not affect the propagating waves significantly. However, the resolution of a subwavelength imaging system is critically dependent on the reconstruction of the evanescent waves, or part of the evanescent wave spectrum, by the LHM slab. This reconstruction is in turn critically dependent on the slab's constitutive parameters, and the slight mismatch of 0.03% in the real part has an important impact on the resolution of the image as we shall see hereafter. It is important to note that this small perturbation in the real part of the constitutive parameters has often been overlooked and the imaginary parts with a value in the same order are typically considered to be the main contributor for limiting the image resolution. By comparing the simulation results and analytical calculations, we demonstrate that the simulated image resolution of an LHM perfect lens is mainly limited by this mismatch. In other applications such as the simulation study of surface plaritons at LHM/RHM interfaces where the matching condition is required, the understanding of this limitation in FDTD can also be very important.

Permeability and Permittivity of Metamaterials Determined by the Field Summation Method

J.-M. Lerat, N. Mallejac, and O. Acher
CEA Le Ripault, France

Negative index materials have been recently demonstrated using adequate topologies of metallic inclusions exhibiting both engineered permeability and permittivity [1]. The opportunities associated to these so-called metamaterials, first envisioned 40 years ago, are continuously expanding to new field of applications and extended wavelengths.

The effective parameters ε and μ are fundamental quantities in the conception of a metamaterial. As a consequence, it is of foremost importance to be able to enhance our ability to predict these quantities for different inclusion topologies, and retrieve them from experimental results. A method has been proposed [2] to determine the effective parameters of heterogeneous materials, from the knowledge of the fields inside the material. This paper shows that this method can be fruitfully applied to the determination of permeability and permittivity of a metamaterial.

As an example, a composite consisting of resonant permeability inclusions has been considered. The fields in the composite have been determined using HFSS commercial software. The permeability and permittivity have been deduced using this field summation method. Reflexion and transmission coefficients have been computed from these values, and are compared with raw numerical prediction by HFSS. It is evidenced on Fig. 1 that a satisfactory agreement is observed.

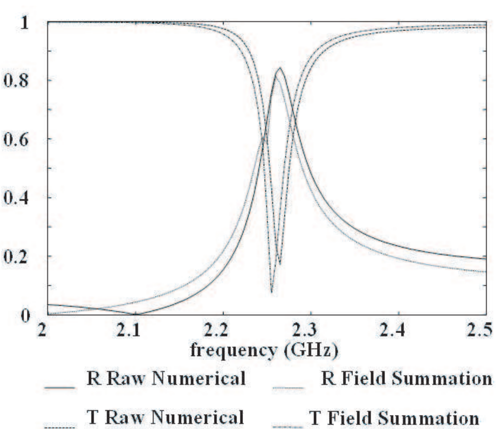

Figure 1: Reflection and transmission coefficient derived from effective parameters obtained by field summation, and compared to raw numerical results, for a composite made of split ring resonators.

Different types of composite materials are considered. In some cases, the field summation method indicates that it is not adequate to describe a metamaterial through an homogenization approach at frequencies close to the resonance. This observation may account for some difficulties in retrieving effective parameters from experimental results, and the scarcity of direct experimental determinations of ε and μ on metamaterials.

REFERENCES

1. Smith, D. R., J. B. Pendry, and M. C. K. Wiltshire, *Science*, Vol. 305, 788, 2004.
2. Acher, O., A. L. Adenot, and F. Duverger, *Phys. Rev. B*, Vol. 62, 13748, 2000.

Session 1A3a
Scattering and Propagation in Random Media and Rough Surfaces

Designer Emissivities

T. A. Leskova and A. A. Maradudin
University of California, USA

The emissivity of an object is defined as the ratio of the brightness temperature $T_{B\nu}$ emitted by the object to its actual physical temperature T_{phys}, under the assumption that the object is at a constant physical temperature [1], $T_{B\nu} = e_\nu(\theta, \phi)T_{phys}$. In this equation the subscript ν refers to the polarization of the brightness temperature, while (θ, ϕ) are the polar and azimuthal angles of observation. Kirchhoffs law [2] relates the emissivity $e_\nu(\theta, \phi)$ to the reflectivity of the surface, $e_\nu(\theta, \phi) = 1 - r_\nu(\theta, \phi)$, where the reflectivity $r_\nu(\theta, \phi)$ is the fraction of the power scattered from the surface when $a\,\nu = p$, s wave is incident on it from the direction (θ, ϕ). Since the reflectivity of a surface is affected by its roughness [3], it follows that its emissivity is affected by the roughness. The question then arises, can one design a random surface that produces an emissivity with a specified wavelength dependence at a fixed angle of emission?

We investigate this question for a one-dimensional random surface defined by $x_3 = \zeta(x_1)$. The region $x_3 > \zeta(x_1)$ is vacuum, while the region $x_3 < \zeta(x_1)$ is a perfect conductor. This surface is illuminated by an s-polarized plane wave of frequency ω, whose plane of incidence is the x_1x_3 plane. We represent the surface profile function in the form $\zeta(x_1) = nb < x_1 < (n+1)b$, with $n = 0, \pm1, \pm2, \ldots$ Here b is a characteristic length, and the $\{d_n\}$ are independent, identically distributed random deviates. The probability density function (pdf) of d_n, $\langle\delta(\gamma - d_n)\rangle = f(\gamma)$, where the angle brackets denote an average over the ensemble of realizations of $\zeta(x_1)$, is therefore independent of n. In the Kirchhoff approximation, which we use due to its simplicity, the reflectivity is given by $r_s(\theta_0, \omega) =\mid F((2\omega b/c)\cos\theta_0) \mid^2$, where θ_0 is the polar angle of incidence, and $F(\nu) = \int_{-\infty}^{\infty} d\gamma f(\gamma)\exp(-i\nu\gamma)$. Thus, if we wish to have a particular frequency dependence of the emissivity $e_s(\theta_0, \omega)$ at an angle of emission θ_0, we have to solve the equation $\mid F((2\omega b/c)\cos\theta_0 \mid= [1 - e_s(\theta_0, \omega)]^{1/2}$ to obtain $f(\gamma)$. This is done iteratively by the use of a modified Gerchberg-Saxton algorithm [4]. From the result a long sequence of $\{d_n\}$ is generated by the rejection method [5], from which a realization of the surface profile function is generated. To validate the approach described, the emissivity produced by the resulting surface is calculated by solving the scattering problem numerically for a particular example.

REFERENCES

1. Johnson, J. T., R. T. Shin, J. A. Kong, L. Tsang, and K. Pak, *IEEE Trans. Geosci. Remote Sensing*, Vol. 37, 8, 1999.
2. Tsang, L., J. A. Kong, and R. T. Shin, *Theory of Microwave Remote Sensing*, Wiley, New York, 1985.
3. Baylard, C., J.-J. Greffet, and A. A. Maradudin, *J. Opt. Soc. Am.*, Vol. A10, 2637, 1993.
4. Gerchberg, R. W. and W. O. Saxton, *Optik*, Vol. 35, 237, 1972.
5. Press, W. H., S. A. Teukolsky, W. T. Vetterling, and B. P. Flannery, *Numerical Recipes in Fortran, 2nd Edition*, Cambridge University Press, New York, 281–282, 1992

On the Application of the Radiative Transfer Approach to Scattering from a Random Medium Layer with Rough Boundaries

S. Mudaliar
Air Force Research Laborotory/SNHE, USA

The problem of scattering from a random medium layer with rough boundaries is a difficult one. People have used the phenomenological radiative transfer approach to solve this problem. This approach is conceptually simple and yet very effective for studying multiple scattering processes. Here one uses the transport equations corresponding to the random medium of the layer and then imposes the transport theoretic boundary conditions [1]. Although this procedure appears to be heuristically sound, it is not clear what approximations are involved, and under what conditions such an analysis may be used for the problem at hand. One way to better understand this radiative transfer approach is to compare and relate it to the statistical wave approach. For the case of unbounded random media it has been demonstrated how the ladder-approximated Bethe-Salpeter equation reduces to the radative transport equation [2]. We found that this procedure can be applied to a random medium layer with planar boundaries and arrive at the radiative transport system as given in [1]. For the case of the problem of random medium layer with rough boundaries we have developed two different statistical wave approaches. In the first approach we assume that we know the solution to the problem without volumetric fluctuations. The second approach is based on the solution of the problem where all the fluctuations of the problem vanish. A key step in both approaches is the representation of the problem as a suitable integral equation which incorporates volumetric scattering and surface scattering. This integral equation is then used to derive equations for the first and second moments of the fields. Use of Wigner transforms in the ladder-approximated Bethe-Salpeter equation leads us to equations of radiant intensities. One important requirement to obtain this result is that the fields be quasi-uniform. This implies that localized spectra of waves travelling in different directions are weakly correlated compared to those travelling in similar directions. In the first wave approach we imposed the 'weak surface correlation' approximation in order to perform averaging over surface fluctuations. With this approximation we find that the integral equation system is identical to that of the radiative transfer approach. In our second wave approach the volumetric and surface fluctuations are treated in a unified manner. The equations for radiant intensities obtained by this approach are different from that of the radiative transfer approach. In order to understand the differences, we translated our integral equation system into a system of integro-differential equations. These integro-differential equations are identical to those used in the radiative transfer approach. However, the boundary conditions are quite different; they are a coupled system of integral equations. The important difference is that we have a set of nonlocal boundary conditions as opposed to those used in radiative transfer approach, where they are localized relations. We need to impose additional assumptions on our results to arrive at the boundary conditions similar to those of radiative transfer. Physical implications of all these characteristics are discussed in this paper. This study has thus enabled us to better understand the meaning of the radiative transfer approach as applied to our problem.

REFERENCES

1. Ulaby, F. T., R. K. Moore, and A. K. Fung, *Microwave Remote Sensing*, Vol. 3, Artech House, 1986.
2. Barabanenkov, Y. N., A. G. Vinogradov, Y. A. Kravtsov, and V. I. Tatarskii, *Izv VUZ Radiofiz* 15, 1852–1860, 1972.

Polarization Dependent Backscatter Cross Sections of Composite Random Rough Surfaces for Normal to Near Grazing Incidence

E. Bahar
University of Nebraska, USA

P. Crittenden
Air Force Institute of Technology, USA

The small height/slope perturbation solutions, for the vertically and horizontally polarized backscatter cross sections of random rough surfaces have significantly different dependence upon the incident angle. Thus, for highly conducting surfaces, the ratio of vertically to horizontally polarized backscatter cross sections based on these solutions becomes very large for grazing angles of incidence and the ratio is independent of the roughness characteristics. The corresponding backscatter cross sections based on the physical optics solutions are polarization independent and the ratio is also independent of the roughness characteristics.

Ample experimental data, however, indicate that at near grazing angles of incidence the vertically and horizontally polarized backscatter cross sections of the earth surface, can be of the same order of magnitude and they are also significantly large than the values predicted by both physical optics and small perturbation theory. A unified full wave approach is used to express the backscatter cross sections as weighted sums of two cross sections. The first, associated with the larger scale rough surface height is given by the physical optics cross section, multiplied by the magnitude squared of the smaller scale rough surface height characteristic function. The second is the cross section associated with the smaller scale surface height, modulated by the slopes of the larger scale surface. When the composite rough surface is characterized by a continuous surface height spectral density function, it becomes necessary to judiciously separate the smaller scale surface from the lager scale surface. It is shown that this can be done using the unified full wave approach by seeking stationary solutions to the cross sections over a wide range of the variational parameters $r = \langle h_s^2 \rangle / \langle h^2 \rangle$ where $\langle h_s^2 \rangle$ and $\langle h^2 \rangle$ are the mean square heights of the smaller scale surface and the total surface respectively. These stationary values for the polarization dependent backscatter cross sections at grazing incidence can be practically equal and they are also significantly larger than the corresponding physical optics and perturbation results. These investigations also impact on the feasibility of relating the backscatter cross section to the remote sensing of moisture content of soil surfaces over gently undulating fields.

Time-reversal Strategies for Extended Target Imaging and Focusing, and Clutter Nulling

E. A. Marengo
Northeastern University, USA

Time-reversal (TR) imaging has been shown (see [1], and the references therein) to be a useful strategy for super-resolved imaging of M point targets from the multistatic response matrix (MRM) K measured by an array of $N > M$ co-located transmitters and receivers. This method works even if there is significant multiple scattering among the targets. For the particular non-multiply scattering case the MRM $K = \sum_{m=1}^{M} \tau_m g(\mathbf{x}_m) g^{*\dagger}(\mathbf{x}_m)$ where $\dagger$ denotes the adjoint, the τ_m's are the target scattering strengths, the $g(\mathbf{x}_m)$'s are linearly independent N-long Green function vectors or "propagators" corresponding to the target locations $\mathbf{x}_m$, and the $g^*(\mathbf{x}_m)$'s are the associated "backpropagators". If (u_i, v_i, λ_i) is the singular system of K, where $K_{u_i} = \lambda_i v_i$, then if $\lambda_i = 0$ the inner product $u_i^\dagger g^*(\mathbf{x}_m) = 0$ for all $m = 1, 2, \ldots, M$ so that in the absence of additive noise the TR MUSIC pseudospectrum $P(\mathbf{x}_m) = (\sum_{\lambda_i=0} |u_i^\dagger g^*(\mathbf{x}_m)|^2)^{-1}$ peaks at the correct target locations while in the presence of noise it yields an image of the targets. In this theory there is a single propagator $g(\mathbf{x}_m)$ and its companion backpropagator $g^*(\mathbf{x}_m)$ per point target. But, as is well known (see [2–4]), for extended targets whose size is not small relative to the smallest probing wavelength one must associate a set of propagators and backpropagators per each target (they depend on both the target's shape and position). The question then arises how to optimally generalize TR imaging when the targets are extended. This generalization is desirable for realistic applications in ground-penetrating radar, SAR imaging, and inverse scattering of large objects. A treatment based on the Born approximation is given in ([5]) which focuses on extended targets that have a uniform scattering potential. The present work considers the more general exact scattering regime and non-uniform scatterers, and also provides a new framework to treat space-time information in TR. The general theory is based on the fact that for a broad class of problems the MRM K essentially takes the more general form $K \simeq \sum_{m=1}^{M} \sum_{q=1}^{\alpha_m(\mathbf{x}_m)} \tau_{m,q} \pi_m^{(q)}(\mathbf{x}_m) [\Pi_m^{(q)}]^\dagger(\mathbf{x}_m)$ where $\alpha_m(\mathbf{x}_m)$ is a finite number of degrees of freedom corresponding to the relevant signal-to-noise ratio (SNR) and where the $\pi_m^{(q)}(\mathbf{x}_m)$'s and $\Pi_m^{(q)}(\mathbf{x}_m)$'s form respective sets of propagators and backpropagators *per target*. The generalized form of the pseudospectrum valid for extended targets can then be shown to be $P(\mathbf{x}_m) = (\sum_{\lambda_i=0} \sum_{q=1}^{\alpha_m(\mathbf{x}_m)} |u_i^\dagger \Pi_m^{(q)}(\mathbf{x}_m)|^2)^{-1}$ which theoretically peaks at the correct target locations. This method and yet more generalized variants of it are validated in this talk with the aid of computer simulations.

The proposed approach can be implemented for cases of increasing complexity ranging from known targets, to targets of partially known support, to completely unknown targets whose support one attempts to deduce from the data. An application emphasized in this talk is imaging of an extended target in the presence of certains kinds of clutter which do not limit the information space versus data space dimensionality restrictions of all TR approaches. This includes ways of suppressing the clutter by reducing the data subspaces that are associated mainly to clutter (interference) which enhances signal-to-interference ratio. Another application, within the medical context, is the minimally invasive focusing of wave energy in a target surrounded by clutter (e.g., surrounding organs).

REFERENCES

1. Gruber, et al., *J. Acoust. Soc. Am.*, Vol. 115, 3042–3047, 2004.
2. Chambers, D. H. and J. G. Berryman, *IEEE Trans. Antenn. Propagat.*, Vol. 52, 1729–1738, 2004.
3. Chambers, D. H. and A. K. Gautesen, *J. Acoust. Soc. Am.*, Vol. 109, 2616–2624, 2001.
4. Chambers, D. H., *J. Acoust. Soc. Am.*, Vol. 112, 411–419, 2002.
5. Zhao, H., *SIAM J. Appl. Math.*, Vol. 64, 725–745, 2004.

A New Fractal-based Approach to Model Scattering from Natural Surfaces with Hurst Exponent H(R)

A. K. Sultan-Salem and G. L. Tyler
Stanford University, USA

Natural surfaces have properties, such as the root-mean square (RMS) slope, which depend on the horizontal scale, R, over which they are estimated. Fractal surface models mimic these observed scale-dependent characteristics and, thus, have come to play an important role in the study of wave scattering from different types of natural rough surfaces. Franceschetti et al. [1], for instance, used the Kirchhoff approximation and a fractional Brownian surface model to develop a practical fractal-based scattering law. Their law subsumes as special cases the Hagfors and Gaussian scattering laws, widely used to model scattering from planetary surfaces, when the Hurst exponent parameter, H, of the fractal model equals 1/2 and 1, respectively. The exponential scattering law, which is a better modeler of the scattering behavior from certain surfaces, is not covered by the fractal-based scattering law of Franceschetti et al., however. In order to find a fractal counterpart to the exponential law, we allow the Hurst exponent to be a function of horizontal scale, $H(R)$. Given an exponential scattering law, whose parameters are obtained through fitting backscatter radar cross section observations, an integral equation is solved, via the Hankel transform, to obtain the Hurst exponent and, consequently, the RMS slope of the surface as a function of horizontal scale [2]. This approach can be extended to provide a scale-explicit parameterization of surfaces for which near-nadir quasi-specular observations are available, and whose scattering behavior is modeled by any linear combination of the aforementioned scattering laws or any others that have a Hankel transform.

REFERENCES

1. Franceschetti, et al., *IEEE Trans. Antennas Propag.*, 1405–1415, Sept. 1999.
2. Sultan-Salem, A. K. and G. L. Tyler, "Generalized fractal-based laws for scattering from planetary surfaces: a unifying scale-explicit paradigm," *J. Geophys. Res.*, in press.

A Semi-rigorous Method for Scattering from 2D Rough Heterogeneous Surfaces

P. Mallet[1,2], C. A. Guérin[1], A. Sentenac[1], and J. P. Segaud[2]

[1]Universite Paul Cezanne, France
[2]ONERA Centre de Toulouse, France

Scattering from three-dimensional rough heterogeneous media is a challenging problem that can hardly be addressed by the classical numerical methods (FDTD, Coupled-Dipole Approximation, ...) due to the cost of computing over a large three-dimensional domain.

We propose an efficient numerical method to calculate scattering from two-dimensional rough surfaces on top of an assembly of random inclusions. The roughness has large scales compared to radiation wavelength and the scatterers are small particles that radiate like dipoles.

Our approach is semi-rigorous as multiple scattering between particles and between surface and scatterers are accounted for. The Kirchhoff Approximation (KA), however, is used to compute the electric and magnetic currents produced at the interface.

In the KA, the surface currents depend only on the local incident field on the surface, which is the sum of the incident beam and fields scattered by all the particles. The latter are the dipolar response of each particle excited by both the field radiated by the surface currents and the field steeming from the other particles. All these interactions are expressed trough operations on the (unknown) dipolar moments of the scatterers. Finding these dipolar moments then amounts to solve a linear system of size 3N, N being the number of scatterers.

Once this is done, surface currents can be made explicit, as well as the field scattered above by the heterogeneous surface.

Some numerical test cases will be presented. A cross-comparison with other methods will be made on simple geometries to validate the results.

Session 1A3b
Interaction of Microwaves with Vegetation

Scattering by a Vertical Tree Trunk over a Flat Ground: A Comparison between Analytical and Numerical Approach

P. de Matthaeis and R. H. Lang
The George Washington University, USA

Most microwave models of forests neglect the near field interaction of the trunk and the surface of the ground. In this paper we investigate this interaction and compare the result with the standard analytical approach. Plane wave scattering by a vertical trunk over a flat lossy ground is considered.

The problem is first treated numerically. Using a surface integral equation formulation, the method of moments is used to determine the equivalent surface currents on the finite cylinder. The procedure exploits the rotational symmetry of the cylinder, and employs a dyadic Green's function for the half space. From the equivalent surface currents the bistatic scattering coefficient is evaluated. In the analytical approach, the contribution from the ground is taken into account in the computation of the scattering coefficient in the form of a double bounce effect between the cylinder and the flat ground.

The numerical results are compared to the approximate analytical approach for frequencies from 200 MHz to 2 GHz. It is seen that the approximate approach losses accuracy as the frequency decreases. However, it is noted that the approximate analytical method is computationally much faster.

Experimental and Model Investigation about Forest Emission at L Band

A. D. Vecchia, P. Ferrazzoli, and L. Guerriero
Tor Vergata University, Italy

M. Guglielmetti, M. Schwank, and H. Flühler
Institute of Terrestrial Ecology, Switzerland

C. Mätzler
Institute of Applied Physics, Switzerland

In the near future important projects, aimed at monitoring soil moisture and land properties by L band spaceborne radiometers, are foreseen. In particular, technological efforts are being done for the development and launch of SMOS and HYDROS. Since these systems will collect microwave signatures at large scale, the contribution of surfaces covered by forests must be investigated. In fact, forests cover a large fraction of land, so that several pixels will be affected, partially or even totally, by their presence.

Up to now, most of theoretical and experimental studies about microwave interaction with forests have been based on active systems. Therefore, presently available results about emissivity are rather limited and sparse. New efforts are required to estimate the emission due to forest components and attenuation introduced over soil emission, which are important to fully exploit the potential of future L band radiometers.

In this work, results of model simulations and recent experiments are described and compared against each other. The model is based on routines, developed at Tor Vergata University in recent years, representing electromagnetic effects of trunks, branches, leaves, and soil. Single effects are then combined in order to simulate the emission of the whole medium. This basic electromagnetic software has recently been joined with a set of basic allometric relationships, available in the literature for several forest categories. This allows us to estimate forest emission without need of very detailed ground truth.

Experimental data were collected during the autumn 2004 in the Research Centre Jülich (Germany). The L-Band 1.4 GHz radiometer ELBARA, as well the X-Band 11.4 GHz radiometer MORA, were installed looking in the upward direction in a mixed hardwood forest. The average height of trees was about 20 meters, and the leaf fall process was monitored. Measurements with ELBARA allow distinguishing the horizontal and the vertical polarisation, and the antenna beamwidth is 12 degrees. In November 2004, the ELBARA radiometer was located above the same forest, looking downward from a 100 m tower. The experiment was repeated after covering the soil with a metallic foil.

The theoretical model has been adapted to the structural and geometrical properties of the forest. It was run in order to simulate the cases of upward looking radiometer and downward looking radiometer in absence and presence of the metallic foil. Comparisons between simulated and measured data are shown. The model represents several basic properties of experimental data. Some critical points, requiring further work, are identified.

Angular Normalization of ENVISAT ASAR Data over Sahelian Grassland Using a Coherent Scattering Model

A. Monsiváis[1], **I. Chênerie**[1], **F. Baup**[1,2], **E. Mougin**[2], **and K. Sarabandi**[3]

[1]Université Paul Sabatier, France
[2]CNES/CNRS/UPS, France
[3]The University of Michigan, USA

ENVISAT-ASAR has the capability of working at different spatial resolutions. This characteristic makes the ENVISAT satellite an excellent tool for the remote sensing of landscapes. Moreover, the choice of polarization allows focusing the observation on particular scattering mechanisms. For instance, in the case of the Sahelian grassland, the main contribution at HH polarization can be contributed to scattering from the soil surface whereas at VV polarization the main contribution is from the vegetation.

Seasonal measurements are acquired at different incidence angles. For temporal soil and vegetation parameters retrieval it is necessary to normalize the radar data for the angular behavior of the radar backscatter. A simple method for characterizing the angular behavior is by plotting the measurements of the backscattering coefficient during the dry season (stationary target) as a function of the incidence angle and considering that this angular dependence is conserved throughout the rainy season as well. However, this method is not sufficiently precise for data gathered in the rainy season since the scattering mechanisms of the vegetation and soil are different. Instead, we propose the use of a coherent scattering model for vegetation in order to carry out a more precise angular normalization. With this method, a higher precision is obtained for the normalization of the backscattering coefficient at VV polarization during the rainy season, in which the main contribution to the backscatter is attributed to vegetation.

The procedure for determining the angular normalization factor is as follows:

1. Determination of the soil contribution from the backscattering coefficient data at HH polarization during the dry season.

2. Simulation of the backscattering coefficient as a function of both time (during the growing season) as a function of incidence angle $\sigma(t, \theta_i)$ employing the roughness parameters obtained from Step 1 and ancillary data (vegetation type, density, etc.). This allows for a first-order correction to gentle angular variations of backscattering coefficient.

3. Determination of the angular normalization factor plot of normalized backscattering coefficient σ_{θ_0} (normalized to mean incidence angle) as a function of time to monitor long term temporal variations.

This method can be applied to the data gathered at both HH and VV polarizations.

Model Approaches for Scattering and Extinction of Thin Stems

A. D. Vecchia, **P. Ferrazzoli**, **and L. Guerriero**
Tor Vergata University, Italy

In the recent years, important advances in microwave remote sensing of crops were achieved. The availability of spaceborne SAR systems, as well as airborne campaigns, made several radar signatures available over agricultural fields. In some cases, also detailed ground truth are available. Moreover, several new theoretical efforts led to refine scattering models of vegetated fields. In spite of these important advances, discussion is still open about important topics. Several works are aimed at refining the techniques to combine the contributions of different scattering sources within vegetated media. However, also single element representation requires further work.

Detailed ground truth collected during experimental campaigns indicated that the stem diameter measured by a meter was appreciably higher than the diameter obtained by using weight measurements and information about wet and dry matter density. This discrepancy may be explained by stem hollowness, which is evident in the mature phase of the cycle for some crops, like wheat.

In this work different approaches, adopted to represent scattering and extinction of wheat stems, are presented and compared against each other. Adopted models for stems are: i) full cylinder with diameter equal to the one measured by a meter; ii) full cylinder with "equivalent" diameter, obtained by weight measurements; iii) hollow cylinder, with external and internal diameters obtained by using both meter and weight measurements. A specific electromagnetic routine, derived for the third case, is described.

Backscattering coefficients of wheat fields, simulated using the three techniques, are compared to each other at different frequencies, angles and stages of growth. Also extinction coefficients are compared. It is shown that "equivalent" and "hollow" cylinder techniques lead to similar results, while "full" cylinder technique leads to appreciably different results. For the C band case, some comparisons with experimental data, collected by ERS-2 SAR and ENVISAT ASAR, are presented. Better agreements are achieved by using the "equivalent" and "hollow" cylinder approaches.

Session 1A4
Bioelectronics and Medical Electromagnetics

A Review of the Mechanisms of Interaction between the Extremely Low Frequency Electromagnetic Fields and Human Biology

H. A. Sadafi[1], Z. Mehboodi[2], and D. Sardari[2]

[1]Royal Melbourne Hospital, Australia
[2]Amirkabir University, Iran

Studies of the biological effects and any health related consequences of extremely low frequency (ELF) electromagnetic fields (EMF) have been going on for over half a century however with contradictory outcomes. Hence, it is now necessary to stress on standardizing the EMF-health research experiment procedures in order to enable such experiments become replicable and results comparable. In 1998, a review of several of the ELF EMF human biological interaction mechanisms regarding field intensities and frequencies was presented to the Australian Radiation Laboratory of Commonwealth Department of Community Services and Health in 1988 by Andrew W. Wood. Wood's 1988 assertion of the importance of understanding the interaction mechanisms did not alter even after a decade when the NIEHS RAPID (http://www.niehs.nih.gov/) gathering of world experts produced their statement, in which quoted, there have been experiments on possible mechanism/s in support or refutation of the various proposals however none were replicated. Valberg (Valberg *et al.*, 1997) also summed up some but failed to include all the claimed proposed mechanisms at the time. This paper is to present a complete list of the allegedly possible interaction mechanisms to date.

This paper will also report on an academic research on computer modeling of biological effects of ELF EMF using one of the proposed mechanisms. The research reported here has generally aimed at modeling the proposals using computer. The initial phase of this effort has concentrated on Ca effect as the number of publications referencing that was considerable. Calcium is a key element in the biological performance of every organ in the human body. Thus it deemed imperative to study the effect of EMF on Ca channels of a living cell.

Furthermore, considerations for setting standards in EMF experimental research protocols are recommended. Developing a standard protocol allows results of future experiments to be comparable; and, the chance of replicability in EMF-health improve, which this aspect has indisputably been absent in EMF research projects thus far. Replication is desirable mainly because it eliminates bias, artifact and systematic errors. Replication is almost impossible in the case of epidemiological studies however in experimentation is possible if the details are specified in full. To authenticate any effect of MF, it is not satisfactory to present experimental results without reporting the experimental settings in their entirety.

Calculating SAR in two Models of the Human Head Exposed to Mobile Phones Radiations at 900 and 1800 MHz

S. Khalatbari, **D. Sardari**, **and A. A. Mirzaee**
Amirkabir University, Iran

H. A. Sadafi
Royal Melbourne Hospital, Australia

Since the 1990's, use of mobile phones has augmented worldwide generating a public concern as to whether frequent utilization of such devices is unsafe. This provoked EMF researchers to find suitable techniques of assessing radiation blueprint and exposure hazards if any. Most research groups focused on two techniques: experimental measurements and finite-difference time-domain (FDTD) computations. Computation of the specific absorption rate (SAR) generated by cellular phones inside two models of the human head is presented in this paper. Two models of mobile phones were considered working at 900 and 1800 MHz bands according to the Global System for Mobile Communication. Radiated energy distributions and averaged SAR values in 1 g and 10 g of tissue were computed inside the models of head using FDTD. Computations were compared with a realistic head model constructed with the MRI scans.

The distribution of the local SAR in the head was similar to that of the simplified head models. The maximum local SAR calculated was 53.43 W/kg and the maximum SAR(10 g) was 2.96 W/kg, both for 1 W output power from the antenna.

The results indicated the area of the maximum local SAR was situated in outer layer of skull, where muscle and skin were. The important parameters in absorbed energy in the head were the type of antenna, current distribution and the distance between head and antenna. The head models used for simulation proved as insignificant parameter in the calculations.

Total Body Water Measured by Electromagnetic Resonant Cavity Perturbation

D. A. Stone and M. P. Robinson
University of York, UK

B. Oldroyd and J. Truscott
University of Leeds, UK

A. Wright
MRC Human Nutritional Centre, UK

We recently demonstrated a novel method for determining human total body water (TBW) intended for patients suffering abnormal hydration using an electromagnetic resonant cavity perturbation (RCP) approach [1]. RCP relies on asking a volunteer to lie in a large cavity resonator and changes in its resonant frequency, f_{res}, are observed due to the consequent perturbation of the dielectric properties. Utilising the relationship that water content correlates to these dielectric properties at radio frequencies, it has been shown that the measured response of these parameters enables determination of body water [2]. Measurements are made using an automated network analyser operating in the transmission mode (measuring S_{21} or S_{12}). The sensitivity can be demonstrated by asking a volunteer to drink a small amount of liquid between measurements, and is better than one litre. Although the sensitivity varies from subject to subject, we have shown that by fitting a second-order polynomial to the variation of the gradient versus the mass-to-height ratio, we are able to develop a prediction equation applicable to a wide range of ages and body types. Moreover, we have validated these equations by conducting a cross-validation study using three reference methods; our predictions of TBW have been shown to compare favourably.

Method: A rectangular electromagnetic screened room is utilised as an R.F cavity, which resonates at 59 MHz when energy is coupled into the room. Two monopole probes are mounted on the ceiling of the room and couple to the required vertical E-field (TE_{101} mode). Twenty-nine healthy volunteers were recruited and asked to lie in the centre of a screened room at York University, UK, before and after drinking 1.25–2 litres of water and isotonic fluid. For the cross-validation study, a further eighteen volunteers were invited to participate in a series of experiments at the Centre for Bone and Body Composition at the Leeds General Infirmary, UK. TBW for each volunteer was measured using three existing techniques; isotope dilution, dual X-ray absorptiometry and bio-impedance analysis. These volunteers were also measured in the screened room at York University.

Results: A combination of the isotope dilution data and the corresponding measurements of Δf_{res} taken in the screened room at York have been used to cross-validate the RCP prediction equations. Although a Bland and Altman plot was used to correct a -2 litre drift in the data, agreement between the results is highly significant ($r = 0.95$, $p < 0.001$). Precision is also encouraging; the standard deviation of 37 paired measurements is 2.6 KHz, whilst resolution for the validation group ranges from 350–800 ml.

Conclusions: Predictions of TBW using electromagnetic RCP are favourable compared with reference methods; data is accurate and repeatable, and furthermore, resolution is better than 1 litre. This leads to confidence in the integrity of the proposed technique.

REFERENCES

1. Robinson, M. P., J. Clegg, and D. A. Stone, "A novel method of studying total body water using a resonant cavity: experiments & numerical simulation," *Medicine in Physics and Biology*, Vol. 48, 113–125, 2003.
2. Stone, D. A and M. P. Robinson, "2003 total body water measurements using resonant cavity perturbation techniques," *Medicine in Physics and Biology*, Vol. 49, 1773–1788, 2004.

Influence of Electric Field Variation on Intracelluar K+ Ion Variations and Its Implication on Electrochemical Treatment

H. B. Kim[1], **S. B. Sim**[2], **S. Y. Ahn**[1,3], **W. Chang**[4], **J.-H. Li**[4], **and Y.-L. Xin**[4]

[1]Solco Biomedical Institute, Korea
[2]Catholic University, Korea
[3]Coll. Nat. Sci. of Seoul National University, Korea
[4]China-Japan Hospitality Hospital, China

Electrochemical Treatment(EchT) has been applied clinically to patients with diseases of hemangioma, lung and liver tumors, and so on.

In EchT, high electric field induces damage in the cells, first on the membrane than any other cell organelles due to higher resistance of the phospholipid bilayers in the cell. The field-induced voltage drop mainly occurs on the membrane. Moreover, because the cell dimension is a few orders of magnitude larger than the thickness of the cell membrane, the strength of the induced electric field within the membrane is hundred to thousand times higher than the apparent strength of the applied field. Such electric field may result in damage of the membrane phospholipid bilayer and membrane proteins, and thus change the potential of voltage-gated ion channels, especially potassium channels. In this study, we present the study on the variation of intracellular potassium ions via the confocal microscopy, and by increasing the strength of applied electric field from 5 V and up between two electrodes 5 mm apart.

Qualitative Analysis of Human Semen Using Microwaves

A. Lonappan, A. V. Praveen Kumar, G. Bindu, V. Thomas, and K. T. Mathew
Cochin University of Science and Technology, India

Microwave engineering now a days plays a vital tool in diagnostic and therapeutic medicine. A quality evaluation of human semen at microwave frequencies using the measurements made at different intervals of time by cavity perturbation technique in the S-band of microwave spectrum is presented in this paper. Semen samples were also examined in the microscopic as well as macroscopic level in clinical laboratory. It is observed that conductivity of semen depends upon the motility of sperm and it increases as time elapses, which finds applications in forensic medicine.

Microwave Thermotherapy — Technical and Clinical Aspects

J. Vrba, L. Oppl, J. H. Trefna, T. Drizdal, and R. Zajicek
Czech Technical University, Czech Republic

J. Kvěch and J. Kubeš
Institute of Radiation Oncology, Czech Republic

We would like to describe our new technical results dealing with microwave thermotherapy in the cancer treatment. Our research interest is to develop applicators for deep local heating and for intracavitary cancer treatment as well. Basic evaluation of clinical results is presented.

Deep Local and Regional Applicators

Microwave thermotherapy (hyperthermia) is being used for cancer treatment since early 80's in many countries around the world. Since 1981 we were interested in the local external applicators working at 434 MHz and 2450 MHz. These applicators were used here in Prague for the treatment of more then 500 patients with superficial or subcutaneous tumours (up to the depth of approximately 4 cm). Now, following new trends in this field, we continue our research in two important directions:

–deep local and regional applicators,

–intracavitary applicators.

For the deep local thermotherapy treatment we develop above all waveguide type applicators based on the principle of evanescent mode waveguide, which is our specific solution and original contribution to the theory of microwave hyperthermia applicators. This technology enable us:

–to design applicators with as small aperture as necessary also for the optimum frequency range for deep local and/or for regional thermotherapy treatment (the frequency band between 27 and 70 MHz).

–using our technology we need not to fill the applicator by dielectric (necessary for deep penetration into the biological tissue - i.e., up to 10 centimetres under the body surface).

–two to four of such applicators can be also used for regional treatment.

Waveguide type applicators are often used in the local external hyperthermia treatment of cancer and other modifications of microwave thermotherapy as they offer very advantageous properties, above all:

–depth of penetration of the EM energy approaching the ideal case of plane wave,

–low irradiation of the energy in the vicinity of the hyperthermia apparatus,

–very good impedance matching, i.e., perfect energy transfer to the biological tissue.

We have studied waveguide applicators heating pattern for the aperture excitation at above and at under the cutoff frequency. It has helped us to get analytical approximations of the electromagnetic field distribution in the treated area of the biological tissue. The most important results for the effective heating depth d can be characterised as follows:

–at high frequencies (above approx. 1000 MHz) the depth of effective heating d is above all a function of frequency f (skin effect),

–bellow approx. 100 MHz d is the dominantly function of the diameter D of applicator aperture ($d = 0.386D$).

Clinical Results

In the case of cancer treatment the long term statistics of clinical results can be described as follows:

Complete Response of Tumor 53%

Partial Response of the Tumor ...31%

No Significant Response 16%

which corresponds to results obtained also by other groups in Europe.

*This research is supported by Grant Agency of the Czech Republic, project: "Microwave Imaging for Biomedical Applications" (102/05/0959) and by the research program MSM6840770012 "Transdisciplinary Research in the Area of Biomedical Engineering II" of the CTU in Prague, sponsored by the Ministry of Education, Youth and Sports of the Czech Republic.

Relative Absorption of Electromagnetic Energy in Adjacent Tissues

Y. V. Narayana[1], **G. N. Devi**[2], **and G. S. N. Raju**[3]

[1]ANITS Engineering College, India
[2]55-1-26, J.R. Nagar, Venkojipalem, India
[3]AU College of Engineering, India

The hypothermia is an effective form of therapy over the years. In this technique, the elevated temperatures are used for the treatment. It is possible to make use of the heat generated as a result of raise in temperature for effectively treating the tumors and cancerous tissues. This is possible by allowing electromagnetic energy to incident on the effective tissues for defined intervals.

For effective applications of such methods, the knowledge of the electromagnetic energy absorption in different biological tissues is required. In fact, the absorption depends on frequency and the characteristics of the tissues.

In the present work, some studies are made to evaluate the relative absorption of electromagnetic energy for different pairs of adjacent tissues. It is well known that, the permitivity, conductivity are also functions of frequency and they differ from tissue to tissue.

The different orientations of the electric field of the electromagnetic wave are considered for computing the above mentioned data. From the data obtained in the present work, the relative absorption of electromagnetic energy is found to vary for each pair of tissues. It is also found to be dependent on the polarizations of the electromagnetic wave that is incident on the tissues. The data of the present work is useful for the design of radiation sources.

Detection and Identification of Bio-medical Materials Possessing Chirality Using the Mueller Matrix

E. Bahar
University of Nebraska-Lincoln, USA

Since bio-medical materials possess some degree of chirality, the specific impact of chirality on the Mueller Matrix elements is analyzed. The canonical solutions for electromagnetic propagation in chiral media are the right and left circular polarized waves. Therefore, initially the effects of chirality on the circular like and cross polarized reflection coefficients are obtained.

It is shown that to within first order in the chirality parameters, only the circular, like polarized reflection coefficients (right to right, left to left) are modified. However since the Mueller Matrix elements are usually expressed in terms of linear like and cross polarized scattering coefficients, the corresponding expressions for the linear polarized reflection coefficients are determined. It is shown that only the linear, cross polarized reflection coefficient are modified. As a result (to within first order in the chirality parameter) only the eight quasi off diagonal elements of the Mueller Matrix are effected by the chiral property of the bio-medical materials. This reinforces the experimental observations from previous scattering experiments that the quasi off diagonal Mueller Matrix elements could provide a basis for detection and identification of bio-medical materials.

The analysis provides the explicit relationship between the quasi off diagonal elements and the degree of chirality of the bio-medical material. Thus it is possible to determine whether the chiral effects are sufficiently large to provide the accuracy necessary to conduct species-level discrimination in the present of spurious contributions due to surface roughness, etc. The explicit dependence of the Mueller Matrix elements (due to chirality) upon frequency and angles of incidence is also determined. Thus it is possible to optimize the impact of chirality on the Mueller Matrix in order to improve the feasibility of species level discrimination.

Co-design Planar Antenna for "UWB"

T.-P. Vuong, **Y. Duroc**, **and S. Tedjini**
Institute National Polytechnique de Grenoble, France

G. Fontgalland
LEMA de l'Universidade Federal de Campina Grande, Brazil

In this paper a wide band antenna to cover the UWB band is proposed. One of the main features of this antenna is the rejection frequency in the Wi-Fi band (around 5.2 GHz). The analysis results of the antennas parameters, S_{11}, VSWR and the radiated pattern, are presented. The communications, in special wireless, are in the top of attention of researchers. The need of a high velocity bit transmission rate and the great number of services that restrict the free operation band ask for new solutions to the communications systems. The UWB (Ultra Wide Band) technology seems to be very prominent for this application, since it operates in a large band with very low power transmission. The antenna in the UWB applications plays an important hole. This is the reason why it is in focus. In this study for a new antenna, before goes to step measurement, a commercial electromagnetic software CST microwave Studio version 5.0 is used to simulate antennas parameters. The antenna geometry was simulated using a dielectric with relative permittivity $\varepsilon_r = 4.4$. The geometry obtained here is optimized to reduce antenna dimensions. The co-design antenna (Fig. 1) presents the behavior of a classical large band antenna and the behavior of a rejection band structure. In our case, the rejection was selected to be around the Wi-Fi band (5.2 GHz). From Fig. 2, we can see that the new proposed antenna works with reflection coefficient bellow of -10 dB in the band of 3.1 to 4.75 GHz and from 5.6 to 13.2 GHz.

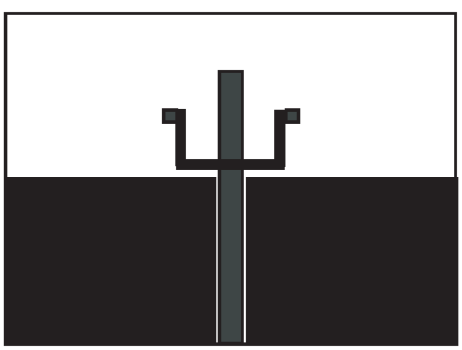

Figure 1: Co-design of studied patch antenna.

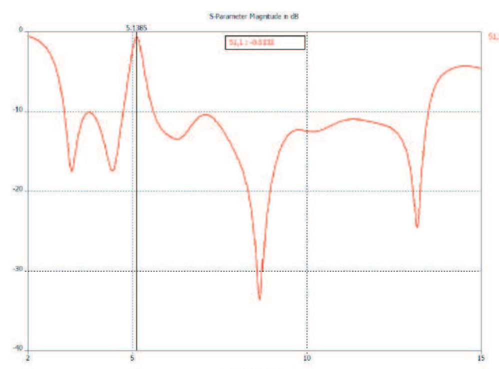

Figure 2: Parameter S_{11} of the UWB antenna.

Session 1A5
Microelectronic Packaging

A Hybrid Time-domain Method for Electromagnetic Problems in Microelectronic Packaging

T. Xiao, M. Chai, and Q. H. Liu
Duke University, USA

Computational electromagnetics for the design simulation of microelectronic packaging problems faces a great challenge because of the complex fine geometrical details in the chip level compounded with the large scale of the package. A time-domain approach such as the finite-difference time-domain method with a uniform grid requires a large number of discretization points to solve such mixed-scale problems. This issue is especially challenging for package-level problems.

In this work, we develop a hybrid time-domain technique that combines several methods for the efficient modeling of microelectronic packaging problems: (a) the enlarged cell technique (ECT) for the conformal FDTD method, (b) the alternating direction implicit conformal finite-difference time domain (ADI-CFDTD) method, and (c) the pseudospectral time-domain (PSTD) method. The ECT eliminates an important limitation, i.e., the reduction in the time step size, in the CFDTD method, and removes the staircasing error in the FDTD method for curved conductors. Similarly, the ADI-CFDTD method removes this staircasing error, and is especially useful for regions with electrically small features. The PSTD method, on the other hand, is efficient for large homogeneous regions. Therefore, combining all these methods in our hybrid time-domain technique is attractive as it makes use of their advantages while avoiding the disadvantages in each of these methods. The interface conditions between different regions of these methods are provided by the Riemann solver to ensure the stability. We will demonstrate the efficacy of this hybrid method by solving large-scale package level EMI/EMC problems.

Effects from the Thin Metallic Substrate Sandwiched in Planar Multilayer Microstrip Lines

L. Zhang and J. M. Song
Iowa State University, USA

Accompanied with the increasing integrated density and operation frequency in VLSI circuits and semiconductor chips, the special consideration on signal integrity and interconnect becomes more critical and essential for the circuit design process, which attracts years of attention and research effort. Although many new multilayer silicon technologies such as deep-submicron technology, hierarchical wiring topology or other types of multilevel interconnect structures are introduced to enable great efficiency of semiconductor integration, it also brings up with challenges as that, from the perspective of signal integrity, these complicated structures of interconnect network make circuits much vulnerable to the substrate coupling of noise, power supply noise, ground bounce, crosstalk, ringing, antenna effects etc. Therefore, the interconnect existing within such integrated circuit, especially the multilayer lossy structures, is one research-focused topic. As one feasible solution, very thin high-conductive substrates are added into multilayer structures as ground or current return to depress or shield away the harsh effects with improvement of transient performance. However, this multilayer lossy structure is highly dispersive at radio and microwave frequency due to the skin depth can be in the order of the microns, which may be much larger than the metal thickness of the profile.

Compared with the previous work of planar multilayer microstrip line, which starts with the usual hypothesis of the perfect ground plane or impedance boundary condition (IBC), and the work considering the effects of the signal strip with finite conductivity or thickness, this paper focuses on the effects of this thin but highly conductive substrate in the middle substrate. The immittance approach, as one of the spectral domain approaches (SDA), and complex root searching method are used for one simplified model of multilayer microstrip line proposed. The corresponding 2-dimensional Green's function of multilayer microstrip line is deduced and the Galerkin's method is applied to solve the related eigenvalue problem numerically. Thus the dispersion and propagation attenuation of multilayer open microstrip are simulated numerically finally. The field distribution and the transmission-line characteristics of interconnects, such as resistance, inductance, capacitance, and conductance (RLCG) per unit length for transmission-line parameter models, are also calculated.

From the numerical results, it is found that, in both lossy (metal-insulator-silicon structure such as Si-SiO_2) and lossless configurations (thin metal between lossless dielectric microstrip line), at lower frequency range, this thin metal substrate can excite slow waves reported previously. Such strong slow wave phenomenon can attributes to the coupling of electromagnetic wave between the substrates above and below this thin metal substrate, which can be shown in the field distribution. And accordingly, the frequency dependent transmission-line characteristics of interconnects, such as RLCG per unit length, have changed remarkably.

Modeling of Randomly Rough Surface Effects on Absorptions by Conductors at Microwave Frequencies

X. Gu and L. Tsang
University of Washington, USA

H. Braunisch
Intel Corporation, Components Research, USA

Methods for modeling the impact of randomly rough conductor surface on the power absorption by conductors of high-speed interconnects are presented. The roughness of the interface, especially in microelectronic packaging based on organic materials, is often used to facilitate the adherence of the copper structures to the dielectric layers. Since the speed of interconnects is rapidly increasing to the multi-GHz region, the propagation and radiation at the shorter wavelength can cause the roughness of the surface to have significant effects on signal integrity. Existing commercial software tools do not allow users to model the surface roughness of the substrates accurately. There only exist simple empirical models with limited or unknown validity.

We model the effects of a random rough surface on the absorption by a metallic surface at microwave frequencies using 2-D and 3-D small perturbation methods. The results depend on the characteristics of rough surfaces: the RMS height, correlation length and correlation function. We further show the similarity with and differences from Morgan's classical result. The power absorption by a metallic surface is quantified through the development of the solution of electromagnetic fields on the rough dielectric-metal interface. The analysis leads to the extraction of frequency-dependent power attenuation for each given metal roughness profile.

We demonstrate the method for random Gaussian and exponential rough surfaces. We also extract the rough surface profiles from real measured surface data on PCBs and packages. Results are illustrated for the frequencies of interest that extend up to 50 GHz. Statistical results are further obtained from Monte-Carlo simulations. The roughness profiles are up to 4 microns in RMS height with correlation lengths 0.3 to 3 times the RMS heights.

Krylov Model Order Reduction of Finite Element Models of Packaging Structures with Embedded Frequency-dependent Multiports

H. Wu and A. C. Cangellaris
University of Illinois at Urbana-Champaign, USA

In an effort to tackle the complexity of the electromagnetic analysis of the signal and power distribution networks (referred to, in the following, as SDN and PDN, respectively) in state-of-the-art integrated electronic systems, their decomposition into several parts and the development of hierarchical models for some of the resulting portions is often utilized. The term "hierarchical" is used here to define a model development process where the electromagnetic properties of different portions of the structure under modeling are described in terms of models of different degrees of complexity and, hence, accuracy, the choice of which is dictated by the specific attributes of the structure and the modeling objectives. A most representative example of a structure for which such hierarchical analysis can be applied is the electromagnetic quantification through modeling of noise generation and coupling in multi-layered substrate with multiple power and ground planes and multiple signal layers sandwiched between the planes. Assuming that multi-conductor transmission line (MTL) models can be used for the coupled interconnects in the nets, the complexity of the finite element mesh for the multi-layered substrate is simplified significantly. An integrated model for the combined SDN and PDN system, which is needed for the accurate quantification of switching noise generation and coupling is then obtained by embedding the MTL models in the finite element model, through the proper interfacing of the two models at the signal vias. Considering the fact that different types of models can be used for the coupled interconnects (ranging from lumped RLCG models for short sections, to more accurate transmission line theory-based models, or even comprehensive electromagnetic models extracted either through a full-wave solver), the hierarchical nature of the resulting model is evident.

This paper presents a methodology for the direct generation of reduced-order macromodels of the hybrid models obtained from the application of the aforementioned hierarchical modeling process. More specifically, we are concerned with finite element-based models that include frequency- dependent macromodels for portions of the SDN and/or PDN, described in terms of a multiport transfer function matrix with its elements cast in terms of rational functions of the complex frequency $s = j\omega$. The proposed methodology utilizes Krylov subspace-based methods for the direct generation of compact (low-order) macromodels of the overall structure. Like in the application of Krylov subspace methods for the direct model order reduction of finite element models of packaging structures including lumped elements [1], the resulting methodology allows for the construction of the overall multiport macromodel over a broad frequency interval, at essentially the cost of a single frequency point solution of the finite element system.

The proposed methodology will be presented and its validity and efficiency will be demonstrated through its application to typical SDN and PDN structures. The paper will conclude with a discussion of some issues pertinent to the passivity of the generated reduced-order macromodel.

REFERENCES

1. Wu, H. and A. C. Cangellaris, *IEEE Trans. Microwave Theory Tech.*, Vol. 52, 2305, 2004.

Enabling Accelerated Boundary-element Design Tools for Packaging and Interconnects

S. Chakraborty and V. Jandhyala
University of Washington, USA

For today's high-speed, high-density electrical packaging, while analysis tools based on boundary element methods are particularly efficient due to the development of fast algorithms that solve these matrix equations in near linear time, the need for design tools has not been met. For boundary element methods, such a tool would necessitate the ability of incremental solution, wherein small changes in designs would not require a complete simulation pass. The development of such a design tool is rendered more challenging because boundary element methods, solved by method of moments techniques, lead to full matrices. Changing the location or design of a component would alter entire rows and columns of these matrices, and therefore increase even the setup cost linearly.

A novel approach to localize the effects of incremental design of spatially separated components within the method of moments is presented. The technique proceeds by isolating the component under design in a closed mathematical surface. This surface bifurcates the overall simulation problem: the interior problem includes the interaction of the component and its surface, and the exterior problem is related to the surface and the remainder of the global problem. The overall gain of this method is that the setup cost is only related to the local problem of the component, the surface, and the interaction between these two. Moreover, for direct solvers, a Schur-complement based scheme can also accelerate subsequent solves, by presenting the remainder of the matrix in a factorized form as a numerical Green's function for the localized problem.

Noise Source Characterization on the PDN for EMI

M. Lai[1], **V. Ricchiuti**[2], **A. Orlandi**[3], **B. Archambeault**[4], **G. Antonini**[3]
D. J. Pommerenke[1], **and J. L. Drewniak**[1]

[1]University of Missouri Rolla, USA
[2]Siemens C.N.X., Italy
[3]University of L'Aquila, Italy
[4]IBM, USA

Noise resulting from IC activity is easily distributed throughout an electronic design as a consequence of a low-impedance power distribution network in a multi-layer printed circuit board. Both EMI and SI problems can result as a consequence. The passive portions of the PDN are being successfully modeled with full-wave formulations, as well as circuit extraction approaches, which provide design insight and methodologies for the PDN. However, in order to determine specific total capacitance needed, as well as quantify the voltage on the PDN, a suitable noise source model is needed for the ICs. This work details a frequency-domain approach for extracting current noise source models from swept-frequency methods.

The core and I/O activities in a common IC have different contributions to the global noise level in the full system. In order to better understand and quantify the specific weight of each, a methodology for estimating these two distinct but simultaneous noise sources is being developed. The estimation of the noise current by means of S-parameters and power spectra measurements is proposed here for a 208 pin, 155.52 MHz clock FPGA characterized by two voltage logic levels, 1.8 V for the core and 3.3 V for the I/O. From the measurement of the power spectra at the two logic levels in a position that can be considered coincident with the FPGA itself and from 2-port S-parameters measurement, it is possible to model the noise currents sources associated with the core and I/O respectively. The method is validated by estimating the same noise current sources also from a remote location from the FPGA itself, and it is done by adequately taking into account the effect of the transfer impedance between the ports and the FPGA. The effect of the SMA connectors used to perform the measurement is removed by means of a de-embedding procedure. The noise current sources are fully characterized in terms of magnitude and phase by means of a Hilbert transform procedure using the measured power spectra. In order to take in account only the effect of the activity of the FPGA, the power spectra are filtered from the effect of the external clock. The obtained noise current sources can also be characterized in terms of different load conditions by changing the number of I/O outputs simultaneously switching, allowing the estimation of an upper and lower limit for the sources.

Fast Method for Analysis of Electromagnetic Bandgap Structures Used in Power Delivery Networks

A. Tavallaee and R. Abhari
McGill University, Canada

Electromagnetic Bandgap (EBG) structures are increasingly used in high-speed digital and mixed-signal electronic circuits as the efficient means of power/ground noise suppression and port isolation. In order to provide these functions, the EBG structure is incorporated in the power delivery network (PDN) of an electronic circuit. In a conventional method of system implementation, this modified PDN is distributed within the layers of a printed circuit board, whereas in modern microelectronic chip design and system packaging, it can be embedded in the substrate. In all these scenarios, design engineers need to employ fast and accurate methods to account for the added frequency-selective features of the modified PDN in circuit simulations.

Floquet-Bloch theorem has been used for decades to obtain the dispersion equations of periodic structures and thereby to predict the passband/stopband frequencies. Recently, this analysis technique has been adapted to two-dimensional (2-D) transmission-linebased geometries and applied to a number of metamaterials and metallo-dielectric EBG structures to examine their overall modal characteristics. The method can rapidly predict the frequency band diagram. However, it does not include computing complex propagation constants.

In this work, a similar approach is adopted to characterize the PDNs containing EBG structures, as they can be efficiently modeled by 2-D transmission line circuits. Moreover, a general formulation is developed to account for the losses introduced in the network due to imperfect conductors, lossy dielectrics and lumped passive elements representing the series/parallel periodic loadings. The overall incurred loss in signal transmission through such networks is investigated by obtaining the frequency response, H(f). The method benefits from the fact that it is derived from analytical solutions, thus resulting in rapid production of band diagrams with accuracy comparable to fullwave simulators. Furthermore, it has the advantage that frequency is specified as an input parameter and the dispersion equation is solved for the complex propagation constant. Simulation results for a few EBG structures, such as the mushroom-type proposed by Sievenpiper, will be shown to demonstrate the efficiency and capability of the method.

Extraction of Chip Power Delivery Current and Activity Variations

I. Kantorovich, V. Drabkin, C. Houghton, and J. St. Laurent
Intel Corporation, USA

Power delivery (PD) noise, current and activity variation are major indicators of chip and package performance. A prerequisite to determine PD current and chip activity variation is knowledge of impedance of power delivery system (PDS) impedance on-die. New technology requirements push the impedance of on-chip PDS into the milliohm and sub-milliohm region, where difficulties in measurement setup, calibration and compensation of parasitics in VNA measurements [1] increase dramatically. On-die impedance measurement is a special challenge, because it must be performed under operating conditions, when only on-die voltage can be measured accurately, while on-die current measurement is problematic, except for DC current. Recently we proposed an approach [2], in which measurements are conducted for controlled periodic step-wise computer process containing long periods of unchanged chip activities. For this process, high and low DC currents far from transitions can be measured in independent experiments. It is more difficult to reconstruct transition current. We discuss two methods of the transition current reconstruction in the paper. They are based on chip representation as a variable current source and a variable resistor. The latter representation requires measurement of variable resistance in the step-wise process. Current is determined from Ohm's law applied in the time domain, while impedance of power delivery system is determined applying Ohm's law in the frequency domain. The current waveform in the variable resistor representation has ripples similar to that shown by the measured voltage. The difference in impedance determined from the two methods is most pronounced near power delivery resonances and is higher for chips with higher Q-factors. Using the proposed methodology we can also measure transfer impedance which can provide information on power delivery at any point of die, package or PCB. We discuss two different ways of generating a step-wise computer process: by running a pre-characterized set of computer instructions and toggling clock frequency. Usually the measured step response voltage is corrupted by random noise or regular noise introduced by computer code or measurement instrumentation. The paper considers methods of noise identification and exclusion. Once the impedance of the power delivery system is known, one can determine di/dt for any computer process. Details of current measurements are discussed in the paper. We can also measure effective variable conductance of the chip, which can be viewed as quantification of chip activity.

REFERENCES

1. Novak, I., "Measuring milliohms and picohenrys in power distribution networks," DesignCon 2000, Santa Clara, 2000.
2. Kantorovich, I., C. Houghton, S. Root, and J. St. Laurent, "Measurement of low impedance on chip power supply loop," *IEEE Transactions on Advanced Packaging*, Vol. 27, 10–14, 2004.

High Speed and Low Noise Packaging Design Methodologies for 40 Gbps SerDes Channel with PBGA Type Package

D. G. Kam[1], **J. Yu**[2], **H. Choi**[2], **K. Bae**[2], **J. Kim**[3], **D.-K. Jeong**[3], **C. Lee**[2], **and J. Kim**[1]

[1]Korea Advanced Institute of Science and Technology (KAIST), Korea
[2]Amkor Technology Korea, Korea
[3]Seoul National University, Korea

A 40 Gbps package solution that uses merely cheap wire-bonding plastic ball grid array (PBGA) technology is presented. Since such a high speed is well beyond the reach of conventional package designs, a number of techniques are devised to achieve the bandwidth for transmitting a 40 Gbps NRZ bit stream with a single differential channel: to shorten the bonding wires for critical signals even by cutting power/ground rings partially, to use low-loss RF substrate, to prohibit return current from transitioning layers by modifying conventional stack up and ball distribution, to use shielding structure for critical signals, and to remove some balls to reduce the length of 40 Gbps channel on a package. The effect of each technique is examined quantitatively by simulation and measurement, from which some of the techniques described above are adopted. The package type is determined as four-layer wire-bonding PBGA that also accommodates on-package decoupling capacitors for power integrity and a heat slug for thermal dissipation. Post-layout full wave simulation shows considerable possible improvement of channel performance. A prototype package is fabricated by Amkor Technology Korea. A test board is also fabricated by using low-loss PTFE material. The insertion loss of the overall channel is measured to be less than 3 dB up to 40 GHz. Finally the eye-diagram measured on the test board verifies the proposed techniques to be working solution of high speed and low noise package design for 40 Gbps SerDes channel with PBGA type package.

3D-SOP Millimeter-wave Functions for High Data Rate Wireless Systems Using LTCC and LCP Technologies

J.-H. Lee, D. Thompson, S. Pinel, J. Papapolymerou, and M. M. Tentzeris
Georgia Institute of Technology, USA

Millimeter-wave (mmW) electronics for commercial applications, such as short-range broadband wireless communications and automotive collision avoidance radars, require low-manufacturing cost, excellent performance, and high level of integration. The multilayer LTCC System-On-Package (SOP) approach is very well suited for these requirements because it offers a great potential for passives' integration and enables microwave devices to be fabricated with high reliability, while maintaining the low cost. The very mature multilayer fabrication capabilities of LTCC up to 100+ GHz enable the replacement of broadside coupling by vertical coupling and make LTCC a competitive solution to meet millimeter wave design requirements. As an alternative, Liquid Crystal Polymer (LCP) is an organic material that offers a unique low-cost all-in-one solution for high frequency designs due to its ability to act as both a high-performance flexible substrate ($\varepsilon_r = 2.9 - 3.1, \tan\delta = 0.002 - 0.004$) and a near-hermetic package for multilayer modules. These characteristics make LCP very appealing for many applications and it can be viewed as a prime technology for enabling system-on-package RF and mmW designs. In this paper, we present the development of various advanced 3-D LTCC and LCP system-on-package architectures enabling a complete passive solution for compact, low cost wireless front-end systems to be used in RF and mmW frequency ranges. The 3D embedded functions, which have been developed, include slotted patch resonator filters for achieving compactness and great compromise between size and power handling and directional filters to provide easy and compact solutions for different applications, such as mixing and multiplexing.

One important function that can be easily integrated in multilayer modules is filtering. In order to maintain their properties in compact topologies, band pass filters are commonly realized using slotted patch resonators in mmW frequencies due to their miniaturized size, the great compromise between size and power handling and their easy-to-design layout. In this paper, one single mode slotted patch filter (1-pole) with a transverse cut on each side has been designed and embedded in LTCC ($\varepsilon_r = 5.4, \tan\delta = 0.0015$) for 38–40 GHz applications such as vehicular communications. The patch filter ($1.02\,\mathrm{mm} \times 1.02\,\mathrm{mm}$) has been optimized in aim of 6.5% bandwidth, 39 GHz center frequency, and < 3 dB insertion loss. Such a structure has been developed from the commonly used half-wavelength square patch at 39 GHz by adding one transverse cut on each side leading to a significant reduction of the patch size and a good power handling. The desired coupling coefficients are obtained by inserting the feedlines and the single resonator into different metal layers. The stripline filters are excited through vias connecting the top metal with the next underlying metal, enabling the package to prevent radiation loss. The experimental results of the filter agree very well with simulation data, demonstrating a minimum insertion loss of 2.3 dB, the return loss > 18.2 dB over pass band, and bandwidth about 6.4%.

The LCP filter design we developed exploits the ripple near the cut off frequency of a Tchebyscheff low pass filter to create a band pass response. The initial low pass filter has been implemented by cascading two low impedance sections. Two slots have been added in each of these low impedance sections to enhance the ripple amplitude, and a ripple of 10 dB in amplitude has been measured. Then an open stub creating a transmission zero at 36 GHz has been added to enhance the rejection up to -35 dB in the lower band. Capacitive feeding can be used to remove the low frequency pass band if it is required resulting in a pass-band response centered at 60 GHz and a relative 3 dB bandwidth of 15% with minimum insertion losses as low as -1.5 dB. A ripple of $+/-0.15$ dB has been measured over a bandwidth of 6 GHz centered at 60 GHz.

Session 1A6a
Steerable Reflect-array Antennas

Principles of Synthesis of Steerable Reflect-array Antennas

O. G. Vendik
Electrotechnical University, Russia

Reflect-array antennas are being developed during many years. Recently the reflect-arrays were suggested as structures with an electronically steered radiation pattern. Such a steerable reflect-array antenna can be used as a low cost version of a phased array antenna for a wide commercial application. The synthesis of steerable reflect-array antennas, as a synthesis of any antenna, should be realized by solving two problems: external antenna problem and internal antenna problem. The first one includes the investigation of the antenna radiation pattern. The second one concerns a design of the structure providing the required amplitude-and-phase distribution along the antenna aperture. Any reflect-array antenna consists of primary radiator or illuminator and a reflecting surface. The primary radiator provides the amplitude distribution with a minimum spillover loss. Sophisticated design technique was used to diminish a constructive space occupied by the radiator [1]. The reflected surface is covered by a large number of small reflectors in form of microstrip vibrators or patches. The vibrators or patches are connected with tunable devices (varactor diodes [2] or ferroelectric tunable capacitors [3]), which serve for controlling the phase of wave reflected by each small reflector.

The external antenna problem is established on the theory of antenna array. The both distance between the small reflectors and geometry of the array are responsible for the directivity, the beam width, and the side lobe level of the antenna. The phase of reflected waves has to meet two principal demands: 1) Transformation of spherical wave front given by the primary radiator into the plane wave, 2) Availability of a phase gradient along the array, which corresponds to the beam deflection required. If the linear size of the array is much higher than the wavelength, the phase shift incursion along the array can be much higher than 360°. In this case the phase distribution is corrected by reset of the phase to $n \times 360°$, where $n = 1, 2, 3, \ldots$. Such a phase correction is well known as a characteristic feature of Fresnel mirror. In order to provide a low side lobe level, the phase correction in a discrete array should be installed with a reasonable correctness.

The internal antenna problem consists in finding the phase shift required for each small reflector. Remarkable feature of a tunable reflector made as a microstrip vibrator or a patch in combination with a tunable device is that the 360° phase shift of the reflected wave can be provided with only one tunable device (varactor or tunable capacitor). It should be reminded that for a realization of a transmission-type phase shifter one needs at least 8 tunable devices. The optimum phase shift of each tunable reflector must be found as a result of a correct simulation and realized by application of the biasing voltage generated by a specified controller.

Commonly, simulation of the phase shift required is performed with a numerical technique. The result of the phase shift simulation is used for designing the reflect-array antenna and must be included in the driving program of the biasing voltage controller. The both problems mentioned above can be sufficiently simplified, if the simulation by the numerical technique is replaced by using a correct analytical model. The development of the analytical models of all components of reflect-array antenna is an urgent problem, which solution is important for a realization of a cheap reflect-array antenna for mass production.

REFERENCES

1. Pilz, D. and W. Menzel, *Electron. Lett.*, Vol. 34, No. 9, 832–833, April 1998.
2. Sievenpiper, D. F., et al., *IEEE Trans. Antennas Prop.*, Vol. 51, 2713–2723, Oct. 2003.
3. Romanofsky, R., J. Bernhard, et al., *IEEE MTT-S*, 00TH 1D 1, 2000.

Tunable Impedance Surfaces for Low-cost Beam Steering and Conformal Antennas

D. Sievenpiper
HRL Laboratories LLC, USA

HRL Laboratories has developed a tunable impedance surface that enables a low-cost electronic beam steering. It consists of a lattice of resonant elements that are interconnected with their neighbors by varactor diodes. The surface provides a frequency dependent phase shift for reflected waves, which depends on the resonance frequency of the resonators. By varying the reverse bias voltage on the varactors, we can locally tune the resonance frequency, creating a programmable phase shifting surface. This is used to steer or focus microwave energy.

The tunable surface can also be used with a conformal feed. In this implementation, we excite surface currents with a small antenna located directly adjacent to the surface. We tune the surface to create a periodic grating structure, and the surface waves leak off at an angle determined by the period of the surface impedance. This implementation eliminates the protruding structure required by a space feed, resulting in a complete antenna structure that is electrically thin. We have shown that this concept can also be used on curved surfaces, so the antenna can be conformal to arbitrary shapes.

Unique Issues and Features of a Scanning Reflectarray Antenna Based on Ferroelectric Thin Film Phase Shifters

R. R. Romanofsky
NASA Glenn Research Center, USA

Evolving high data rate communications systems demand greater attention to subtle aspects of information theory and electromagnetic engineering. As the ratio of signaling bandwidth to carrier frequency decreases, less familiar phenomenon influence system performance. Some interesting effects are expected to appear if the trend toward wide-band scanning phased array antennas and bandwidth-efficient, high-speed modulators continues. Indeed there is a growing demand for efficient, low-cost phased array antennas. The reflectarray is an alternative to directly-radiating phased array antennas and promises higher efficiency at reduced cost. The ferroelectric reflectarray involves phase shifters based on coupled microstrip patterned on $Ba_xSr_{1-x}TiO_3$ films, that are laser ablated onto $LaAlO_3$ substrates. These devices outperform their semiconductor counterparts from X- through and K-band frequencies. There are special issues associated with the implementation of a scanning reflectarray antenna, especially one realized with thin film ferroelectric phase shifters. This paper will discuss these issues which include modulo 2π effects and phase shifter transient effects on bit error rate, scattering from the ground plane, relevance of phase shifter loss and presentation of a novel hybrid ferroelectric/semiconductor phase shifter, and the effect of mild radiation exposure on phase shifter performance.

Design of a Steerable Reflect-array Antenna with Semiconductor Tunable Varactor Diodes

M. D. Parnes
MPA, Haofe Street 8, Ashkelon, 78172, Israel

O. G. Vendik
Electrotechnical University, Russia

V. D. Korolkov
Resonance, Engels Street, Bldg. 27, St. Petersburg, 194156, Russia

The demonstrator of a steerable reflect-array antenna was designed as a system of dipoles loaded by varactor diodes. The GaAs varactors of type 3A606 produced in Russia were used. The microwave response of a dipole loaded by varactor has been simulated in framework of a circuit analytical model described in MATHCAD media. Change of the varactor capacitance in the range 0.2–0.9 pF was provided by the control voltage 0–20 V. The periodical structure of dipoles is conditionally depictured as a set of waveguides with electric and magnetic walls. Each dipole loaded by varactor is included in a separate waveguide. The waveguide section is presented as a transmission line short circuited at the back side and open to free space at the front side as an elementary radiator. The waveguide is shunted by the dipole, which is loaded by the varactor and can be presented as a resonant tank. Some elements of the model have been taken from [1–3].

The phase shift of the dipole-waveguide-radiator reflection coefficient was achieved in the range 0–320 degrees. The result of applying the circuit analytical model has been verified by the full-wave analysis based on HFSS software.

The correct simulation of the phase shifts, which are peculiar to each dipole, made possible to design a steerable reflect array. The array consists of 20 dipole structured as two parallel lines. The operational frequency is 10 GHz, the length of the dipole is 9.2 mm, the spacing between dipole is 18 mm. The doubleside metallized Duroid with $\varepsilon = 2.4$ and thickness of 1 mm was used as a substrate. Dipole structure was manufactured by a photolithographic process and the varactors were fixed with a surface mount technology.

Developed system of the control voltage provides obtaining the phase shift along the dipole structures, which is necessary for transformation of a spherical phase front of a prime radiator into the plane phase front with a required declination. Experimental investigation revealed the radiation pattern with the beam width 8 degrees scanned in the angle ± 45 degrees and the side lobe level of -15 dB.

Mentioned above analytical model of dipole loaded by a tunable varactor has been used as a basis for a simple procedure of designing the steerable reflect-array antenna, which can be offered as a cheap version of steerable antenna for a mass production.

REFERENCES

1. Chang, D. C. and M. C. Huang, *IEEE Trans. Antennas Propagat.*, Vol. 43, 829–834, Aug. 1995.
2. Boccia, L., F. Venneri, et al., *Proc. IEEE Antennas Propagat. Soc. Int. Symp.*, Vol. 3, 132–135, 2002.
3. Pilz, D. and W. Menzel, *Electron. Lett.*, Vol. 34, No. 9, 832–833, April 1998.

Modeling of Low-profile Reflect Array Antenna

M. S. Gashinova and O. G. Vendik
St.-Petersburg Electrotechnical University, Russia

Microstrip reflectarray antenna exploits operational principles of traditional parabolic reflector antenna and microstrip patch phased array [1–4]. Such a combination allow to ovecome two disadvantages of both standart antennas. It is common difficulty to overcome a 30 dB gain limit of phased array because of lossy feeding network. The conventional high-gain antennas are the parabolic reflectors. Being the very efficient radiators they are bulky and massive. A flat microstrip refletarray is being developed as a compact high-gain antenna [2]. Low loss is conditioned by the sizes of most radiators are far from ones of resonant half-wavelength radiators used usually with transmission lines for phase adjustment as well as by absence of feeding networks. Such an antenna is to be designed to convert spherical wave radiated by feed horn antenna into plane wave by phasing of reflected wave due to adjusting the patch sizes and arranging them by principle of Fresnel mirror.

The basic configuration of antenna includes a feed horn antenna and a printed reflectarray. Rectangular patches arranged in a planar aperture based on metal backed substrate will reradiate illuminated energy into space. Each radiator's phase is adjusted to make total reradiated field cophasal and concentrated in a specific direction. The phasing method is to use a variable size patches to form the front of reflected wave.

The phases of the reflected wave have to be attainable in the range from 0 to 360 degree. However the range of real array is, usually, less then 360 degree [4] and, besides, the gap of unreliazable phases exists for twisting reflectarray. The effect of parameters of whole structure such as the thickness of the substrate layer, distance between patches on non-linear dependence of phase angle on sizes has been evaluated.

A code has been developed for the design of multilayer printed reflectarrays, which adjusts the sizes of patches to achieve a progressive phase for dual linear polarisation according to both twisting and focusing requirements. The design code is based on the Spectral Domain Method of Moments (MoM) for lossy mutilayer periodic structures and normal incidence of a plane wave [1, 5]. Specific entire-domain basis functions are proposed to achieve a high convergence and accuracy of MoM.

The simulation model includes several assumptions such as periodicity and infinity of array, which allow us to analyse an elementary waveguide cell with two pairs of opposite electric and magnetic walls. In reality finite array of not quite independent patches should be analysed. The contribution of the edge patches of arrangement on gain and radiation pattern have been estimated.

To validate the design method, a series of reflectarray antennas operating at different frequencies with and without twisting effect have been designed and manufactured [6]. A good agreement was obtained between predicted and measured radiation patterns for both polarisations. The measured gains were not less then 32 dB.

The code developed can be broaden to be used as a basis of designing a steerable reflect array antenna with tuneable capacitors included in each patch reflector.

REFERENCES

1. Pilz, D. and W. Menzel, *Electron. Lett.*, Vol. 34, No. 9, 832–833, April 1998.
2. Menzel, W., D. Pilz, and M. AI-Tikrit, *IEEE Antenna's and Propagation Magazine*, Vol. 44, No. 3, 25–29, June 2002.
3. Encinar, J. A., *IEEE Trans. Antennas Propagat.*, Vol. 49, 1403–1410, October 2001.
4. Tsai, F.-C. E. and M. E. Bialkowski, *IEEE Trans. Antennas Propagat*, Vol. 51, No. 10, 2953–2962, October 2003.
5. Pilz, D. and W. Menzel, *Asia-Pacific Microwave Conference Proc.*, Hong Kong, 225–227, December 2–5, 1997.
6. Parnes, M. D., V. D. Korolkov, M. S. Gashinova, I. A. Kolmakov, Ya. A. Kolmakov, and O. G. Vendik, *Trudy VUZov Rossii*, *Radioelectronics*, in Russian, Vol. 1, 56–59, 2005.

Increasing Efficiency or Bandwidth of Electrically Small Transmit Antennas by Impedance Matching with Non-foster Circuits

S. E. Sussman-Fort[1,2], and R. M. Rudish[1]

[1]EDO Corporation, USA
[2]State University of NY, USA

We have previously reported [1] the experimental realization of a stable, low-power high-Q VHF *non-Fostercapacitor*. This is an active one-port circuit element whose reactance-versus-frequency slope is *negative*. Our experimental verification showed that a non-Foster capacitor can reduce mismatch loss of electrically-small *receive* antennas over substantial bandwidths, thereby improving their sensitivity.

When used to cancel the reactance of an electrically-small *transmit* antenna, a non-Foster capacitor will be subjected to excessively high voltage in order to radiate even a moderate amount of power. We have previously reported [2] that we can mitigate this high voltage first by resonating the antenna with a conventional passive reactance, and then by canceling the reactance of this combination with a non-Foster tuned circuit. We also demonstrated the performance of stable non-Foster tuned-circuits. Initially, our tuned circuits were configured for operation in a simple, but relatively inefficient, class-A bias mode. Subsequently, we configured a composite device as a parallel connection of an NPN and a PNP transistor to operate in a more efficient class-B mode. Both class-A and class-B circuits were constructed with low-power devices.

Now, we report on our efforts to increase the power output capability and efficiency of these circuits to render them practical for realistic transmit antenna applications. We show that non-Foster transmit matching of electrically-small antennas is much more broadband than any passive matching circuit. The power efficiency of the antenna and its class-B biased non-Foster matching circuits is also better than that achievable for a passively matched transmit antenna.

REFERENCES

1. *IASTED International Conference on Antennas, Radar and Wave Propagation*, Banff, Canada, Arp. 2005.
2. *Twenty-Ninth Annual Antenna Applications Symposium*, Allerton Park IL, Sept. 21–23.

Session 1A6b
Antennas and Resonators

Admittance Characteristics of Open Slot Radiators

G. S. N. Raju and Y. V. Narayana
AU College of Engineering, India

The inclined slots cut in the narrow wall of a rectangular waveguide are commonly used for producing horizontally polarized waves. Moreover, slots of resonant length as radiating elements in the array are preferred in most of the applications. But it is not possible to accommodate the slots of resonant length in the narrow wall of standard X-band rectangular waveguide. Hence they are protruded into the broad wall and are analyzed by several Researchers. It is found from the literature and also from our investigations that the protruded pieces of slots into the broad wall lead to undesired polarized components.

In the view of the above facts, a slot of resonant length is accommodated in the present work by increasing only the narrow wall without disturbing broad wall dimensions. The analysis involves plane wave spectrum approach and the admittance characteristics of the slot are obtained. The resultant double integrals are evaluated numerically after testing for convergence.

The arrays of such slots are extremely useful for the design of planar arrays and if the inclination of the slots from broad side is made small, the horizontal polarization is found to be almost maintained.

For the design of large arrays, slots of low conductances are found to be desirable. The low conductances are obtained by controlling width, length, inclination of the slots. The narrow wall dimensions has become an additional parameter for the design of the Arrays in the present work. The admittance data presented is extremely useful for the design of both linear and planar arrays.

Wide Axial Ratio Bandwidth Circular Polarized Dielectric Resonator Antenna

R. Chair[1], **S. L. S. Yang**[2], **A. A. Kishk**[1], **K. F. Lee**[1], **and K. M. Luk**[2]

[1]University of Mississippi, USA
[2]City University of Hong Kong, Hong Kong

Dielectric resonator antenna (DRA) has attracted considerable interest due to its inherent advantages of light weight, small size, low cost, ease of excitation and less conductor loss compared to patch antennas. DRAs can be made with different materials with a wide range of permittivities. DRAs have been designed to provide a variety of performance characteristics, such as wide band, dual band and circular polarization. In particular, with suitable design, the impedance bandwidth of a DRA element can attain 30% or more.

In [1], a 45° rotated rectangular DRA with permittivity 10.8 is excited by a narrow rectangular slot. It radiates circularly polarized waves with 6.6% axial ratio (AR) bandwidth. Wider AR bandwidth (in the range of 10% − 20%) designs reported in the literature usually involve either complex excitation or in the array form [2, 3].

In this paper, using a stair case structure, a simple aperture coupled DRA with wide AR bandwidth is presented. The 45° rotated stair DRA is excited by a microstrip line through a narrow rectangular slot. Using rectangular DR shapes with a length to width ratio of 1.9, two degenerate orthogonal modes are excited, generating circular polarization. The measured results show an impedance matching impedance bandwidth ($S_{11} <$ -10 dB) of 36.6% with $\varepsilon_r = 12$ and a measured AR bandwidth (AR < 3-dB) of 10.6%, with stable broadside radiation patterns. The AR bandwidth of the proposed simple DRA is comparable to more complicated designs reported in the literature. Simulation (from HFSS) and measured results show good agreement.

REFERENCES

1. Oliver, M. B., Y. M. M. Antar, R. K. Mongia, and A. Ittipiboon, "Circularly polarized rectangular dielectric resonator antenna," *Electron. Lett.*, Vol. 31, No. 6, 418–419, Mar. 1995.
2. Haneishi, M. and H. Takazawa, "Broadband circularly polarized planar array composed of a pair of dielectric resonator antennas," *Electron. Lett.*, Vol. 21, No. 10, 437–438, May 1985.
3. Pang, K. K., H. Y. Lo, K. W. Leung, K. M. Luk, and E. K. N. Yung, "Circularly polarized dielectric resonator antenna subarrays," *Microwave and Optical Tech. Lett.*, Vol. 27, No. 6, 377–379, Dec. 2000.

Radiation Q and Efficiency of Ideal Dipoles inside a Spherical Shield

J. C.-E. Sten and A. Hujanen
Technical Research Centre of Finland, Finland

In this paper an account is given of the effects of a semitransparent (low-loss) dielectric or magnetic shield on the operation of electrically small antennas. An obvious motivation for the work is that mobile terminal antennas are nowadays often embedded within the equipment. Two parameters form our principal interest here; 1: the quality factor, Q, computed from the ratio between the energy stored and the power accepted by the antenna, and 2: the radiation efficiency, η, or the proportion of radiated power to net power delivered to the antenna. Our approach is theoretical; we describe a method for calculating these quantities for azimuthally symmetric electric (TM) and magnetic (TE) multipoles surrounded by a semitransparent spherical shield of variable thickness, dielectric and magnetic constants with losses. Thus, a boundary value problem for the electromagnetic fields is formed. For its solution, a matrix method is applied to relate the transverse field components at each pair of adjacent interfaces. The method is hereupon applied to the case of a shield consisting of a single homogeneous layer. The Q and efficiency for such a structure are determined by computing numerically the energy stored in the near field of the multipole as well as the power radiated and dissipated in the shield. The performances of TM and TE multipole radiators are compared as a function of frequency. Hence, it is seen that even a very thin layer of a lossy dielectric considerably degrades the radiation efficiency at low frequencies, however, more severely for electric dipoles than for magnetic ones. Therefore, the electric dipole has a lower radiation Q than its magnetic counterpart. However, with a growing frequency the differences between the two types of dipoles are seen to balance. Low-frequency series expansions as well as high-frequency asymptotic expansions of the efficiency are given to elucidate the importance of the material parameters of the shield. We also derive some closed-form expressions for the dielectric permittivity of the shield and its outer and inner radii, which minimises the Q.

Theory of Size Reduction of DRA Resonators

A. A. Kishk
University of Mississippi, USA

Dielectric resonator antennas have found increase interest because of their many advantages as efficient radiators. In the X-band and higher the antenna size is very small, but at low frequencies the antennas size may not be suitable and one has to use very high dielectric constant in order to reduce the size, but the bandwidth decreases dramatically because of the high quality factor. Since for mobile personal communications, the radiation patterns are not very critical. Another method to reduce the antenna size with wide bandwidth is desired. Here we propose a method of size reduction that was used successfully with microstrip patches [1]. The method depends on the nature of the mode excited within the full size resonator. It is well known that a perfect electric conductor (PEC) passing by a plane with zero tangential electric fields or only orthogonal electric field can be replaced with a PEC plate without disturbing the original field distribution and thus reducing the space by half and keeping the same resonant frequency of the antenna. This is corresponding to reducing the antenna size to half. This is actually what is used with the DRA antennas above a PEC. If the mode has a plane of symmetry with respect to the geometry and excitation and parallel to the E-plane of the antenna, the electric fields on this plane will be laying along the plane and the magnetic fields will be orthogonal to this plane. This plane could be replaced by a perfect magnetic conductor (PMC) without disturbing the field distribution and thus keeping the same resonant frequency and reducing the antenna size to half. However, there is no natural PMC to be used. Therefore, the reduction of the size using this plane needs to be considered carefully. Although, artificial magnetic conductors can be realized, this will not serve the purpose of size reduction because these materials to be useful its size might be larger than the size of the antenna itself.

The fields inside the dielectric resonator of the high dielectric materials see the dielectric surface as nearly magnetic conductor. Such an assumption is by itself is a useful argument that makes us believed that this plane exits naturally if the dielectric materials of one half are removed. Of course, such an assumption becomes better as the dielectric constant increases.

Demonstration of this argument will be presented by several DRA designs that keep the bandwidth of the full size DRA even after the size reduction that could be more than 75% of the full size DRA.

REFERENCES

1. Kishk, A. A., et. al., *IEEE Transactions on Antennas and Propagation*, Vol. 52, No. 1, January 2004.

Waveform Prediction of a Pulse Communication Link between Antennas Modeled by a Combination of Thin-wires

F. Sagnard[1,2] **and G. El Zein**[1]

[1]IETR, UMR 6164, INSA, France
[2]Université de Marne-La-Vallée, France

In recent years, there has been a growing interest in the transient radiation of electromagnetic fields to meet the needs for the development of wireless systems for various applications. In this context, the emerging Ultra-Wide Band (UWB) radio technology appears as an attractive solution for the development of high-data rate, very low-power and short range wireless systems for numerous applications in communications, networking, radar, imaging, and positioning systems. Such a technology relies on the transmission of a series of modulated short pulses (less than 1 ns) which are characterized by a broadband spectrum (greater than 500 MHz with a fractional bandwidth of more than 20%). Because of the very wide frequency band of the excitation signal, novel studies concerning the modeling and the characterization of the propagation channel and of the antennas have to be achieved. In particular, the antennas play an important role as a part of the pulse-shaping process in the spatio-temporal domain, and the propagation channel is responsible for the generation of a large number of multipath issued from the different interactions of the radio signal with the surrounding objects.

To highlight the influence of link parameters such as the shape and duration of the pulse excitation, the geometric characteristics of the transmitting and receiving antennas and of the link, and the dielectric properties of constitutive materials of the propagation channel, we have developed a modeling tool, under a graphical interface, based on analytical relations to represent a transient communication link between conductive antennas in the presence of a multipath channel. The analytical modeling proposed appears as an extension of previous developments as it addresses the transient analysis of several 2D or 3D antenna geometries (V-dipole, bow-tie, butterfly, TEM horn...) using a combination of linear thin-wire dipoles, and it allows to consider a variety of pulse shapes, and particularly the successive derivatives of the Gaussian pulse. We have considered two types of dipoles: at first, infinite conductive dipole elements in the presence of a load at the feed point to take into account impedance mismatches, and secondly resistive loaded dipoles based on the Wu and King formulation to prevent from reflection at the top ends in order to satisfy broadband characteristics. For the modeling of the propagation channel, we consider a multi-layer material in the free-space between both antennas, or a statistical multi-path channel based on the Turin approach. Different types of plots allow to analyze the waveforms and the energy of the signal at each stage of its propagation from the transmitter to the receiver. Moreover, we have developped several algorithms to characterize quantitatively the distortion phenomenon caused in the process of radiation and transmission through building materials. The problem of optimization of the radiating characteristics of the transmitting antennas in a specific direction has been addressed: parameters such as the pulse duration and the antenna size appear particularly critical.

The approach presented in this paper reveals to be a convenient tool for the study and the analysis of transient waveforms involved in an UWB link. It allows to better understand results issued from numerical simulations and experimental measurements to further design UWB systems.

Session 1A7
Microwave and Optical Devices, Propagation

Fabrication of Multimode Interference Devices Based on Ge-doped Silica-on-silicon Waveguides by HC-PECVD and RIE

G.-D. Peng and Z. Jin

The University of New South Wales, Australia

Multimode interference devices based on Ge-doped silica-on-silicon waveguides are fabricated by HC-PECVD and RIE. The thin film deposition and etching process are optimized to achieve good optical devices. Silica layer particle control is studied for the thin film deposition. It is found that the preheating time is related to silica layer particle distribution. Using photoresist as masks for RIE simplifies the process. The waveguide shape profile is optimized by different RIE parameters. The optimal process balances the waveguide shape, surface smoothness, and etching rate. Good performance multimode interference devices have been realized.

On the Spatial Characterstics of Cellular Mobile Channel in Low Antenna-height Environments

N. M. Khan, **M. T. Simsim**, **R. Ramer**, **and P. B. Rapajic**
The University of New South Wales, Australia

In order to exploit the spatial dimens ion efficiently, reliable channel models are required which can lead to the design of effective signal processing schemes. Physical channel models are the continuing efforts in this regard. Several approaches have been suggested for the distribution of scatterers. The two most common distributions are the uniform [1] and Gaussian [2,3]. The latter has been identified as more practical in the literature. Gaussian Scatterer Density Model (GSDM) [2] proposes Gaussian Distributed Scatterers clustered around mobile station (MS). Since, in low antenna-height indoor environments, scatterers also exist in the vicinity of base station(BS). So a more generalized scattering model is needed for such environments.

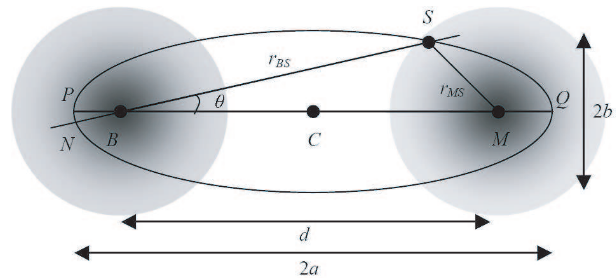

Figure 1: Physical channel model.

In this paper, we use the generalized Eccentro-Scattering physical channel model proposed in [3] to derive the probability density function (pdf) of the Angle of Arrival (AoA) of the multipath signals at BS from Gaussian distributed scattering regions around MS and BS for indoor environments.

We assume Gaussian distributed scatterers to be confined in an elliptical shaped scattering disc (see Fig. 1) whose eccentricity can be altered according to the maximum delay and the distance between MS and BS. A Gaussian model of the spatial pdf of scatterers around MS and BS can be written as,

$$p_{R_{BS},\Theta}(r_{BS},\,\theta) = \frac{\parallel r_{BS} \parallel}{2\pi\sigma_{MS}^2} \exp\left\{-\frac{\parallel r_{BS} - r_{BM} \parallel^2}{2\sigma_{MS}^2}\right\} \tag{1}$$

$$p_{R_{BS},\Theta}(r_{BS},\,\theta) = \frac{\parallel r_{BS} \parallel}{2\pi\sigma_{BS}^2} \exp\left\{-\frac{\parallel r_{BS} \parallel^2}{2\sigma_{BS}^2}\right\} \tag{2}$$

where σ_{MS} and σ_{BS} are the standard deviations of the distributions of scatterers around MS and BS, and θ is the AoA of the multipaths at BS from the scatterer S. All other parameters are explained in Fig. 1. From (1), (2) and Fig. 1, the final closed-form expression for the pdf of AoA can be written as

$$\begin{aligned} p_\Theta(\theta) = \frac{\Omega}{2\pi}\left[1 + \exp\left(\frac{-d^2}{2\sigma_{MS}^2}\right) - \exp\left(\frac{-(4a^2 - 4ad\cos\theta + d^2)^2}{8\sigma_{MS}^2(2a - d\cos\theta)^2}\right) - \exp\left(\frac{-(4a^2 - d^2)^2}{8\sigma_{BS}^2(2a - d\cos\theta)^2}\right)\right] \\ + \frac{\Omega d\cos\theta}{2\sqrt{2\pi}\sigma_{MS}} \exp\left(\frac{-d^2\sin^2\theta}{2\sigma_{MS}^2}\right)\left\{\mathrm{erf}\left(\frac{d\cos\theta}{\sqrt{2}\sigma_{MS}}\right) + \mathrm{erf}\left(\frac{4a^2 - 4ad\cos\theta + d^2\cos 2\theta}{2\sqrt{2}\sigma_{MS}(2a - d\cos\theta)}\right)\right\} \end{aligned} \tag{3}$$

where Ω is the normalizing constant. Eq. (3) is helpful in finding correlation statistics of the channel.

REFERENCES

1. Liberti, J. C. and T. S. Rappaport, "A geometrically based model for line-of-sight multipath radio channels," in *Proc. 46th IEEE Veh. Technol. Conf.*, 844–848, April-May 1996.
2. Janaswamy, R., "Angle and time of arrival statistics for the Gaussian scatter density model," *IEEE Trans. Wireless Commun.*, Vol. 1, No. 3, 488–497, July 2002.
3. Khan, N. M., M. T. Simsim, and P. B. Rapajic, "A generalized spatial model for all cellular environments," in *Proc. IEEE SympoTIC'04*, Slovak Republic, 33–38, October 2004.

Investigating the Standard Deviation of the Distribution of Scatterers in Cellular Environments

M. T. Simsim, N. M. Khan, R. Ramer, and P. B. Rapajic
University of New South Wales, Australia

Physical and statistical properties of the scatterers existing between transmitter and receiver have to be studied in order to design reliable channel models. Wireless signal propagation changes in different environments according to scatterers' density. It is reasonable to assume that the majority of scatterers are located closer to mobile station (MS) and the density of scattering points decreases as the distance from MS increases [1, 2]. Gaussian, Laplacian, exponential, and hyperbolic distributed scatterers are examples of scattering models employing this principle of tapering-off of scatterers. For instance, Gaussian Scatter Density Model (GSDM) [1, 3] assumes Gaussian (normal) distribution for the scattering points around MS. Thus, the value of standard deviation of the distribution of scatterers, σ, plays an important role in determining the width of the scattering region and, hence, in applying the model to a specific environment.

If the density of scattering points decays sharply as the distance from MS increases, then the probability density function (pdf) of Angle of Arrival (AoA) of the multipath signal at BS will have rapidly decaying tails. Thus, the model accounts only for scatterers in the close vicinity to MS, which will have the major effect on the received signal at BS. On the other hand, if the density of scattering points decays slowly as the distance from MS increases, then the pdf of AoA of the multipath signal at BS will have heavy tails. In this case, the model accounts also for farther scatterers from MS, which have considerable effect on the received signal at BS.

A general rule of thumb was proposed in [1] for the first order approximation of the standard deviation based on experimental data. It was assumed that the stronger multipath echoes that arrive at BS shortly after Line of Sight (LoS) signal are due to scattering points close to MS while multipath echoes with larger delay values are due to scattering points farther from MS. The study in [3] found that the pdf of AoA depends on a single parameter which represents the ratio of the distance between BS and MS, D, and the standard deviation of the distribution of Gaussian distributed scatterers around MS, σ. Recently, a model for NLoS propagation in street-guided environment has been reported in [2], where it was found that $\sigma = 1/6\times$ street width is the best value for the standard deviation to fit field measurements of Power Azimuthal Spectrum (PAS). In [4], the value of standard deviation was related to cross correlation of the fading between antenna elements spaced by distance d, $\rho(d)$, and the wavelength of the carrier frequency, λ, as, $\sigma = \sqrt{\frac{\lambda^2 ln(\rho(d))}{-4\pi d^2}}$. Here, several techniques are studied for predicting accurate values for the standard deviation of the distribution of scatterers. We examine several measurement campaigns for different cellular environments in order to deduce information about the actual distribution of scatterers in these environments.

REFERENCES

1. Lotter, M. P. and P. van Rooyen, "Modeling spatial aspects of cellular CDMA/SDMA systems," *IEEE Commun Lett*, Vol. 3, No. 5, 128–131, 1999.
2. Chen, Y. and K. Dubey, "Parabolic distribution of scatterers for street-dominated mobile environments," *IEEE Trans. Veh. Technol.*, Vol. 54, No. 1, 1–8, January 2005.
3. Janaswamy, R., "Angle and time of arrival statistics for the Gaussian scatter density model," *IEEE Trans. Wireless Commun.*, Vol. 1, No. 3, 488–497, July 2002.
4. Ward, C., M. Smith, A. Jeffries, D. Adams, and J. Hudson, "Characterising the radio propagation channel for smart antenna systems," *Electronics & Communication Engineering Journal*, Vol. 8, No. 4, 191–200, August 1996.

Mathematical Modeling of Nonlinear Waves and Oscillations in Gyromagnetic Structures by Bifurcation Theory Methods

G. S. Makeeva[1], O. A. Golovanov[2], and M. Pardavi-Horvath[3]

[1]Penza State University, Russia
[2]Penza Military Institute of Artillery, Russia
[3]The George Washington University, USA

The vector field bifurcation approach and its numerical implementation for the rigorous mathematical simulation of nonlinear phenomena in microwave, mm-wave ferrite or composite semiconductor/ferrite devices were developed. The bifurcation points of nonlinear Maxwell's operator for the three-dimensional boundary problems, stated and solved rigorously (i.e., considering the full Maxwell's equations with the nonlinear equations of motion for magnetization in ferrites and transport carriers in semiconductors) were analyzed using numerical methods.

The electromagnetic field is represented as decomposed into a series of weakly nonlinear wave fields. A linearized Maxwell's operator matrix was determined. The propagation constants of weakly nonlinear waves or the eigenfrequencies of weakly nonlinear oscillations were found using bifurcation points. The Cauchy problem for the system of ordinary differential equations was formulated. The electrodynamical analysis of strong nonlinear waves excited by the fields of weakly nonlinear waves was performed.

Using the bifurcation dynamics of Maxwell's equations the nonlinear wave interactions in the strongly nonlinear planar ferrite or semiconductor/ferrite inserts loaded into the strip-slot waveguiding or resonator structures were analyzed (from the harmonic frequency terms at the 'soft' non-linear stage to the region of 'hard' non-linearity). The nonlinear propagating of electromagnetic waves, magnetostatic or spin waves in the strip-slot ferrite film waveguiding structures were modeled. The nonlinear wave phenomena, including frequency multiplication, parametric excitation of waves, spin-wave instability process, were investigated taking into account constrained geometries.

This approach has a high likelihood of success in investigating nonlinear phenomena in new microwave/millimeter-wave ferrite devices for frequency multiplexing/filtering, limiters, noise rejectors, signal-noise ratio enhancers, and pulse compressing devices.

Miniaturized Cross-slotted Dual-mode Filter for Mobile and Satellite Communications

S. Shen[1], **G. M. Banciu**[2], **and R. Ramer**[1]

[1]University of New South Wales, Australia
[2]National Institute of Materials Physics, Romania

A new, compact, narrow band, low loss, dual-mode cross-slotted filter is proposed and developed. The compactness and improved filter characteristics of this square filter makes it suitable for mobile and satellite communications. The dual-mode filter consists of simple star-type geometry slot lines crossing a square patch. Two additional fringe slots are also introduced on each side of the square patch. The external coupling is capacitive and was achieved through external lines, which are placed at a right angle. The conventional square patch dual-mode filters offer simple design and good power handling capability, however they require larger size than the dual-mode loop filters for the same frequency band. The novelty of this proposed structure consists in significant size-reduction and the ability to control the central frequency and the bandwidth; our proposed dual-mode filter is 37% smaller than a conventional patch dual-mode filter for the same frequency band. The filter was simulated using Sonnet Software, both lossless and lossy cases being considered, and was fabricated on a Rogers?substrate with a dielectric constant of 10.8. The star-type geometry dual-mode filter presents two transmission zeros on each side of the pass-band, and improved filter characteristics over the conventional ones. The perturbation was introduced using a difference between the lengths of the diagonal slots. It is found that the resonant frequency of the filter with 1% fractional bandwidth could be shifted down to below 900 MHz, for the use in the mobile and satellite communications.

REFERENCES

1. Zhu, L., P. M. Wecowski, and K. Wu, "New planar dual-mode filter using cross-slotted patch resonator for simultaneous size and loss reduction," *IEEE Trans. on MTT*, Vol. 47, 650, 1999.
2. Casinese, A., A. Andreone, M. Barra, C. Granata, P. Orgiani, F. Palomba, G. Panariello, G. Pica, and F. Schettino, "Dual mode superdonducting planar filters based on slotted square resonators," *IEEE Trans. on Applied Superconductivity*, Vol. 11, No. 1, 2001.
3. Hsieh, L. H. and K. Chang, "Dual-mode quasi-elliptic-function bandpass filters using ring resonators with enhanced-coupling tuning stubs," *IEEE Trans. on MTT*, Vol. 50, 1340, 2004.
4. Curtis, J. A. and S. J. Fiedziuszko, "Miniature dual mode mnicrostrip filters," *IEEE Microwave Symposium Digest*, 1991.
5. Banciu, M. G., G. L. jewski, A. Ioachim, L. Nedelcu, N. Militaru, A. Shen, and R. Ramer, "New planar compact dual mode filters for mobile communications," *CAS Proceedings to International Semiconductor Conf.*, 2004.
6. Guglielmi, M. and G. Gatti, "Experimental investigation of dual-mode microstrip ring resonators," *The 20th European Microwave Conference Digests, Budapest-Hungary*, 901–906, 1990.

Near-field Scatterers and Mutual Coupling in Multi-antenna Systems

S. Krusevac and R. A. Kennedy
Australian National University and National ICT, Australian

P. B. Rapajic
University of Greenwich, UK

Communication systems use antenna arrays to increase the communication capacity by exploiting the spatial properties of the multi-path channel. Providing high capacity requires independence of the channel matrix coefficients, a condition generally achieved with wide antenna element spacing. For many subscriber units, such separations are unrealistic, and the resulting antenna mutual coupling can impact the communication system performance. The prior studies have presented important findings concerning the effect of mutual coupling on spatial correlation in closely spaced antenna arrays. But, they often disagree in terms of whether mutual coupling is advantageous or disadvantageous. In the multi-antenna systems, the mutual coupling is due to antenna element separation, geometry of array and antenna elements, frequency, substrate thickness and constant and near field scatterers-NFS. All these parameters are known for a given array, except near field scatterers. In order to get better insight into the mutual coupling effects in the multi-antenna system, we include the near-field scatterers in theoretical investigation. The occurrence of NFS can not be controlled, they appear randomly. Thus we investigate impact of NFS on the spatial correlation for different distribution functions of near-field scatterers. In addition, the modal analysis approach is presented in order to obtain closed-form expressions for the spatial correlation function for narrow-band signals for a wide variety of scattering distribution functions. We investigate spatial correlation in the multi-antenna system for different NFS distribution in the close vicinity of receive antenna arrays. Relatively close NFS can cause array blindness, but at the same time they can perturb antenna pattern to result in lower spatial correlation level. The scatterers relatively far from antenna array can behave like multi-path scattering object and increase the environment richness. Our simulation results confirm that near field scatterers increase the mutual coupling between the antenna elements. Hence, they act as decreasing factor on spatial correlation for rich far-field scatterers environments. While, for poor scattering environment they act as increasing factor on spatial correlations.

Current-induced Bistability and Dynamic Range of Microwave Generation in Magnetic Nano-structures

A. N. Slavin and V. S. Tiberkevich
Oakland University, USA

We give a simple picture of magnetization dynamics in magnetic multi-layers under the action of spin-polarized current. Based on the idea that the main effect of the current I is the creation of negative damping $GI_{\_} = {}_{\_} - sI$, we explained both the current-induced bistability and microwave generation in a finite range of currents. In the absence of current the magnetization vector in a "free" layer of a magnetic layered structure has at least two equilibrium orientations: one stable ("bottom" state), corresponding to the minimum of the magnetic energy and one unstable ("top" state), corresponding to the maximum of the energy. Since the effective damping created by spin-polarized current is negative, at a certain critical current $I_{c\_} = {}_{\_}G/s$ the total effective damping $Gtot_{\_} = {}_{\_}G_{\_} + {}_{\_}GI$, where G is the natural positive damping, could become negative not only for the "bottom" state of magnetization orientation, but also for the "top" state. When that happens the "bottom" (initially stable) state loses itsstability, while the "top" (initially unstable) state, in contrast, becomes stable. The change of stability for each state happens, in general, at the different values of current. The "bottom" state becomes unstable at $I_{c\_} = {}_{\_}Imin$, thus allowing precession of magnetization with microwave frequency, while the "top" state becomes stable at $I_{c\_} = {}_{\_}Imax$, thus stopping any magnetization precession. If $I_{min\_} < {}_{\_}I_{max}$ there exists a finite range $I_{min\_} < {}_{\_}I_{\_} < {}_{\_}I_{max}$ of currents in which the system demonstrates microwave oscillations of magnetization. In the opposite case $Imin_{\_} > {}_{\_}Imax$ the precessional dynamics could not exist at all, and with the current variation in the interval $I_{min\_} < {}_{\_}I_{\_} < {}_{\_}I_{max}$ the system becomes bistable, i. e., it switches between two stable states corresponding to the minimum and maximum of the magnetic energy. We derived simple analytical expressions for both threshold currents $Imin$ and $Imax$ and compared our results with available experimental data.

Nonlinear Self-phase-locking in an Array of Current-driven Magnetic Nano-contacts

A. N. Slavin and V. S. Tiberkevich
Oakland University, USA

Recently it was shown that spin-polarized current passing through a thin magnetic layer can excite microwave magnetization precession in this layer. It was also demonstrated experimentally that the frequency of microwave generation in a current-driven magnetic nano-contact can be phase-locked to the frequency of a small external sinusoidalcurrent added to the constant bias current. In this work we theoretically investigate the possibility of self-phase-locking of an array of magnetic nano-contacts by self-induced dipolar magnetic field. First, we consider an isolated nano-contact driven by a constant bias current and determine the conditions of its phase-locking to the frequency of a small external microwave signal, which can be created either by microwave magnetic field or by microwave modulation of the bias current. We show that, in contrast with the case of a usual microwave oscillator, the mechanism of phase-locking in a nano-contact is strongly nonlinear: due to the strong dependence of the precession frequency on the precession amplitude even small changes in the oscillation amplitude can result in matching of the generated frequency to the frequency of the external signal. This nonlinear frequency matching mechanism leads to a significant increase in the frequency bandwidth of phase-locking D (up to $\sim 300\,\text{MHz}$). Bandwidth D has a non-trivial dependence on the magnetization angle, showing a well-pronounced minimum for the magnetization angle at which the coefficient of the nonlinear frequency shift is zero. We used the results obtained for an isolated nano-contact to determine the conditions for self-phase-locking of an array of nano-contacts, and found that the self-phase-locking in an array is practically possible when the distance between individual contacts is $\sim$ 10 times larger than the nano-contact radius even if the inhomogeneous distribution of the frequencies generated by individual nano-contacts is as large as 10%.

Adaptive Turbo Multiuser Decision Feedback Detection for DS-CDMA on Unknown Multi-path Channels

V. D. Trajkovic[1], **P. B. Rapajic**[2], **and R. A. Kennedy**[1]

[1]National ICT Australia, Australia
[2]University of Greenwich, UK

In this paper we propose an adaptive turbo multiuser detection (MUD) on unknown multi-path channels. The analyzed multi-user scheme is Successive Decision Feedback Detector (S-DFD), which means that users are detected on one-by-one basis and they are cancelled successively by use of decision feedback. An adaptive LMS algorithm is used to estimate MUD coefficients. Binary Phase Shift Keying (BPSK) in combination with Direct Sequence Code Division Multiple Access (DS-CDMA) is analyzed, which means that information is first coded using convolutional encoder, and then modulated and spread using randomly chosen spreading sequences for each user.

Our analysis shows that the adaptive realization employing the LMS adaptive algorithm, outperforms (in terms of Bit Error rate (BER)) the conventional detection that combines a standard Minimum Mean Square Error (MMSE) solution and decoding concatenated in a turbo scheme. A standard solution means that the MUD coefficients are obtained applying the MMSE criterion and assuming perfect knowledge about the received spreading sequences after multi-path propagation and perfect decision feedback.

The reason behind this is that during the Turbo detection process the assumption about perfect decision feedback becomes highly unreliable that must be taken into account while determining S-DFD coefficients. Decision feedback error propagation becomes particularly severe at low Signal-to Noise Ratio (SNR) or highly loaded, heavy interference systems when number of users exceeds the spreading gain. On the other hand, the adaptive LMS detection does not assume the perfect decision feedback while adjusting the filter coefficients and it always set the coefficients providing that the output error is orthogonal on the received sequence. This means that it automatically takes into account the feedback error propagation providing an unbiased MMSE solution that does not assume perfect feedback and, consequently, deliver better BER results. In addition to better BER performance, another advantage of the adaptive detection is that it does not require knowledge about system parameters, such as spreading sequences, multi-path channels etc, but the MUD parameters are estimated during the training process.

In our work, we analyze various multi-user scenarios. This includes unsaturated systems, where number of users K is smaller than the spreading gain N ($\rho = K/N < 1$) and overloaded case, i.e., the number of users K is larger than the spreading gain ($\rho > 1$). We also analyze single- and multi-cell cases. In single cell situation, all users are assumed to be within one cell and during the multiuser detection process multi-user turbo detector detects all signals, one-by-one, in a turbo-like process. However, in a multi-cell scenario, there is a certain number of users located outside the cell of interest that cannot be detected and, consequently, they represent unknown interferers whose influence may significantly degrade the performance of the analyzed turbo MUD. Our simulation results show that the adaptive turbo MUD always exhibits better or at least identical BER performance relative to the conventional MMSE turbo MUD. We show that SNR gain grows with the increasing number of users within the system and the most remarkable improvement is obtained for the overloaded case. For this particular scenario, the conventional MMSE turbo MUD cannot perform detection properly, while the adaptive detector still achieves relatively good BER performance.

A Novel Approach for Tunable Filters

R. R. Mansour and R. Zhang
University of Waterloo, Canada

The paper presents a new concept to implement tunable lowpass filters by employing slot resonators etched in the ground plane. The tunability is achieved with the use of switches to change the effective length of the slots on the ground. A tuning range of more than 60% has been obtained. The concept is attractive since the Q of the switching elements play a little role in determining the insertion loss of the filter. The structure is useful where the emphasis is on out-of-band interference suppression. The validity of the proposed concept is demonstrated by considering 4-slots and 10-slots lowpass filters. RF MEMS switches are integrated on the ground plane to short circuit the slots. The simulated and measured results of the tunable filters exhibit an excellent agreement with a remarkable insertion loss and tuning range performance.

Session 1A9
Novel Methods for Solving the Forward and Inverse Problems of Radiative Transport

Analytical Cumulant Solution of the Radiative Transfer Equation for Light Scattering in Turbid Media

W. Cai, M. Xu, X. Ni, and R. R. Alfano
City University of New York, USA

We will discuss an analytical solution of the time-dependent radiative transfer equation in an infinite uniform medium with an arbitrary phase function using cumulant expansion, and compare the theoretical results with the Monte Carlo simulation and experiments.

The expression of the exact spatial cumulants of light distribution function, up to an arbitrary high order, at different angle and time have been derived. We plan to briefly review this derivation. The first cumulant represents the center of the distribution, and the second cumulant represents half-width of spread of the distribution, which can be fast and exactly calculated using the analytical expression. The photon distribution function is expressed by a Gaussian distribution for late times and for backscattering, or by a reshaped distribution for transmission at early times, with exact center and exact half-widths. The computed time-resolved profiles match with that of the Monte Carlo simulation.

The analytical cumulant approach is extended for solution of the polarized (vector) radiative transfer equation. Our computation shows that in the backscattering case circular polarization helicity flips with increase of the size of scatters. These results are compared with our recent experimental results using circular polarization. Approach for including the semi-infinite and slab boundaries is tested, and the results are shown.

Radiative Transport in Rotated Reference Frames

G. Y. Panasyuk, **J. C. Schotland**, and **V. A. Markel**

University of Pennsylvania, USA

We have proposed a novel method for solving the linear radiative transport equation (RTE) in a three-dimensional macroscopically homogeneous medium. The method utilizes the concept of locally rotated reference frames and can be used with an arbitrary phase function of a random medium consisting of spherically-symmetrical microscopical scatterers. The angular dependence of the specific intensity written in the spatial Fourier representation is obtained as an expansion into spherical functions defined in reference frames whose z-axes coincide with the direction of the Fourier vector k. In practice, this expansion is truncated at the maximum order $l_{\max}$. Boundary conditions have been considered in the slab and half-space geometries.

We have applied the method to (i) calculation of the RTE Green's function for different values of the absorption and scattering coefficients, μ_a and μ_s, and the asymmetry parameter g within the Henyey-Greenstein model for the phase function [1, 2], and (ii) to generation of forward data for an inverse problem of optical tomography [3]. In particular, we have demonstrated in [3] that the spatial resolution of images obtained in optical tomography is not limited to the fundamental length scale of one transport mean free path.

Angular dependence of the specific intensity I due to a unidirectional point source is illustrated in the figure (see caption for numerical values of relevant parameters). An accurate value of the specific intensity at $\theta \approx \pi/2$ ($\approx 10^{-3}$ relative error) was obtained at $l_{\max} = 34$. Note that for smaller values of $l_{\max}$, such as $l_{\max} = 10$, the result is still grossly inaccurate and can even be negative.

REFERENCES

1. Markel, V. A., "Modified spherical harmonics method for solving the radiative transport equation," *Waves in Random Media*, Vol. 14, L14, 2004.
2. Panasyuk, G. Y., J. C. Schotland, and V. A. Markel, "Radiative transport equation in rotated reference frames," preprint at http://arxiv.org/abs/math-ph/0505054.
3. Panasyuk, G. Y., J. C. Schotland, and V. A. Markel, "Superresolution and corrections to the diffusion approximation in optical tomography," *App. Phys. Lett.* Vol. 87, 101111, 2005.

Numerical Solution of the Radiative Transport Equation for Modulated Imaging of Tissues

A. D. Kimn
University of California, USA

We develop a novel numerical method to solve the radiative transport equation in a slab with an inhomogeneous absorption coefficient for modulated imaging of tissues. In modulated imaging of tissues, the incident light is modulated spatially permitting the sampling of the solution in the spatial frequency domain. We use the iterated source method to handle the integral operator. For the angle variables, we use the discrete ordinate method. We use a Fourier pseudo-spectral method to treat the transverse spatial variables. We use a semi-implicit method to solve the resulting discretized system of equations. We show numerical results using this method of direct images using spatially modulated illumination.

Inverse Transport with Diffusion-type Measurements

G. Bal
Columbia University, USA

Inverse problems in optical tomography consist of reconstructing the optical properties of tissues from boundary measurements of photon intensities that are usually averaged in the angular variable, e.g., when only currents are available at the domain boundary. Whereas an fairly extensive mathematical theory exists on the reconstruction of optical parameters from full (phase-space) measurements in transport theory, very little is known about reconstructions from angularly averaged measurements. We will review recent results obtained recently on the subject.

Hybrid Solution Methods for the Radiative Transport Equation

S. Arridge and M. Schweiger
University College London, UK

T. Tarvainen, **V. Kolehmainen**, **M. Vauhkonen**, **and J. Kaipio**
University of Kuopio, Finland

Optical Tomography based on the Diffusion Approximation (DA) is a well established field of research. Despite the success of the DA in modelling optically thick regions, it is well known that under certain conditions it is no longer valid, in particular, near sources and interfaces, and in low scattering or high absorption regions. Under these circumstances, attention has turned to the more accurate, and computationally more expensive Transport Equation, which in optics is usually referred to as the Radiative Transfer Equation (RTE). A very large body of literature exists for solving this equation with differing computational complexity.

A general method for the RTE involves the representation of the angular variation as well as the spatial variation in terms of an implicit or explicit basis. Full solutions to the transport equation which require a large number of angular basis functions become prohibitively expensive. However, the detailed representation of the angular variation may not be required over the whole domain. In this paper we consider a system where the angular order of basis is adapted, leading to a reduction in the overall system size.

We compare some alternative strategies:

1. a hybrid DA/RTE approach where two different models are explicitly developed and coupled with an interface condition

2. a variable order basis methods where the angular variation is developed in orthogonal basis functions. The coupling of different orders is achieved by truncating the basis expansion at different orders, which imposes a Dirichlet condition on a set of implicit interfaces.

We show results in particular for the parts of domains close to sources, and to non-scattering void regions.

Fourier-Laplace Structure of the Inverse Medium Problem for the Radiative Transfer Equation

J. C. Schotland
University of Pennsylvania, USA

There has been considerable recent interest in the inverse problem of optical tomography. The usual approach to this problem makes use of the diffusion approximation (DA) to the radiative transfer equation (RTE). Within the accuracy of the DA, it is possible to formulate the linearized inverse problem in terms of the inversion of a suitably defined Fourier-Laplace transform which relates spatial fluctuations in the optical absorption of a random medium to the intensity of light transmitted through the medium. In this talk I will discuss analogous results which hold beyond the DA. In particular, it is shown that by making use of the plane-wave expansion for the Green's function of the RTE that a generalized Fourier-Laplace structure arises in the inverse medium problem for the RTE. This is joint work with Arnold Kim and Vadim Markel.

A PDE-constrained Optimization Algorithm for Frequency Domain Optical Tomography

A. H. Hielscher, **K. Ren**, **X. Gu**, **A. K. Klose**, **and G. Abdoulaev**
Columbia University, USA

Diffuse Optical Tomography (DOT) is a fast developing new medical imaging modality that use near-infrared light to probe various sections of the human body. The light from laser diodes is deliver through optical fibers to several locations on the surface of the body part under investigation. Measurements of backreflected and transmitted light intensities at other positions on the surface are recorded and analyzed. The technology for making these measurements is nowadays readily available and has mainly been applied to breast and brain imaging. However, a major challenge that still remains is the development of efficient numerical schemes that transform these data into useful cross-sectional images of the interior.

In this work, we present a novel approach to solving the inverse problems encountered in optical tomography. We have implemented a PDE-constrained optimization method that uses a finite-volume method for the discretization of the frequency-domain radiative transport equation (RTE). The finite-volume discretization gives rise to an algebraic nonlinear programming problem that is solved using the iterative augmented Lagrangian method. By simultaneously updating both radiance and optical properties, the method solves the forward and inverse problems in optical tomography all at once. In this way, the computing time is greatly reduced as compared to traditional unconstrained optimization methods, during which one has to repeatedly solve the forward problem many times. We tested and quantified the performance of the algorithm for various combinations of mesh sizes, noise, regularization parameters, initial guesses, optical properties and measurement geometries. Besides the speed of the code, we compared image qualities by defining a correlation coefficient ρ as well as a deviation factor δ.

In the cases that involve image reconstruction from synthetic measurement data we observe 10-30-fold decrease in computing time for the constrained optimization code compared to the unconstrained optimization code. The regularization parameter β has some influence on the computing time, but with reasonable values on the order of $\beta \sim 10^{-7}$ to 10^{-9}, the computational time changes less than 20%. In general, reconstruction of both absorption and scattering together took longer than reconstructions of only the scattering coefficient or only the absorption coefficient. As expected the correlation coefficients ρ and deviation factors δ worsen as the signal-to-noise ratio decreases. Similarly δ decrease substantially as the (homogeneous) initial guess is not chosen close to the optical properties of the actual background medium. Interestingly ρ is only weakly affected by the initial guess. As long as the optical properties are chosen within 50% of the actual background medium ρ changes by only 10-20%. Finally δ and ρ do not change once the mesh is fine enough so that the average size of finite volumes becomes less than the average scattering mean free path $(1/\mu_s)$. Another positive aspect of the augmented Lagrangian method is that it maintains storage requirements that are comparable to requirements encountered in unconstrained optimization methods.

*This work was supported in part by the National Institute of Arthritis and Musculoskeletal and Skin Diseases (grant no 5R01 AR046255-05) and the National Institute of Biomedical Imaging and Bioengineering (grant no R01 EB001900-01).

Session 1P1
Poster Session 2

Mobile Wireless Communication System Antennas for 260MHz-band

H. Kawakami
Antenna Giken Corp., Japen

There is the 1/4 wavelength antenna until now as an automotive radio devices antenna. It replaces it recently, and the half-wave antenna type (the SN antenna) has been commercialized. It is desired that the height is low for the antenna mounted the car. There is often that whether the antenna becomes unnecessary and antenna has been damaged, when the place with the restriction in the height is passed. Only it was low that this paper was completed the car height, and the antenna in which to have the electric field that as 1/4 wavelength, the main radiation beam turns in the front face direction, and that it is equivalent to half-wave antenna is possible was developed.

Though 1/4 wavelength antenna of the helical conformation existed until now, it has not come to the detailed design. This paper in making the height in the helical element division to be being constant, it was decided by the change of pitch and diameter of the spiral dimension of optimum conditions. That is to say, the height made producing monopole antenna with reduction helical conformation of half-wave length composition of the SN antenna to be 300 mm or less as the condition. VSWR did that they are 2.0 less than in use frequency band and that the disconnection of not damaging element is easy, even if there is the resiliency, and even if it collides, etc. with the condition, and the excellent and characteristic thing was obtained gains, directionalities, SWR, etc. The gain improvement is the antenna equipment as a possible structure on this antenna with the finite reflector plate, which is small with shortening helical antenna as radiating element in the roof of emergency dead weight of Fire Defense Agency.

Compact Surface-mount UWB Monopole Antenna for Mobile Applications

T. Y. Wu, **C. L. Tang**, **and A. C. Chen**
Industrial Technology Research Institute, Taiwan

In the recent years, short range and high data rate wireless communication is applied in multimedia device. UWB radio technology can meet these requirements. Planar antennas have many advantages, such as low profile, small size and easy to fabricate, which are suitable for portable devices. There are several UWB planar antenna designs, including planar half-disk antenna [1], planar horn antenna [2], and metal-plate antenna [3], have been reported.

In this paper a novel surface-mount ultra-wideband (UWB) monopole antenna with a compact size of only $12.5 \times 9 \times 1.5$ mm is obtained by folding a metal-plate onto a low-profile rectangular-box foam base is presented. The lowest resonant frequency and the highest resonant frequency of proposed antenna was controlled by length and width of the metal-plate. Broadband matching technique is the key point in UWB antenna design. By carefully adding a matching slit on the upper side of metalplate, the antenna can achieving good impedance matching over a very wide bandwidth. The optima size of the matching slit in this study is about 1×3 mm, and the impedance bandwidth defined by 2:1 VSWR is 7.97 GHz (3.03–11.0 GHz). The far-field radiation characteristic across UWB band of the proposed antenna is also studied. It shows a monopole like radiation pattern and antenna gain is about 3.0 dBi.

The proposed antenna has a compact structure, which makes it easy to fit in any possible margin within the housing of a mobile/hand-held wireless device, thus leading to an internal UWB antenna. It is also suitable for surface-mountable manufacturing process, so as to reduce the production cost. Details of the antenna design and experimental results of the constructed prototypes will be discussed in the upcoming presentation.

REFERENCES

1. Yang, T. and W. A. Davis, "Planar half-disk antenna structures for ultra-wideband communications," *IEEE Antenna Propagat. Soc. Int. Symp. Dig.*, Vol. 3, 2508–2511, 2004.
2. Lee, S. H., J. K. Park, and J. N. Lee, "A novel CPW-FED ultra-wideband antenna design," *Microwave Opt. Technol. Lett.*, Vol. 44, 393–396, 2005.
3. Wong, K. L., T. C. Tseng, and P. L. Teng, "Low-profile ultra-wideband antenna for mobile phone applications," *Microwave Opt. Technol. Lett.*, Vol. 43, 7–9, 2004.

TEC Measurements through GPS and Artificial Intelligence

V. Barrile, **M. Cacciola**, **F. Cotroneo**, **F. C. Morabito**, **and M. Versaci**
Univ. Mediterranea, Italy

The ionosphere is a very dynamic region that couples strongly with thermosphere and magnetosphere systems. Due to its dispersive nature, GPS differential code and carrier phases at L1/L2 frequencies can be computed. From these, the Total Electron Content (TEC) may be derived as the integral of the local electron density along the path between the satellite and the receiver. TEC, in fact, is defined as the total number electrons in the ionized plasma contained in an imaginary tube ($1\,\mathrm{m}^2$ cross section) between a GPS satellite and the GPS receiver. As the plasma density changes with time of day, season and solar activity, changes in TEC reflect of near-Earth space dynamics. The amount of TEC is very important because it provides two-dimensional cross-section maps of the ionosphere's electron density, with significant improvements in: mono-frequency satellite measurement; GPS and SAR imagery of geophysical phenomena (volcano deformations or subsidence detection); detection of ionospheric disturbances like geomagnetic storms, ionospheric scintillation and post-seismic perturbation, with space weather implications.

Nowadays, Kalman filters and stochastic estimations are used to calculate TEC, in order to obtain empirical ionospheric model. In our work, a new solving method is proposed; it involves Artificial Intelligence algorithms and structures in order to improve calculation performances and to reduce calculation elapsed times.

Reliability and Availability of GPS Measures in Airport Landing Systems

V. Barrile, M. Cacciola, and F. Cotroneo
Univ. Mediterranea, Italy

In last decade, the air traffic managed by all airports in the world is considerely increased. Consequently, it is also increased the requirement of technological solutions which are able to improve safety level, int the various phases of flight assistance including the most demanding phase of flight: aircraft approach and landing.

Among the considered solutions, the best reliable ones involve GPS receivers in order to establish airplane positions. Advantages of this solution are above all referred to moderate costs and precision of positioning. However navigation systems such as GPS (Galileo, GLONASS) cannot be considered as high available systems. In fact, because of "unintentional RF interferences" (environment pollution) or terroristic attacks through "Antenna Jamming" and "Code Contamination" techniques, the offered service can be stopped.

In our work, these problems has been analysed and some solutions are suggested when GPS system is used to control landing phase, in order to improve the safety and also to assure a short-range precision during the whole landing procedure.

Electromagnetic Scattering by Rough Surfaces with Spatially Varying Impedance

M. Spivack and N. S. Basra
University of Cambridge, UK

A method is given for evaluating electromagnetic scattering by an irregular surace with spatially varying impedance. This allows examination of the effects of impedance variation and the resulting modification of rough surface scattering. Expressions are derived for the coherent field for both flat and rough surfaces, taking the form of effective impedance conditions.

Many applications of wave scattering from rough surfaces are complicated by the involvement of further scattering mechanisms. Radar propagating over a sea surface, for example, may encounter refractive index variations in the evaporation duct or spatially varying impedance due to surface inhomogeneities. This is an even greater problem in remote sensing over forest or urban terrain. The great majority of theoretical and numerical studies, most focusing on surface roughness, nevertheless treat such effects in isolation. Roughness is usually the dominant feature but impedance variation may produce further multiple scattering. Experimental validation of scattering models in complex environments remains a major difficulty, exacerbated by the lack of detailed environmental information, and it is therefore crucial to distinguish and identify sources of scattering. In addition, while numerical computation in these cases may be feasible for the perfectly reflecting surface, it can become prohibitive for more complex environments, particularly in seeking statistics from multiple realisations.

This study is motived by these considerations. We have sought to provide an efficient means to evaluate the effect of impedance variation and its interaction with surface roughness, and to derive descriptions of the resulting coherent or mean field, for both flat and irregular surfaces.

Results have been derived by use of an operator expansion: Surface currents (from which scattered fields are determined) are expressed as the solution of an integral equation, in which the effect of impedance variation is separated. The solution is written in terms of the inverse of the governing integral operator, and provided the impedance variation is not too large this inversion can be expanded about the leading term.

Development of the Pulsed Direct Current Iontophoresis and Its Clinical Application

M. Akimoto
Kanto Gakuin University, Japan

M. Kawahara, **M. Matsumoto**, **and H. Matsubayashi**
I.C.I. Cosmetics Japan, Japan

The skin is a primary area of body contact with the environment and is the route by which many chemicals enter the body. The delivery of drugs into and through the skin has been an important area of research for many years. And percutaneous absorption is also one of the most important phenomena in cosmetic research. Generally, the stratum corneum is the main barrier limiting the passive transdermal diffusion of a lot of drugs, and this function is very important factor for the development of transdermal therapeutic system. To overcome some of these limitation, in recent years, several approaches have been proposed including chemical and physical enhancing method. Iontophoresis can be defined as the process of increasing the rate of penetration of ions into or through a tissue by the application of an external electric field across the tissue. Iontophoresis is being increasingly investigated as a technique for enhancing the penetration of ionic drugs across skin. In this work, ionic transport through the skin is characterized by two electrochemical techniques: impedance spectroscopy, and pulsed-current iontophoresis. Impedance spectroscopy was used to investigate the electrical response of skin to different ions, applied currents and fields. The dielectric measurements were performed using automatic swept-frequency network and impedance analyzers. The frequency range 5 Hz to 10 MHz was covered by an HP–4192A impedance analyzer. Open-ended co-axial probes were used to interface the measuring equipment with the samples in all cases. An equivalent circuit of skin is a resistor in series with a parallel combination of a resistor and a capacitor. The stratum corneum shows two important electrical features. First, it tends to become polarized as an electrical field is applied continuously. Second, its impedance changes with the frequency of the applied electrical field. Therefore, as an electrical field with direct current is applied in a continuous manner to the stratum corneum to facilitate the permeation of charged molecules, an electrochemical polarization may occur in the skin. To avoid the counterproductive polarization, the current should be applied in a periodic manner, which is called pulsed direct current. The pulsed direct current generating iontophoretic delivery system also was developed. In vivo pharmacodynamic studies in diabetic animals suggested that the systemic bioavailability of peptides and proteins are dependent upon the electronic variables of the iontophoretic delivery device, e.g., frequency, on/off ratio and intensity of the current applied, physiochemical parameters. The mechanism of iontophoresis transdermal transport of peptide macromolecules are analyzed. A non-parenteral method for the delivery of macromolecules such as insulin was developed by using a pulsed direct current mode transdermal iontophoretic technique. The intensity of current, frequency, on/off ratio and mode of waveform were found to play an important role in the transdermal iontophoretic delivery. Low current intensity and short treatment duration were found to be adequate to obtain equivalent blood glucose control compared with that using conventional direct current iontophoresis. More extensive investigations on various aspects of this system are necessary to obtain optimum parameters of pulsed mode for transdermal iontophoretic delivery of dermatology.

Design of Reduced-size Branch-line Couplers with Series Capacitors

T. Kawai, **Y. Kokubo**, **and I. Ohta**
University of Hyogo, Japan

Branch-line couplers are widely used in microwave and milimeter-wave circuit systems such as balanced mixers, balanced amplifiers, phase shifters, and etc. Since conventional couplers designed based on the distributed circuit theory tend to waste chip area in MICs or MMICs, especially at low frequencies, thus many research efforts have been devoted to reduce the size of couplers. Here, we treat branch-line couplers with series capacitors at each input/output port as shown in Fig. 1(a) and design reduced-size couplers based on the equivalent admittance approach. Fig. 1(b) exhibits the theoretical scattering parameters for the compact coupler that the electrical length of branchlines is 60°. As shown in this figure, the fractional bandwidth is about 10% for -20 dB return loss. This value is comparable to that of the conventional branch-line coupler. The validity of this design technique is demonstrated by electromagnetic simulator (Sonnet em) assuming that the glass substrate with dielectric constant of 4.8 and thickness of 0.5 mm, respectively. Fig. 2 shows the circuit pattern of simulation for the proposed coupler designed at center frequency of 3 GHz. In this circuit, input/output ports and branch-lines are constructed of coplanar waveguides (CPWs). Metal- Insulate-Metal (MIM) capacitor is constructed with the air gap ($Gap = 3\,\mu m, area = 0.3\,mm^2$) under the CPW center conductor near each port junction. In order to avoid the parasitic slot-line mode, air bridges are added near the junctions. Simulation results given by plots in Fig. 1(b) generally agree with the theoretical results. We demonstrate that the size reduction of about 50% can be achieved with maintaining the property comparable to that of the conventional couplers. Experiment verifications will be our feature works.

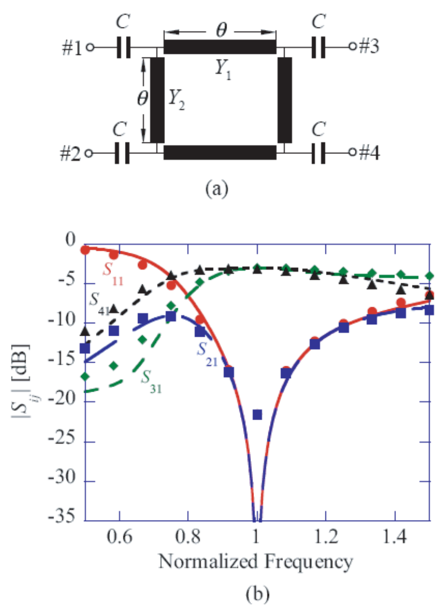

Figure 1: (a) Circuit construction and (b) frequency characteristics of scattering parameters of branch-line coupler with series capacitors ($Y_1 = 0.50, Y_2 = 0.35, C = 0.83, \theta = 60°$).

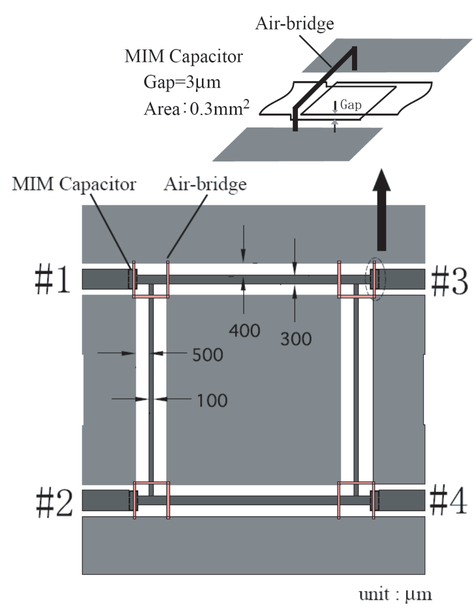

Figure 2: Circuit pattern of a proposed coupler.

Plane Wave Scattering by an Array of Pseudochiral Cylinders

M. Polewski, R. Lech, and J. Mazur
Gdansk University of Technology, Poland

This paper presents the analysis of electromagnetic plane wave scattering by cylindrical objects made of pseudochiral material located in free space.

Presented approach is based on the Iterative Scattering Procedure (ISP) [1] and allows to define the total scattered field from arbitrary configurations of cylinders. To take into account practical applications two layered cylindrical object is defined. As shown in Fig. 1 the inner dielectric or metallic core is covered with the pseudochiral material. For configuration from Fig. 1 assuming TM^z excitation and homogeneity of the field along z axis, the following wave equation is obtained [1, 2].

$$\rho\frac{\partial}{\partial\rho}\Big(\rho\frac{\partial E_z}{\partial\rho}\Big)+k_o^2\varepsilon_z\mu\rho^2E_z+\frac{\mu}{\mu_\rho}\frac{\partial^2E_z}{\partial\phi^2}=0 \tag{1}$$

It is important to note that the elements $\varepsilon_z\neq\varepsilon$ and $\mu_\rho\neq\mu$ indicate the pseudochirality effect in the considered cylinder.

The results of numerical experiment for the configuration of three pseudochiral cylinders have been presented in Fig. 2. It can be noticed that the level of side lobes for pseudochiral cylinders (Fig. 2b) decreases significantly in comparison to the configuration of dielectric posts (Fig. 2a).

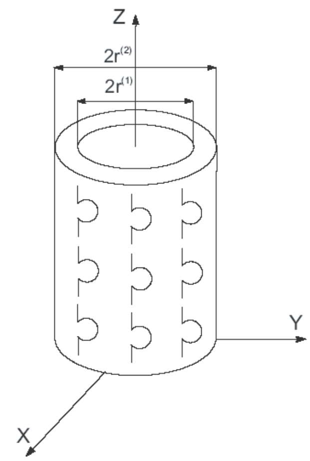

Figure 1: Pseudochiral cylinder geometry.

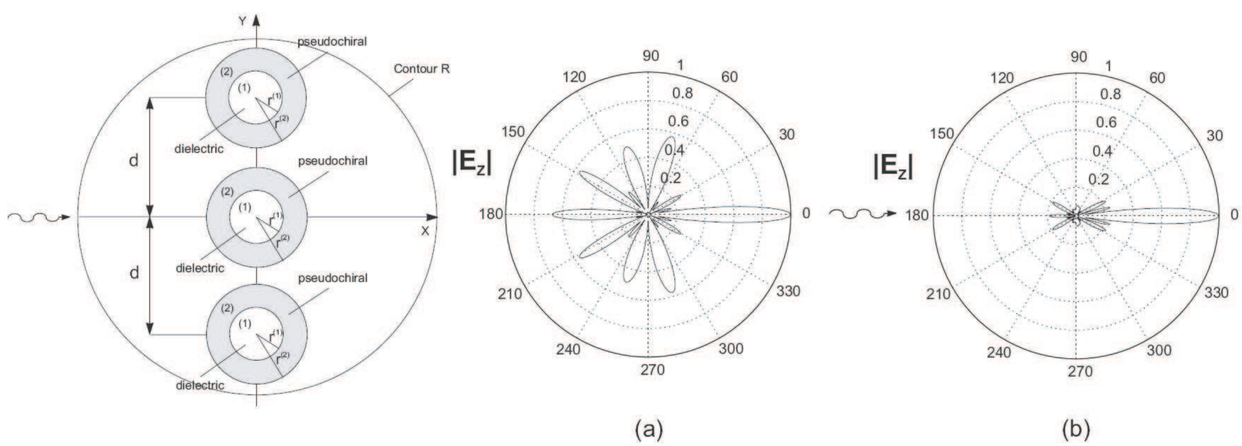

Figure 2: Scattering characteristics of $|E_z|$ for TM^z excitation from three pseudochiral cylinders. Plane wave excitation along x-axis direction. Dimensions: $r^{(1)}=0.4\lambda$, $r^{(2)}=0.75\lambda$, $R=3\lambda$, $d=2\lambda$, $\rho=100\lambda$, $M=N=26$: (a) dielectric cylinders: layer (1) $\varepsilon^{(1)}=2$, layer (2) (host medium) $\varepsilon^{(2)}=4$, $\varepsilon_z^{(2)}=4$, (b) pseudochiral cylinders: layer (1) $\varepsilon^{(1)}=2$, layer (2) $\varepsilon^{(2)}=4$, $\varepsilon_z^{(2)}=9$, $\mu^{(2)}=1$, $\mu_\rho^{(2)}=1.5$.

REFERENCES

1. Polewski, M. and J. Mazur, “Scattering by an array of conducting, lossy dielectric, ferrite and pseudochiral cylinders,” *Progress in Electromagnetic Research, PIER 38*, 283310, 2002.
2. Engheta, N. and M. M. Saadoun, “Novel pseudochiral or Ω-medium and its applications,” *Proc. of PIERS91*, Cambridge, MA, 339, July 1991.

Electromagnetic Field for Randomly Oriented Particle Located in Laser Beam

Y. P. Han and H. Y. Zhang
Xidian University, China

There are a lot of practical applications involving particle, such as particle size measurements using a phase Doppler instrument, light scattering by aerosols in atmosphere, trapping the particle in laser tweezers, the absorption in the human head of electromagnetic waves emitted by hand phones and the effect of radomes (spheroidal dielectric covers) on radar and communications antennas. Many investigations on the scattering from particle have been carried out GLMTs describe the interaction between an arbitrary shaped beam and a class of scatterers exhibiting a regular surface. In GLMTs, the most difficult task concerns the description of the illuminating beam. Gouesbet et al. have provided approaches for expansions of the incident shaped beam propagating parallel to the coordinate axis (i.e., an off-axis beam).

In this paper, we provide the description of the arbitrarily shape beam, for example, a plane wave or a Gaussian beam, for any angle incidence by virtue of the Generalized Lorenz-Mie theory. The incident beam is decomposed into an infinite series of elementary constituents, such as partial wave or plane waves, with amplitudes and phases given by a set of beam-shape coefficients. We derive the transformation of spherical vector wave functions with reference to the two different spherical coordinate systems under rotated translation and obtain the general expression of beam shape coefficients $g_{n,TE}^{ms}$, $g_{n,TE}^{\prime ms}$, $g_{n,TM}^{ms}$, $g_{n,TE}^{\prime ms}$ for the randomly oriented scatterer.

Once the beam-shape coefficients in coordinates are determined, the solution of scattering for arbitrary shaped beam by a particle is obtained by means of the method of separation of variables. The fields are expanded in the terms of the spherical vector wave functions. The unknown coefficients of scattered and internal electromagnetic fields are determined by solving a system of linear equations derived from the boundary conditions. The exact analytic solution of scattering from a randomly oriented axisymmetric particle with an arbitrarily shaped beam illumination can be obtained by means of the method of separation of variables. Also, the numerical results for the beam scattering properties for particle is given. The associated code, developed under Matlab, is suitable for computing the scattering properties of the randomly oriented particles, allowing one to extensively investigate the dependence of scattering properties on the particle size, shape, refractive index, magnitude and location of beam waist. This study is suggestive and useful for interpretation of electromagnetic scattering phenomena from oriented particles.

Corrector Packaging for Heating inside a Domestic Microwave Oven

A. Rhattoy and S. Bri
Université Moulay Ismail Meknes, Morocco

M. Audhuy-Peudeceder
ENSEEIHT-INPT, France

In this paper, we demonstrate that an adapted packaging improves the microwave cooking. The electromagnetic and thermal functions of the packaging are studied. This applicator is constituted of a slot array or a metallic bar array which is positioned on a metallic box filled with an alimentary product. The slot array purpose is to homogenise the power distribution inside the metallic box and to minimise the coupling degree between the product, the microwave oven and the generator. It is possible to control the electromagnetic fields by means of the packaging that becomes a second oven in the first oven. In this case the field calculation is realised by the Finite Element Method. We have calculated the width of the slots, the distance between them and the height of the slot array in relation to the product according to the following criteria: Electromagnetic fields inside the product should be uniform and independent of the fields in the oven, the input impedance of the cavity should be constant wherever the position of the product in the oven.

A WEB Application for Electromagnetic Structures

A. S. B. Lopes, **F. M. Sales Junior**, **and J. R. S. Oliveira**
CEFETRN/NUTEL, Brazil

Several structures in electromagnetic applications were studied along the last decades and the results have been published in reports, papers and magazines. With the success of Internet applications, it's important to think how we could use it to permit users to resolve some simple problems using a browser to inform some characteristics of a structure and receive the result of his research. Structure like transmission lines, antennas, planar circuits are, sometimes, analyzed using approximates equations that are enough to some applications. So, we can use them to construct a WEB interface to receive the data and to show the results.

In this paper, a WEB interface is constructed to solve problems of transmission line, antennas and planar circuits and used as a tool to analysis and synthesis of such structures. The objective is use, initially, closed equations to characterize some transmission lines presenting results for characteristic impedance, resistance, inductance, capacitance, loss conductor, loss in dielectric and attenuation.

In the analysis of antennas, some types are considered, like monopole, dipole, helicoidal, yagi, microstip and others. The variables to be analyzed are resonant frequency, gain, radiation pattern and quality factor. It is important in a WEB application, the graphical behavior of some electrical parameters, like frequency versus length or height.

Other application of special importance for designers is the synthesis of transmission lines, antennas and circuits. The WEB interface allows the filling in some fields with the desired electric parameters and the output presents the physical characteristics of such structure.

This kind of WEB applications is been projected to be also used as a didactic tools for teaching electromagnetic concepts to the CEFETRN's students in analysis of electromagnetic concepts and some projects. The final objective is to obtain a portal that grows with the addition of new devices. This growth can be done by any person involved in the project in any place of the world using the WEB management tool.

Computation of Resonant Frequencies of Any Shaped Dielectric Resonators by CFDTD

A. Shahvarpour and M. S. Abrishamian
K. N. Toosi University of Technology, Iran

Dielectric resonators(DRs) have helped achieving the miniaturization of many active and passive microwave components, such as oscillators, filters and antennas. Nowadays they are used widely in mobile telecommunications and optical instruments such as optical couplers and filters. To design such components, designers must have the knowledge of predicting the shape and resonant frequency response of usable dielectric resonators. Numerical methods such as Method Of Moment(MOM), Finite Element Method(FEM) and Finite Difference Time Domain(FDTD), are useful tools for simulating those problems. The MOM & FEM are usually in frequency domain and we need to inverse a large matrix to solve the problem. Fortunately, FDTD is in time domain and by one run, we can have a large bandwidth response of our system.

We have prepared a program code for determining resonant frequencies of DRs by using CFDTD (Conformal Finite Difference Time Domain) which is used for curved surfaces such as cylindrical and spherical shapes in Cartesian coordinate. In Figure, the resonant frequency response of a thin dielectric spherical layer that can be useful for improving the achievement of Whispering Gallery Modes, which are produced in spherical DRs, is shown. In the Figure, the analytical and numerical results are compared, and a good agreement is achieved.

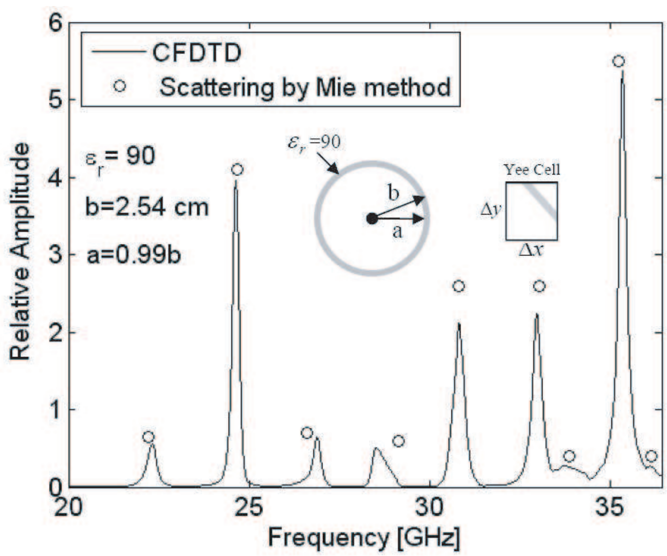

Figure 1: Resonant frequencies of a thin dielectric spherical layer.

*The authors wish to thanks Iran Telecom Research Center for encouragement and sponsoring this work.

A Novel Transmission Line Model for Analyzing Bowtie Patch Antennas

K. Moussakhani and A. Ghorbani
Amirkabir University of Technology, Iran

The transmission line method is known to be reasonably accurate and have good efficiency especially in numerical calculation as well as it can be applied for modeling of antennas arrays. In this paper a novel transmission line model is presented for analysis of bowtie patch antenna of finite length, placed on a dielectric substrate as shown in Fig. 1. The purposed model uses two slots for modeling the radiation from patch sides. Each radiation slot is presented by parallel equivalent admittance. Also mutual coupling, effect of slots length limitation as well as the influence of the side slots on the radiation conductance is taken into account implicitly in this model.

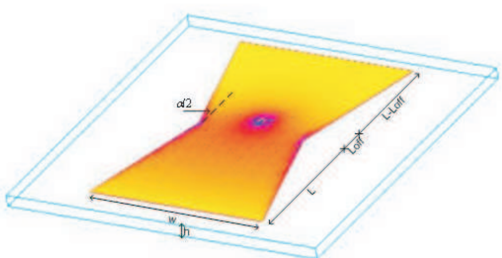

Figure 1: Antenna structure.

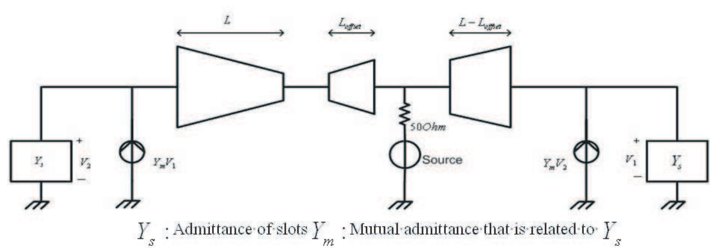

Figure 2: Purposed model.

More over we have used taper transmission line instead of common microstrip line for modeling bowtie shaped patch as shown in Fig. 2.The offset of feed location has been considered by dividing the taper line into three sections as can be seen in Fig. 2. Also admittance and controlled source equations that used for rectangular patch antenna are modified to take into account the current distribution on bowtie patch and shape of side slots, and flare angle dependent correction functions are implied to improve mutual coupling formulation.

The results obtained by this method compared with method of moment for several bowtie patch antennas and the results are in good agreements. In Fig. 3 typical results obtained for return loss is compared with MoM and as can be observed there is good agreement and conformity between them. Also we tried to calculate the error deviation between our method and MoM and observed that less than 3% error can be achieved.

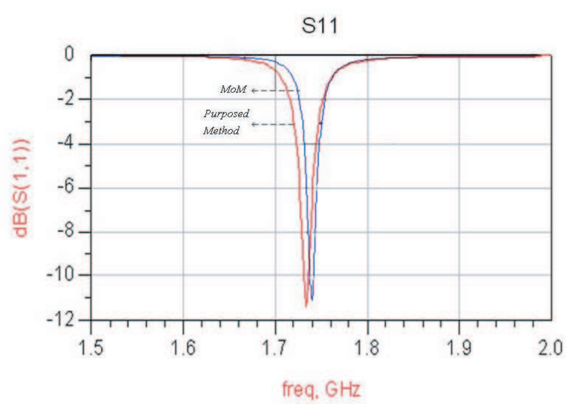

L=18.75, W=25.2, H=1.6
$L_{offset} = 1.6$, $\varepsilon_r = 4.4$, $\alpha = 30°$

Figure 3: Return loss versus frequency.

This result shows that this model can be successfully apply to predict the input characteristics of bowtie patch antenna as well as similar configuration. Also using this model one can analyze effect of each part of antenna separately and optimized parameters of antenna individually in quickest time.

Session 1P2
Electromagnetic Modeling in Optoelectronics

Simulation of Self-assembled Photonic Crystals with Embedded Waveguide Using FDTD Method

J.-U. Lee[1], **K.-H. Baek**[1], **C. Olson**[1], **D. M. Kim**[1,2], **and A. Gopinath**[1]

[1]University of Minnesota, USA
[2]Kookmin University, Korea

Photonic crystals (PCs) with three-dimensionally periodic structures and omnidirectional photonic bandgaps (PBGs) within certain wavelength ranges have attracted extensive interest in their various potential applications in integrated photonics and optics. Artificial planar, line, or point defects embedded in the PCs, which allow propagating or localizing light, are required for the applications. One of the 3-D PBG structures, self-assembled PCs (inverse opals) with embedded defects has been investigated widely due to its simple and low-cost fabrication process. Ordered templates with close-packed face centered cubic structure may be built by the colloidal spheres, and is selectively removed after infiltrating a semiconductor material with high-refractive index into the interstitials of spheres.

A complete numerical characterization of the self-assembled PCs with a defect is essential for guiding the design process and obtaining a deeper insight into the physics of PCs. One of the numerical techniques, the Finite Difference Time Domain (FDTD) method for simulating the interaction of electromagnetic fields with material structures has become a well-established tool for the analysis of PCs. For predicting the PC behaviors and designing proper applications, we need to accurately model the PCs and their applications using the FDTD method.

In this paper, the numerical analysis using FDTD method for 3-D self-assembled inverse opal structures with embedded line defects is discussed. No previous results of such investigation have been reported. To confirm the existence of specific PBGs of self-assembled PCs, we calculated photonic band structures and transmittance spectrum using the MIT Photonic-Bands program based on Plane-Wave method and the Rsoft Fullwave FDTD codes, respectively. The simulation results for the 3-D PCs with close-packed air spheres surrounded by silicon suggest that the air spheres with diameter of 870 nm are required for a PBG at wavelength of 1550 nm, and the band structure of 3-D inverse opal shows an omnidirectional PBG exists. A line defect, Si_3N_4 rectangular channel waveguide embedded in the 3-D self-assembled PCs was used for the propagation simulations of light at wavelength of 1550 nm and the transmission spectrums of the waveguides were measured using the FDTD codes. We confirmed that guided wave propagation occurred along the Si_3N_4 guide within the PBG. Simulation results on both the 2-D and 3-D inverse opals with embedded waveguides will be presented at meeting.

Modal Analysis and Beam Propagation in Bent Fibers

G. R. Hadley
Sandia National Laboratories, USA

After three or four decades, fiber optics is still finding new applications both in communications and more recently in high-power lasers and amplifiers for medicine and materials processing. These new applications often require bending the fiber to ensure single mode operation and therefore maintain a high brightness output. Bent fibers also offer a means for polarization control. In these cases numerical models are needed that accurately handle the radiation loss resulting from the bending while keeping all relevant field components. To this end, we have developed a suite of tools for modeling bent fibers that address these issues. Our numerical models are triangular-grid finite difference based in cylindrical coordinates so that radiation loss is naturally handled as a curvilinear coordinate system effect, rather than by artificially adding on an index ramp as is typically done. Our suite of codes includes both full vector and semivectorial eigenmode solvers and beam propagation codes. These tools have recently been modified to include Kerr effect nonlinearities, and thus both the model derivation and its applications for predicting self-focusing effects in MW fiber amplifiers will be presented.

Hybrid Methods for Efficient Electromagnetic Simulation

T. M. Benson, **P. Sewell**, **A. Vukovic**
C. Christopoulos, **D. W. P. Thomas**, **and A. Nosich**
University of Nottingham, UK

Simulation of the electromagnetic behavior of very general structures is a common activity in many branches of science and technology and many techniques have been proposed and exploited for this purpose. The use of general-purpose time-domain numerical techniques such as the Finite Difference Time Domain (FDTD) [1] and Transmission Line Modeling (TLM) methods [2] is becoming widespread, due to their flexibility and relative ease of use. These techniques offer the flexibility to deal with relatively arbitrary geometries and a wide range of material properties. Unfortunately, the flexibility of numerical simulation tools is often bought at the expense of computational efficiency, both in terms of run times and memory consumption. In particular, their space discretizing nature means that they do not effectively model free-space regions.

Alternative Integral Equation approaches to both frequency and time domain simulations intrinsically incorporate our physical understanding of the relatively simple behavior of electromagnetic fields in uniform spaces [3, 4]. There is no need to terminate the calculation window with artificial absorbers as the kernel of the integral equation intrinsically contains the correct asymptotic behavior at infinity. We will show that such formulations can offer clear computational advantage, especially when the problem space considered contains large uniform regions or the geometry cannot readily be spatially discretized without stair-stepping error.

Having considered these two alternative approaches to electromagnetic simulation we will go on to discuss hybrid simulation techniques, where different simulation tools are used to model those parts of a particular problem to which they are best suited. By embedding a numerical algorithm such as TLM within a global region described by the Integral Equation method, and coupling tools together through a suitable interface, an overall efficiency saving can be achieved [5].

REFERENCES

1. Taflove, A., "Computational electrodynamics: the finite-difference time-domain method," Artech House, Norwood, MA, 1995.
2. Christopoulos, C., "The transmission-line modeling method: TLM," *IEEE Press*, Piscataway, NJ, 1995.
3. Boriskina, S. V. and A. I. Nosich,, "Radiation and absorption losses of the whispering-gallery-mode dielectric resonators excited by a dielectric waveguide," *IEEE Trans. Microwave Theory Tech.*, Vol. 47, 224–231, 1999.
4. Fedotov, F. V., A. G. Nerukh, T. M. Benson, and P. Sewell, "Investigation of electromagnetic field in a layer with time varying medium by volterra integral equation method," *J. Lightwave Technology*, Vol. 21, 305–314, 2003.
5. Lindenmeier, S., L. Pierantoni, and P. Russer, "Hybrid space discretising integral equation methods for numerical modelling of transient interference," *IEEE Trans. on Electromagnetic Compatibility*, Vol. 41, 425–430, 1999.

Applying Oblique Coordinates in the Method of Lines

S. F. Helfert
University of Hagen, Germany

The Method of Lines (MoL) has been proven as an efficient tool for modeling waveguide structures in the microwave area and in optics. Depending on the structure under study various coordinate systems like Cartesian or cylindrical ones have been introduced. Formulas for arbitrary rectangular coordinates can be found in [1].

With such expressions the MoL has been used to analyze photonic crystal structures (PCs) with a square lattice. In contrast, the shape of the elementary cells in hexagonal structures is not rectangular (see Figure 1(a)). Motivated by papers found in the literature (e.g., [2–4]) an algorithm was developed that uses oblique coordinates. In the references given above algorithms for the TE-polarization (2D) were described. Here, expressions for the analysis of 3D-vectorial structures are derived. The formulas were applied to compute the band-structure of PCs with a hexagonal lattice. The results for the TE-polarization and the Γ-M band are shown in Figure 1(b). Also included are the values at the edges from the literatrue [5]. A good agreement is recognizable.

Oblique coordinates are also suitable to examine tilted waveguides. Results will be compared with those obtained with a step approximation in Cartesian coordinates.

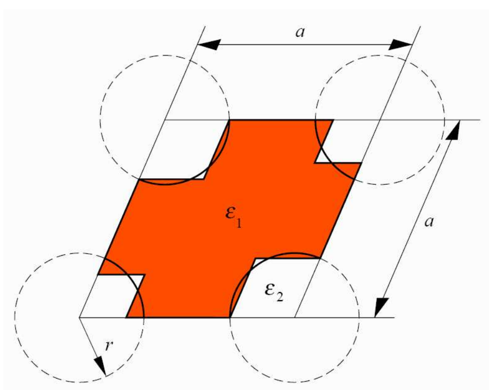

(a)

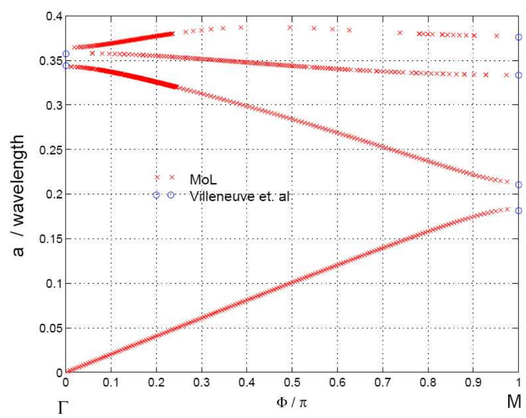

(b)

Figure 1: a) Elementary cell of a hexagonal photonic bandgap structure and b) determined band structure compared with [5].

REFERENCES

1. Pregla, R., "Modeling of optical waveguide structures with general anisotropy in arbitrary orthogonal coordinate systems," *IEEE J. of Sel. Topics in Quantum Electronics*, Vol. 8, 1217–1224, Dec. 2002.
2. Yamauchi, J., J. Shibayama, and H. Nakano, "Propagating beam analysis based on the implicit finite-difference method using the oblique coordinate system," *OSA Integr. Photo. Resear. Tech. Dig.*, San Francisco, USA, 19–21, Feb. 1994.
3. Benson, T. M., P. Sewell, S. Sujecki, and P. C. Kendall, "Structure related beam propagation," *Opt. Quantum Electron.*, Vol. 31, 689–703, Special issue on optical waveguide theory and numerical modelling, 1999.
4. Sewell, P., T. M. Benson, S. Sujecki, and P. C. Kendall, "The dispersion characteristics of oblique coordinate beam propagation algorithms," *J. Lightwave Technol.*, Vol. 17, No. 3, 514–518, 1999.
5. Villeneuve, P. R., S. Fan, S. G. Johnson, and J. D. Joannopoulos, "Three-dimensional photon confinement in photonic crystals of low-dimensional periodicity," *IEEE Proc.-Optoelectron.*, Vol. 145, No. 6, 384–390, 1998.

Mixed-mode Optical Design for Optoelectronic Applications

N. Danz, D. Michaelis, P. Schreiber, C. Wähter, and U.-D. Zeitner
Fraunhofer Institute for Applied Optics and Precision Engineering, Germany

This paper aims to highlight the variability of tools and methods which are required for the optical design of optoelectronic systems, which may include sources, receivers, refractive and diffractive micro-optical elements as well as waveguides and photonic crystals.

What details of the character of the electromagnetic field in a design are to be considered strongly depends on the systems geometry. High refractive indices and geometry features at wavelength scale or below require vectorial analysis, whereas low index contrast, small numerical aperture (NA) and field diameters well above the wavelength may allow for simple ray optics. If the optical system includes quite different media and different length-scales, due consideration is needed in order to determine a possible design flow which is both sufficiently accurate and numerically feasible. If approximations are unavoidable, the cross-check of the results with complementary methods is a must in order to achieve reliability of the design prior to fabrication. Thus, a variety of different design tools has to be at hand within the design process, for e.g., fibre to photonic crystal coupling, diffractive correction, and light extraction from OLED devices, for example.

If the coupling from a telecom fibre to a defect waveguide in a photonic crystal by means of free-space micro-optics is considered, it is intuitively clear that FDTD isn't applicable for the whole geometry, whereas considerable parts of the system are best handled with ray-tracing, simply. In order to improve design efficiency, a semi-analytical model to calculate the transmission from the focal field (foc) to the intended waveguide mode (w) as an integral over a coupling plane (cp)

$$T=\frac{\left|\iint\limits_{(cp)} dxdy\left[\vec{E}^{(t)^*}_{Foc}\times\vec{H}^{(t)}_{W}+\vec{E}^{(t)}_{W}\times\vec{H}^{t^*}_{Foc}\right]_z\right|^2-\left|\iint\limits_{(cp)} dxdy\left[\vec{E}^{(t)}_{Foc}\times\vec{H}^{(t)}_{W}-\vec{E}^{(t)}_{W}\times\vec{H}^{t}_{Foc}\right]_z\right|^2}{\iint_{(cp)} dxdy\left[\vec{E}^{(t)^*}_{Foc}\times\vec{H}^{(t)}_{W}+\vec{E}^{(t)}_{W}\times\vec{H}^{(t)^*}_{Foc}\right]_z}$$

can be used advantageously [1], which is based on the reciprocity theorem for photonic crystal waveguides [2]. To confirm the result, FDTD is a proper means now since the volume required for the analysis just allows for a discretisation which fits into a PCs memory.

Diffractive elements in micro-optical systems call for separate investigation. Scalar diffraction theory turns out to be a simplified approximation if e.g. diffractive corrections are applied to high NA micro-lenses. In order to incorporate efficiencies and phases for different diffraction orders accurately in an overall design, rigorously coupled wave analysis applied to grating problems is an adequate means. The coupling of grating analysis and a ray-trace engine is a must, too, if light extraction from OLEDs by means of periodic structures is investigated. Furthermore, for the OLED device the coupling of light from the radiating dipoles into slab guided and leaky modes requires special consideration, since this may reduce the overall device efficiency remarkably. There, a Green-functions based analysis tool is an adequate means for design improvements.

Although commercially available design tools nowadays offer a wide range of functionality, these examples which all stem from applied research show that the diversity of optical applications requires that the designer can fall back to different design tools, to appropriate interface tools, and to a sufficiently broad knowledge in electromagnetics.

REFERENCES

1. Michaelis, D., et al., "Coupling coefficients of photonic crystal waveguides," SPIE, Vol. 4987, 114–125, 2003.
2. Michaelis, D., et al., "Reciprocity theorem and perturbation theory for photonic crystal waveguide," *Phys. Rev. E* , Vol. 68, 065601(R), 2003.

Modelling of Time-varying Phenomena in Electroabsorption Modulators

A. Vukovic, E. Bekker, P. Sewell, and T. M. Benson
The University of Nottingham, UK

Modern RF electroabsorption modulators are important devices as they directly determine the bandwidth, speed and operational frequency of dense wavelength division multiplexing (DWDM) and optical time division multiplexing systems (OTDM). In these systems they are commonly used for short pulse generation, data encoding and clock recovery. In order to enable systems achieve higher speed, bandwidths and lower costs an efficient modelling tool that would enable deeper insight into the physical behaviour of the modulator and its existing problems and limitations is needed.

The principal operation of a RF electroabsorption modulator relies on the interaction of the optical electromagnetic wave with the time-varying medium whose complex dielectric constant is modulated by a microwave wave. The optical wave is confined by a complex semiconductor geometry and the modulation of the dielectric constant is done in a relatively small region of a multiple quantum well (MQW). It is well known that a temporal change of the dielectric permittivity in an open and semi-open medium causes transformation of the original plane wave into reflected and transmitted waves of different frequencies and same wave numbers [1, 2]. In the time-varying waveguide the change of the permittivity directly affects not only the frequency of the incident wave but also the spatial distribution of the wave which further complicates the problem.

One of the major limitations in the performance of RF modulators is the temporal variation of the frequency and this is measured through the chirp parameter.

Numerical methods such as the Finite Difference Time Domain (FDTD) and the Transmission Line Modelling (TLM) method can in general be used to model time-varying phenomena but they do not allow for the physical investigation of the problem. On the other hand exact analytical methods have been confined to a few special cases of infinite and semi-infinite media [1, 2] and slab waveguides [3].

This paper investigates a semi-analytical Time Domain Spectral Index (TDSI) technique [4] that enables efficient modelling of propagation of the optical signal through a time-varying rib waveguide and is suitable for predicting the chirp parameter. For the complex case of a time-varying dielectric waveguide, invariant in the z-direction, the solution of the wave equation yields waves (incident and reflected) having new frequencies and preserved wavenumbers. The new spatial wave distribution of the secondary waves is obtained by reversing the original spectral wave problem of the TDSI and solving for a new frequency. The amplitudes of all incident and reflected waves are solved using the Galerkin approach with triangular and Gaussian basis functions. The method is verified for cases of temporal dielectric change in an open region and a slab waveguide and then extended to include an air-clad waveguide. The method is applied to model the chirp parameter in a typical electroabsorption waveguide.

REFERENCES

1. Morgenthaler, F., "Velocity modulation of electromagnetic waves," *IRE Trans. On Microwave Theory and Technique*, 167–172, 1958.
2. Fante, R., "Transmission of electromagnetic waves into time-varying media," *IEEE Trans ons Antennas and Propagation*, Vol. AP-19, No. 3, 417–424, 1971.
3. Nerukh, A., P. Sewell, and T. M. Benson, "Volterra integral equations for nonstationary electromagnetic processes in time-varying dielectric waveguides," *J. of Lightwave Techn.*, Vol. 22, No. 5, 1408, 2004.
4. Bekker, E., A. Vukovic, P. Sewell, and T. M. Benson, "A novel hybrid approach for modelling of electroabsorption modulators," 7^{th} *International Conference on Transparent Optical Networks ICTON*, 147–151, 2005.

High-Q Photonic Crystal Microcavities in Diamond

S. Tomljenovic-Hanic[1], **M. J. Steel**[2,1], **and C. M. de Sterke**[1]

[1]University of Sydney, Australia
[2]RSoft Design Group, Inc., Australia

There has recently been great interest in optical microcavities based on photonic crystal slabs (PCS) [1–3]. Almost all of these studies consider a two-dimensional PCS composed of a hexagonal array of cylindrical air holes in a silicon dielectric slab ($n \approx 3.4$). In this study, the material chosen is diamond ($n \approx 2.4$) because of its unique possibilities for demonstrating quantum entanglement of N-V centres. The photonic crystal geometry is potentially advantageous in achieving entanglement, since it can enable strong confinement in cavities and optical coupling between different centres [4].

The quality factors of defects in PC slabs are strongly influenced by the position and widths of the photonic band gaps (PBG). Consequently, the first step is to design an infinite periodic structure without a cavity. Subsequently, the finite structure including the cavity defect can be optimized to obtain the highest quality factor possible. We find that the PBG widths of diamond PCS are comparable with silicon-based PCS whereas the positions of corresponding gaps differ. Consequently the in-plane quality factors for the two materials are similar, whereas the out-of-plane factor for diamond is smaller.

The optimization of optical cavity design, i.e., further tuning of the quality factor is possible by modifying the geometry of the lattice structure surrounding the cavity. For example Noda et al. constructed a cavity by three missing air holes in a row of a silicon slab with hexagonal lattice structure [1, 2]. They optimized the structure by shifting the left and right air holes outwards. We apply a similar method to the diamond based structure and find that high-Q microcavities can be designed in this material.

*This work was produced with the assistance of the Australian Research Council (ARC) under the ARC Centres of Excellence Program. CUDOS (the Centre for Ultrahigh-bandwidth Devices for Optical Systems) is an ARC Centre of Excellence.

REFERENCES

1. Akahane, Y., T. Asano, B. S. Song, and S. Noda, *Nature*, Vol. 425, 944, 2003.
2. Akahane, Y., T. Asano, B. S. Song, and S. Noda, *Opt. Express*, Vol. 13, 1202, 2005.
3. Srinivasan, K. and O. Painter, *Opt. Express*, Vol. 11, 579, 2003.
4. Salzman, J., S. Prawer, and D. Jamieson, *Photonic Crystal Devices and Systems in Diamond*, Provisional Patent, CCID 131000480.

Nonlinear Pulse Propagation and Modulation Instability in Periodic Media with and without Defects

V. Grimalsky[1], **S. Koshevaya**[2], **J. Sanchez-Mondragon**[1]
M. Tecpoyotl-Torres[2], **and J. Escobedo-Alatorre**[2]

[1]National Institute for Astrophysics, Mexico
[2]Autonomous University of Morelos, Mexico

The nonlinear propagation of EMW in periodic media is of great interest due to the possibility to accumulate energy in periodic media within the stop band and, therefore, the input intensity levels for observation of nonlinear phenomena are quite low [1]. For resonant interactions, also it is possible to realize matching conditions, which are not possible in uniform media. Some papers analyze both resonant multiwave interactions and self-action of EMW in nonlinear periodic media [1, 2]. As usually, the nonlinearity is assumed as moderate, and the nonlinear dynamics is described within a framework of coupled equations for slowly varying amplitudes of interacting waves. Also, a method based on a slow variation in time was proposed, which seems more adequate as ones based on coupled equations [3].

The presence of defects in periodic structure leads to narrow regions of transmission within the stop-band. In this case, the application of coupled equations for counter propagating waves becomes doubtful, and a more general approach is needed [3]. Also, the influence of defects on the dynamics of modulation instability of long pulses is of a great interest. The present paper considers numerical simulations of the pointed above phenomena. For a correct description of the nonlinear dynamics, it is necessary also to take into account the wave dissipation and possible transverse diffraction.

The results of simulations have been demonstrated an essential influence of defects within the periodic structure on the nonlinear propagation of EM pulses, even if the carrier frequency is chosen within the stop band of the structure with a defect. This can be explained by a quite wide spectrum of the input pulse, and the ? of such a spectrum is within the transmission region due to the defect. This situation is analogous to the nonlinear propagation of short spin-dipole waves in the vicinity of the cut-off frequency [4]. The dynamics of modulation instability also changes in the presence of the defect. The diffraction can affect essentially the modulation instability dynamics.

REFERENCES

1. Gupta, S. D, "Nonlinear optics of stratified media," *Progress in Optics.*, Vol. 38, 3–84, Elsevier, Amsterdam, NL, 1998.
2. Escobedo-Alatorre, J., J. Sanchez-Mondragon, M. Torres-Cisneros, R. Selvas-Aguilar, and M. Basurto-Pensado, "A device approach to propagation in nonlinear photonic crystal," *Optical Materials*, Vol. 27, No. 7, 1260–1265, 2005.
3. Scalora, M. and M. E. Crenshaw, "A beam propagation method that handles reflections," *Opt. Commun.*, Vol. 108, 191–196, 1994.
4. Burlak, G., V. Grimalsky, S. Koshevaya, and P. Marquez-A., "Dynamics of magnetostatic wave solitons in the vicinity of frequency cut-off," *Journ. of Magn. Magn. Mater.*, Vol. 237, No. 1, 97–103, 2001.

Nonlinear Vector Finite Element Simulation of Optical Photonic Devices

A. Fisher[1], **D. White**[2], **and G. Rodrigue**[1]

[1]University of California, USA
[2]Lawrence Livermore National Laboratory, USA

Continual research of new optical devices for use in the communication industry has led to the possibility of using the nonlinear optical response of various materials. Using these nonlinear effects, researchers have been designing switches, logic gates, and frequency generators with increasing complexity in both functioning and geometry. The high degree of complexity in functioning makes analysis of these devices through analytical approximation incomplete. Significant progress in understanding these devices has been made through the use of simulation using nonlinear Finite Difference Time Domain (FDTD) schemes. While the FDTD schemes are highly computationally efficient, the increasing geometric complexity of these devices is becoming a problem for the FDTD approach given its highly restrictive geometry constraints.

We present a nonlinear Vector Finite Element Method (VFEM) scheme that involves discretizing Maxwell's equations using Nedelec edge and face bases. The VFEM scheme is capable of simulating instantaneous third order nonlinear processes such as the the kerr effect, and four wave mixing. The VFEM scheme is also capable of handling the complicated 3 D geometries found in many of the newer optical photonic devices with a high degree of accuracy. Also, our VFEM scheme includes methods for reducing the high computational cost of nonlinear finite element methods, thereby making larger simulations possible.

In addition to presenting this new scheme, we will also present a series of tests to show that the scheme is capable of simulating the intricacies of optical photonic devices. These tests include simulations of classical nonlinear optical effects that can be compared with analytical approximations. The tests also include some comparisons to FDTD schemes on less complicated geometries. Finally, with a reasonable degree of confidence in the accuracy of the scheme, we will present novel simulations of some optical photonic devices.

Modelling of Bragg Gratings and Application in Cascaded Cavities

A. Melloni, F. Morichetti, and M. Martinelli
Politecnico di Milano, Italy

Nowadays advanced electromagnetic numerical methods and powerful computing availability allow the analysis of most of the optical structures and devices with a great accuracy. These methods (FDTD, FEM, ...) can be extremely accurate but often they are extremely time and memory consuming, especially if 3D structures are considered. Whilst an electromagnetic approach is undoubtedly convenient for the analysis of the linear behavior, for the non-linear analysis, synthesis and optimizations of more complex devices they are often of poor utility.

In this contribution we explain how an accurate modelling of a simple building block, like the Bragg reflector, can be of great aid in both linear and nonlinear analysis of complex circuits, such as cascaded coupled cavities. The concept of using an equivalent circuit instead of a more physical description of the device is well grounded in both electronic and microwave domain and can be applied advantageously also in the optical field.

A possible equivalent circuit of the Bragg grating shown in Figure 1(a) is composed by an ideal partially reflecting mirror (r, t, φ_0) placed between two sections of propagating regions (L_e, n_0), as shown in Figure 1(b). The reflectivity r and the equivalent length L_e can be determined analytically, numerically or experimentally [1].

In the nonlinear domain the equivalent circuit can powerfully maintain its validity, provided that the nonlinear coefficient of the two sections L_e is given by $n_{2e} = n_2 L_p / 2L_e$ where n_2 is the nonlinear refractive index of the material and L_p is the effective nonlinear length, defined as the distance over which the nonlinearity really acts. By integrating the electric field over the physical length of the grating, it is found that the nonlinear length is equal to the penetration depth $L_p = tanh(kL)/kL$, that is the group length (k being the grating coupling coefficient). To show the potentialities of such an approach, let's consider two cascaded cavities defined by three gratings (detailed data of the structure can be found in [2]). The spectral behavior in the linear regime of the whole structure is the bell-shaped response centered at 1.55 μm shown in Figure 2. As the input power increases, the spectral response shifts toward the right and deforms under the effect of the Kerr nonlinearity. For high power levels, a bistability region appears on the right side of the response, close to the band-edge. The nonlinear response, both in frequency and time domain, can be computed very efficiently and a comparison with results obtained with electromagnetic simulators show a very good agreement.

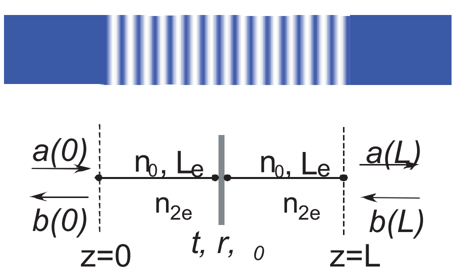

Figure 1: a) Generic bragg grating; b) its linear and nonlinear equivalent circuit.

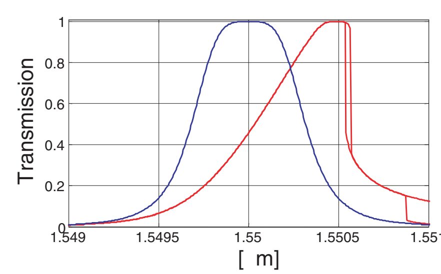

Figure 2: Spectral transfer function of two cascaded cavities in linear and nonlinear regime.

REFERENCES

1. Melloni, A., et al., "Equivalent circuit of bragg gratings and its application to fabry-perot cavities," *JOSA A*, Vol. 20, No. 2, 273–281, 2003.
2. *Slow-wave Task of the European COST Action P11–WG2*, http://w3.uniroma1.it/energetica/

Spectral-element Discontinuous Galerkin (SEDG) Simulations for Metallic Nanoparticles

M. Min and P. F. Fischer
Mathematics and Computer Science Division, USA

We present higher-order computational methods to study the dynamic nature of electromagnetic waves interacting with metallic nanoparticles where strong surface plasmon excitations can occur. In the study of light interacting with a nanoscale object, a particular computational issue is that the problem includes sharp discontinuities in the dielectric function along the surface of the nanoscale object. In such cases, standard lower-order methods such as FDTD method require considerable computational work in order to achieve a certain expected accuracy. The drawback comes from the slow rate of convergence of the methods for problems whose solutions have less regularity in smoothness. We propose to use higher-order numerical techniques with phase-preserving nature: a spectral-element discontinuous Galerkin (SEDG) method. The method is based on multidomain body-conforming approach. The exponential accuracy of this method without stair-stepping phenomena will be discussed. Computational performance of 3D structures and simulation for metallic nanosphere waveguide will be demonstrated.

Session 1P3a
Microwave Remote Sensing of Snow

Assessing the Impact of Measurement Spatial Resolution on Passive Microwave Observations of Snow from the Cold Land Processes Experiment

R. E. J. Kelly[1,2], **M. Tedesco**[1,2], **E. J. Kim**[1], **J. L. Foster**[1], **and D. K. Hall**[1]

[1]University of Maryland Baltimore County, USA
[2]NASA/Goddard Space Flight Center, USA

The NASA Cold Land Processes Experiment (CLPX) conducted in 2002 and 2003 provides a unique opportunity for hydrologic scientists to investigate snow hydrology processes from a multitude of ground, aircraft and satellite-based measurements. Aircraft passive microwave observations at 10, 18, 21, 37 and 89 GHz frequencies from NOAA's Polarimetric Scanning Radiometer (PSR) enable studies to be conducted that investigate the microwave responses from snow fields at different spatial scales.

In this paper, a study is described that uses CLPX PSR measurements at 10, 18 and 37 GHz to characterize the spatial variability of the passive microwave response of snow within three Mesocell Study Area (MSA) at medium to coarse spatial resolution scale lengths. PSR observations are spatially averaged to simulate instantaneous field of view observations ranging from 500 m to 25 km in size. Geostatistical analysis is applied to characterize the passive microwave response of snow in the three MSAs at each spatial scale. Ground-based snow field survey measurements made by CLPX scientists, and ancillary geospatial data sets of the MSAs (such as digital elevation models and vegetation cover) are combined in a simple model to represent snow depths and snow water equivalent fields. A geostatistical characterization of the survey-based fields is conducted and compared with the geostatistics of the multi-scale passive microwave scale observations. The effect of observing snow fields at different spatial resolutions, especially with respect to the impact on representativity of snow field variability, is discussed.

Spatial Scaling Behavior of Brightness Temperatures during CLPX and Appropriate Satellite Sensor Resolution

E. J. Kim[1] and M. Tedesco[2]

[1]NASA Goddard Space Flight Center, USA
[2]GEST-NASA Goddard Space Flight Center, USA

Accurate estimates of snow water equivalent and other properties play an important role in weather and hydrological forecasting and climate modeling over a range of scales in space and time. Such estimates also have important uses in natural hazard forecasting (e.g., melt-related floods) and water resource applications such as agriculture and hydropower, and there is a strong heritage for the retrieval of snow parameters using passive microwave remote sensing techniques.

Improving the spatial resolution of new passive microwave satellite sensors is a major desire in order to (literally) resolve subpixel heterogeneity effects on the accuracy of retrievals, but limited spacecraft and mission resources impose severe constraints and tradeoffs. In order to maximize science return while mitigating risk for a sensor concept, it is essential to understand the scaling behavior of snow in terms of what the sensor sees (brightness temperature) as well as in terms of retrieved quantities (snow water equivalent, SWE). NASA's Cold Land Processes Experiment-1 (CLPX-1: Colorado, 2002 & 2003) was designed to provide data to measure these scaling behaviors for varying snow conditions in areas with forested, alpine, and meadow/pasture land cover.

We will use observations from CLPX-1 ground, airborne, and satellite passive microwave sensors to examine and evaluate the scaling behavior of brightness temperatures and retrieved SWE across scales from meters to 10's of kilometers.

The conclusions will provide direct examples of the appropriate spatial sampling scales of new sensors for snow remote sensing. The analyses will also illustrate the roles and spatial scales of the underlying phenomena (e.g., land cover) that control subpixel heterogeneity.

SAR Remote Sensing of Snow Parameters in Norwegian Areas — Current Status and Future Perspective

R. Storvold, E. Malnes, and K. A. Hogda
Norut IT, Norway

S.-E. Hamran, K. Mueller, and K. Langley
University of Oslo, Norway

The paper present results from a series of European and national projects on remote sensing of snow parameters. Currently, SAR data are only available at C-band frequencies. Other frequencies such as L-band or Ku-band may be favorable in several contexts, but current C-band SAR data may still be used and further developed to a more mature level. In particular, the advent of wide swath SAR data has provided frequent data sets at medium spatial resolution, that can be used to monitor snow parameters operationally.

We will present results from a snow covered area monitoring service developed for Norway and Sweden. The service, which is based on Envisat ASAR wide swath data, produces snow cover maps on average 3–4 times per week. The resulting time series gives a unique data set for studying the snow cover as it rapidly retreats during the melting season, and is of high value to hydropower companies.

Snow water equivalent is the key parameter for hydrological applications. Several means to retrieve SWE from SAR data have been proposed. Norut IT has so far focused on using repeat pass interferometry to measure SWE since SWE change is directly proportional to the interferometric phase change. The technique has been demonstrated, but scarceness of usable interferometric baseline pairs has so far not allowed wide spread applicability of the technique.

A future SAR using Ku-band frequency as carrier will might solve the problem of retrieving SWE. Since backscatter at Ku-band frequency is more sensitive to SWE, it is likely that robust SAR methods can be invented for this purpose. It will, however, be extremely important for the scientific community to validate the retrieval algorithms against in-situ data. The authors have developed an innovative validation concept using Ground-penetrating radars at the same carrier frequencies as the space borne SARs to validate EO data in an efficient manner. The concept has been studied at C-band frequencies on glaciers at Svalbard, and we hope to build a similar platform for Ku-band frequencies, and this will be used to validate model based retrieval algorithms.

Electromagnetic Models for Passive Microwave Remote Sensing of Snow and Application to Experimental Data

M. Tedesco
GEST-NASA Goddard Space Flight Center, USA

E. J. Kim
NASA Goddard Space Flight Center, USA

Several electromagnetic models have been described in the literature for modeling radiometric signatures of snow-covered terrains. Understanding how each model simulates the radiometric behavior of a snowpack, exploring the conditions under which the different models display the best agreement can provide insights for developing retrieval techniques, as well as possible model improvements.

In this study, we use four widely-used electromagnetic models to simulate the brightness temperatures of six different snow classes at different frequencies and observation angles. The snow classes considered here account for a majority of the types of snow occurring in the northern hemisphere. The models considered are the following: a model based on Dense Media Radiative Transfer Theory, a model based on the Strong Fluctuation Theory, the Helsinki University of Technology (HUT) model and the Microwave Emission of Microwave Layered Snowpacks (MEMLS) of the Institute of the Applied Physics, Berne.

We discuss the different approaches taken by each model, the required input parameters and the sensitivity of the electromagnetic quantities involved (e.g., brightness temperatures, extinction coefficient) to the input parameters. We compare the brightness temperatures simulated by means of the electromagnetic models for the six classes and analyze the causes of the observed differences.

Finally, we drive all four models with snow parameters derived from recent field data (e.g., the NASA Cold Land Processes experiment) and evaluate the outputs against observed brightness temperatures observations.

Session 1P3b
Remote Sensing and Imaging

On the Analysis of Geophysical Networks from Multiscale DEMs

L. T. Tay, **B. S. D. Sagar**, **and H. T. Chuah**
Multimedia University, Malaysia

A lot of information can be extracted from digital elevation models (DEMs) and it offers scientists with invaluable information in terrain characterization. Regions with varied degrees of concavity and convexity represent various degrees of terrain complexities. These complexities explain various physiographic and geomorphic processes. The abstract structures of concave and convex zones represent the valley and ridge connectivity networks respectively. These two unique topological networks have immense use in characterizing the surficial terrain quantitatively via morphometry, hypsometry, allometric scaling and granulometry. The main objective of this paper is to present a method based on morphological transformations in extracting the network and fractal techniques in terrain characterization. We analyze the intereferometrically derived DEM of Cameron Highlands and Tioman region of Malaysia. Cameron Highlands region comprises a series of mountain stations at altitudes between 500 m and 1300 m whereas Tioman region is parts of an Island with altitude ranges from sea level to 500 m.

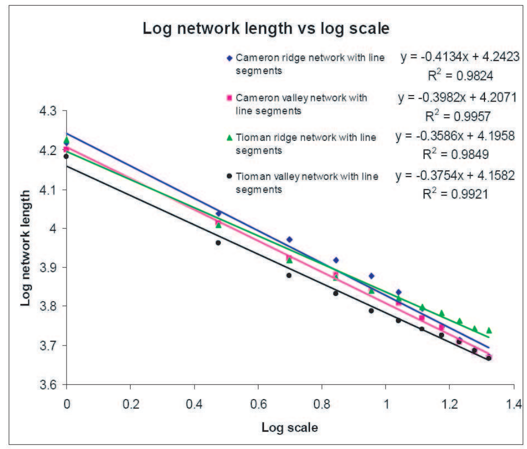

Figure 1.

We employ multiscale nonlinear morphological transformations to generate DEMs at multiple resolutions and to extract channel and ridge networks from these multiscale DEMs. We provide a simple scaling law from the relationship shown by considering the lengths of unique networks derived from multiscale DEMs as functions of radius of the structuring element. It is shown as a simple resolution-independent power-law dimension in the form of $l \sim r^{\alpha}$, where l and r denote length of network at different scale and radius of structuring element respectively. α as the scaling exponent, is the fractal dimension of network. This relationship depict that similar trends have been followed for both ridge and valley connectivity networks and describes the scaling properties of the terrain where the density of the networks decreases as the resolution decreases. The plot of network lengths as functions of radius of structuring element is in logarithm values (figure below). The gradients of best fit lines of these plots indicate that the rate of change in the lengths of the networks, across multiple resolutions. The complexities and intricacies of valley and ridge network change with various types of topography, therefore network length is considered as an important parameter for complex geometry of valley and ridge. We prove that hilly terrain (Cameron Highland region) possesses higher value of exponent as compared to non-hilly terrain (Tioman region). The reason is the rate of change in elevation of hilly terrain across resolution is higher than non-hilly terrain. Relatively, the network intricacies will change more rapidly for hilly terrain. Further analyses of these two networks provide the morphologies of convex ones and hillslopes. The length criterion and fractal dimensions of networks can be used as a powerful criterion for the classification among sub-basins in a large basin. Basins with different topography structure have different network geometry and densities. Emerging river network patterns can be considered to relate with basic underlying physical mechanisms involved in the formation of landscapes of varied complexities. The differences will be reflected by the fractal dimension as this exponent is computed based on network densities across multiple scales.

Buried Cylinders Geometric Parameters Measurement by Means of GPR

B. A. Yufryakov and O. N. Linnikov
Scientific and Technical Centre of System Modeling, Russia

In [1, 2] the method for estimation of cylindrical objects radii based on results of selected contour reflected signals hyperbolic approximation was proposed. The velocity of signal propagation is considered as known and direct least-square method of hyperbolic adjustment for 2D-radarogramms is used.

In this paper the interactive technique of 3D-data processing is proposed. It allows to estimate simultaneously the velocity of signal propagation in the medium and parameters of cylindrical objects, i.e., orientation, radius, length and depth of occurrence. Operator participation in data processing allows to smooth the errors of reflected signal registration and to obtain exact and visual representation of hidden cylindrical objects.

The technique proposed is based on frontal method of GPR 3D-data interpretation [3]. This technique selects from the whole bulk of registered GPR data the first arrival of wave fronts from the recorded signals reflected from objects. These selected surfaces in the signal space will be referred to as frontal hodographs.

For frontal hodographs of cylindrical objects in interactive regime of GPR data analysis it is possible to select sections being orthogonal to cylinder axe. These sections are hyperbolas, their form define unambiguously the velocity of signal propagation in the medium V, cylinder radius r and depth of occurrence h. However, modest accuracy of frontal hodograph registration does not allow to use these functional dependence directly. Therefore it is proposed to operator to select approximating hyperbola by means of software tools. The parameter set V, r and h which gives the best approximation will be the set of measured parameters. Such technique can be easily used both for monostatic and for bistatic systems. Vertical section through hyperbola vertex will show the space location of cylinder axe (azimuth angle θ and tilt angle φ), as well as cylinder length.

The technique developed is realized in the GPR software module "Defectoscope" [4]. In the paper the results obtained by this technique in real measurements for various cylinders in the box with sand are presented.

The parameters of cylindrical objects measured by this technique can be used both for immediate interpretation of observed objects and for automatic formation of objects reflecting surfaces on their frontal hodograph according to [3].

REFERENCES

1. Shihab, S., W. Al-Nuaimy, and A. Eriksen, "Radius estimation for subsurface cylindrical objects detected by ground penetrating radar," *Tenth Intern. Conference on Ground Penetrating Radar*, Delft, The Netherlands, 319–322, June 2004.
2. Al-Nuaimy, W., S. Shihab, and A. Eriksen, "Data fusion for accurate characterisation of buried cylindrical objects using GPR," *Tenth Intern. Conference on Ground Penetrating Radar*, Delft, The Netherlands, 359–362, June 2004.
3. Yufryakov, B. A., B. S. Surikov, Y. G. Sosulin, and O. N. Linnikov, "A method for interpretation of ground-penetrating radar data," *Journal of Communications Technology and Electronics*, Vol. 49, No. 12, (English Translation of *Radiotekhnika i Elektronika*), 1342–1356, December 2004.
4. Andryukhin, A. N., O. N. Linnikov, V. N. Trusov, B. A. Yufryakov, V. Y. Bodrov, and Y. G. Sosulin, "Pulse GPR with optoelectronic sensor," *Tenth Intern. Conference on Ground Penetrating Radar*, Delft, The Netherlands, 187–190, June 2004.

Automatic Ground Clutter Rejection Processing Using Doppler-angle Domain Image Features Based Processing (DAIP)

H. Deng
The University of North Texas, USA

For airborne radar systems, the ground clutter received through antenna sidelobe poses a serious threat to effective ground moving target detection. Traditionally Space-Time Adaptive Processing (STAP) is widely used in airborne radar system for ground clutter and jammers. The joint space-time processing is necessary for ground clutter rejection because the ground clutter couples between space domain and time domain due to the platform movement. However, successful implementation of STAP requires accurate estimation of the clutter covariance matrix in real time. The "training" data used for clutter estimation is normally obtained by sampling the secondary units that are spatially adjacent to the primary detection unit with the assumption that the clutters in the primary and secondary units are statistically Independent and Identically Distributed (IID). Since the ground clutter is inhomogeneous in nature, finding sufficient IID secondary data for clutter estimation poses the most serious challenge to successfully implementing STAP algorithm. In this work, a novel Doppler-Angle domain Image feature based Processing (DAIP) technique is to be developed for effective ground clutter rejection processing without using secondary data. The airborne radar system collects the echo data in space-time domain by transmitting multiple coherent pulses and receiving data from each element of an antenna array. STAP suppresses interference by "whitening" interference signals and further integrates target signal through two-dimensional matched filtering in the time-space domain. The proposed DAIP, however, transforms the collected time-space data directly into the Doppler-angle domain; hence, both target signal and interferences are coherently integrated through the transform. The discrimination processing of target and interference signals for target detection is performed based on their different features on the Doppler-angle plane without actually filtering out interference signals.

The target signal is a concentrated point in the transform domain. Jammer signals on the Doppler-angle plane are straight lines parallel to the Doppler axis. Ground clutter on the plane is normally a tilted ridge or even multiple parallel ridges dependent on the ratio of the platform moving speed to the radar Pulse Repetition Frequency (PRF). The thermal noise is statistically uniformly spread in the Doppler-angle plane through the 2-D Fourier transform. Therefore, in the Doppler-angle domain, the structure of target signal is conspicuously different from that of ground clutter or jammer, i.e., target signal is concentrated and interferences are extended. It is further noted that moving target signal generally does not overlap with clutters on the Doppler-angle plane because of their different Doppler frequencies. Hence, based on the above observations DAIP algorithm is to be developed for automatic rejection of ground clutter. The first step of DAIP is to transform radar data collected in the space-time domain to an image in the Doppler-angle domain through two-dimensional Fourier transform. Subsequently, a clamping processing is applied to all pixels of the transformed images to remove the white noise. Following the clamping processing, the remaining non-zero pixels are either target signals or interferences (clutter or jammer). The feature extraction of the clamped image is carried out by clustering non-zero pixels into pixel blocks consisting of consecutively connected non-zero pixels through an image segmentation algorithm called region growing. With the segmentation processing, the image becomes a collection of pixel blocks that are either target or interference. Target detection for a pixel block is based on pixel concentration level, which may be measured by a metric called block size.

The processing results in the work indicate that DAIP can effectively reject ground clutter and detect ground moving targets based on distinguishing features of target and interference in the Doppler-angle domain. Without requirement of estimating clutter covariance, DAIP is particularly suitable for applications in highly inhomogeneous or unknown clutter environment.

InSAR with Multiple Baselines—Comparison of Height Retrieval and Phase Unwrapping Techniques

M. C. Yeung[1], **W. D. Wong**[1], **B.-I. Wu**[1], **Y. Hara**[2], **and J. A. Kong**[1]

[1]Massachusetts Institute of Technology, USA
[2]Mitsubishi Electric Corporation, Japan

This study investigates both interferometric SAR (InSAR) post processing height retrieval techniques as well as phase unwrapping techniques when we use three satellites (and hence three baselines). Potential advantages of this configuration are explored and compared with the original 2-satellite method. For height retrieval, 3 methods were compared. The first approach is data averaging—3 interferograms retrieved per look are grouped into pairs, with the 2 best selected to be averaged to produce a better estimate of the digital elevation map (DEM). The second approach is the unambiguous range magnification (URM) method, which expands the unambiguous wrapped phase range by taking advantage of the observation that phases for different satellites wrap at different rates because of different distances and geometries relative to the same terrain pixel. Thus, the wrapped phase range is increased multiple fold from 2π without doing any phase unwrapping. This eases the reliance on phase unwrapping when performing height retrieval. The third approach is the maximum likelihood estimator (MLE), which uses URM to predict the closest phase estimate which best fits most of the data sets available.

It is shown that for multiple flyover looks, the data-averaging method is an efficient and computationally inexpensive method to obtain improved retrieved heights. The MLE technique is asymptotically favorable over the data averaging method, which may or may not be the case in a real situation. The URM method performs the worst among the 3, since it relies on the shortest baseline for unwrapping—unfortunately, the shortest baseline is most susceptible to noise.

For 3D phase unwrapping, we introduce the 3D Projection method, which uses the geometry of the satellite configuration to create constraints for the values of the phase differences. Noise, which moves phase points away from the "line segments" which define such constraints, can be filtered out if we manually adjust the phases such that they once again obey the constraints. The results show that this method works better than if such a processing step was not taken.

Effect of Rain on Zenith Path Sky Noise Temperature at 29.9 GHz at Tropical Site Amritsar

P. Sharma
Guru Nanak Dev University, India

I. S. Hudiara
KC College of Engg., India

M. L. Singh
Guru Nanak Dev University, India

Rain has long been recognized as the major and foremost factor that causes fading of wireless communication systems. The effect is dependent on the various factors such as the site (location of the communication link or satellite), frequency of the operation, and of the elevation. The present communication is an abstract from the long term microwave propagation measurement program being going at CRL, GNDU, Amritsar since 2001.

Here the results in the form of rain rate and corresponding variation in sky noise temperature have been presented. The corresponding values of the zenith path attenuation have also been derived.

The rain rate has been measured with tipping bucket type rain guage having resolution 0.254 mm and corresponding sky noise temperature with zenith looking Dicke type radiometer at 29.9 GHz installed at CRL, GNDU, Amritsar, Punjab, India.

Enhanced Detection and Classification of Buried Mines with an UWB Multistatic GPR

A. J. Dumanian
MIT Lincoln Laboratory, USA

C. Rappaport
Northeastern University, USA

We present a resonance-based classification technique for the identification of plastic-cased antipersonnel (AP) land mines buried in lossy and dispersive soils under rough surfaces by a stepped-frequency ultra-wideband (UWB) downward-looking ground penetrating radar (GPR) with an array of receivers. For this application the multistatic ground probing sensor is positioned just above the ground surface and operates from UHF to C-Band frequencies. Novel physics-based models based on the finite difference frequency domain (FDFD) technique simulate the characteristic resonating multi-aspect target frequency responses for several realistic buried land mine detection scenarios. Matched filter detection results are presented which assess the GPR's performance in identifying a simulated mine buried under a rough surface at varying depths in dry sand and a dispersive clay loam soil from other false targets such as buried rocks.

*This work was sponsored by the Department of the Air Force under Air Force Contract No. FA872105-C-0002 and by CenSSIS, the Center for Subsurface Sensing and Imaging Systems under the Engineering Research Centers Program of the National Science Foundation (Award EEC-9986821). Opinions, interpretations, conclusions, and recommendations are those of the author and are not necessarily endorsed by the United States Government.

Electrical Properties of Titan Surface from Cassini Scatterometer and Radiometer Measurements

H. A. Zebker and L. Wye
Geophysics Stanford University, USA

We observe Titan, Saturn's largest moon, using active and passive microwave instruments carried on board the Cassini spacecraft. The 2.2-cm wavelength penetrates the thick atmosphere and provides measurements at resolutions from 10-200 km over much of the moon surface. Here we seek to explain Titan's simultaneous high reflectivity and high emissivity, using a layered model in which a gray body emissive material is overlain by a nearly lossless but complex icy layer. The lossless layer is required to produce the high radar returns through coherent backscattering, while the absorptive substrate is needed to produce high radiative temperatures. We use angle diversity to separate a Hagfors? like surface scattering term from a diffuse volume scattering term in the radar echo, and retrieve dielectric constants ranging 1.5 to greater than 3 for much of the surface. The specular term also yields surface slope distributions from a few degrees rms to greater than 15 degrees in different regions. The reduction of the radiometry data also gives dielectric constants over the same range, but the average properties of Titan favor the lower values. Dielectric constants of 1.7 are indicative of frozen hydrocarbon materials such as methane or ethane, while water ice has a dielectric constant of 3.2. If the surface is composed largely of water ice, it would have to be unconsolidated material such as snow where the bulk electrical properties are reduced by the fractional volume of material. Many small scale features are seen and differ both in emissivity and reflectivity from the average values, and likely give clues to the nature of geologic processes occurring on the surface.

Preliminary Detection of the Dangerous Meteorological Phenomena and Selections Closed Objects by the Help Radar with Variable Polarization

A. B. Shupiatsky
141700 Moscow Region, Dolgoprudny, Russia

The review of theoretical and experimental studies of meteorological events and reflections from ground and structures on it, covered by deposits, fogs and other meteorological object by dual-polarization radars are presented. Theoretical and experimental foundations of the polarization methods of detecting dangerous weather phenomena are made. Theoretical models of polarization characteristics (linear and elliptical) of radar signals from different kinds of clouds and precipitation are worked out and described. From common case of elliptically polarization is shows sensibility echo signal from microstructure of reflected particles. A choice of optimal polarization may by make.

Algorithms of the detection of a variety of hydrometeors and optimal polarization are discussed. Creation of algorithms of connection of microstructure and dangerous weather phenomena with polarization characteristics of radar signals are presented. Requirements to the equipment and up-dating of existing radars are formulated. These algorithms and requirements were realized on basis of polarization airborn and ground dual-polarization weather radars. These diversity-polarization radar are described.

Methods and means for remote detection of pre-storm state, increased electrical activity, zones of icing , hail and shower clouds, heavy precipitation, turbulence and other weather phenomena and conditions which are dangerous for flights of air vessel and human activities. It is necessary to note one more important developed direction in polarizing radiometeorology. It is a bistatic mode of reception of signals. With this mode considerably extends information of the polarizing characteristics of a signal. Theoretically and experimentally is shown, that with reception of signals not only with a return corner of dispersion of 180 degrees, but also in a general case with other corners of dispersion, volume of the information about reflecting object considerably extends. So from the point of view of meteorological tasks the detection of large particles in a cloud, spectrum of their distribution, phase structure is possible. The theoretical substantiation developed a technique and the equipment for realization of this mode of operations is resulted.

The prospects of application SAR in radiometeorological researches are discussed. One of the basic advantages of such aerials are an opportunity to operate the form of the diagram of a direction, to form some diagrams of the various form, that is very important with sounding volumetric diverse meteorological objects. Thus the high speed of scanning, opportunity of adaptation to varying external conditions for example, formation of failures on interfering reflections, opportunity is reached many functional of use, that is simultaneous maintenance of search, detection and support of various objects. So, the application of SAR in meteorological researches allows:

1. Quickly to translate the diagram of a direction from one part meteorological object on other or on other close located object, that is very important for comparison with evolution of a cloud especially with artificial influences.
2. Opportunity of adaptation to quickly varying conditions.
3. It is essential to raise resolution in space.
4. To operate during supervision the form of the diagram of a direction and quantity petals of it, that allows to minimize unnecessary reflections and to allocate researched object.

There are also other important qualities of use of SAR in meteorology. However these aerials are complex and also main while expensive for meteorological researches. Nevertheless progress in development and use of such aerials is obvious.

Apparently Abnormal Satellite Thermal Signals of Infrared Band as a Thermal Plateau on the Sea Surface

S. Nakamura
Kyoto University-Retired/Geophysical Advisor, Japan

The author has had studied about the thermal pattern as a thermal plateau or a pinnacle which was obtaibed by a directly monitoring of the satellite signals. A dynamical model is introduced for realizing this thermo plateau on the sea surface. A supporting thermal pattern is shown as well as the related meteorological data.

Session 1P4
Recent Advances in Bioelectromagnetics Research on Mobile Telephony and Health

Recent Advances in Bioelectromagnetics Research on Mobile Telephony and Health — An Introduction

S. Lang
Nokia Corporation, Finland

By the end of year 2005, it has been estimated that there will be about two billion mobile subscriptions and by the year 2010 the amount will increase up to about three billion. Huge advances have been made in the research and development in the wireless communications technology during the past two decades. However, the rapidly increased use of mobile phones and establishment of mobile base station networks has led to concerns that radiofrequency (RF) energy could possibly cause some unexpected adverse health effects in humans. It has been suggested, for example, that mobile phone use induces brain tumors or promotes brain cancer development, or have other unknown effects on central nervous system. These concerns have led to extensive media debates and also — sometimes — hasty sciencepolitical decisions to initiate extensive biomedical research programs in several countries around the world.

It is not widely known that biological and health effects of RF energy have been studied for about 60 years. Currently, there are about 1500 published studies related to RF health research, covering various disciplines from biophysics to epidemiology, usually defined as bioelectromagnetics research. Moreover, there are about 200 studies ongoing and about 100 reported but not published. All these studies can be found at WHO EMF database (http://www.who.int/peh-emf/en/). Current safety guidelines, such as established by the International Commission on Nonionizing Radiation Protection (ICNIRP) and IEEE, are based on this extensive research database. No adverse health effects have been shown to occur below these science-based safety limits.

Recent advances in multidisciplinary bioelectromagnetics research addressing mobile telephony and health issue have significantly increased our knowledge about fundamental scientific questions in this area. Improved dosimetry and exposure design have made it possible to conduct well-controlled biomedical experiments. Several carefully conducted theoretical biophysical analyses have also increased our understanding about the responses of cell macromolecules to RF energy. However, inconsistent molecular biological findings have raised questions whether the observed changes are real and whether they have any significance on human health. In this regard, part of the biomedical research community has forgotten a fundamental rule that an observed effect cannot be considered established if it has not been independently replicated and confirmed by other researchers. RF energy — cancer link has been rejected by recent carefully conducted animal studies. However, inconsistent epidemiological findings and misinterpretation of epidemiological data continue to create confusion in mobile telephony — cancer debate in many countries.

There are also other relatively intensive arguments ongoing, which interest many stakeholders, including general public, scientific community, massmedia, governmental regulatory bodies, politicians, and industry. A few popular ones are: does mobile phone use affect human brain electrical activity, are children more vulnerable to RF exposure than adults, do base station RF emissions possess a health risk to humans, are there any RF signal-specific effects. In these debates it is — unfortunately — often overlooked what rigorous scientific findings tell us and what is just anecdotal evidence.

RF Interactions with Biological Molecules and Processes: Quantifying Thermal and Non-thermal Mechanisms

A. R. Sheppard
Loma Linda University, USA

Electromagnetic fields can have direct effects on mobile ions, atoms, and molecules within mechanism-specific constraints for field strength, temporal scale, and spatial dimensions. Threshold conditions for several mechanisms can be estimated from the field magnitude, frequency, and modulation that might satisfy criteria for biophysical interactions of potential physiological significance. The vast parameter space over which technological devices operate indicates the need for fundamental approaches that could apply to many of the established and speculative biophysical mechanisms.

Temperature is a fundamental parameter of biochemistry. It also is the most comprehensive and best-established measure for effects on whole organisms and small regions of tissue. "Microthermal" effects occurring over small distances and lasting brief times have been proposed as a way to focus heating at microscopic and molecular scales. However, thermal diffusion limits temperature changes over cellular dimensions to $\approx 10^{-12}\,K$, even for the extremes of exposure obtainable with common devices. For many years, laboratory reports of differences between the biological effects of CW vs. pulsed and amplitude-modulated RF have stimulated interest in modulation-dependent mechanisms. Heating, which is proportional to E^2 or H^2, is inherently non-linear and could be a basis for some demodulation of pulsed or amplitude modulation at low rates, but the controversial effects reported with definitively non-thermal exposures require other mechanisms, particularly above ≈ 1 to 10 MHz where nonlinearities of transmembrane ionic flux become insignificant [1–3]. The principles of thermodynamics show that various nonlinear interactions between a RF field and a biological system produce characteristic spectral signatures that could be detected by spectroscopy with exceptionally high sensitivity [4]. For example, for a proposed experiment, a detection sensitivity of -127 dBm in an experimental cavity corresponds to ≈ 10 to 100 photons/s/cell at a nonlinearly-produced 1^{st} harmonic [5]. This sensitivity suggests that if harmonic and other frequency signatures of nonlinearity are absent, the nonlinearities of biological matter are so weak that physiological effects are unlikely.

In general, phenomena reported at nonthermal power levels imply the existence of resonant absorption, such as in rhodopsin where a tuned response underlies the high photon efficiency of vision. Similarly, tuned absorption in the RF range would indicate greater sensitivity than thermal absorption, which occurs over a broad bandwidth. Quantitative models and experiment show that such resonances cannot occur below the low-infrared region, particularly because of damping by macromolecular collisions with water molecules [6].

Mechanisms that are inherently statistical, such as stochastically altered binding to DNA, allow estimates for the probability of consequences from the long-term accumulation of rare effects. Assuming an Arrhenius process, even integrating low probability events over years yields so few errors that it would be impossible to detect them against normal background errors.

*Supported by MMF, Motorola, Nokia.

REFERENCES

1. Pickard, W. F. and Y. H. Barsoum, *J Membr Biol*, Vol. 61, No. 1, 39–54, 1981.
2. Barsoum, Y. H. and W. F. Pickard, *Journal of Membrane Biology*, Vol. 65, 81–87, 1982.
3. Pickard, W. F. and F. J. Rosenbaum, *Mathematical Biosciences*, Vol. 39, 235–253, 1978.
4. Balzano, Q. and A. R. Sheppard, *Bioelectromagnetics*, Vol. 24, No. 7, 473–482, 2003.
5. Balzano, Q., *Bioelectromagnetics*, Vol. 23, 278–287, 2002.
6. Prohofsky, E. W., *Bioelectromagnetics*, Vol. 25, No. 6, 441–451, 2004.

Research of Interactions of EM Field and Biological Systems

J. Vrba[1], **L. Vannucci**[2], **P. Peschke**[3], **J. Kvěch**[4], **J. Kubeš**[5], **F. Vozeh**[6], **and M. Vojtisek**[7]

[1]Czech Technical University, Czech Republic
[2]Institute of Microbiology, Czech Republic
[3]German Cancer Research Institute, Germany
[4]FN Motol, Czech republic
[5]Institute of Radiation Oncology in Prague, Czech Republic
[6]Charles University, Czech Republic
[7]National Institute of Health, Czech Republic

Abstract: Paper deals with new results obtained by several research projects in the field of interactions of EM field and biological systems.

1. Introduction: In present time 4 research institutions in the Czech Republic run research projects focused on studies of interactions between EM field and biological systems. In this contribution we would like to give more details about that projects and obtained results —both technical (i. e., developed exposition systems) and biological as well.

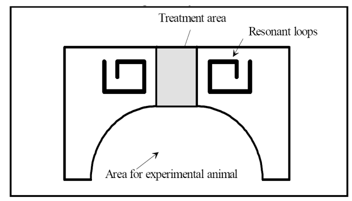

Figure 1: Arrangement of discussed microwave hyperthermia applicator.

Three of that projects (1 in Germany and 2 in Czech Republic) are basic research for simulation of the microwave hyperthermia treatment. Other two project are focused on simulation of the case of exposition by mobile phone.

2. Applicator for German Project: The main goal of the planned biological experiment is a hyperthermia treatment of the experimentally induced pedicle tumours of the rat to verify the feasibility of ultrasound diagnostics and magnetic resonance imaging respectively to map the temperature distribution in the target area of the treatment. That means to heat effective volume of approximately cylindrical shape (diameter approx. 2 cm, height approx. 3 cm). Temperature to be reached is $41°C$ or more (i. e., temperature increase of at least $4°C$ from starting point $37°C$), time period of heating is 45 minutes.

Considering the necessary effective heating depth for the planned experiments, we have found 915 MHz to be suitable frequency. As an excellent compatibility of the applicator with non-invasive temperature measurement system (ultrasound or NMR) is a fundamental condition for our project, we should have to use non-magnetic metallic sheets of minimised dimensions to create the conductive elements of the applicator. Therefore the applicator itself (see Fig. 1) is created by two inductive loops tuned to resonance by capacitive elements [4, 5]. Dimensions of these resonant loops were designed by our software, developed for this purpose. Coupling between coaxial feeder and resonant loops (not shown in Fig. 1) as well as a mutual coupling between resonating loops could be adjusted to optimum by microwave network analyser.

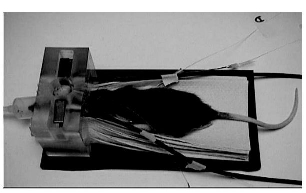

Figure 2: Photograph of the discussed applicator.

The position of the loops is fixed by perspex holder. There is a special cylindrical space for experimental animal in lower part of this perspex holder. As the heated tissue has a high dielectric losses, both loops are very well separated and so no significant resonance in heated area can occur. From this follows, that either the position of the loops with respect to heated area or the distance between the loops is not very critical.

First measurements to evaluate the basic properties of the discussed applicator were done on agar phantom of muscle tissue:

- evaluation of basic microwave properties (transfer of EM energy to the ?
- evaluation of compatibility with US and NMR,
- calculation and measurement of SAR and temperature distribution and its homogeneity.

An Initial Approach to *in Silico* Bioelectromagnetics for RF Exposures

J. C. Weaver, T. R. Gowrishankar, A. T. Esser, D. A. Stewart, K. C. Smith, and Z. Vasikoski
Massachusetts Institute of Technology, USA

Introduction. Our group has developed an initial capability for creating and solving single cell and multicellular models that involve interactions with nonionizing electromagnetic fields from essentially dc to ~2 GHz, and estimates of biochemical change. Interactions can range from weak (e.g., animal navigation, environmental exposures at power line frequencies) to strong (e.g., some telecommunication waveforms, conventional and supra-electroporation with potential medical applications). **Methods.** Our approach involves interactions on multiple spatial scales (e.g., molecules and membranes, cellular organelles, single cells, multiple irregular cells in close proximity, tissue level and whole body) and temporal scales of ns to hours [1–5]. The biological system models consist of a large number of interconnected models. The purpose is estimating field-induced biochemical change, using local models for candidate biophysical mechanisms that couple the field to ongoing biochemical processes. *In silico* (computer-based) assessments can provide rapid, approximate information for large numbers of exposures with different magnitudes and waveforms, a capability partly analogous to high throughput screening. **Results.** We have achieved an initial modeling/screeing capability that is applicable at the multicellular, cellular and subcellular levels. Solutions to a biological system model: (1) describe the microscopic field redistribution due to the applied field (microdosimetry), and (2) estimate the biochemical change due to biophysical mechanisms assigned within the system model. Our microdosimetry models can be combined with anatomic whole body models developed by others for macrodosimetry (typically ~ mm scale) in humans and laboratory animals. This approach can aid the design and interpretation of experiments involving biological effects of nonionizing electromagnetic fields ranging from dc to microwave frequencies. This provides the possibility of preliminary exposure assessment for many different waveforms *in silico*. The estimated biochemical change due to a particular electromagnetic field exposure is based on known biophysical mechanisms (presently heating, voltage-gated channels and electroporation; others can be added). This allows competing in uences to also be considered quantitatively with initial testing of a hypothesis that a particular biophysical mechanism might cause a biological effect [6]. **Support.** NIH grant RO1–GM63857 and a AFOSR/DOD MURI grant on Subcellular Responses to Narrowband and Wideband Radio Frequency Radiation.

REFERENCES

1. Gowrishankar, T. R. and J. C. Weaver, "An approach to electrical modeling of single and multiple cells," *Proc. Nat. Acad. Sci.*, Vol. 100, 3203–3208, 2003.
2. Stewart, D. A., T. R. Gowrishankar, and J. C. Weaver, "Transport lattice approach to describing cell electroporation: use of a local asymptotic model," *IEEE Transactions on Plasma Science*, Vol. 32, 1696–1708, 2004.
3. Gowrishankar, T. R., C. Stewart, and J. C. Weaver, "Electroporation of a multicellular system: asymptotoic model analysis," *Proceedings of the 26th Annual International Conference of the IEEE EMBS 2004*, 5444–5446, San Francisco, 2004.
4. Gowrishankar, T. R., D. A. Stewart, G. T. Martin, and J. C. Weaver, "Transport lattice models of heat transport in skin with spatially heterogeneous, temperature-dependent perfusion," *Biomed. Eng. Online*, Vol. 3, 42, 2004.
5. Stewart, D. A., T. R. Gowrishankar, and J. C. Weaver, "Skin heating and damage by millimeter waves: Theory based on a skin model coupled to a whole body model (in preparation)."
6. Vaughan, T. E. and J. C. Weaver, "Molecular change signal-to-noise criteria for interpreting experiments involving exposure of biological systems to weakly interacting electromagnetic fields," *Bioelectromagnetics*, Vol. 26, 305–322, 2005.

FDTD Calculations of Specific Energy Absorption Rate in a Seated Voxel Model of the Human Body

R. P. Findlay and P. J. Dimbylow
Health Protection Agency, UK

Finite-difference time-domain (FDTD) calculations have been performed to investigate the frequency dependence of the specific energy absorption rate (SAR) in a seated voxel model of the human body. The seated model was derived from the anatomically realistic voxel phantom NORMAN in the standard standing position with arms to the side. Exposure conditions studied were vertically polarised plane-wave electromagnetic fields between 10 MHz and 3 GHz. The frequency range chosen incorporates the whole-body SAR resonance region. The resolution of the voxel model was 4 mm for frequencies below 100 MHz and 2 mm for those above this. Additionally, the 4 mm and 2 mm calculations were overlapped in the 100 MHz to 300 MHz range to investigate the dependence of SAR on voxel resolution. A reduction in the voxel size from previous work at 4 mm allowed the whole-body SAR to be calculated at these higher frequencies.

SAR values are presented as a function of frequency. Results show that the whole-body SAR resonance peak for the seated adult model occurs at a higher frequency and is less well defined than that of the standard standing adult phantom. Additionally, in the sitting posture a second, smaller resonance peak is found to occur at a slightly higher frequency than that of the main resonance condition. Layer absorption plots and images of SAR absorbed in individual voxels demonstrate the way in which the body, when in a sitting posture, absorbs the incident electric field at these frequencies.

Use of Anatomically Correct Head Models and Higher Dielectric Values to Study SAR Difference between Children and Adult's Head and Eye Tissues

J. Keshvari and S. Lang
Nokia Research Center, Finland

The increasing use of mobile communication devices, especially mobile phones by children, has triggered discussions whether there is a larger radio frequency (RF) energy absorption in the heads of children compared to that of adults.

There have been many studies investigating SAR in child and adult heads using various exposure scenarios and head models. Most of the researchers investigating SAR in the head of adults and children have used down-scaled adult head models to represent the child head. Use of down-scaled head models in the calculation of SAR and temperature has been criticized frequently indicating that a down-scaled adult head model cannot reliably represent a child head when investigating the RF energy distribution. All of those studies have assumed the same value for dielectric parameters in child and adult head models. These are criticized in scientific communities by many researchers commenting that, children organs are not fully developed, they differ not only from anatomical point of view but also their tissue composition is different, with higher water content. Therefore, use of down-scaled head models and same dielectric values may give rise to incorrect exposure assessment and misleading conclusions in terms of health risk assessment.

The aim of this presentation is:

- To compare SAR in 4 different anatomically correct MRI based head models using the same dielectric values for all models.
- To compare SAR in 3 different anatomically correct MRI based head models when the dielectric values are increased from 5 to 20%.

A series of FDTD simulations were carried out to study the localized volume-averaged SAR distribution in 4 different MRI based head models.

The main finding of this study is that the distance of antenna from the exposed tissue, tissue composition and anatomical differences between head models can explain differences in the RF energy absorption between anatomically correct MRI-based adult and child models. In the case of eye region exposure, both anatomical parameters and tissue composition differences between the models affect the calculated SAR levels. Moreover, the results show that the head size does not appear to be a key parameter in the near-field RF exposure. In summary, there is no systematic difference in the RF energy absorption between anatomically correct MRI-based child and adult head models.

Increasing conductivity or both conductivity and permittivity at the same time would not necessarily cause an increase in SAR. In many cases the SAR decreases. Same increase in dielectric value would not cause same SAR variation in different models (individuals). The SAR variation because of increase in dielectric values is very much dependent on the anatomy and tissue layer composition of the exposed region.

Overview of RF Genotoxicity Research

M. L. Meltz
University of Texas Health Science Center at San Antonio, USA

One of the major issues in the area of electromagnetic field bioeffects is whether or not radiofrequency radiation, in the range of frequencies being used in wireless technologies and mobile/cell telephones, is genotoxic. While there have been a number of reviews, including those which present relative numbers of positive versus negative results, one of the most extensive reviews was that published in December, 2003 [Meltz, M. L., "Radiofrequency Exposure and Mammalian Cell Toxicity, Genotoxicity, and Transformation," Bioelectromagnetics 6: S196–S213]. This review went beyond comparing pluses and minuses, and addressed technical deficiencies found in many of the published papers. Genotoxicity has been of significant importance in the chemical and drug industries; positive results observed in validated in vitro assays are a signal to manufacturers (and regulators) that the chemical/drug they are hoping to develop (or which is already in the environment) has at least the potential to cause mutations in cells in vivo. This suggests that the chemical therefore has the potential to be an initiator in the carcinogenic process, although this may or may not lead to a tumor in an animal, and further may or may not lead to a tumor in a person. A positive result in one in vitro assay is never by itself enough to make a decision; in addition, exposure of animal models to gain additional information about tumor formation before making a decision about carcinogenic potential is considered essential. The results of the above listed paper, which examined data from studies up to and including those published in the year 2002, was that the overwhelming weight of the evidence did not support the hypothesis that RF exposures at different frequencies and exposure levels (SARS) caused toxicity, genotoxic (DNA and chromosomal) damage, synergistic interactions with genotoxic chemicals, phenotypic mutations (limited data), or micronuclei (although suggestive evidence indicating the possibility was available at that time). This presentation will extend the genotypic summary to include more recent publications, including those from the REFLEX program, to see if the weight of evidence has been changed or further supported.

Does Long-term Radiofrequency (RF) Exposure of Laboratory Animals Affect Cancer, Survival and General Health

J. A. Elder
Motorola Florida Research Labs, USA

Objective: To review long-term exposure studies examining whether radiofrequency (RF) energy causes/promotes cancer or affects survival and general health of laboratory animals.

Methods: In three tables, this report summarizes more than 30 studies of cancer in laboratory animals exposed to RF energy published since 1962. The first table indicates whether or not a statistically significant increase was observed in cancer incidence as well as effects on survival and body mass, if reported. For each of the studies, information is provided on animal species (mice and rats), frequency (and modulation), dose rate (specific absorption rate, SAR), exposure conditions, cancer model, number of animals per group and reference. A second table presents the 15 studies in which animals were exposed for 12–25 months. Thus, about 50% of the studies employed long-term exposures of one year or longer in duration; in 13 studies, animals were exposed for 18-25 months. Significantly, 9 publications describe lifetime exposure studies in which mice and rats were exposed for 24–25 months, the average lifetime of these animals. A third table lists the studies by cancer model (spontaneous tumors, genetically-modified animals, chemically-induced tumors, ionizing radiation-induced tumors and models employing injected tumor cells).

Results: Two studies ([1, 2]) reported that RF exposure had a "protective" effect on cancer development but such results are not supported by the overall evidence. Likewise, the results in three papers ([3–5]) describing carcinogenic effects in RF-exposed animals are not supported by the weight of evidence in the scientific literature that includes follow-up studies addressing the effects reported in Chou, et al. and Repacholi, et al.. Three follow-up studies to the Chou, et al. study failed to confirm an association between RF exposure and an increase in cancer incidence ([6–8]). The follow-up investigation of the experiment by Rephacholi, et al., ([9]) by Utteridge, et al., ([10]) used eight times as many animals and four exposure levels (0.25, 1, 2, and 4 W/kg) and did not confirm an increase in tumors. Two studies reported changes that could not be replicated in the same laboratory ([11, 12]).

Conclusion: The scientific weight of evidence in more than 30 long-term cancer studies in laboratory animals shows no adverse effect of RF exposure up to two years in duration at dose rates up to 4 W/kg on 1) survival, 2) body mass, an indicator of general health status, and 3) carcinogenic processes (initiation, promotion and co-promotion).

*Supported by Motorola

REFERENCES

1. Preskorn, et al., *J. Surg. Oncol.*, Vol. 10, 483, 1978.
2. Adey, et al., *Rad. Res.*, Vol. 152, 293, 1999.
3. Szmigielski, et al., *Bioelectromagnetics*, Vol. 3, 179, 1982.
4. Chou, et al., *Bioelectromagnetics*, Vol. 13, 469, 1992.
5. Rephacholi, et al., *Rad. Res.*, Vol. 147, 631, 1997.
6. Toler, et al., *Rad. Res.*, Vol. 148, 227, 1997.
7. Frei, et al., *Bioelectromagnetics*, Vol. 19, 20, 1998.
8. Frei, et al., *Rad. Res.*, Vol. 150, 568, 1998.
9. Rephacholi, et al., *Rad. Res.*, Vol. 147, 631, 1997.
10. Utteridge, et al., *Rad. Res.*, Vol. 158, 357, 2002.
11. Bartsch, et al., *Rad. Res.*, Vol. 157, 183, 2002.
12. Anane, et al., *Rad. Res.*, Vol. 160, 492, 2003.

Epidemiologic Assessment of Cancer Risk from Mobile Phone Use: Where are We

A. Auvinen[1,2], A. Lahkola[1], K. Tokola[1], and P. Kurttio[1]

[1]SSTUK–Radiation and Nuclear Safety Authority, Finland
[2]University of Tampere, Finland

More than a dozen epidemiological studies have addressed the possible risk of cancer associated with mobile phone use. Overall, the evidence is reassuring, as risk estimates are close to unity and confidence interval relatively narrow. However, most studies have been based on relatively small number of long-term users. When the analysis was restricted to long-term use of mobile phones, some indication of increased risk was found for acoustic neurinomas. Also, effect related to use on the same side as where the tumor was diagnosed could not be excluded. Despite the substantial volume of research some increase in risk cannot be ruled out at the moment. Knowledge could be further advanced by improving exposure assessment rather than increasing the number of case-control studies. Prospective cohort study is a gold standard in epidemiology and would substantially advance our understanding of the possible health effects of radiofrequency electromagnetic fields emitted by mobile phones.

Enzymatic Alteration of Rat Brain Chronically Exposed to Low Level Microwave Radiation

R. Paulraj and J. Behari
Jawaharlal Nehru University, India

There has been a growing concern among the public regarding the potential human health hazard of exposure to microwave radiation by these appliances. These radiations affect certain growth related enzymes. They are (i) protein kinase C (PKC), a key enzyme involved in the transduction of signals conveyed from membrane receptors to the intra-cellular region of action of hormones, growth factors and cytokines (ii) ornithine decarboxylase (ODC), a rate-limiting enzyme in the polyamine biosynthesis.

Present work describes the effect of low level microwave radiation on calcium dependent protein kinase activity (PKC) and ornithine decarboxylase activity on developing rat brain. Thirty days old Wistar rats were exposed 2 h/day for 35 days at different frequencies. Exposure was carried out in a specially designed anechoic chamber.

After the exposure the whole brain, hippocampus, and hypothalamus tissue were dissected out and used for estimation of PKC and ODC. Radio labeled P^{32} ATP and C^{14} Ornithine were used for estimation of PKC and ODC activity respectively.

A statistically significant decrease in PKC activity was observed in exposed group as compared to their control counterpart. It is notable that activity on hippocampus showed a significant decline as compared to hypothalamus and the rest of the brain. On the other hand a statistically significant increase in the ODC activity was observed. It is inferred that prolonged exposure to these radiation causes significant alteration in the brain tissue, suggesting a transductive coupling to the cytoplasm. These results indicate a possibility that this type of radiation may also affect membrane bound enzyme such as PKC and ODC, which are associated with the cell proliferation and differentiation. It is suggested that the alteration in these enzymes may affect the behavioral pattern as well as learning and memory functions in developing rat.

Investigation of 900 MHz Electromagnetic Radiation for Effects on Permeability of the Blood Brain Barrier

L. E. Anderson
Duke University, USA

L. B. Sasser and J. E. Morris
Pacific Northwest National Laboratory, USA

Statement of Objective: A study was conducted to examine blood brain barrier (BBB) integrity in animals exposed to GSM RF signals. Significant features include use of an exposure system comparable to that employed in an earlier French study (Dr. Aubineau) with associated detailed dosimetry, multiple exposure levels along with positive controls, and a blind experimental design.

Methodology: Exposure rockets were constructed modeling those used in the French study. Each animal, exposed or sham exposed, were acclimated to the rockets over a 3 day period, after which they were exposed or sham exposed to 1.0 or 4.0 W/kg (brain SAR) for two hours using loop antennas similar to the French study. The antennas were calibrated with documented performance values by IT'IS (Zurich, Switzerland). Agreement with data from the original antenna was outstanding for the antennas fabricated for this study. Male Sprague Dawley rats were canulated in the ascending aortic vessel for introducing fluorescently labeled dextran into the brain immediately prior to exposure. The fluorescent dextran (MW of 70 kdal. and 10 kdal.) is labeled with Oregon Green dye with an absorbance/emission maxima at 496/524 nm respectively.

Analysis: Immediately following exposure, animals were euthanized and brains were perfused with ice cold 4% formaldehyde in phosphate buffered saline. Subsequent to in situ perfusion, brains were removed into 4% PBS at 5 degrees C for 24 hours, followed by 48–72 hours in cold 30% sucrose (in PBS). Brains were then quick frozen using liquid nitrogen and kept at -80 degrees C until preparations for histological analyses. To insure the blind nature of the study, preparation of histological samples and fluorescent analyses of brain tissues were performed by Dr. Nissi Varki and Dr. Kelly Doran (University of California, San Diego)

Results: Six animals were used per exposure condition with analyses ongoing. Preliminary results indicate that fluorescence is limited to the vessel walls with no appreciable extravasation into surrounding brain tissue in animals exposed as well as sham exposed to the GSM signal. No differences have been observed in animals exposed to either the 4 or 1 W/kg levels of exposure.

Mobile Phone Use and Health. Self-rated Health, Neurocognitive Function, Neurophysiological Effects Using 900 MHz Wireless Communication Signals. A laboratory-based Exposure Study

B. B. Arnetz[1,2], T. Ǎkerstedt[3], N. Kuster[4], A. Lowden[3], M. Berg[5]
C. Wiholm[1], S. Ebert[4], S. D Moffat[2], and L. Hillert[6]

[1]Uppsala University, Sweden
[2]Wayne State University, USA
[3]IPM, Karolinska Institutet, Sweden
[4]Swiss Federal Inst of Technology, Switzerland
[5]Uppsala University Hospital, Sweden
[6]Stockholm Centre for Public Health, Sweden

There is a rapid increase in the use of mobile phones and other wireless devices. Does exposure to such wireless devices impact on human health and well-being Even though there have been a number of reports purporting that mobile phone use elicits health complaints, including skin sensation, headache, difficulties concentrating, sleep disturbance, and fatigue among mobile phone users (mobile phones and cancer risks are not the subject of our current research) , findings have been difficult to reproduce. Some studies, however, have indicated effects of radiofrequency fields (RF) on self-reported symptoms, cognitive functions, blood pressure, brain waves (EEC), and sleep while other studies have not been able to confirm initial findings.

There is lack of sufficiently large, interdisciplinary, well-controlled, laboratory-based studies of the possible non-cancerous and short-term effects from GSM 900 MHz wireless communication signals.

In the present study we have assessed short-term self-rated and neurophysiological effects from laboratory controlled exposure to RF (GSM 900 MHz). Each person is his/her own control. Following a night of adaptation, participants are either exposed to a sham or actual 900 MHz exposure situation. Later, they are brought back for a third sham or real exposure night.

The study investigates the impact from GSM 900 MHz wireless signal exposure, using a double-blind set-up. Outcome measures include:

- Self-rated health, symptoms and belief about actual exposure
- Physiological (individual physiological response patterns), including blood pressure, hormones, and EEG, and
- Social (stress induced through tests during the exposures)

The study is ongoing. All exposures are expected to be completed by February, 2006, and the final report is due late fall 2006.

The study will offer us a better understanding whether day-time phone use is associated with changes in self-rated health, hormonal pattern, mental and cognitive functions as well as night-time sleep and related functions.

The study was approved by the ethical committee at Uppsala University.

Session 1P5
Modelling, Imaging and Inversion of Large-Scale Electromagnetic Data

On the Low-frequency Modeling of Coupled Obstacles Buried in Earth-like Medium

A. Breard, G. Perrusson, and D. Lesselier
CNRS-SUPÉLEC-UPS, France

The work considered here focuses onto the characterization of homogeneous volumetric obstacles buried in a Earth-like homogeneous or half-space medium in the induction regime. Fields of application are in the magnetic probing of natural or artificial objects buried in subsoil at some distance from the air/soil interface.

By characterization, it is meant identification of number, locations and main electrical and geometrical features of these obstacles. The latter are assumed to be penetrable with somewhat higher conductivity than the one of the embedding medium (more resistive cases are also worthwhile). A typical obstacle geometry is the versatile yet simple ellipsoidal one and degenerate shapes. Usually one could assume two (or a small number of) such obstacles with different semi-axes and conductivities, somewhat close (in terms of the skin depth) to one another and lying in the near-field of a (vertical) magnetic dipole or a (horizontal) electrical current loop (the source), the magnetic field induced by the electromagnetic interaction being collected nearby at several locations along a borehole (within the Earth) or on a planar surface (above the Earth interface) and possibly at several frequencies variations of impedance of coil receivers could be considered as well.

The first step is to put together a proper modeling tool of the interaction. One is considering, inspired in that matter by earlier work for a single obstacle, G. Perrusson *et al.* Conductive masses in a half-space Earth in the diffusive regime: Fast hybrid modeling of a low-contrast ellipsoid, *IEEE Trans. Geosci. Remote Sens.* **38** 1585-1599 (2000), the extended Born approximation allied to traditional low-frequency asymptotics fields and all pertinent quantities are expanded in positive integer powers of (jk), k complex wavenumber of the exterior medium.

Thus, one is able to express the secondary electrical currents within the obstacles as volume integrals of products of source-independent depolarization tensors times primary fields, the coefficients up to power 3 in (jk) of the said tensors being expressed in closed-form for ellipsoidal shapes in their eigen co-ordinate systems, the coefficients of the primary fields being known or having been derived lately as well up to pertinent orders in both homogeneous and half-space cases for the sources indicated above.

Then, further simplification comes from the fact that, when the obstacles are small enough, the quantities which matter are the tensor coefficients at their centers times their volumes. Since the electrical excitation field at the center of one given obstacle appears as the sum of the primary field and the field due to all other obstacles, one easily arrives at a set of linear equations which yield the total electrical currents at every center (with closed-form solution for two obstacles); the magnetic fields they radiate or (via reciprocity) variations of probe impedances follow. Since all quantities are expanded into powers of (jk) coefficients of the series expansions are obtained in practice. Notice that one has to carefully book-keep all needed changes of coordinate systems from an absolute one to those of the ellipsoidal obstacles.

In this contribution, one will show how the machinery (a version of Lax-Foldy theory of multiple scattering, refer, e.g., to H. Braunisch, Methods in Wave Propagation and Scattering, PhD Thesis, MIT (2001), for a pure magneto-quasistatic development), can be worked out and how numerical results it provides compare with those from brute-force approaches and other approximations in various configurations. Time permitting, and depending upon the pace of the present investigation, retrievals of those obstacles using a differential evolution method will be considered briefly.

NSA Calculation of Anechoic Chamber Using Method of Moment

T. Sasaki, Y. Watanabe, and M. Tokuda
Musashi Institute of Technology, Japan

Normalized site attenuation (NSA) is usually analyzed by using the ray tracing method and the finite difference time domain (FDTD) method. But the analytical accuracy of the NSA deteriorates in the low frequency band below several hundreds MHz because the ray tracing method approximates an electromagnetic wave as an optical ray. We cannot use this method because we will analyze the NSA characteristic in low frequency such as using power line communication. On the other hand, FDTD method can analyze NSA characteristics in the low frequency band below several hundreds MHz [1], but this method cannot be used to calculate the NSA of an anechoic chamber with a cross section of a non-rectangular shape, as shown in Figure 1.

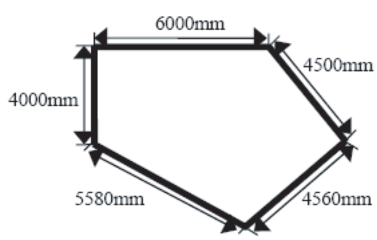

Fig. 1: Shape of anechoic chamber for analysis.

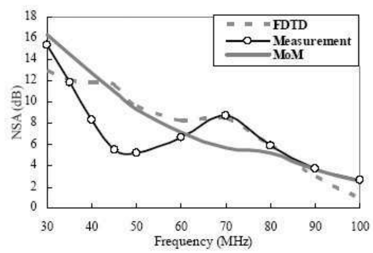

Fig. 2: NSA characteristics of the fully anechoic chamber.

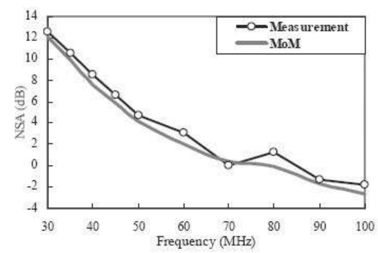

Fig. 3: NSA characteristics of the semi anechoic chamber.

So we propose the calculation method of NSA characteristic using the method of moment (MoM). MoM is able to imitate a cross section of a non-rectangular shape because this method imitates the object using the many wires. The shape of the anechoic chamber is composed of wire meshes and the electromagnetic wave absorber imitates the wire meshes with limited electric conductivity. In this study, we calculated NSA characteristic of the anechoic chamber with the shape of rectangular in order to examine the ability of using MoM. Figures 2 and 3 are case of the NSA calculation results using MoM. Figure 2 shows NSA characteristics of the fully anechoic chamber at horizontal polarization and Figure 3 shows NSA characteristics of the semi anechoic chamber at horizontal polarization. The calculation results using the FDTD method and the measured results are obtained from [1]. In Figure 2, the NSA characteristics calculated by the MoM in the frequency range from 30 to 100 MHz almost correspond with the measured results as well as FDTD method. In Figure 3, the calculation result of MoM agrees with the measurement result very well.

As a result, it is conformed that imitating the electromagnetic wave absorber by using wire meshes with limited electric conductivity is effective and the NSA characteristics can be calculated by using the MoM. Future tasks are to improve calculation accuracy and calculate NSA of the anechoic chamber with nonrectangular shape as shown in Figure 1.

REFERENCES

1. Takiguchi, Y., E. Kimura, and M. Tokuda, "NSA characteristics of anechoic chamber using fdtd method," *4th European Symposium on Electromagnetic Compatibility (EMC Europe 2000 Brugge)*, Vol. 1, 257–262, 2000.

Optimal Grids for the Forward and Inverse Electric Impedance Tomography Problems

F. Guevara Vasquez and L. Borcea
Rice University, USA

V. Druskin
Schlumberger-Doll Research, USA

In Electrical Impedance Tomography (EIT) one seeks to find the conductivity inside a body rom electrical measurements at its surface. This is an ill-posed inverse problem and finding appropriate parametrizations of the unknown is a crucial question.

We begin by reviewing optimal grid results for an 1D inverse problem [1], that gives a rigorous way of choosing an appropriate parameterization of the conductivity. The main idea is to fit the measurements exactly with a resistor network, and to interpret the resistors as local averages of the conductivity over the grid cells of a finite differences discretization. Next, we show how we can profit from a linearization of the resistors to improve over the performance of optimal grids in the 1D EIT forward problem.

Lastly, we discuss a generalization of the 1D methods to the 2D EIT inverse and forward problems, and show numerical results.

REFERENCES

1. Borcea, L., V. Druskin, and L. Knizhnerman., "On the continuum limit of a discrete inverse spectral problem on optimal finite-difference grids," *Comm. Pure Appl. Math*, Vol. LVIII, 1231–1279, 2005.

Finite-difference Solution of the 3D EM Problem Using Integral Equation Type Preconditioners

M. Zaslavsky, **S. Davydycheva**, **V. Druskin**, **L. Knizhnerman**,
A. Abubakar, **and T. M. Habashy**
Schlumberger-Doll Research, USA

The CSEM marine problem requires fine gridding to account for sea bottom bathymetry and to model complicated targets. This results in large computational costs using conventional finite-difference solvers. To circumvent these problems, we employ a volume integral equation approach for preconditioning and to eliminate the background, thus significantly reducing the condition number and dimensionality of the problem. We consider and compare two types of preconditioners, one is based on a magnetic field formulation and the other is based on what is referred to as the dissipative approach by singer. Theory and preliminary numerical results will be presented.

An Effective Inversion Method Based on the Padé Via Lanczos Process

R. F. Remis
Delft University of Technology, The Netherlands

In the Padé Via Lanczos (PVL) process, the response of a full-order system is approximated by a Padé approximation which captures the essential features of the full system on a certain time interval or frequency band of interest. The Padé approximations can be computed in a stable manner via the Lanczos algorithm. In this paper we apply the PVL process to effective inverse electromagnetic scattering problems. Specifically, our objective is not to look for the true and in general position dependent medium parameters of some object, but to look for so-called effective medium parameters instead. These effective parameters are position independent and are determined by minimizing a well-defined objective function. This minimization procedure is carried out by visually inspecting the objective function. Such an approach is possible since the PVL process provides us with a single Padé approximation for scattered fields produced by a whole range of homogeneous medium parameters. We will illustrate our approach by a number of numerical experiments for single and multiple frequency data.

Inversion of Large-scale Electromagnetic Data through the Iterative Multizooming Reconstruction of Nonmeasurable Equivalent Current Densities

M. Donelli[1], **D. Franceschini**[1], **M. Benedetti**[1], **A. Massa**[1], **and G. L. Gragnani**[2]

[1]University of Trento, Italy
[2]University of Genoa, Italy

In the framework of the inversion of electromagnetic data, several methodologies consider the introduction of an equivalent current density defined into the dielectric domain to be reconstructed. One of the main drawbacks of these approaches is their "difficulty" to reconstruct the so-called "nonradiating" (or "nonmeasurable") components of the equivalent current density. Hence the obtained solution may suffer from a strong low-pass effect. In order to overcome this drawback, *Habashy et al.*, [1] presented a reconstruction method where the problem of nonmeasurable currents was addressed through a successive steps process. Taking into account the guidelines suggested in [1], *Gragnani et al.*, [2] proposed a nonlinear procedure based on the reconstruction of the measurable components of the equivalent current density by means of the singular value decomposition of the discretized Green's operator. Such components are then inserted into a nonlinear equation whose unknowns are the nonmeasurable components as well as the dielectric properties of the investigation domain. Then, a nonlinear functional is defined and minimized by means of a standard steepest-descent procedure.

Even though the results obtained by taking into account the nonmeasurable current density were better than the ones of the minimum-norm solution, the method demonstrated some inaccuracies or faults due to the presence of the local minima. Moreover, the choice of a suitable representation for the nonradiating currents represented an open problem partially addressed.

In this paper, these problems are faced through an integrated strategy based on an innovative stochastic method and on an iterative multizooming procedure. Since the existence of nonradiating components is equivalent to the Green's integral operator having a null-space and one way to decrease the size of the null space is to let the equivalent current density have fewer degrees of freedom, it is convenient to approximate this density with a smaller number of basis or unknowns, e.g., by using a coarse grid in the domain under test [3]. Consequently, the reconstructed profile presents a poor spatial resolution because of the inappropriate sampling step. Therefore, an iterative multizooming process is considered. Starting from a coarse representation, the method iteratively defines a subgridding of the support of the equivalent current density successively improving the representation of the current by minimizing the nonlinear cost function defined in [2]. In order to avoid local minima problems, an innovative minimization technique based on the particle swarm optimizer (PSO) [4] is used.

REFERENCES

1. Habashy, T. M., M. L. Oristaglio, and A. T. de Hoop, "Simultaneous nonlinear reconstruction of two-dimensional permittivity and conductivity," *Radio Sci.*, Vol. 29, 1101–1118, 1994.
2. Gragnani, G. L. and S. Caorsi, "Inverse-scattering method for dielectric objects based on the reconstruction of nonmeasurable equivalent current density," *Radio Sci.*, Vol. 34, 1–8, 1999.
3. Chew, W. C., Y. M. Wang, G. P. Otto, D. Lesselier, and J. Ch. Bolomey, "On the inverse source method of solving inverse scattering problems," *Inverse Probl.*, Vol. 10, 547–553, 1994.
4. Donelli, M. and A. Massa, "A computational approach based on a particle swarm optimizer for microwave imaging of two-dimensional dielectric scatterers," *IEEE Trans. Microwave Theory Techn.*, Vol. 53, 1761–1776, 2005.

QN Inversion of Large-scale MT Data

A. Avdeeva[1] **and D. Avdeev**[1,2]

[1]Dublin Institute for Advanced Studies, Ireland
[2]Russian Academy of Sciences, Russia

Nonlinear electromagnetic inversion techniques are commonly based on an iterative minimization of a classical Tikhonov type regularized cost functional. To solve such a minimization problem gradient type methods such as Quasi-Newton (QN) are used, because they require calculation of gradients of the cost functional only, while at the same time avoiding calculations of second-derivative terms. However, the inherent disadvantages of these approaches are that: i) the iterative sequence may converge very slowly and ii) memory storage that is proportional to $M \times M$ is required, where M is the number of conductivities to be recovered. This latter requirement makes three-dimensional (3D) QN inversion impractical to implement. To overcome problem (i) we applied an adjoint method for analytical calculation of the gradients of the cost functional for the case of the one-dimensional (1D) magnetotelluric (MT) problem. To handle the second problem (ii) the limited-memory variant of the QN method (LMQNB) was employed. This method requires storage that is proportional to $2 \times Ncp \times M$, where Ncp is the number of correction pairs (practically, only a few). The numerical implementation of the LMQNB method has been tested on a synthetic MT impedance dataset calculated for a layered earth model at several periods. With these examples it is shown that the analytical calculation of gradients indeed accelerates the QN inversion by many times and it is demonstrated that only a few correction pairs are enough to produce reasonable results. The above improvements open the way to implement the QN method to solve the fully 3D MT inverse problem as it is demonstrated in an accompanied presentation by Avdeev & Avdeeva.

2.5 D Algorithm for Tomographic Imaging of the Deep Electromagnetic Geophysical Measurement

A. Abubakar, **T. M. Habashy**, **V. Druskin**, **D. Alumbaugh**, **P. Zhang**, **and M. Wilt**
Schlumberger, USA

L. Knizhnerman
Central Geophysical Expedition, Russia

Electromagnetic methods are essential tools for the appraisal of a reservoir because of their sensitivity to the resistivity (conductivity) which is a function of the fluid saturation. One of the traditional electromagnetic techniques for well logging is the induction single-well measurement. This technique is employed both as a wireline technology and as a measurement while drilling to estimate near well-bore resistivity. This induction logging measurement has a sensitivity of up to a few meters from the well and is a function of the separation between the transmitter and receiver and frequency of operation. To reach deeper into the reservoir, a cross-well electromagnetic induction technology was developed. The system operates very similar to the single-well logging tool however with transmitter and receiver deployed in separate wells. During a cross-well survey the receivers are lowered into one well, initially to the bottom of the survey-depth interval. Then the transmitter is lowered into the second well and is moved to log the entire survey-depth interval. During logging the transmitter broadcasts electromagnetic signals at a number of pre-prescribed frequencies while at the receiver well these signals are recorded. After the transmitter run is completed the receiver array is moved to the next depth station in the survey interval and the process is then repeated until the entire depth interval has been covered. After the data set has been collected, an inversion process is applied to convert the electromagnetic signals to a resistivity distribution map of the region between the wells.

This inverse process is one of the most challenging parts of the effort to make this cross-well technology work since it requires one to solve a full nonlinear inverse scattering problem, which is usually ill-conditioned and non-unique. Moreover, when the number of the model parameters to be inverted is large, the inversion can be very time-consuming. In order to carry out the inversion within a reasonable time, we employ a finite-difference code as a forward simulator. In this forward code the configuration is numerically discretized using a small number of cells determined by the optimal grid technique. The resulting linear system of equations representing the discretized forward problem has to be solved in each inversion step. To solve this system, we use a LU decomposition method that allows us to obtain the solution for all transmitters simultaneously. Furthermore, in order to be able to use the optimal grid without sacrificing accuracy we use an anisotropic material averaging formula. All these features help in reducing the computational time for constructing sensitivity kernel and for calculating the data misfit. For the inversion method, we employ a constrained Gauss-Newton minimization scheme where the inverted model parameters are forced to lie within their physical bounds by using a nonlinear transformation procedure. We further enforce a reduction in the cost function after each iteration by employing a line search method. To improve on the conditioning of the inversion problem, we use two different regularizers. The first is a traditional L_2-norm regularizer, which allows a smooth solution. The second is the so-called weighted L_2-norm regularizer, which can provide a sharp reconstructed image. The trade-off parameter which provides the relative weighting between the data and the regularization part of the cost function is determined automatically to enhance the robustness of the method. We will present results from simulated data as well as from field measurements to demonstrate the capabilities of the developed algorithm.

A Rigorous Three-dimensional Magnetotelluric Inversion

D. Avdeev[1,2] **and A. Avdeeva**[2]

[1]Russian Academy of Sciences, Russia
[2]Dublin Institute for Advanced Studies, Ireland

The Limited-Memory Quasi-Newton method with simple Bounds (LMQNB) has been applied to develop a novel fully three-dimensional (3D) magnetotelluric (MT) inversion technique. This nonlinear inversion is based on iterative minimization of a classical Tikhonov type regularized cost functional. But instead of the usual model space of log resistivities, the approach iterates in a model space with simple bounds imposed on the conductivities of the 3D target. The LMQNB requires storage that is proportional to $2 \times Ncp \times M$, where the M is the number of conductivities to be recovered and Ncp is the number of the correction pairs (practically, only a few). This is much less than requirements imposed by other Newton type methods (that usually require storage proportional to $N \times M$, or $M \times M$, where N is the number of data to be inverted). The LMQNB convergence to the solution is drastically accelerated by analytical calculation of the gradients of the cost functional. The gradients are calculated using an adjoint method based on EM field reciprocity. The inversion involves all four entries of the MT impedance matrix. The powerful integral equation forward modelling code x3d by Avdeev et al. (2002) is employed as an engine for this inversion. Convergence, performance and accuracy of the LMQNB inversion are demonstrated on 3D MT synthetic, but realistic, examples.

Contrast Source Inversion of 3D Electromagnetic Data

P. M. van den Berg
Delft University of Technology, The Netherlands

A. Abubakar and T. M. Habashy
Schlumberger-Doll Research, USA

This paper discusses the full vector three-dimensional inverse scattering problem. We consider the determination of the location and the electromagnetic composition of a bounded object in a homogeneous embedding from measurements of the scattered electromagnetic wavefield, when the object is illuminated by a known single frequency wavefield. To solve this large-scale nonlinear inversion problem, we apply the so-called multiplicative regularized contrast source method. In this MR-CSI method we reconstruct the complex permittivity contrast and the so-called contrast sources (the product of the contrast and the fields) by minimizing a cost functional in which the residual errors in the electric field equations occur. This minimization is carried out alternatingly. In each iterative step we update the contrast and the contrast sources each using one conjugate gradient step so that the total computational complexity of the method is equal to the complexity of solving only two forward problems. By operating in this manner solving a full three-dimensional vector nonlinear inverse scattering problem is feasible. Further this method is equipped with total variation type regularization. This regularization is included as a multiplicative constraint, so that the regularization parameter needed in the minimization process is determined automatically. The multiplicative type of regularization handles noisy as well as limited data in a robust way without the usually necessary *a priori* information. We illustrate the performance by presenting some inversion results from 3D electromagnetic experimental data.

Further, we discuss an inversion method to invert not only the complex electric contrast but also the magnetic contrast of a three-dimensional object. The contrast source inversion is extended by introducing both the electric contrast sources and the magnetic contrast sources. Further, an extended cost functional is introduced in which the residual errors in both the electric and magnetic field equations occur. Additionally, the multiplicative regularization is extended such that the spatial variations of both the electric and magnetic contrast are minimized. Numerical examples using simulated data are presented to demonstrate the capabilities of this extended MR-CSI method.

Session 1P6a
Volume and Rough Surface Scattering: Theory and Photonic Applications

Phase Fluctuations in Scattered Radiation

S. M. Watson
University of Central Florida, USA

K. D. Ridley
QinetiQ, UK

Fluctuations in scattered radiation are of considerable practical and theoretical interest [1]. Perhaps due to the prevalence of direct detection systems at optical wavelengths, as well as the relative difficulties encountered in phase sensitive systems, phase statistics and correlations would appear to have received considerably less attention than corresponding results for intensity. Freund and Kessler obtained the phase autocorrelation of a complex Gaussian field from the two-point joint density [2], a calculation that Middleton had performed in earlier investigations [3]. As noted by Sebbah et al., [4], the results from these investigations are applicable to the wrapped phase, or phase modulo 2π, and not the unwrapped phase that can take on arbitrary values. However, there are instances when the variance of the unwrapped or cumulative phase is of most interest, such as characterizing transit times in diffuse waves [5], wavefront sensing and interferometry [6]. In this talk we present unwrapped or cumulative phase results following scattering from one-dimensional phase screens and extended random media. Analytical results are obtained in weak and strong fluctuations regimes, which provide a benchmark for numerical simulations that allow insight under all fluctuation conditions.

REFERENCES

1. Inshimaru, A., *Wave Propagation And Scattering In Random Media*, IEEE Press, 1997.
2. Freund, I and D. A. Kessler, "Phase autocorrelation of random wave fields," *Opt. Commun.*, Vol. 124, 321–332, 1996.
3. Middleton, D., *An Introduction To Statistical Communication Theory*, IEEE Press, 1996.
4. Sebbah, P., O. Legrand, B. A. van Tiggelen, and A. Z. Genack, "Statistics of the cumulative phase of microwave radiation in random media," *Phys. Rev. E.*, Vol. 56, 3619–3623, 1997.
5. Van Tiggelen, B. A., P. Sebbah, M. Stoytchev, and A. Z. Genack, "Delay-time statistics for diffuse waves," *Phys. Rev. E.*, 7166–7172, 1999.
6. Wheelon, A. D., *Electromagnetic Scintillation I. Geometrical Optics*, Cambridge University Press, 2005.

Scattering of an Electromagnetic Wave from 3-dimensional Rough Layers: Small-amplitude Method and Small-slope Approximation

G. Berginc
Thales Optronique S. A., France

C. Bourrely
Centre de Physique Thérique, France

The scattering of electromagnetic waves from randomly rough surfaces have been extensively studied in different domains such as radio-physics, geophysical remote sensing, ocean acoustics, surface optics and recently plasmonics where metallic surfaces have a dielectric coating. Our purpose is to show how light can interact with several randomly rough surfaces. In this paper, we consider an electromagnetic polarized plane wave incident on a three-dimensional dielectric film with one or two randomly rough surfaces. We assume that the randomly rough surfaces are Gaussian and statistically independent: a Gaussian probability density function is assumed for the random rough surface heights and the autocorrelation function is a Gaussian function. We study two hypothesis, we consider three-dimensional structures bounded by two-dimensional weakly rough surfaces or by two-dimensional randomly rough surfaces with small-slope.

In the case of weakly randomly rough interfaces, we use the small-amplitude perturbation theory, we have generalized the integral equations called reduced Rayleigh equations in the case of a three-dimensional layer with weakly randomly rough interfaces. The electromagnetic polarized plane wave is incident on a dielectric layer whose mean thickness is constant. The dielectric layer is deposited on a metallic film. Illustrative examples are presented for the bistatic diffuse component of the electromagnetic field.

In the second part of the paper, we discuss the extension of the theory using the small-slope approximation method. We study structures with two-dimensional randomly rough surfaces, including scattering from free-standing films or films on a substrate, one or both of whose surfaces are randomly rough. The fourth order term of the perturbative development is required if we want to take into account the interactions between the two randomly rough surface. Some simulations will be given and compared with the small-amplitude perturbation method.

This analysis is relevant to problems of laser cross-section calculation, remote sensing of irregular layered structures and remote detection of chemical coatings.

Fast Modeling of Reflectance Image of Turbid Medium with Full-field Illumination

C. Chen, **R. S. Brock**, **D. W. Pravica**, **X.-H. Hu**, **and J. Q. Lu**
East Carolina University, USA

Reflectance imaging with oblique full-field illumination is a powerful tool for non-invasive determination of internal structure of turbid materials and diagnosis of lesions in human tissues. Extraction of structural information from the reflectance imaging data, however, requires quantitative modeling of light transportation and distribution in the turbid medium. Radiative transfer theory offers an accurate model and often has to be realized through Monte Carlo simulations, which is time consuming due to its statistical nature. In contrast, the diffusion approximation to the radiative transfer theory can be solved analytically but only applicable to the distribution of multiply scattered photons.

Based on previous studies of radial distribution of reflected light with single-fiber illumination [1–3], we compared different hybrid models that combine the Monte Carlo simulation with calculations based on the diffusion approximation of radiative transfer theory. On the basis of these results, we investigated a hybrid model that is most appropriate for full field illumination in which photon tracking in the Monte Carlo simulation is truncated to significantly increase the calculation speed. The contribution to the reflected light distribution at the surface of the imaged medium by the truncated photons is obtained from the analytical solution of the diffusion equation for these multiply scattered photons. We will present the numerical results on the validity and applicability of this fast hybrid method for modeling reflectance images with fullfield illumination and its potential use in the inverse determination of internal stricture in turbid medium.

REFERENCES

1. Farrell, T. J., M. S. Patterson, and B. Wilson, "A diffusion theory model of spatially resolved, steady-state diffuse reflectance for the noninvasive determination of tissue optical properties in vivo," *Med. Phys.*, Vol. 19, 879–88, 1992.
2. Wang, L. and S. L. Jacques, "Hybrid model of Monte Carlo simulation and diffusion theory for light reflectance by turbid media," *J. Opt. Soc. Am. A*, Vol. 10, 1746–1752, 1993.
3. Alexandrakis, G., T. J. Farrell, and M. S. Patterson, "Monte Carlo diffusion hybrid model for photon migration in a two-layer turbid medium in the frequency domain," *Appl. Opt.*, Vol. 39, 2235–2244, 2000.

Optical Tomography of Arbitrarily Shaped Object with Randomly Rough Boundaries

G. Berginc and M. Jouffroy
Thales, France

This paper presents the results of research designed to fulfill two main objectives including development of laser reflectance modeling of complex convex or concave objects with randomly rough boundaries and investigation of tomographic reconstruction of these objects.

This paper addresses the utility of physics based modeling of the laser backscattering of complex rough targets. The physics based model, we present in this paper, is designed to provide accurate results but to also include all of the electromagnetic interaction mechanisms. To model the laser interaction with the randomly rough surface, we use the second order Small-slope Approximation method. Because the problem, we consider in this paper, is three-dimensional, all the scattering coefficients (coherent and incoherent component of the electromagnetic field) are functions of the azimuth angles, and the cross-polarized terms do not vanish. We define, in this case, the Mueller matrix, which gives all the combinations of the polarization states of the scattered electromagnetic waves. The randomly rough surfaces of the complex object are characterized by electromagnetic parameters (permittivity...) and roughness parameters (standard deviation of rough surface height and autocorrelation function). One of the great advantages of this physics based model is its extensibility. Electromagnetic interactions of higher levels of complexity can be added to the model. Illustrative examples are presented for laser scattering from large convex objects. Our model addresses also transparent structures. With this model, we can obtain high temporal resolved laser backscattering from complex objects.

In the second part of the paper, we investigate algorithms for tomographic reconstruction of complex objects. The reconstruction is based on compilations of time-resolved optical backscattering obtained at various angles. The laser backscattered energy at various angles is calculated by our reflectance modeling of complex objects. We use our model to generate sets of data, with which we can compare the different models of reconstruction. We compare direct back-projection method, filtered back-projection method, Fourier-Radon method and stochastic method. We analyze the stability of the different methods when we add noise to the laser backscattering.

Statistical Distribution of Field Scattered by 1-Dimensional Random Slightly Rough Surfaces

R. Dusséaux and R. de Oliveira
Université de Versailles Saint-Quentin en Yvelines, France

We consider the 1–D scattering problem by a perfectly conducting surface illuminated by a monochromatic plane wave. The surface is a plane with a local cylindrical Gaussian perturbation assumed to be stationary, ergodic and centred so that for each realization of the surface, the spatial average value over the modulated zone is zero. Outside this zone, the scattered field, due to the deformation, can be represented by a superposition of a continuous spectrum of outgoing plane waves the so-called Rayleigh integral [1]. In the far-field zone, the Rayleigh integral is reduced to the propagating waves contribution and the method of stationary phase leads to the classical expression of the far field [2]. Under the first-order Small Perturbation Method [3], we show that:

- The incoherent intensity is not proportional to the power spectrum of the surface.
- The real part and imaginary part of the field are uncorrelated Gaussian stochastic variables with zero mean values and unequal variances.
- The probability density of the field amplitude is given by the Hoyt distribution [4] and the phase distribution is not uniform.

REFERENCES

1. Dusséaux, R. and R. de Oliveira, "Scattering of a plane wave by 1–dimensional rough surface—study in a nonorthogonal coordinate system," *Progress in Electromagnetic Research PIER*, Vol. 34, 63–88, 2001.
2. Born, M. and E. Wolf, *Principles of Optics—Electromagnetic Theory of Propagation Interference and Diffraction of Light*, Appendix III (Oxford, Pergamon), 1980.
3. Ishimaru, A., *Wave Propagation and Scattering in Random Media*, (New York: Academic).
4. Beckmann, P. and A. Spizzichini, "The scattering of electromagnetic waves from rough surfaces," (Oxfor, Pergamon), 1963.

Experimental and Theoretical Studies of Specular and Diffuse Scattering of Light from Randomly Rough Metal Surfaces

E. I. Chaikina, E. R. Méndez, and A. G. Navarette Alcalá
Centro de Investigación y de Educación Superior de Ensenada, México

A. A. Maradudin and T. A. Leskova
University of California, USA

We present experimental results for the reflectivity of two-dimensional randomly rough metal surfaces, as well as the contribution to the mean differential reflection coefficient from the light scattered incoherently by such surfaces. The measurements were done with s- and p-polarized light. The samples were fabricated on photoresist and coated with gold. Their surface profiles constitute good approximations to Gaussian random processes with a Gaussian surface height autocorrelation function. The measurements were done in the infrared at a wavelength of 10.6 μm. The experimental results for the reflectivity are compared with the results of small-amplitude perturbation theory, phase perturbation theory, and self-energy perturbation theory, and with results obtained on the basis of the Kirchhoff approximation. Rough surfaces with rms heights a small fraction of the wavelength of the incident light were employed, so that meaningful comparisons with the results of the perturbation theories could be made. In the case of the light scattered incoherently, the experimental results are compared with results obtained by means of the Kirchhoff approximation and with the results of small-amplitude perturbation theory and phase perturbation theory. The theoretical results for the reflectivity obtained on the basis of phase perturbation theory are closest to all the experimental results in both s and p polarization. Phase perturbation theory also produces the best overall agreement with the experimental results for the contribution to the mean differential reflection coefficient from the incoherent component of the scattered light for in-plane, co-polarized scattering, although small-amplitude perturbation theory produces better results in p polarization for samples with very small transverse correlation lengths of the surface roughness.

Session 1P6b
Guided Waves

Guide-Wave Propagation on 2D Doubly-Periodic Clusters of Multi-Port Resonators

R. A. Speciale
Research and Development Inc., USA

The recently introduced Tilted-Ellipse Representation of Standing-Wave Patterns [1, 2] provides a fast and inexpensive way for extracting the multi-dimensional, complex scattering-matrices of very large, multi-port microwave systems, by performing computer-simulations of large-scale experimental-measurements that would require a very complex and expensive multi-port Automated Vector Network Analyzer, and a long data-acquisition time. That simulation method is based on the results of a rigorous mathematical analysis [1, 2] of the simultaneous propagation of forward- and backward-waves along virtual measurement lines, connected to the ports of the microwave systems being simulated. That measurement-simulation method is currently being applied to the study of guided-wave propagation on 2D doubly-periodic clusters of directly-coupled, multi-port cylindrical resonators. Very large reductions of the problem-dimensionality is attained, by combining diakoptiks and symmetry-analysis. The complex scattering-matrix of C_{6V}-symmetric unit-cells is circulant, and symmetric around its main-diagonal, due to reciprocity, so that it may be specified using only the first three elements of its first row. Similar order-of-magnitude dimensionality-reductions are attained by interconnecting unit-cells in progressively-larger clusters having the same C_{6V}, and diagonal symmetry. The smallest cluster including only seven cylindrical-resonators is shown in Figure 1.

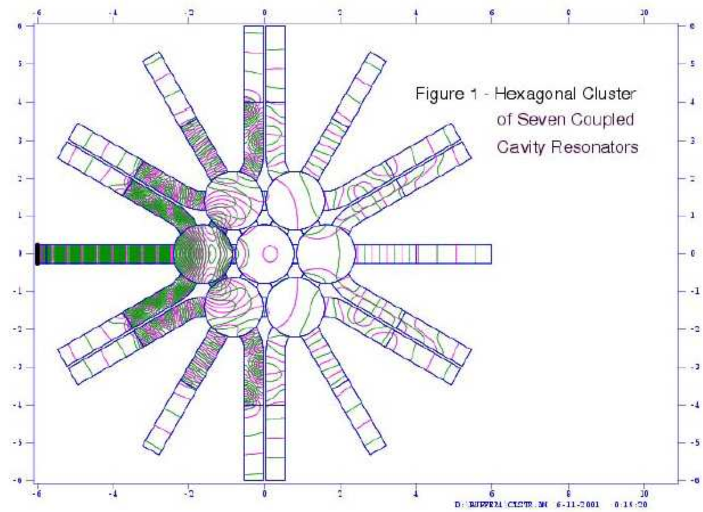

Figure 1:

Guided-wave propagation on such clusters of directly-coupled resonators is being characterized around the resonant frequencies of the TM_{010} and TM_{110} modes, including excitations generating left-/right-hand circular polarizations.

REFERENCES

1. Speciale, R. A., "Computing the scattering matrix of multiport systems," *PIERS 2004*, Pisa, Italy, 2004.
2. Speciale, R. A., "The tilted-ellipse representation of standing-wave patterns," *ACES 2004*, Syracuse, NY, 2004.

Dispersion Characteristics of Coplanar Waveguides at Subterahertz Frequencies

J. J. Zhang and T. Y. Hsiang
University of Rochester, USA

We present experimental and simulated studies of the dispersion characteristics of coplanar waveguides (CPWs) at subterahertz frequencies. Two types of CPWs were studied, those with wide ground planes and those with narrow ground planes. In both cases, simulations closely followed the experimental results, thus giving us a basis for implementing the simulations in circuit-design modes for a wide range of such waveguides.

A Multi Conductor Transmission Line Model for the Evaluation of the Rotor Shaft Voltages in Adjustable Speed Drive Motors

B. de Vivo[1], **C. Petrarca**[2], **V. Tucci**[1], **and M. Vitelli**[3]

[1]University of Salerno, Italy
[2]University of Naples "Federico II", Italy
[3]Second University of Naples, Italy

The use of switching devices, such as IGBTs, characterised by high switching frequencies and very low switching times in new generation pulse width modulation (PWM) inverters has increased the efficiency and performances of Adjustable Speed Drives (ASDs) for industrial and traction applications. However, such systems may be affected by disadvantages like over voltages at the motor terminals, when long cables are used between the drive, and the generation of rotor shaft voltage, due to the capacitive couplings in the motor (between the windings and the rotor and between the rotor and the stator). The shaft voltage may cause the breakdown of the lubricating film in the bearings. The resulting impulsive currents, by damaging the bearing elements shorten the component life, which in turn seriously affects the ASD reliability. For this reason, it is of great importance to develop numerical models able to predict the shaft voltage so as to estimate the currents flowing through the bearings. Several works, based on either concentrated or distributed circuit models, have been proposed for the evaluation of the shaft voltage magnitudes for several motors sizes. However, the results obtained by such approaches suffer from approximations and simplifications in the considered circuit model.

Therefore, in the present paper, a numerical model able to accurately predict the shaft voltage in high power induction motor for traction applications fed by a PWM inverter is presented. The windings of the motor are modeled by a multi conductor transmission line (MTL), whereas the cables between the source and the motor are described by a single transmission line. The effect of wave propagation and reflection and of the frequency-dependent distributed losses is considered by using a time-domain equivalent circuit to represent the MTL. A semi-analytical method, based on the perturbation theory of the spectrum of symmetric matrices, is adopted. The parameters of the MTL are obtained either analytically or numerically by using a commercial software (Maxwell® by Ansoft). The effects of the rise time and amplitude of the input voltage together with the length and the electrical characteristics of the cables are considered.

Frequency-selective Power Transducers: Hexagonal Ferrite Resonator-semiconductor Element

M. Y. Koledintseva
University of Missouri Rolla, USA

For many applications, it is necessary to obtain adequate information about mm-wave (30-300 GHz) spectra of signals (spectral power density, peak power of pulse signals, integral power in the given frequency band, width and central frequency of spectrum) [1, 2]. Typically, equipment for measuring power parameters of electromagnetic signals contains a primary measuring transducer and a secondary processing/displaying unit. A primary measuring power transducer converts energy of electromagnetic oscillations in the different kind of energy (e. g., thermal, mechanical, etc.), or an electromagnetic signal which is easy and convenient to register and quantify with the secondary processing and indicating unit. Most of microwave and mm-wave power meters and detectors are not frequency-selective. Their application for "fine" spectra measurements needs additional high-Q filters and cumbersome calibration of a mm-wave receiving path. Heterodyne-type spectrum analyzers and measuring receivers typically have a problem with numerous parasitic channels of reception, which is an especially difficult problem for the analysis of mm-wave spectra of signals of middle and higher intensity levels (more than 1 mW of continuous power).

The power transducers proposed in this paper allow for frequency-selective measuring of mm-wave power parameters. Frequency selectivity is assured by a monocrystalline hexagonal ferrite resonator (HFR). An advantage of applying of a HFR is its high intrinsic field of magnetic crystallographic anisotropy, so it does not need massive bias magnetic systems for achieving ferromagnetic resonance [2]. In the transducer, the HFR is in a direct contact with a semiconductor element. The semiconductor element may be a Hall-element slab, or an unpackaged chip diode (or a transistor). The mm-wave power absorbed by the hexagonal ferrite resonator at the ferromagnetic resonance converts to heat in the HFR, and the heat flux penetrates through the body of a semiconductor element with current flowing in it. Since this structure is placed in the bias magnetic field, a number of thermo/electro/magnetic phenomena accompany the known Hall-effect in a semiconductor. They cause a voltage additional to that of the Hall-effect. This happens only when the frequency of the mm-wave signal falls into the ferromagnetic resonance curve of the hexagonal ferrite, and assures frequency selectivity of power conversion. The conversion coefficient of a power transducer on the structure "HFR-semiconductor element" is analyzed using the power balance equation. It is shown that increasing thermal sensitivity of a semiconductor element and assuring a good thermal contact with the HFR leads to better sensitivity and higher conversion coefficient of a power transducer. Some experimental results in 8-mm waveband with the designed power transducers based on HFR-Hall element and HFR-unpackaged transistor will be presented.

REFERENCES

1. Kitaytsev, A. and M. Koledintseva, "Physical and technical bases of using ferromagnetic resonance in hexagonal ferrites for electromagnetic compatibility problems," *IEEE Trans. EMC*, Vol. 41, No. 1, 15–21, February 1999.
2. Koledintseva, M., A. Kitaitsev, V. Konkin, and V. Radchenko, "Spectrum visualization and measurement of power parameters of microwave wide-band noise," *IEEE Trans. IM*, Vol. 53, No. 4, 1119–1124, August 2004.

Analysis of Guided Modes in Shielded Slot Line

F. Kuroki and K. Miyamoto
Kure National College of Technology, Japan

Guided modes in a shielded slot transmission line were analyzed. This transmission line consists of slotted metal strips inserted in a below cutoff parallel metal plate waveguide as shown in Fig. 1. The TEM mode as shown in Fig. 2(a) can propagate in the slot area as the lowest dominant mode, while the higher modes as shown in Fig. 2(b) may propagate in the metal strip regions. With this in mind, we calculated the cutoff wavelength based on the transverse resonant method. Figs. 3(a) and (b) show the quarter cross section and its transverse equivalent transmission-line circuit. From this equivalent circuit, the cutoff wavelength of the Nth higher mode was given by

$$\lambda_c = \frac{1}{N - \frac{1}{\pi}\tan^{-1}\frac{B_s}{Y_0^{(1)}}}\left\{w - s + \frac{\lambda_c}{\pi}\tan^{-1}\frac{B_a}{Y_0^{(1)}}\right\},$$

where B_a and B_s correspond to susceptances at the side edges of the metal strip, and $Y_0^{(1)}$ is the characteristic admittance of the TM mode propagating along the transverse equivalent transmission-line. The susceptances were calculated by the variational method for waveguide discontinuities. Fig. 4 shows the calculated and measured dispersion curves of the dominant TEM mode and the 1^{st} higher mode. Agreement between the theory and measurement was quite satisfactory, and thus the validity of this analytical procedure was confirmed.

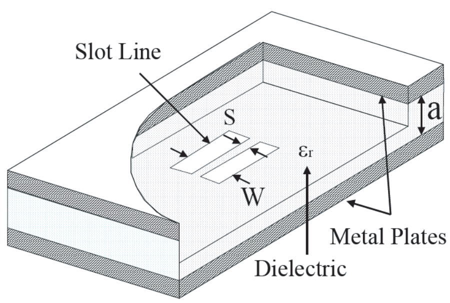

Figure 1: Structure of shielded slot line.

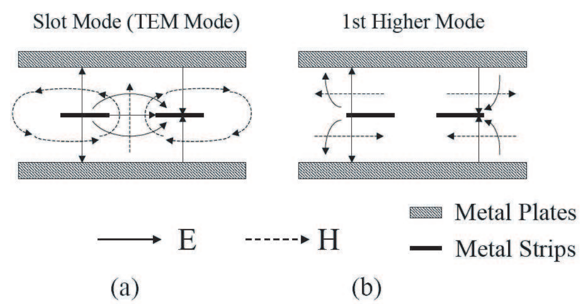

Figure 2: Field distributions of (a) slot mode and (b) 1^{st} higher mode.

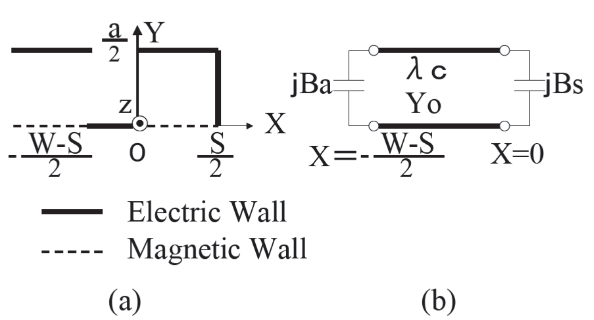

Figure 3: Analytical model. (a) Quarter cross sectional view, (b) Transverse equivalent transmission-line circuit.

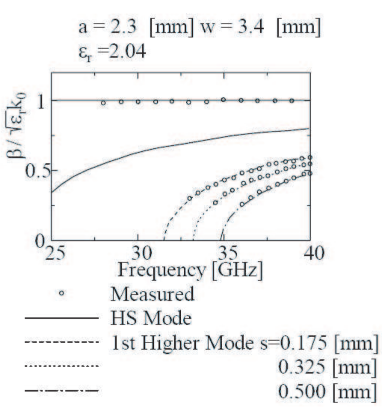

Figure 4: Calculated and measured dispersion curves of guided modes in shielded slot line.

Propagation of Light in Random Waveguide Systems with Slightly Random Imperfections

A. Komiyama
Osaka Electro-Communication University, Japan

From the interest in the crosstalk [1] in an image fiber which is used to transmit directly an optical image, the propagation properties of light in one-dimensional waveguide systems with random geometrical imperfections have been discussed based on the couple mode theory [2, 3]. In the numerical discussion [2] the propagation constants of the modes are generated by using a series of random normal numbers and the coupled mode equation is numerically solved. Although there is no essential difficulty, the numerical calculations for a large system with a very long correlation length are a time consuming task. Besides from the numerical results it is difficult to understand the whole of the dependence of the propagation properties on the structure parameters of the system. In the theoretical discussion [3] the perturbation solution of the couple mode equation is used. Consequently the results obtained are applicable only to the case of a short correlation length.

In this paper a propagation problem of light in a one-dimensional waveguide system composed of an infinite number of cores is treated based on the coupled mode theory. In the system sizes of the cores change slightly along the fiber axis and the propagation constant of the mode is a random function of propagation distance. A solution of the coupled mode equation is derived in a series form with the solution of the coupled mode equation for an ordered system as an initial term. The solution is applicable to the whole range of the correlation length. Using the solution the equations describing the average amplitude and the average power are derived. The equations include two coefficients, the mode coupling coefficient and the damping factor. Light launched into a core spreads over the system with propagation and the light power is transformed into the incoherent power. The mode coupling coefficient determines how light spreads and the damping factor determines the rate of the transformation of the light power into the incoherent power. The mean free path can be obtained from the distance dependence of the damping factor. When the correlation length tends to infinity the mean free path tends to infinity and light propagates coherently in the system. For short correlation lengths the damping factor is proportional to the correlation length. The result agrees with the result obtained using the perturbation solution [3]. For long correlation lengths the damping factor increases gradually compared with the linear dependence on the correlation length.

REFERENCES

1. Komiyama, A. and M. Hashimoto, *IEICE Trans.*, E77-C, 1808–1813, 1994.
2. Komiyama, A. and M. Tokimoto, *IEICE Trans.*, E83-C, 1849–1854, 2000.
3. Komiyama, A., *Proceedings of 2004 URSI EMT-S*, 260–262, 2004.

Session 1P9
Numerical Method

An Efficient *hp* Adaptive Finite Element Solver for Time-harmonic Electromagnetic Fields

V. Hill, O. Farle, P. Ingelstrom, P. Nickel, and R. Dyczij-Edlinger
Saarland University, Germany

Thanks to its great flexibility in modelling geometry and material properties, the finite element (FE) method is a widely used tool for the numerical analysis of electromagnetic devices. With the FE method, there are two different ways of improving the accuracy of numerical solutions. In case of p enrichment, the degrees of the basis functions are increased whereas, in case of h refinement, the element sizes are decreased. When the fields are smooth, p enrichment yields exponential convergence, whereas h refinement is always limited to algebraic rates of convergence. On the other hand, when singularities are present, the performance of p schemes is poor whereas nonuniform h methods succeed in keeping the rate of convergence unchanged. Since real world configurations typically involve both regions of smooth fields and localized areas of rapid field variations or even singularities, p enrichment and h refinement should be viewed as complementary rather than competing techniques.

The FE method we propose in this paper combines hp adaptivity with fast solution techniques. As for h refinement, we construct sequences of nested tetrahedral meshes which allow for subregions of greatly varying refinement levels, and impose special restriction operators to make the FE basis functions maintain proper continuity conditions. The resulting FE spaces are perfectly nested, which makes them very well-suited for advanced geometrical multi-grid solvers exploiting local sub-meshing techniques.

Regarding p enrichment, a set of hierarchical $\mathcal{H}(\mathrm{curl})$ conforming basis functions developed by one of the authors is employed. It is of the incomplete order type, features explicit basis functions for higher order gradients as well as increased sparsity within the stiffness matrix, and possesses interpolation properties that greatly simplify h refinement and hence bridge the gap to the before mentioned method. Our basic building block for a fast solver in the p domain is a multiplicative Schwarz method.

One challenge with hp schemes is that the aspects of multi-grid schemes for h refinement and Schwarz methods for p enhancement can no longer be considered separately. In fact, there are many ways to cycle back and forth between a low-order FE space over a coarse mesh and a high-order space over a fine discretization, and it turns out that the corresponding algorithms differ greatly in their computational complexity.

In our talk we will give the details of the proposed hp adaptive FE solver. We will demonstrate the efficiency of the new approach by a number of numerical examples.

Challenges for Computational Electromagnetics for Low Frequencies

W. C. Chew[1], **M. K. Li**[1], **Y. A. Liu**[1], **Z. G. Qian**[1]
J. Xiong[1], **L. Sun**[1], **I. T. Chiang**[1], **L. J. Jiang**[2], **and Y. H. Chu**[3]

[1]University of Illinois, USA
[2]IBM TJ Watson Research Center, USA
[3]Agilent Technologies, USA

Full wave electromagnetic simulation of circuits in computer technology is a challenging problem, as it is in the domain where wave physics meets circuit physics, namely, it is the "twilight zone". In this regime, electromagnetic field does not behave fully as waves, but meanwhile, simple circuit theory such as KCL and KVL cannot fully capture the physics of the electromagnetic interaction. In this regime, two kinds of breakdown occur for computational electromagnetics: the low-frequency breakdown due to the inaccuracy in the integral equation, and the low-frequency breakdown in accelerators such as the fast multipole algorithm.

When the size of a geometry structure is much smaller than a wavelength, it is necessary to use a quasi-Helmholtz decomposition of the surface current to preclude the breakdown of the integral equation. Such a decomposition is achieved by using either the loop-tree basis or the loop-star basis for the quasi-Helmholtz decomposition. In this manner, the physics that corresponds the world of the capacitors, and that that corresponds to the world of the inductors can be correctly captured.

When the size of the geometry structure is comparable to wavelength, Rao-Wilton-Glisson (RWG) functions can be used to expand the current on the structure to capture the wave physics. Low-frequency breakdown problem can be delayed by using higher precision calculations when RWG functions are used.

As for the solution accelerator, we have recently proposed the mixed-form fast multipole algorithm that can work seamlessly from static to the microwave regime. It is both accurate and error controllable, as well as being memory efficient. However, there exist structures where both wave physics and circuit physics are important. This could be a large structure with many excruciating details as happens in a computer circuit, but the overall platform size is not small. In that case, it is more expedient to put Huygens' equivalence boxes around each region with fine details, and decouple the exterior problem from the interior problem. This can be regarded as having replaced a region with fine details with an N-port representation. Inside the Huygens' boxes, low-frequency techniques can be used to solve the problem so that low-frequency physics is correctly captured, with the ensuing geometry details. Outside the Huygens' boxes, when wave-like interactions are computed, less number of unknowns is needed to capture the wave physics, but meanwhile, the ability to model fine details is not foregone.

Multi-level Multiplicative Schwarz Preconditioner for Solving Matrix Equations from DD-FE-BEM Formulation

K. Z. Zhao and J.-F. Lee
The Ohio State University, USA

A symmetric coupling between finite and boundary elements for solving electromagnetic wave radiation and scattering problems in $\mathbb{R}^3$ has been recently proposed by Vouvakis et al., [1]. The new formulation results in a symmetric complex matrix equation which is free of internal resonances, and the spectral radius of the couplings between finite and boundary elements is bounded by 1. Moreover, the formulation is also allowing non-conformal couplings between FEM and BEM, and thus, offers great modeling versatility for solving real-life complex problems. By non-conformity, we mean that the surface triangulations of the FEM and the BEM do not need to be the same, as well as the flexibility of choosing different order of basis functions for FEM and BEM portions separately.

This paper addresses the practical issue of how to solve the resulting symmetric complex matrix equations efficiently. As is well known that in order to solve large sparse matrix equations (or even dense matrix equations, for that matter) efficiently using iterative solution, such as Conjugate Gradient (CG) methods, the most critical ingredient is the preconditioner. In the authors' group, we have developed over the years a robust preconditioner, termed p-MUS (p-type MUltiplicative Schwarz), for preconditioning the matrix equations from the application of the vector finite elements [2]. We extend the p-MUS to the current DD-FE-BEM formulation, and treating the BEM block as another "abstract" domain, and construct three possible preconditioners: an inner-outer loop domain decomposition preconditioner, an additive p-type Schwarz method, and a Multi-level MUltiplicative Schwarz (M-MUS) preconditioner for solving the resulting DD-FE-BEM matrix equations. Various numerical examples, including both radiation and scattering problems, will be presented and comparisons of the three preconditioners will be discussed as well in the presentation.

REFERENCES

1. Vouvakis, M., K. Zhao, S. Seo, and J.-F. Lee, submitted to *IEEE Trans AP*.
2. Lee, J.-F. and D. K. Sun, *IEEE Trans. MTT*, 864–870, 2004.

Higher Order Hierarchical FEM Solutions with Enhanced Efficiency and Practicality

B. M. Notaroš, M. M. Ilić, and A. Ž. Ilić
University of Massachusetts Dartmouth, USA

Recently, computational techniques based on using electrically large curved elements for geometrical modeling (large domains) and higher order basis functions for field modeling have been employed within the framework of the finite element method (FEM), with an objective to significantly reduce the number of unknowns and computational resources for a given (high) accuracy when compared to low-order small-domain solutions. However, these advantages become evident and convincing only if the large-domain FEM approach is carefully planned and implemented. This paper addresses several numerical aspects of the higher order implementation and presents some new advancements in the context of hierarchical curl-conforming polynomial vector basis functions on generalized hexahedral finite elements [1], which are all crucial for making this approach an efficient and practical analysis and design tool for engineers.

Hierarchical curl-conforming vector basis functions enable using different orders of field approximation in different elements for efficient selective discretization of the solution domain. We demonstrate very effective higher order FEM models of complex structures consisting of both very large and very small elements of very different shapes. We also discuss some of the algorithms for the higher order hexahedral mesh generation. Although hierarchical polynomials are inherently ideal for p-refinement of solutions, for general structures it must be combined with an h-refinement. We show excellent convergence properties for several hp-refined meshes and discuss possible further improvements of the technique.

Hierarchical basis functions generally have poor orthogonality properties, which results in FEM matrices with large condition numbers. The ill-conditioning is principally caused by a strong mutual coupling between the pairs of higher-order functions defined on the same (electrically large) generalized hexahedron, which become increasingly similar to one another as the polynomial degrees increase. In order to reduce this coupling, basis functions with better orthogonality properties have to be utilized. We show that higher order large-domain hierarchical curl-conforming FEM vector basis functions constructed from standard orthogonal polynomials and their modifications on generalized curvilinear hexahedral elements exhibit a very slow increase of the condition number of the FEM matrix with increasing the field-approximation orders and a very dramatic reduction of the condition number for high orders as compared to the technique in [1] using field expansions based on simple power functions (the reduction is as large as fourteen orders of magnitude in some cases).

To ensure that the CPU time per unknown in higher order solutions is comparable to that in low-order solutions, rapid and accurate recursive procedures are needed for evaluation of elements of FEM matrices. We show how important for the efficiency of the solution is that computation algorithms avoid redundant operations related to the indices for basis and testing functions and for geometrical representations within all of the interactions in the FEM solution, as well as the summation indices in the Gauss-Legendre integration formulas. In addition, it is crucial that the topological analysis of the problem and assembly of the connectivity matrix are also done in an optimal way that minimizes the total number of nonzero elements and ensures a similar level of sparsity of system matrices as for low-order solutions.

REFERENCES

1. Ilić, M. M. and B. M. Notaroš, "Higher order hierarchical curved hexahedral vector finite elements for electromagnetic modeling," *IEEE Transactions on Microwave Theory and Techniques*, Vol. 51, 1026–1033, March 2003.

Combining an FEM Domain Decomposition Method with BEM for Accurate Antenna Array Analysis

M. N. Vouvakis[1], **S.-C. Lee**[2], **K. Z. Zhao**[2], **S. M. Seo**[2], **and J.-F. Lee**[2]

[1]University of Massachusetts-Amherst, USA
[2]The Ohio State University, USA

Finite Element Method-Domain Decomposition (FEM-DD) methods have been proven very efficient and effective numerical techniques for the analysis of Maxwell's equations. Among other advantages, it suffice to stress their parallelization ability, ability to systematically couple different numerical methods into hybrid schemes, efficient exploitation of geometrical redundancies and symmetries, and relaxing meshing and adaptive meshing strategies. On the other hand, in light of the resent fast Integral Equation developments, see for example MLFMA, AIM, P-FFT, etc. Boundary Element Methods (BEM) are best suited for the fast analysis of unbounded problems.

This paper attempts to modularly couple the two approaches. The result is a very robust, accurate and efficient method for unbounded electromagnetic problem analysis. The method is extremely efficient when repeating structures are involved in the computational domain. The FEM-DD is coupled with BEM using DD concepts. In other words, the FEM-DD and BEM are viewed as another domain level in the domain decomposition. In overall this is a 2-level DD, where the inner level of the DD is the FEM-DD whereas the outer level DD is the coupled FEM-DD and BEM problem. The method is non-conforming thus it allows for maximum exploitation of geometry repetitions, local adaptation schemes and efficient structured BEM solvers. The overall method is variational and free of internal resonances. Various solutions strategies will be proposed.

New results of the coupled FEM-DD and BEM will be given. Comparisons with other methods, convergence curves and computational statistics will be presented in order to demonstrate the accuracy, efficiency and versatility of the method. Some results on real-world challenging radiation and scattering problems such as very large antenna arrays, hybrid radomes and EBGs will be presented.

Session 2A1
Waves on Metamaterial Elements and Their Applications

Subwavelength Tunneling of Electromagnetic Waves

H. Wen[1], **B. Hou**[2], **and W. J. Wen**[2]

[1]The University of British Columbia, Canada
[2]The Hong Kong University of Science and Technology, China

Under certain conditions, the transmission of electromagnetic waves through subwavelength metallic meshes was enhanced. The metallic mesh (hereby referred to as layer B) is sandwiched between two identical layers in three configurations: split ring arrays, metallic plates with periodic fractal slots, and plastic plates with periodic metallic fractals. The *split rings/metallic mesh/split rings* structure demonstrates some unique electromagnetic (EM) characteristics. It is found that the transmittances of EM waves are significantly enhanced at certain frequencies near the stop bands of the split rings. While the metallic plates with periodic fractal slots (layer A) and plastic plates with periodic fractals (layer C) are a complementary pair (ie an inverse version of each other), in an ABA or CBC configuration, the composite is found to exhibit multiple transmission peaks which do not appear when layer B alone is used. The phenomena of subwavelength tunneling is caused by electromagnetic enhancement at and between the interfaces of the different layers, induced by local resonances of the two outer plates. The simulations indicate that, for the *split rings/metallic mesh/split rings* structure, two different physical mechanisms are responsible for the transmissions: negative refractive index effect, and electromagnetic wave tunneling when EM waves penetrate through negative permittivity substrates sandwiched between two high permittivity slabs. For the ABA and CBC configurations, the nature of the resonance, electrical or magnetic, is a determinant of locating the transmission peak of the composite, either on the left or the right of the sandwiching layer.

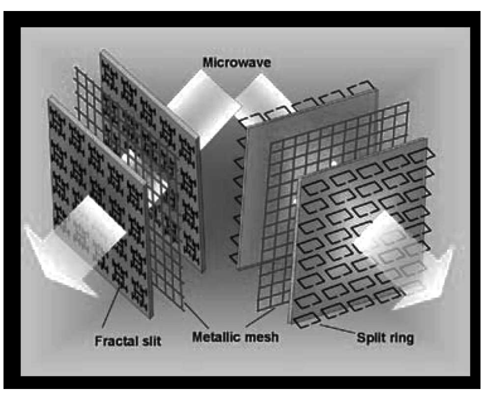

Figure 1: The structural configurations of sandwiched EM metamaterials.

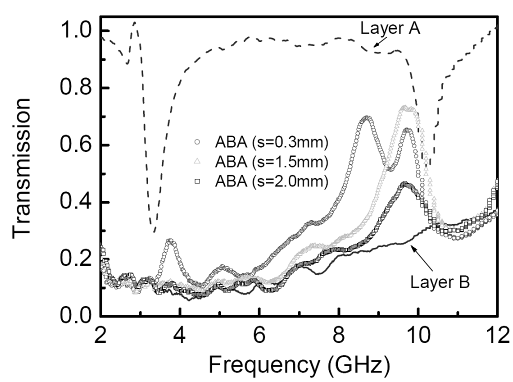

Figure 2: The measured normal transmissions of layer A and B as well as the ABA layers at various separations.

Reflection at the Boundary of Two Periodic Media: a Generic Approach Applicable to Metamaterials

L. Solymar and R. R. A. Syms
Imperial College, UK

One of the central problems of metamaterials research is concerned with the incidence of a plane electromagnetic wave upon a periodic medium [1]. A particularly simple solution, by neglecting the transition layer and higher order modes, for the reflection coefficient has been recently obtained by Tretyakov [2] for the one-dimensional case. An alternative approach to reflection at the boundary of two two-dimensional periodic media consisting of coupled optical waveguides was presented by Syms [3] in the 1980s. His basic idea was to write the recursion equation across the boundary (taking two columns on each side), assume the solution in the form of an incident, a reflected and a transmitted waves and treat interaction between nearest neighbours only. The latter approach is adopted in the present paper to derive generic reflection and transmission coefficients valid for a variety of periodic media which can be described by the nearest neighbour approximation. To show the generality of the expressions examples are given for acoustic waves, plasma waves on nanoparticles (both longitudinal and transverse polarisations), waves on loaded dipoles (both in the axial and in the side-by-side configuration) and magnetoinductive waves on magnetically coupled resonant metamaterial elements (both axial and planar configurations). Potential applications will be discussed

REFERENCES

1. Smith, D. R., W. J. Padilla, D. C. Vier, S. C. Nemat-Nasser, and S. Schultz, *Phys. Rev. Lett.*, Vol. 81, 4184, 2000.
2. Tretyakov, S., *Analytical modeling in applied electromagnetics*, Artech House, Boston, 2000.
3. Syms, R. R. A., "Perturbation analysis of nearly uniform coupled waveguide arrays," *Appl. Opt.*, Vol. 25, 2988–2995, 1986.

Waves on Coupled Lines of Resonant Metamaterial Elements: Theory and Experiments

A. Radkovskaya
M.V. Lomonosov Moscow State University, Russia

O. Sydoruk and E. Shamonina
University of Osnabrück, Germany

C. J. Stevens and D. J. Edwards
University of Oxford, UK

L. Solymar
Imperial College, UK

The coupling and the resulting power transfer between two parallel magnetoinductive waveguides consisting of resonant metamaterial elements were first discussed by Shamonina and Solymar [1]. It was shown that in the lossless case full power transfer is possible between the two waveguides. A particularly interesting case arises when the two waveguides are shifted relative to each other parallel to their axes. At its most general the theory is formulated in terms of five mutual inductances, i.e., each element is coupled to its nearest neighbour in the same waveguide and to the three nearest elements in the parallel waveguide. The resulting dispersion curves have two branches with a stop band between them. The pass band and the power transfer are shown to be fast varying functions of the shift. It is shown further that the power transfer between the two waveguides may vary as much as 40 dB (minimum transmission when the frequency of operation appears to be in the stop band) so that the effect can serve as an efficient switch.

The experiments are performed in the frequency range of 0.3–0.9 GHz using two waveguides parallel to each other consisting of spiral resonant elements in the planar configuration. The first element of waveguide 1 was excited from below by a small loop protruding at the end of a coaxial cable. The receiver consisting of a similar loop was scanned above waveguide 2 measuring the magnetic field at positions corresponding to the centres of the elements. The measured values of the current distribution in waveguide 2 and the measured power transfer between the waveguides are shown to be in good agreement with the theoretical predictions.

REFERENCES

1. Shamonina, E. and L. Solymar, *J. Phys. D: Appl. Phys.*, Vol. 37, 362, 2004.

Quasi-static Waves on Resonant Elements in Non-chiral Periodic Media and Metamaterials: a Historical Survey

L. Solymar
Imperial College, UK

E. Shamonina
University of Osnabrück, Germany

Due to the interest in filters and in slow-wave-structures for microwave tubes several researchers derived dispersion characteristics and discussed their applications both for one-dimensional and two-dimensional cases. The existence of both forward and backward waves were shown, and the relationship between phase and group velocities were examined. This early work done in the 50 s and 60 s by Mourier [1], Atabekov [2] and Silin [3] will be discussed followed by plasma waves on nanoparticles as presented by Quinton et al. [4], Brongersma et al. [5], and Weber and Ford [6]. Similar waves were shown to be able to propagate along loaded, electrically coupled metallic rods (called electric dipoles in this context) [7], or along a set of magnetically coupled loops [8, 9]. Due to their origin these latter waves were called magnetoinductive waves. These additional waves may be excited by an incident electromagnetic wave but they are not dependent on them. They have a separate existence. The similarities and differences between the various waves will be stressed and possible applications [9–13] including near field imaging and near field manipulation such as waveguiding or focusing will be discussed.

REFERENCES

1. Mourier, G., "Circuits a structure periodique a deux et trois dimensions. Applications possibles aux tubes a ondes progressive," *L'Onde Electrique*, Vol. 38, 95–100, 1958.
2. Atabekov, G. I., *Linear Network Theory*, Pergamon Press, Oxford, 1965.
3. Silin, R. A. and V. P. Sazonov, *Slow Wave Structures*, Boston SPA, Eng, National Lending Library for Science and Technology, 1971.
4. Quinton, M., A. Leitner, J. R. Krenn, and F. R. Aussenegg, *Opt. Lett.*, Vol. 23, 1331, 1998.
5. Brongersma, M. L., J. W. Hartman, and H. A. Atwater, *Phys. Rev. B*, Vol. 62, R16356, 2000.
6. Weber, W. H. and G. W. Ford, *Phys. Rev. B*, Vol. 70, 125429, 2004.
7. Tretyakov, S. A. and A. J. Viitanen, *El. Eng.* Vol. 82, 353, 2000.
8. Shamonina, E., V. A. Kalinin, K. H. Ringhofer, and L. Solymar, *Electron. Lett.* Vol. 38, 371, 2002.
9. Shamonina, E., V. A. Kalinin, K. H. Ringhofer, and L. Solymar, *J. Appl. Phys.*,Vol. 92, 6252, 2002.
10. Freire, M. J., R. Marques, F. Medina, M. A. G. Laso, and F. Martin, *Appl. Phys. Lett.*, Vol. 85, 4439, 2004.
11. Nefedov, I. S. and S. A. Tretyakov, *MOTL*, Vol. 45, 98, 2005.
12. Freire, M. J. and R. Marques, *Appl. Phys. Lett.*, Vol. 86, 182505, 2005.
13. Shamonina, E. and L. Solymar, *J. Phys. D: Appl. Phys.* Vol. 37, 362, 2004.

Wave Propagation in Grounded Dielectric Slabs with Double Negative Metamaterials

W. Shu and J. M. Song
Iowa State University, USA

Double negative (DNG) metamaterials, which have both negative permittivity and negative permeability, have been attracting much interest in recent years. They are being extensively studied for their novel properties in guidance, radiation, and scattering of electromagnetic waves. In some of the previous works, exotic properties in grounded dielectric slab have been reported, such as the cutoff of the first TM mode, the special regions of TM surface modes for which the curve of effective dielectric constant ϵ_{eff} versus normalized thickness $d = \lambda_0$ does not increase monotonically, and the potential to suppress all surface waves.

In our work we show that, for grounded dielectric slab with lossless, isotropic, and homogeneous DNG medium, not only TM surface modes but also TE surface modes have special regions within which two different eigen modes exist: one exhibits the backward property since the power propagated in dielectric slab is more than in the air, therefore the total power flow direction is opposite to the phase velocity; the other has more power propagated in air region, so the total power flow direction is the same as the phase velocity.

The evanescent surface modes are studied using graphical method. It is shown that a proper evanescent surface mode can exist which is impossible with double positive (DPS) medium. Unlike the normal surface mode which has sine and cosine standing wave in dielectric slab, evanescent surface mode exponentially decays in both slab region and air region. It is also found the shapes of dispersion curves for evanescent surface modes are highly dependant on material and structure parameters. Like normal surface modes, the evanescent surface modes can be suppressed under certain conditions.

It is desirable to know the complete spectrum of waveguide structure, especially when dealing with discontinuity problems using mode matching method. The complete proper spectrum of the grounded dielectric slab with DPS medium consists of a set of discrete surface modes and a continuous radiation spectrum. Besides these, the proper spectrum of grounded dielectric slab with DNG medium includes one evanescent surface mode and infinite number of complex surface modes. It is proved that the complex modes are always improper with DPS medium while they are always proper with DNG medium, whose fields exponentially decay in both transverse and longitudinal directions. They do not carry away power in these two directions, acting as reactive fields.

Finally, the conditions for surface wave suppression suggested by P. Baccarelli and his colleagues are examined and loosened to necessary and sufficient conditions. These thorough criteria give us more freedom to design the substrate of patch antenna to increase radiation efficiency and reduce edge-diffraction effects.

On the Microstrip Characterization of Artificial Magneto-dielectric Structures

C. R. Simovski[1,2], **P. Ikonen**[1], **and S. Tretyakov**[1]

[1]Helsinki University of Technology, Finland
[2]St. Petersburg Institute of Fine Mechanics and Optics, Russia

Wideband measurement methods are needed for extracting effective material parameters of artificially engineered composite materials to enable further development and optimization of these materials. It is obvious that resonator based measurement techniques fail to fulfill the ultimate goal of wideband characterization. Therefore, waveguide measurement methods become necessary. Depending on the characterized material sample, usually two basic guiding structures are utilized: small scatterers or homogeneous blocks of material can be measured using a parallel-plate waveguide or a (quasi-)TEM transmission line, usually a normal microstrip line. Building a parallel-plate waveguide operating at low frequencies (1–3 GHz) is practically difficult, thus, we propose to use a microstrip line. In this presentation we demonstrate an experimental characterization process targeted to extract the material parameters of a uniaxial artificial magneto-dielectric sample with resonant properties. We extract the parameters from measured S-parameters of loaded and empty microstrip line. It is shown that the proposed technique is suitable for characterizing the properties of the material over a rather wide frequency range excluding the thickness resonance bands. We use the comparison of S-parameters of the material block under test and a reference block with known permittivity and no magnetic properties. The novelty of our work is related with modifications of the known characterization methods. These modifications are required when the following three factors simultaneously disturb the characterization procedure:

1. The network analyzer cannot be calibrated with respect to the actual input ports but with respect to the cable connectors, because the properties of two cable connectors and therefore the electric distance between the calibration point and the input ports is unknown.

2. The wavelength in the empty waveguide is not exactly equal to that of free space, and we do not know the possible error.

3. The reference dielectric block with known material parameters (that is used in the proposed comparative method) does not fill the effective cross section of the microstrip line completely.

Traveling Waves along the Metasolenoid

L. Jylhä, S. Maslovski, and S. Tretyakov
Helsinki University of Technology, Finland

A new magnetic particle called "metasolenoid" was introduced in [1, 2], see Figure 1. It consists of a stack of closely packed metallic single split-ring resonators. In the lowest-order resonant mode the metasolenoid can be used as a magnetic inclusion [1], but in its higher order modes it can be used as a high-quality resonator [2]. At higher modes, the magnetic field is mostly concentrated inside the solenoid, where are no metallic parts. The field distribution is quite similar to that inside volume resonators. Therefore, the quality factor of a metasolenoid can be much higher than the quality factor of an ordinary microstrip resonator.

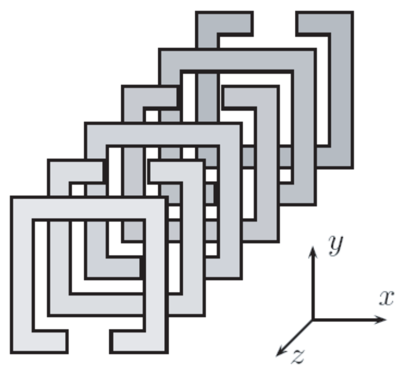

Figure 1: Geometry of the metasolenoid.

In this study, we focus on the use of the metasolenoid as a wavequiding structure. Eigenmodes in a wavequide made of coupled capacitively loaded wire loops were studied also in [3, 4], but there only the interaction between the neighboring loops was taken into account. Such approach is valid only if the separation between the loops is of order of the loop radius or larger, i.e., when the interaction between the loops is weak. In this study, the interaction between the rings that are not neighbors is also taken into account. Therefore, structures with small separations between the rings can be studied. When the separation between the rings is small, the coupling between them is strong and the waveguide is capable to support slow waves with very short wavelength.

Metasolenoids can find applications in the design of delay lines, filters, and resonant magnetic sensors.

REFERENCES

1. Maslovski, S., P. Ikonen, I. Kolmakov, S. Tretyakov, and M. Kaunisto, "Artificial magnetic materials based on the new magnetic particle: metasolenoid," *Progress in Electromagnetics Research*, Vol. 54, 61–81, 2005.
2. Jylhä, L., S. Maslovski, and S. Tretyakov, "High-order resonant modes of a metasolenoid," *Journal of Electromagnetic Waves and Applications*, Vol. 19, No. 10, 1327–1342, 2005.
3. Shamonina, E., V. A. Kalinin, K. H. Ringhofer, and L. Solymar, "Magnetoinductive waves in one, two, and three dimensions," *J. Appl. Phys.*, Vol. 92, 6252, 2002.
4. Shamonina, E. and L. Solymar, "Magneto-inductive waves supported by metamaterial elements: components for a one-dimensional waveguide," *J. Phys. D: Appl. Phys.*, Vol. 37, 362, 2004.

Plasmonic-polaritonic Photonic-prystal Superlattices as Left-handed Metamaterials

V. Yannopapas
University of Patras, Greece

A. Moroz
Wave-scattering.com, Germany

Left-handed metamaterials come in two basic types, namely those based on purely dielectric periodic structures, or as periodic metallic microstructures exhibiting electric and magnetic resonances [1]. The purely dielectric metamaterials are characterised by rather low wavelength-to-structure ratio (typically less than 2:1). On the other hand, the metamaterials based on metallic microstructures, the most prominent example of which are those consisting of split ring resonators (SRRs) and wires, are truly subwavelength structures with wavelength-to-structure ratio at least 5:1. Here, we present a new set of artificial structures which can exhibit a negative refractive index band in excess of 6% in a broad frequency range from deep infrared to terahertz range [2]. The structures are composites of two different kinds of non-overlapping spheres, one made from inherently non-magnetic polaritonic and the other from a Drude-like material. The polaritonic spheres are responsible for the existence of negative effective magnetic permeability whilst the Drude-like spheres are responsible for negative effective electric permittivity. The resulting negative refractive index structures are truly subwavelength structures with wavelength-to-structure ratio 14:1, which appears almost by 50% higher than it has been achieved so far. Our results are explained in the context of the extended Maxwell - Garnett theory [3] and reproduced by the calculations based on the layer Korringa-Kohn-Rostoker method, an ab initio multiple scattering theory [4, 5].

REFERENCES

1. Pendry, J. B., "Negative refraction," *Contemp. Phys.*, Vol. 45, No. 3, 191–202, 2004.
2. Yannopapas, V. and A. Moroz, "Negative refractive index metamaterials from inherently non-magnetic metamaterials for deep infrared to terahertz frequency ranges," *J. Phys.: Condens. Matter*, Vol. 17, No. 25, 3717–3734, 2005.
3. Ruppin, R., "Evaluation of extended Maxwell-Garnett theories," *Opt. Commun.*, Vol. 182, Nos. 4–6, 273–279, 2000.
4. Stefanou, N., V. Yannopapas, and A. Modinos, "Heterostructures of photonic crystals: frequency bands and transmission coefficients," *Comput. Phys. Commun.*, Vol. 113, No. 1, 49–77, 1998.
5. Stefanou, N., V. Yannopapas, and A. Modinos, "MULTEM 2: A new version of the program for transmission and band-structure calculations of photonic crystals," *Comput. Phys. Commun.*, Vol. 132, Nos. 1-2, 189–196, 2000.

Electroinductive Waves on Chains of Resonators

M. Beruete[1], **M. J. Freire**[2], **R. Marqués**[2], **F. J. Falcone**[1], **and J. D. Baena**[2]

[1]Universidad Pública de Navarra, Spain
[2]Universidad de Sevilla, Spain

A new kind of waves supported by chains of resonators drilled on a metallic substrate is presented. Propagation of energy comes as a consequence of the electric coupling between these resonators. Therefore, these waves are termed as electroinductive waves (EIWs). They can be interpreted as the dual counterpart of the so called magnetoinductive waves (MIWs) [1–3], which are due to the mutual inductance between chains of resonators. The unit cell of the analyzed structure is formed by the dual or "complementary" (in Babinet's sense) particle of the split ring resonator (CSRR), recently reported in [4]. This unit cell, as well as its circuit model, is shown in the Figure. In order to show the existence and excitation of the reported EIWs, analytical calculations, electromagnetic simulations and experiments have been carried out. Both, simulations and experiments show a very good agreement with the analytical model.

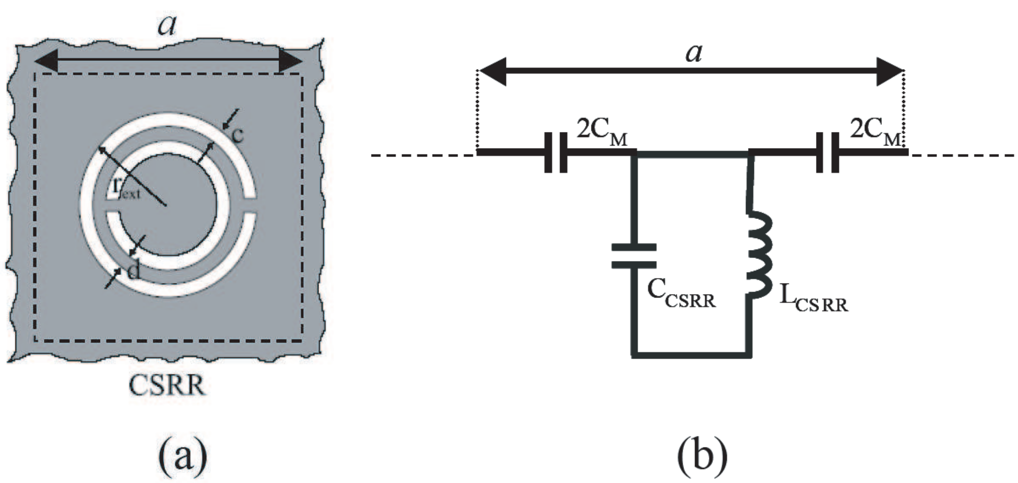

REFERENCES

1. Shamonina, E., V. A. Kalinin, K. H. Ringhofer, and L. Solymar, *Electron. Lett.*, Vol. 38, 371, 2002.
2. Shamonina, E., V. A. Kalinin, K. H. Ringhofer, and L. Solymar, *J. Appl. Phys.*, Vol. 92, 6252, 2002.
3. Shamonina, E. and L. Solymar, *J. Phys. D*, Vol. 37, 362, 2004.
4. Falcone, F., T. Lopetegi, M. A. G. Laso, J. D. Baena, J. Bonache, M. Beruete, R. Marques, F. Martin, and M. Sorolla, *Phys. Rev. Lett.*, Vol. 93, 197401, 2004.

New Experimental Results and Physical Interpretation of a Near-field Planar Magneto-inductive Lens for 3D-subwavelength Imaging

M. J. Freire, R. Marqués, and J. D. Baena
University of Seville, Spain

Near-field sub-wavelength imaging has been proposed in the optical frequency range by using a planar silver slab [1] and in the microwave regime by using a magnetized ferrite slab [2]. In both cases the physical mechanism involving the imaging is the amplification of the evanescent Fourier harmonics of the electromagnetic field coming from the source by means of the excitation of surface waves in the slab interfaces. More recently a near-field lens operating in the microwave regime based on the excitation of surface magnetoinductive (MI) waves in a twodimensional (2D) planar array of inductively coupled resonators has been reported [3]. The device consists of two parallel 2D arrays of broadside coupled split ring resonators (BCSRR). A loop input antenna is used as field source and a similar output antenna is used to measure the image. The reported device shows 3D super resolution (see Figure 2). After these encouraging results new prototypes were fabricated and a physical interpretation of the results is in progress [4]. The aim of this contribution is to present these new experimental results, altogether with its physical interpretation.

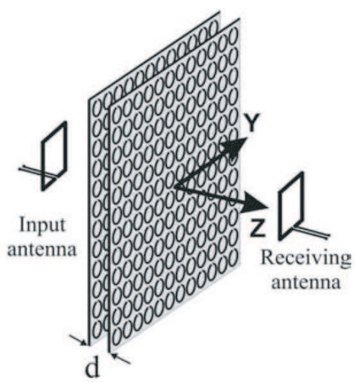

Figure 1: Sketch of the experimental setup.

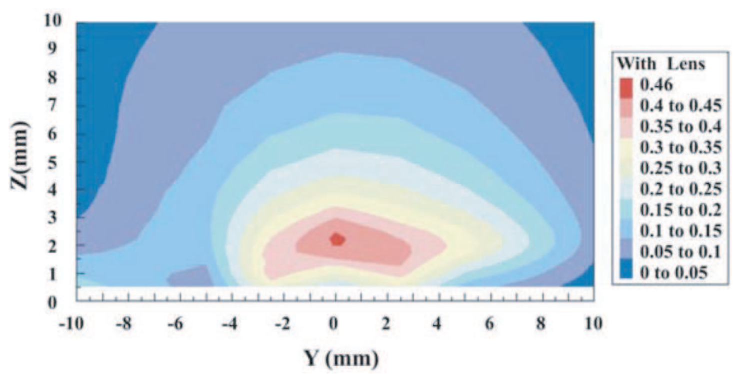

Figure 2: Measurement of the transmission coefficient between the antennas in the device of Figure 1.

REFERENCES

1. Fang, N., H. Lee, C. Sun, and X. Zhang, *Science*, Vol. 308, 534, 2005.
2. Marques, R., F. Mesa, and F. Medina, *App. Phys. Lett.*, Vol. 86, 023505, 2005.
3. Freire, M. and R. Marques, *App. Phys. Lett.*, Vol. 86, 182505, 2005.
4. Marques, R., F. Mesa, M. Freire, and J. D. Baena, *Proc. of the ICECOM05 Conf.*, Dubrownik, Croatia, 2005.

Analysis and Visualization of Fields and Waves inside a PEMC Waveguide

A. H. Sihvola, **I. V. Lindell**, **and M. Pitkonen**
Helsinki University of Technology, Finland

The PEMC medium is a special type of metamaterial which is a generalization of the well-known concepts of PEC (perfect electric conducting) and PMC (perfect magnetic conducting) media. Perfect electromagnetic medium is characterized by an admittance-type parameter $M = \cot\vartheta$, and the choices of $\vartheta = 0$ and $\vartheta = \pi/2$ give the PEC and PMC cases, respectively. For the basic properties of PEMC media, see [1–3].

The effect of the PEMC boundary is that the field that is incident on it will suffer a rotation in polarization. Hence it is a non-reciprocal actor in the electromagnetic problem. (In fact, the suggested realizations of PEMC elements require gyrotropic materials; either ferrites or magnetized plasma -type antisymmetric material parameter responses.) As the ordinary metal waveguide serves as a structure where longitudinal propagation is combined with reflection resonances in the transverse direction, we can expect interesting effects to be found in the behavior of electromagnetic fields that are transmitted through a waveguide with walls made of PEMC material.

We have analyzed the electric and magnetic fields in PEMC waveguides for propagating modes. The field structure is obviously dependent on the M parameter and it can be seen to approach uniformly the well-known fields of waveguides with PEC or PMC walls. The effect of finite value of the PEMC parameter M is that the transverse fields are no longer orthogonal, at the walls the electric field has a tangential component and both electric and magnetic fields have longitudinal components, forming paired loops. In the presentation we shall visualize these effects in various ways.

REFERENCES

1. Lindell and Sihvola, *J. Electro. Waves Applic.*, Vol. 19, No. 7, 861–869, 2005.
2. Lindell and Sihvola, *IEEE Trans. Antennas Propagat.*, Vol. 53, No. 9, 3005–3011, September 2005.
3. Lindell and Sihvola, *IEEE Trans. Antennas Propagat.*, 3012–3018.

Session 2A2
Plasmonic Nanophotonics

Optical Response of Metal Nanoparticle Chains

K. H. Fung and C. T. Chan
The Hong Kong University of Science and Technology, China

The excitation of surface plasmon on metal nanoparticles is interesting to many researchers because of its variety of applications. By arranging nanoparticles in different ways, many interesting properties can be observed [1]. For metal nanoparticle chains, there is a red (blue) shift on the plasmon resonant frequency for longitudinal (transverse) excitation. Numerical and experimental results on this splitting of plasmon resonant frequency for Ag nanoparticle chains with diameters around 10 nm are compared by Sweatlock et al. recently [2]. They used finite integration techniques (which may contains artifacts) for the numerical calculations [2]. Here, we present the results calculated by the multiple scattering theory (MST) and the ways to understand the results using simple models.

MST calculations are performed on the extinction of finite silver nanosphere chains embedded in glass matrix. The transmission and reflection of an infinite 2D arrays of silver nanospheres are also calculated to understand the interaction between nanoparticle chains. The results are in agreement with recent experiments. The splitting of plasmon-resonance modes associated with different polarizations of the incident light is further understood by employing simple models. Results on the effect of order and disorder in nanoparticle chains are also presented.

REFERENCES

1. Kreibig, U. and M. Vollmer, *Optical Properties of Metal Clusters*, Springer, Berlin, 1995.
2. Sweatlock, L. A., S. A. Maier, H. A. Atwater, J. J. Penninkhof, and A. Polman, *Phys. Rev. B*, Vol. 71, 235408, 2005.

Focusing Using Single-negative Medium

J. Li and C. T. Chan
The Hong Kong University of Science and Technology, China

A thin slab of single negative material, such as a silver slab, is known as the poorman's version of the perfect lens proposed by Pendry. It can also act as a super lens in the sense that it can break the classical diffraction limit for the TM wave in the near field. In this work, we analyze the condition for image formation for a thin (nanoscale) slab and show that there exists quantized conditions for the optical path in order for a slab to behave like a lens, and both the silver (single negative) thin slab and the perfect (double negative) lens become special cases of such condition. This quantization serves to be an extension of the focusing criteria. Moreover, by employing an additional resonance configuration, high transmittance of light can be induced and the lens functions like the perfect lens, and yet it is much simpler in structure. This improvement follows directly from the established quantization rule.

Fabrication and Characterization of High Sensitivity Visible Light Photonic Crystal Biosensors

N. Ganesh and B. T. Cunningham
University of Illinois at Urbana-Champaign, USA

We report the fabrication and characterization of improved Photonic Crystal (PC) biosensors operating in the visible region of the electromagnetic spectrum (instead of infrared) and based on a nanoporous low refractive index surface structure. These devices display a high degree of sensitivity to surface-specific bimolecular interactions and very low sensitivity to nonspecific bulk refractive index variations. Such properties are extremely attractive in a biosensor, as the Signal to Noise Ratio (SNR) is improved and consequently the detection resolution of the bio-assay is enhanced. Rigorous Coupled Wave Analysis (RCWA) is used to model the device and show that its superior characteristics arise from stronger confinement of evanescent electric fields close to its surface (Figure 1). Electron Beam Lithography (EBL) is used to fabricate a nano-structure 'mold' (Figure 2) from which nano-replicas are created using PDMS stamps at high throughput and low cost. The replicated nanostructures are coated with a high refractive index dielectric (TiO_2) to form the final device (Figure 3). Results of the Bulk Sensitivity and Surface Sensitivity of the device are reported and compared to devices operating in the same manner but in longer wavelength regimes.

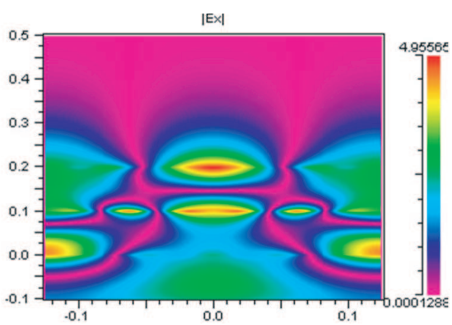

Figure 1: RCWA modeling results showing strongly confined electric fields at resonance.

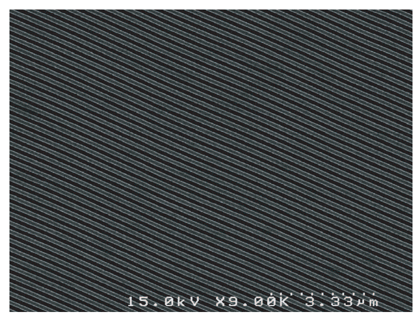

Figure 2: SEM micrograph of the surface structure of the 'mold' from which devices are made. The structure is comprised of linear features, with a period of 250 nm.

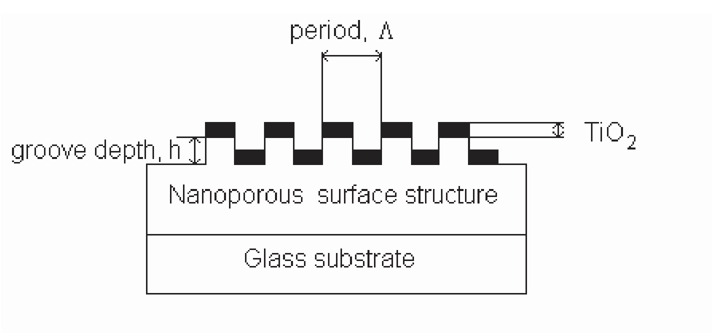

Figure 3: Cross section structure of the photonic crystal device. The resonance wavelength depends on the values of h, Λ and thickness of the TiO_2 layer.

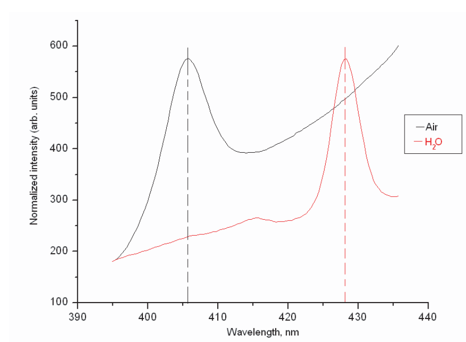

Figure 4: Normalized reflectance spectra shift of the PC device in air (black) and water (red) corresponding to a bulk refractive index change.

Thermal Emission by Photonic Micro-textured Surfaces

J. T. K. Wan and C. T. Chan
Hong Kong University of Science and Technology, Hong Kong

Ordinary metallic photonic crystals (PCS) have photonic band gaps in which the density of states is suppressed. Thermal emission of photons is suppressed in those frequencies, and is enhanced in other frequencies. We considered the thermal emission property of a photonic crystal and compared it with that of a simple micro-textured surface. The proposed micro-textured surface exhibits a similar optical thermal emission spectrum with that of a photonic crystal. In addition, the present proposed topology also suppress emission in low frequencies. This simple and yet effective surface structure inspires new directions in fabricating thermal emitting materials.

Calculation of Scattering from Polyethylene Particles Compared with Terahertz Measurements

L. M. Zurk[1], **B. Jouni**[1], **F. Farahbakhshian**[1], **D. P. Winebrenner**[2]
E. Thorsos[2], **M. R. Leahy-Hoppa**[3], **and L. M. Hayden**[3]

[1]Portland State University, USA
[2]University of Washington, USA
[3]University of Maryland, USA

The Terahertz (THz) portion of the electromagnetic (EM) spectrum that lies between the microwave and infra-red spectrums ($1\,\mathrm{THz} = 10^{12}\,\mathrm{Hz}$) and has remained almost entirely unexplored due to difficulties in the generation and detection of energy at these frequencies. With the advent of ultrafast optical laser technologies, the ability to generate and detect energy is enabling the exploration within this so-called THz-gap. One potentially promising application of THz spectroscopy is the detection of explosive materials, and initial measurements indicate that explosives may have unique spectral characteristics in this region. However, the scattering physics that gives rise to these signatures is only beginning to be explored, and may be critically effected by the granular composition of most explosive materials.

In this paper, formulations for the EM scattering from collections of spherical scatterers are developed and applied to granular materials representative of explosive materials. Calculations are presented for pellets comprised of polyethylene (PE) powder. This spectrophotometric grade powder is manufactured by Sigma-Aldrich and has been used as a pellet binder in experiments focused on the detection of RDX explosive. In this paper, the transmission characteristics of PE itself are computed using a random media model consisting of uniformly distributed Mie spheres with a log-normal size distribution. The result of the Monte Carlo computation is compared with FTIR spectroscopy acquired from PE samples obtained from two different manufactured bins, and the two bins were observed to have markedly different grain size distributions. As expected, the observed scattering is strongly grain-size dependent. Implications and future research on this topic are discussed in the context of evaluating the ability to use THz spectroscopy for explosives detection.

Slow Electromagnetic Waves and Resonance Phenomena in Photonic Crystals

A. Figotin and I. Vitebskiy
University of California at Irvine, USA

The problem of slowing down electromagnetic (EM) waves has been extensively discussed in the literature. Such a possibility can be useful in a variety of microwave and optical applications. Our objective is to compare different ways to achieve this effect in linear dispersive media such as photonic crystals. A very low group velocity $v_g = \partial\omega/\partial k$ corresponds to stationary points of the dispersion relation $\omega(k)$. In periodic layered media, the dispersion relations can develop only three kinds of stationary points. Assuming that the values ω_s and k_s correspond to a stationary point, the above three possibilities can be defined as follows

1. The vicinity of a band edge, where $\omega - \omega_s \sim (k - k_s)^2$
2. The vicinity of a stationary inflection point, where $\omega - \omega_s \sim (k - k_s)^3$.
3. The vicinity of a degenerate band edge, where $\omega - \omega_s \sim (k - k_s)^4$.

The case 1 relates to a common EM band edge, it can be found in any periodic array. By contrast, the cases 2 and 3 can only occur in periodic arrays with special geometry [1-6]. In all three cases the group velocity v_g vanishes as ω approaches ω_s. But when the efficiency of conversion of incident light into the slow mode is concerned, the three cases are fundamentally different from one other. Consider plane EM wave incident on semi-infinite photonic crystal with dispersion relation having a stationary point at $\omega = \omega_s$. What happens if the wave frequency ω approaches ω_s? Let S be the energy flux associated with the slow wave transmitted inside the crystal. It turns out that in the vicinity of photonic band edge (case 1), the energy flux S of the transmitted wave vanishes along with the group velocity $v_g = \partial\omega/\partial k$. This implies total reflection of the incident wave as $\omega \to \omega_s$.

By contrast, in the vicinity of stationary inflection point (case 2), the energy flux $\boldsymbol{S}$ remains finite even at $\omega = \omega_s$, contrary to the fact that the wave group velocity vanishes. The latter implies that the wave amplitude inside the photonic crystal increases dramatically. In steady-state regime, the incident wave with $\omega = \omega_s$, after entering the periodic structure, gets almost 100% converted into a non-Bloch frozen mode with the energy density growing quadratically with the distance from the photonic crystal boundary. Thus, the case 2 provides ideal conditions for slowing down the EM wave by a semi-infinite photonic crystal.

Finally, in the vicinity of degenerate band edge (case 3), the energy flux $\boldsymbol{S}$ vanishes, similarly to what we had in the vicinity of a regular band edge (case 1). At the same time, the electromagnetic energy density inside the periodic structure now becomes enormous, similarly to what takes place in the vicinity of stationary inflection point (case 2).

Finite bounded periodic structures supporting the frozen mode regime, can also display a giant Fabry-Perot cavity resonance associated with the degenerate photonic band edge [6]. In contrast to the regular transmission band edge resonance, in the case of degenerate band edge the field intensity enhancement is proportional to the forth degree of the number of layers in the stack. This allows to drastically reduce the dimensions of the resonant cavity without compromising on performance. This effect can be realized not only in bounded photonic crystals, but also in a waveguide environment, as well as in a finite array of coupled resonators.

REFERENCES

1. Figotin, A. and I. Vitebsky, *Phys. Rev. E*, 63, 066609–1–17, 2001.
2. Figotin, A. and I. Vitebskiy, *Phys. Rev. B*, 67, 165210–1–20, 2003.
3. Figotin, A. and I. Vitebskiy, *Phys. Rev. E*, 68, 036609–1–16, 2003.
4. Ballato, J., A. Ballato, A. Figotin, and I. Vitebskiy, *Phys. Rev. E*, 71, 036612–1–12, 2005.
5. Figotin, A. and I. Vitebskiy, arXiv:physics/0504112 v2 19 Apr 2005.
6. Figotin, A. and I. Vitebskiy, *Phys. Rev. E*, 72, 036619–1–12, 2005.

The Dispersion Relations of the Sub-skin-depth Metal Particles

S. C. Chen
Far East College, Taiwan

T. M. Chang and D. P. Tsai
National Taiwan University, Taiwan

According to Maxwell's equations, if sizes of conductors are much larger than the incident wavelength, the electromagnetic fields are forbidden inside the conductor, only a very thin layer is penetrated by electromagnetic fields, this thin layer is the so-called "skin depth". Under optical waves, the skin depth is about 20 nanometers for noble metals, thus, if the size of the metal particle is less than the skin depth, the particle will be possible to be full of the electromagnetic fields. Based on such point of view, it is easy to understand why the absorption of optical waves only happened in sub-micro particles [1].

There are some interesting phenomena should be further studied in the sub-skin-depth optics. For example, the internal electric field of the optical wave can excite volume plasmons, for classical electromagnetic theories, volume plasmons can be excited only when the incident frequency is higher than the plasma frequency [2]. It means that both the surface plasmon and volume plasmon are able to coexist in sub-skin-depth space, the coupling of these two type plasmons suggests that the dispersion relation of the sub-skin-depth particle should be quite different from the classical one. We will try to derive the novel dispersion relation from fundamental theories and verify it by experiments and numerical simulations.

REFERENCES

1. Messinger, B. J., K. U. Von Raben, and R. K. Chang, "Local fields at the surface of noble-metal microspheres," *Phys. Rev. B*, Vol. 24, No. 2, 649, 1981.
2. Raether, H., "Surface plasmons on smooth and rough surfaces and on gratings," Springer-Verlag, 1988.

Photonic Crystal Made of Dichroic Filters

M. Beruete[1], **M. Sorolla**[1], **and I. Campillo**[2]

[1]Public University of Navarre, Spain
[2]Labein Centro Tecnológico, Spain

By using a convencional dichroic filter operating in the Millimeter Waves, made of a metallic plate of 0.5 mm thickness drilled with a two dimensional hole array with 4 mm hole diameter and 5 mm geometrical period in both transversal dimensions, we have designed a Photonic Crystal consisting of stacking several plates separated by air with a longitudinal geometrical period of 2 mm. In spite of the fact that the longitudinal periodicity predicts a bandgap around 85 GHz, a lower bandgap is also present at 57 GHz due to transversal periodicity. Possible applications as frequency selective surfaces are discussed.

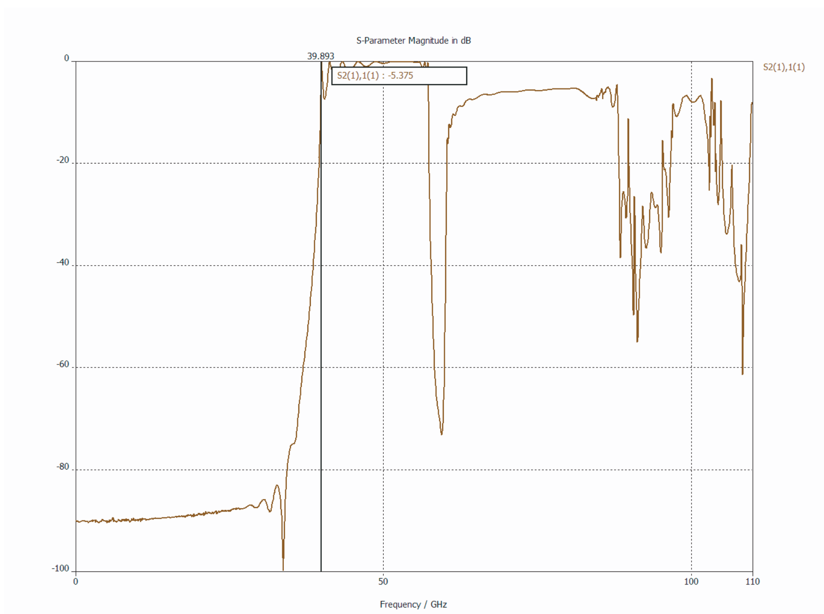

REFERENCES

1. Goldsmith, P. F., "Quasioptical Systems–Gaussian Beam," *Quasioptical Propagation, and Applications*, IEEE Press, 1998.
2. Joannopoulos, J. D., R. D. Meade, and J. N. Winn, *Photonic Crystals: Molding the Flow of Light*, Princeton Univ. Press, Princeton, NJ, 1995.

Magnonic-photonic Crystals with Application to Tunable Microwave Devices

S. A. Nikitov[1], **C. S. Tsai**[2,3], **Y. V. Gulyaev**[1], **and Y. A. Filimonov**[1]

[1]Russian Academy of Sciences, Russia
[2]University of California, USA
[3]National Taiwan University, Taiwan

Magnonic and magneto-photonic crystals based on magnetic materials have become a field of increasing interest in recent years. One- and two-dimensional (1-D and 2-D) periodic layer structures can be engineered by varying the magnetic properties such as magnetization and anisotropy using magnetic-non-magnetic, all-magnetic, ferro- and anti-ferromagnetic lattices. A variety of tunable microwave and magnetooptic devices based on propagation of magnetostatic (or spin) waves in such magnonic and magneto-photonic crystals can be envisaged.

In this work, the dispersion and bandgap characteristics of magnetostatic waves propagating in 1- and 2-D magnonic and magneto-photonic crystals are first formulated using Maxwell's and Landau-Lifshitz equations. Specifically, the 2-D periodic structure with magnetization inhomogeneity facilitated by creating 2-D array of holes in yttrium iron garnet (YIG) ferromagnetic thin films are analyzed in detail. The resulting dispersion characteristics depend on the periodicity and depth of the holes as well as the bias magnetic field. The corresponding experimental studies were carried out at the frequencny range of 2.0 to 6.0 GHz. The measured dispersion characteristics of the magnetostatic waves show magnetic field-dependent bandgaps. Such magnetically-tunable frequency bandgaps should facilitate control and processing of microwaves. The findings of both theoretical and experimental studies will be presented.

*Supported by the Russian Foundation for Basic Research, Russia and Academia Sinica, Taiwan.

Session 2A3
New Applications of Radar for Non-destructive Testing

Detection of Groundwater by Ground Penetrating Radar

S. I. Elkhetali
Academy of Graduate Studies, Libya

This paper addresses the application of ground probing radar (GPR) to detection of groundwater from relatively deep aquifers in a desert environment. Tests of signal processing techniques to improve the detectability of a weak signal in noise and interference are reported. The study is based on simulated images from structures that have the potential of storing groundwater. Highly attenuation weak echoes from deeper ground strata are difficult to detect because they are contaminated by noise, interference, filtering (selective attenuation of higher frequencies), direct coupling between antennas and dispersion. All these effects are included in the simulation.

To increase the signal to noise ratio to achieve a reasonable probability of detection and false alarm, various processing schemes are possible, typically employing analogue, binary (double threshold) and digital processing. Different system architectures are compared to improve detectability. First impulse and stepped frequency systems were compared. Then there is more emphasis on the stepped frequency and different architectures are compared.

Monograms showing how losses vary as functions of depth and attenuation and how the signal to noise ratio is improved by processing are provided.

The difficulty of detecting a weak signal being reflected from a deep interface in the presence of noise and interference is compounded by electronic components being non-ideal. System effects are studied. A successful detection is obtained when the SNR are adequate to provide an acceptable probability of detection and false alarm. Automatic detection and classification by artificial neural networks is tried to classify geologic subterranean features for aiding and speeding the process and to overcome lack of experts on the field.

Detection of Buried Objects in Periodic Structures with Ground Penetrating Radar Mounted on Moving Vehicles

P. Falorni, L. Capineri, and L. Masotti
University of Florence, Italy

C. G. Windsor
116, New Road, East Hagbourne, OX11 9LD, UK

The aim of this paper is the analysis and the development of algorithms capable to detect anomalies in periodic structures by using an ultra-wide-band (UWB) Ground Penetrating Radar. These inspection methods based on GPR are commonly used for surveys of civil structures like rebar underneath a road or a bridge or more recently for landmines detection along railway tracks. In these cases a radar with an array of antennae is generally mounted on a moving vehicle which allows the acquisition of radar signals at a certain velocity. In order to detect variations of the inspected area in real time it is necessary to develop quick signal processing methods also capable to account for the unavoidable variation of the background measurable with radar (e.g., period of the bars distance in the railway or the thickness of a layer in a road).

Among several possible methods available in the literature (physical model based or image processing based) we decide for the homomorphic deconvolution of radar signal based on the Cepstrum [ref 1]. This technique has been chosen according to the assumption that the received radar signal is generated by the convolution of the transmitted signal and the characteristic function of the object. To prove this assumption we synthesized signals of some buried landmines with the convolution model and we compared with the experimental one. In the case of the rebar or pipes buried in concrete layers, this assumption is still valid considering that the radar central wavelength is much comparable to the object size and the characteristic object function becomes simpler. This trial on simple objects was needed to set the algorithm parameters. Then we have simulated several cases of interest for GPR surveys like variation of object dimensions, variation of the periodic pattern, variation of the periodic buried objects lateral distance and different values of signal to noise ratio. The method included a moving window approach to calculate variations in the acquired signals and requires an initialization step (initial pattern estimation). Other methods based on Fourier Transform have also been investigated.

Finally the algorithm was applied to an experimental dataset of rebar buried in a 4 cm thick concrete layer separated by 12 cm. The signals are acquired in a bridge with a 1.5 GHz central frequency UWB radar along a distance of 7 m. The results are an average distance of rebar 15.5 cm with standard deviation 2.3 cm. A processing time of 0.5 s with acquisitions at pulse repetition frequency of 32 kHz was found to be compatible with a vehicles velocity of about 6 km/h.

REFERENCES

1. Oppenheim, A. V. and R. W. Shafer, *Digital signal processing*, Prentice Hall, London, 1975.

Development of High Speed GPR for Railtrack Assessment

S. Bandyopadhyay[1], **J. Gascoyne**[2], and **W. Al-Nuaimy**[1]
[1]University of Liverpool, UK
[2]Zetica, UK

Rapid and non-destructive evaluation of the quality of the railway infrastructure, specifically the under-track ballast, is a growing concern worldwide, and GPR has demonstrated its ability to provide such an evaluation, within the constraints of the available technology. This paper presents the results of ongoing research into the development of a high-speed train-mounted multiple-antenna GPR system for non-destructive assessment of the railway trackbed. By travelling on trains in service and at line speeds, such an inspection system can significantly improve the efficiency and cost-effectiveness of maintaining and renewing railway under-track ballast. The paper addresses the issues of antenna shielding against electromagnetic interference, electromagnetic compatibility tests, antenna choice, configurations and positioning, as well as optimal methods for triggering, registration, and post-processing.

Methods for triggering an array of GPR antennas and transferring control between multiple systems are investigated and detailed, as are techniques for coordinating different data sets, namely, multi-frequency GPR arrays, multiple video sequences, GPS positioning data, GIS location data and other track data, in order to fuse the data layers both before and after interpretation within the existing rail model. The paper further details the design and implementation of the control units, the GPR event marker system and data fusion layers prior to processing and interpretation. Results are resented from the UKs first high-speed (60 mph) train-mounted GPR trials.

Automatic Processing of Train-mounted GPR Data for Ballast Inspection

A. Doshi and W. Al-Nuaimy
University of Liverpool, UK

Until very recently, inspection of railtrack using high-speed GPR was not possible due to hardware technology limitations. With the development of newer and faster GPR systems, the prospect of high-speed GPR inspection of rail ballast has become very real, and there is increased interest in developing interpretation algorithms capable of dealing with the large volumes (typically gigabytes) of GPR data that result from such surveys. Such computational tools are required to process and interpret the multi-channel GPR data in a robust, consistent and reliable manner, and present the results in a manner consistent with industry expectations and regulations.

This paper presents recent developments towards new GPR data interpretation software enabling fast, reliable and automated processing of multiple data sets of unlimited size. Specifically, algorithms have been designed for processing the GPR data to reduce the effect of background and clutter using novel signal and image processing techniques. Techniques have been formulated for minimising/eliminating the effect of sleepers (steel and concrete) on high speed rail GPR data. Interactive semi-automated layer picking routines have been designed for pinpointing the ballast-subgrade interface, and for identifying surface anomalies such as AWS magnets and footbridges. Automated and semi-automated methods are presented for ballast dielectric modelling based on the data interpretation and any available corroborative information such as core samples. This allows automatic depth calibration and profiling. Finally, pattern recognition techniques have been been developed to characterise spent or fouled ballast from clean ballast, and have been employed in conjunction with neural networks to automatically characterise the quality of the ballast sub-track by determining the level and nature of degradation in ballast. Results are presented from a number of high-speed trials in the UK.

Frequency and Time Domain Error in Buried Target Radar Signature Extraction

I. van den Bosch[1], **P. Druyts**[1], **M. Acheroy**[1], **and I. Huynen**[2]

[1]Royal Military Academy, Belgium
[2]Microwaves and Communications laboratory, Belgium

The ground-penetrating radar (GPR) model developed by van den Bosch et al., [1] allows for the extraction of the target radar signature, in theory free from the antenna signal artifacts (internal re ections, emission and reception equivalent currents amplitudes and the multiple re ections) and from the soil response. For this, the radar system has to be characterized for determining the antenna operational parameters H_i (antenna internal re ections), H_t^2 (antenna transmission and reception) and H_f (antenna scattering), and a measurement above the soil without the target has to be performed in order to extract its radar signature R_S. With this in hand, one is able to recover the target signature R_T by using the method developed in [1], where comparisons between extracted and computed target signatures have been made, and excellent agreement has been found.

However, real world conditions are far from the laboratory settings in which the experiments were performed. The operational parameters of the antenna can be wrongly estimated. In our experience, these parameters are strongly dependent upon the strength with which the waveguide is attached to the VNA. On another hand, the soil EM parameters, namely the dielectric permittivity and magnetic permeability, can—and do—vary greatly from point to point, therefore an estimation of those parameters or of R_S may not correspond to the reality of the ground surrounding the buried target.

In this work, the relative error on the target signature is decomposed into a weighted sum of the relative errors on the terms that participate to the total radar signal. It is shown how the frequency domain magnitudes of these weights are inversely proportional to the magnitude of the target signature. Special attention is devoted to the error due to wrong soil radar response estimation. Its consequences are thoroughly examined in the time domain, which allows for an intuitive yet rigorous interpretation of the resulting degradation of target discrimination against the background.

REFERENCES

1. Van den Bosch, I., P. Druyts, S. Lambot, I. Huynen, and M. Acheroy, "Accurate and efficient modeling of monostatic GPR signal of dielectric targets embedded in stratified media," *Proceedings of the Progress in Electromagnetics Research Symposium (PIERS)*, 251–255, Hangzhou, Zhejiang, China, August 2005.

GPR Ground Bounce Removal Methods Based on Blind Source Separation

J.-X. Liu, **B. Zhang**, **and R.-B. Wu**
Civil Aviation University of China, China

Downward looking ground penetrating radar (GPR) has been considered a viable technology for landmine detection. For such a GPR with the antennas positioned very close to the ground surface, the reflections from the ground surface, i.e., the ground bounce, are very strong and can completely dominate the weak returns from shallowly buried plastic mines. Hence, one of the key challenges of using GPRs for landmine detection is to remove the GB as completely as possible without altering the landmine return.

In this paper, GB removal methods based on Blind Source Separation (BSS) are investigated, including Independent Component Analysis (ICA) based method and Blind Instantaneous Signal Separation (BISS) based method. First, a modified ICA based method is presented. In this method, an eigenimage based Independent Components (ICs) selection strategy combined with non-homogeneous detector (NHD) is given, which is fully automatic. A BISS based method is also proposed for GB removal. This method can be applied in various environments as ICA, but it has much less number of extracted components than ICA's, and this can reduce the computational load. Experimental results show that the proposal methods exhibit excellent performance.

Detection and Characterization of Targets Buried Below a Rough Surface

K. Belkebir, **O. Cmielewski**, **A. Litman**, **M. Saillard**, **and H. Tortel**
CNRS, France

The problem of detection and characterization of an object buried at very low depth beneath a rough surface is addressed. At least two approaches have been proposed to solve such an inverse problem. One of them consists in reconstructing simultaneously both the scatterer and the surface profile. One can also proceed in two steps: first, the surface profile is reconstructed from the early-time response to ultra-wide band signals, and the corresponding Green's function is built numerically. The second step deals with the reconstruction of a scatterer embedded in a (rough) stratified medium. However, both methods assume that the buried object has been previously detected and localized, since only a small area around the scatterer is considered. Here, the whole signal processing scheme is described, from detection to inversion, assuming that a multi-static and multi-frequency data set is available, from measurements of the scattered field along a piece of line.

The problem of detecting the target is tackled by analyzing the frequency averaged Wigner-Ville function as applied to the data and does not require any assumption about the signature of the target. We will present two ways of characterizing the target.

The first one is performed using the iterative solution derived from the Newton-Kantorovitch algorithm as applied to the Wigner-Ville function instead of the scattered field as it is usually done. Indeed, if this built-in function is well adapted to the detection of the object and performs a good clutter rejection, our hope is that an inversion procedure based on its optimization allows us to use a forward model involving a flat interface instead of rough surface, the contribution of the latter being considered as noise. Such an approach permits us to save a lot of time since it involves the standard half-space Green's function.

In the second approach we have first used a new type of correlation of the scattered fields in order to obtain an estimation of the surface profile. A direct solver based on a finite element method has been built in order to take into account the reconstruted surface profile. A "level-set" type method coupled with this solver has been used in an iterative process in order to recover the shape of the buried scatterer.

The efficiency of both approaches will be illustrated via numerical experiments and comparisons will be reported.

Non-Destructive Evaluation of Dielectric Structural Materials by Holographic Subsurface Radar

S. Ivashov[1], V. Razevig[1], A. Sheyko[1], I. Vasilyev[1], and T. Bechtel[2]

[1]Bauman Moscow State Technical University, Russia
[2]Enviroscan, Inc., USA

The existing methods of non-destructive testing of structural and building materials or components have a number of disadvantages. X-ray devices, for example, require two-way approach to the observed detail. This is complicated sometimes and more often even impossible. X-ray devices are widely used in medicine, for hand-luggage control in airports and in technological processes where two-way approach to the object to be examined has no problems as a rule. Ultrasonic equipment has proved to be ineffective in media containing a great number of micro cracks and heterogeneities. Its main application is the examination of relatively homogeneous media with few defects and inclusions, for example, metal details of relatively large dimensions.

From this point of view, the microwave devices are the most promising as they make possible the use of reflective sounding, i.e., transmission and reception of electromagnetic waves is performed from one side of the sounded surface. It enables to examine walls, ceilings and decorative elements and so on in ready-for-service buildings. Thus, it is possible to control the quality of their construction and repair. When using a specially designed antenna, the proposed method also makes it possible to examine corners between walls. This is hardly possible otherwise. Another advantage of radar sounding is a relatively large wavelength λ in the used microwave band, at which there is no reflection from minor natural heterogeneities of media under investigation, for example, by cracks and small (compared to λ) technological hollows in bricks and other construction materials. By choosing wavelength of emitted signal, it is possible to carry out preliminary selection of heterogeneities in surveyed object in view of features of a task.

However, taking into account that water possesses a very high permittivity of 80, cracks filled with moisture have high contrast. This effect can be used in practice. While constructing and reconstructing, concrete structures or their parts, which are under the level of the construction site ground, have to be sealed to prevent water intrusion. This type of structures includes underground garages, automobile parking places, underground pedestrian crossings, and etc. This problem becomes especially actual in spring and autumn when the soil water level is high.

The recent disastrous loss of Space Shuttle Columbia has aroused the great demand in new methods and devices for non-destructive testing and evaluation of the Space Shuttle Thermal Protection System heat protection tiles, as well as the external fuel tank insulating foam. Various approaches have been suggested for determining the integrity of the tiles and foam. However last flight Space Shuttle Discovery has shown that the difficulties with diagnostics of heat protection system are not overcome till now.

The radar under consideration was originally designed for producing non-destructive microwave images of construction details, buried land mines, and etc. The preliminary investigations indicated that its high resolution and sensitivity to cracks or voids, and variations in the subsurface moisture content of materials under inspection could be useful in providing early warning of hidden, incipient problems in the Shuttle protection systems.

This holographic radar method differs from traditional surface-penetrating radar (which typically uses impulse signals) in the simplicity of equipment design and the considerably smaller aperture of scanning antennae. These innovations allow improvement in the spatial resolution of surface-penetrating radar images. It is noteworthy that the effective detection depth of this method is less than that of traditional impulse radars. Nevertheless, for many applications, the holographic radar will provide sufficient detection depth. A good example is the space shuttle heat protection system, which has tile thickness in the range of 4.3–10 centimeters. Another extremely important advantage of this holographic radar technology is the possibility that it can image, without reverberation, dielectric materials that lie above a metal surface as in case heat protection cover. Such materials cannot effectively be inspected non-destructively with traditional time-domain impulse radar technology.

Some experiments concerning surveying of construction details and foam above metal plate will be presented in full paper.

Session 2A4
Non-linear Inverse Problems in Electromagnetic Medical Imaging

Inverse Electromagnetic Scattering Problems for Partially Coated Objects

F. Cakoni, D. Colton, and P. Monk
University of Delaware, USA

We consider the three dimensional electromagnetic inverse scattering problem of determining information about a coated object from a knowledge of the electric far field patterns corresponding to time harmonic incident plane waves at fixed frequency. To fix our ideas we consider a anisotropic dielectric obstacle (partially) coated by a thin layer of a highly conducting material, which is modelled by a transmission boundary value problem with conducting transmission condition on the coated part. No a priori assumption is made on the connectivity of the scattering obstacle nor on the extent of the coating, i.e., the object can be either fully coated, partially coated or not coated at all. We present an algorithm for reconstructing the shape of the scattering obstacle together with an estimate of either the surface impedance or surface conductivity. Numerous numerical examples are given showing the efficaciousness of our method.

A High-order Finite Element Method for Electrical Impedance Tomography

S. Pursiainen and H. Hakula
Helsinki University of Technology, Finland

Electrical impedance tomography (EIT) is a non-invasive imaging technique where a conductivity distribution inside a domain is reconstructed from voltage measurements at the boundary. The voltage data is generated by injecting currents into the domain. This is an ill-conditioned non-linear inverse problem. Small measurement or forward modeling errors can lead to unbounded fluctuations in the reconstructions. The present work focuses on applying the high-order finite element method (p-FEM) to the EIT forward problem, which is to determine the boundary voltages given the conductivity and the injected currents. In the traditional finite element method (h-FEM), the polynomial degree of the element shape functions is relatively low and the discretization error is reduced by increasing the number of elements. Whereas in p-FEM, the polynomial degree is increased and the mesh-size is kept constant. The advantage of p-FEM over h-FEM is that the discretization error converges more rapidly to zero as a function of the number of unknowns. In this work, high-order discretization of the forward problem and efficient solution of the corresponding linear systems are discussed. It is also considered, how a priori knowledge of the conductivity distribution can be incorporated into the reconstruction process when using p-FEM. Numerical experiments are presented.

The Linear Model for Chirp-Pulse Microwave Computerized Tomography: an Analysis of the Applicability Limitations with an Application to Mammography

A. M. Massone
CNR-INFM, Italy

M. Bertero, M. Piana, and F. Conte
Universita' di Genova, Italy

M. Miyakawa
Niigata University, Japan

Chirp-Pulse Microwave Computerized Tomography (CP-MCT) is a multifrequency imaging modality developed at the Department of Biocybernetics, Niigata University, Niigata, Japan which provides map of temperature variations in biological tissues, via temperature dependence of the attenuation and/or phase constant of the microwave. In a series of papers a linear model for data reduction in CP-MCT has been formulated, whereby a CP-MCT projection is given by a blurred version of the Radon transform of the contrast and the blurring is described by the impulse response of the device. In this talk the applicability limitations of this model will be discussed and the influence of diffraction and refractive effects will be investigated. We will also present the simulation of a mammographycal experiment computed by means of an FD-TD technique and the effectiveness of a reconstruction algorithm based on the linear model will be studied.

An Improvement of Born Approximation Based on the Linear Sampling Method

M. Brignone
Università di Genova, Italy

M. Piana
Università di Genova, Italy

J. Coyle
Monmouth University, USA

We consider the inverse scattering problem of determining the refractive index of an inhomogeneous body from measurements of the far-field pattern at fixed frequency. Under Born approximation conditions this problem can be reduced to a Fourier transform inversion problem with limited data. In this talk we describe a reconstruction approach where the linear sampling method is applied to obtain a priori information on the support of the scatterer and an out-of-band extrapolation procedure is performed by means of a projected iterative algorithm. Applications to two-dimensional examples show that this approach may provide notable super-resolution effects.

Computational Validation of a Particle Filtering Approach to the Solution of the Magnetoencephalography (MEG) Inverse Problem

A. Sorrentino and M. Piana
Università di Genova, Italy

The problem of estimating the parameters of a source dipole from dynamical measurements of the magnetic field in a simulated magnetoencephalography (MEG) experiment is addressed by means of a Bayesian approach computed with a particle filtering technique. In particular, we validate this method in the presence of volume currents and accounting for the neuronal origin of the noise affecting the measurements. The effect of encoding a priori information in the prior density distribution function is also tested.

Resolution and the Linear Sampling Method

J. Coyle
Monmouth University, USA

R. Aramini
Universitá di Trento, Italy

The linear sampling method (LSM) is a visualization scheme for frequency domain inverse problems that provides an image of the profile of the scatterer. In particular, the method consist of plotting the norm of a regularized solution, g, to a linear Fredholm equation of the first kind at points in a grid that cover a region where the unknown scatterer is thought to be located. The profile of the scatterer is then characterized by the fact that the norm of g increases without bound as the sampling points approach the boundary of the scatterer. A tremendous advantage of the LSM is that it is not computationally expensive to implement and no a priori knowledge of the physical traits of the scatterer are needed. It is, however, the case that several questions remain regarding the choice of sampling grid and the effects on the resolution of the profile. This talk will focus on both illustrating the difficulties that one may encounter as well as offer possible solutions to this problem.

Robust Design of the Field in Medical Electromagnetic Systems

P. Lamberti, G. Spagnuolo, and V. Tucci
University of Salerno, Italy

The field uniformity in a region as large as possible plays a great role in the design of medical electromagnetic systems, in the case both of Magnetic Resonance Imaging (MRI) and Electron Paramagnetic Resonance (EPR). However the inevitable uncertainty and tolerance on the design parameter due to the component derive and manufacturing processes can lead the system to work in an unexpected range of field value and with low uniformity. The field robustness in presence of that variation can be obtained performing a nominal system design that guarantees the operation in a low field sensitivity region of the parameter space.

In this paper we introduce a robust design approach based on Interval Analysis (IA) and Finite Element Method (FEM). In particular we show the using of FEM in conjunction to the Design of Experiment to obtain a v-variate polynomial expression of the field in the centre of the working volume as a function of the parameter $f(x_1, x_2, \ldots, x_v)$, where v is the number of parameter design. The robustness analysis of such polynomial function by means of the IA allows to select a region of low field variability in the parameter space, i.e. the robust nominal design $(x_{10}, x_{20}, \ldots, x_{v0})$ respect to a variation of $\pm\delta_i$ around each parameter nominal value. The robustness of a solution is obtained looking to the width of the complete Taylor series of the polynomial function around the nominal solution while the real variables, i.e., the v parameter design, and the real operations are substituted respectively with interval variables and operations. Such interval variables $X_i = [x_{i0} - \delta_i, x_{i0} + \delta_i]$, for $i = 1, \ldots, v$, are symmetric intervals, centred in the correspondent parameter nominal values $(x_{10}, x_{20}, \ldots, x_{v0})$ and with radius of variation equal to the particular variations δ_i.

In this paper an example of the proposed approach at the design of an EPR is reported while the robustness is checked by means of a Monte Carlo analysis.

A Class of Non-iterative Methods Applied to Microwave Tomography at a Fixed Frequency

H. Haddar
INRIA Rocquencourt, France

The imaging problem at study consists into finding the location and the shape of inhomogeneous and possibly anisotropic inclusions embedded into a homogeneous medium from electromagnetic measurements at a fixed frequency. We consider the cases where the wavelength is of the same order of magnitude as the inhomogeneities size. We shall investigate imaging techniques based on the sampling method formalism: the inhomogeneities are visualized by constructing an indicator function whose evaluation at a given point (sampling point) requires to solve an ill posed linear problem.

The first one is the classical linear sampling method that requires the computation of the Green tensor for the background medium, which may turn out to be numerically very costly, even for simple configurations where analytical expressions can be derived. The second one is an alternative approach based on the reciprocity gap functional [2, 1] that avoids the computation of this tensor. However, it requires the knowledge of both the electric and magnetic field at a given surface. This method is also shown to have a more general setting than the linear sampling method, allowing for instance a large flexibility in the choice of the indicator function. This choice can be exploited to enhance the performance of the method if some a priori information is known about the type of inhomogeneities.

The numerical efficiency and limitations of both methods will be discussed in the talk.

Time-domain Image Reconstruction in an Experimental Prototype for Breast Cancer Detection

A. Fhager, **P. Hashemzadeh**, **and M. Persson**
Chalmers University of Technology, Sweden

Microwave tomography is rapidly developing into a promising imaging technique that could be useful in many different applications where a non-invasive detection of internal dielectric properties is required. Such a technique could be very useful in mammographical imaging in the search for breast cancer tumours. There is a considerable benefit in using microwaves in the diagnosis of breast cancer tumours due to a significant contrast in the dielectric properties between tumour and surrounding tissue compared to X-rays where the contrast could be as low as a few percent.

We have developed an experimental prototype of an electromagnetic tomographic system for microwave imaging of the breast together with a time-domain conjugate-gradient image reconstruction algorithm. The FDTD formulation is used to model the electromagnetic problem and for solving the forward scattering problem. The inverse problem is solved iteratively by minimising a cost functional containing the difference between the measured scattered field and the corresponding simulated field. Gradients are computed from solutions of the adjoint Maxwell equations and a line search is made to find the minimum of the functional. The measurements are made using a circular array of dipole antennas and conducted in frequency domain. Time-domain signals are synthesised by means of an inverse Fourier transform.

In this paper we present our latest advances on optimising the resolving capabilities and accuracy in the reconstructed image. This includes both experimental and algorithmic issues. We also evaluate the performance of the imaging method by reconstruction of tissue like phantom objects.

Session 2A5
Computational Methods in Electromagnetics

Analysis of EM Scattering and Radiation Using Characteristic Basis Function Method with Plane Wave Spectrum Approach

X. F. Que and Z.-P. Nie
University of Electronic Science and Technology of China, China

Characteristic basis function method (CBFM) can be used to analyze the electromagnetic scattering and radiation properties of PEC object, especially for periodic structure. Characteristic basis functions (CBFs) are higher level expansion functions for unknown induced current, which can be considered as numerical basis functions for each block. The CBFM reduces the matrix size to a small and manageable level. The most CPU-intensive part in CBFM is to compute the matrix vector product. The couplings between all the discretized elements should be calculated and used twice, one for generating the CBFs and the other for constructing the system matrix, which is an intolerable procedure when dealing with electrically large object of arbitrary shape.

In this paper, the plane wave spectrum (PWS) approach is used to accelerate the matrix vector product. Only near-field interaction will be calculated directly. This method also realizes a saving in the memory requirement. Unlike FMM and MLFMA, no iterative methods are needed because a reduced matrix will be obtained, which is typically 3 orders of magnitude smaller for a moderate size problem when compared to the conventional MoM and can be solved by direct inversion.

We use the CBFM/PWS technique to analyze the large antenna arrays and scattering problems of arbitrary conducting objects. Numerical examples validate the accuracy and efficiency of this method.

REFERENCES

1. Prakash, V. V. S. and R. Mittra, "Characteristic basis function method: a new technique for fast solution of integral equations [J]," *Microwave and Optical Technology Letters*, Vol. 36, No. 2, 95–100, 2003.
2. Yeo, J. H., V. V. S. Prakash, and R. Mittra, "Efficient analysis of a class of microstrip antennas using the characteristic basis function method," *Microwave Optical Technology Letters*, Dec. 2003.
3. Song, J., C. C. Lu, and W. C. Chew, "Multilevel fast multipole algorithm for electromagnetic scattering by large complex objects [J]," *IEEE Trans.*, AP-45, 1488–1492, 1997.

The Structures of Fields of Standing Axisymmetric Spherical Electromagnetic Waves with High Localization of Intensity of Electrical and Magnetic Fields

M. V. Pavlova and Y. A. Zyuryukin
Saratov State Technical University, Russia

In the present work the mathematical simulation of standing axisymmetric spherical electromagnetic waves in isotropic medium is carried out. It was supposed, that at centre of a coordinate system a certain receiver of converging spherical waves is, and also the device, capable to realise phase shift of this received wave, and element, that emits this delayed wave as a wave, diverging from centre. The analytical expressions for components standing spherical $E-$ and $H-$ of waves, depending on a phase shift of diverging spherical wave concerning converging are obtained. The equations of lines of force taking a phase shift into account, which define electrical lines of force for $E-$wave and magnetic lines of force for $H-$wave, are obtained. The pictures of lines of force of fields of standing spherical electromagnetic waves, that define new variety of modes with high localization and strength of intensity of electrical and magnetic fields are calculated and constructed.

The Electromagnetic Effect of Different Sources on Pin-fin Heatsinks

S. B. Chiu and J. H. Chou
National Cheng Kung University, Taiwan

Due to the geometric features of heatsinks, the heatsinks may have adverse effects on electromagnetic radiation as the operating frequency of electronic devices increases to the gigahertz range. Different electromagnetic sources are often used in various practical applications. Thus the influence of electromagnetic interference (EMI) from different sources on heatsinks needs to be considered.

A finite difference time domain (FDTD) technique is used to investigate to the EM effect of different sources on pin-fin heatsinks. Seven fin configurations are investigated; namely, one without any fin, a metal block fin, and five pin fins with pin numbers of 2×2, 3×3, 4×4, 5×5, 6×6 respectively. Two types of excitation sources are studied, including a smooth compact pulse and a modulated Gaussian pulse with frequencies ranging from 0.8 GHz to 10 GHz.

The computational results show that at the low frequency of 0.8 GHz, for both types of excitation sources, only the heatsink with 6×6 pins exhibits obvious resonant phenomenon in electric fields. The difference lies in the extent of resonant levels. The resonant effect is larger for the case with modulated pulse source. At 4 GHz, the resonant behavior occurs at all fin configurations except the 3×3 pin-fin heatsink, irrespective of the difference in excitation sources. At this operating frequency, the resonant points and radiated magnitudes caused by the heatsinks for two sources are similar. At 10 GHz, multiple resonant points are observed. Furthermore, the resonant points move toward a distribution of high frequencies for the case of the smooth compact pulse excitation source. In contrast, the spectrum distribution resulted from the modulated Gaussian pulse source is concentrated mostly at discrete frequencies. In other words, the response due to different excitation source is insignificant at lower operation frequencies. But at higher operation frequencies, the difference in excitation sources can be significant and should be careful interpreted.

A Fast Solution of Combined Field Volume Integral Equation for EM Scattering

X. C. Nie, N. Yuan, Y. B. Gan, and L. W. Li
National University of Singapore, Singapore

The volume integral equation (VIE) approach is one of the most popular methods for electromagnetic scattering problems due to its flexibility in treating inhomogeneous objects. However, so far, VIE has been applied only to objects with non-magnetic materials (*i.e.*, $\mu = \mu_0$), and thus only the solution of the electric field volume integral equation (EFVIE) was considered. Materials with non-trivial permeability are often encountered in realistic applications, and hence, there exists a need to extend VIE to scatterers with arbitrary permeability (μ) and permittivity (ε).

In this paper, a combined field volume integral equation (CFVIE) is presented and solved for scattering from objects with arbitrary permittivity and permeability. Since the material has permeability (μ) that is different from the background medium, a magnetic volume current is required in addition to the electric volume current. This resulted in a coupled EFVIE and MFVIE (magnetic field volume integral equation), known as the combined field volume integral equation (CFVIE). The CFVIE is then solved using method of moments (MoM) to obtain the two unknown functions. However, as is well known, the traditional MoM cannot handle electrically large objects due to excessive memory requirement and computational complexity. To alleviate this problem, we need to leverage on recently developed fast algorithms, such as conjugate gradient fast Fourier transform (CG-FFT) method, multilevel fast multipole algorithm (MLFMA), adaptive integral method (AIM) and pre-corrected fast Fourier transform (P-FFT) method. However, all these algorithms have been restricted to FFVIE for purely dielectric objects so far. For CFVIE, the CG-FFT method is not applicable as the resultant matrix equation does not possess Toeplitz property. In contrast, the irregular-mesh-based P-FFT and AIM methods remain usable, although the extension is not trivial.

In this paper, we extended the P-FFT method to CFVIE to facilitate analysis of large inhomogeneous scatterers. The P-FFT method avoids the filling and storage of the usual coefficient square matrix. In the implementation of the P-FFT method, two sets of projection operators are constructed for the projections of the electric and magnetic sources, respectively. In addition, two sets of interpolation operators are also applied to the computation of vector/scalar potentials and the curl of vector potentials, respectively, in the support of the testing functions. The interpolation operators operate only on the Green's function, and thus are valid for any kind of basis functions. The resultant method has a memory requirement of O(N) and a computational complexity of O($N\log N$) respectively, where N is the number of unknowns. Due to the significant reduction in computational requirements as compared to the traditional MoM, the present method can analyze complex dielectric and magnetic objects of much larger sizes.

Broadband MLFMA for Electromagnetic Scattering by Dielectric Objects

H. Wallén, S. Järvenpää, P. Ylä-Oijala, and J. Sarvas
Helsinki University of Technology, Finland

In this talk we present a broadband algorithm for the electromagnetic scattering by a homogeneous dielectric object in the 3D space. For handling a large number of unknowns we use a broadband multilevel fast multipole algorithm (MLFMA).

In order to make the iterative solver for MLFMA to converge sufficiently fast, we use a well-conditioned Mueller surface integral equation formulation [1], which provides a broadband formulation for this field problem. One obtains this formulation by writing the EFIE and MFIE equations at both sides (1 and 2) of the surface of the object for the unknowns $\mathbf{J} = \mathbf{n} \times \mathbf{H}$ and $\mathbf{M} = -\mathbf{n} \times \mathbf{E}$, $\mathbf{n}$ being the outer unit normal of the surface, and then combining the equations as

$$-\alpha_1(MFIE_1) + \alpha_2(MFIE_2) \text{ and } \beta_1(EFIE_1) - \beta_2(EFIE_2)$$

with multipliers $\alpha_j = 2\mu_j/(\mu_1 + \mu_2)$, $\beta_j = 2\epsilon_j/(\epsilon_1 + \epsilon_2)$, $j = 1, 2$.

In our broadband MLFMA [2] we use the traditional MLFMA for levels with division cube side-length $\geq \lambda/2$, λ being the wavelength, and for levels with smaller cube sidelengths we use an MLFMA based on the spectral representation of the Green's function. In the Mueller formulation the exterior and the interior of the object need MLFMA procedures of their own because they have different wave numbers.

In each iteration step for the matrix-vector product, we need to compute the fields $\mathbf{E}^{\mathbf{sc}}$ and $\mathbf{H}^{\mathbf{sc}}$ due to the given surface currents $\mathbf{J}$ and $\mathbf{M}$. We get the components of the matrix-vector product by adding these currents, multiplied by suitable constants, and by taking inner products with the relevant testing functions.

The outgoing fields are presented by their radiation patterns. For translating the outgoing fields $\mathbf{E}^{\mathbf{sc}}$ and $\mathbf{H}^{\mathbf{sc}}$ from a division cube Q to incoming plane-wave expansions in a non-nearby cube we only need to store the radiation and incoming wave patterns of $\mathbf{E}^{\mathbf{sc}}$, because both $\mathbf{E}^{\mathbf{sc}}$ and$\mathbf{H}^{\mathbf{sc}}$ are obtained directly from them. These patterns are computed easily from $\mathbf{J}$ and $\mathbf{M}$ in Q, and they are stored in three Cartesian components to make the interpolation and anterpolation procedures work in an efficient manner.

We demontrate the resulting broadband MLFMA algorithm by a numerical example, where the bistatic RCS is computed for dielectric spheres with diameters varying from $\lambda/100$ to 3λ and using several levels in MLFMA. A good agreement with the Mie-series results are obtained with reasonable numbers of iterations.

REFERENCES

1. Ylä-Oijala, P. and M. Taskinen, *IEEE Trans. Antennas Propagat.*, Vol. 53, No. 10, 3316–3323, Oct. 2005.
2. Wallén, H. and J. Sarvas, *Progress in Electromagnetics Research*, Vol. 55, 47–78, 2005.

Arbitrary Lagrangian Eulerian Electromechanics in 3D

R. Rieben, **B. Wallin**, **and D. White**
Lawrence Livermore National Laboratory, USA

We present results from an effort to couple the equations of electromagnetic diffusion with the equations of arbitrary Lagrangian-Eulerian (ALE) hydrodynamics. The electromagnetic diffusion equations are discretized using a novel mixed finite element method coupled with a generalized Crank-Nicholson time differencing scheme. At each discrete time step, electromagnetic force and heat terms are calculated and coupled to the hydrodynamic equations in an operator split approach. We present preliminary results from a fully coupled electromechanical simulation as well as results concerning advection techniques for electromagnetic quantities.

Hybrid Numerical Simulation of Micro Electro Mechanical Systems

M. Greiff, U. B. Bala, and W. Mathis
University of Hanover, Germany

In order to develop a simulation model for micro-electro-mechanical systems (MEMS) it is necessary to understand their components and the interaction between them. A MEMS can be described by its electrical and mechanical behavior. Therefore a simulation model has to include a mechanical and an electrical part. Since these parts are not independent the calculation has to accomplish a coupling between them. In this work this is done by passing the electric force calculated by the electrical part to the mechanical part (Fig. 1). Using this force the mechanical part is able to calculate the mechanical deflection and return it to the electrical part. This iterative process has to be repeated in a loop. Furthermore, often for an accurate simulation of MEMS multi-scale aspects must be taken into account.

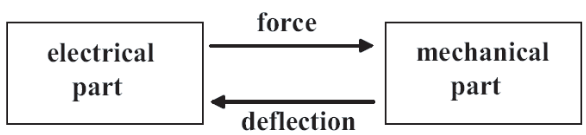

Figure 1: Mechanical and electrostatic part.

A typical example for a MEMS is the electrostatic force microscope (EFM) (Fig. 2). An EFM is used to scan electric forces near a charged surface. It consists of a cantilever and a tip which is run over the surface under investigation. In this work the mechanical part including the cantilever and the tip is modeled by using a beam model. Though the whole EFM scanning process is dynamic all transient processes are assumed to be slow. Therefore the electric behavior is mainly determined by the electrostatic field. For the calculation of the electrostatic field several aspects as possible nonlinearities in the sample, high electric field values near the tip and the different size of cantilever and tip have to be taken into account. Therefore a hybrid numerical simulation method that combines the finite element method (FEM), the boundary element method (BEM) and the method of fundamental solutions (MFS) is implemented in this work. Since the scanning process is dynamic the FEM mesh has to be adapted to the time dependent geometry near the tip. This is achieved by using the arbitrary Lagrangian Eulerian method (ALE). A typical simulation result is given in Fig. 3.

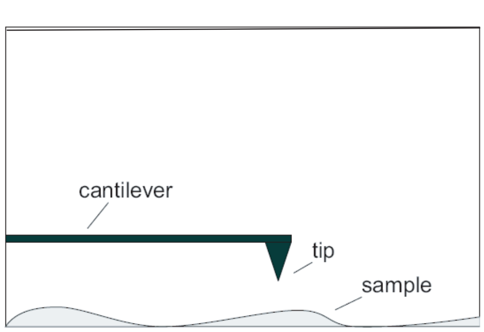

Figure 2: Electrostatic force microscope.

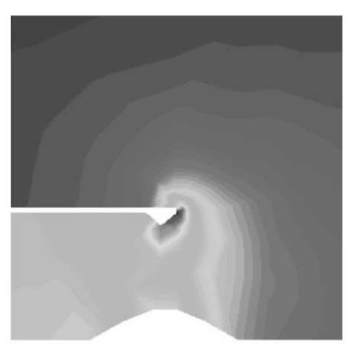

Figure 3: Simulated electrostatic field.

EM Field Induced in Inhomogeneous Dielectric Spheres by External Sources

G. C. Kokkorakis, **J. G. Fikioris**, **and G. Fikioris**
National Technical University of Athens, Greece

The electromagnetic field induced in the interior of inhomogeneous dielectric bodies by external sources can be evaluated by solving the well-known electric field integrodifferential equation (EFIDE). For spheres with constant magnetic permeability μ, but variable dielectric constant $\varepsilon(r, \theta, \varphi)$ a direct, mainly analytical solution can be used even in case when the inhomogeneity in ε renders separation of variables inapplicable. This approach constitutes a generalization of the hybrid (analytical-numerical) scalar method developed by the authors in two recent papers, for the corresponding acoustic (scalar) field induced in spheres with variable density and/or compressibility. This extension, by no means trivial, owing to the vector and integrodifferential nature of the equation, is based on field-vector expansions using the set of three harmonic surface vectors, orthogonal and complete over the surface of the sphere, for their angular (θ, φ) dependence, and Dini's expansions of a general type for their radial functions. The use of the latter has been shown to be superior to other possible sets of orthogonal expansions and as far as its convergence is concerned it may further be improved by properly choosing a crucial parameter in their eigenvalue equation. The restriction to the spherical shape is imposed here to allow use of the well-known expansion of Green's dyadic in spherical eigenvectors of the vector wave equation.

Spatial-spectral Hybrid Method in Calculation of Capacitances and Inductances of Ring Conductors in a Stratified Medium

T. J. Dufva
Helsinki University of Technology, Finland

J. C.-E. Sten
VTT Technical Research Centre of Finland, Finland

In addition to generic numerical integration equation methods in electromagnetics, there is also a need for simplier algorithms for some basic geometries. These algorithms may be used as efficient and accurate models for some RF-components, for example, or they may served as benchmarks for more generic algorithms. An example of such algorithms is the one presented earlier by the authors [1]. The paper treats the calculation of the capacitances and inductances of the system of thin ring conductors in a stratified medium. These parameters were found by solving the surface charge and current distributions on the rings by using Galerkin method and the spectral method. The present work generalises the above algorithm for thick ring conductors.

The spectral method utilising an integral transform in the transverse plane is commonly used in the analysis of planar structures in a stratified medium. This is because the solution of the Green's function is more straightforward in the spectral domain. However, if the coupling integrals between the basis functions are to be evaluated in the spatial domain, the tedious inverse transform of the spectral Green's function must be carried out for every integration point. Another solution is to calculate the coupling integrals in the spectral domain. Unfortunately, the infinity integrals which arise are also laborious due to the highly oscillating and slowly decaying integrands. The so-called spatial-spectral hybrid method exploits the benefits of the pure spectral method but avoids the most troublesome integrals. In the method the Green's function and the coupling integrals are divided into two parts. The first part of the Green's function includes the primary point source and the first reflections from the interfaces of the medium, found from the image theory. The corresponding parts of the coupling integrals are evaluated in the spatial domain. The rest of the Green's function and the corresponding parts of the coupling integrals are calculated in the spectral domain. Although the integrands are oscillating like in the pure spectral method, they decay exponentially because the asymptotic part of the spectral Green's function is contained in the first part evaluated in the spatial domain.

The unknown surface charge and current distributions on the faces of the conducting rings are estimated as superpositions of entire-domain basis functions. Each of the basis functions includes the correct edge behaviour and together they constitute a complete and quickly converging expansion for the distributions. The integral transforms of the basis functions needed in the method are found in analytic form.

REFERENCES

1. Dufva, T. J., and J. C.-E. Sten, "Quasi-static variational analysis of planar spiral conductors," *Journal of Electromagnetic Waves and Applications*, Vol. 16, No. 7, 957–976, 2002.

Session 2A6
Antennas

Synthesis of Aperture-Field Distributions for of High-Gain Phased Arrays

R. A. Speciale
Research and Development Inc., USA

Recent analytical and numerical studies of rather unusual aperture-field distributions for high-gain phased arrays have generated some interesting new results, while leading to a deeper insight, and understanding of the underlying radiation process. The planar, circular-aperture distributions analyzed were synthesized as weighted linear combinations of **TE** and **TM** cylindrical wave-modes with equal azimuth symmetry order $\boldsymbol{m}$. The **TE** and **TM** cylindrical modes used were mathematically defined as linear combinations of the W. W. Hansen's **M** and **N** basis vector-fields, using only Bessel functions of the first kind to express the radial dependence of the five **TE**, and of the five **TM** field-components. The closedform expression of the radial component $\boldsymbol{S}_R^*$ of the Complex Poynting Vector shows that the radial energyflow density of the combined **TE** and **TM** aperture-fields is identically zero, *everywhere* in the half-space above the $\mathbf{z} = 0$ plane of the aperture, for any values of the radial and azimuth coordinates $\boldsymbol{r}$ and $\boldsymbol{\varphi}$, and of the symmetry order $\boldsymbol{m}$. Further, the imaginary part of the vector product $\boldsymbol{S}_R^*$, that represents *reactive power flow* in the radial direction, also becomes identically zero, when the two mode-types are linearly combined with equal weights. At the same time, however, the axial component $\boldsymbol{S}_{\mathbf{Z}}^*$ of the Complex Poynting Vector of the combined **TE** and **TM** fields is non-zero, and is oriented along the positive z-axis, thus generating a broadside high-gain beam. It appears then that the linear combination of **TE** and **TM** cylindrical wave-modes, with equal order $\boldsymbol{m}$, results in the total cancellation of the radial, active-energy flow, *everywhere* in the $\mathbf{z} \geq 0$ radiation half-space, at all radial, azimuth, and axial positions. The results of preliminary computations, with $\boldsymbol{m} = 1$, show that the electric-field components $\mathbf{E_r}$, $\mathbf{E}_\varphi$ and $\mathbf{E_z}$ have a decaying oscillatory radial dependence, while the axial component $\boldsymbol{S}_z^*$ of the Complex Poynting Vector is sharply peaked at the center of the circular aperture. The azimuth component $\boldsymbol{S}_\varphi^*$ of the Complex Poynting Vector is zero a the center of the aperture, and has a mostly non-decaying oscillatory radial dependence. The axial ratio $\rho = \mathbf{E}_\varphi/\mathbf{E_r}$ is exactly equal to **1** on axis (at the center of the aperture), thus representing circular polarization, and goes through poles and zeros with increasing radius. The radiation pattern in the near-, Frenel, and far-field is being determined by using the Green's function, and by combining all the components of the **E** and **H** fields. Present analysis efforts aim at determining an optimum aperturetruncation radius, and an optimum radial *filtering (or windowing)*. As no rigorous procedure is as yet known for determining the optimum combination of truncation radius and radial filter shape, a rather heuristic approach is being used. It has been determined that the new, unusual aperture-distribution may be represented by a continuous spectrum of planar waves, where all the spectrum components have propagation vectors **K** oriented at a constant angle $\boldsymbol{\gamma}$ relative to the broadside z-axis, and phases that are linearly dependent on the azimuth angle $\boldsymbol{\varphi}$. As a consequence, the resulting total phase-front appears to have the shape of a circular helical-surface, similar to a corkscrew. It has been concluded that the radiated beam, generated by that distribution, appears to be the microwave equivalent of an *optical vortex*.

REFERENCES

1. Stratton, J. A., *Electromagnetic Theory*, Chapter VII, 392.

Advanced Design of Phased Array Beam-Forming Networks

R. A. Speciale
Research and Development Inc., USA

Recent fundamental results [1] in the theory of linear, multi-port networks have enabled a costeffective, higher-reliability design for electronically-steered phased arrays. The referenced paper documents and proves that, by including a properly designed beam-forming network, it becomes possible to feed an array and steer its beam, using a much reduced number of expensive and critical phase- and amplitude-controlled sources, while at the same time completely eliminating the adverse effects of element coupling. Those cost and reliability advantages are however only attainable if the structure of the beam-forming network used establishes a pattern of *synergistic connectivity*, where *each* controlled source simultaneously feeds *all* the array elements, and *each* array element is simultaneously fed by *all* the sources. The closed-form expressions (31)–(34) of the referenced paper completely specify the requirements that the beam-forming network used must satisfy, and establish a rigorous basis for its synthesis. Those new results are based on a generalization of the classical concepts of *scalar* image impedance, and of *scalar* image-transfer function for two-port networks, to the new concepts of multidimensional image-impedance *matrix*, and of multidimensional image-transfer function *matrix* for linear multi-port networks. Electronically-steered phased arrays provide unsurpassed agility and high angular resolution in beam-pointing, and the capability of adaptive, multifunction performance. Such highly desirable features are however only attained at the price of high cost, extreme complexity, and limited reliability. Indeed, electronically-steered phased arrays are most frequently designed as activeaperture system, that include a large number of semiconductor devices and beam-steering controlelements, embedded in the physical array structure, and directly connected with the array radiating elements. The phased arrays used in radar systems use transmit/receive modules (T/R), essentially tiny radar, each nested behind a radiating element, in a half-wavelength square-section of the total array aperture. Because of the well-known low power-efficiency of semiconductors, a large heat-flux is developed locally, thus generating a complex cooling problem. Finally, notwithstanding technology advances the semiconductor devices and beam-steering control-elements still are the most expensive components of electronically-steered phased array, and cost-effective designs would only be attained by reducing their total number. Such reduction are only feasible by including a non-symmetric, multiport beam-forming network between a reduced number of active devices and the array radiating elements. Such beam-forming network would necessarily be non-symmetric, because of including an n-port interface on the side of the active devices, and an N-port interface on the side of the array radiating elements, with $n < N$. The use of a reduced number of beam-steering control-elements appears possible, by considering that current active apertures have the capability of generating a large number of useless aperture distributions, that do not produce any practical radiation pattern. Also, the angular resolution of beam-steering may be reduced by steering the beam in finite increments, each only a fraction the -3 dB beam-width. The recent fundamental results in the theory of multi-port networks have been attained by introducing a generalization of the classical concept of *scalar* image impedance of two-port networks, to that of image-impedance *matrices*. Similarly, the classical concept of *scalar* image-transfer function of two-port networks, has been generalized to that of image-transfer function *matrices*. These generalizations have made possible the design of non-symmetric beam-forming networks, that are simultaneously impedance-matched to the external environment at both interfaces, while having prescribed two-way transfer functions between two interfaces with different number of ports ($n < N$).

REFERENCES

1. Speciale, R. A., "Advanced design of phased array beam-forming networks," *IEEE Antenna and Propagation Magazine*, Vol. 38, No. 4, 22–34.

Slotline Leaky Wave Antenna with a Stacked Substrate

J. Machac, J. Zehentner, and J. Hruska
Czech Technical University, Czech Republic

All kinds of open planar transmission lines are predisposed to excite leaky waves. Space leaky waves can be utilized in leaky wave antennas, which have been known for nearly 50 years [1]. The first microstrip leaky wave antenna was described in [2], and the slotline antenna in [3]. We have designed, fabricated and measured several slotline leaky wave antennas [4]. Their drawback is radiation into two main beams, one above and one below the substrate. We turned therefore to the conductor–backed slotline (CBSL), and designed and fabricated various antennas with a thick substrate [5]. They radiate only into the one main beam. From the fabrication point of view it is more convenient to use a stacked substrate. One layer is formed by a thin commercially available substrate, while the second layer is filled with air. The cross-section of the CBSL with a stacked substrate is shown in Fig. 1. The radiation pattern of a CBSL antenna with a stacked substrate has one rather wide main lobe and radiates also backward and below the bottom metallization. The side lobe level (SLL) varies from -6 to -10 dB. The level of the lobes directed under the substrate is about -13 dB comparing to the main lobe. The main lobe tilts slightly in the forward direction with the frequency. The width of the main lobe at half power (FWHP) decreases with frequency. The background reflector perpendicular both to the slot and to the substrate effectively shapes the radiation pattern. Two antennas with the reflector were designed with the aid of the CST Microwave Studio and then fabricated. The antenna with the reflector and the ground conductor of the same size as the substrate reduces the side lobes to -17 dB, and the radiation below the substrate to -20 dB. It has a narrower main beam than the antenna without the reflector. The background conductor, being larger than the antenna substrate by 30 mm on the side and front walls, further reduces the radiation below the substrate to -23 dB. The SLL is now -17 dB from 6.5 to 6.75 GHz. The FWHP varies around 17.5 deg with the frequency, which is considerably less than the FWHP of the original antenna. The parameters of the radiation pattern of this antenna are shown in Fig. 2. The paper presents the versatility of the slotline leaky wave antenna design.

Figure 1: Cross-section of the CBSL with a layered substrate.

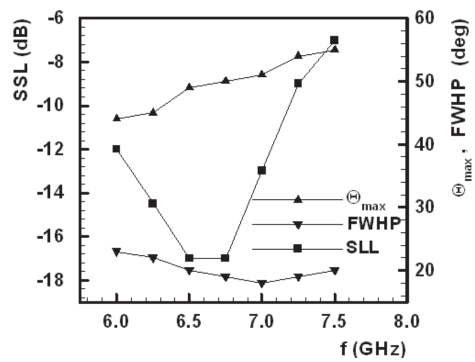

Figure 2: Measured side lobe level, full width of the main lobe at half power and the angle of maximum radiation of the antenna with the reflector larger than the substrate.

*This work has been supported by the Grant Agency of the Czech Republic under project 102/03/0449 “New circuit devices for communication technology”.

REFERENCES

1. Zurker, F. J., “Surface and leaky-wave antennas, in antenna engineering handbook,” H. Jasik, ed., McGrew Hill, New York, 1961.
2. Menzel, W., “A new traveling wave antenna in microstrip,” Vol. 33, 137–140, AEü, 1979.
3. Sheen, J. -W. and Y. -D. Lin, “Propagation characteristics of the slotline first higher order mode,” *IEEE Trans. Microwave Theory Techn.*, Vol. MTT-46, No. 11, 1774–1781, Nov. 1998.
4. Zehentner, J., J. Machac, P. Lorenz, and J. Mrkvica, “Planar slot-patch antenna,” *33rd European Microwave Conference*, Proceedings, London, UK, Vol. 3, 223–226, October 2001.
5. Machac, J., J. Zehentner, and J. Hruska, “Conductor-backed slotline antenna,” *34th European Microwave Conference*, Proceedings, Amsterdam, Netherlands, Vol. 2, 1205–1208, October 2004.

Coplanar Multi-line Antenna Design for Thin Wireless Terminal

K. Takei, Y. Shirakawa, and M. Ikegaya
Hitachi Cable Ltd., Japan

To improve portability of wireless apparatus, recently their shapes have been required thinner and thinner. On the other hand, responding starts of several kinds of multi-media wireless services, ex. wireless LAN (WLAN), 2.5/3 G cellar phone, terrestrial digital TV and etc., it is necessary to provide multi-mode antennas. The coplanar line antenna (CPLA), which consists of finite a self ground and strip lines around it, is suitable for thin shape multi-mode antenna [1]. This antenna has been widely used as multi-mode WLAN antenna for mainly notebook PC application. CPLA can be designed using simple modified transmission line theory, which is obtained by replacing conventional line with new line having a complex transmission constant due to radiation loss [2]. For the purpose of applying CPLA to smaller and thinner wireless apparatus, i.e., handy phone, PDA, and pocket PC, we propose the coplanar multi-line antenna (CPMLA), which has multi-stacked strip lines around the self ground.

To realize CPMLA in the limited small space of smaller and thinner terminal, we must analyze more precise antenna pattern, which is made under 0.5–1 mm line and space rule in stead of 2–4 mm rule of conventional CPLA. Direct EM analysis by using numerical method, i.e., FEM, FDTD, and Method of Moment, consumes huge computational time. An antenna design with computer is equal to searching out the candidate structure by using suitable searching algorithm and fast EM calculation required too many times in its algorithm. To realize the actual computer design of CPMLA, we have developed a novel design method by using the modified transmission line theory.

The novel design method is based on conventional design method of coupling transmission lines. Since strip lines of CPMLA are arranged on one ideal plane, we approximately consider only a multiple coupling between neighbor two strip lines. Different relative locations of these lines cause different self impedance of them. Because the conventional method assumes the same self impedance and the same mutual impedance caused of the coupling between neighbor lines, the scattering matrix of a multi-line structure is derived analytically. To obtain a scattering matrix of a multi-line structure with different self impedances, we have developed a recursive algorithm for such a scattering matrix as follows.

$$\overline{Z}=\begin{bmatrix}\alpha_1 & \beta & 0 & 0\\ \beta & \alpha_2 & \ddots & 0\\ 0 & \ddots & \ddots & \beta\\ 0 & 0 & \beta & \alpha_N\end{bmatrix},\quad \begin{vmatrix}\alpha_1-\lambda_i & \beta & 0 & 0\\ \beta & \alpha_2-\lambda_i & \ddots & 0\\ 0 & \ddots & \ddots & \beta\\ 0 & 0 & \beta & \alpha_N-\lambda_i\end{vmatrix}=0,\quad \begin{matrix}\alpha_1 x_1^i+\beta x_2^i=\lambda_i x_1^i\\ \beta x_1^i+\alpha_2 x_2^i+\beta x_3^i=\lambda_i x_2^i\\ \vdots\\ \beta x_{N-1}^i+\alpha_N x_N^i=\lambda_i x_N^i\end{matrix}$$

$$\overline{Z}={}^t\,\overline{T}\,\overline{S}\,\overline{T}=\begin{bmatrix}x_1^1 & \cdots & x_N^1\\ \vdots & \vdots & \vdots\\ x_1^N & \cdots & x_N^N\end{bmatrix}\begin{bmatrix}z_1 & 0 & 0\\ 0 & \ddots & 0\\ 0 & 0 & z_N\end{bmatrix}\begin{bmatrix}x_1^1 & \cdots & x_1^N\\ \vdots & \cdots & \vdots\\ x_N^1 & \cdots & x_N^N\end{bmatrix}$$

The final equation shows that impedance matrix Z is converted into diagonal scattering matrix S. Therefore, dividing CPMLA structure along longitudinal direction of the strip line into a short period without discontinuity along this direction, EM performances can be calculated by the modified transmission line theory. Moreover, connecting each short period with the cascade matrix of conventional circuit theory according to the CPMLA topology, we can design a multi-mode antenna, ex. 800/1500/1900 MHz 3-mode antenna sized of $40 \times 50 \times 0.03$ mm.

REFERENCES

1. Japanese patent application 2001-085484.
2. Japanese patent application 2004-305873.

Effect of Distant Scatterers on MIMO Fading Channel Tracking

N. M. Khan and R. Ramer
University of New South Wales, Australia

This paper considers the problem of a wireless multi-input multi-output (MIMO) fading channel tracking, when a strong distant scattering cluster is present in the area in addition to the local scattering zone around the mobile. Time-varying fading channels are dynamic in nature and their tap values in signal processing depend significantly on the distribution of the angle of arrival (AOA) $p(\psi)$ at the mobile station. We assume N_T-input, N_R-ouput MIMO communication system where each receiver antenna observes a linear combination of all transmitted data sequences, each distorted by ISI, under white Gaussian noise [1]. Using state-space approach, a MIMO system operating over time-varying channel, can be modeled as, [1, 2].

$$h_l^{(m,j)}(i+1) = \alpha_l^{(m,j)} h_l^{(m,j)}(i) + v_l^{(m,j)}(i+1) \tag{1}$$

$$r^{(j)}(i) = \sum_{m=1}^{N_T} \sum_{l=1}^{L^{(m,j)}} h_l^{(m,j)}(i) x^{(m)}(i-l) + n^{(j)}(i) \tag{2}$$

where $h_l^{(m,j)}(i)$ is the lth tap of the impulse response of order $L^{(m,j)}$ between the mth input $x^{(m)}(i)$ (with $m = 1, \ldots, N_T$), and the jth ouput $r^{(j)}(i)$ (with $j = 1, \ldots, N_R$), of the time-varying MIMO channel, at time instant i. $x^{(m)}(i)$ is the transmitted signal from transmitter m, and $r^{(j)}(i)$ is the received signal at receiver j. $v_l^{(m,j)}(i)$ and $n^{(j)}(i)$ are i.i.d. process and measurement noises and $\alpha_l^{(m,j)}$ is the autoregressive (AR) coefficient of lth tap and accounts for the variations in the channel due to spatially dispersed multipath signals affected by the maximum Doppler shift $f_D^{(l)}$ [1–3].

$$\alpha_l = E\{h_l(i) h_l^*(i-1)\} = \int_{-\pi}^{\pi} p(\psi) e^{-j2\pi f_D^{(l)} T \cos(\psi)} d\psi \tag{3}$$

where T is the symbol duration. In rural or sub-urban areas, when mobile travels at fast speed under the influence of a dominant distant scatterer (e.g., hill), the distribution of the AOA, $p(\psi)$ deviates from the uniform shape (a common assumption usually made to find correlation statistics [1–3]), and can be written as,

$$p(\psi) = \Omega \frac{R^2 + 4D\cos(\psi - \psi_D)\sqrt{R^2 - D^2 \sin^2(\psi - \psi_D)}}{\pi R^2} \tag{4}$$

where R is the radius of the distant scattering cluster, D is the distance of its center from the mobile, ψ_D is the angle it makes with the virtual line of sight at mobile and Ω is the normalizing constant.

A variety of models may be used with different values of D, R and ψ_D depending on the terrain and geography of the area to obtain α_l, which can then be exploited in fading channel tracking algorithms using (1) and (2).

REFERENCES

1. Komninakis, C., C. Fragouli, A. H. Sayed, and R. D. Wesel, "Multi-input multi-output fading channel tracking and equalization using Kalman estimation," *IEEE Trans. Signal Proc.*, Vol. 50, No. 5, 1065–1076, May 2002.
2. Khan, N. M. and P. B. Rapajic, "Use of state-space approach and Kalman filter estimation in channel modeling for multiuser detection in time-varying environment," in *Proc. Intl. Workshop Ultra-Wideband Sys.*, No. 1052, Finland, June 2003.
3. Jakes, W. C., *Microwave Mobile Communications*, John Wiley, New York, 1974.

Planar Small Antenna Module for Global Positioning System

T. Ogawa and K. Takei
Hitachi Cable Ltd., Japan

Prototype of a novel planar antenna module for Global Positioning System (GPS) is developed. The antenna module consists of a circularly polarized antenna and two stages of low noise amplifiers. The size of this module is $28\,\text{mm} \times 15\,\text{mm} \times 2\,\text{mm}$. The module works in 3 V voltage operation. The module is small, thin and lightweight, which is suitable for mobile navigation equipments.

The circularly polarized antenna receives 1575 MHz right-handed circularly polarized wave which is used on GPS. The antenna consists of two layered metal patterns. These layers are connected each other by via hole. The metal pattern is formed on both sides of one PCB. Electrical size of the antenna is about $\lambda/8$ square. Our antenna is quite smaller than a conventional ceramic patch antenna commonly used for GPS equipments of $\lambda/2$ square size. The smaller size of this antenna enables to use conventional PCB with high dielectric constant ($\varepsilon r = 10$) instead of relatively expensive ceramic block. Actual antenna size is about 12 mm square.

The antenna consists of a lot of rectangular small metal segments. We analyzed induced currents on each segment using method of moment to calculate axial ratio and input impedance of the antenna. We defined two directional currents I_v and I_h, which are perpendicular to each other, on each segment. The axial ratio (AR) is calculated as shown in equation (1). The axial ratio of designed antenna is about 2.5 dB (less than 3 dB). Therefore this antenna can receive GPS signal successfully in spite of small electrical size.

$$|AR| = \left|\frac{|I_L| + |I_R|}{|I_L| - |I_R|}\right| \quad I_L = I_V + I_H\angle 90^\circ \quad I_R = I_V\angle 90^\circ + I_H \quad I_V = \Sigma I_v \quad I_H = \Sigma I_h \tag{1}$$

The antenna and the low noise amplifier are formed on PCB. The two layered antenna is formed on both sides of PCB. Circuit pattern of two stages amplifiers is formed on one side, and ground plane is formed on the other side. On calculation of the axial ratio, we considered currents, which are induced on the antenna and the ground plane.

High gain design of first stage amplifier causes capacitive input impedance ($200 - j100\,\Omega$) of FET. Therefore, we designed antenna impedance about $200 + j100\,\Omega$ to achieve conjugate matching. The impedance of the conventional $\lambda/2$ patch antenna is about $50\,\Omega$. However, the input impedance of the low noise amplifier is not $50\,\Omega$. Therefore conventional design method requires large scale matching circuit with distributed lines. Our design method successfully omits such large scale matching circuit because it is possible to design antenna impedance and axial ratio simultaneously. We chose bipolar transistor at second stage of the amplifier to achieve output impedance around $50\,\Omega$. Hence the module can be connected to conventional demodulator directly.

REFERENCES

1. *Japanese Patent Application 2001-085484*.
2. Takei, K., *Proc. PIERS*, 154, Singapore, 2003.
3. Takei, K., et al., *Proc. China-Japan Joint Meeting on Microwaves*, 166–169, Harbin, 2004.
4. Takei, K. and T. ogawa, *Proc. ICECom*, Dubrovnik, Croatia, 2005.

Interaction of Electromagnetic Field from Cellular Base Station Antennas on Cardiac Pacemakers

R. Kubacki[1], **M. Wnuk**[2], **and J. Sobiech**[1]

[1]Military Institute of Hygiene and Epidemiology, Poland
[2]Military University of Technology, Poland

Background. The aim of this study was to investigate the possible interaction of pulsed electromagnetic (EM) fields affecting the cardiac pacemakers. Pulse modulated fields typical for cellular GSM system have been considered for this study. In the literature, only interaction of electromagnetic field emitted from cellular handsets to pacemakers has been described. It has been proved that this kind of radiation is rather "safe" for pacing process. Only in same lit-erature a minimum safety distance of few centimeters from handset to the patient body was suggested. Nevertheless, no one assesses the threshold of electric field strength when pace-makers change the shape of emitted pulses or even when they inhibit of the pacing process. This is because measurements of electric field in the vicinity of handset is difficult and there is a need to assess all components of electric field vector. However, there is no information about possible interaction of radiation emitted from base station antennas on pacemaker functions. This information whether electromagnetic field from base stations can be danger for pace-makers is important for people dwelling in the vicinity of these antennas.

Our intention was to recognize whether the radiation from GSM base stations can affect pacemaker functions. All investigations were carried out in the anechoic chamber where the level of exposure and type of polarization can be precisely determined.

Methods. The base station panel antenna (Kathrein antenna type 738573) has been chosen as a source of EM field. The antenna has been fed from external generator and amplifier allowing to expose of pacemakers to EM field up to 300 W/m^2. Microwaves (940 MHz) have been modulated with 577 μsec pulses and 867 Hz repetition frequency - every second time slot was fulfilled. In this case EM field is a pulse modulation function comparable to field emitted from base station antennas when base station is linked with 4 persons. Each pacemaker was situated in anechoic chamber with 3 typical orientation (polarization) regarding to the electric vector of the incident field. To find the susceptibility threshold to electromagnetic interference all ori-entations of pacemakers were sought to find the critical polarization of electric field.

Results. Pacemakers signals have been analyzed in function of power density of incident microwaves and the following changes in pacemaker signals have been studied:

-changes of the amplitude and shape of pulses,

-changes of the repetition frequency of the pulses

-falling out of one or few pulses,

-the inhibition of the pacing process.

Values of electric field strength when the above changes occurred were found. Nevertheless, it should be underlined that the above changes occurred in strong electromagnetic field and they are dependent of the type of pacemakers and polarization of the electric field.

Computer-Simulation of Near-Field Phased-Array Radiation-Pattern Scanning

R. A. Speciale
Research and Development Inc., USA

The recently introduced Tilted-Ellipse Representation of Standing-Wave Patterns [1, 2] provides a fast and inexpensive way for extracting the multi-dimensional, complex scattering-matrices of very large, multi-port microwave systems, by performing computer-simulations of large-scale experimental-measurements, that would require a very complex and expensive multiport Automated Vector Network Analyzer, and a long data-acquisition time. That simulation method is based on the results of a rigorous mathematical analysis [1, 2] of the simultaneous propagation of forward- and backward-waves along virtual measurement lines, connected to the ports of the microwave systems being simulated. That analysis has shown that the mutual correlation between the imaginary components, and the real components of the standing-wave fields, along the length of each virtual measurementline, can be quantitatively represented by the parametric equations of a tilted-ellipse, centered on the origin of a Cartesian frame. Clearly, very significant time- and cost-savings are attained by simulating complex S-matrix experimental-measurements, when the system under simulated test has a very large number of ports ($n \gg 4$), and/or a very large number of propagating modes. Most remarkably, measurement-simulations may be performed at early stages of system design, as no prototype is required. The S-matrix measurement-simulation method described in [1, 2] makes even possible the HPC-simulation of the multi-dimensional scattering-matrix measurements required to perform near-field scans of the radiation-pattern of electronically-steered phased-array (Figure 1).

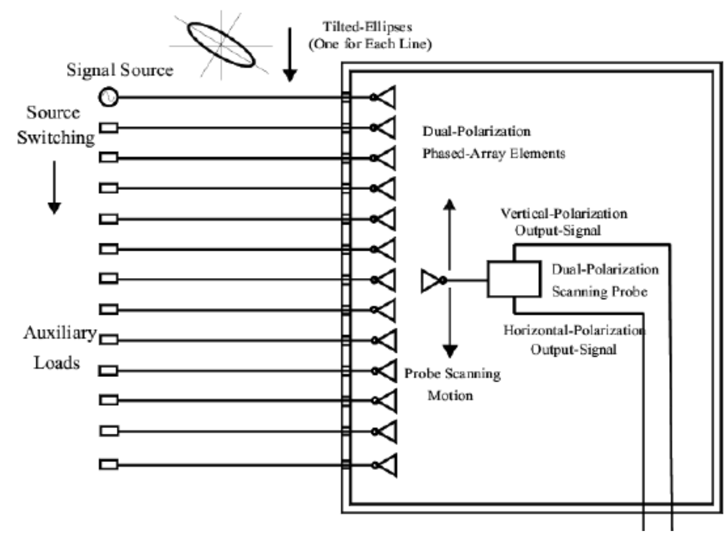

Figure 1: Phased-array in a near-field scanner.

The tilted-ellipse representation of the standing-wave patterns along each virtual line, may be used to compute the magnitudes and the phases of the forward-wave and backward-wave vectors, at any arbitrary point along all the virtual measurement-lines. The mathematical results of the previously-reported analysis of the simultaneous propagation of the forward and backward waves [1, 2], express the complex values of the forward-wave vectors, and of the backward-wave vectors, as functions of the distance from each system port, by using the semi-axes $\boldsymbol{a}$ and $\boldsymbol{b}$ of the ellipse, and the tilt-angle δ of its major axis. The new measurement-simulation performs therefore the very same wave-extraction function that, in an actual experimental measurement-session, would require the use of many Vector-Reflectometers, each composed of two directional couplers, and of a vector-voltmeter.

REFERENCES

1. Speciale, R. A., "Computing the scattering matrix of multiport systems," *PIERS 2004*, Pisa, Italy, 2004.
2. Speciale, R. A., "The tilted-ellipse representation of standing-wave patterns," *ACES 2004*, Syracuse, NY, 2004.

Dual Frequency Rectangular Microstrip Patch Antenna with Novel Defected Ground Structure

J. Sun, E.-P. Li, and Y.-J. Zhang
Institute of High Performance Computing, Singapore

Frequency operated microstrip antenna have already attracted much attention due to the practical application in communication systems. There are normally two ways to generate two operating frequency: using multi-resonator and using reactive load on the antenna structure. The reactive element can be lump element or just special structure, e. g., short pins or slot etched on the patch. By proper design, the slot will not modify the desired mode but perturb the undesired mode. Some researchers have realized more sophisticated slot design, i. e., meander shape slot on the both edge of the patch to further reduce the patch size [1]. More recently, the photonic bandgap structure has draw great attention on the electromagnetic engineering. The photonic bandgap concept (PBG) applied in electromagnetic engineering could be referred to as electromagnetic bandgap (EBG). Since the basic concept is the same and only different frequency range is involved, we could still use the term PBG to refer to the EBG related structure. It is interesting that some researchers has used the PBG structure on the ground plane to suppress the high order harmonics for the microstrip patch antenna [2], others use the PBG structure on the ground plan of the PCB board to enhance the signal integrity, i.e., to reduce the cross talk or to increase the signal to noise ratio. In this paper, we study the rectangular patch antenna with defected ground structure (DGS). This DGS structure in the ground plane is only under the feeding miscrostrip line and does not present under the microstrip patch, so that the radiation through the ground plane can be controlled to a low level. The DGS consists of three tapered photonic bandgap structure in parallel, which is similar to the design of low pass filters in [3], however, only half of the tapered photonic bandgap structure is used for our purpose. The microstrip patch antenna with DGS under the feeding stripline is shown in Fig. fig:1, where $r_1 = 1.5\,\mathrm{mm}$, $r_2 = 1.2\,\mathrm{mm}$, $r_3 = 1.0\,\mathrm{mm}$, $r_4 = 0.8\,\mathrm{mm}$, $p_1 = 3.5\,\mathrm{mm}$, $p_2 = 4.5\,\mathrm{mm}$, $W = 12.45\,\mathrm{mm}$, $L = 16\,\mathrm{mm}$. A commercially available package, CST Microwave Studio, is used to simulate the return loss using the 3-D FDTD method. Adaptive meshing scheme is adopted to obtain convergence results. The return loss for the conventional stripline feed microstrip patch antenna and our proposed structure is shown in Fig. 2. It is very interesting to note that the novel structure has two effects on the behaviour of the return loss. First, the high frequency harmonics were greatly suppressed; second, a dual frequency operation mode (the frequency ration is around 1.3) is presented. By tuning the PBG structure parameters, the second operating frequency can be shifted lower or higher in certain range.

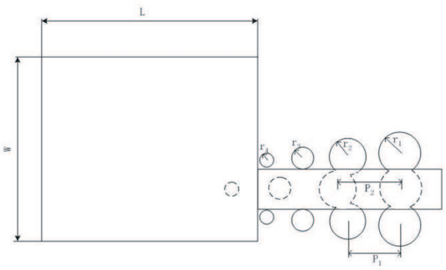

Figure 1: A microstrip patch antenna on a PBG defected ground plane.

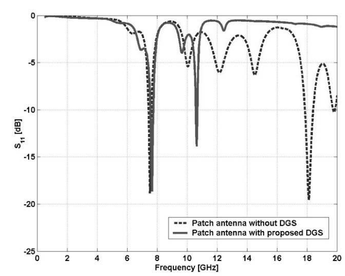

Figure 2: Return loss for the conventional microstrip antenna and proposed antenna.

REFERENCES

1. Gao, S.-C., L.-W. Li, T.-S. Yeo, and M.-S. Leong, "FDTD analysis of a slot-loaded meandered rectangular patch antenna for dual-frequency operation," *IEE Proc. -Microw. Antennas Propq.,* Vol. 148, No. 1, 65–71, 2001.
2. Liu, H., Z. Li, X. Sun, and J. Mao, "Harmonic suppression with photonic bandgap and defected ground structure for a microstrip patch antenna," *IEEE Microwave and Wireless Components Letters,* Vol. 15, 55–56, 2005.
3. Bozzetti, M., A. D'Orazio, M. DeSario, V. Petruzzelli, F. Prudenzano, and F. Renna, "Tapered photonic bandgap microstrip lowpass filters: design andrealisation," *IEE Proc. -Microw. Antennas Propq.,* Vol. 150, No. 6, 459–462, 2003.

Modeling of High Power Broadband THz Antennas

A. S. Podgorski, **J. T. MacGillivray**, **and W. D. Prather**
Air Force Research Laboratory, USA

The term THz is currently applied to electromagnetic spectrum contained between 100 GHz and 10 THz. This region of electromagnetic spectrum remains virtually unused, despite many advantages that it could provide in the area of imaging and communication. During the last 25 years the only usage of the THz spectrum was attributed to narrow-band molecular spectroscopy for Earth, planetary and space sciences. What hampered the developments in the THz area was the lack of commercially available instrumentation.

The uniqueness of the THz technology is related to the fact that, as well as providing the information on structural images of objects it could also be used for spectroscopy—to provide information on materials. At the molecular level, the biologists will have a valuable new tool as the rotations and vibrations of the DNA molecules lie in the THz range.

Current developments of THz technology fall into two categories: active and passive. Active THz technology involves firing THz-rays at an object and analyzing the radiation transmitted and reflected back. However, all objects at normal temperatures are constantly emitting relatively low levels of THz-rays, which can be detected with sensitive instruments. Because of the low level of the detected signals, the passive THz systems have to be narrowband, but the active THz systems do not need to be restricted to the narrowband. Therefore, we can expect that the future system might be active and passive, and they can be narrowband as well as broadband.

Anticipating that by extending the frequency range into the THz region the substantial losses can occur in the antenna, which is generally the longest part of the broadband generating system, we decided to concentrate the effort on modeling the antenna using the FDTD code. Although the plan is to reach 10 THz, the first broadband antenna was designed to operate in the 100 GHz to 1 THz frequency range only. The antenna was designed to ensure gain of 50 dB and output peak power level of 0.1 MW. The design of the antenna was based on a TEM-Horn Antenna that operated successfully up to 100 GHz.

Our estimate indicates that the FDTD modeling of BGF antennas operating in the 100 GHz to 1 THz, will require approximately $10,000 \times 500 \times 400$ cells and as such it could only be done using super-computers. To allow easy implementation of the antenna model into the FDTD Code, while using super-computer, four different versions of a 3-D model of the broadband antenna were prepared and considered.

The publication will present the results of this very extensive modeling effort.

Session 2A9
Space-Time Dynamics of Pulsed Beam Fields in Complex Media

Uniform Signal Contribution of the Step Function Modulated Sine Wave

N. A. Cartwright and K. E. Oughstun
University of Vermont, USA

A canonical problem of central importance in the theory of ultrawideband pulse propagation through temporally dispersive, absorptive materials is the propagation of a step function modulated signal through a dielectric material that exhibits anomalous dispersion. One method in which a closed-form approximation to the propagated pulse may be obtained is application of asymptotic expansion techniques to the Fourier integral representation. For a linearly-polarized plane-wave pulse traveling in the positive z-direction with the temporal behavior on the plane $z = 0$ given by

$$E(0,t) = u(t)\sin(\omega_c t), \tag{1}$$

the propagated pulse on the plane $z > 0$ is given exactly by the Fourier-Laplace integral

$$E(z,t) = \frac{1}{2\pi}\Re\left\{ i\int_{ia-\infty}^{ia+\infty} \frac{i}{\omega-\omega_c}\exp\left[\frac{z}{c}\phi(\omega,\theta)\right]d\omega\right\}. \tag{2}$$

Here, $u(t)$ denotes the step function, ω_c is the *carrier frequency* of the input pulse, $\phi(\omega,\theta)$ is the *complex phase function*

$$\phi(\omega,\theta) \equiv i\frac{c}{z}\left(\tilde{k}(\omega)z - \omega t\right) = i\omega\left[n(\omega) - \theta\right], \tag{3}$$

where $\tilde{k}(\omega) = (\omega/c)n(\omega)$ is the *complex wavenumber*, $\theta = ct/z$ is a dimensionless space-time parameter, and a is a real constant greater than the abscissa of absolute convergence for the initial field $E(0,t)$. The problem then is to evalute the contour integral (2) for all $\theta > 1$, the field given by (2) vanishing identically for all $\theta \leq 1$.

Asymptotic expansion techniques were first applied to (2) by Brillouin in 1914 [Brilluoin, *Ann. Phys.* **44** (1914)]. His analysis showed that the propagated field is comprised of two precursors and the main signal as

$$E(z,t) = E_S(z,t) + E_B(z,t) + E_c(z,t), \tag{4}$$

where $E_S(z,t)$ is the Sommerfeld precursor, $E_B(z,t)$ is the Brillouin precursor and $E_c(z,t)$ is the signal contribution. Later analysis by Oughstun and Sherman [*Pulse Propagation in Causal Dielectrics*, Springer-Verlag (1984)] using uniform expansion techniques showed that Brillouin's results were quantitatively incorrect in several important space-time regions. However, their expansion exhibited several discontinuities in its description of the propagated signal. Here, corrections to this previous research (in particular, to the signal contribution) are presented which results in a completely uniform asymptotic description of the propagated pulse.

Fast Time Domain Integral Equation Solver for Simulation of Propagation of Wide-band Pulses through Dispersive Media

E. Bleszynski, **M. Bleszynski**, **and T. Jaroszewicz**
Monopole Research, Thousand Oaks, USA

We present recent results on the analytical formulation and representative applications of the fast time domain integral equations specially tailored to problems interaction of wideband pulses with dispersive media. The algorithm takes advantage of the the block-triangular and block Toeplitz structures of impedance matrix in temporal indices, and of the Toeplitz structure of far-field component of the impedance matrix in spatial indices, hence allowing for the simultaneous compression in space and time. Furthermore, since the algorithm relies only on the translational invariance of the Green function, its computational cost is independent of the degree of dispersion of medium. An additional advantage of the method is its applicability to problems involving Green functions given in either tabulated or analytic forms.

An important practical element of the underlying time-domain integral formulation is that instead of using the customary integral equation operators involving the Green function and its derivatives, we construct effective integral equation operators equal to (i) the Fourier transform of the dispersive medium Green function, (ii) the Fourier transform of the product of the dispersive medium Green function with the inverse of dielectric permittivity.

Some of the most recent enhancements of our time-domain capabilities include numerically efficient modeling of specific time-localized waveforms, such as linear combinations of hermite polynomials. There is a need for such particular solver numerical capability in the context of several current and future medical and military potential applications. We derived compact analytical expressions for the projections (on spatial and temporal basis functions) of the incident wave represented as a superposition of hermite polynomials. A particular example of practical interest belonging to this class of waveforms is the "Mexican hat" wave-form, expressible as a linear superposition of Hermite polynomials up to the second order. We implemented the resulting formulation in the code module generating the incident wave projection on Rao-Glisson-Wilton (RWG) basis functions defined on triangular patches, and on pulse or band-limited (approximate prolate spheroidal) temporal basis functions.

We present numerical results for scattering on an arbitrarily sharped homogeneous dielectric body of a "conductive Debye" material, in which the electric permittivity is given by the Debye formula with an added conductivity term. The computations are carried out using a surface-integral equation formulation, involving matrix elements of free-space and dispersive dielectric Green functions. We evaluate the matrix elements of the dispersive medium Green function by means of integration in the complex frequency plane. We discuss some aspects of numerical quadrature in evaluation of integrals along branch cuts with singular (but integrable) behavior of branch-cut discontinuities.

We show validation results for a dielectric sphere, for which we compare scattered pulse shapes obtained from our time-domain integral equations with those synthesized using Mie solutions.

*This work is supported by the AFOSR grant F49620-01-0504.

Observation of Precursor-like Behaviour of Ultra-fast Pulses Propagating in Water

A. Fox[1], **U. Österberg**[1], **X. Gu**[2], **and R. Trebino**[2]

[1]Dartmouth College, USA
[2]Georgia Institute of Technology, USA

We have measured temporal, spectral and absorptive characteristics of broadband optical pulses around 800 nm propagating through pure water. The bandwidth of our pulses varied between 10 nm to 100 nm and the temporal pulsewidth varied between 60 fs to 2 ps and the pulse repetition rates were either 1 kHz or 80 MHz. The distances the pulses propagated through water varied between 0.3 meters to 6.1 meters. All measurements were performed under strictly linear conditions.

Our absorption measurements showed non-exponential decay as a function of path length. Pulses of varying temporal widths, bandwidths, chirps, and repetition rates were compared with simulated classical absorption predictions for statistically significant deviations. Deviations occurred for low repetition rates and pulse lengths shorter than approximately 500 fs. For the 60 fs pulses we observed 2 orders of magnitude less absorption after approximately 6 meters of propagation through water compared to 2 ps long pulses which absorbed according to Beer's law.

The temporal and spectral measurements were performed using cross-correlation frequency-resolved optical gating (XFROG). The XFROG technique records a spectrogram which enables us to extract both amplitude and phase information of the short optical pulses exiting from the water tube. These spectrograms clearly showed the breakup of a Gaussian pulse into three distinct pulses with different arrival times. The pulses were also centered at different carrier-frequencies and they had developed different types of chirp.

Using the theory developed for calculating the temporal energy velocity of propagation in an absorbing and dispersive medium [1] in conjunction with proven experimental data for both the real and imaginary part of the dielectric function of water [2] we were able to qualitatively relate our pulse breakup with that of points of stationary phase.

These observations are believed to be the manifestation of precursor activity.

REFERENCES

1. Lisak, M., "Energy expressions and energy velocity for wave packets in an absorptive and dispersive medium," *J. Phys. A: Math. Gen.*, Vol. 9, 1145–1158, 1976.
2. Segelstein, D. J., "The complex refractive index of water," M. Sc. Thesis, Department of Physics, University of Missouri-Kansas City, 1981.

Optimal Waveform Design for Imaging with an Active Array

L. Borcea
Rice University, USA

G. Papanicolaou
Stanford University, USA

C. Tsogka
University of Chicago, USA

We consider in this paper broadband array imaging of distributed reflectors by sending probing signals from one or more sources at the array and then recording the scattered echoes at all array elements.

We address the question of optimally choosing the waveform send by the array in order to construct the best possible image of the target for a given signal to noise ratio of the data. This is different from the problem of selecting the optimal waveform so as to maximize the received power at the array. The solution to this problem is known and its main drawback is that it corresponds to sending a narrowband waveform that peaks at the resonance frequency of the reflectors. That is because maximizing the power is equivalent to iterative time reversal, or, the singular value decomposition of the impulse response matrix. The resulting narrow-band waveform gives strong scattered echoes, but it is bad for imaging because lack of bandwidth means no range resolution and no statistical stability in clutter.

We propose instead to determine the source power allocation and waveforms with an optimality criterion based on the quality of the image. The main idea is to determine the waveform by solving an optimization problem using an appropriate measure that quantifies the quality of the image. The optimization problem is then solved subject to constraints such as limiting the power at the array and asking for an acceptable signal to instrument noise ratio at the receivers.

Analytic Pulsed-beam Communication Channels

G. Kaiser
Center for Signals and Waves, USA

Let $G(x_r - x_e)$ be the causal Green function for the wave equation in four space-time dimensions, representing the signal received at the space-time point x_r due to an impulse emitted at the space-time point x_e. Such emission and reception processes are highly idealized since no signal can be emitted or received at a precise point in space and at a precise time. We present a simple model for *extended* emitters and receivers by continuing G analytically to a function $\tilde{G}(z_r - z_e)$, where $z_e = x_e + iy_e$ is a complex space-time point representing a circular pulsed-beam emitting antenna dish centered at x_e and radiating in the direction of y_e and $z_r = x_r - iy_r$ is a complex space-time point representing a circular pulsed-beam receiving antenna dish centered at x_r and receiving from the direction of y_r. The analytic Green function $\tilde{G}(z_r - z_e)$ represents the *coupling amplitude* between the emission and reception dishes. The space components of y_e and y_r give the spatial orientations and radii of the dishes, while their time components determine the duration and collimation of the emission and reception processes. Causality requires that the orientation vectors y_e and y_r must belong to the future cone V_+ in space-time. The directivity D of the communication channel is a non-negative convex function on V_+, *i.e.*, $0 \leq D(y_r + y_e) \leq D(y_r) + D(y_e)$. That is, the directivity of the channel can be no better than the sum of its emission and reception components.

Weak Lacunae of Electromagnetic Waves in Dilute Plasma with Anisotropy

S. V. Tsynkov
North Carolina State University, USA

As has been shown in our previous work, the Maxwell equations of electromagnetic field do not, generally speaking, satisfy the Huygens' principle, unless the electromagnetic waves propagate through a very simple medium, such as the vacuum or a dielectric with static response. Accordingly, lacunae and the sharp aft fronts of the waves will not, generally speaking, exist in the corresponding solutions because of the propagation after-effects. However, for an important case of the high-frequency transverse electromagnetic waves in dilute plasma, the governing equations reduce to the Klein-Gordon equation. The latter is not Huygens' per se, but it turns out that lacunae can still be identified in its solutions, although in an approximate sense. The aft fronts for these "weak lacunae" can be clearly observed, but they may not be as sharp as in the pure Huygens' case. Moreover, it can be shown that the "depth" of a weak lacuna, i.e., the magnitude of its residual field relative to the magnitude of the field inside the primary wave packet, is controlled by the dimensionless ratio ω_{pe}/ω, where ω_{pe} is the Langmuir frequency and ω is the dominant carrying frequency of the waves, $\omega_{pe} \ll \omega$.

The aforementioned study has been carried out for the isotropic dilute plasma with the parameters close to those of the Earth's ionosphere. It is known, however, that the actual ionospheric propagation may be noticeably affected by the magnetic field of the Earth. This field makes the plasma anisotropic and also introduces an additional temporal scale into the model given by the electron cyclotron frequency Ω_{ee}. The cyclotron frequency is typically about an order of magnitude lower than the Langmuir frequency. In the current work we show that the additional effect of the Earth's magnetic field on lacunae for the case of high-frequency transverse propagation is small. Quantitatively, it is about Ω_{ee}/ω times smaller than the previously studied effect of the primary wave dispersion in plasma, where $\Omega_{ee} < \omega_{pe} \ll \omega$.

Qualitative Methods in Inverse Electromagnetic Scattering

F. Cakoni
University of Delaware, USA

Since the invention of radar, scientists and engineers have striven not only to detect but also to identify unknown objects through the use of electromagnetic waves. A significant step forward in the resolution of this problem was the use of synthetic aperture radar (SAR). However, (SAR) suffers from limitations arising from the incorrect model assumptions which ignore both multiple scattering and polarization effects. In recent years, in an effort to overcome the limitations of such an incorrect model, considerable effort has been put into the development of nonlinear optimization techniques which avoids incorrect modeling assumptions. The success of such an approach is based on strong a priori knowledge of the scattering object and hence is inappropriate for many, if not most, practical applications. In view of the problems inherent in the weak scattering and nonlinear optimization approaches to target identification, a new class of methods has been developed in the past few years loosely called qualitative methods in inverse scattering theory. The main theme of this talk is the use of one such qualitative method, the linear sampling method, to solve inverse electromagnetic scattering problems. In particular, we will discuss the imagining of objects imbedded in a known inhomogeneous media using electromagnetic radiation at a fixed frequency.

Session 2P1
Nanostructures and Metamaterials for RF and Optical Applications

Exotic Waves in Chains of Silver Nanospheres

C. R. Simovski[1,2], A. J. Viitanen[1], and S. A. Tretyakov[1]

[1]Helsinki University of Technology, Finland
[2]St. Petersburg Institute of Fine Mechanics and Optics, Russia

A transversal mode with zero group velocity and non-zero phase velocity that can exist in chains of silver nanospheres in the optical frequency range is theoretically studied. In such chains at a certain special frequency a monochromatic source excites the standing wave in an infinite chain, and as a result we obtain an optical resonator without spatial bounds. It is shown that the external source radiating a narrow-band non-monochromatic signal excites in the chain a mixture of standing and slowly traveling waves. The standing wave component (named as *resonator mode*) is strongly dominating. The physical reason of such a regime is an unusual distribution of power flux over the cross section of the chain. The study shows that the axial Poynting vector is negative on the chain axis and changes its sign at a certain distance ρ_0 from it, so that the total energy flux of the pulse turns out to be positive. The most part of the pulse energy propagating along the chain in the positive direction returns back inside a narrow spatial channel centered at the chain axis. Since the chain period for such a regime is obviously small compared to the wavelength in free space, the energy is concentrated in a subwavelength spatial region. Besides of very efficient slow-wave lines these chains can be also used for subwavelength localization of the light energy. The possible application for obtaining subwavelength images is discussed.

Next, chains with alternating spheres that differ by diameters (or, perhaps, covered with dielectric material) — two-phase chains — are studied. A small change of polarizabilities of spheres in these two sub-arrays results in new interesting properties. One of them is a significant broadening of the propagation band. For the case of the longitudinal polarization of spheres there is a narrow stop-band at the center of the band of eigenfrequencies, and one can obtain a high-quality band-stop filter. A single-phase chain of silver nanospheres can be considered as a filter with a narrow pass-band whose remarkable property is the subwavelength localization of the field. Two-phase chains behave as band-stop filters, also with subwavelength localization of the field. Other interesting features of this structure are also discussed.

Light Scattering on 2D Nanostructured Resonant Gratings

N. V. Ilyin, **I. G. Kondrat'ev**, **N. V. Sapogova**, **and A. I. Smirnov**
Institute of Applied Physics, Russia

Lately, a great success has been achieved in creating metamaterials based on resonant metal elements (e.g., left-handed media and films with embedded metal nanoparticles). Peculiar electromagnetic properties of such metamaterials open new prospects for creating various focusing/guiding electrodynamic systems and converters of frequency and angle spectra of electromagnetic radiation.

This paper studies nanostructured gratings made up by metal nanoparticles (specifically, silver) embedded in the dielectric, which are capable of maintaining quasi-static modes. The special emphasis is devoted to following specified types of gratings: row of periodical cylinders and square grating of spheres. The problem of a diffraction of a plane electromagnetic wave on such structures has been solved within the dipolar-interaction approximation. The equations for the tangential and normal components of the effective field have been obtained. The frequency dependences of the refraction, transmission, and absorption coefficients on the grating parameters (its period, refractive index of the dielectric, Q-factor of individual electrostatic resonances) have been obtained and analyzed. Besides, it has been shown that considered structures are capable of maintaining quasi-static modes. The basic properties of considered gratings have been analyzed and compared.

The research performed demonstrates that it is possible to use single-layer structures consisting of nanosized metal elements as frequency filters and decelerating systems in the IR and optical bands.

New Resonant Elements for Isotropic Magnetic Metamaterials

J. D. Baena[1], L. Jelinek[2], R. Marqués[1], and J. Zehentner[2]

[1]University of Sevilla, Spain
[2]Czech Technical University, Czech Republic

In 1999 Split Ring Resonator (SRR), as a unit cell of negative permeability media, was first introduced by Pendry [1]. Afterwards, Smith et al., [2] analyzed an array of wires and SRRs obtaining an artificial medium with simultaneously negative permittivity and permeability. This was the first realization of a left-handed medium which was theoretically studied by Veselago [3] several decades ago. However, this and subsequent realizations were highly anisotropic. A first attempt towards the design of isotropic magnetic metamaterials was made by Gay-Balmaz and Oliver Martin [4], who obtained a 2D isotropic SRR. The SRR is not the unique candidate for artificial quasi-isotropic medium, as was demonstrated by using Ω particles in [5]. More recently, an SRR based proposal for isotropic magnetic metamaterial design has been presented [6].

The main aim of this work is to design particles from which an isotropic media can be made. Really, no material composed by periodical arrangement of unit cells can be fully isotropic. However, in many cases the behavior of such system can be characterized by second order tensors (e.g., the electric, magnetic or magnetoelectric polarizability tensors), without considering tensors of higher orders. The cubic structures of Figs. 1 and 2 show the group of symmetry of the cube, thus being candidates for fully isotropic magnetic metamaterials [6]. In addition, it can be shown that the sub-group generated by the four operations $(\mathbf{I}, -\mathbf{I}, \mathbf{C}_{4\mathrm{x}}\mathbf{C}_{4\mathrm{y}}, \mathbf{C}_{4\mathrm{y}}\mathbf{C}_{4\mathrm{x}})$ also provides isotropic tensors. An example of an isotropic resonator invariant by this group of symmetry (in fact a modification of a previous proposal [7]) is shown in Fig. 3. A modification of Fig. 2 which substitutes the four gaps broadside-coupled SRR (BCSRR) by a simpler two-gaps BC-SRR is also invariant by the aforementioned symmetry group. Finally, the elimination of the inversion (-**I**) operation may lead to bi-isotropic magnetic media.

Figure 1.

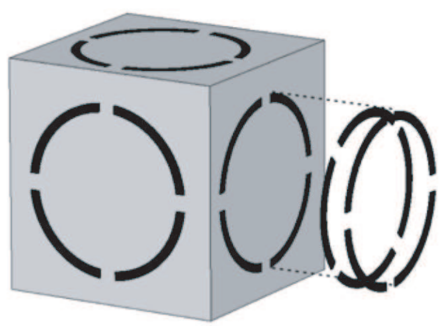

Figure 2.

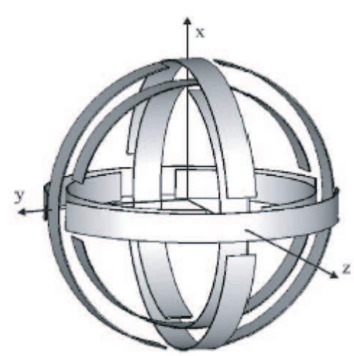

Figure 3.

REFERENCES

1. Pendry, J. B., et al., *IEEE Trans. on MTT*, Vol. 47, 2075, 1999.
2. Smith, D., et al., *Phys. Rev. Lett.*, Vol. 84, 4184, 2000.
3. Veselago, V., *Soviet Physics USPEKHI*, Vol. 10, 509, 1968.
4. Gay-Balmaz, P. and O. J. F. Martin, *Appl. Phys. Lett.*, Vol. 81, 939, 2002.
5. Simovski, C. R. and S. He, *Phys. Lett. A*, Vol. 311, 254, 2003.
6. Koschny, Th., L. Zhang, and C. M. Soukoulis, *Phys. Rev. B*, Vol. 71, 121103(R), 2005.
7. Marqués, R., J. D. Baena, J. Martel, F. Medina, F. Falcone, M. Sorolla, and F. Martin, *Proc. of the ICEAA'03*, 439, Pisa, Italy, Sept. 2003.

Modified Equivalent Circuit Model of Microwave Filter with LTCC Technique

Y. L. Qin, **A. Fang**, **J. Hu**, **W. W. Zhou**, **and M. Zhang**
Zhejiang University of Technology, China

Because microwave products in the consumer electronics market is continuous development, device and component manufacturers to seek new advanced integration, packaging and interconnection technologies, as size, cost and performance are critical factors for the success of a microwave product. One of the most promising integration technologies is the multilayer low temperature co-fired ceramic technology (LTCC). In this technology, passive components, such as inductors, capacitors and filters, are integrated into multilayer LTCC substrate.

The purpose of this paper is to address the special method that should be considered for designing LTCC microwave filter. It is given how to get equivalent circuit about multilayer ceramic microwave filter that is striplines configuration or LC configuration, especially, modified equivalent circuit model is proposes, which relation between the concentrate parameters and physical dimension of LTCC microwave filter is discussed. Then the capacitance and inductance matrix of LTCC microwave filter is got using the fast multipole method. Finally, two microwave filters are designed by the novel design method of field-circuit and HFSS. The novel design method of field-circuit is high efficiency, so the design components time can be shortened.

Design of a Metafilm-composite Dielectric Shielding Structure Using a Genetic Algorithm

J. Huang[1], M. Y. Koledintseva[1], P. C. Ravva[1], J. L. Drewniak[1]
R. E. Du Broff[1], B. Archambeault[2], and K. N. Rozanov[3]

[1]University of Missouri-Rolla, USA
[2]IBM Co., USA
[3]Russian Academy of Sciences, Russia

Many practical applications require shielding structures having specified frequency characteristics. Metafilms buried in composite layers or layers of commercially available dielectrics may increase S.E. in the frequency band of interest, or assure desirable frequency-selective effects.

An analytical model for a shielding structure containing both bulk composite layers and planar metafilms (MFs) made of perfect electric conductors is presented. It allows for synthesis of shielding structures using a robust and quickly converging genetic algorithm (GA) [1]. Composite dielectrics containing conductive inclusions at dilute concentrations (below the percolation threshold) can be modeled using the Maxwell Garnett formulation [1]. MFs can be of two different types: patch or aperture. Their frequency responses, specifically, transmission (T) and reflection (Γ) coefficients in a plane-wave formulation, are calculated based on polarizabilities determined by the particular pattern geometry. T and Γ of a patch-type MF are derived using the generalized sheet transition conditions (GSTC) [2]. For aperture-type MF, the Babinet's duality principle [3] is used to map the results from the complementary problem. T and Γ for a single-layered MF are represented in a unified matrix form for any angle of incidence. Any MF buried in a host dielectric can be decomposed into three types of basic elements: a host composite slab, interface between media, and an MF inside the homogeneous host medium. Each basic element is described by a corresponding T-matrix [4], and the total T-matrix of the stack is the sequential product of individual T-matrices. T and Γ of the stack is easily derived from the total T-matrix. If there are two or more MFs, the distance between them justifies the condition of neglecting higher-order mode interactions.

Before the synthesis process, a designer should have some initial information based on a particular application of the shielding under design. The requirements for the desired frequency response of the structure should be known, and the designer should decide which shielding mechanism may be preferable — reflective, absorptive, or combination. An appropriate number of composite layers, the total maximum thickness, and reasonable ranges of electromagnetic parameters of layers for the initial search pool should be specified. To ensure manufacturability, the designer needs some a priori data on ingredients available and technologically appropriate. The GA helps to choose the best geometry of MF patterns, thickness of layers, and appropriate constitutive parameters of each composite layer.

REFERENCES

1. Koledintseva, M. Y., et. al., "Engineering of composite media for shields at microwave frequencies," *Proc. IEEE EMC Symposium*, Vol. 1, 169–174, Chicago, IL, August 2005.
2. Kuester, E. F., et. al., "Averaged transition conditions for electromagnetic fields at a metafilm," *IEEE Trans. AP*, Vol. 51, No. 10, Part 1, 2641–2651, October 2003.
3. Lee, S. W., et. al., "Simple formulas for transmission through periodic metal grids or plates," *IEEE Trans. on AP*, Vol. 30, No. 5, 904–909, September 1982.
4. Weber, R. J., "Introduction to microwave circuits: radio frequency and design applications," *New York: IEEE*, Ch. 2, 25–27, 2001.

Towards Nano-scales in Photonics

M. Soljačić, **A. Karalis**, **E. Lidorikis**, **and M. Ibanescu**
MIT, USA

L. V. Hau
Harvard University, USA

J. D. Joannopoulos
MIT, USA

We will discuss possible solutions to several key fundamental problems in nanophotonics. The goal of nanophotonics is to explore and manipulate photons at scales (in space, time and energy) that are orders of magnitude smaller than anything previously possible. To accomplish this, one needs to constrain visible or near-infrared photons (the preferred mode of operation: $\lambda \sim 1\,\mu$m) into scales compatible with nanotechnology: 10–100 nm. One also needs to drastically reduce the operational power of optical devices, eventually even down to single photon operating energies.

Most of these problems could be tackled by Surface Plasmon (SP) based devices. SPs enable constraining, and manipulation of light at scales compatible with nanophotonics. Unfortunately, SP-supported designs suffer from two other major disadvantages: huge losses (characteristic of plasmonic materials), and small bandwidth (since SPs are resonance-supported phenomena). We will present a novel class of surface plasmon (SP) assisted components that can overcome all of these difficulties. We will show results of a detailed theoretical and numerical study of the underlying physical mechanism driving these novel SP components.

For a long time, there was a widespread belief in the optics community that alloptical signal processing is not feasible because of the weakness of ultra-fast non-linear effects. There are two most commonly used approaches to enhance non-linear effects. One is to use a material that has as large a non-linear response as possible. The other approach involves finding a structure whose geometrical properties optimize non-linear response. As far as materials go, Electro-Magnetically Induced Transparency (EIT) materials have by far the strongest non-linear response in nature: Kerr non-linearities 12 orders of magnitude larger than in GaAs have been measured in EIT systems recently, thus making EIT-materials the most non-linear materials in nature. Concerning the structural enhancement of non-linearities, Photonic Crystal (PhC) micro-cavities are superior to all other proposed systems: one can design tiny ($O(\lambda^3)$), low operational power (e.g., few tens of mW), ultra-fast (bit rate $>=$ 40 Gbit/sec) devices suitable for any kind of all-optical signal processing, that can be implemented in common optical materials (AlGaAs, As_2Se_3...). We will present a detailed theoretical and numerical investigation of the possibility of combining the unparalleled non-linear properties of EIT materials, with superb opportunities of PhC micro-cavities for structural enhancement of non-linear effects in order to produce an all-optical non-linear device that can be operated at extraordinarily low (even single photon) energy levels.

Design and Measurement of a Four-port Device Using Left-handed Metamaterials

Z. M. Thomas, T. M. Grzegorczyk, B.-I. Wu, X. D. Chen, and J. A. Kong
Massachusetts Institute of Technology, USA

A left-handed metamaterial can be designed such that the frequency dispersive nature of the constitutive parameters results in a change in the sign of refraction with frequency for a specified incidence angle [1]. A four-port device is designed that utilizes this property and reflection to separate an signal incident from port 1, into three distinct bandwidths. Power transmitted at the metamaterial interface is later collected at a port corresponding to either positive or negative refraction accordingly (ports 3 and 4). Power in the band of frequencies where the dominant effect is reflection is collected at a third output port (port 2).

Designing the device requires the selecting of an appropriate metamaterial that will support negative refraction in some bandwidth, and positive refraction in another. The incidence angle should be selected such that these properties can be realized, and a third band exists where reflection is dominant. Because the energy transmitted into the metamaterial must also exit the metamaterial before being detected at either of the two transmission ports, the geometry affecting the exit angle must also be considered and specified. Ideally the transmitted power exits the metamaterial with minimal internal reflection and is directed directly towards the appropriate port.

We present a design of the four-port device that utilizes the split-ring resonators introduced in [2]. This structure can achieve a Lorentz type dispersion relation [3]. The rings are all oriented in the same direction resulting in dispersion in one component of the permeability tensor. The ring design dimensions are supplied from [4] and the dispersive behavior is verified by simulation followed by applying the retrieval algorithm in [5]. After investigating and specifying the design parameters we find that a wedge of the material can be fashioned to achieve the desired properties. The device is constructed for measurements inside a parallel plate waveguide. Measurements are taken at the edge of a parallel plates utilizing SMA to X-band waveguide adapters. The X-band corresponds to the resonance region of the split-ring resonators. Measurements are made on a vector network analyzer and are found to be consistent with analytical expectations.

REFERENCES

1. Smith, D. R. and D. Schurig, "Electromagnetic wave propagation in media with indefinite permittivity and permeability tensors," *Phys. Rev. Lett.*, Vol. 90, No. 7, 077405, February 2003.
2. O'Brien, S. and J. B. Pendry, "Magnetic activity at infrared frequencies in structured metallic photonic crystals," *J. Phys.: Condens. Matter*, 6383–6394, June 2002.
3. Shelby, R. A., D. R. Smith, and S. Schultz, "Experimental verification of a negative index of refraction," *Science*, Vol. 292, 77–79, April 2001.
4. Wang, W., "Directive antenna using metamaterial substrates," *MIT Masters Thesis*, June 2004.
5. Chen, X., T. M. Grzegorczyk, B.-I. Wu, J. P. Jr., and J. A. Kong, "Improved method to retrieve the constitutive effective parameters of metamaterials," *Phys. Rev. E*, Vol. 70, No. 016608, 1–7, 2004.

Embedded-circuit Meta-materials for Surface Wave Suppression

H. Mosallaei
Northeastern University, USA

Suppressing surface waves is a very challenging task in electromagnetics. Many researchers have proposed different configurations to stop the surface wave propagation. One of the most efficient ways has been based on the use of periodic dielectric and metallo-dielectric Electromagnetic Band-Gap (EBG) structures [1–2]. However, the periodicity of such structures is comparable to the wavelength and at least a few periods are required to achieve high isolation which is not very appropriate in the design of small size devices and systems.

In this paper a novel approach based on negative μ materials for suppressing the surface waves is offered. To accomplish this, Embedded-Circuit Loops (ECL), realizing artificial molecules, are printed on a low dielectric material. For a magnetic excitation polarized along the axis of the loops, the designed meta-material presents negative permeability property. In the negative μ region, the wave is stopped and cannot penetrate through the material [3]. Unlike traditional EBGs the periodicity of ECL can be a very small fraction of a wavelength ($< 0.05\lambda$). Fig. 1(a) depicts the geometry of a 1-layer ECM. The transmission coefficient for a plane wave illuminating a very thin layer of a ECM is shown in Fig. 1(b). The stop-band behavior is clearly demonstrated.

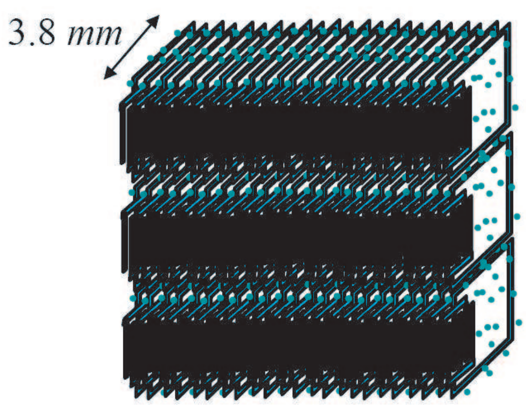

(a)

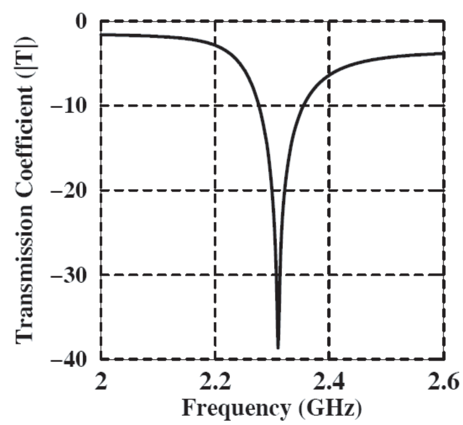

(b)

Figure 1: (a) Embedded-Circuit Metamaterial and (b) its performance.

REFERENCES

1. Rahmat-Samii, Y. and H. Mosallaei, "Electromagnetic band-gap structures: classification, characterization, and applications," *IEE International Conference on Antennas and Propagation*, UMIST, Manchester, UK, 2001.
2. Yang, F. and Y. Rahmat-Samii, *IEEE Trans. Antennas Propagat.*, Vol. 51, No. 10, 2936–2946, Oct. 2003.
3. Sarabandi, K. and H. Mosallaei, "Novel artificial embedded circuit meta-material for design of tunable electro-ferromagnetic permeability medium," *IEEE International Microwave Symposium*, Philadelphia, Pennsylvania, 2003.

Double Clad Fiber Laser with Frequency Selecting by Double Clad Fiber Bragg Grating

T. Wu[1] **and Z.-D. Xue**[2]

[1]LongYan University, China
[2]Fuzhou University, China

It is always using F-P linearity cavity in double clad fiber lasers. The cavity is composed of one dichroic mirror and fiber end Fresnel reflector (reflectivity nearly 4%). This is a defect and unstable cavity. It cannot exactly select frequency, and the line width of the laser is extensive. In some applications requiring wavelength strictly, this kind of laser is limited. As a rule Bragg gratings that compose a laser cavity are fabricated in a high germanosilicate host fiber and then spliced with an Yb3+−doped active fiber. Difference of parameters of the two kinds of fibers leads to dditional losses of both pump and signal. A double-clad fiber Bragg grating which was fabricated in the core of Yb3+−doped double-clad fiber using the phase-mask method is reported. This kind of grating is used as the output mirror of the D-shape inner cladding Yb3+−doped double-clad fiber laser. The fiber length is 10 m and 20 m respectively. The laser operating near 1058 nm with stable and narrow FWHM (3 dB bandwidth is 0.329 nm) is realized. The maximum output power laser is 570 mW. Finally, these experimental results are analyzed theoretically. A double clad fiber Bragg grating remarkably greatly improves the Spectrum properties of laser, and the anticipative wavelength of laser can be achieved. For the splice loss in cavity of the DCFL is very little, the bulk of the DCFL is reduced. It is also shown that wavelength-definite, narrow linewidth, high-efficiency, high-beam-quality laser performances can be achieved, which are of great interest for many important applications.

Ferroelectric PSTO and Mn: BSTO Thin Films for Wireless Microwave Elements

Z. Yuan[1], **S. W. Liu**[2], **and C. L. Chen**[1]

[1]University of Texas at San Antonio, USA
[2]University of Arkansas, USA

Ferroelectric thin films have broad applications in electronic, optoelectronic, optical, acoustic and microwave devices areas. Especially, there has been a significant increasing need of films in wireless microwave communications, such as microwave phase shifters, filters, and oscillators. Currently, ferroelectric BSTO and PSTO thin films are considered to be very promising candidates for room temperature tunable microwave elements because of their high dielectric tunability and relative low dielectric loss.

Recently, we have focused on the improvement of dielectric properties of the highly epitaxial ferroelectric thin films. A novel method of 2% Mn additional-doping technique was adapted to the pure BSTO/MgO films. The as-growth films were characterized by x-ray diffraction and transmission electron microscopy to understand the microstructure, crystallinity, epitaxy behaviors. The microstructural studies reveal that both BSTO and PBCO thin films are c-axis oriented with excellent single crystalline and excellent epitaxial behavior although both BSTO and PBCO film have large lattice mismatch with (001)MgO substrate at about 6% and 7.5%, respectively. The epitaxial relationships were found to be $(001)_{\text{films}}//(001)_{\text{MgO}}$ and $[100]_{\text{film}}//[100]_{\text{MgO}}$.

To understand the dielectric properties of the as-grown PSTO and Mn:BSTO films, high frequency dielectric measurements were employed to analyze the dielectric properties of Mn: BSTO and PSTO thin films. A significant improvement of dielectric property of the as-grown Mn: BSTO films was achieved with large tenability of 80% at 40 KV/cm, very large dielectric constant value of 3800 and extra low dielectric loss of only 0.001 at 1 MHz measuring frequency and room temperature. The mechanisms responsible for this improvement concern the fact that the acceptor dopants Mn^{2+} can compensate for the electrons generated form the oxygen vacancies, whose hopping between different titanium ions will induce the dielectric loss. The high frequency (10-30 GHz) dielectric measurements demonstrate that the Mn: BSTO films are excellent in both dielectric property and very low insertion loss values of only 0.2 dB at 10 GHz and more than 1.5 dB at 30 GHz. On the other hand, the high frequency dielectric property measurementson the as-grown PSTO/MgO thin films exhibit a high dielectric constant value of 1420 at zero-bias and a very large tunability at 34% under bias field 40 Kv/cm up to 20 GHz. In summary, these results indicate that highly epitaxial Mn: BSTO and PSTO thin films are good candidates for developing the high-frequency, room-temperature tunable microwave.

Chain of Metamaterial Nanospheres as Leaky-wave Nanoantennas at Optical Frequencies

A. Alù[1,2] and N. Engheta[1]

[1]University of Pennsylvania, USA
[2]University of Roma Tre, Italy

The theory for designing a traveling-wave or a leaky-wave antenna is well established at microwave frequencies. At these frequencies usually a waveguide structure with some radiating defects or corrugations periodically arranged in space can produce a guided beam that leaks some energy into free space. Under proper conditions on the periodicity and the guidance of the energy, this may produce a directive beam with potential applications in several fields. The advent of metamaterials, i.e., artificially engineered materials with unconventional properties not common in nature, has raised new interest in different areas including the leaky-wave antenna design. In particular, a proper design of planar metamaterial circuit boards has been shown by others to produce a compact leaky-wave antenna with interesting performance, in terms of the possibility of scanning the angle of radiation from end-fire to back-fire by varying the frequency of operation, without any cut-off at broadside [1, 2].

Extending these concepts to the optical frequencies can offer exciting possibilities and useful applications. However, such extension does not only involve the scale reduction, since materials (e.g., noble metals) behave differently in different frequency regimes. The recent interest in plasmonic resonances and related phenomena, however, has raised the attention on a possible new paradigm for extending the circuit concepts from lower frequencies into the visible domain. We have shown in [3] how nanocircuit elements can be envisioned at these frequencies and how they can be properly connected in order to synthesize a complex nanocircuit. In [4] we have followed this analogy to consider optical nano-transmission-lines by properly arranging nanoinductors and nanocapacitors. Following the same analogy, and exploiting linear chains of plasmonic particles interleaved with non-plasmonic gaps, here we show theoretically how it is possible to design highly directive leaky-wave antennas at optical frequencies with future potentials in communications and nanotechnology. A different way of designing leaky-wave antennas using periodically modulated epsilon-negative nanorods has recently been studied theoretically [5]

In the present work, we show the conditions on the plasmonic particles composition and on the geometrical properties of the chain for supporting such resonant modes and consequently for building directive nanoantennas at optical frequencies. We also propose some design examples and we verify the results with full-wave simulations utilizing realistic materials (e.g., silver) with dispersive properties and ohmic losses included.

REFERENCES

1. Grbic, A. and G. V. Eleftheriades, *IEEE Trans. Antennas Propagat.*, Vol. 50, 1494, 2002.
2. Lim, S., C. Caloz, and T. Itoh, *IEEE Microwave & Wireless Components Lett.*, Vol. 14, 277, 2004.
3. Engheta, N., A. Salandrino, and A. Alù, PRL, Vol. 95, 095504, 2005.
4. Alù, A. and N. Engheta, *Proc. of URSI GA*, New Delhi, India, Paper No. 99, 2005.
5. Li, J. and N. Engheta, "2005 annual meeting of the optical society of america," *Frontiers in Optics*, Tucson, Arizona, October 16-20, 2005.

Epsilon-near-zero (ENZ) Materials as Insulators for Nanocircuit Elements

M. G. Silveirinha[1,2] and N. Engheta[1]

[1]University of Pennsylvania, USA
[2]Universidade de Coimbra, Portugal

There has been a growing interest in research on metamaterials with negative parameters, i.e., double-negative (DNG) or single-negative media [1, 2]. However, metamaterials with other unconventional material parameters have also attracted a great deal of attention. One class of such materials is the media in which the relative permittivity and or permeability is near zero. These materials, which can be referred to as epsilon-near-zero (ENZ) or mu-near-zero (MNZ), have been the subject of study recently [3, 4]. We have shown theoretically that electromagnetic or optical waves may be able to tunnel through very narrow channels or waveguide bends filled with ENZ materials, and that this property can play an interesting role in reducing the reflectivity at certain waveguide bends. It has also been shown that zero-index materials can be used to narrow the far-field pattern of an antenna embedded in the medium and to transform curved wavefronts into planar ones.

In the present work, we explore another interesting feature of ENZ materials, namely, their role as insulators for nano-scale circuit elements at the infrared (IR) and visible frequencies. The concept of circuit elements in the optical domains, i.e., nanoinductors, nanocapacitors, and nanoresistors has been introduced recently [5], in which it was suggested that plasmonic and non-plasmonic nanoparticles can behave as circuit elements, i.e., inductor and capacitor, at optical frequencies. One of the interesting questions in this context is the following: "Can we have an equivalent of "insulators" or "shields" for such nanocircuit elements at the optical frequencies that minimizes the coupling between the circuit elements?". One possible answer to this question is the use of ENZ layers as insulating shields around optical nanoelements. Our theoretical analysis has shown that such layers can, under certain circumstances, indeed act as insulators supporting zero displacement current, resulting in the confinement of the displacement current inside the nanoparticles. Therefore, ENZ-shielded nanocircuit elements can be regarded as elements with lesser leakage coupling among neighboring nanoelements.

In this talk, we will present some of our theoretical results, and we will forecast some future ideas and potential applications for this concept.

REFERENCES

1. Ziolkowski, R. W. and N. Engheta (Guest editors), Special issue of *IEEE Transactions on Antennas and Propagation on metamaterials*, Vol. 51, No. 10, October 2003.
2. Itoh, T. and A. A. Oliner (Guest Editors), Special issue of *IEEE Transactions on Microwave Theory and Techniques*, Vol. 53, No. 4, April 2005.
3. Engheta, N., M. Silveirinha, A. Alù, and A. Salandrino, "Scattering and reflection properties of low-epsilon metamaterial shells and bends," *2005 International Conference in Electromagnetics in Advanced Applications*, Turino, Italy, September 12–16, 2005.
4. Ziolkowski, R. W., "Propagation in and scattering from a matched metamaterial having a zero index of refraction," *Physical Review E*, Vol. 70, 046608, 2004.
5. Engheta, N., A. Salandrino, and A. Alù, *Physical Review Letters*, Vol. 95, 095504, August 2005.

Leaky-mode Resonance Properties of Periodic Lattices and Their Applications

R. Magnusson and Y. Ding
University of Connecticut, USA

Subwavelength periodic photonic crystal slabs and waveguide gratings exhibit strong resonance effects. For periodic elements with weak dielectric-constant contrast, strong surface-localized fields with high Q-factors are found. As the modulation amplitude increases, the Q-factor falls and the resonant spectra broaden. These guided-mode resonance effects arise when an incident electromagnetic wave is coupled by a second-order grating to a leaky waveguide mode supported by the thin-film system. Such resonance effects can be applied to implement new photonic devices. For example, optical reflection (bandstop) filters with narrow spectral linewidths can be realized since the coupling of the external wave into the leaky, reradiated mode occurs over narrow parametric ranges. Resonant bandstop optical filters with high efficiencies (∼98%) and narrow lines (∼1 nm) have been experimentally verified in the near-IR spectral region. New resonant biosensors can be developed based on these concepts.

This paper provides analytical, numerical, and experimental results elucidating the nature of resonant leaky modes associated with periodic refractive-index lattices. It is shown by numerous simulations that single-layer subwavelength periodic leaky-mode waveguide films with binary profiles can be applied to fashion optical elements that provide a remarkably broad variety of spectral characteristics. These sparse elements even with one-dimensional periodicity can function as new types of narrow-line bandpass filters, polarized wideband reflectors, polarizers, polarization-independent elements, and as wideband antireflectors. The work presented addresses fundamental phenomena essential for development of subwavelength leaky-mode resonant device technologies. The associated physical properties are explained in terms of the photonic band structure and its relation to the structural symmetry of the elements. The interaction dynamics of the leaky modes at resonance contribute to sculpting the diverse spectral bands observed by numerical simulations. The leaky-mode spectral placement, their spectral density, and their levels of interaction are shown to be fundamentally important in understanding device operation. These results demonstrate potentially new dimensions in optical device design and may provide complementary capability with thin-film optics.

In addition to applications in the photonic band, it is of interest to consider applicability of guided-mode resonance effects in lower frequency spectral regions. For example, devices operating in the THz region are potential candidates. Thus, computed results are presented to illustrate key properties of resonant THz elements such as spectral profiles and resonance efficiencies with respect to the structural parameters defining the device.

Slow-than-light Transportation of Microwave through Subwavelength Fractal Slots

B. Hou, W. J. Wen, and P. Sheng
The Hong Kong University of Science and Technology, China

Recently, we have found that high electromagnetic wave transmissions can be achieved for a metal plate perforated by slots arranged in fractal geometry at wavelengths much larger than the cross sectional dimensions of fractal slots, and that the transmission is independent on the incident angle, plate thickness, or array periodicity [1,2]. Now, we investigate the wave transportation in time domain through the subwavelength fractal slots at the transmission peak. Both experimental and theoretical results reveal a slow-than-light phenomenon. For example, the time delay can reach 1.3 ns for a microwave pulse to propagate through a 7.7 mm thick metal plate with the fractal slots, which means a reduced group velocity of c/50. The time delay or the reduction in group velocity for a metal plate of thickness given is determined solely by the geometric of fractal slots, because the transmission is caused by a subwavelength resonance which is the transversal shape resonance localized in the metallic slots with axial wave number $k = 0$. The time delay can also be tuned by filling dielectrics into the fractal slots where the fields undergo a significant enhancement.

REFERENCES

1. Zhou, L., W. Wen, C. T. Chan, and P. Sheng, "Mechanisms for high electromagnetic wave transmissions," *PIERS 2005* , Hangzhou, China, 2005.
2. Wen, W., L. Zhou, B. Hou, C. T. Chan, and P. Sheng, "Microwave resonant transmission through subwavelength fractal slots," to be published.

Session 2P2
Surface Plasmon Photonics

Plasmons in nearly Touching Metallic Nanoparticles: Singular Response in the Limit of Touching Dimers

I. Romero[1], **J. Aizpurua**[1], **G. W. Bryant**[2], **and F. J. G. de Abajo**[1,3]

[1]Donostia International Physics Center (DIPC), Spain
[2]National Institute of Standards and Technology, USA
[3]Centro Mixto CSIC-UPV/EHU, Spain

We study the optical properties of pairs of spherical gold nanoparticles for light incident with its polarization parallel to the interparticle separation vector. Both the absorption of this system and the light scattering strength exhibit resonant features that shift in frequency when the separation between particles is varied. Distances close to the point of particle percolation are discussed in detail, where a rich structure of resonant features shows up. The evolution of overlapping spheres from the point where they touch to the point where they merge into a single sphere shows a resonant feature that shifts towards the far infrared region immediately in the limit when the spheres touch at a single point.

Temporal and Spectral Eependence of the Nonlinear Optical Properties of $Au\!:\!Al_2O_3$ and $Cu\!:\!Al_2O_3$ Composite Films

H. Fernández, R. Del Coso, J. Solis, J. Gonzalo, and C. N. Afonso
Instituto de Óptica, CSIC, Spain

Third order optical non-linearities in metal-dielectric nanocomposites have received considerable attention over the last years. These nanocomposites show large third order susceptibilities in the vicinity of the surface plasmon resonance with ultrafast build-up times. These characteristics make them promising for several applications in the field of information technologies like all-optical switching, signal regeneration or high speed demultiplexing [1]. Particularly, a very large third order nonlinear optical susceptibility has been recently reported for Cu nanocomposites near the percolation threshold that has been related to the appearance multiple particle interactions and giant local field enhancement effects [2].

The aim of this work is to investigate the spectral and temporal dependence of the third order non-linear response of Cu and Au nanocomposites embedded in Al_2O_3 with large metal volume fractions. Alternate pulsed laser deposition (PLD) is used to produce the samples. The nanocrystals are organized in layers that are separated by Al_2O_3. The total number of nanocrystal layers are of 10 and 5 respectively for the case of the $Cu\!:\!Al_2O_3$ and $Au\!:\!Al_2O_3$ samples while the spacing layers are 6 nm - thick and in both cases. In order to analyse the effect of the metal content and morphology in the non-linear optical properties of the nanocomposites, the dimensions and shape of the nanocrystals in each layer have been varied in different samples by increasing the metal content up to a limit close to the percolation threshold. The nonlinear optical properties of the films have been analyzed by degenerate four wave mixing and z-scan in the wavelength interval from 500 to 620 nm using laser pulses durations in the 100 fs - 10 ps interval.

For all the nanocomposites analysed (Cu and Au, and no matter the metal volume fraction), at wavelengths close to that of the surface plasmon resonance, the third order susceptibility values determined with laser pulses in the ps range are considerably higher (five to twenty times) than the ones obtained under fs laser pulses. The observed increase of the third order susceptibility for increasing pulse durations is bigger in the Cu than in Au nanocomposites. In both cases the third order susceptibility value observed saturates for pulse durations around 5 ps. These results are discussed in terms of the different physical mechanisms contributing to the effective third order susceptibility of the nanocomposites, including the possible contribution associated to the ultrafast heating of the nanoparticles related to the temperature dependence of their dielectric function.

REFERENCES

1. Cotter, D., R. J. Manning, K. J. Blow, A. D. Ellis, A. E. Kelly, D. Nesset, I. D. Phillips, A. J. Poustie, and D. C. Rogers, "Nonlinear optics for high-speed digital information processing," *Science*, Vol. 286, 1523–1528, 1999.
2. Coso, R. D., J. R. Isidro, J. Solis, J. Gonzalo, and C. N. Afonso, "Third order nonlinear optical susceptibility of $Cu : Al_2O_3$ nanocomposites: from spherical nanoparticles to the percolation threshold," *J. Appl. Phys.*, 95, 2755–62, 2004.

Flasmon Spectroscopy of Metallic Nanoparticles Close to Dielectric Substrates. Analysis of Particle-substrate Interaction Effects

F. Moreno and F. González
University of Cantabria, Spain

Plasmon spectroscopy of metallic nanoparticles has been a very active field of research during the last decade [1]. The excitation of lacalized plasmons, or plasmon resonances, in small metallic particles generates strong local electric fields very close to the particle surface. This enhancement of the electric field finds many applications that have generated new technologies in the nanoscopic world [1].

It is well known that the spectrum of plasmon resonances depends on the size and shape of the individual particles and also on the particle-particle interaction when the particle density is high and multiple scattering is important. This interaction modifies the spectrum in such a way that dipolar resonances shift (normally th the red) and other multipolar resonances appear [2, 3]. Usually, in experimental works with nanoparticles, these are grown inside a dielectric high-refractive-index matrix ($GaAs$, TiO_2, *a-Si*, *etc.*) in order to shift the resonance to the visible part of the spectrum [4, 5]. This matrix is ,in turn, located on a flat substrate, which normally is dielectric. In these works, particle shape and size, and particle-particle interaction are considered in order to account for the structure of the resonance (either, peak position or shape). Because of the presence of the substrate, particle-substrate interaction is another source of modification of the spectrum of the plasmon resonance, which can contribute to the shift of the dipolar component and also to the appearance of new resonances of higher orders, but it has not been considered so far.

In this research, we present a systematic numerical study of the scattering crosssection of a small metallic particle (Ag) immersed in a dielectric medium of refractive index n and located at a given distance above flat, dielectric substrate of refractive index n' ($> n$, $< n$). The geometry is restricted to the 1D case, which has been shown to be successful in dealing with this kind of electromagnetic problem [2]. The study is made as a function of both the distance to the substrate and the angle of incidence, the latter case to analyze the effect of the component of the incident electric field when it is parallel/perpendicular to the substrate. The numerical work has been performed by using exact numerical techniques based on the application of the Extinction Theorem of the Physical Optics [6], where the authors have previously studied scattering for both far and near field approximations [7, 8].

REFERENCES

1. Prasad, P. N., *Nanophotonics*, John-Wiley, 2004.
2. Kottmann, J. P. and O. J. F. Martin, *Opt. Exp.*, Vol. 8, No. 12, 655, 2001.
3. Kelly, K. L., et al., *J. Phys. Chem. B*, Vol. 107, 668, 2003.
4. Klar, T., et al., *Phys. Rev. Lett.*, Vol. 80, No. 19, 4249, 1998.
5. Mertens, H., et al., *Appl. Phys. Lett.*, Vol. 85, No. 8, 1317, 2004.
6. Vesperinas, M. N., *Scattering and diffraction in physical optics*, John-Wiley, 1991.
7. Valle, P. J., et al., *Phys. Rev. B*, Vol. 51, No. 19, 13681, 1995.
8. Moreno, F., et al., *Appl. Phys. Lett.*, Vol. 68, No. 22, 3087, 1996.

Metallic Photonic Band Gap Structures for Laser Applications

F. H'Dhili[1,2], T. Okamoto[1], J. Simonen [1,3], and J. Simonen [1,4]

[1]RIKEN Nanophotonics Laboratory, Japan
[2]Tunis El Manar University, Tunisia
[3] University of Joensuu, Finland
[4]Osaka University, Japan

We report on a two dimensional plasmonic crystal laser structure that utilizes a thin Ag film for the generation of long range surface plasmons (LRSPs) and a layer of the organic semiconductor tri(8-hydroxyquinoline) aluminum (Alq3) doped with the laser dye 4-dicyanmethylene-2-methyl-6-(p-dimethylaminostyryl)-4H-pyran (DCM) as active medium. The dispersion diagram of this structure exhibits a plasmonic bandgap in the dye emission wavelength range. At the flat bandedge, the groupe velocity tends to zero, so that the density of surface plasmon modes is high. This yields a lasing action. However, the device suffers from the energy dissipation (metal absorption, unwanted radiation, etc.). We suggest few ways to minimize the effect of this problem. First, we propose the use of LRSPs characterized by a low loss coefficient. To this end, we investigate theoretically and experimentally the best conditions for the excitation of these modes. A strong emission is observed compared to that from a planar structure. These modes provide a high performance when the dye thickness is about 100 nm, a value consistent with the numerical findings. In addition, we demonstrate that the use of a spacer layer significantly increases the emission efficiency. We further suggest a new design for the laser structure for minimal radiation loss.

Surface-plasmon Polariton Scattering from a Finite Array of Nanodefects on Metal Surfaces

J. A. Sánchez-Gil
Instituto de Estructura de la Materia, Spain

T. A. Leskova and A. A. Maradudin
University of California, USA

We investigate theoretically and numerically the propagation and scattering of surface plasmon-polaritons (SPPs, evanescent waves, bounded to the interface, resulting from a blend of surface plasmons and photons) on surfaces structured with nano-defects. The formulations are based on the reduced Rayleigh equations obtained by imposing either the continuity conditions or the impedance boundary condition, rigorously accounting for all the scattering channels: SPP reflection and transmission, and radiative leakage. The scattering of SPP (both CW and pulsed excitation) in the visible and near IR by single (nano/micro)-defects [1, 2] and finite arrays of nano-defects [3] on an otherwise planar metal interface is studied; both are specially relevant in micro/nano-Optics of SPPs.

In particular, we analyze the range of parameters (defect size and number) for which high SPP reflection efficiency (low radiative losses and negligible SPP transmission) is achieved within a SPP band gap [3, 4], neglecting ohmic losses (justified for array lengths significantly shorter than the SPP inelastic length): Smaller defects play better as SPP mirrors (e.g., efficiency above 90% for Gaussian ridges/grooves with sub-30 nm height and half-width) than larger defects, since the latter yield significant radiative losses [3]. The impact of absorption in real metals on the efficiencies is discussed. Finally, the existence of localized states within the gap (of interest in resonant scattering or filtering) is studied upon introducing vacant sites, anomalous defects, etc.).

REFERENCES

1. Sánchez-Gil, J. A. and A. A. Maradudin, *Opt. Lett.*, 28, 2255, 2003.
2. Sánchez-Gil, J. A. and A. A. Maradudin, *Opt. Express*, 12, 883, 2004.
3. Sánchez-Gil, J. A. and A. A. Maradudin, *Appl. Phys. Lett.*, 86, 251106, 2005.
4. Kretschman, M., T. A. Leskova, and A. A. Maradudin, *Opt. Commun.*, 215, 205, 2004.

How Light Emerges from an Illuminated Finite Array of Subwavelength Holes

L. Martín-Moreno[1], **A. Degiron**[2,4], **F. Przybilla**[2], **C. Genet**[2], **J. Bravo-Abad**[3]
F. J. Garcia-Vidal[3], **and T. W. Ebbesen**[2]

[1]Universidad de Zaragoza-CSIC, Spain
[2]Universite Louis Pasteur, France
[3]Universidad Autónoma de Madrid, Spain
[4]Duke University, USA

The extraordinary optical transmission (EOT) through periodic arrays has been extensively studied both experimental and theoretically since its discovery. However, to the best of our knowledge, all theoretical studies have concentrated on the case of an infinite array. By combining experiment and theory, we have analyzed the influence of the inherent finite size of the arrays. We find an unexpected spatial distribution of transmitted light which is both strongly anisotropic and extremely sensitive to the angle of incidence of the impinging light. This behaviour is explained by a simple model that takes into account the edges of the array and its effect on the emission pattern.

Experimental Realization of a Low Profile Metallic Bull's-Eye Antenna

M. B. Diaz
Universidad Pública de Navarra, Spain

The very promising results, reported at optical wavelengths, of enhanced transmission phenomena through subwavelength apertures in corrugated metallic films and in hole arrays have stimulated the interest in this emergent research topic [1,2]. For the case of optical wavelengths, one-dimensional arrays of very narrow slits have been theoretically analyzed and two types of transmission resonances were predicted [3,4], coupled surface plasmon polariton (SPP) resonances and slit waveguide modes. Corrugated planes are well known for antenna engineers, but it has been recently demonstrated that the enhanced optical transmission phenomenon can be fully described by means of the excitation of a leaky mode, being in this case a leaky plasmon mode [5,6]. This leaky mode enhances the aperture field at the entrance face, and also creates a narrow-beam pattern at the output region. By using reciprocity principle, it is shown that the two enhancement effects are equal. A microwave scaled version of these experiments can drive to new potential applications. In this work, a further step of these concepts that opens potential applications for very low profile feeder antennas is presented. Simulation as well as experimental results of a low profile metallic Bull's-Eye antenna are shown envisaging their potential application in communication systems. These structures can be considered as a kind of metamaterial where enhanced transmission and beaming is possible.

Transmission of Light through a Thin Metal Film with Periodically and Randomly Corrugated Surfaces

B. Baumeier, **T. A. Leskova**, **and A. A. Maradudin**
University of California, USA

We calculate the transmission of p- and s-polarized light, incident normally from vacuum, through a thin metal film deposited on a semi-infinite dielectric substrate. The vacuum-metal and metaldielectric interfaces are one-dimensional rough interfaces defined by $x_3 = -\zeta(x_1)$ and $x_3 = -H + \zeta(x_1)$, respectively, where the function $\zeta(x_1)$ has the form $\zeta(x_1) = d \sum_{n=-\infty}^{\infty} \exp[-(x_1 - nb - d_n b)^2/a^2]$, with $0 \leq d \leq H/2$. In this expression the $\{d_n\}$ are independent, identically distributed random deviates drawn from a uniform distribution. By means of a rigorous numerical approach the transmissivity of a single realization of the film is calculated as a function of the wavelength of the incident light, the amplitude d, and the width of the distribution from which the $\{d_n\}$ are drawn. Results for silver and gold films show that in comparison with the transmissivity of a film with planar surfaces ($d = 0$), the transmissivity is strongly enhanced in the case of a film with a periodically modulated thickness ($d_n \equiv 0$) for light of both p and s polarization even for moderate values of $d\,(= 0.2\,\mathrm{H})$. In the case of p polarization the transmissivity is further enhanced at the wavelengths of the surface plasmon polaritons supported by the scattering system. The enhancement of the transmissivity for both polarizations of the incident light is further increased as the amplitude d is increased up to $d = 0.4\,\mathrm{H}$. In the presence of nonzero randomness in the function $\zeta(x_1)$ the enhancement of the transmissivity in both polarizations is decreased for a given value of d from its value in the absence of the randomness, but a significant enhancement remains even when d_n is allowed to take values in the interval $(-0.2, 0.2)$. Thus, periodicity is sufficient to produce a significantly enhanced transmissivity, but it is not necessary.

Terahertz Surface-plasmon Polariton Scattering from Semiconductor Groove Arrays: Gap Formation and Switching

M. Kuttge and J. Gómez-Rivas
FOM-Institute for Atomic and Molecular Physics, The Netherlands

J. A. Sánchez-Gil
Instituto de Estructura de la Materia, Spain

We present experimental and theoretical results of terahertz surface plasmon polaritons (SPPs) propagating on gratings structured on semiconductor surfaces. Single-cycle pulses of terahertz radiation, focused on a gap formed by a razor blade closed to the interface, are used to excite SPPs in a broad frequency range. Time-domain measurements are performed by out-coupling the transmitted SPPs to radiated waves in a similar manner. A theoretical framework is presented that allows us to investigate the scattering of terahertz SPPs by arrays of sub-wavelength defects on semiconductors. The formulation is based on the reduced Rayleigh equation resulting upon imposing an impedance boundary condition. The efficient SPP scattering on the semiconductor periodic structure introduces significant dispersion and modifies the SPP propagation, leading to a rich phenomenology.

A stop gap, or a frequency range where SPPs are Bragg reflected, is observed on doped-Si surfaces. This gap depends strongly on the Si doping density and type. The resonant scattering at the edge of the gap reduces the group velocity by more than a factor of 2. The measurements show a good agreement with our numerical calculations [1].

Based on approximate estimations of the SPP gap broadening with temperature in the case of indium antimonide samples with rectangular grooves, numerical calculations are carried out to determine the spectral dependence of all the SPP scattering channels (reflection, transmission, and radiation) in the immediate vicinity of that gap. The thermally-induced SPP switching nearby the lower SPP band edge is investigated as a function of groove parameters (size and number), providing the most suitable configurations. Near-field intensity maps are presented that shed light onto the SPP scattering and switching physical mechanisms [2].

Our experimental results demonstrate indeed SPP switching for deep grooves. Since the above approximation is no longer valid for such groove depth, we make use instead of the formally exact Green's theorem surface integral equations to calculate the spectral dependence of the SPP transmission at different temperatures. Comparisons with experimental results yield good agreement [3].

REFERENCES

1. Gómez-Rivas, J., M. Kuttge, P. H. Bolivar, H. Kurz, and J. A. Sánchez-Gil, *Phys. Rev. Lett.*, 93, 256804, 2004.
2. Sánchez-Gil, J. A. and J. Gómez-Rivas, *Phys. Rev. B (submitted).*
3. Gómez-Rivas, J., J. A. Sánchez-Gil, M. Kuttge, P. H. Bolivar, and H. Kurz, *Appl. Phys. Lett. (submitted).*

Surface Modes in Structured Metal Surfaces

F. J. G. de Abajo[1,2] **and J. J. Sáenz**[3]

[1]Consejo Superior de Investigaciones Científicas, Spain
[2]Donostia International Physics Center (DIPC), Spain
[3]Universidad Autónoma de Madrid, Spain

Surface-bound modes in metamaterials forged by drilling periodic hole arrays in perfect-conductor surfaces will be explored by means of both analytical techniques and numerical solution of Maxwell's equations. It will be shown that these metamaterials cannot be described in general by local, frequency-dependent permittivities and permeabilities for small periods compared to the wavelength, except in certain limiting cases. New related metamaterials are shown to exhibit optical properties that are elucidated in the light of our simple analytical approach.

Refraction of Surface Polaritons by a Surface Lens

B. Baumeier, T. A. Leskova, and A. A. Maradudin
University of California, USA

J. A. Sánchez-Gil
Instituto de Estractura de la Materia, C.S.I.C., Spain

The scattering of surface plasmon polaritons by spatially localized surface defects has been studied both theoretically [1, 2] and experimentally [3]. Such scattering processes lead not only to a reflected surface plasmon polariton but also to radiation of electromagnetic waves into the vacuum above the metal surface on which the surface plasmon polariton propagates. When a surface plasmon polariton propagating along a metal surface impinges at oblique incidence on an extended linear surface defect such as a linear groove or a ridge on an otherwise planar surface, the translational invariance along the surface structure imposes a conservation law on the tangential components of the wave vectors of all waves excited by the interaction of the surface plasmon polariton with the structure, namely the reflected and transmitted surface plasmon polaritons as well as the radiated bulk waves. This is Snells law for surface plasmon polaritons. When the surface defect is formed from a different material, e.g., a dielectric film, so that in the region of the defect the surface plasmon polariton has a different wavenumber, the surface polariton is refracted at the boundary of the defect. In the present work we consider the transformation of surface plasmon polaritons at surface structures that are formed by a film on a planar (or corrugated) metal surface. In particular we are interested in the case where the boundary between the clean metal surface and the film is a parabola, for which the surface profile function is given by $\zeta(x_1, x_2) = d\theta(x_1 - ax_2^2)\theta(x_1)$, where $\theta(z)$ is the Heaviside unit step function, and d is the thickness of the film, and the case where the film has an elliptic shape for which $\zeta(x_1, x_2) = d\theta(1 - (x_1/a)^2 - (x_2/b)^2)$. The refraction of surface polaritons at the boundary of such structures on a metal surface leads to a focusing of the transmitted surface waves. The reduced Rayleigh equations for a vacuum/film/metal system with two two-dimensional rough interfaces are derived and solved numerically. The parameters of surface defects allowing an efficient focusing of surface plasmon polaritons are determined.

REFERENCES

1. Sánchez-Gil, J. A., *Appl. Phys. Lett.*, Vol. 73, 3509, 1998.
2. Shchegrov, A. V., I. V. Novikov, and A. A. Maradudin, *Phys. Rev. Lett.*, Vol. 78, 4269, 1997.
3. Okamoto, T., K. Kakutani, T. Yoshizaki, M. Haraguchi, and M. Fukui, *Surface Science*, Vol. 544, 67, 2003.

Session 2P3
Physics Based and Statistical Methods in Subsurface Imaging

A Novel Modeling and Inversion Method to Image Weakly Scattering Sub-cellular Structure

E. Karbeyaz and C. Rappaport
Northeastern University, USA

Non-invasive assessment of the health of an embryo or a single cell is an open issue of critical importance for the success of certain procedures like in vitro fertilization. To achieve this goal, we need a three dimensional understanding of the investigated structure, such as how mitochondria are distributed within the cell, or how many cells reside in the embryo. Advanced microscopy can provide both amplitude and phase information from multiple views, but obtaining detailed volumetric information is challenging. In particular, imaging mitochondria is usually quite difficult since there may be 100,000 of these tiny low-contrast scatterers overlapping each other within the cell.

Although the electromagnetic properties of cellular structures exhibit slight variations relative to the background, methods based on the Born approximation are not suitable to image these objects since their overall electrical sizes are quite large when they are probed in or near the visible spectrum, and the observed scattered light is in the farfield of the cell.

In this work, we present a novel method to image these objects in two dimensions, which is based on the expansion of the target object function in terms of Fourier-Bessel coefficients, and an alternative approximation for the total fields within the scatterer. This approximation satisfies the continuity of the total tangential fields at the object-background boundary for each circular mode using the known incident and observed scattered fields, and takes into account the fact that the refractive index distribution along structures being investigated varies slightly around a known mean value. The resulting linear system of equations is solved via Tikhonov regularization for the unknown expansion coefficients. This approach can be readily extended to more realistic 3D cases.

To illustrate the method, a number of Finite-Difference Time-Domain (FDTD) simulations involving cells models with miscellaneous organelle distributions, such as aggregated, perinuclear, cortical mitochondria distributions, have been performed. Basic ideas of the FDTD method, such as total-field scattered-field formulation, near to far field transform, PML absorbing boundary condition have been employed to obtain the far zone scattered fields due to the cell models under plane wave illumination. These far zone scattered fields have been utilized to form the image of the probed objects. Remarkably accurate reconstructions of the general density distribution of the subcellular structure have been obtained.

The Effective Permittivity of Inhomogeneous Objects Reconstructed by Inverse Scattering Methods

N. V. Budko and R. F. Remis
Delft University of Technology, The Netherlands

The notion of effective permittivity originates from the effective medium theory (EMT), where a medium randomly inhomogeneous on a micro-scale is represented as a homogeneous bulk material. There exist many different formulas that give the effective permittivity in terms of the permittivities, sizes, and shapes of the microscopic constituents. Normally one tries to find an expression which would suit all possible illumination and measurement conditions. The problem is, in fact, an inverse scattering problem, and as such can be investigated using the standard inversion methodology. In particular, we have looked at it in the context of *effective inversion*, i. e. inversion with very limited scattered field data where it is impossible to reconstruct an inhomogeneous subsurface target, but may be possible to recover its effective permittivity having an approximate knowledge of the outer shape of the object. That latter shape is often the result of simple linearized imaging algorithms, such as the travel-time tomography and the sampling method. The difference with the EMT is that, strictly speaking, the reconstructed effective permittivity suits only some particular illumination and measurement configuration. Yet our results indicate that the reconstructed effective permittivities are closely related to the permittivities of the constituents. On the other hand, the inverse scattering approach is much more rigorous as far as the reconstruction of the effective permittivity is concerned, than the general but approximate techniques of the EMT. For example, no statistical assumptions are needed and the inhomogeneities do not have to be electrically small.

This time we shall talk about a very fast and efficient numerical method specifically designed for the effective inversion problem. As common in inverse scattering, the problem is nonlinear and therefore requires repetitive solution of the associated forward scattering problem. In its turn the forward problem has to be solved by one or another iterative algorithm. Hence, the solution of the inverse problem requires multiple runs of an iterative scheme. Most of the work in such a scheme is done at the stage of construction of the so-called Krylov subspace. In the effective inversion case, however, the once constructed Krylov subspace can be re-used, thereby significantly reducing the computational order of the inverse problem. With the help of this reduced-order algorithm various inhomogeneous targets can be analyzed with little computational effort. Special attention will be paid to the dispersion of the reconstructed effective permittivity.

Neural Networks as Statistical Indicator of Breast Cancer Using Scattered Electromagnetic Data

P. Rashidi, D. Woten, J. Lusth, and M. El-Shenawee
University of Arkansas, USA

In this work we will present the application of neural networks as a preprocessor in breast cancer imaging. In our previous work on imaging breast cancer using microwave modality, we observed that the reconstruction of shape and location of three-dimensional tumor required several CPU hours on a Hewlett-Packard Alpha Server DS25. We are proposing to avoid the high computational expenses of these algorithms by initially processing the data using neural networks, which have been used recently in predicting breast cancer based on mammography or magnetic resonance imaging data. In these applications, the neural network was used to replace radiologists or physicians interpretations. The major advantage of using neural networks lies in its real time results. We are proposing to train neural networks on data based on scattered electromagnetic fields from the breast with and without a tumor. The basic idea is to train the neural network on synthetic data and then test it on different data with added noise. The neural network will statistically indicate the presence or absence of a tumor. In case of a suspicious abnormality in the breast, our three-dimensional imaging algorithm will be used to reconstruct the tumor.

Our preliminary results show that when neural networks were trained with a reasonable amount of noise, they successfully predicted the cancer. In determining the utility of a neural network, the systematic approach espoused by Goodman was taken. First, a logistic regression model was constructed. After determining the linear weights for one set of synthetic data (fifty samples without a tumor, ten with), the model was tested on a second similar, but independent, set. Based upon the performance of the model on the new data, a non-linear model was indicated. The choice for a non-linear model was a single-hidden-layer neural network with full interconnections between layers. Experiments showed that the network's hidden layer could be composed of as few as two nodes and still achieve perfect prediction on the independent set. Moreover, training the network on the second set and testing on the original achieved the same result. Finally, an inferential analysis of a network trained on the combined data sets will be performed to yield the most important linear and non-linear aspects of the imaging data.

Some New Results for Shape Reconstruction in 3D Low-frequency Electromagnetic Induction Tomography Using Level Sets

O. Dorn
Universidad Carlos III de Madrid, Spain

Recently the application of low-frequency electromagnetic fields has been discussed for probing geophysical test sites over distances of up to several hundred metres. This can be used for example in petroleum engineering for characterizing a reservoir, or in environmental imaging applications for tracking pollutant plumes above the ground-water table. The mathematical treatment of these problems is quite challenging since 2D approximations typically yield only very poor results, and the problems are furthermore severely ill-posed. Therefore, the problems need to be treated as fully 3Dinversion problems from relatively few data for the system of Maxwells equations. We will present and discuss some new developments for a shape reconstruction approach which is able to reconstruct in a stable way geophysical structures from few low-frequency electromagnetic data. The method is based on an artificial evolution of a level set function characterizing the unknown shapes. Numerical examples in 3D are presented for shape reconstructions from synthetically created data with different types of noise added.

Single Value Decomposition and Degree-of-ill-posedness Assessment in Microwave Imaging

P. M. Meaney, Q. Q. Fang, and K. D. Paulsen
Dartmouth College, USA

In all Gauss-Newton iterative microwave imaging scenarios, there are a number of parameters related to the overall configuration that can impact the resultant image quality. These include signal frequency, amount of measurement data, number of property parameters reconstructed, etc. Overall, the four most important constituents comprising the system and algorithms are the measurement data, accurate forward solution, parameter update and the sensitivity map in the form of the Jacobian matrix. The latter encodes rich information regarding system performance and algorithm efficiency.

In this presentation we explore the singular value decomposition (SVD) of the Jacobian matrix and adopt the notion of degree-of-ill-posedness, α [1], developed by Brander and DeFacio [2] for the inverse Born approximation. While these previous discussions were developed for analytical expressions of the Jacobian matrix, we have applied minor approximations to our standard imaging algorithms to generate the numerically-based nodal-adjoint expression for constructing the Jacobian matrix [3]. This has facilitated convenient computation of the degree-of-ill-posedness for multiple system parameter studies. We have also applied this only to the first iteration of the Jacobian matrix to simplify the overall discussion while being able to observe important trends with respect to parameter variation. We have also restricted this analysis to a circular antenna array geometry with the single point sources configured close to the target under investigation.

We have studied three important algorithm parameters in simulation which have important implications with respect to hardware implementation and overall system performance: signal frequency, amount of measurement data and number of property parameters reconstructed. In general, the results match previous intuitive notions; i.e., that increased frequency and increased measurement data improve α. However the results with respect to the number of inverse parameters are somewhat counter-intuitive in that α improves even well after the number of parameters has exceeded the amount of independent measurements ($\mathrm{N_{sources}} \times \mathrm{N_{receivers}}/2$). Historically, groups have worked to collect more independent data than parameters reconstructed at considerable system expense. This latter result confirms observations we have made with our microwave system in both phantom and clinical imaging sessions and also for the near infrared imaging system being developed at Dartmouth College [4, 5]. These analyses have provided important insights as we work toward robust clinical implementation.

*This work was supported by NIH/NCI grant # R01 CA80139.

REFERENCES

1. Hansen, P. C., "Rank-deficient and discrete ill-posed problems: numerical aspects of linear inversion," SIAM, Philadelphia, 1997.
2. Brander, O. and B. DeFacio, "The role of filters and the singular value decomposition for the inverse Born approximation," *Inverse Problems*, Vol. 2, 375–393, 1986.
3. Fang, Q, P. M. Meaney, and K. D. Paulsen, "Singular value analysis of the Jacobian matrix in microwave image reconstructions," *IEEE Trans. Ant. Propag.*, 2005 (submitted).
4. Meaney, P. M., Q. Fang, et al., "Microwave breast imaging with an under-determined reconstruction parameter mesh," *IEEE Int. Symp. Biomedical Imaging*, Arlington, VA, 1369–1372, 2004.
5. Poplack, S. P., K. D. Paulsen, et al., "Electromagnetic breast imaging C average tissue property values in women with negative clinical findings," *Radiology*, Vol. 231, 571–580, 2004.

Radar Detection of Subsurface Objects Using Correlation Imaging

S. Matzner[1], **L. M. Zurk**[1], **and A. I. Timchenko**[2]

[1]Portland State University, USA
[2]National Academy of Sciences of Ukraine, Ukraine

The radar detection of objects below a rough surface is an active area of research motivated by the problem of detecting shallowly buried land mines. The primary challenge for this approach is the extremely low signal-to-noise ratio between the return from the buried object and the reflected return from the rough surface. The weakness of the former is due to the low dielectric contrast between the buried object and the enclosing soil, as well as the lossiness of the soil medium. The strength of the latter is due to the random roughness of the surface. In this work, correlation imaging is employed to separate the return from the rough surface from that originating from the object by correlating radar measurements made at multiple angles. We incorporate a probabilistic weighting function (filter) to further enhance the effectiveness of correlation imaging, taking into account the random phase variation of the buried object return due to the rough surface.

The electromagnetic scattering is computed using a dyadic Greens function which describes the scattering from a half-space medium with planar boundary, and spherical objects embedded below this boundary. An approximate solution is obtained using a perturbation technique to yield expressions for the scattered field as a function of the viewing geometry (incident and scattering angles), object placement, and soil dielectric properties. The rough surface height variation is assumed to have a Gaussian distribution.

To evaluate the effectiveness of the correlation processing, we simulate the response of a monostatic Synthetic Aperture Radar with a linear viewing geometry that illuminates each ground patch from different angles. The samples from each patch are then used to measure the correlation:

$$C(\vec{r}_p) = \sum_{m=1}^{N} \sum_{n=1}^{N} E_p(\vec{k}_m) E_p^*(\vec{k}_n) e^{2i(\vec{k}_n - \vec{k}_m)} W(\vec{k}_m, \vec{k}_n)$$

where $\vec{r}_p$ is the patch location, N is the number of radar positions, $E_p(\vec{k}_m)$ is the electrical field received from the pth patch due to excitation from the mth source position, and $W(\vec{k}_m, \vec{k}_n)$ is the weighting function.

Our previous results showed that this approach was effective at reducing the clutter to allow detection of buried objects when the modeled scattering response is computed to first order. In this work, we extend the scattering model to consider second order scattering terms so that the return from the buried object after scattering from the random surface is taken into account. This term contains small variations in both the magnitude and the phase of the buried object return, and reduces the correlation between independent measurements. To compensate for this, a new weighting function is applied based on the assumed statistical properties of the rough surface. For a Gaussian surface, the weighting function has a normally distributed phase term that is centered at the assumed object depth, z_0. Results are presented that show the robustness of this approach to inaccuracies in the assumed depth and the width (σ) of the probability distribution.

Statistical and Adaptive Signal Processing for UXO Discrimination for Next-generation Sensor Data

S. L. Tantum, Y. Q. Wang, and L. M. Collins
Duke University, USA

Until recently, detection algorithms could not reliably distinguish between buried UXO and clutter, leading to many false alarms. Over the last several years modern geophysical techniques have been developed that merge more sophisticated sensors, underlying physical models, statistical signal processing algorithms, and adaptive training techniques. These new approaches have dramatically reduced false alarm rates, although for the most part they have been applied to data collected at sites with relatively benign topology and anomaly densities. On more challenging sites, performance of even these more modern discrimination approaches is still quite poor. As a result, efforts are underway to develop a new generation of UXO sensors that will produce data streams of multi-axis vector or gradiometric measurements, for which optimal processing has not yet been carefully considered or developed. We describe a research program to address this processing gap, employing a synergistic use of advanced phenomenological-modeling and signal-processing algorithms. The key foci of the program are (1) development of new physics-based signal processing approaches applicable to the problem in which vector data is available from such sensors; and (2) development of the theory of optimal experiments to guide the optimal design and deployment of the new sensor modalities. Here, we present initial results using simulated data obtained with our phenomenological models that indicate that optimal processing of features extracted from multi-axis EMI data can provide substantial improvements in discrimination performance over processing of features extracted from single-axis data. This research was supported by the Strategic Environmental Research and Development Program (SERDP) under project UX-1442.

A Lossy Half-space Green's Function Forward Model and Inversion Method for Geophysics Problem

H. Zhan, **C. Rappaport**, **M. Farid**, and **E. L. Miller**
Northeastern University, USA

Sensing and detection of dense non-aqueous phase liquids (DNAPLs) in soil is very significant and beneficiary for geo-environmental engineering, but challenging due to uncertain and hard to determine wave characteristics through soil media. The detection task may be possible by discriminating dielectric property contrast between DNAPL pools and saturated soil background. Despite least invasiveness of ground penetration radar (GPR), but due to its depth limitations, other alternatives should be implemented to detect DNAPLs. Sensing the subsurface volume between boreholes using cross-well radar (CWR) is an innovative and non-invasive technique, which is effective for deep investigations.

In this work, an analytical model is developed to approximate CWR sensing in infinite half-space lossy media in the frequency domain. Half-space dyadic Green's function in integral form for a vertical polarized dipole source is derived. Integration for angles goes far into evanescent range. To analyze the reflection behavior of a spherical wave onto a planar interface at oblique angle, plane wave decomposition technique is used to replace the spherical wave with a collection of all modes of plane waves. Fresnel reflection theory is utilized to investigate each plane wave reflection due to the planer interface. The Born approximation is employed as a linear model for a shape-based inversion, developed to localize the object. This localization is possible assuming the contrast between the clutter and lossy background as a priori information.

The forward model is validated via CWR experiment. Soil parameters (relative dielectric constant, and loss tangent) variance with frequency is approximated with a quadratic polynomial. Calibration of soil parameters is conducted comparing the results with experimental CWR data, using an iterative low-order parameterized optimization technique that involves both magnitude and phase information. Forward model and CWR experimentation results agree well over broad frequency range. Localization and reconstruction of the object is implemented using non-linear least square optimization by minimizing a cost function that calculates the misfit between the predicted numerical simulation and experimental observation. The proposed inversion method generates satisfying preliminary results, which are validated by numerical experiments.

Optimal Ultrasonic Surface Displacement and Velocity Estimation in the Presence of Surface Roughness

P. Ratilal, N. Donabed, and C. Rappaport
Northeastern University, USA

D. Fenneman
US Army RDECOM CERDEC Night Vision and Electron., USA

An analytic model is developed for the ultrasound field reflected off a moving surface in the presence of random surface roughness for an ultrasonic displacement sensing system in bistatic configuration. The model incorporates the beampattern of both the source and receiver ultrasound transducers as well as spectrum of the rough surface. Conventional approaches for estimating surface displacement and velocity amplitudes based on the laser vibrometer, such as coherent interferometry and incoherent doppler shift spectra, are applied to the ultrasound system. Simulation with the model indicates that surface displacement and velocity estimation is highly dependent upon measurement geometry such as the area of surface insonified and angle of incidence of the system, height and correlation length scales of the rough surface, and frequency and duration of the ultrasound pulse. The model is then applied to determine an optimal measurement scheme for the ultrasound displacement sensor in land-mine confirmation.

One-dimensional Inverse Scattering: Localization of Planar Interface

R. Barresi, **G. Leone**, and **R. Solimene**
Università degli Studi Maediterranea di Reggio Calabria, Italy

The problem of localization of a planar interface in a layered medium from the knowledge of the scattered electromagnetic field is set as an inverse problem within the frequency domain.

This problem has practical interest in many disciplines, as civil engineering and geophysics, because in many applications the subsurface can be considered as a planarly layered medium and the unknown position of interfaces are to be determined. In particular, in civil engineering, an important application is the localization and the determination of the depth of voids embedded in masonries of ancient buildings. Other promising applications concern the assessment of the widths of asphalts or the evaluation of the position of metal inclusions, e.g., sheets or fine meshes reinforcement. In geophysics, the determination of underground stratification is very important.

The problem is often considered in time domain by the search for successive reflections within received reflected field; however sometimes, because of the finite available bandwidth, later reflections due to deeper interfaces are 'buried' by oscillations of earlier responses. We choose to deal with the problem in the frequency domain and found that multiple reflections allow to improve the resolution in the localization. In the formulation we assumed that the dielectric properties of the layered medium are known.

Consider first the localization of a single interface within a layered medium. Since the relation between the scattered field and the position of the unknown interface is non linear; we reformulate the problem by introducing a Dirac distribution [1] centred on the unknown position and derive a linear operator linking such an unknown distribution to the scattered electric field. Next, we invert this operator by the Singular Value Decomposition (SVD) and use the truncated SVD (TSVD) as regularizing algorithm.

In the case of two-layered media, the operator to be inverted is a finite Fourier transform with limited data whose SVD has been well studied and is known in closed form. The resolution [1] is independent of the threshold of truncation of the SVD, that is of the uncertainties on data, due to the typical step-like behaviour of the singular values.

In the case of a three-layered lossless medium, in the search for the second interface, the operator can be recast as the summation of an infinite number of Fourier transforms in correspondence of successive bouncing of the waves inside the layer and a numerical investigation of the SVD of the relevant operator shows the curve of the singular values as successive steps corresponding to each reflection. When only the first two contributions are taken into account [2], an analytical estimate can be performed in some circumstances. The main results is that the achievable resolution can be improved with respect to the single interface case, according to the available uncertainty level on data.

Numerical experiments confirm the main conclusions. In addition the approach has been successfully employed to experimental data, in order to find the position and the width of a void layer inside a masonry of tuff. A procedure amounting to iteratively locating successive interfaces has been established. Calibration data collected in reference geometries make it available the scattered field at each step needed for the inversion.

REFERENCES

1. Pierri, R., A. Liseno, and F. Soldovieri, "Shape reconstruction from PO multi-frequency scattered fields via the singular value decomposition approach," *IEEE Trans. on Antennas and Propagat.*, Vol. AP-49, No. 9, 1333–1343, Sept. 2001.
2. Solimene, R. and R. Pierri, "Localization of a planar perfect-electric-conducting interface embedded in a half-space," in print on *Journal of Optics A: Pure and Applied Optics*.

A Unified Surface Source Model for Discrimination of Subsurface Metallic Objects by Magnetometry and UWB Electromagnetic Induction

F. Shubitidze[1], K. O'Neill[1,2], S. Billings[3], L. Pasion[3], and D. Oldenburg[4]

[1]Dartmouth College, USA
[2]USA ERDC Cold Regions, Research and Engineering Lab, USA
[3]Sky Research Inc., USA
[4]UBC Geophysical Inversion Facility, Canada

Clean up of land and water from subsurface metallic objects, particularly unexploded ordnance, still remains the number one military environmental problem. This process requires two steps: first a signal from a metallic object has to be detected and second, from the detected signal the object of interest must be distinguished from widespread pieces of metallic clutter. Recent studies have shown that magnetic and time or frequency domain electromagnetic induction (EMI) sensing technologies are the most promising approaches for UXO detection. In EMI the practical depth of penetration of the target by EMI signals is determined by the input frequency and target's conductivity and permeability. Signal clutter due to the dielectric heterogeneity of the surrounding environments or other non-metal material is negligible. Since, most if not all UXOs are metal, or contain substantial amounts of metals, they can easily be detected, but it is extremely difficult to discriminate them reliable from non-hazardous items. In order to overcome the discrimination problem, joint and cooperative (typically magnetic and EMI) approaches have been proposed. In these approaches magnetic and EM forward models have different parameterizations. Therefore when attempting joint or cooperative inversions, constraints imposed by one data set (for example magnetic) on the other (EM) is partially active — because of forward models.

In order to use all information obtained from each data set, this paper presents a unified source model applicable for any combination of magnetic and frequency or time domain EM data, for any sensor configuration and for any input waveform. In this approach, the EMI field from a given object is generated by a reduced set of surface sources: magnetic charges for a dry soil (free space approximation) or magnetic dipoles for relatively high conductivity host media such as seawater. These sources are distributed on a fictitious spheroid, which surrounds the object. First an input primary magnetic field is decomposed into fundamental spheroidal modes. Then, for each input spheroidal mode, a full low frequency EMI problem is solved via the method of auxiliary sources. Finally, for efficiency the EMI responses are reproduced by the reduced (few) set of sources, which is stored inside a library. Once all these processes are completed the full EMI problem for any transmitter/receiver can be easily solved by carrying out a spheroidal decomposition of the primary field and simply superposing the stored modal solutions. In time domain cases the EMI responses from the reduced set of sources are generated from frequency data for different waveforms using the inverse Fourier transform. In this paper, the first comparisons between the proposed model and real data in time and frequency domains will be presented and demonstrated for different waveforms. Finally, the method will be applied to the UXO discrimination problem.

Session 2P4
Neural Network and/or Remote Sensing Inversion Problems

Neural Networks for Satellite-Based Estimation of Precipitation

F. W. Chen
MIT Lincoln Laboratory, USA

This presentation provides an overview on the use of neural networks in precipitation estimation.

Neural networks provide a useful method for learning mathematical relationships using a representative sample of data. These are especially useful in situations where the relationships between variables are extremely complicated and simulations based on physical models are inadequate or computationally expensive.

Approaches to precipitation estimation can be classified into two groups: model-based and statistics-based. Model-based methods involve tuning parameters to match observations and then using the parameters to obtain precipitation rate. Statistics-based methods correlate brightness temperature observations with ground truth measurements. The physics of precipitation is extremely complicated and existing physical models do not adequately capture all of the variation of precipitation. Moreover, repeatedly running radiative transfer calculations can take a lot of time while neural net computations are much simpler.

Chen and Staelin (IEEE Trans. Geosci. Remote Sensing, 41(2), 2003) have developed a method for estimating precipitation using the passive microwave radiometer AMSU-A/B (Advanced Microwave Sounding Unit) aboard the NOAA-15, NOAA-16, and NOAA-17 satellites. The method applies spatial filtering and signal separation to extract information relevant to precipitation. The outputs of this signal processing component are then fed to a neural network. This method was trained using data from the NEXRAD ground-based radar network as ground truth and shows reasonably good agreement at 15-km resolution.

*This work was sponsored by the National Oceanographic and Atmospheric Administration under Air Force contract FA8721-05-C-0002. Opinions, interpretations, conclusions, and recommendations are those of the author and not necessarily endorsed by the United States Government.

Neural Network Retrievals of Atmospheric Temperature and Moisture Profiles from High-resolution Infrared and Microwave Sounding Data

W. J. Blackwell
Massachusetts Institute of Technology, USA

A novel statistical method for the retrieval of atmospheric temperature and moisture (relative humidity) profiles has been developed and evaluated with sounding data from the Atmospheric InfraRed Sounder (AIRS) and the Advanced Microwave Sounding Unit (AMSU). The algorithm is implemented in three stages. First, the infrared radiance perturbations due to clouds are estimated and corrected by combined processing of the infrared and microwave data. Second, a Projected Principal Components (PPC) transform is used to reduce the dimensionality of and optimally extract geophysical profile information from the cloud-cleared infrared radiance data. Third, an artificial feedforward neural network is used to estimate the desired geophysical parameters from the projected principal components.

The cloud-clearing of the infrared radiances was performed by the AIRS Science Team using infrared brightness temperature contrasts in adjacent fields of view and microwave-derived estimates of the infrared clear-column radiances to estimate and correct the radiance contamination introduced by clouds. The PPC compression technique was used to reduce the infrared radiance dimensionality by a factor of 100, while retaining over 99.99% of the radiance variance that is correlated to the geophysical profiles. This compression allows the use of smaller, faster, and more robust estimators. A single-layer feedforward neural network with approximately 3000 degrees of freedom was then used to estimate the geophysical profiles at approximately 60 levels from the surface to 20 km.

The performance of this method (henceforth referred to as the PPC/NN method) was evaluated using global (ascending and descending) EOS-Aqua orbits co-located with ECMWF fields for a variety of days throughout 2003 and 2004. Over 350,000 fields of regard (3×3 arrays of footprints) over ocean and land were used in the study. Retrieval performance compares favorably with that obtained with simulated observations from the NOAA88b radiosonde set of approximately 7500 profiles. The PPC/NN method requires significantly less computation than traditional variational retrieval methods, while achieving comparable performance.

*This work was sponsored by the National Oceanic and Atmospheric Administration under Air Force contract FA8721-05-C-0002. Opinions, interpretations, conclusions, and recommendations are those of the author and not necessarily endorsed by the United States Government.

Ozone Profiles Retrieval: Intercomparison between Neural Networks Inversion and Other Estimation Techniques

M. Iapaolo[1], **F. Del Frate**[1], **and S. Casadio**[2]

[1]Università di Roma Tor Vergata, Italy
[2]Karl Franzens University of Graz, Italy

The Global Ozone Monitoring Experiment (GOME) is a nadir-viewing broadband spectrometer (240–790 nm) of moderate resolution (0.2–0.4 nm) on board the European ERS-2 spacecraft which has been operational since mid 1995. Its measurements allow the retrieval of global distributions of ozone and a number of chemically associated atmospheric trace gases, such as NO_2, BrO, $HCHO$, $OClO$ and SO_2. GOME is the first in a series of European space-borne ozone monitoring instruments; it has been followed by the SCanning Imaging Absorption spectroMeter for Atmospheric CHartographY (SCIAMACHY) on Envisat (2002) and by the Ozone Monitoring Instrument (OMI) on EOS-Aura satellite (2004), and it will be continued by GOME-2 series on the EUMETSAT Metop-1, 2, 3 satellites, planned to be launched in 2006.

Most important for climate and environmental application is the retrieval of vertical ozone profiles, which yield pertinent information on the ozone distribution in the stratosphere and the upper troposphere exploiting the spectral information of the Hartley and Huggins bands in the UV range. Recently, a retrieval methodology based on neural networks (NNs) has been proposed; such a technique is very attractive for its capability to provide a real-time accurate solution of the inversion problem, as required to process the huge volume of data that characterize the continuous observation of the atmosphere from a satellite platform. In this study all GOME spectral measurements from July 1995 to June 2003 have been successfully processed. The effectiveness of the retrieval algorithm has been tested, and the accuracy of the retrieved ozone profiles has been evaluated performing an extended inter-comparison with similar products provided by other instruments and inversion techniques. The Improved Limb Atmospheric Spectrometer (ILAS), a limb-scanning instrument boarded on the Japanese satellite ADEOS, and a series of lidar stations belonging to the Network for Detection of Stratospheric Changes (NDSC) have been considered in this work. Tropical, mid-latitude and high-latitude regions have been considered during the inter-comparison, either in the Northern or in the Southern Hemisphere, and the results have been critically analized.

Application of Artificial Neural Networks and Genetic Algorithms to the Retrieval of Snow Parameters from Passive Microwave Remote Sensing Data

M. Tedesco[1,2] **and E. J. Kim**[2]

[1]University of Maryland Baltimore County, USA
[2]NASA Goddard Space Flight Center, USA

Monitoring the quantity, distribution and dry/wet state of snow provides vital information for applications such as weather and natural hazards forecasting, use of water resources for domestic and hydropower applications.

The retrieval of snow parameters from microwave remote sensing data is based on the inversion of relationships between the snow parameters and electromagnetic quantities. It is rarely possible to perform this inversion in a strictly analytical way and numerical techniques are often used. In some cases, the problem of inverting these relationships is solved by using a linear regression between the snow parameter of interest and a combination of electromagnetic quantities (e.g., Chang's algorithm for the retrieval of SWE). In other cases, iterative techniques based on the solution of the radiative transfer equation can be used (e.g., the HUT iterative inversion technique).

Numerical techniques such as Artificial Neural Networks (ANN) and Genetic Algorithms (GA) can also be used for the inversion of the radiative transfer equations. In this study we separately evaluate the capabilities of both ANN- and GA-based techniques to retrieve snow parameters from space-borne brightness temperatures at 19 and 37 GHz collected by the SSM/I and/or AMSR-E radiometers, with particular emphasis on snow depth. The two techniques are applied to different datasets collected over different areas and the results are compared with ground measurements. We also evaluate the advantages and disadvantages of the two techniques in terms of computational time and potential applications to retrievals of snow parameters close for near-real-time applications. We compare the performances of the ANN- and GA-based techniques with those of the most well known algorithms described in the literature: Chang's algorithm, the Helsinki University of Technology iterative algorithm and the Spectral Polarization Difference algorithm.

On the Robustness of Neural Network Algorithms for Oil Spill Detection

E. Angiuli, F. Del Frate, S. Di Giosia, and L. Salvatori
Università Tor Vergata, Italy

In this paper we present the potentialities of Neural Network algorithms for detection of oil spill. Previous works have demonstrated how neural networks are a valid instrument for this type of analysis. In fact, an artificial neural network (NN) may be viewed as a mathematical model composed of many nonlinear computational elements, named neurons, operating in parallel and massively connected by links characterized by different weights. This particular structure makes neural networks very stable and robust when there are sensible input variations. For this study, multilayer perceptrons (MPL) have been considered, which have been found to have a suited topology for classification and inversion problems. The network input is a vector containing the values of a set of features characterizing an oil spill candidate. The output is a value, included between 0 and 1, representing the probability that the candidate is an oil slick. The classification performance has been evaluated on a data set of ERS-SAR and Envisat-ASAR images containing examples of oil spills and look-alikes. To test the robustness of the algorithm, we have grouped all the collected examples into different subsets considering two main factors: the different SAR instrument (ERS-SAR or Envisat-ASAR) and the natural noise characterizing the image. For this latter case the standard deviation of the backscattering values of the sea surface has been considered as a general noise index. Several nets have been designed using in turn different subsets for the training phase and the performance of each net has been tested on different subsets, either similar or dissimilar to those used in the training. The neural algorithm gives generally satisfactory results, however the performance is clearly affected by the type of examples included in the training set. This effect has been investigated throughout a systematic analysis.

Neural Network Ozone Retrieval System for Total Ozone and Ozone Profile Retrieval from Gome Uv/Vis Spectra (Nnorsy-gome)

A. K. Kaifel[1], **M. D. Müller**[2], **and J. Kaptur**[1]

[1]Zentrum für Sonnenenergie-und Wasserstoff-Forschung, Germany
[2]NASA Goddard Space Flight Center, USA

The Neural Network Ozone Retrieval System (NNORSY) was developed during the last years for total ozone and ozone profile retrieval from UV/VIS spectra of ERS-2 GOME and total ozone column retrieval from IR NOAA-TOVS satellite data. Version 1 of NNORSY GOME ozone profile retrieval was implemented for real-time processing of GOME data at the DLR-DFD up to the failure of the tape recorder of ERS-2 in July 2003 ($http : //wdc.dlr.de/data_products/SERVICES/GOMENRT/inde-x.html$). Latest developments for NNORSY-GOME Version 2 yielded further improvements of retrieval accuracy and was applied to the whole GOME data time range in order to generate a more than 9 year global ozone profile data set with high vertical resolution.

For training ozonesonde data are used reaching from ground up to about 25 km and satellite ozone profile measurements from SAGE, HALOE and POAM covering the height range from 60 km down to tropopause height level. This means that the neural network have to deal with incomplete target data during training. Therefore training algorithms have to be developed to handle partial training with incomplete target vector.

This paper first presents the solution we developed for partial training as well as application to ozone profile retrieval from GOME UV/VIS spectra for reprocessing whole GOME level 1 data set ranging from July 1995 to the end of 2004. These yields to a consistent global ozone profile data set stretching from ground up to 60 km height at 1 km sampling rate. Comparison with other independent satellite ozone profile data products (e.g., MLS) as well as extensive geophysical validation against ozonesonde data will also be shown.

NNORSY processing is very fast and resulting GOME ozone profile product has about the same or better accuracy as classical optimal estimation based retrieval schemes which makes NNORSY a candidate for further real-time processing on current or upcoming satellite sensors like OMI on EOS-AURA or GOME-2 on METOP.

Analysis of Urban SAR Data Using Morphological Pre-processing and Neural Networks

J. A. Benediktsson[1], **S. O. Sigurjonsson**[1]
G. Lisini[2], **P. Gamba**[2], **J. Chanussot**[3], **and J. R. Sveinsson**[1]

[1]University of Iceland, Iceland
[2]University of Pavia, Italy
[3]LIS / INPG, France

Classification of high-resolution remote sensing images from urban areas has been addressed in [1] and [2] using two main steps:

- feature extraction based on the construction of a differential morphological profile which characterizes each pixel both in terms of intensity and in terms of local geometry.
- classification based on a neural network (eventually after selection of the most significant features).

In this paper, a further evolution of [1] and [2] is presented and applied in neural network classification of an AIRSAR image of Los Angeles, California. For the feature extraction step, two different approaches are used for the construction of the morphological profile of each pixel: 1) alternating sequential filters (ASF) and 2) the applications of openings and closings with linear structuring elements under varying angles. The effect of using speckle filtering prior to the construction of the morphological profiles is also investigated. In the paper, the maps obtained from the classification of the different morphological profiles are used for classification and street tracking.

From the data, street extraction is made in two steps. The first one is aimed at trying and discarding the "blobs" that do not possess the usual characteristics of the roads such as elongation. This is made by a routine hat tries and associate each "blob" present in the filtered image to a "street prototype" database [4]. If the shape of the blob under test is too different from the ones found in the database, it will be removed from the image. It is possible to remove even only a part of the entire blob that shows too peculiar features. The second step uses modified Hough transform routine [5] for real road extraction.

To evaluate the quality of the extracted street network, quantitative indexes are computed, including the correctness and completeness indexes [5]. Both of them require the knowledge of the true network and provide a means to understand to what extent the extracted networks is similar to the reference one. In particular, completeness represents the fraction of ground truth length extracted while correctness is the fraction of segments' length belonging to actual roads.

REFERENCES

1. Pesaresi, M. and J. A. Benediktsson, "A new approach for the morphological segmentation of high-resolution satellite imagery," *IEEE Transactions on Geosciene and Remote Sensing*, No. 2, 309–321, 2001.
2. Benediktsson, J. A., J. A. Palmason, and J. R. Sveinsson, "Classification of hyperspectral data from urban areas based on extended morphological profiles," *IEEE Transactions on Geoscience and Remote Sensing*, No. 3, 480–491, 2005.
3. Acqua, F. D., P. Gamba, and G. Lisini, "Road map extraction by multipledetectors in fine spatial resolution SAR data," *Canadian J. Remote Sensing*, Vol. 29, No. 4, 481–490, Aug. 2003.
4. Acqua, F. D. and P. Gamba, "Detection of urban structures in SAR images by robust fuzzy clustering algorithms: the example of street tracking," *IEEE Trans. Geosci. Remote Sensing*, Vol. 39, No. 10, 2287–2297, Oct. 2001.
5. Wiedemann, C. and H. Ebner, "Automatic completion and evaluation of road networks," *Int. Arch. Photogramm. Remote Sensing*, Vol. 33, 976–986, 2000.

Speckle Reduction of SAR Images Using Independent Component Analysis

C. H. Chen and X. J. Wang
University of Massachuetts Dartmouth, USA

Synthetic aperture radar (SAR) images are often degraded by multiplicative speckle noises. Appearing to be randomly granular, SAR image speckle noise is resulted from phase variations of radar waves from unit reflectors within a resolution cell. Its existence is undesirable, since it degrades image quality and affects the task of human interpretation and evaluation. SAR image speckle noise reduction has been a well studied subject for over twenty years, notably by J. S. Lee, D. T. Kuan and many others.

In this paper the neural network based independent component analysis(ICA) technique is presented that shows experimentally more signficant speckle noise than those reported by other researchers. The ICA method employed makes use of fastICA algorithm for the basis images and a classification procedure to assign the basis image to signal (edge) space or the speckle (texture) space, with the assumption that the two spaces are independent. The coefficient associated with the signal space basis image is going through a nonlinear transform while the coerfficient associted with the speckle space is set to zero. The image is then reconstructed from the resulting signal space.

The SAR images considered with 250×350 pixels for the experimental comparison have nine channels with PLC bands and three polarizations. They cover the agricultural area near the village of Feltwell, UK. The comparison of ratio of standard deviation to mean clearly indicates that our method is signficantly better in most image channels.

Table 1: Ratio comparison.

	Original	Our method	Wiener filter	Lee method	Kuan method
Channel 1	0.6362	0.2723	0.5597	0.3072	0.5765
Channel 2	0.6298	0.2581	0.4358	0.3154	0.5203
Channel 3	0.5842	0.2407	0.3976	0.3018	0.5276
Channel 4	0.3682	0.2196	0.3097	0.2640	0.3437
Channel 5	0.3596	0.3087	0.3164	0.2785	0.3272

Markov Random Fields and Neural Network for Improving Multi-source Data Interpretation

P. Gamba, G. Trianni, and S. Caorsi
Università di Pavia, Italy

There is currently a big need for methods aimed at improving the exploitation of multi-source data for earth observation. This is caused by the increasing number of image sources providing different kinds of information about the earth for oceanic, meteorological, terrestrial applications. These sources may be very different in their nature, and consequently also the spatial and spectral resolution of their data sets may be also very different.

In this work we are interested to land cover analysis, especially in urban areas, where the huge spatial variability of the environment requires usually data coming from many sensors to generate a satisfactory and reliable interpretation of the scene. This process, labeled as data fusion, has been performed using various approaches, from statistical methods [1], to Dempster- Shafer theory [2], and also by means of neural networks [3]. Here we propose a basic procedure based on a Markov Random Field but with the aid of neural network for extracting the a priori probability density functions for the land cover classes. Moreover, a comparison with all neural network chains for data fusion in urban areas [4] is provided, in order to understand the advantages and drawbacks of the approach. As a matter of fact, taking into account some simple local interactions at the scale of a single pixel and its neighbors, MRF models show a complex global behavior, which is the principal reason of their popularity among the scientific community. One drawback of MRF is that they may have prohibitive computational costs. To our aim, we found out that ICM (iterated conditional mode) was the most useful algorithm. Still, neural network trained for spatial (re)classification may be equally effective, and maybe more suitable to continuously spatially changing environments. So, this work provides an interesting comparison between the two techniques, both based on a initial pixel-based classification performed by a Fuzzy ARTMAP classifier.

For our tests, the area around the town of Pavia (Northern Italy) has been chosen. The city of Pavia has already been widely analyzed for other purposes and therefore a detailed ground information, together with other results, may be used for analysis and comparison [5]. So, we collected some ERS-1/2, Envisat (ASAR) and Landsat TM and ETM images of the town and performed our classification based on the MRF and NN approaches. The multi-source data have been co-registered one to the others and to the corresponding ground truth. We want to remark here that in defining the MRF classification model, we made some choices as the energy function present in the Gibbs function, the pixel number contained in the neighborhood of each pixel, and the optimization algorithm, which are peculiar to urban areas, and thus were chosen to make the approach more suited to the target area.

REFERENCES

1. Welch, R. and M. Elehers, “Cartographic feature extraction with integrated (SIR-B) and landsat TM images,” *Int. J. Remote Sensing*, Vol. 9, 873–880, 1988.
2. Lehrer, N., G. Reynolds, and J. Griffith, “Initial hypothesis formation in image understanding using an automatically generated knowledge base,” *Proc. Workshop Image Understanding*, 521–537, Los Angeles, CA, February 1987.
3. Jakubowicz, O., “Autonomous reconfiguration of sensor systems using neural nets,” in *Proc. SPIE: Sensor Fusion*, 197–203, Orlando, FL, April 1988.
4. Gamba, P. and B. Houshmand, “An efficient neural classification chain for optical and SAR urban images,” *International Journal of Remote Sensing*, Vol. 22, No. 8, 1535–1553, May 2001.
5. Gamba, P., “A collection of data for urban area characterization,” *Proc. of IGARSS04*, Vol. 1, 69–72, Anchorage (USA), September 2004.

Neural Networks for the Electromagnetic Near Field Subsurface Sensing

S. Caorsi and G. Cevini
University of Pavia, Italy

This paper is intended to give an assessment of the application of a neural network approach to the electromagnetic sensing of subsurface scenarios. The neural network approach is used to obtain a reconstruction of the geometric and dielectric properties of buried geometries. Besides, the focus is on the exploitation of aspect-limited electromagnetic data coming from near field measurements, such as those available at the terminals of a ground penetrating radar equipment. This topic is related to many practical applications in environmental and civil engineering, such as, for example, the subsurface mapping of utilities or contaminants, or the monitoring of the subsoil conditions, for buildings, roads or railroads maintenance purposes.

The problem of reconstructing the geometric and dielectric characteristics of buried scenarios is usually formulated as an inverse scattering one. Since, usually, only few parameters can be investigated in order to characterize the unknown target, learning-by-examples techniques have recently been applied to face inverse scattering problems. As a matter of fact, a neural network can be trained to approximate the functional relation between the electromagnetic available measurement data and the unknown characteristics of the scatterer, through the exploitation of a set of examples representative of the problem at hand. Thus, the a-priori information must be effectively exploited to construct a representation of the investigated problem.

The proposed approach is seen to provide a geometrical and physical characterization of buried objects by considering both frequency-domain aspect-limited data (amplitude and phase of the measured scattered field) and time-domain aspect-limited data [1–3]. Different measurement configurations have been tested (both bistatic and multi-offset setups). Besides, we have also considered the problem of reconstructing the properties of layers embedded in a host medium in order to test the potentialities of the neural network approach to reconstruct the subsoil composition. Again, different measurement configurations have been taken into account.

Numerical results will be presented assessing the capabilities of a neural network approach to exploit electromagnetic data to face the reconstruction of subsurface scenarios. Moreover, we also monitored the computational burden of the approach in order to give some indications on the computational resources requirements. The collected data will serve the purpose of underlining, on the one hand, the advantages and, on the other hand, the limitations of the proposed approach.

REFERENCES

1. Caorsi, S. and P. Gamba, "Electromagnetic detection of dielectric cylinders by a neural network approach," *IEEE Trans. on Geoscience and Remote Sensing*, Vol. 37, 820–827, 1999.
2. Bermani, E., S. Caorsi, and M. Raffetto, "Microwave detection and electromagnetic characterization of cylindrical objects from amplitude-only data by means of neural networks," *IEEE Trans. on Antennas and Propagation*, Vol. 50, 1309–1314, 2002.
3. Caorsi, S. and G. Cevini, "An electromagnetic approach based on neural networks for the GPR investigation of buried cylinders," *IEEE Geoscience and Remote Sensing Letters*, Vol. 2, 3–7, 2005.

Combination Approaches in Neural Classifiers Fusion for Image Classification

K.-S. Chen
National Central University, Taiwan

Y.-C. Tzeng
National United University, Taiwan

In this paper, three different weighting policies: variance reduction technique, rms distance weighting, and average distance weighting, in the use of multiple neural classifiers for image fusion are investigated and compared. The fusion procedures are categorized by their input/output characteristics in five categories: data in data out, data in feature out, feature in feature out, feature in decision out, decision in decision out. It is seen that data fusion are held at different levels and is divided into three levels: raw data level fusion, feature level fusion, and decision level fusion. In this paper, we take the decision level fusion. The performance of each method of combination is evaluated with fusion of multi-polarization SAR and optical images. As for classifier, a single neural network was used to classify both SAR and optical images, although different types of classifier may be used to different data sources. Experimental results show that the classification accuracy is dramatically improved by the proposed method. For weighting method that combines the pre-classification results, it indicates that the rms distance weighting and the average distance weighting perform comparatively and both outperform that of using the variance reduction technique.

Cloud Cover Assessment of Quickbird Imagery Using NEURANUS Software

Z. Bergen
Digital Globe, USA

The success of Cloud Cover Assessment (CCA) of satellite imagery is highly dependent on band coverage. We present a constrained problem where existing arvchive imagery requires assessment in a production environment and band coverage is limited. We utilitize NEURANUS software to build an artificial neural net (ANN) for creating classified images from Quickbird imagery. The advantage of ANNs for production work is that a confidence measure is inherent in the process, and low confidence images may be processed according to existing semi-automated techniques. The resulting thematic layers are translated into polygon coverages in an Oracle Spatial database. In addition, we present a current approach to cloud assessment resulting from the low confidence cases of the ANN.

Retrieving Cloud Information with Neural Network Ensembles

D. G. Loyola R.
German Aerospace Center (DLR), Germany

The global distribution and the physical properties of clouds in the Earth's atmosphere are of great importance for a number of disciplines including weather forecasting, climate change, hydrology and atmospheric chemistry/physics. An increasing number of satellite based sensors measure the backscattered solar light, which in one way or other depends on the clouds properties. The accurate and fast retrieval of clouds information solving this inverse problem is an area of active research. This paper presents a novel approach for retrieving macrophysical cloud information out of the oxygen A-Band using neural network ensembles. The absorption depth in the oxygen A-band in and around 760 nm, depends on the cloud coverage, the cloud-top height and the optical depth of the cloud. Radiative transfer models are used to simulate the oxygen A-band absorption and neural networks are trained to retrieve cloud information using these simulations. The neural networks basically compute the inverse of the radiative transfer model, but this inversion is an ill-posed problem. Therefore an ensemble of distinct inverse solvers (neural networks) is combined to produce a more robust and less sensitive retrieval algorithm. The resulting system is extremely fast, and the retrieved cloud information compares well with that of traditional algorithms and with cloud information obtained from other sensors.

Neural Networks for Tropospheric Profiling from GPS-LEO Radio Occultation

P. Basili[1], **S. Bonafoni**[1], **P. Ciotti**[2], **and E. Maltempi**[1]

[1]University of Perugia, Italy
[2]University of L'Aquila, Italy

Global Positioning System (GPS) receivers placed on a Low-Earth Orbit (LEO) satellite allow the sounding of the Earth's troposphere and ionosphere evaluating the additional delay, due to the refractivity index, of a radio signal when passing through the atmosphere.

This radio occultation technique in recent years has been exploited to obtain profiles of refractivity, temperature, pressure and humidity in the troposphere, and several investigations have demonstrated that the retrieval accuracies are comparable with traditional atmospheric sensing techniques. Even though the atmospheric refractivity profiling by radio occultation is a well-defined problem, care must be taken to analyse factors affecting the occulted signal (multipath, satellite motion etc.) and to compute the temperature, pressure and humidity profiles from the refractivity profile. The accuracy of tropospheric profile estimation is affected by the use of proper boundary conditions and by the presence of water vapour in the atmosphere, that complicates the interpretation of refractivity. In fact the recovery of tropospheric profiles in wet conditions requires knowledge of temperature derived from independent observations (i.e. radiosoundings or ECMWF data).

In this work a retrieval method based on neural networks is proposed to overcome the constraint of temperature profile availability at each GPS occultation. We have trained a neural network with refractivity profiles as input computed from the geometrical occultation parameters of the CHAMP satellite provided by the Information System and Data Center (ISDC) of GeoForschungsZendrum (GFZ) (Potsdam).

The outputs are the dry and wet refractivity profiles obtained from the contemporary ECMWF data. We have considered a feedforward neural networks with the Levenberg-Marquardt algorithm for a fast training. The output decomposition of the wet and dry refractivity allow to obtain temperature, pressure and humidity profiles without the knowledge of the temperature ones as independent source of information.

Session 2P5
Electromagnetic Modeling and Inversion and Applications 1

New GL Method and Its Advantages for Resolving Historical Difficulties

G. Q. Xie, F. Xie, and J. H. Li
GL Geophysical Laboratory, USA

In this paper, we proposed two type new electromagnetic integral equation systems

$$\begin{bmatrix} E(r) \\ H(r) \end{bmatrix} = \begin{bmatrix} E_b(r) \\ H_b(r) \end{bmatrix} + \int_{\Omega} \begin{bmatrix} G_E^J(r', r) & G_H^J(r', r) \\ G_E^M(r', r) & G_H^M(r', r) \end{bmatrix} \begin{bmatrix} ((\sigma + i\varepsilon) - (\sigma_b + i\omega\varepsilon_b))E_b(r') \\ -i\omega(\mu - \mu_b)H_b(r') \end{bmatrix} dr', \tag{1}$$

and its dual integral equation systems. The 6×6 diagonal EM parameter matrix is for isotropy, and 6×6 full matrix for anisotropy materials. Based on these EM integral equation system, we proposed the new GL EM modeling and inversion algorithms. Our GL EM method based on the magnetic differential integral equation has been published first in the world in PIERS 2005 in Hongzhou. We used finite step iterations exactly to solve these integral equation system or the new EM and seismic differential integral equations in finite sub domains. The Global EM wave field are improved successively by the Local scattering EM wave field in the sub domains. In the FEM and FD method, the large matrix equation, inaccurate and complex absorption condition on artificial boundary, the cylindrical and spherical coordinate singularities, and ill posed in inversion are historical difficulties. The Born approximation is only used for low contrast material. The GL method is completely different from FEM, FD, and Born approximation. Our GL modeling and inversion resolved these historical difficulties. Only 3×3 or 6×6 small matrices are needed to solve in the GL method; There is no any artificial boundary for infinite domain is needed in the GL method; In the GL method, the cylindrical and spherical coordinate singularities are removed. Our GL method combines the analytic and asymptotic method and numerical method perfectly. It is more accurate than FEM and FD method and Born likes approximation. The GL method is available for all frequencies and high contrast materials. The GL solution has $O(h^2)$ convergent rate if the trapezoid and mid point integral is used. In particular, if the Gaussian integral are used, the GL solution has $O(h^4)$ super convergence. The GL is a high perform parallel algorithm with self parallelization properties. The FEM and FD scheme of high order PDE are complicated. Fortunately, the GL method has very simple scheme. In particular, the GL method has no scheme or half scheme such that it has half mesh and no mesh. The FEM and FD scheme only used Riemann integral. In the GL method, we can use both of Riemann and Lebeger integral that induces meshless method. We developed software for 3 D/2.5 D EM, seismic, acoustic, flow dynamic, and QEM modeling and inversion. Our GL modeling and inversion can be useful for geophysical and Earthquake exploration, environment science and engineering, nondestructive testing, steel and metal casting, weather radar, medical, Earth magnetic, antenna, and heating conductive imaging, space sciences and lunar and sun and stars electromagnetic and light exploration. The GL QEM modeling and inversion can be useful for studying micro optical physical and biophysics properties in nanometer materials and biophysics materials. The GL and AGILD method resolve the poles coordinate difficulties in Navier–Stocks flow atmosphere simulation and Earth and Space EM field.

REFERENCES

1. Xie, G. Q., J. H. Li, and F. Xie, "New global and local electromagnetic field (GL) modeling and inversion," PIERS2005 in Hangzhou, 68, 2005.
2. Xie, G. Q., F. Xie, and J. H. Li, "GL EM modeling and inversion based on the new EM integral equation," Report of GLGEO, GLP05001, GLGEO has copyright and patent for the GL method, 2005.

Optical Distance and Optical Distance Difference in Moving Systems

G. Korom
Faraday Institute for Theoretical Physics, Hungary

It is shown based on a gedanken-experiment, that the difference of the two wave-propagations and the "optical" path difference (OPD), or more simply the optical distance (OD) is the same only in systems resting in the conductive medium. In case of moving sources and moving observers, the OD is equal with the actual distance of the source and the observer from each other in the phase-space, and is not necessarily equal with the length of the wave propagation across the medium. It has turned out that the phase difference of the amplitude-splitted, and later reunited electromagnetic vibrations in the Michelson-Morley experiment will not change while the speed difference of the Ether-wind is changing, and/or the Michelson Interferometer is rotating. Only phase shifts with equal magnitude will occur at the observers, but the interferometer is insensitive to these shifts, and the observed frequency remains constant because of a double Doppler effect. Consequently, the circular interference fringes observed on the screen will not be dislocated. These results urge the revision of the significance of the Theories operating with relativity of Time and absolute constant light speed, refusing the existence of the Ether. Besides the widely used, derived terminology of "*Optical Path Difference*", author suggests to use — as for the future — the equivalent, directly measurable "*Optical Distance*", and finally, also the "*Optical Distance Difference*" because it describes much better the real physical events going on in the Michelson-Morley experiment.

An Incremental Inductance Approach to Proximity Effect Calculations of Differential Striplines

S. Asgari and M. Tsuk
Ansoft Corporation, USA

The performance of the high-speed digital integrated circuits depends on how well the signal waveforms are controlled on the coupled interconnecting transmission lines whether on-chip or off-chip. Hence, to preserve the signal integrity of the transmitted waveforms traveling with high speed through interconnecting lines requires the designer to analyze a broad band of frequencies.

Meanwhile in many applications, for example the printed circuit board (PCB) layout designs, the differential traces are pushed close to one another. This is done so as to save board space. As a result, the differential impedance will go down for closely spaced lines. Also, the effect of tight coupling decreases the effective trace width causing skin effect loss. This will result in intense concentration of magnetic flux near the corners of the traces, inducing substantial peaking of the current density at the corners. The proximity effect illustrates itself as the concentration of current around the periphery of the signal conductors and the reference planes. The proximity effect increases especially at the very high frequencies.

While usually different 2D and 3D field solvers such as Ansoft's SI2d and HFSS are used to do a more elaborate surface resistance calculation, no closed form equations that we know of are available to do an adequate approximation of the proximity effect even for the simpler case of symmetric differential striplines. In this paper, we derive closed form equations for the effective surface resistance matrix of symmetric edge-coupled differential stripline based on Wheeler's incremental inductance rule while incorporating the proximity effects of the lines. This methodology can be generalized to non-symmetric as well as multi-coupled lines.

The paper is organized as follows. In section II, we review Wheeler's incremental inductance rule and set up the general formulas needed to solve for the resistance matrix. In section III, we present the closed form equations for the resistance matrix and summarize the equations for the case of differential stripline. In section IV, we show few examples and simulation results which demonstrate the usefulness of our approach as compared to that of Ansoft's SI2d as well as Moments method (MOM) calculations. Finally we end the paper with concluding remarks and future extension of the work.

Matlab Simulink Based DQ Modeling and Dynamic Characteristics of Three Phase Self Excited Induction Generator

A. Kishore, R. C. Prasad, and B. M. Karan
Birla Institute of Technology, India

In this paper, DQ-modeling approach for Transient State analysis in the time domain of the three-phase self-excited induction generator (SEIG) with squirrel cage rotor is presented along with its operating performance evaluations. The three-phase SEIG is driven by a variable-speed prime mover (VSPM) such as a wind turbine for the clean alternative renewable energy in rural areas. Here the prime mover speed has been taken both as fixed and variable and results has been analyzed. The basic Dynamic characteristics of the VSPM are considered in the three-phase SEIG approximate electrical equivalent circuit and the operating performances of the three-phase SEIG coupled by a VSPM in the Transient state analysis are evaluated and discussed on the conditions related to transient occurs in the system and speed changes of the prime mover.

Estimation of Higher Order Correlation between Electromagnetic and Sound Waves Leaked from VDT Environment Based on Fuzzy Probability and the Prediction of Probability Distribution

A. Ikuta, **M. Ohta**, **and H. Ogawa**
Prefectural University of Hiroshima, Japan

Some studies on the mutual relationship between electromagnetic and sound waves leaked from electronic equipment in the actual working environment have become important recently because of the increased use of various information and communication systems like the personal computer and portable radio transmitters, especially concerning their individual and/or compound effects on a living body.

On the other hand, the actual observed data often contain fuzziness due to confidence limitation in sensing devices, permissible errors in the experimental data, and quantizing errors in digital observations. Therefore, in oreder to evaluate precisely the objective electromagnetic and sound environments, it is desirable to estimate the mutual relationship between electromagnetic and sound waves based on fuzzy observations.

In this study, a signal processing method considering not only linear correlation but also the higher order nonlinear correlation information is proposed on the basis of fuzzy observation data, in order to find the mutual relationship between electromagnetic and sound waves leaked from an electronic information equipment. More specifically, by applying the well-known fuzzy probability to an expression on the multi-dimentional probability distribution in an orthogonal expansion series form reflecting hierarchically various type correlation information, a method to estimate precisely the correlation information between each variable from the conditional moment statistics of fuzzy variables is proposed as a trial. The effectiveness of the proposed theory is experimentally confirmed by applying it to the observation data leaked from VDT periphery in the actual work environment.

Single Phase Single Stage AC/DC Converter with High Input Power Factor and Tight Output Voltage Regulation

A. K. Jha
Birla Instt. of Technology, India

B. G. Fernandes
Indian Institute of Technology, India

A. Kishore
Birla Instt. of Technology, India

Proposed converter integrates an input current shaper and an isolated DC-DC converter with a shared switch and PWM controller. The work in the direction to eliminate the problem of high DC bus voltage stress without compromising the high input power factor and tight output vpltage regulation. It is low cost efficient AC/DC converter. It is applicable for DC power below 200 W. The concept behind the proposed converter is "Direct Power Transfer". DPT scheme utilizes some power directly from PFC cell to output without processing through DC-DC cell. Due to the reduction in power processing as earlier converter efficiency is more. This converter is apllicable for all medium power electronic equipment.

A New Generalized Space Vector Modulation Algorithm for Neutral-point-clamped Multilevel Converters

P. Purkait and R. S. Sriramakavacham
Birla Institute of Technology, India

Neutral-point-clamped converter are increasing applied in industrial drive systems as they allow the use of lower voltage devices in higher voltage applications, provide reduced output voltage total harmonic distortion (THD), and can develop lower common mode voltage. Several distinct modulation strategies have been proposed in the past for eliminating the common mode voltage, providing low THD output voltage or reducing the neutral point current ripple. However each of these strategies improves the performance of the converter in one view point while loosing performance in other view point. A new generalized space vector modulation technique is proposed. Analytical model and simulation results are presented.

Improved Mesh Conforming Boundaries for the TLM Numerical Method

I. J. G. Scott and D. de Cogan
University of East Anglia, UK

The numerical simulation of wave propagation in bounded space using differential-based models generally encounter spatial discretisation problems. If the boundaries do not conform to the precise discretisation of the mesh, then errors can arise. Accuracy can be improved by either bulk or local mesh refinement, but the penalty is an increased computational load.

This has been an acute problem for those who use the Transmission Line Matrix (TLM) method. The simplicity of the technique lies in the scattering of impulses from nodes which are located on a Cartesian mesh. These travel along connecting transmission lines and arrive simultaneously at adjacent nodes after a time interval, Δt. It is conventional in TLM to place boundaries half way between nodes (although any other integral half distance is also possible). If at time $k\Delta t$ an E-field analogue impulse starts off from a node which is located a distance $\Delta x/2$ from a perfectly reflecting surface, it will arrive at the boundary at time $(k+1/2)\Delta t$. Following reflection and inversion it will return to the same node at time $(k+1)\Delta t$. This is quite a restriction, but if a boundary is placed at some other distance, then the return of the impulse may be out of synchronism with the others on the mesh and cannot be treated using existing TLM schemes.

TLM modellers have adopted coping strategies, e.g., [1]. Müller et al [2] use a reference plane located at $\Delta x/2$ from a surface-adjacent node. The distance of the real boundary from this plane represents an additional/subtractional length, l of line of characteristic impedance, Z_0. They then use an impedance transformation, replacing this by a length, $\Delta x/2$ of line of impedance, Z_B so that the impedance observed at the reference plane remains unchanged, but the time of arrival of pulses is now in synchronism with all other pulses in the modelling space. The mesh is still a discretised Cartesian system, but the transmission lines at the interface are redefined so that propagating signals perceive a smooth boundary. Although this mesh transformation scheme is very effective, the resulting expressions have a recursive component. As the TLM iterative process progresses, there is a need to store all previous values; the computational load is greater than conventional stepped-boundary TLM.

In our paper we adopt a similar approach, but propose a scheme where the need for recursion is avoided. This is achieved by a relocation of the reference plane. What was previously a separate recursion is now integrated into the normal TLM scattering process. In our analysis we estimate the error limits that arise as a result of the assumptions that we make. Practical implementations (e.g., cylindrical resonator) and comparison with analytical results (e.g., horn antenna) demonstrate a significant improvement in accuracy.

REFERENCES

1. Jaycocks, R. and S. Pomeroy, *UViC First International Workshop on Transmission Line Matrix (TLM) Modelling-Theory and Applications*, University of Victoria, British Columbia (Canada), 269–272, 1–3 August, 1995.
2. Mueller, U., A. Beyer, and W. J. R. Hoefer, *IEEE Trans. on Microwave Theory and Techniques*, MTT-40, 2267–2271, 1992.

A Fast Matlab-based 3D Finite Difference Frequency Domain (FDFD) Method and Its Application to Subsurface Scatterers

Q. Z. Dong and C. Rappaport
Northeastern University, USA

The FDFD electromagnetic model computes wave scattering by directly discretizing Maxwell's equations along with specifying the material characteristics in the scattering volume. No boundary conditions are need except for the outer grid termination absorbing boundary. We use a sparse matrix Matlab code with generalized minimum residue (GMRES) Krylov subspace iterative method to solve the large sparse matrix equation, along with the Perfectly Matched Layer (PML) absorbing boundary condition. The PML conductivity profile employs the empirical optimal value from [1–3].

The sparse Matlab-based model is about 100 times faster than a previous Fortran-based code implemented on the same Alpha-class supercomputer. The 3D FDFD model is easily manipulated; it can handle all types of layer-based geometries if the target region is less than 25% of the total computational space.

Several cases have been investigated. The scattered electromagnetic fields due to spherical and elliptic mine-like TNT targets buried in simulated Bosnian soil are computed and compared to reference solutions. The electric field distribution of a cylindrical air void in soil is computed and compared with analytical models. Multiple buried scatterer problems are easily specified and analyzed with FDFD. This method is particularly well-suited to rough surface and volumetric inhomogeneity applications.

REFERENCES

1. Marengo, E., C. Rappaport, and E. Miller, "Optimum PML ABC conductivity profile in FDFD," *IEEE Transactions on Magnetics*, Vol. 35, 1506–1509, 1999.
2. Winton, S. and C. Rappaport, "Specifying PML conductivities by considering numerical reflection dependencies," *IEEE Transactions on Antennas and Propagation*, Vol. 48, No. 7, 1055–1063, July 2000.
3. Rappaport, C., M. Kilmer, and E. Miller, "Accuracy considerations in using the PML ABC with FDFD Helmholtz equation computation," *Int. J. Numer. Modeling*, Vol. 13, 471–482, Sept. 2001.

Modeling Electromagnetic Scattering from Particles

M. J. Berg, **C. M. Sorensen**, **A. Chakrabarti**, **and M. I. Mishchenk**
Kansas State University, USA

Particles of both spherical and nonspherical shape are often encountered in the natural environment. Examples include atmospheric clouds and aerosols. Light scattering from these particles creates radiative forcing effects that influence the Earth's climate [1]. Additionally, electromagnetic scattering from a particle can provide information about the physical properties of the particle in an unintrusive manner. Furthermore, applications of electromagnetic scattering to remote sensing of physical systems of single or multiple particles requires a detailed knowledge of the interaction between the particle and the field. We apply the Discrete Dipole Approximation (DDA) to study electromagnetic scattering from single spherical and nonspherical particles. Our aim is to quantify simple patterns in the scattering process which aid in characterizing the physical properties of a scattering particle [2, 3]. We also examine in detail how an electromagnetic field interacts with a particle at the microscopic level to establish the macroscopic scattering, absorption and extinction cross sections.

REFERENCES

1. Mishchenko, M. I., "Scattering, absorption, and emission of light by small particles," Cambridge, 2002.
2. Sorensen, C. M. and D. J. Fischbach, "Patterns in mie scattering," *Opt. Commun.*, Vol. 173, 145–153, 2000.
3. Berg, M. J., C. M. Sorensen, and A. Chakrabarti, "Patterns in mie scattering: evolution when normalized by the rayleigh cross section," *Appl. Opt.*, In Press, 2005.

The Spectral Expansion on the Entire Real Line of Green's Function for a Three-layer Medium in the Fundamental Functions of a Nonself-adjoint Sturm-liouville Operator

E. G. Saltykov
Moscow State University, Russia

Green's function $u(z,x)$ satisfies the Helmholtz equation with the delta function on the right-hand side and the radiation condition. The function u has a logarithmic singularity at the source position $M'(z',x')$. At the points of discontinuity of the coefficient in the Helmholtz equation, the function $u(z,x)$ satisfies the matching conditions for the function and its normal derivative. We consider the Helmholtz equation under the assumption that z, z', x, x' belong to the real axis R. We set that the coefficient in the equation depends on the one variable z and represents three complex constants.

To find the solution, we consider the Fourier expansion of u with respect to the variable x [of which the coefficient in the equation is independent]. Using the Cauchy theorem, we reduce the Fourier integral in the upper or the lower half of the complex plane of a spectral parameter to two integrals over the edges of the cuts passing through the ramification points.

We have thereby obtained the expasion of Green's function in the fundamental functions, which are finite on the entire real line solutions of the ordinary sturm-liouville equations with the complex coefficients.

The spectrum consists of two half-lines parallel to the real axis on the complex plane of a spectral parameter and going in the positive direction of the real axis.

The case of a three-layer medium which is considered in this paper is the generalization of the case of a two-layer medium which was considered in [1].

REFERENCES

1. Saltykov, E. G., *Differents. Uravn.*, Vol. 38, No. 5, 687–691, 2002.

Simulation of Electromagnetic Fields of Electromagnetic in Separator

X. F. Tan
Hunan Institute of Science and Technology, China

Electromagnetic Separator are high performance devices utilizing a powerful magnetic force for separation of magnetic foreign matter form raw material. Electromagnetic Separator is widely applied to metallurgical industry, mining industry, power industry, seaports, cement and construction material. Even in the developing industry jof garbage disposal, the separator is used to recover the iron and steel materials mixed in the scrap stock. The finite element program generating system FEPG is one of finite element method software, which can generate source program. Magnetic potential and magnetic density of magnetic field of Electromagnetic Separator have been studied. The results could help us to know the principle of Electromagnetic Separator well. However, there is still boundary condition and singularity treatment and large matrix cost in the FEM method. These historic difficult are overcame by AGILD and GL method. Recently Hunan KMD electrical company used GL geophysical Laboratory's AGILD and GL parallel electromagnetic modeling method for KMD stirring electromagnetic field simulation and obtained excellent result and obtained dynamic rotation magnetic imaging first in the world. We will use AGILD modeling for our Separator simulation

REFERENCES

1. Xie, G. Q., J. Li, and J. H. Li, "New AGILD EMS electromagnetic field Modeling," *Progress In Electromagnetics Research Symposium 2005*, Hangzhou, China, August 22-26, 2005.
2. Xie, G. Q., J. H. Li, E. Majer, D. Zuo, and M. Oristaglio, "3-D electromagnetic modeling and nonlinear inversion," *Geophysics*, Vol. 65, No. 3, 804, 2000.

Session 2P7
Electromagnetic Theory and Dielectric Waveguides and Antennas

Theory of Rain Fades; Measurement Done at Ku-band Satellite Link in a Tropical Region

V. Kumar and V. Ramachandran
University of the South Pacific, Fiji

The results on rain attenuation measurements made on 11.65 GHz signal from INTELSAT 701 at Suva (Lat.: 18.08° S, Long.: 178.3° E), a tropical region, during the period of Apr'02–Mar'03 are presented in this paper. Rainfall at Suva was often frequent and heavy with average accumulation per month exceeding 150 mm. In the tropics, heavy rainfall has intense pockets of rain surrounded by larger regions of less intense rainfall. Rain-rate and attenuation measurement showed good correlation, since the site had a high elevation angle of 68.5, which increases the probability of having only one rain cell in the propagation path. Deep fades (> 7 dB) on 11.65 GHz were often short lived. They collectively occurred for 7.4 hrs of year at the site and were mostly recorded during the evening hours. Fading occurs through the process of absorption (minor) and scattering (major) by water droplets present in the propagation path. The finite conductivities of the water droplets make it an imperfect dielectric (complex quantity) medium and at 11.65 GHz, attenuation due to absorption is calculated to be 0.015 dB/km. The absorption coefficient (α) increases with frequency. The process of attenuation by scattering is determined by the scattering parameter δ, which is a function of the radii of the raindrops and the frequency of the signal. At the observed frequency, Rayleigh scattering happens when it is drizzling and in cloud and fog where each molecule in a droplet behaves like an individual dipole which scatters the radiowave in all directions. Mie scattering occurs at high rain-rate where the drop size is comparable or larger than the wavelength, hence, the Fresnels' relation for the reflection and transmission of the EM wave at the boundary of two media (water and air) of different refractive indices are applicable. The imperfection in the dielectric constant leads to a complex transmission coefficient and as a result, causes the received signal to be depolarized.

The Characteristics of Millimetre-wave Gyrotropic Magnetic Material for Use in Quasi-optical Non-reciprocal Devices

B. Yang, R. S. Donnan, and D. H. Martin
Queen Mary, University of London, UK

Ferrites materials are employed in many millimetre-wave and sub-millimetre-wave applications such as radar, imaging, communications, electron spin resonance and precision measurement. The use of quasi-optical techniques are preferable for millimetre-wave systems over waveguiding for the propagation and manipulation of signals as they afford low power losses, wide bandwidths and high power handling capabilities.

Large numbers of quasi-optical Faraday rotators utilize magnetically soft ferrite material. These devices are biased by using large external magnets. Quasi-optical Faraday rotators that used permanently magnetized ferrites were first examined by Martin et al. [1] who surveyed a number of ferrites and produced an isolator with 17 dB isolation and 1.0 dB insertion loss at 115 GHz. This work was extended and improved upon by Webb [2] who produced W-band isolators having 30 dB isolation and an insertion loss of < 0.5 dB.

The objective of our research is to focus on selecting magnetically-hard ferrite materials, which are ideally suited to operate in high frequency (> 90 GHz) quasi-optical non-reciprocal devices.

In this paper we present the static magnetic characteristics of a candidate material, which is suited for use in high-performance non-reciprocal device operating at frequency above 90 GHz. Further, we theoretically examine the determination of a ferrite's magneto-optical constants from complex amplitude reflectance and transmittance measurements, and assess the stability of such determinations upon measurement practice.

REFERENCES

1. Wylde, R. J., "Gaussian beam-mode circuits for millimetre wavelengths," Ph.D. Thesis, Queen Mary University of London, 1985.
2. Webb, M. R., "Millimetre wave quasi-optical signal processing systems," Ph.D. Thesis, St Andrews, 1992.

"Wiggly-line" Perturbation Applying to Ground Plane Aperture for Multispurious Rejection in Microstrip Parallel Coupled Line Filter

M. Moradian and M. R. Hajhashemi
Isfahan University of Technology, Iran

S. V. Mirmoghtadaie
Isfahan University, Iran

In this paper a suitable method is presented which allows removing the spurious pass-bands of a parallel coupled-line bandpass filter. This configuration is constructed by applying wiggly line perturbation to the ground plane slot widths. First ground-plane slot dimensions are optimized for compensating the unequal modal electrical lengths using a commercially available electromagnetic simulator IE3D [1]. Using this method the double frequency spurious band associated with unequal even/odd electrical lengths can be suppressed or meaningfully reduced [2], then the slot widths is modulated with sinusoidal perturbations. The periods of the sinusoidal perturbations are selected according to desired spurious bands that must be rejected. Finally, in essential conditions, only the widths, gaps spacing and lengths of the coupled-line filter may be optimized to overcome the first passband perturbation. If the sinusoidal perturbations are applied to strip widths the first passband may be perturbed and optimization of coupled line dimensions is difficult [3]. With the proposed method undesired harmonic passbands of the filter are rejected. In addition optimization of coupled line dimensions is done easily.

REFERENCES

1. Zeland Software Inc., IE3D Manual, 2004.
2. Velázquez-Ahumada, M. D. C., J. Martel, and F. Medina, "Parallel coupled microstrip filters with ground-plane aperture for spurious band suppression and enhanced coupling," *IEEE Trans. Microwave Theory and Thechniques*, Vol. MTT–52, 1082–1086, Mar 2004.
3. Nerukh, A., P. Sewell, and T. M. Benson, "Volterra integral equations for nonstationary electromagnetic processes in time-varying dielectric waveguides," *J. of Lightwave Techn.*, Vol. 22, No. 5, 1408, 2004.
4. Lopetegi, T., M. A. G. Laso, F. Falcone, F. Martin, J. Bonache, J. Garcia, L. Pérez-Cuevas, M. Sorolla, and M. Guglielmi, "Microstrip "wiggly-line" bandpass filters with multispurious rejection," *IEEE Microwave Wireless Compon. Lett.*, Vol. 14, 531–533, Nove 2004.

Design of a Non-uniform High Impedance Surface for a Low Profile Antenna

M. Hosseini[2], **A. Pirhadi**[1,2], **and M. Hakkak**[1,2]

[1]Tarbiat Modares University, Iran
[2]Iran Telecommunication Research Center (ITRC), Iran

A Non-Uniform High Impedance Surface (NU-HIS) is proposed against a Uniform HIS (U-HIS). As in Fig. 1(b) and(c), both surfaces are one dimensional and made of parallel wires with a length a little less than $\lambda/2$ around the resonance frequency. It is well known that the radiation of antennas very close to PEC ground is very poor as a result of the inherent behavior of the PEC ($\Gamma = -1$). If

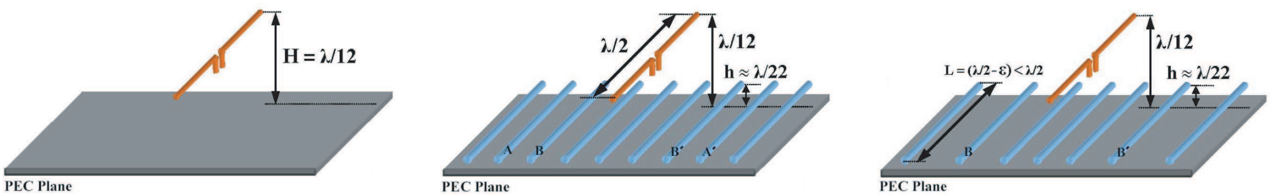

(a) (b) (c)

Figure 1: The geometry of the dipole antenna located over a) PEC, b) U-HIS, c) NU-HIS.

PEC is replaced by a HIS showing a very high wave impedance to the arriving wave, the complex surface exhibits $\Gamma \approx 1$; Therefore, the radiation improves. To show the effect of the proposed surfaces a half wavelength dipole antenna is placed over three different surfaces, PEC, U-HIS, and NU-HIS (see Fig. 1), while the dipole height is fixed and very close to the surface ($\approx \lambda/12$). These three EM problems are analyzed numerically by MoM. The results are shown in Fig. 2. As in Fig. 2(a), for a dipole near a PEC, there is no resonance in Z_{in}. As a result, the VSWR is very poor. Using a U-HIS formed by putting uniformly-placed wires close to the PEC plane, as in Fig. 1(b), the VSWR improves very much (see Fig. 2(b)). Now the main idea of this work is applied by removing the two wires A and A' in Fig. 1(b) and aptly shifting the positions of B and B' sideward. This way, a Non-Uniform or tapered HIS is formed as in Fig. 1(c). Fig. 2(c) shows the VSWR and Z_{in} of this surface. As observed, the bandwidth on VSWR increases.

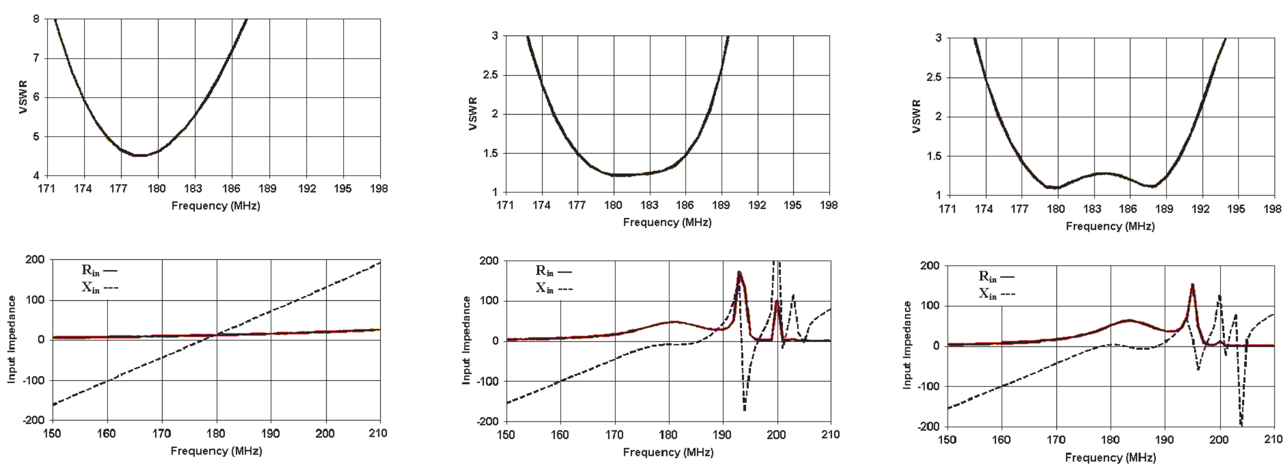

(a) (b) (c)

Figure 2: VSWR and input impedance of the dipole located over a) PEC ground plane, b) U-HIS, c) NU-HIS.

Axial Focusing Properties of Cosine-Gaussian Beam by a Lens with Spherical Aberration

Q. F. Wang, **X. Q. Wang**, **L. Wang**, **J. J. Lin**, **J. S. Tang**, **and K. Sheng**
Southwest Jiaotong University, China

Based on the expression for the axial light intensity of cosine-Gaussian beam by a lens with spherical aberration, the influence of the coefficient of the spherical aberration and Fresnel number of Gaussian beams on the axial intensity distribution is discussed. The numerical results show that for the lens with negative spherical aberration, near the best focal point, the axial light intensity changes slowly with the changing of propagation distance. So, the negative spherical aberration may be an approach for achieving the flattened laser intensity distribution alone propagation axis. When the parameters of the beam and the optical system satisfy some conditions, there are two axial light intensity maxima which are located on both sides of the geometrical focus of focused cosine-Gaussian beam. For the lens without spherical aberration, the maximum light intensity, or the best focal point is on the left side of the geometrical focus. For the lens with positive spherical aberration, the best focal position can leap to the right side of geometrical focus, z_{f2} from the left of it, z_{f1}, when the value of Fresnel number of Gaussian beams N_w changes, it is so-called focal switch. With the increasing of the coefficient of the spherical aberration kS_1, relative transition height $\Delta z_f = | z_{f1} - z_{f2} |$ increases, but the value of critical Fresnel number $(N_w)_c$ decreases. For example, when the coefficient of the spherical aberration equals 0.5 and 0.3, and, the critical Fresnel number equals 7.03 and 8.68 (when the transition occurs), the relative transition height Δz_f equals 0.246 and 0.146 respectively. It is also shown that when the coefficient of the spherical aberration is small, the value of critical Fresnel number $(N_w)_c$ decreases rapidly as the kS_1 increases. After about $kS_1 = 0.3$ the value of $(N_w)_c$ decreases slowly.

Some Applications of the High-mode-merging Method

J. S. Tang[1], **X. Q. Wang**[1], **L. Wang**[1]
S. Y. Cao[1], **Z. Wang**[2], **J. Gao**[1], **and K. Sheng**[1]

Southwest Jiaotong University, China
NC A&T State University, USA

Waves guided along dielectric step discontinuity can be described by a a multi-port network [1] and it is simplified as a two-port network with the influence of high-modes retaining [2]. These results can be used for treat dielectric strip waveguide, even more complicated structures. Some numerical results are got for a strip and a groove dielectric waveguide some kind of resonant phenomena also is obtained. Some comments on this method and some suggestions are given furthermore as follows:

(1) The results for all methods accord one another pretty good in certain accuracy, especially for the first two that the results are more closed each other.

(2) The results of three methods give similar tendency of changing.

(3) The EDC method is still useful in some cases because it is rather simple and easy for calculations and with clear physical meaning. A significant defect is that it can't give the loss.

(4) There is some kind of periodic phenomena existing. The reflection coefficients, both argument and modulus, and loss of them are varying with the width of waveguide periodically. It is coincide with the conclusion of [3].This phenomena can be seen as resonance , but the mechanism of it is remained to be explained further. It is also indicated that the high-mode-merging method is correct.

(5) In high-mode-merging method, the coupling between TE modes and TM-modes has not been considered. It is also one of the defects of this theory.

(6) In the original theory of [1], two parallel perfect conductive planes are needed. So, the waveguide discussed here is not open absolutely. If the upper one of them moved far enough, it almost can be seen as an open one approximately. If we want to remove the upper conductive plane, we'll get infinite number of continuous high modes it is a problem of continuous spectrum and is out of the topic of this paper.

The cascade network method is not confined to solve only symmetric system like single strip dielectric waveguide but also can be extended to treat some more complicated structures, such as finite periodic strip(groove) dielectric waveguide, the curved surface dielectric waveguide etc.

REFERENCES

1. Peng, S. T. and A. A. Oliner, "Guidance and leakage properties of a class of open dielectric waveguides: part I-mathematics formulation," *IEEE Trans. on. MTT*, Vol. MTT-29, 843–855, Sept. 1981.
2. Tang, J. S., S. Kemin, and G. Jun, "The high-mode-merging technique for dielectric waveguides," PIERS 2006 Procedings, 142–146, Hangzhou, China, Aug. 2005.
3. Peng, S. T., A. A. Oliner, I. T. Hsu, and A. Sanches, "Guidance and Leakage properties of a class of open dielectric waveguides: Part II-New physical effects," *IEEE Trans. on MTT*, Vol. MTT-29, 855- 869, Sept. 1981.

Analysis of Circular Cavity with Metalized Dielectric Posts or Corrugated Cylinders

R. Lech and J. Mazur
Gdansk University of Technology, Poland

This paper presents the analysis of electromagnetic wave scattering by cylindrical objects located arbitrarily in a circular cavity. The general configuration of the resonators to be investigated is shown in Figure 1. The posts structures can be either homogenous along the height of the resonator or homogenous along their circumference. The first kind of posts is composed of metalized dielectric, cylindrical rod or fragments of metallic cylinder as depicted in Fig. 1(a), while the latter is a corrugated metallic cylinder (see Fig. 1(b)). The proposed structures can be utilized as a key building elements of combline and tunable filters and measurements resonators.

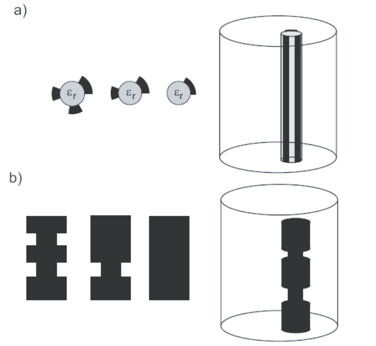

Figure 1: Analyzed structure. a) metlized dielectric, cylindrical post in circular cavity; b) corrugated metallic cylinder in circular cavity.

In both cases the exact full-wave theory based on the mode-matching method is applied to analyze the structures. Both TE and TM modes are considered simultaneously in the analysis. Additionally, to elim-inate the phenomenon of relative convergence when sharp metallic edges are presents, the analysis includes the edge condition. A set of integral equations in the tangential electric fields at the interfaces are derived and solved with te use of the basis functions which contain as much as possible information on the behavior of these fields at all sharp metallic edges [1, 2].

This ensures numerical efficiency and fast convergence of the method. The resonance frequencies of the investigated resonators are accurately determined. Validity and accuracy of the approach will be verified by comparing the results with Quick Wave FDTD Simulator, FEM method and experiment. A good agreement with FDTD method for a couple examples was obtained and presented in the tables below.

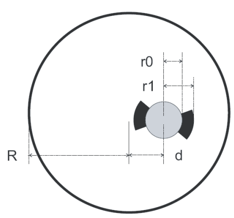

Data: $r_0 = 5$mm; $r_1 = 10$mm; $R = 30$mm; $H = 100$mm; $d = 0$mm and $d = 10$mm; the resonance frequencies are in GHz

$d = 0$mm			$d = 10$mm		
p	Our Results	FDTD Method	p	Our Results	FDTD Method
0	6.21	6.23	0	5.389	5.398
	6.541	6.565		6.456	6.470
	7.582	7.598		7.056	7.067
1	6.362	6.382	1	5.589	5.597
	6.697	6.718		6.620	6.637
	7.728	7.747		7.162	7.169
2	6.779	6.797	2	6.148	6.150
	7.142	7.154		7.088	7.067
	8.152	8.166		7.446	7.450

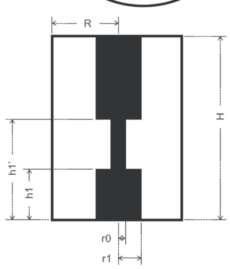

Data: $r_0 = 5$mm; $r_1 = 10$mm; $R = 30$mm; $H = 100$mm; $d = 0$mm and $d = 10$mm; $h_1 = 20$mm; $h_1' = 40$mm; the resonance frequencies are in GHz

$d = 0$mm	
Our Results	FDTD Method
2.880	2.895
3.960	3.945
4.930	4.922

$d = 10$mm	
Our Results	FDTD Method
2.894	2.904
2.994	3.020
3.964	3.961
4.036	4.035
4.838	4.820
4.842	4.834

REFERENCES

1. Amari, S., S. Catreux, R. Vahldieck, and J. Bornemann, "Analysis of ridged circular waveguides by the coupled-integral-equations technique," *IEEE Transaction on Microwave Theory and Techniques*, Vol. 46, No. 5, May 1998.
2. Lech, R., M. Polewski, and J. Mazur, "Scattering in junction by posts consisting of a segment of conducting cylinder," *IEEE Transaction on Microwave Theory and Techniques*, Vol. 51, No. 3, 998–1002 March 2003.

UWB Textile Antennas for Wearable Applications

M. Klemm and G. Troester
Swiss Federal Institute of Technology, Switzerland

Wearable computing is a new, fast growing field in application-oriented research. Steadily progressing miniaturization in microelectronics along with other new technologies enables wearable computing to integrate functionality in clothing allowing entirely new applications. Integration in textiles ideally combines such requirements since clothing offers unobtrusiveness, a large area and body proximity. However, such electronic devices have to meet special requirements concerning wearability. Ultra-wideband (UWB) is an emerging wireless technology, recently approved by FCC. In low/medium data-rate applications, like wearable computing, UWB offers low-power operation and extremely low radiated power, thus being very attractive for body-worn, battery-operated devices.

In this paper we present new ultra-wideband (UWB) textile antennas for wearable applications. These antennas are made entirely of textiles. As a conductor we have used metalized textile with the surface resistivity of $0.1\,\Omega/\mathrm{sq.}$, which offer low ohmic losses. As the dielectric substrate, very thin (0.5 mm) textile with dielectric constant 2.6 (extracted from measurements). This textile dielectric was chosen due to a relatively high dielectric constant and a small thickness. Prior textile antennas (e.g., [Klemm, EuMW 2004]) were usually composed of dielectric materials with ε_r only slightly higher than 1, and thicknesses of 4–6 mm. Therefore, a new feature of our antennas is that they could be easily integrated directly into clothing, rather than being attached.

We have realized different types of thin UWB textile antennas, both in microstrip and coplanar (CPW) techniques. To our best knowledge, these are the first CPW-fed textile antennas reported in the open literature.

Due to the limited space, in Fig. 1(a) we present only one example of the manufactured UWB textile antenna: CPW-fed textile UWB disc monopole antenna. In Fig. 1(b) we compare measured (two prototypes) and simulated return loss (RL) characteristics, which agree relatively well. Both measured antennas have RL below 10dB from 3.4 GHz to 10.2 GHz.

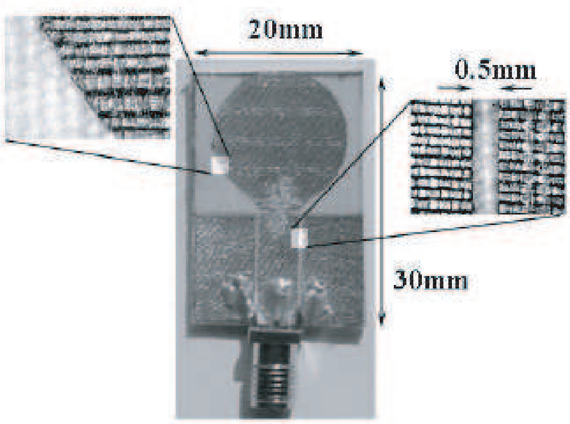

(a)

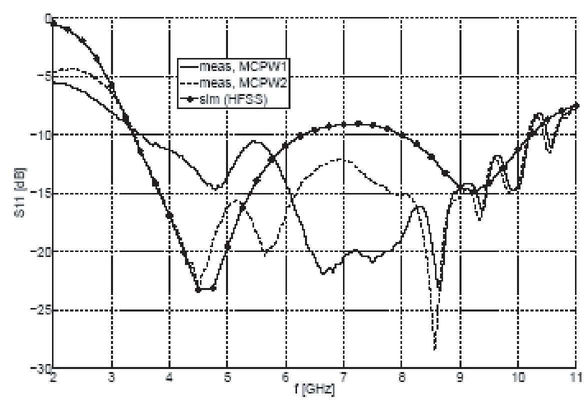

(b)

Figure 1: The CPW-fed UWB disc monopole antenna: a) photo, b) Measured (two realizations) and simulated return loss characteristics.

Propagation of Strong Electromagnetic Waves in Semiconductors with S-shaped Current Voltage Characteristics

Y. G. Gurevich and J. E. Velázquez-Pérez
Universidad de Salamanca, Spain

It is well known that some semiconductors exhibit a S-shaped dependence of the electron temperature with the local electric field. Usually such dependence leads to the same kind of dependence in the current-voltage characteristics [1, 2].

In this work we will present the theory of the propagation of strong electromagnetic waves in such media. In our study we have found that a semi-infinite semiconductor when excited with a strong electromagnetic wave will exhibit an internal discontinuity of the electrical permittivity. The position of this discontinuity is found to be a function of the magnitude of the electromagnetic wave (E_0).

From the an application point of view, this property can be exploited to design a Fabry-Pérot interferometer. The thickness of this interferometer can be modulated by E_0. As a consequence of the above described, the reflectance value will exhibit an oscillatory dependence with the magnitude of the electromagnetic wave.

REFERENCES

1. Volkov, A. F. and S. M. Kogan, *Sov. Phys. Uspekh.*, Vol. 96, 633, 1968.
2. Baas, F. G. and Y. G. Gurevich, *Sov. Phys.*, JETP, Vol. 28, 572, 1969.

Effect of Surface Defects on the Amplification of Anomalous Transmission in Dielectric and Metallic Photonic Band Gap Materials: Calculation and Experimental Verification

S. Massaoudi, A. Ourir, and A. de Lustrac
Université Pairs-Sud, France

We study the distribution of defects on dielectric and metalic Photonic Band Gap materials. We'll show that the surface defects lead to the amplification of anomalous transmission and excitation of the new electromagnetic modes. These properties allow very interesting applications, such as controlable antennas with high directivity, or compact demultiplexer for WDM [1]. The dielectric and metallic PBG-prisms, which we studied are made of dielectric or metallic rods disposed in an isosceles right-angled triangle.

The Results of the Dielectric PBG-prism

The Fig. 1(a) shows the radiation pattern measured at 16 GHz of a prism without defect.

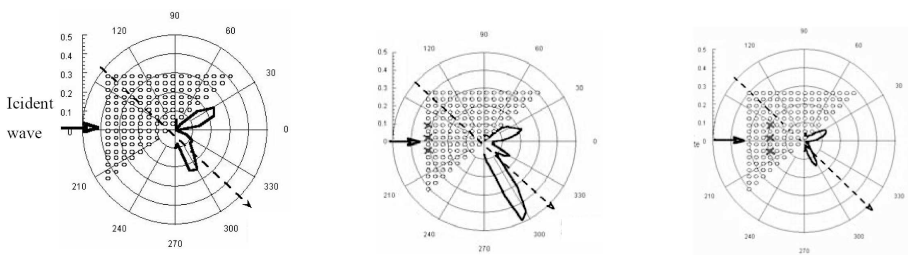

(a) (b) (c)

Figure 1: Measured near field radiation pattern at 16 GHz. a) Perfect PBG-prism, b) The PBG-prism with three cavities (in red) placed on the surface, and c) The PBG-prism with three defects inside.

The Fig. 1(b) gives the radiation pattern measured at 16 GHz of a prism with three defects on the surface of the dielectric. The Fig. 1(c) shows the radiation pattern measured at the at 16 GHz of a prism with three defects inside.

The Results of Metallic PBG-prism

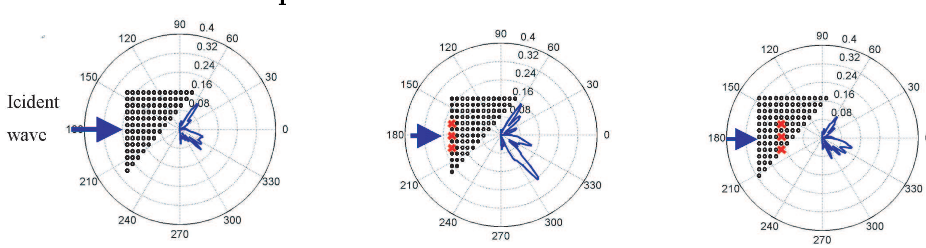

(a) (b) (c)

Figure 2: Measured near field radiation pattern at 12 GHz of metallic PBG-prism. a) Perfect PBG-prism, b) The PBG-prism with three cavities (in red) placed on the surface, and c) The PBG-prism with three defects inside.

The Fig. 2(a) shows the radiation pattern measured at 12 GHz of a prism without defect. The Fig. 2(b) gives the radiation pattern measured at 12 GHz of a prism with three defects on the surface of the dielectric. The Fig. 2(c) shows the radiation pattern measured at the at 12 GHz of a prism with three defects inside.

REFERENCES

1. Lustrac, A. de, T. Brillat, F. Gadot, and E. Akmansoy, "The use of controllable photonic band gap (CPBG) materials: an antenna application," *Optical-and-Quantum-Electronics*, Vol. 34, Nos. 1–3, 265, January–March 2002.

Dielectric Waveguide Filter with Cross Coupling

D. S. Jun, **H. Y. Lee**, **D. Y. Kim**, **S. S. Lee**, **E. S. Nam**, **and K. I. Cho**
Electronics and Telecommunications Research Institute, Korea

Recently, commercial millimeter wave applications such as 60 GHz communication systems or 77 GHz autonomous cruise control highly require surface mountable planar millimeter wave band-pass filters with a narrow bandwidth for low cost and compact integration of RF (Radio Frequency) front-ends. Metallic rectangular waveguide filters result in high production costs and bulky integration to planar circuits.

In this paper, we describe newly developed three resonator dielectric waveguide filters. The reduction in the number of resonators contributes to the compact, which is smaller than the previous three resonator dielectric waveguide filters. To improve stop band rejection for filters with a smaller number of resonators, cross coupling between 1st and 3rd resonators is introduced by twodimensional arrangement of resonators, which provides an attenuation pole at the higher frequency side of the pass band. The coupling between resonators is introduced by three-dimensional arrangement of resonators, which expect low cost and compact integration of RF front-end modules.

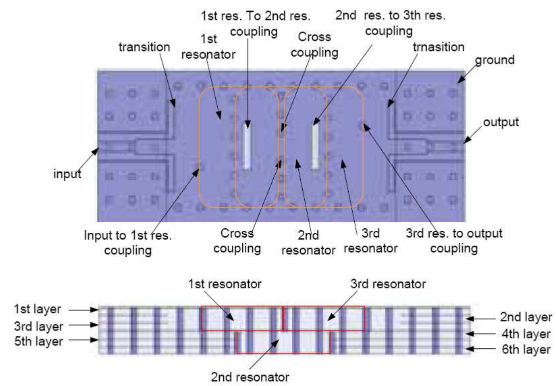

Figure 1: Schematic layout of BPF.

The waveguide structure is by forming metallized through holes in a dielectric substrate with metallized surfaces. In order to cross coupling for attenuation pole, the resonators are arranged twodimensionally. The structure facilitates realization of cross coupling by the space between though holes. T-shaped waveguide to GCPW (Ground Coplanar Waveguide) transitions lead to input/output ports, which enable flip chip bonding or external system probe connecting. The space between though holes around the input/output port must be sufficiently narrow to avoid propagation of the waveguide mode within the waveguide because a wide spacing can cause unwanted coupling. Also, the space between though holes of the waveguide structure must be sufficiently narrow to decrease radiation loss because a wide spacing can cause to increase insertion loss.

Planar dielectric waveguide filters with cross coupling were developed for 60 GHz band applications. The filters were fabricated using LTCC (Low Temperature Cofired Ceramics) for transceiver module. These filters will be applied to high-speed wireless communication systems.

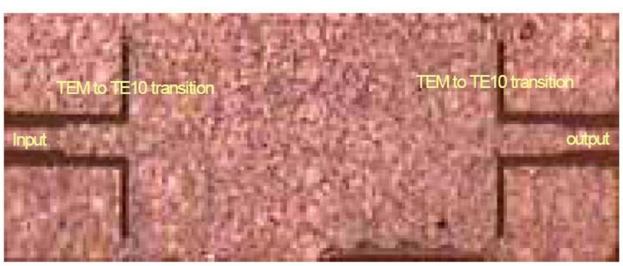

Figure 2: Photograph of a fabricated BPF.

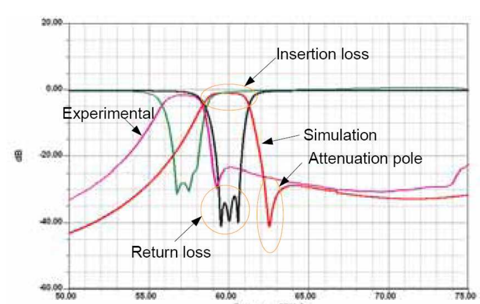

Figure 3: Experimental and simulation results of BPF.

Session 2P9
Time Reversal Techniques in Electromagnetics

Time Reversal: From Acoustics to Electromagnetism

M. Fink
University Denis Diderot, France

Time-reversal invariance is a very powerful concept in classical and quantum mechanics. In the field of acoustics and electromagnetism, where time reversal invariance also occurs, time-reversal experiments may be achieved simply with arrays of transmit-receive antenna, allowing an incident wave field to be sampled, recorded, time-reversed and re-emitted.

Time reversal mirrors (TRMs) may be used to study random media and complex reverberating structures. Common to these complex media is a remarkable robustness exemplified by observations that the more complex the medium between the probe source and the TRM, the sharper the focus. This property is related to the fact that TRMs work with broadband signals, contrary to phase conjugated mirrors. TRMs open the way to new signal processing's that interest imaging, detection and telecommunications.

Due to the limited frequency range of acoustics waves (KHz and MHz), TRMs have been first developed in this field of Acoustics. They have plenty of applications including ultrasonic therapy, medical imaging, non destructive testing, telecommunications, underwater acoustics, seismology, sound control and domotics. An overview of these fields will be presented.

Time reversal within the GHz range is now possible and it is now applied with Electromagnetic waves. A comparison of the TRM possibilities in Acoustics and Electromagnetism will be discussed.

Practical and Theoretical Aspects of Time Reversal of Electromagnetic Waves

J. de Rosny, G. Lerosey, and M. Fink
Université Paris 7, France

Since 1990, the time reversal of ultrasonic waves is studied at laboratoire Ondes et Acoustique from Paris, France. Experimental as well as theoretical aspects of Time Reversal are explored.

Very recently, the first experiment of time reversal of microwave electromagnetic waves was performed at our laboratory. In this experiment, the time-reversed electromagnetic wave was focused on a single antenna. Since then, we have built two 8-antenna arrays that lead us to measure the spatial focusing. With this new set-up, it was essential to have a better understanding of all the aspects of time reversal of Electromagnetic waves. It exits only a few previous theoretical works on time reversal of electromagnetic waves. However most of the time, they only address a few particular aspects of time reversal of Electromagnetic Waves. Here we would like to propose a theory that makes the link between fundamental and technical aspects of time reversal. Thus in a first part, we discuss general aspects of reversibility of Maxwell Equation. We generalized the concept of time reversal cavity, first introduced in acoustic, to the case of electromagnetic waves. We show that the time-reversed wave is linked to the imaginary part of the dyadic Green's function. However this fundamental approach of time reversal is not sufficient since the electromagnetic wave field is generated and recorded by the way of antenna. Then we describe the time reversal experiment in terms of currents and potentials. The equivalent electric schema of a two-antenna time-reversal experiment is proposed. The influence of the two antennas is taken into account by the way of a 2 by 2 mutual impedance matrix. We recall the link that exists between impedance matrix and dyadic Green's function. The theory is then generalized to linear array of antennas. We show that the time-reversed wave on the array is linked to the real part of the mutual impedance. Technically, an antenna is always loaded, i.e., the antenna is connected to the ground by the way of impedance in order to provide an impedance matching. Therefore we explain the influence of such loads on the focusing. Most of our experiments are performed in a electromagnetic reverberant chamber. We show how the reverberation leads to retrieve the time-reversed Green's function even with a few time-reversal antennas. The presentation will be illustrated with experimental results and numerical results.

Experimental Wideband Time Reversal of Microwaves

G. Lerosey, **J. de Rosny**, **A. Tourin**, and **M. Fink**
Universite Paris 7, France

Time reversal (TR) has been studied for a quite long time in ultrasound, and it has been shown that it is able to focus both in space and time a wave. In a recent paper we have shown that it is possible to time-reverse microwaves without the need to fully digitize the impulse response as it is done with ultrasound. In fact the interesting part of a radio frequency modulated signal being in its complex envelop, one has only to digitize the baseband impulse responses, to time reverse them and phase conjugate the carrier. This allowed the study of such a process with high frequencies using nowadays electronic components, but it was carried with a narrow bandwidth (2 MHz). TR communications have first been successfully performed with acoustic signals in underwater schemes. Recently we have studied the use of ultrasonic TR in a small-scaled indoor environment to characterize its benefits and drawbacks when doing ultra wide band communications. We have underlined that it drastically decreases the time spreading of the signals and allows spacial focusing of the information. The drawbacks are that it also creates inter-symbol interferences due to the fact that the medium is never exactly symmetric in time and that the number of sensor is never infinite. Some of these characteristics have also been addressed theoretically for the electromagnetic case. In this presentation we go further in the study as we developed a wide bandwidth time reversal mirror (up to 250 MHz of bandwidth) in order to have all information on the temporal and spatial focusing properties and to do the first real experiments of wideband TR communications. To that end, we have used separated components that were available commercially. The carrier frequency is generated at 2.45 GHz, the baseband signals come from a dual channel arbitrary waveform generator with 1 GS/s sampling, the modulation is achieved with an IQ modulator with a bandwidth of 250 MHz. The acquisition of the signals is made with a 4-channel 20 GS/s sampling digital scope. The down conversion and processing of the data is achieved numerically with Matlab because nowadays commercial demodulators have smaller bandwidth than the one we needed. In addition to this setup, which stands for a single channel time reversal mirror (TRM), we used two 8-channels switches in order to emulate a 8 channel TRM by linearity, the 8 other antennas being used as receiving antennas. This setup allowed us to study different part of electromagnetic TR process which will be described in this paper. All the experiments were conducted in an electromagnetic reverberating room with a Q factor of 30, because the emitting power of the setup did not allow in-room experiments. Further work will be done in a typical indoor setup, with a more powerful amplifier. In a first part, the temporal compression is investigated as a function of the bandwidth and the number of emitting antennas. A special attention is given to the gain in amplitude that is due to the TR temporal compression in terms of signal to external noise ratio. The effect of the correlation between antennas is also discussed and its effect on the TR sidelobes is shown. In the second part a clear evidence of the spatial focusing of a TR experiment is given. To that end, the 8 channel TRM is used to send a pulse on one antenna of a 8 antenna array receiver. The 8 receiving antennas are quarter-wavelength antennas on a ground plane. That way the field is scanned in the neighborhood of the focus point with model antennas. The result is compared to the analytical functions for spatial correlations of electromagnetic fields in 3 D, while taking the coupling into account. Finally, using the results of the above sections, the 8 channel TRM is used to send information to between 1 and 8 receivers that are 0.5 wavelength apart. It is shown that although no precoding nor error correcting code are used, high data rate communications can be achieved with a significant binary error rate, especially in a noisy environment.

Electromagnetic Super-resolution Time-reversal Nulling

D. D. Stancil, **A. G. Cepni**, **B. E. Henty**
Y. Jiang, **Y. Wei**, **J.-G. Zhu**, **and J. M. F. Moura**
Carnegie Mellon University, USA

A novel approach to exploiting multipath for communications and radar detection is time-reversal focusing. In this approach, the multipath is used to focus RF energy on a desired receiver or radar target. In a rich multipath environment, the energy can be focused onto a region roughly the size of 1/2 wavelength even if a line-of-sight is not present.

With suitable modifications to the time-reversed signals, it is possible to create a situation where the multiple paths interfere destructively at a desired location, resulting in a null rather than a focused spot. This technique can be useful for removing the effects of extraneous clutter in radar applications, or to minimize interference to an unintended receiver in communications applications.

In this talk we describe recent experiments in which we have demonstrated time-reversal nulling in both the frequency and time domains, and applied the technique to enhancing the detection of changes in an environment probed by radar. Two types of experiments are presented. The first type consists of frequency domain experiments using multiple antennas or synthetic aperture arrays, and involve bandwidths of up to 2 GHz. These experiments are performed in an open laboratory environment with controlled amounts of clutter. The second type consists of experiments performed in the time domain using a reverberant cavity formed by sections of HVAC duct capped on both ends. These experiments use single transmit and receive antennas and bandwidths up to 36 MHz.

Decomposition of the Time Reversal Operator for a Small Scatterer of General Shape

D. H. Chambers
Lawrence Livermore National Laboratory, USA

Many applications of time reversal to imaging and target characterization require decomposition of the time reversal operator. This is typically accomplished by applying the singular value decomposition to the multistatic response matrix of an array. The number and character of the singular values depends not only on the number of resolvable targets, but also on the particular scattering characteristics of each target. An understanding of how the scattering physics determines the singular values could lead to new methods of characterizing targets when direct imaging is difficult. In this paper we review the decomposition of the time reversal operator for a general planar array and a single small spherical target. We show how the conductivity and permittivity of the sphere can create up to six distinguishable singular values for a fully polarimetric array. We then extend this analysis to a small ellipsoidal scatterer and show how orientation and eccentricity modifies the behavior of the singular values and singular vectors. Results for the limiting cases of a disk and a rod will be presented. We show how orientation could be estimated by rotating an array and tracing the behavior of the singular values as a function of rotation angle.

This work was performed under the auspices of the U. S. Department of Energy by the University of California, Lawrence Livermore National Laboratory under Contract No. W-7405-Eng-48. Research partially supported by DARPA.

Time Reversal Based Multi-tone Imaging Algorithm

H. K. Zhao
University of California, USA

We develop an direct imaging algorithm using an active array. This imaging algorithm is based on time reversal technique and principal component analysis of the response matrix for the active array. The key point is to locate and visualize strong scattering events. The algorithm is very simple and does not need any forward solver. Also multiple-frequencies and multiple-measurements can be superposed naturally. Resolution based thresholding can be used to deal with highly noisy data. Stability and accuracy of of the algorithm for extended target and in random medium will be demonstrated.

Selective Focusing of Ultrawideband Fields in Dispersive and Continuous Random Media via DORT

M. E. Yavuz and F. L. Teixeira
The Ohio State University, USA

In lossless and stationary media, invariance of the wave equation under time-reversal (TR) enables optimal refocusing of time-reversed signals. In practice, this can be achieved using a TR antenna array (TRA), where received signals due to a (unknown) scatterer(s)/source(s) are retransmitted back to the original media in a time-reversed fashion. As the time-reversed signals backpropagate in the medium, they interfere constructively (due to phase conjugation) at the original source position(s) resulting in focusing capabilities that can be used to aid in detection and imaging problems. Under certain conditions, focusing obtained by TR can even outperform the classical diffraction limit, characterizing *superresolution*. Ultrawideband (UWB) operation and multiple scattering in the background media are some of the factors that can enhance the focusing resolution in TR applications via frequency decorrelation and spatial decorrelation, respectively. As a result, TR techniques can be particularly attractive in scenarios where strong multiple scattering occurs. Such conditions exist, for example, in subsurface sensing applications where the intervening soil media are in general inhomogeneous. However, information about the soil constitutive parameters is often incomplete and can only be described in a statistical sense via random medium models. A further advantage of TR techniques in this case is that, under UWB operation, they are *statistically stable*, i.e., they do not depend on the particular realization of the random media, but only on its statistical properties.

Here, we apply a method based on the decomposition of the time-reversal operator (DORT) to study a selective focusing approach for UWB subsurface sensing scenarios where the inhomogeneity of soil medium is modeled by *continuous* random medium models with prescribed first and second order statistics (spatially fluctuating random permittivities and correlation functions), and including frequency dispersive effects.

In order to exploit the UWB operation, this method is implemented over the entire available bandwidth in a consistent fashion. While direct TR would produce focusing around all scatterer locations, DORT allows *selective* focusing on the desired scatterer(s). We will study the effects of first and second order medium statistics on the DORT performance and focusing properties. Since frequency-dispersion breaks the TR invariance, several compensation methods for dispersive effects will be compared. Noise sensitivity of the eigenvalues (and corresponding excitation eigenvectors) will be studied towards using it as a criterion to distinguish (distributed) background clutter eigenvalues from those that correspond to distinct (discrete) scatterers. Throughout this study, we restrict ourselves to limited aspect array configurations.

Broadband Time Reversal Scheme for Target Detection in Highly Cluttered Field

J.-G. Zhu, **Y. Jiang**, **J. Moura**, **D. D. Stancil**, **Y. Jin**, **A. G. Cepni**, **and B. E. Henty**
Carnegie Mellon University, USA

In electromagnetic wave propagation, utilizing time reversal scheme, focus with superresolution has been experimentally demonstrated in highly cluttered environment [1, 2]. Based on such concept, a modified time reversal scheme based on the utilization of antenna array has also been developed to substantially enhance the target detection in highly cluttered environment. The spatial nullifying scheme results in a virtual elimination or substantial suppression of the scattering on the clutter while enabling automatic energy focusing on the target [3, 4]. In this paper, we present a time reversal scheme along using only a single antenna and a broad band illumination of a highly cluttered field for target detection.

Consider a single target in a cluttered field. A short pulse, corresponding to a broad spectral bandwidth, is broadcast from a single transmitter to the field. Echoes from the field with and without the target presence are recorded by a single receiver. The difference signal between the echoes with and without target is time reversed and mathematically rebroadcast to the field. The final received echo is used for an energy detector to assess the presence of the target. Figure 1 shows a 2-D FDTD simulation of a cluttered field along with a target. The scatters and the target are all identical square cross-sectioned metallic objects. AWGN is added to the receiver prior to the mathematical time reversal operation. Figure 2 shows the ROC curve for comparison between results of the broadband time reversal scheme the simple change detection.

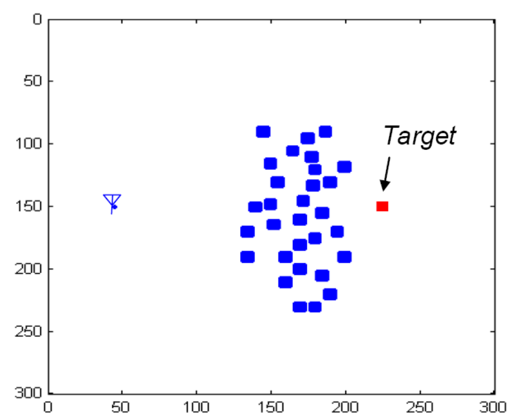

Figure 1: Cluttered field and target used in simulation.

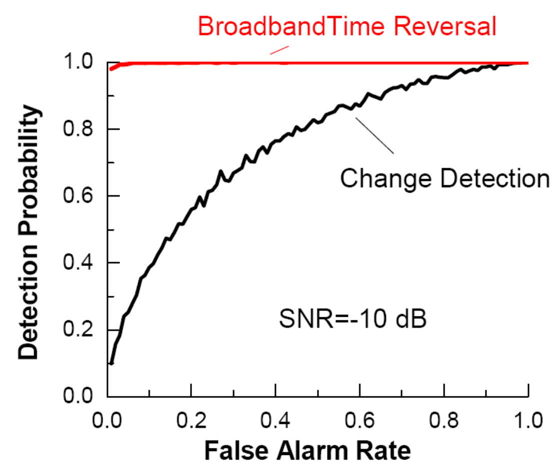

Figure 2: Calculated ROC curve using an energy detector.

REFERENCES

1. Lerosey, G., et al, *Phys. Rev. Lett.*, Vol. 92, 194301, 2003.
2. Henty, B. and D. Stancil, *Phys. Rev. Lett.*, Vol. 93, 243904, 2004.
3. Zhu, J. G., et al, *Antennas and Propagation Society International Symposium*, Vol. 4B, 135–138, 2005.
4. Moura, J. M. F., et al, *ICSSP05 Proceedings.*, Vol. 4, iv/1121, 2005.

Session 3A1a
Automatic Classification of Spectral Signatures and Scattering Patterns

A New Approach to Polarimetric SAR Image Classification

J. Yang, T. Xiong, and Y.-N. Peng
Tsinghua University, China

In this paper, a Generalized Optimization of Polarimetric Contrast Enhancement (GOPCE) is employed for supervised polarimetric synthetic aperture radar (SAR) image classification. The GOPCE introduced by the authors [1] is the extension of Optimization of Polarimetric Contrast Enhancement (OPCE), and it includes three optimal coefficients associated with the Cloude entropy and two special similarity parameters [2] in addition to the optimal polarization states. For classification, we first classify a polarimetric SAR image into several sets: $C_1, C_2, \ldots C_m$ and the mixed sets $C_{1,2}, C_{2,3}, \ldots C_{m-1,m}$ by some parameter (e. g., span), based on the polarimetric SAR data of the training areas. Then a mixed set is divided into two classes by using the GOPCE for several times. For comparison, we also use the Maximum Likelihood (ML) classifier, based on the complex Wishart distribution [4]. The classification results of a NASA/JPL AIRSAR L-band image over San Francisco by two approaches are listed in Table 1 and Table 2, respectively, demonstrating the effectiveness of the GOPCE based classifier.

Table 1: Classification results by the proposed method.

GOPCE	Sea area	Quasi-natural surface	Woods area	Urban area
Sea area	**96.89%**	3.11%	0%	0%
Quasi-natural surface	0.75%	**98.43%**	0.82%	0%
Woods area	0%	4.56%	**95.41%**	0.03%
Urban area	0	0	9.00%	**91.00%**

Table 2: Classification results by the Maximum Likelihood classifier.

ML	Sea area	Quasi-natural surface	Woods area	Urban area
Sea area	**98.30%**	1.57%	0.05%	0.08%
Quasi-natural surface	0.35%	**96.74%**	2.21%	0.7%
Woods area	0%	5.6%	**92.17%**	2.24%
Urban area	0%	6.84%	2.8%	**90.36%**

REFERENCES

1. Yang, J., G. Dong, Y. Peng, et al., "Generalized polarimetric contrast enhancement," *IEEE Geosci. Remote Sensing Lett.*, Vol. 1, No. 3, 171–174, 2004.
2. Yang, J., Y. N. Peng, and S. M. Lin, "Similarity between two scattering matrices," *Electron. Letters*, Vol. 37, No. 3, 193–194, Feb. 2001.
3. Yang, J., Y. Yamaguchi, W.-M. Boerner, and S. M. Lin, "Numerical methods for solving the optimal problem of contrast enhancement," *IEEE Trans. Geosci. Remote Sensing*, Vol. 38, No. 2, 965–971, 2000.
4. Lee, J. S., M. R. Grunes, and R. Kwok, "Classification of multi-look polarimetric SAR imagery based on complex Wishart distribution," *Int. J. Remote Sensing*, Vol. 15, No. 11, 2299–2311, 1994.

Soft Computing and Neural Adaptive Techniques for High Accuracy Data Classification

E. Binaghi and I. Gallo
Università degli Studi dell'Insubria, Italy

In this present work we intend to survey the recent salient experiences and main results obtained by our group in the field of Soft Computing and Neural Learning for Pattern Recognition.

To document our first significant research activity, we present a supervised classification model integrating fuzzy reasoning and Dempster-Shafer propagation of evidence; the model is built on top of connectionist techniques to address classification tasks in which vagueness and ambiguity coexist. The salient aspect of the approach is the integration within a neuro-fuzzy system of knowledge structures and inferences for evidential reasoning based on Dempster-Shafer theory. In this context the learning task can be formulated as the search for the most adequate "ingredients" of the fuzzy and Dempster-Shafer frameworks such as the fuzzy aggregation operators, for fusing data from different sources and focal elements, and basic probability assignments, describing the contributions of evidence in the inference scheme. The new neural model allows us to establish a complete correspondence between connectionist elements and fuzzy and Dempster-Shafer ingredients, ensuring both a high level of interpretability and high performance in classification.

A second salient experimental work developed by our group concerns contextual classification of remote sensing images. Many cases of remote sensing classification present complicated patterns that cannot be identified on the basis of spectral data alone, but require contextual methods which base class discrimination on the spatial relationships between the individual pixel and local and global configurations of neighboring pixels. However, the use of contextual classification is still limited by critical issues, such as complexity and problem dependency. We present a contextual classification strategy for object recognition in remote sensing images in an attempt to solve recognition tasks operatively. The salient characteristics of the strategy are the definition of a multiresolution feature extraction procedure exploiting human perception and the use of soft neural classification based on the Multi-Layer Perceptron model. Three experiments were conducted to evaluate the performance of the method-ology, one in an easily controlled domain using synthetic images, the other two in real domains involving built-up pattern recognition in panchromatic aerial photographs and high resolution satellite images.

The last work presented is representative of recent research interest focusing on 3D image analysis. In particular the work investigates the potential of neural adaptive learning to solve the correspondence problem within a two-frame adaptive area match-ing approach. A novel method is proposed based on the use of the Zero Mean Normalized Cross Correlation Coefficient integrated within a neural network model which uses a least-mean-square delta rule for training.

Two experiments were conducted for evaluating the neural model proposed. The first aimed to produce dense disparity maps based on the analysis of standard test images. The second experiment, conducted in the biomedical field, aimed to model 3D surfaces from a varied set of SEM (Scanning Electron Microscope) stereoscopic image pairs.

A Method to Solve an Acoustic Scattering Problem Involving Smart Obstacles

F. Zirilli
Universitá di Roma La Sapienza, Italy

In the context of time harmonic acoustic scattering we formulate an Inverse problem involving smart obstacles and we propose a method to solve it. A smart obstacle is an obstacle that when hit by an incoming acoustic wave tries to pursue a given goal circulating a suitable pressure current on its boundary. A pressure current is a quantity whose physical dimension is pressure divided by time.

The goals pursued by the smart obstacles that we have considered are the following ones: to be undetectable or to appear with a shape and/or acoustic boundary impedance different from its actual ones eventually in a location in space different from the actual location. We fix our attention on obstacles that pursue the goal of being masked that is obstacles that try to appear with a shape and an acoustic boundary impedance different from their actual ones. As a special case of masked obstacles we consider the case of furtive obstacles, that is obstacles that try to be undetectable.

We consider the following time harmonic inverse scattering problem: from the knowledge of several far fields generated by the smart obstacle when hit by known time harmonic waves, the knowledge of the goal pursued by the smart obstacle and of its acoustic boundary impedance reconstruct the boundary of the obstacle.

A method to solve this inverse problem that generalizes the so called HERGLOTZ function method used in inverse obstacle scattering is proposed. This method is based on the definition of two HERGLOTZ functions, one for the acoustic field scattered by the smart obstacle and one associated to the pressure current through an auxiliary variable. Under some hypotheses the HERGLOTZ functions are determined from the knowledge of the far fields. The knowledge of the HERGLOTZ functions makes possible the reconstruction of the boundary of the smart obstacle using ad hoc equations. Two numerical experiments that validate the method proposed are presented.

The website http://www.econ.univpm.it/recchioni contains a general overview of the work on scattering done in the past years.

A Neural Adaptive Algorithm for Feature Selection and Classification of Hyperspectral Data

I. Gallo
Università degli Studi dell'Insubria, Italy

Recent applications of Pattern Recognition and in particular of Image Analysis and Classification deal with high dimensionality data. In this context, the use of automated classification procedures is still limited by the lack of robust methods able to cope with the intrinsic complexity of high dimensionality and the consequent Hughes phenomenon, implying that the required number of labelled training samples for supervised classification increases as a function of dimensionality. The problem can be addressed in two complementary ways: identify a classification model less sensitive to the Hughes phenomenon and/or reduce the dimensionality of data and redundancies by applying feature selection strategies. Neural networks seems to be very good candidates for simultaneous feature selection and classification. In view of these considerations, I designed an experimental study to investigate the robustness of a non conventional classification model when dealing with high dimensionality data.

In particular this work presents a supervised adaptive classification model built on the top of Multi-Layer Perceptron, able to integrate in a unified framework feature selection and classification stages.

The feature selection task is inserted within the training process and the evaluation of feature saliency is accomplished directly by the back-propagation learning algorithm that adaptively modifies special bell functions in shape and position in order to minimize training error. This mechanism of feature selection avoids trial and error procedures which imply several training stages.

The model includes a method to determine whether a hidden unit should be removed or maintained. This pruning mechanism is fundamental for training speed up and in many cases leads to a hidden layer with only the minimum number of neurons i.e., two. An important aspect of this method is that it avoids to retrain the network after removal of a neuron and relative synapses, because the neuron was excluded by the learning procedure.

The adaptive model is conceived as a composition of full connected neural networks, each of them devoted to selecting the best set of feature for discriminating one class from the others.

Performances were evaluated within a Remote Sensing study aimed to classify MIVIS hyperspectral data. Inside the classification problem, a comparison analysis was conducted with Support Vector Machine and conventional statistical and neural techniques. The adaptive neural classifier performed a selection of the most relevant features and showed a robust behaviour operating under minimal training and noisy situations.

Moreover, experimental results on standard datasets confirm that this feature selection strategy achieves a competitive behaviour with respect to the other methods considered.

Classification of Single Particle Optical Scattering Patterns

G. F. Crosta
Università degli Studi Milano - Bicocca, Italy

Some experimental methods such as *TAOS* [1] are capable of collecting the light scattered by single airborne particles in the micrometer size range when the latter are illuminated by a triggered laser source (wavelength = 532 nm). Data consist of intensity patterns (Fig. 1) collected in a suitable solid angle at a high rate (>100 patterns per second).

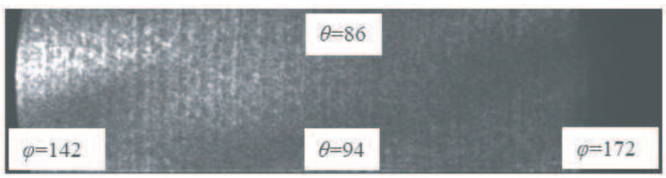

Figure 1.

Typical scattering pattern (***a07b03b***) produced by an aerosol particle from skid braking tests on a car racing track. Aerosol was collected by an 8-stage impactor device, re-suspended in water and injected into the *TAOS* apparatus.

There is no known theoretical method capable of dete rmining the particle size, shape and complex refractive in dex from such incomplete data. As a consequence a heu ristic algorithm was developed, which relies on spectrum enhancement for feature extraction and on principal com ponents (*PC*) analysis for classification. Spectrum en hancement of an image includes spatial differentiation, possibly of fractional order, followed by non-linear transformations aimed at separating structure from tex ture. *PC* analysis maps each input pattern into a point in the *PC* space. The classifier was trained with the aim of maximizing discrimination between suitable sets of *TAOS* patterns e.g., those labelled 1 and 2 in Fig. 2. New sets of patterns e.g., those from skid braking aerosol particles (labelled 4), were then submitted to the classifier. The result is also displayed by Fig. 2. From the PCs of a given pattern one can estimate how much the shape of the particle deviates from the spherical one.

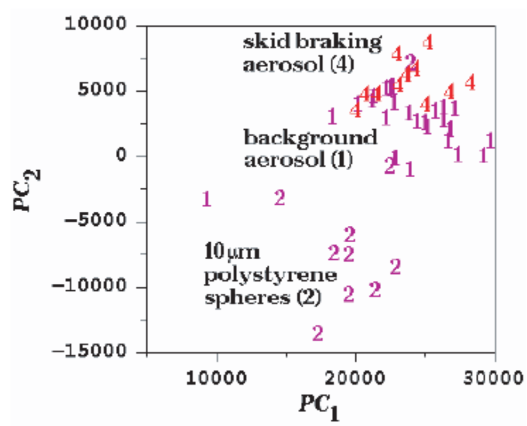

Figure 2: Classification of TAOS patterns from environmental aerosol particles: train on{1,2}→recognize{4}, $142.88432 < \varphi < 168.517815$, $86.083414 < \vartheta < 93.948435$, Exec = w05, $\delta = 45$deg, $p = 2.2$, $d + 1 = 10$, axis = u_1, $0 <= |u| <= 255$, dim[{PC}] = 10.

REFERENCES

1. Holler, S., S. Zomer, G. F. Crosta, Y.-L. Pan, R. K. Chang, and J. R. Bottiger, "Multivariate analysis and classification of two dimensional angular optical scattering (TAOS) patterns from aggregates," *Applied Optics*, Vol. 43, No. 33, 6198–6206, 2004.

Feature Extraction by Fractional Order Differentiation

G. F. Crosta
Università degli Studi Milano - Bicocca, Italy

The spectrum enhancement algorithm has been used for some time for separating structure from texture and extracting features from images (including optical scattering patterns) for automatic classification and recognition. The relevant definition and properties of spectrum enhancement and the relation of the latter to fractional differentiation are outlined below.

Let $Q\Omega$ denote a square of sidelength L and $\mathcal{T}$ the surface of the torus obtained by glueing the opposite sides of $Q\Omega$ together. Assume the grayscale image is modeled by a function $Qg[\boldsymbol{x}]$, $\boldsymbol{x} \equiv \{x_1, x_2\} \in Q\Omega$, which is continuous on $\mathcal{T}$. Next let $Q\Omega$ be discretized by a square grid of steplength ℓ. Let $\boldsymbol{u} \equiv \{u_1, u_2\}$ be the spatial frequency vector. Then the discrete FOURIER transform $G[\boldsymbol{u}]$ of $Qg[.]$ is supported in the square $0 \leq |u_1|, |u_2| \leq u_{max} = L/2\,\ell - 1$ cycles/image. Let $\boldsymbol{u}$ be represented in polar coordinates $\boldsymbol{u} \equiv \{u, \theta\}$. Denote by $|G[\mathrm{u}]|^2$ the power spectral density. Let Θ denote an arc symmetric with respect to either axis ($\boldsymbol{u}_1$ or $\boldsymbol{u}_2$) and let the normalized, arc-averaged spectral density profile be the function $s[.]$ of $u = |\boldsymbol{u}|$ defined in $0 \leq u \leq u_{max}$ (cycles/image) according to

$$s[u] = \frac{1}{|\Theta|} \int_{\Theta} 10\mathrm{Log}_{10} \left[\frac{|G[u]|^2}{|G[0]|^2} \right] u\, d\theta, \tag{1}$$

where $|\Theta|$ is the length of Θ and obviously $|G\,[0]|^2 \neq 0$ for any non-degenerate image. Let $m[u]$ be a model spectral density such that

$$m^{(p)}[u] = 0, \quad 0 \leq u \leq 1; \quad m^{(p)}[u] = -10\mathrm{Log}_{10}[u^p], \quad u \geq 1 \quad \text{cycles/image}, \tag{2}$$

where p (>0) is the model exponent. Then, the $m^{(p)}[.]$-enhanced spectrum $h[u]$ is defined by

$$h[u] = s[u] - m^{(p)}[u], \quad 1 \leq u \leq u_{\max}. \tag{3}$$

Intuitively, the function $h^{(p)}[.]$ represents deviations of $s[.]$ from the model $m^{(p)}[.]$. The values of L, u_{max}, $|\Theta|$, p are determined by the intended application.

Assume the image is not degenerate. Then the following properties can be shown to hold.

a) If p satisfies $p/2 = N$ (>0), integer, then the tempered distribution $H^{(p)}[\boldsymbol{u}]$ defined by

$$H^{(p)}\,[u] = |u|^p\, \frac{|G\,[u]|^2}{|a_{0,0}|^2} + \delta\,[u]\,, \tag{4}$$

has the following representation in terms of FOURIER transforms ($\mathcal{F}$) of derivatives of $Qg[.]$:

$$H^{(p)}[u] = \frac{1}{|a_{0,0}|^2} \sum_{n=0}^{N} \binom{N}{n} \left| \mathcal{F}\left[\frac{\partial^N Qg}{\partial^{(N-n)} x_1 \partial^n x_2} \right] \right|^2 + \delta\,[u]\,. \tag{5}$$

b) If $p/2$ is not an integer, then fractional derivatives and anti-derivatives of $Qg[.]$ of net order $p/2$ appear in the representation of $H^{(p)}[\boldsymbol{u}]$ and the sum in Eq. (5) is replaced by a binomial series.

c) In either case, if all FOURIER coefficients satisfy $|a_{l,m}|^2 \geq \varepsilon > 0$ the relation between $H^{(p)}[.]$ of Eq. (4) and the enhanced spectrum $h^{(p)}[.]$ of Eq. (3) is

$$h[u] = \frac{10}{|\Theta|} \int_{\Theta} \mathrm{Log}_{10}\,[H[u]]\, u\, d\vartheta. \tag{6}$$

Session 3A1b
Seabottom Electromagnetic Imaging and Detection Technologies

Modeling and Inversion of Marine CSEM Data

K. Hokstad[1], T. Røsten[1], and E. Gundersen[2]

[1]Statoil Research Centre, Norway
[2]Statoil, Stavanger, Norway

The principle of the marine controlled-source electro-magnetic (CSEM) technique used for remote detection of hydrocarbons (HC), is described by Ellingsrud et al., (2002). A horizontal electrical dipole (HED) emits an ultra-low frequency (0.1–5 Hz) electromagnetic (EM) wavefield into the underlying seabed and downwards into the subsurface. EM energy is rapidly attenuated in the conductive seafloor sediments. In high resistive layers such as HC-filled sandstones and at a critical angle of incidence the energy is guided along the layers and attenuated less. The detection of this guided and refracted energy is the basis of marine CSEM in HC exploration.

Before interpretation of the CSEM data is possible, extensive data processing is required. Important processing steps include: (1) window-based Fourier transform from time to frequency, (2) separation of down-going and up-going (scattered) fields, (3) depth migration, and (4) full inversion, estimating subsurface conductivity. Here we will focus on the last two processing steps; depth migration and inversion, and the use of forward wavefield simulations as part of the necessary workflow.

Zhdanov et al., (1996) introduced frequency-wavenumber (fk) and finite-difference depth migration methods for CSEM data, based on familiar ideas from seismic imaging (Claerbout, 1985). There are, however, important differences in migration of CSEM data, compared to seismic data: First, the attenuation of EM-fields in a conducting subsurface is very strong, and ultra-low CSEM data suffer significantly from dispersion. Second, the conductivity contrast at the sea floor is usually significant. Third, the horizontal and vertical conductivity can differ significantly, which leads to strong anisotropy.

The migration methods mentioned above does not handle EM-wavefield amplitudes correctly. In fact their seismic counterparts, were never assumed, nor designed, to do so. Hence, the result of depth migration is only a structural image of conductivity contrasts. To compute estimates of the subsurface conductivity, full inversion must be used. In steepest-decent and conjugate-gradient inversion schemes (Newman et al., 1997), the gradient in the first iteration provides a structural image of the subsurface. In seismic imaging the gradient calculation is referred to as reverse-time migration (Mittet et al., 2005).

A subsurface conductivity anomaly is not a unique hydro-carbon indicator. It may be due to other resistive bodies or layers in the subsurface, such as salt and igneous intrusions (sills) or regional trends (e.g., basin thickening). In the interpretation of marine CSEM data for HC exploration, these anti-models must be considered. In a typical workflow, numerical forward modelling is used to simulate and evaluate all realistic scenarios. The EM results are used, together with other information, e.g., seismic data, to risk exploration prospects before drilling decisions are made. In the presentation we will show examples from marine CSEM field data, and discuss some of Statoils experience using this technology.

REFERENCES

1. Claerbout, J. F., *Imaging the Earth Interior*, Blackwell Sci. Publ, 1985.
2. Ellingsrud, S., M. C. Sinha, S. Constable, L. M. MacGregor, T. Eidesmo, and S. Johansen, "Remote sensing of hydrocarbon layers by Sea Bed Logging (SBL): results from a cruise offshore Angola," The Leading Edge, Vol. 21, 972–982, 2002.
3. Mittet, R., F. Maaø, O. M. Aakervik, and S. Ellingsrud, "Depth migration of SBL data," *Ann. Internat. Meetg. Eur. Ass. of Geoscientists. and Engineers*, Exp. Abstracts, H08, 2005.
4. Newman, G. A. and D. L. Alumbaugh, "Three-dimensional massively parallel electromagnetic inversion-I. Theory," *Geophys. J. Int.*, Vol. 128, 345–354, 1997.
5. Zhdanov, S. M., P. Traynin, and J. R. Booker, "Underground imaging by frequency-domain electromagnetic migration," *Geophysics*, Vol. 61, 666–682, 1996.

Experience with the Three-dimensional Imaging of Marine Controlled Source Electromagnetic Data for Hydrocarbon Exploration

J. J. Carazzone and D. A. Pavlov
ExxonMobil Upstream Research Company, USA

Experience with the three-dimensional inversion of frequency domain, controlled, multi-source, electromagnetic data collected in the deep water marine environment suggests that the derived resistivity images can, under appropriate conditions, play a useful role in commercial hydrocarbon saturation predictions. Significant technical challenges exist in the simulation and inversion of these data.

The Marine Controlled Source Electromagnetic (MCSEM) surveys conducted by ExxonMobil beginning in 2002 provide data for which electromagnetic imaging offers a significant potential due to the relatively high spatial density of the electric field recordings, the low level of anticipated noises and the excellent electrical coupling provided by the marine environment. Unfortunately, significant technical issues are presented by the large subsurface volume probed by low frequency electromagnetic recordings, the large dynamic range of the recorded data, the large number of source positions, and the three-dimensional nature of the anticipated targets. Inversion results at locations offshore of West Africa illustrate the progress made in confronting these technical difficulties and progress toward the goal of establishing a new class of hydrocarbon exploration tools.

Electromagnetic soundings in conductive sediments are heavily constrained by the skin-depth phenomena to a very narrow range of frequencies which must both successfully penetrate to maximum target depth and also resolve significant conductivity variations between the sea bottom and the target zone. The implied frequency range for targets of practical interest varies from approximately 1/16 Hz to 2 Hz and the skin depth from 2 km to no less than 0.2 km. On these scales reservoir targets are unquestionably three dimensional objects for which two dimensional approximations are either inappropriate or unnecessarily restrictive. Sediments and seawater are assumed to exhibit conductivity values ranging from about 6 s/m to values in the range of 0.01 s/m in well saturated hydrocarbon reservoirs. Only three general techniques for simulation and, therefore, inversion of Maxwell's equations (in the frequency domain) are available for three-dimensional models: integral equations (IE), finite difference (FD), and finite element (FE). Weak scattering approximations, particularly of the distorted wave type, may have some domain of application (yet to be shown) due to the limited range of subsurface conductivity values anticipated. However, these methods may face difficulties associated with the large size of the domain of unknown subsurface resistivities sought by the inversion process. The availability of a massively parallel FD approach dictated its selection for this undertaking versus a more sophisticated FE approach restricted in scope to a single processor platform. Inversion results reported in this presentation use both amplitude and phase information derived from the ocean bottom electric field recordings.

Application of inversion technology to MCSEM datasets from offshore of West Africa over both hydrocarbon reservoir and non-reservoir locations shows that hydrocarbon data signatures, particularly for the electric field component parallel to the applied transmitter current, can be effectively imaged into three dimensional resistive bodies which are often broadly consistent with existing seismic structures. Carefully processed MCSEM data has repeated been found to fit likely three dimensional models to a very high percentage of electric field energy, frequently exceeding 95%. Inverted resistivity images displayed against the more conventional dense seismic depth images illustrate the potential for the new MCSEM tool in hydrocarbon exploration.

New Advances in 3D Imaging of Sea-bottom EM Data for Offshore Petroleum Exploration

M. S. Zhdanov
University of Utah, USA

During recent years a significant progress has been made in developing new mathematical methods and computer codes for interpretation of the sea-bottom electromagnetic (EM) data for offshore petroleum exploration. In this paper I present an overview of effective imaging techniques, which include the fast sea-bottom EM imaging based on the principles of electromagnetic migration, different types of integral representations for EM responses in the receivers, and regularized inversion. Electromagnetic migration, similar to seismic migration, is based on a special form of downward continuation of the observed field, which can be computed as a solution of the boundary value problem for the adjoint Maxwell's equations, in which the boundary values of the migration field on the earth's surface are determined by the observed EM data. It is shown that EM migration can be treated as an approximate solution of the corresponding EM inverse problem.

Another approach is based on iterative quasi-linear (QL) inversion with the accuracy control using rigorous integral equation (IE) method. In the framework of this approach the background conductivity may be formed by a layered formation, or may be described by arbitrary conductivity distribution. This allows us to incorporate known information about the geoelectrical structures in the inversion and keep it unchanged during the inverse process.

The new imaging methods are tested on the typical models of the sea-bottom EM surveys for offshore petroleum exploration, including magnetotelluric (MT) surveys and Seabed Logging (SBL) synthetic data.

Three Dimensional Electromagnetic Modeling and Inverison of Seabottom Electromagnetic Data

G. A. Newman and M. Commer
Earth Sceinces Division, USA

Modeling and inversion of low frequency (10 to 0.1 Hz) seafloor electromagnetic data present significant technical challenges because of the enormous quantity of data that is acquired during a field experiment. The problem is further compounded because transmitter-receiver offsets easily exceed ten's of kilometers and the large subsurface volumes that are sensed beneath the sea floor are inherently three-dimensional (3D) in the context of hydrocarbon exploration. Thus modeling and inverting such data is no simple task. There are several methodologies available to treat the problem and here we focus on finite-difference FD methods. Because FD solutions to the 3D time harmonic Maxwell's equations in the quasi-static limit can be solved relatively rapidly on distributive computing platforms, these methods have the flexibility to treat the large scale nature of the problem. Nevertheless much work remains in accelerating 3D FD solutions to the forward and inverse modeling problems. Here we are investigating a variety of approaches. For the forward problem we present some preliminary results of solution acceleration using multigrid (MG) as a preconditioner for Krylov subspace iteration methods that are used to solve sparse, large-scale, linear systems that arise from the finite difference approximation of 3D Maxwell equations. With the inverse problem we present some results for preconditioning the inverse iteration based on approximate adjoint methods for nonlinear conjugate gradient and Gauss-Newton optimization strategies. Because 100's to 1000's of solutions to the forward modeling problem are required with either optimization strategy, MG methods also offer the potential for significant speedup in the context of inverse modeling.

A Critical View about Marine Controlled Source EM Data Interpretation

P. Dell'Aversana
Eni S.p.A., Italy

The Sea Bed Logging (SBL) or Marine Controlled Source Electromagnetic (MCSEM) method is aimed at detecting and characterising resistive layers, possibly corresponding with hydrocarbon bearing reservoirs.

The basic principle driving the interpretation of the Marine CSEM data is that electric field magnitude and phase vs. offsets (recorded by a series of receivers deployed at sea floor) will show different trends as a function of the resistivity distribution and depending on water depth.

An interpretation approach that is commonly used in the hydrocarbon industry is based on the assumption that, if a proper reference receiver is selected (for instance in correspondence of an area where hydrocarbon absence has been proven), the normalised magnitudes and phases vs. offset (i. e., the observed data vs. the reference data) can represent an indication of resistive layers, possibly associated with presence of hydrocarbons.

In that framework normalized magnitudes significantly higher than 1 at intermediate to far offsets can be interpreted in terms of subsurface resistivity anomalies. Using a similar approach, also the normalised phases are assumed to be indicators of resistivity anomalies.

It is not difficult to show that, especially in shallow water environment (300–400 m), the above assumptions can be misleading.

If a "perfect" up-down wave separation is performed many of the ambiguities can be avoided. The problem is that a perfect elimination of the airwave effect cannot be guaranteed in any case. The risk is the production of artefacts and misleading interpretation.

An additional open question is about the choice of the reference receiver. Other misunderstandings can be originated by effects due to the presence of resistive layers above and below the target, by the variations of water depth along the acquisition profiles, by the presence of noise and so on.

In this work we clarify better the above concepts using simple synthetic tests and real data. Our goal is to show how the interpretation techniques based on normalised plots should be integrated with a an approach massively based on inversion of MCSEM data.

This is fundamental for an appropriate interpretation, especially if constrained by seismic data, in order to limit the ill-conditioned and ill-posed nature of the inverse electromagnetic problem.

Session 3A2
Optics and Photonics

Numerical Analysis of Light-wave Scattering from Blue Laser Optical Disk Models with Random Rough Surfaces

T. Kojima and T. Kawai
Kansai University, Japan

We have analyzed the scattering of an optical wave from various models of optical disk by numerical simulation methods, e.g., the boundary element method (BEM) or the finite-difference time domain (FDTD) method in the previous paper [1, 2]. In general, the boundary surface between two different layers of multilayered disk structure has more or less microscopic roughness.

In order to consider the influences of the surface roughness on the scattering characteristics, we have presented the numerical simulation of the scattering of a Gaussian beam from optical disk structures with random rough surfaces.

In the present paper, the deterioration of the detected signal characteristics due to the surface roughness is estimated by using numerical simulation models. The computer-generated rough surface model [3] is applied to the multilayered disk structures for blue laser. The scattered light-intensity collected in the aperture of an object lens can be calculated by FDTD method. It is shown that the sum- and differential signal outputs are estimated by using numerically calculated scattered intensity of light. An example of the numerically calculated cross talk characteristics between two adjacent recording marks is also shown and discussed.

REFERENCES

1. Kobayashi, I., T. Kojima, S.-I. Fukai and Y. W. He, "Numerical analysis of light-beam diffraction from magneto-optical disk medium by FDTD Method," *IEICE Trans. Electron*, Vol. E-84-C, No. 9, 1189–1196, Sept. 2001.
2. Kojima, T., H. Hotta and Y. Asano, "Three-dimensional (FD)2TD analysis of light-beam diffraction from phase-change optical disks with land/groove structures," *IEICE Trans. Electron*, Vol. E-86-C, No. 9, 1861–1867, Sept. 2003.
3. Kojima, T. and T. Yamazoe, "Scattering of a focused beam from random rough surface - Analysis by computer simulation," *Proc. of 24th General Assembly of the International Union of Radio Science*, Aug. 1993.

Optically Tunable Photonic Crystal Reflectance Filter

D. W. Dobbs and B. T. Cunningham
University of Illinois at Urbana-Champaign, USA

We have demonstrated a photonic crystal structure whose properties are tunable with laser illumination through the incorporation of a nonlinear dye. Laser illumination causes a change in the bulk refractive index of a polymer that is doped with the dye, leading to controlled tuning of the photonic crystal reflectance spectrum.

The device, shown in Figure 1, consists of a one-dimensional periodic ($\Gamma = 550\,\text{nm}$) surface structure fabricated on a low refractive index plastic substrate that is overcoated with a layer of high refractive index TiO_2. The process is performed over large surface areas on continuous rolls of plastic film. A solution containing 95% polymethylmethacrylate (PMMA) and 5% N-Ethyl-N-(2-hydroxyethyl)-4-(4-nitrophenylazo)aniline by weight is spin-coated onto the structure, resulting in a solid film with a thickness of several microns. When the fabricated structure is illuminated with broadband light at normal incidence with the light polarization perpendicular to the grating lines, a narrow band of wavelengths ($\lambda = 891\,\text{nm}$, $FWHM = 1\,\text{nm}$) is strongly reflected. We have demonstrated that upon laser illumination, the wavelength of the reflection resonance can shift to lower wavelengths by $> 2\,\text{nm}$, and that the resonance returns to its original wavelength when the illumination is turned off. For the resonancetuning effect to be achieved, the wavelength of the laser must be within the absorption spectrum of the dye, which is centered at a wavelength of 500 nm. As shown in Figure 3, we have characterized the switching speed and dependence of the wavelength shift with laser intensity. Because the switching behavior is independent of the polarization of the incident laser beam, the bulk refractive index change is likely caused by the trans-cis excitation of dye molecules. Numerical simulations show that the magnitude of the bulk refractive index change in the dye-doped polymer film is as large as 0.01.

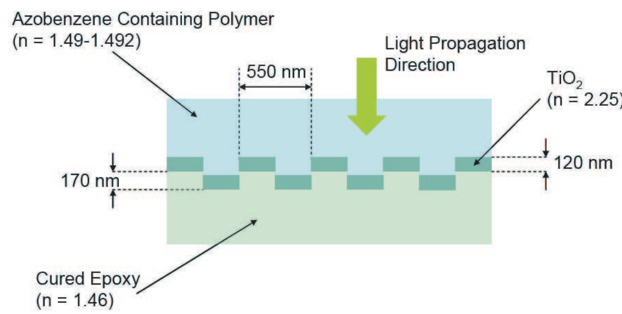

Figure 1.

Because the device structure can be fabricated inexpensively in plastic over large areas, and because a high density of independently addressable locations will be achieved due to lateral optical confinement by the photonic crystal, we expect the new device to find applications in optical computing, storage, switching, and multiplexing.

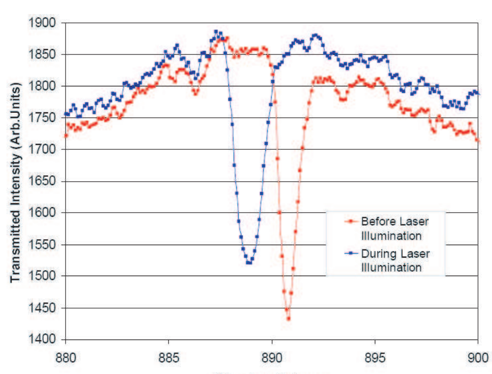

Figure 2.

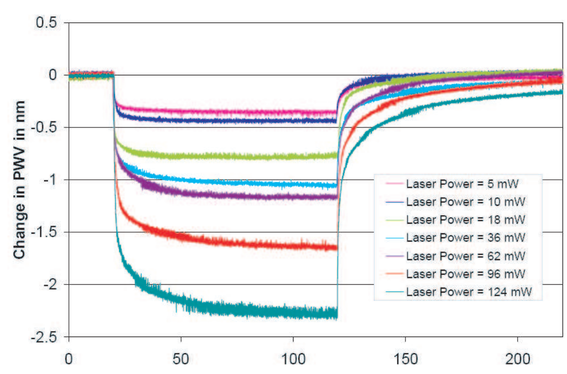

Figure 3.

Focal Switch Effect of Focused Cosine Gaussian Beam

C. J. Peng
Jingdezhen Comprehensive College, China

J. L. Chen
MinJiang University, China

F. X. Lu
Fuzhou Kaixin Real Estate Co., Ltd, China

The light intensity on axis and the focal switch effect of cosine Gaussian beam focused by a thin lens without aperture is studied in detail by using Collins formula. The third-order algebraic equation determining the position of the axial maximum intensity and the formula of the relative transition height are derived. It is shown that the relative focal shift and the focal switch depend on the optical system parameter s/f, beam parameter $\alpha = w_0\Omega_0$, and Fresnel number of beam N_w. Numerical calculation results are presented to illustrate the theoretical predictions. It is shown that if the beam parameter α is smaller than 1, there only exist one axial irradiance maximum, and the focal shift changes slowly with the change of the optical system parameter. So the focal switch of cosine Gaussian will not occur. When the beam parameter α is bigger than 1, the on-axis light intensity is split into two-peaks, which are separately at the both sides of the geometrical focus. The two peaks reach the same height when the optical system parameter s/f equals 1. The relative focal shift changes from negative to positive number, and the focal switch occurs at this point. For example, when the parameters for calculation are Fresnel number of beam $N_w = 2$ and the beam parameter $\alpha = 1.5$, the relative focal shift changes from the left of geometrical focus ($z_{f1} = -0.1779$) to the right of geometrical focus ($z_{f2} = 0.1779$). It is also found that the relative transition height $\Delta z_f = |z_{f1} - z_{f2}|$ increases with the increase of the beam parameter s/f, and decreases with the increase of Fresnel number of beam N_w. Numerical calculation results show that when the beam parameter α is bigger than 1, there exists a hollow between two peaks on the axiswhich becomes deep with the increase of the beam parameter. When the beam parameter is bigger than 3.5, the intensity near the hollow approximately equals zero.

Band-stop Filters in Microstrip Technology with Non-periodic Frequency Responses

I. Arnedo, T. Lopetegi, D. Benito, F. J. Falcone, and M. A. G. Laso
Universidad Pública de Navarra, Spain

Periodic structures have been always an important research issue within the microwave community. One of their well-known drawbacks is that the frequency responses of classical band-stop periodic structures exhibit undesirable stop-bands at the harmonics of the design frequency. On the other hand, Photonic Band-Gap (i.e., band-stop) structures in microwave technology recovered the interest in the periodic structure theory in the last years, proposing a new nondiscrete approach [1] that made possible a huge number of brand new devices. In this paper, single and doublefrequency-tuned Photonic Band-Gap microstrip filters with controlled suppression of the spurious bands at the harmonics of the designed frequencies are presented, based on the Coupled-Mode Theory [2].

Periodic band-stop structures following sinusoidal PBGtype etching profiles in the ground plane of a microstrip line [1, 2] or modulating the upper strip [3] have been profusely reported in the literature. Assuming that only the fundamental quasi-TEM microstrip mode is propagating, its forward and backward waves are related by means of the socalled coupling coefficient, $K(z)$, which is proportional to the first derivative of the impedance to the propagation axis, z [2]. Provided the etching profile or modulated strip-width are periodic, $K(z)$ may be expressed through its Fourier series where K_n are the coefficients of this series. Almost exact analytical expressions may be obtained for the central frequency, $f_n = c \cdot n/(2 \cdot \Lambda \cdot \sqrt{\varepsilon_{eff}})$, rejection level, $|S_{21}|_n = \mathrm{sech}(|K_n| \cdot L)$, and bandwidth between zeroes of reflection, $BW_n = c \cdot |K_n|/(\pi \cdot \sqrt{\varepsilon_{eff}}) \cdot \sqrt{1 + (\pi/K_n \cdot L)^2}$, of the n-th stop-band, which relate these parameters to the n-th coefficient of the Fourier series K_n (being c the speed of light in vacuum, and ε_{eff} the effective relative dielectric permittivity). The previous equations show that in order to suppress all the harmonic pass-bands, we would have to design adequately the perturbation so that $K_n = 0$ for $n \neq \pm 1$, obtaining for instance a nearly sinusoidal strip-width modulation.

Harmonic stop-bands may be observed in measurements for strip-width sinusoidal modulation of a microstrip line with period $\Lambda = \pi/200$ and length $L = 8 \cdot \Lambda$. Perfectly sinusoidal perturbation leads to a quasi-sinusoidal coupling coefficient, which provides not very deep harmonic stopbands. The strip-width modulation is now altered so that $K(z)$ is perfectly sinusoidal ($K_{\pm 1} = 35\, m^{-1}$ and $K_n = 0$ for $n \neq \pm 1$). Now, in measurements, harmonic stop-bands are perfectly suppressed.

Interesting design capabilities can be shown. For instance, for a filter with two stop-bands at 3 GHz and 5 GHz, 20-dB attenuation and 1GHz bandwidth each, a doubly periodic ($\Lambda_1 = 19.12$ mm and $\Lambda_2 = 11.47$ mm) modulation along a $L = 172.08$ mm-long device with $|K_{\pm 1}|_{1,2} = 19.17\,\mathrm{m}^{-1}$ may fulfil these requirements. The agreement between simulation and measurement results is very good.

REFERENCES

1. Laso, M. A. G., T. Lopetegi, M. J. Erro, D. Benito, M. J. Garde, and M. Sorolla, "Multiple-frequency-tuned photonic bandgap microstrip structures," *IEEE Microwave and Guided Wave Letters*, Vol. 10, No. 6, 220–222, June, 2000.
2. Lopetegi, T., M. A. G. Laso, M. J. Erro, M. Sorolla, and M. Thumm, "Analysis and design of periodic structures for microstrip lines by using the coupled mode theory," *IEEE Microwave and Wireless Components Letters*, Vol. 12, No. 11, 441–443, Nov. 2002.
3. Nair, N. V. and A. K. Mallick, "An analysis of a widthmodulated microstrip periodic structure," *IEEE Transactions on Microwave Theory and Techniques*, Vol. 32, No. 2, 200–204, Feb. 1984.

Time-domain Statistics of Multi-layer Optical Filters

H. E. Rowe
Stevens Institute of Technology, USA

We calculate the time-response statistics for multi-layer optical filters with random errors in layer thickness or index of refraction.

Exact statistics have been determined for the reciprocal transfer function in the wavelength domain, using Kronecker product methods. Transfer function statistics are then obtained by applying perturbation theory to these exact results. This is valid because useful devices depart only slightly from their ideal design. These approximate results have been verified by comparison with exact results for special cases. First- and second-order transfer function statistics in the wavelength domain have previously been presented.

The average transfer function, varying with frequency or wavelength, is deterministic. The transfer fluctuations about the average are random. The covariance of the transfer function fluctuations in the wavelength domain has been calculated using the above methods.

The wavelength λ is a natural parameter for calculating transmission statistics. However, we require similar results as functions of frequency f in order to determine time-domain statistics. Thus for a random transfer function, the expected value of the square of the envelope of the impulse response is proportional to the Fourier transform of the covariance of the transfer function.

We separate the transfer function into deterministic and random components:

$$T(f) =< T(f) > +\Delta T(f).$$

The covariance of the random component is

$$C(f_1, f_2) =< \Delta T(f_1)\ \Delta T * (f_2) > .$$

The impulse responses for these two components are their Fourier transforms:

$$G(t) < - >< T(f) >;\ g(t) < - > \Delta T(f).$$

We use the symbol $< - >$ to denote the Fourier transform relationship. The corresponding envelopes for these time functions are $r_G(t)$ and $r_g(t)$. Then $< |r_g(t)|^2 >$, the average square envelope of the random impulse response, is calculated from the covariance C of the random component of the transfer function.

We present results for a 13-layer band-pass optical filter.

REFERENCES

1. Rowe, H. E., *Electromagnetic Propagation in Multi-Mode Random Media*, John Wiley, New York, 1999.
2. Rowe, H. E., "Second-order statistics of multi-layer optical coatings," *PIERS 2002 Proceedings*, 310, July 1–5, 2002.

Direct Light to RF Fiber Antenna

J. Flattery[1], **T. L. Jamison**[2], **and P. Kornreich**[1]

[1]Syracuse University, USA
[2]NASA Goddard Space Flight Center, USA

We are developing an antenna that directly converts a modulated optical signal to microwave radiation. This is useful as an element in a Phased Array Antenna (PAA). Currently signals to each element of a PAA are supplied through an optical fiber. The signal is detected, converted to an electronic form, amplified and applied to the antenna element. The direct optical conversion system eliminates the microwave amplifier at each antenna element. The antenna element consists of a single mode optical fiber that has two dissimilar semiconductor layers at the core cladding boundary as shown in Fig. 1. Since the two semiconductor layer structure does not have inversion symmetry there will be a first order non linear effect which is much larger than higher order non linear effects used in conventional non linear fibers. Two optical signals that differ in frequency by the microwave frequency propagate through the fiber1. The large nonlinearety of the fiber causes mixing of the signals. Signals at the sum and difference frequency are obtained. The difference frequency is the microwave frequency. The fiber will not guide signals at the microwave frequency. These will be radiated by the fiber section. Thus the fiber becomes a microwave antenna. The sum signal is radiated out at the top of the fiber.

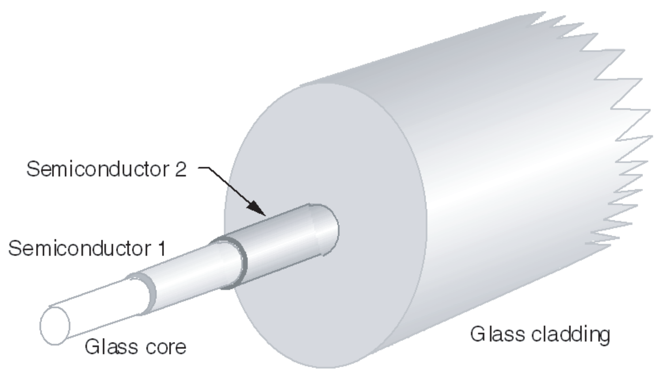

Figure 1: Optical fiber with two thin semiconductor layers at the core cladding boundary.

REFERENCES

1. Zamuda, H., et al., "Photonic generated true time delay phased array applications," USAF Rome Lab Report, No. A532853, Decdmber 1998.

Efficient Tool for Bend Optimization in Photonic Crystals

L. Dekkiche and R. Naoum
University Djillali Liabes of Sidi-Bel-Abbes, Algeria

The realization of efficient sharp and compact waveguide bends is still a challenging task in microoptics. With the introduction of photonic crystals (PC) major interest has also focused on the issue of efficient waveguide bends embedded in PC. There are various proposals for bend design in order to minimize losses. Examples smoothening the sharp bends, introducing cavities or intermediate straight sections or placing smaller holes around the bend.

In this work we use the method of topology optimization to maximize the energy flow through the waveguide and thus reduce unwanted reflections from the waveguide bend to a minimum. We specify a design area in the vicinity of the waveguide and distribute the material in this domain to maximize the energy flow. The flow through the waveguide is found by computing the poynting vector at the output waveguide port.

We have demonstrated $1.55\,\mu$m wavelength light wave through a simple 90° sharply bent waveguide formed in a square lattice two dimensional photonic crystal (2DPC). The in-plane guiding within the planar PC structure is based on a W1 defect waveguide (A single line defect acting as a light channel in the $G-K$-direction) whereas for the vertical light confinement we rely in a slab waveguide formed by the low index contrast material system InGaAsP/InP. To achieve a reasonable bandgap around $1.55\,\mu$m the PC consists of a lattice of holes with a filling factor of 40%. Such propagation has not previously been experimentally confirmed.

The most promising structure was simulated with a 2D-FDTD program. Since we want to use this device around 1550 nm we calculate the lattice constant to be 430 nm and obtain therefore a hole radius of 141.9 nm respectively.

This optimization step has resulted in 2DPC bend that shows a power transmission of at least 100% over a wavelength of 1550 nm.

Statistical Dynamics of Dispersion-managed Optical Solitons

A. Biswas
Delaware State University, USA

The statistical dynamics of dispersion-managed optical solitons is studied in presence of stochastic perturbation term, by the aid of soliton perturbation theory. The super-Gaussian pulses are considered and the corresponding langevin equations are derived and analysed. It is shown that in presence of the perturbation term, the soliton propagates through the fiber with a fixed mean value of the soliton energy.

A Boundary Element Method for the Analysis of Inhomogeneous Photonic Crystals

F. Seydou and T. Seppanen
University of Oulu, Finland

A fast numerical method for determining photonic bandgaps in composite and inhomogeneous dielectric materials is developed.

It is known that for the propagation or scattering of electromagnetic waves in a medium containing M dielectric bodies arranged periodically (photonic crystal), there exist refractive indices for which such structures have bandgaps, i.e., frequencies for which no waves can propagate inside. Such crystals have many technological applications (fiber optics, cellular telephones, semiconductor industry, etc.). The main purpose of this work is precise numerical simulations on novel dispersive and refractive phenomena in photonic crystal waveguides. In detail we study the influence of specially configured crystal inhomogeneities and physical boundary conditions to tailor the performance of planar and finite 2D-photonic bandgap structures. In order to sufficiently high accuracy in the simulations our calculations are based on a rigorous scattering theory for finite size two-dimensional photonic crystals. The results will be compared with other state-of the art algorithms. In particular, we compute the transmitted wave from an incident plane wave and analyze it for different angles of incidence, and we try and find the frequencies that generate the prohibited waves. In this work we choose a method that is based on boundary integral equations. We derive single integral equations on each of the interfaces between two regions by using a hybrid method of layer potentials and Green's formula. The integral equation we need to solve is of Fredholm type and the problem can be shown to be well-posed. Our technique has many distinct advantages. First, since the approximations are made on the boundary we reduce the dimension of the problem from N to $N-1$. Second, our formulation is different than the usual formulation since for dielectrics (in electromagnetic problems), the number of unknowns is reduced by half. The only drawback is that we have, as usual for BIE, dense matrices in the resulted linear algebraic systems. But this can be remedied by using fast multipole algorithms. Details of the numerical implementation and results will be presented. We also analyze the effect of defects, that is the case when periodicity is violated.

Session 3A3
Sensor Array Signal Processing

Survey on Interference Mitigation via Adaptive Array Processing in GPS

D. Lu, Q. Feng, and R. B. Wu
Civil Aviation University of China, China

Global Positioning System (GPS) is a promising navigation system which has been widely used in civil and military applications. However, due to its extremely weak received GPS signal power, it is easily affected by interferences from either intentional or unintentional sources and the positioning precision is degraded severely. Hence, one of the hot topic of using GPS is to cancel the interference as completely as possible with the distortionless of desired GPS signal.

Conventional GPS suppression method is failed to mitigate multiple narrowband interference as well as wideband interference owing to its incapability of differentiating between desired signal and interference in the spatial domain. Yet array signal processing technique can efficiently suppress the above interference according to the spatial information. So it is a trend of GPS interference mitigation. In this paper, from the point of adaptive array processing, we review the existing spatial and space-time interference suppression methods which attempt to mitigate interference before the GPS receiver performs correlation. These methods comprise adaptive nulling technique, spectral self-coherence restoral technique based on the nature of GPS signal, GPS multipath mitigation technique using the vertical array, space-time minimum mean square error and power minimization techniques etc. Also we summarize their performance and applicability by analyzing all these techniques, in which some of our work and opinions are included.

A Simulation Tool for Space-time Adaptive Processing in GPS

W. Y. Zhao, **L. F. Xu**, **and R. B. Wu**
Civil Aviation University of China, China

With the wide use of GPS, it becomes more and more important to improve the positioning accuracy. The GPS signal is very weak, and can be easily interfered. Space-time adaptive processing(STAP) can suppress the jamming not only in the temporal domain, but also in the spatial domain. STAP has now become a good candidates for interference mitigation in GPS

In order to evaluate the performance of various kinds of STAP algorithms, and for the development of novel STAP algorithms. we need to simulate space-time array GPS data with high fidelity and the software GPS receiver. This paper mainly presents a simulation method for space-time GPS data, as well as the simulation of some typical kinds of jammers. The simulation method for software GPS receiver is also introduced. The data that after the process of STAP is computed by the simulated GPS receiver. The simulation results show that the simulation tool is a good platform for the development of STAP algorithms.

Analysis and a Novel Design of the Beamspace Broadband Adaptive Array

W. Liu[1], R. B. Wu[2], and R. Langley[1]
[1]University of Sheffield, UK
[2]Civil Aviation University of China, China

Adaptive beamforming has found numerous applications in various areas ranging from sonar and radar to wireless communications [1]. For arrays to accomplish nulling over a wide bandwidth, tapped-delay lines (TDLs) are employed, resulting in an array withM sensors and TDLs of length J. To perform beamforming with high interference rejection and resolution, we need to employ a large number of sensors and long TDLs, which unavoidably increases the computational complexity of its adaptive part and slows down the convergence of the system. To overcome this problem, the broadband beamspace adaptive array was proposed [2], where several frequency invariant beams are formed pointing to different directions by a fixed beamforming network with two-dimensional (2-D) filters; thereafter the outputs of these beams are combined adaptively by a single weight for each output. Since both the number of beams and the number of selected beams are small, the total number of adaptive weights is greatly reduced.

For this technique to work, the frequency invariant beamforming network needs to meet two conditions, which are imposed explicitly or implicitly. First, the beams formed should have a satisfactory frequency invariant property for the interested frequency band, which is dependent on the required shape of the beam and the temporal/spatial dimension of the corresponding 2-D filter. The more complicated the shape, the more coefficients we need. As the shape is decided by the prototype filter, there is a relationship between the length N of the prototype filter and the dimension of the 2-D filter M and J. As mentioned in [2], the dimension of the 2-D filter should be at least 3 times that of the prototype filter to mainten the shape of the response of the prototype filter. Secondly, the beams formed should not be linearly dependent, otherwise, we will not be able to null out the desired number of interfering signals. This second condition is not mentioned explicitly in [2], but it is a necessary condition.

In our analysis, we will first show that the number of independent beams formed is the same as the length of the prototype filter. Although we can design as many frequency invariant beams as we want, only N of them are independent and at most we can only null out $N-1$ interfering signals. As the array's interference cancellation ability is dependent on both the number of independent beams and the frequency invariant property, there is trade-off between these two factors for a fixed M and J. We may choose a prototype filter with $N = \min\frac{M}{3}, \frac{J}{3}$ for a good frequency invariant property, but when the number of interferences increases and becomes larger than $\min\{\frac{M}{3}, \frac{J}{3}\}$, the array will not be able to null out the additional interferences. Therefore we may need to sacrifice the frequency invariant property a little to increase N. The loss in frequency invariant property can be compensated by the gain in the increasing number of independent beams. As a result, the interference cancellation ability of the array is improved. We will give some simulation results to show this trade-off.

With the above analysis, we propose a new design of the frequency invariant beams, where their main beam directions are uniformly distributed in the combined temporal/spatial space and their independence is guaranteed inherently by the special form of the prototype filter, which is derived from another prototype filter by cosine modulation with appropriately imposed zeros. Simulation result will also be provided to support this new design method.

REFERENCES

1. Godara, L. C., "Application of antenna arrays to mobile communications, Part II: Beam-forming and direction-of-arrival estimation," *Proceedings of the IEEE*, Vol. 85, No. 8, 1195–1245, August 1997.
2. Sekiguchi, T. and Y. Karasawa, "Wideband beamspace adaptive array utilizing FIR fan filters for multibeam forming," *IEEE Transactions on Signal Processing*, Vol. 48, No. 1, 277–284, January 2000.

A Subspace-based Robust Adaptive Capon Beamforming

G. S. Liao, **H. Q. Liu**, **and J. Li**
Xidian University, China

Adaptive beamforming suffers from performance degradation in the presence of mismatch between the actual and presumed array steering vectors of the desired signal, and many approaches have been proposed to improve the robustness of the Capon beamforming. *Li Jian* et al. proposed a robust beamforming method based on maximizing Capon output power. In this paper, we propose a robust subspace approach to adaptive beamforming based on minimizing MUSIC output power. The proposed method involves two steps: the first step is to estimate the actual steering vector of the desired signal based on the subspace technique, and the second is to obtain optimal weight by utilizing the estimated steering vector. Our method belongs to the class of diagonal loading, but the optimal amount of diagonal loading level can be calculated precisely based on the uncertainty set of the steering vector. Moreover, the proposed robust Capon beamforming has an explicit closed-form solution. To obtain noise subspace, the eigen-decomposition is required, which has a heavy computation load, and the number of signals should also be known *a priori.* In order to overcome this drawback, we utilize a POR (Power of R) technique to obtain the noise subspace without eigen-decomposition and knowing the number of signals *a priori.* It approximates the noise subspace of R based on R^{-m} (m is a positive integer) as $m \to \infty$. Surprisingly, *Li Jian's* method is a special case where $m = 1$, and the proposed subspace approach is the case where $m \to \infty$, so we obtained a uniform framework based on the POR technique. This is also an explanation why the proposed subspace approach is superior to *Li Jian's* method. The excellent performance of our algorithm has been demonstrated via a number of computer simulation results.

Signal Processing of Pyroelectric Arrays for Industrial Laser Applications

G. Biagini, L. Capineri, and L. Masotti
Università di Firenze, Italy

M. Mazzoni
CNR-IFAC, Italy

Pyroelectric arrays are widely used for detection of UV-VIS and IR radiation. For their derivative sensor characteristic with respect to temperature their application is addressed to modulated and impulsive radiation. Also for this type of sensors, novel applications require detailed process study and custom signal processing.

For whichever industrial laser application, source diagnostic (temporal waveform, peak amplitude and beam pointing stability, divergence, power density mapping) is claimed, especially for the most involved parameters which determine the efficiency of the process.

Continuos Wave CO_2 laser systems used for cutting metal slabs have long tube arms of large section (5 cm diameter) with knobs supporting mirrors which necessitate to be aligned. To this aim the authors developed large area ($5 \times 5\,\mathrm{cm}^2$) 8×8 elements matrix arrays for a detailed evaluation of the laser spot inside the arm section and its centroid determination. As laser bursts of duration and delay depending on power are currently used for the alignment, we processed the sensor signal for the attainment of the temporal waveforms first of all. Due to the coherence of the laser source one array element is sufficient to diagnostic the laser temporal waveform for source diagnostic. Improved temporal resolution was obtained with special filters extending the flat response region of the sensor bandwidth to higher frequencies. We analysed the bursts and registered the time characteristic of CW regime attainment after the initial transient.

The signals from the matrix arrays were processed after this time by an ACF2101 Burr Brown (switched dual integrator) with *sample* & *hold* function synchronized for all array elements. The front-end analog electronics is formed by 64 dual integrators which, together with the sensors array, constitute the whole device that is fixed at the laser system arm sections. The integrated signals were A/D converted with 10 bits by an Hitachi 32 bit microcontroller equipped with 8 input ports switched by a multiplexer 1 to 8 in a separate device connected to the sensor head. In the electronic design, we optimised the degree of insulation in the hold phase, and we performed the evaluation of the off-set voltages and their influence both on the intensity distribution and the beam spot centroid determination. The first goal was reached by inserting a resistance in parallel with each element and an insulation better than 1% (corresponding to a current two order of magnitude lower than the maximum pyroelectric current).

The signal processing allows for matrix calibration trough normalisation of all the elements responses to the highest value measured in a preliminary calibration phase with a laser of high stability. Owing to the measured linearity in a wide power range (up to 1.5 kW) and different times integration (4–100) ms, the processing allows the choice of the proper time integration for better signal-to-noise ratios with different laser powers. The off-set voltages contributing with noise to an integrated signal also without laser bursts were suppressed by reciprocal subtraction of two-without and with laser burst- sequential acquisitions. Stability of centroid estimation of the order of 0.5 mm has been achieved with 1.5 kW CW Laser in industrial environment.

Optimal Sensor Placement for the Localization of an Electrostatic Source

B. A. Kemp, T. M. Grzegorczyk, and J. A. Kong
Massachusetts Institute of Technology, USA

Electrostatic disturbance sensors have been developed for the passive detection and discrimination of charged bodies [1, 2]. Some proposed applications require the determination of source location or direction of arrival of a small charged object [2], which may be adequately modeled as a moving point charge. Source localization is an inverse problem in that the unknown coordinates of the electrostatic source at some instant in time are determined by the potential measurements from electrostatic disturbance sensors at known locations. This problem is solved by a multidimensional Newton search in the solution space. The solution is the iterative maximum likelihood (ML) estimator in additive white Gaussian noise (WGN), meaning that its performance is efficient in low noise. Since the estimator is iterative, a closed form expression for the solution variance cannot be determined. However, we show via numerical experiment that the iterative electrostatic localization estimator achieves the Cramer-Rao Lower Bound (CRLB) for low measurement noise. Therefore, the closed form expression of the CRLB can be used to represent the performance measure of the iterative estimator in low noise. We apply the expression for the CRLB to optimize the placement of electrostatic disturbance sensors such that for a specified estimator error tolerance, the sensor coverage is maximized at a known measurement noise level. We demonstrate the concept by numerical implementation for the 1D localization problem.

REFERENCES

1. Zank, P. A., E. M. Sutphin, D. W. Buchanan, and T. G. Cehelnik, United States Patent No. 6,900,642, May 31, 2005.
2. Zank, P. A., E. M. Sutphin, D. W. Buchanan, and T. G. Cehelnik, United States Patent No. 6,922,059, July 26, 2005.

Amplitude Estimation of Multichannel Signal in Spatially and Temporally Correlated Noise

K. J. Sohn[1], **H. B. Li**[1], **and B. Himed**[2]

[1]Stevens Institute of Technology, USA
[2]Air Force Research Laboratory/SNRT, USA

Amplitude estimation occurs in numerous signal processing applications. A survey of amplitude estimation techniques for sinusoidal signals with known frequencies in colored noise is found in [1]. While [1] is primarily concerned with *single-channel sinusoidal* signals, we consider amplitude estimation of an *arbitrary multichannel* signal observed in space and time using a sensor array. The observed data is contaminated by a *spatially and temporally correlated* disturbance signal with *unknown* correlation. Among other applications, this problem is encountered in an airborne radar system equipped with multiple antennas (e.g., [2]), where the multichannel signal refers to the space-time steering vector of the antenna array, the amplitude refers to the radar cross section (RCS) of a target, and the disturbance lumps together the thermal noise, radar clutter, and other interferences. Amplitude estimation within such a context would be useful for estimating the spatial and temporal correlation of the disturbance, developing effective target detectors, and finding solutions to several other relevant problems.

To account for its temporal and spatial correlation, our approach is to model the disturbance as a multichannel autoregressive (AR) process. Using extensive real radar data, [2] has shown that multichannel AR models are appropriate and offer efficient representation of the disturbance signal in airborne radars. Our *parametric* approach to the modeling of the disturbance is another major distinction compared to the *non-parametric* approach of [1]. Based on the parametric approach, our problem of interest is to find estimates of the signal amplitude, the AR coefficient matrices, and the spatial covariance matrix of the multichannel signal that drives the AR model. In the sequel, we first examine the optimum ML detector, and show that it involves nonlinear optimization. We then introduce several suboptimal but computationally more efficient LS and WLS amplitude estimators, which can be used to initialize the nonlinear searching involved in the ML estimator. The CRB for the estimation problem is presented as a performance baseline. In our numerical comparison of the different estimators, we focus on the case with *no or very limited training* data, which is of particular interest for applications in non-stationary or dense-target environments (e.g., [3]).

REFERENCES

1. Stoica, P., H. Li, and J. Li, "Amplitude estimation of sinusoidal signals: survey, new results, and an application," *IEEE Transactions on Signal Processing*, Vol. 48, 338–352, February 2000.
2. Román, J. R., M. Rangaswamy, D. W. Davis, Q. Zhang, B. Himed, and J. H. Michels, "Parametric adaptive matched filter for airborne radar applications," *IEEE Transactions on Aerospace and Electronic Systems*, Vol. 36, No. 2, 677–692, April 2000.
3. Michels, J. H., B. Himed, and M. Rangaswamy, "Robust STAP detection in a dense signal airborne radar environment," Signal Processing, special issue on New Trends and Findings in Antenna Array Processing for Radar, Vol. 84, 1625–1636, 2004.

Session 3A4
Microwave Imaging for NDE/NDT Applications

Issues and Problems in 3D Microwave Tomography (and Possible Answers)

I. Catapano[1], L. Crocco[1], M. D'Urso[2], and T. Isernia[3]

[1]Istituto per il Rilevamento Elettromagnetico Dell'Ambiente IREA-CNR, Italy
[2]DIET Università di Napoli Federico II, Italy
[3]DIMET Università Mediterranea di Reggio Calabria, Italy

A large number of papers have been published in the last years concerning 2D inverse scattering problems, while contributions to solution of 3D problems are more recent and relatevely few. Needless to say, accurate and numerically efficient solution procedures of 3D vectorial problems is an extremely relavant topic in applied electromagnetics as it would open the way to new exciting applications. On the other hand, well known difficulties arising in inverse scattering problems (ill-posedness, non-linearity) become an even more serious challenge in this context.

In particular, non linearity of the relationship amongst dielectric (and conductive) characteristics and the scattered fields deserves particular attention in setting solution procedures. As a matter of fact, the so called *false solutions* may occur in case gradient based optimization procedures are used. On the other hand, as their computational complexity grows very rapidly with the number of unknowns, global optimization procedures appear not to be viable in 3D problems herein at hand, due to the possibly very large number of unknowns involved.

All the above considerations claim for methods capable of dealing with 3D problems in a reliable and accurate way, while reducing as much as possible the computational costs and storage requirements. Of course, this is not just a matter of optimizing existing tools, but stimulates development of suitable models and inversion tools.

A first interesting result related to these questions has been recently obtained in the 2D scalar problem, by showing the possibility to achieve quite accurate estimation of the support of the unknown targets from the data themselves before actual inversion. Such a circumstance allow to reduce the number of unknowns in the subsequent quantitative inversion, thus allowing increased robustness against false solutions and ill conditioning problems, as well as faster solution procedures.

A second interesting result, again concerning 2D problems, has been recently obtained by means of a simple rewriting of the scattering equations named Contrast Source-Extended Born (CS-EB) model. This latter has been proved to exhibit a reduction of the degree of non-linearity of the relationship amongst parameters embedding dielectric characteristics and scattered fields as compared to the traditional model, thus furtherly increasing robustness against false solutions in the inversion process and computational efficiency.

The good results obtained in these contexts suggest the extension of these tools to the more demanding 3D vectorial case, which is the subject of the present contribution. As it will be shown during the Conference, the extension of the above tools to the 3D case allows to outperform previous inversion schemes, thus providing useful steps towards quantitatively accurate 3D inverse scattering based imaging techniques.

On the Retrieval of Small Electromagnetic 3-D Scatterers via MUSIC

E. Iakovleva, **D. Lesselier**, **and G. Perrusson**
Laboratoire des Signaux et Systèmes (CNRS-SUPÉLEC-UPS), France

H. Ammari
Centre de Mathématiques Appliquées (CNRS-Ecole Polytechnique), France

The contribution focuses onto the identification of a collection of small volumetric scatterers of unknown number and location embedded within a free or half-space medium. Each scatterer has constant yet arbitrary permittivity, conductivity and permeability (perfectly conducting cases follow from infinite conductivity and null permeability). Time-harmonic receivers and sources are used, typically made of planar arrays of electric or magnetic dipole sources and receivers with prescribed polarization(s) set at some distance (not necessarily in the far field) from the collection. This yields the MultiStatic Response (MSR) matrix that is characteristic of the collection for a set of illuminations and observations — times its conjugate-transpose, it is the time-reversal matrix.

The approach aims at fast numbering, accurate localization, and in best case (well-separated inclusions) at estimates of the electromagnetic and geometric parameters of the scatterers. It is based on MUSIC (MUltiple SIgnal Classification) methodology, enabling us to profit from the eigenvalue structure of the MSR matrix, and it is an involved extension of previous works in 2-D scalar scattering situations, e.g., [1]. Refer also to [2] for original work in the same direction.

The approach is worked out from rigorous asymptotic formulations, vs. average size of the scatterers, of the electric and/or magnetic fields (refer to [3] for related material). The expressions are derived from field integral formulations using the Green dyads of the embedding environment. Notice that one is limiting ourselves thereafter to the leading-order terms of the asymptotic expressions which only involve the (static) electric and magnetic polarization dyads associated to the scatterers.

The asymptotic machinery and the MUSIC-based eigenvalue analysis will be summarized, in line with [4] and a forthcoming SIAM paper.

Main emphasis however will be on the numerical study, to illustrate main features for asymptotically exact, severely noisy data, and/or for data calculated from brute-force numerical codes with no embedded asymptotics. Various configurations of the collection and (ellipsoidal) scatterers thereof, and of source and receiver arrays, will be tackled. Particular attention will be on the case of two close-by scatterers for which electromagnetic coupling matters — the asymptotic formulation provides for this coupling via equivalent scatterers. In addition to displaying MUSIC functionals peaked at the locations of the scatterers and pertinent distributions of eigenvalues, fields due to back-propagation of singular vectors onto the embedding space will be exhibited.

REFERENCES

1. Ammari, H., E. Iakovleva, and D. Lesselier, "A MUSIC algorithm for locating small inclusions buried in a half-space from the scattering amplitude at a fixed frequency," *Multiscale Model. Simul.*, Vol. 3, 597–628, 2005.
2. Chambers, D. H. and J. G. Berryman, "Analysis of the time-reversal operator for a small spherical scatterer in an electromagnetic field," *IEEE Trans. Antennas Propagat.*, Vol. 52, 1729–38, 2004.
3. Ammari, H. and H. Kang, *Reconstruction of Small Inclusions from Boundary Measurements*, Springer, 2004.
4. Ammari, H., E. Iakovleva, D. Lesselier, and G. Perrusson, "Asymptotic field formulations, MUSIC-type retrievals of small 3-D bounded dielectric and/or magnetic inclusions, and their application to dipole source and receiver arrays," *2005 Applied Inverse Probl. Int. Conf.*, Cirencester, 2005.

A Bayesian Approach to Microwave Imaging of Hybrid Targets

O. Féron, B. Duchêne, and A. Mohammad-Djafari
C.N.R.S. - Supélec - Université Paris-Sud 11, France

We deal with an electromagnetic inverse scattering problem where the goal is to characterize unknown objects from measurements of the scattered fields that result from their interaction with a known interrogating wave in the microwave frequency range. This nonlinear and ill-posed inverse problem is tackled from experimental data collected in a laboratory-controlled experiment led at the Institut Fresnel (Marseille, France), which consist of the values of the time harmonic scattered electric fields measured at several discrete frequencies.

The modelling of the wave — object interaction is led through a domain integral representation of the fields in a 2D configuration, where the fields appear to be radiated by the fictitious Huygens-type sources (or contrast sources) induced within the target by the incident wave and equal to the product of the total field by a contrast function representative of the target physical parameters.

The inverse scattering problem, which consists in retrieving this contrast function from the measured scattered fields, is solved by means of an iterative algorithm tailored to the case of objects made of a known finite number of different homogeneous dielectric and/or conductive materials. The latter a priori information is introduced via a Gauss-Markov field for the distribution of the contrast with a hidden Potts-Markov field for the class of materials in the Bayesian estimation framework. In this framework, we first derive the posterior distributions of all the unknowns and, then, an appropriate Gibbs sampling algorithm is used to generate samples and estimate them.

This algorithm is applied to the inversion of two coupled integral equations formulated in terms of the contrast sources in a way similar to that of the contrast source inversion method [1]. However, let us notice a fundamental difference between the CSI method and the one adopted herein: the former is developed in a deterministic framework and consists in minimizing a two-term cost functional by alternately updating the contrast sources and the contrast with a gradient-based method, whereas the latter is developed in a statistical framework, the contrast being then sought as a Gaussian mixture [2] by means of a hidden Markov model.

We have already obtained good results of reconstruction in the TM configuration case. Work is going on to improve the Gibbs sampling algorithm by using the bilinear property of the model and to apply the latter to the TE polarization case.

REFERENCES

1. Van den Berg, P. M. and R. E. Kleinman, "A contrast source inversion method," *Inverse Problems*, Vol. 13, 1607–1620, 1997.
2. Féron, O. and A. Mohammad-Djafari, "Image fusion and joint segmentation using an MCMC algorithm," *J. Electronic Imaging*, Vol. 14, No. 2, ID: 023014, 2005.

A Non-destructive Microwave Approach for the Detection of Multiple Defects in Industrial Products

M. Benedetti, **D. Franceschini**, **A. Massa**, **and A. Rosani**
University of Trento, Italy

M. Pastorino
University of Genoa, Italy

The non-destructive inspection is a key-problem in many industrial processes since the detection of defects or cracks in the products is mandatory. Many tomographic approaches that have been proposed are based on the use of interrogating microwaves and their effectiveness in inspecting dielectric or conductive materials has been demonstrated. A general NDT/NDE problem solved through an inverse scattering technique is still ill-conditioned and non-linear. Unlike standard microwave imaging problems, a lot of *a-priori* information on the scenario under test (the industrial product) is available. In this framework, *Caorsi et al.*, proposed an optimization technique (FGA) [1], where the problem unknowns reduction was achieved by exploiting such an *a-priori* information. A non-destructive inspection is aimed at detecting a single unknown defect inside a known unperturbed host medium lying on a known background. Starting from this assumption, the a-priori information on the unperturbed structure was exploited by means of a suitable Genetic Algorithm (GA). The inverse scattering problem was significantly simplified since the unknowns was reduced to an array of geometric parameters of the defect: its position, size, orientation, and the electromagnetic properties.

Successively, a further improvement was achieved employing the inhomogeneous Green's function [2], which allows a reduction of the region of interest to the area occupied by the crack without increasing the computational burden of the detection process. Such approach (called Inhomogeneous Green's Approach—IGA) obtained a further improvement of the computational burden as well as more accurate reconstructions.

In order to address more realistic problems, this paper presents a new methodology based on the original IGA and able to deal with problems characterized by more complex geometries in comparison to the singlecrack configurations so far considered. Towards this end, two different strategies have been developed both based on the inhomogeneous Green's function [2]. The former is characterized by a set of parallel GA subprocesses, each of them concerned with trial solutions encoding the same number of crack. The best solution is selected among the different crack-length optimal solutions given by each of the GA sub-processes. The second strategy is based on a single GA process where multiple-length chromosomes are defined in order to code contemporarily different solutions characterized by a different number of defects. This approach allows a considerable computational saving, but requires the definition of a new complete class of genetic operators. As far as the numerical validation is concerned, several realistic test cases have been taken into account and the obtained results demonstrate the feasibility as well as the effectiveness of the proposed approaches both in terms of reconstruction accuracy and computational costs.

REFERENCES

1. Caorsi, S., A. Massa, and M. Pastorino, "A crack identification microwave procedure based on a genetic algorithm for nondestructive testing," *IEEE Trans. Antennas Propagat.*, Vol. 49, 1812–1820, Dec. 2001.
2. Caorsi, S., A. Massa, M. Pastorino, and M. Donelli, "Improved microwave imaging procedure for nondestructive evaluations of two-dimensional structures," *IEEE Trans. Antennas Propagat.*, Vol. 52, 1386–1397, 2004.
3. Caorsi, S., M. Benedetti, A. Massa, M. Pastorino, and A. Rosani, "Optimization approaches for the detection of subsurface defects," PIERS2004 in Pisa, Pisa, Italy, S6.01, Mar. 2004.

Improving Inverse Scattering Solution Procedures by Means of a Preliminary Support Estimation: Rationale and Test on Real Data

I. Catapano[1], **L. Crocco**[1], **M. D'Urso**[2], **and T. Isernia**[3]

[1]Istituto per il Rilevamento Elettromagnetico dell'Ambiente IREA-CNR, Italy
[2]DIET Università di Napoli Federico II, Italy
[3]DIMET Università Mediterranea di Reggio Calabria, Italy

Due to the large number of underlying applications ranging from biomedical imaging to near surface geophysical explorations, inverse scattering problems are an important research topic. However, in applying these techniques, one has to solve a non-linear ill-posed inverse problem. This introduces many conceptual and computational complications which affect their actual applicability and effectiveness. As a matter of fact, when dealing with monitoring of regions of large extent, the computational burden becomes often unaffordable. On the other hand, in presence of multiple scattering effects, the inversion cannot be dealt within the framework of linearized models so that non-linearity of the problem becomes a critical point.

In order to devise effective strategies, it is extremely important that some features of the unknown targets can be determined from data without solving the inverse scattering problem. Amongst the other features, geometrical characterization of targets seems to be suitable information.

As matter of fact, this kind of information allows to reduce the computational domain and consequently the number of unknown parameters in the inverse problem, thus increasing the ratio between independent data and unknowns of the inverse problems. This ratio has an important rule in defeating ill-conditioning as well as possible occurrence of false solutions in the inversion process. For all the above, it is clear that a preliminary knowledge of the support of the unknown system of targets may improve the reliability of inversion procedures.

In this contribution, we show the possibility to improve the performances of some inverse scattering solution procedures by means of preliminary support information. To this aim, a two-steps approach aimed at characterizing homogeneous dielectric objects embedded in a homogeneous medium is introduced and discussed. The first step amounts to qualitatively reconstruct the geometrical features throughout the solution of a simple auxiliary problem. In particular, the Linear Sampling Method (LSM) introduced by Colton is applied. Such a method allows to estimate the support of the targets without explicitly solving the inverse scattering problem, but observing the behaviour of an indicator given by the norm of the solution of a linear auxiliary problem. It has to be noted that this information is achbieved in a very fast fashion. Exploiting this information as a constraint, the permittivity profile is then retrieved in the second step by means of a non-linear inversion strategy. To this end, both the Contrast Source Inversion (CSI) method and the recently introduced Contrast Source - Extended Born (CS-EB) one have been tested.

Numerical experiments performed on experimental data collected at the Institute Fresnel of Marseille confirm the usefulness and effectiveness of the proposed two-steps approach. As a matter of fact, independently from the fact one is using CS or CS-EB for the quantitative reconstruction of permittivity, the two-steps approach is capable to achieve accurate reconstructions in many cases wherein the usual approaches get stuck in a false solution.

A Neural Network Approach for Electromagnetic Diagnostic Applications

S. Caorsi and G. Cevini
University of Pavia, Italy

The purpose of the present paper is to investigate the potentialities of the application of neural networks to an electromagnetic diagnostic problem. On the one hand, electromagnetic non-destructive diagnostics is usually referred to the investigation and the reconstruction of not accessible scenarios by the exploitation of measurable data coming from the interactions between electromagnetic waves and the unknown scatterers. Recent years have experienced a relevant interest in developing electromagnetic inverse scattering approaches for NDE/NDT applications (subsurface mapping of underground utilities, detection of mines or unexploded ordnances, archaeological surveys, inspection of industrial products, monitoring of buildings' deterioration and so on). Among other techniques, we are developing approaches based on neural networks to reconstruct the position, the dimension and the dielectric properties of a subsurface object [1, 2].

On the other hand, electromagnetic non-destructive diagnostics also refers to the prediction of the electromagnetic field distribution inside not accessible scenarios. In this case, also, the research areas are manifold. Among others, bioelectromagnetics and its applications are concerned with the investigation of the interactions between electromagnetic waves and biological bodies. In particular, the scientific community is largely interested in developing electromagnetic non-invasive techniques to achieve the prediction of the absorption of the electromagnetic field inside biological bodies exposed to wireless communication systems. A large amount of research efforts have been spent in order to develop solution approaches, mainly based on the solution of the direct scattering problem and thus requiring the exact knowledge of the electromagnetic source and of the dielectric properties of the investigated biological body, which had to be replicated in a reference phantom. Nowadays, some researchers turned to inverse scattering approaches to predict the electromagnetic field distribution inside the human head, since they dont require the modelling of the electromagnetic source [3, 4]. For this research activity, we used a multilayer perceptron neural network to predict the electromagnetic absorption inside a dielectric object which resembles a dielectric reference phantom. The neural network has been trained to approximate the function relating some parameters characterizing the electromagnetic absorption and the available electromagnetic data. On the one hand, we have considered the measurements of the electromagnetic exposure in a limited number of points and on the other hand we have taken into account the measurements of the total field in a limited number of points of an observation domain external to the dielectric object. In this sense, the approach is completely non-destructive.

Several numerical results have been obtained and the potentialities and limits of the proposed techniques have been assessed.

REFERENCES

1. Bermani, E., S. Caorsi, and M. Raffetto, "Microwave detection and electromagnetic characterization of cylindrical objects from amplitude-only data by means of neural networks," *IEEE Trans. on Antennas and Propagation*, Vol. 50, 1309–1314, 2002.
2. Caorsi, S. and G. Cevini, "An electromagnetic approach based on neural networks for the GPR investigation of buried cylinders," *IEEE Geoscience and Remote Sensing Letters*, Vol. 2, 3–7, 2005.
3. Caorsi, S. and A. Massa, "Electromagnetic field prediction inside biological bodies by using an inverse scattering procedure based on a statistical cooling algorithm," *Bioelectromagnetics*, Vol. 21, 422–431, 2000.
4. Caorsi, S., A. Massa, and E. Bermani, "A microwave imaging approach based on amplitude-only data for the reconstruction of the electromagnetic field induced in biological phantoms," *ACES Journal*, Special Issue on "Computational bioelectromagnetics," Vol. 16, 79–89, 2001.

Faithfull Phaseless Microwave Tomography

I. Catapano[1], **L. Crocco**[1], **M. D'Urso**[2], **and T. Isernia**[3]

[1]Istituto per il Rilevamento Elettromagnetico dell'Ambiente IREA-CNR, Italy
[2]DIET Università di Napoli Federico II, Italy
[3]DIMET Università Mediterranea di Reggio Calabria, Italy

In inverse scattering problems, one looks for a quantitatively accurate description of the electrical and geometrical characteristics of an investigated region from the knowledge of a set of incident fields and measures of the corresponding total or scattered fields (both in amplitude and in phase) on a generic surface lying outside the region under test. The development of accurate and reliable techniques for solving this kind of problems is an important challenge because of their potential applications in biomedical imaging, applied geophysics, non invasive subsurface monitoring and non destructive testing and diagnostics.

By leaving aside peculiar characteristics of the different solution approaches existing in the literature, it is important to note the one of the main drawbacks of commonly suggested procedures resides in the need of measuring both amplitude and phase of the scattered fields. In fact, in several areas of applied science it can be very difficult or very expensive (or not possible at all) to measure the phase of a field. In particular, an accurate knowledge of the field phase involves sophisticated measurement equipments, which are more and more expensive as the working frequency increases, so that phaseless measurements are indeed mandatory at optical frequencies. In addition to that, the existence of minimally invasive (only amplitude) probes strongly suggest the adoption of phaseless techniques also at microwave frequencies. In fact, these probes considerably simplify the electromagnetic scenario with respect to classical (amplitude and phase) probes, thus avoiding multiple interactions and the need for probe compensation.

In this contribution a recently introduced approach to inverse scattering from only amplitude measurements of the total field is introduced and tested against experimental measurements taken at the Institute Fresnel of Marseille (corresponding to inhomogeneous scatterers). The basic idea of the adopted inversion technique is to reconstruct the complex scattered field from only amplitude measurements of the total field in a first step and then to solve a standard inverse scattering problem.

The proposed procedure is therefore organized in two different steps. In the first one, the complex scattered field is estimated by minimizing a functional that is the norm of the discrepancy between the measured pattern amplitude distribution and the calculated one. In such a step, a very important point arises in exploiting or, possibly, developing efficient (i.e. with the minimal possible redundancy) representations of the unknown scattered field. The second step, dealing with a standard inverse scattering problem, allows us to obtain an estimate of the dielectric and geometric properties of the system of targets eventually located in the investigated area.

As the proposed inversion technique needs to know both amplitude and phase of the incident field on the measurement curve, a second contribution amounts to demonstrate the possibility of achieving this information from the amplitude distribution of the incident field. The huge amount of knowledge about phase retrieval problems is exploited in such a 'pre-processing' step.

Numerical examples using the above quoted real data fully confirm the possibility to achieve accurate reconstructions in microwave tomography without performing phase measurements.

It is worth to note that this work, opposite to recent contributions, demonstrates the possibility of achieving faithful phaseless microwave tomography without any loss of accuracy as compared to the case wherein amplitude and phase data are available.

A Point Source Method for Reconstructing of Conducting Bodies Buried under a Rough Surface

H. Şahintürk[1], **A. Yapar**[2], **and Y. Altuncu**[2]

[1]Yıldız Technical University, Turkey
[2]Istanbul Technical University, Turkey

Due to large domain of applications such as non-destructive probing, geophysical prospecting, detection of personnel mines, determination of underground tunnels and pipelines etc. the inverse scattering problems related to buried bodies in a known half-space has a particular importance in the inverse scattering theory. As far as we know almost all of the publications related to these kind of problems concern with the bodies buried beneath a planar surface [1, 2]. Whereas in most of the real applications the bodies are buried in layered media having rough interfaces and the roughness have a strong effect on the scattering phenomena as well as reconstruction algorithms. For instance, in the case of bodies buried underground the roughness of the earth surface can potentially modify object scattering returns from those with a flat surface and this affects the reconstruction procedures in a serious way. For that reason the problem has to be considered in its actual conditions. In other words one has to take into consideration the roughness of the interfaces between the layers where the body is located.

The aim of this paper is to address an inverse scattering problem for the perfectly conducting bodies buried in a half-space with rough interface. The body is illuminated by a fixed point source located in the other half-space not containing the body and the scattered field is measured in the some domain in the same region. Through the Green's function of the background medium with rough interface we establish a point-source method for the reconstruction of the location and shape of the obstacle [3]. The method is based on the determination of the total field in the half-space where the body is buried through the measured scattered data. This is done by establishing a reciprocity relation between the incident and scattered fields. Then one reconstructs the object by observing the points where the total field vanishes. The problem is severely ill-posed and Tikhonov regularization is applied. On the other hand the determination of the Green's function constitutes a separate and difficult problem. Here we give a new and general method based on the assumption that the perturbations of the rough surface from the flat one are assumed to be buried objects in a two-part space with planar interface. Modeling the roughness in such a way yields us to formulate the problem as scattering of cylindrical waves from buried homogeneous cylindrical bodies, which is solved through a method based on MoM. Such an approach is very effective for surfaces having a localized roughness, arbitrary rms height and slobe. An illustrative example is given in order to test the accuracy and the applicability of the method.

REFERENCES

1. Akduman, I. and A. Alkumru, "A generalized ART algorithm for inverse scattering problems related to buried cylindrical bodies," *Inverse Problems*, Vol. 11, 1125–1136, 1995.
2. Colton, D., J. Coyle, and P. Monk, "Recent developments in inverse acoustic scattering theory," *SIAM Review*, Vol. 42, No. 3, 369–414, 2000.
3. Potthast, R., "A point-source method for inverse acoustic and electromagnetic obstacle scattering problems," *IMA Jour. Appl. Math.*, Vol. 61, 119–140, 1998.

Broadband Spatiotemporal Differential-operator Representations for Velocity-dependent Scattering

D. Censor
Ben Gurion University of the Negev, Israel

Novel approach, based on spatiotemporal differential-operators, is developed here for broadband, velocity-dependent scattering. Unlike the spectral-domain representations, the new method facilitates a compact formulation for scattering by arbitrary excitation signals, in the presence of moving objects. In free space (vacuum), relativistically exact formulas are developed. After developing the general theory, analysis of relativistically exact free-space scattering by cylinders, and a half-plane, are examined. For cylinders the analysis shows that in the far field pulses are located on circles in the co-moving reference-frame where the object is at-rest. In other reference frames this feature is valid only as an approximation. These results apply also to the diffractive part of the half-plane scattered field. The geometrical-optics contribution is associated with plane-waves and obeys the appropriate transformations. The various zones for these fields in an arbitrary reference-frame are analyzed.

Session 3A5
Electromagnetic Modeling and Inversion and Applications 2

Compact LTCC BPF Design Using Lumped Elements

J. W. Ha and Y. J. Yoon
Yonsei University, Korea

In a filter design, it would be very useful if the orders of it can be reduced without sacrificing the passband response. Especially, it needs an efficient method to decrease the size of filter for the SDMB (Satellite Digital Mobile Broadcasting) in Korea. A low-order, which has a smaller circuit size, is suitable to SDMB device. Therefore, an effective method to design a BPF (Band Pass Filter) with a high skirt selectivity is presented in this paper. Each resonator is separated into inductor and capacitor region [1]. The proposed circuit merges the individual region. LTCC (Low Temperature Co-fired Ceramic) are used because it has the capability of high integration. The 3rd order BPF and the proposed circuits are shown in Fig. 1(a) and (b), respectively. The proposed circuit has fewer resonators than the conventional circuit. Consequently, the size of the proposed BPF is reduced to nearly 20% comparing with the typical 3rd order LTCC filters. The simulated and measured results are shown in Fig. 2. BPF with 3rd order resonator has the passband in SDMB band for -10 dB return loss and provides sufficient interference suppression in 2.4 GHz bluetooth band. Although the resonator is simplified in the modified circuit, it has enough bandwidth as well as stopband rolloff in the received channel. The measured results agree well with the simulation. Thus, it is found that the proposed circuit supports a compact BPF design. The additional process of design will be presented in the symposium.

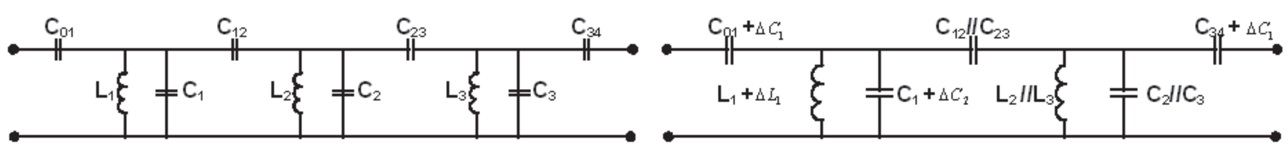

(a) The circuit with three resonators (b) The proposed circuit

Figure 1: Circuits of BPF.

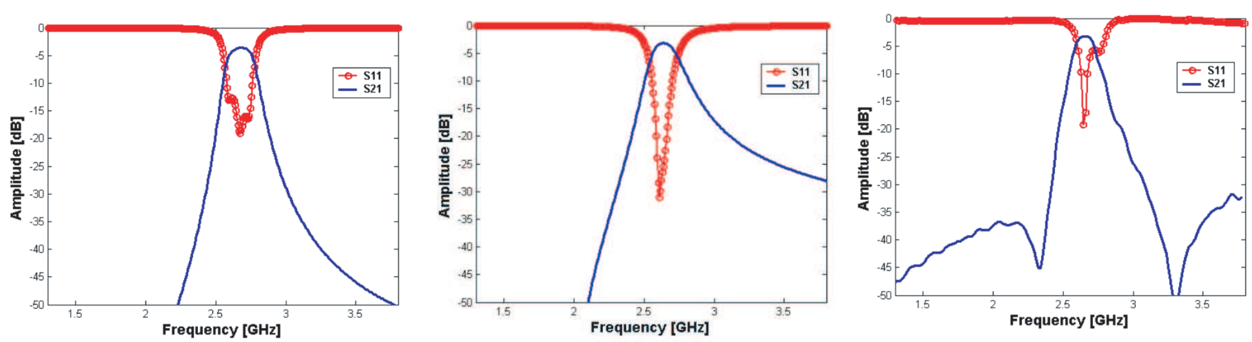

(a) Simulated BPF(3rd order) (b) Simulated BPF (proposal) (c) Measured BPF (proposal)

Figure 2: Comparison of simulated and measured results.

REFERENCES

1. Tang, C.-W., "Armonic-suppression LTCC filter with the step-impedance quarter-wavelength open stub," *IEEE Transactions on Microwave and Techniques*, Vol. 52, No. 2, Feb. 2004.

2.5D AGILD Electromagnetic Modeling and Inversion

G. Q. Xie, **J. H. Li**, **and F. Xie**
GL Geophysical Laboratory, USA

In this paper, we proposed 2.5D AGILD EM modeling and inversion algorithms and software.

We proposed 2.5D magnetic field differential integral equations for EM field on the boundary strip and center strip Ω_s with coordinate poles in cylindrical and spherical coordinate system.

$$H\left(r,r_s\right)\;=\;H_{bo}\left(r,r_s\right)+\oint\limits_{\partial\Omega_i}\frac{1}{\sigma+i\omega\varepsilon}\left(G_b^M\left(r',r\right)\times\nabla\times H\left(r',r_s\right)\right)\cdot d\vec{S}$$

$$-\oint\limits_{\partial\Omega_i}\frac{1}{\sigma_b+i\omega\varepsilon_b}\left(\nabla\times G_b^M\!\left(r',r\right)\times H\left(r',r_s\right)\right)\cdot d\vec{S}+\int\limits_{\Omega_s}\frac{(\sigma+i\omega\varepsilon)-(\sigma_b+i\omega\varepsilon_b)}{(\sigma+i\omega\varepsilon)}E_b^M\!\left(r',r\right)\cdot(\nabla\times H)\!\left(r',r_s\right)dr'$$

A 2.5D magnetic field Galerkin differential equation is proposed on the remainder internal domain. It supposes that the electrical parameters in the rotational direction are uniform. In the cylindrical coordinate system, the electromagnetic (EM) filed is vector functions of the r, θ, and z. However, the electrical parameters are only depended on radial coordinate r and vertical coordinate z. Upon substituting the Fourier serious of the EM field into the strip differential integral equation and Galerkin equation, we developed a new 2.5D AGILD EM modeling and inversion algorithm. The 2.5D AGILD EM modeling and inversion algorithms and software are illustrated and explained in the Figures 1–6. The AGILD modeling and inversion algorithms have the following advantages. (1) It reduced error on the artificial boundary; (2) It reduced the full matrix and the ill posed for inversion; (3) It resolved coordinate singularities in cylindrical and spherical coordinate system in continuous caster, geophysics, singularities in north and south poles for magnetic field in earth and Navier Stokes flow simulation in atmosphere; (4) AGILD has widely applications in geophysics, atmosphere, nano-materials, caster, medical, radio, motor, etc. areas; (5) Applications show that the 2.5D AGILD is fast, accurate, and has reasonable resolution.

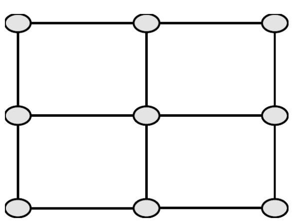

Fig. 1: AGILD forward node scheme.

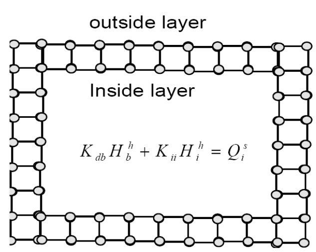

Fig. 2: Inside node layer to outside layer.

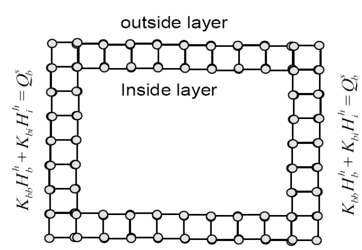

Fig. 3: Outside node layer to inside layer.

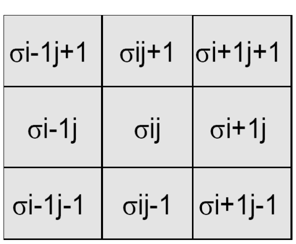

Fig. 4: AGILD inverse block scheme.

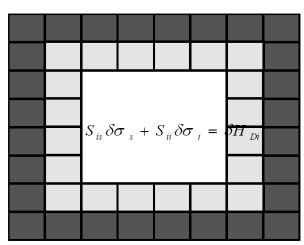

Fig. 5: Inside block layer to outside layer.

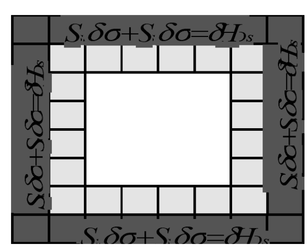

Fig. 6: Outside block layer to inside layer.

REFERENCES

1. Xie, G. Q., J. H. Li, and F. Xie, “Advanced GILD EM modeling and inversion,” *Proceeding of PIERS 2005*, Hangzhou, China, 105–109, 2005.
2. Xie, G. Q., J. H. Li, and F. Xie, “AGILD geophysical and atmosphere imaging, to submit to Proceeding of PIERS 2006 in Tokyo.

Measured Electromagnetic Pulses Verify Asymptotics and Analysis for Linear Dispersive Media

T. M. Roberts
Air Force Research Laboratory, USA

Electromagnetic precursors and other pulses in dispersive media have been studied since 1914. Yet a National Research Council committee recently found few measurements to verify the relevant theories. This talk describes two laboratory verifications of transient-electromagnetic theory that I completed in 2004.

Asymptotics

Petropoulos and I showed in 1996 that the Dirac $\delta(t)$ response of any Debye model will asymptotically approach the closed-form δ response of a classic equation (the advection-diffusion equation) as the depth x greatly exceeds an easily computed quantity that we named the time-domain skin depth. The δ response's peak amplitudes then decay as $x^{-1/2}$ and the full widths at half-maximum (FWHMs) spread as $x^{1/2}$. Similar results were obtained independently by Kelbert and Sazonov, also in 1996. In 1997, Farr and Frost published relevant experimental data for pulses in water and concrete. Because the three groups were unaware of each other and each other's work, their results were profoundly independent.

Petropoulos and my theorem on "element convolution" predicted that Farr and Frost's pulse would propagate in a Debye model of water with peaks $\propto x^{-1/2}$ and FWHMs $\propto x^{1/2}$, approximately. This is evident in Figure 1, where peaks $\times$ FWHMs are constant to within $\pm 1.4\%$ for water, verifying much of the three groups' work.

Exponential Decay

From 1914 until July 4, 2002, apparently, almost every pulse-decay rate predicted for a dispersion model was of the form x^{-const}, called algebraic decay. But decay rates are sensitive to the degree of spectral concentration near $\omega = 0$ (dc). What happens if an incident pulse's spectrum is in a non-infnite band of frequencies separated by a nonzero amount from dc, as broadcast regulations and practicality may require? Each component would travel as e^{ikx}, where $k(\omega)$ is the complexvalued wave number. If $k_i^{\min}$ is the smallest value that Im k has for the material and spectrum at hand, then intuition suggests that the pulse's peak would decay at least as fast as the slowest rate of exponential decay, exp $(-k_i^{\min} x)$.

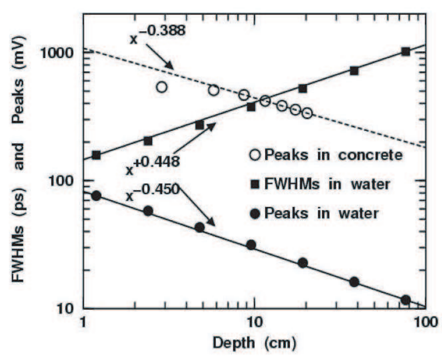

Figure 1: Peaks $\propto x^{-0.450}$ and FWHMs $\propto x^{-0.448}$ for $x > 1$ cm in water. Peaks $\propto x^{-0.388}$ for $x > 8$ cm in concrete.

Five-step derivations of the exponential decay of peak amplitudes and total energies of such pulses are suitable for advanced undergraduates [http://handle.dtic.mil/100.2/ADA411 823, 11–15, Eq. (1) on 51, and 52]. The only assumption is $E(x,t) = \int_{-\infty}^{\infty} e^{i(kx+\omega t)} \tilde{f} e^{i\omega t} d\omega$, where the incident pulse $f(t)$ has Fourier transform $\tilde{f}(\omega)$.

This talk will derive the exponential decay of total energies $\varepsilon(x) = \int_{-\infty}^{\infty} |E(x,t)|^2 dt \leq \exp(-2k_i^{\min} x)$ $\int_{-\infty}^{\infty} |f|^2 dt$ and peak amplitudes $P(x) = \max_t |E(x,t)| \leq \exp(-k_i^{\min} x) \int_{-\infty}^{\infty} |\tilde{f}| d\omega$, where $k_i^{\min}$ is defined two paragraphs above. The result for peak amplitudes ($\mathcal{P}$) was verified in 2002 by four-parameter families of numerical examples for the Debye and Lorentz models. The result for total energies (ε) was verified in 2004 by published measurements.

Electromagnetic Modeling for Interpretation of Airborne SAR Imagery

L. M. Zurk, S. Matzner, F. Farahbakhshian, and R. Toengi
Portland State University, USA

The theory that governs the formation of Synthetic Aperture Radar (SAR) imagery generally assumes that the radar return is due to stationary, isolated, and uncorrelated point scatterers distributed on a flat plane. For most naturally occurring scenes (such as those arising in remote sensing applications) this assumption does not apply. This lack of consideration for the electromagnetic scattering phenomenology limits the useful interpretation of the SAR imagery, and places the burden of recognizing image features on the expertise of the image analyst. In this work, an end-to-end electromagnetic and radar simulation model has been developed to understand and evaluate the appearance of complicated scene features in spotlight SAR images as a function of scene parameters, sensor characteristics, and radar processing approaches. Furthermore, the model can be employed to investigate the potential of advanced physics-based processing techniques that can be used to produce more appropriately-formed image output.

The model uses as input Digital Terrain Elevation Data (DTED) with accompanying information on land cover and/or building structures. The scattering from the terrain is computed using a modified Kirchoff scattering approximation, where the modification takes into account local terrain slopes. The surface roughness is assumed to have a Gaussian distribution with the RMS height and correlation length chosen as appropriate for the specified class of land cover. The scattering model has been developed to emulate the performance of the Lincoln Multi-Mission ISR Testbed (LiMIT). LiMIT is an airborne SAR sensor that was developed and deployed by MIT Lincoln Laboratory, with a recent collection campaign over San Clemente Island as part of the Navy's Silent Hammer Sea Trial experiment. In this talk, an initial comparison of the output imagery of the SAR synthesis model is compared to images acquired by LiMIT during Silent Hammer. Further extensions to the model and concepts for physics-based SAR processing will be presented and discussed.

Forward Problem Solution Using the Finite-difference Time-domain method combined with Frequency Scaling

C. E. Vasios, **L. M. Angelone**, **M. S. Hamalainen**, **J. W. Belliveau**, **and G. Bonmassar**
Harvard Medical School, USA

INTRODUCTION: The estimation of sources underlying measured MEG and EEG signals requires an accurate solution of the static approximation of Maxwell's equations that can be conveniently expressed as the lead field [1], which is the sensitivity distribution of a given MEG sensor or an EEG electrode. In the present state-of-the art approach for lead field estimation (Boundary Element Method, BEM) [2] the head is described with a few compartments with constant and isotropic electrical conductivity. Arbitrary, anisotropic conductivity distributions can be handled with the finite-element and finite-difference methods. This allows taking into consideration thin and highly conductive tissues such as bone marrow, disregarded when using the BEM. We propose a new approach for the lead field computation using the cell-oriented finite-difference time-domain (FDTD) method combined with the frequency scaling technique [3] for low frequencies.

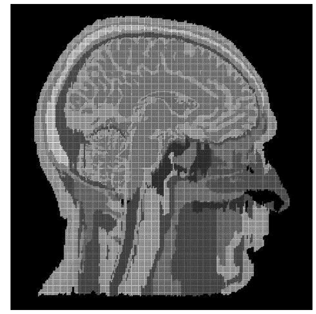

Figure 1: Anatomically accurate $1\times1\times1\,\mathrm{mm}^3$ resolution head model used for induced currents simulations.

METHODS:

Head Model and Electrode Locations: One 29-tissue high-resolution ($1\,\mathrm{mm}^3$) head model (Fig. 1) segmented from the anatomical MRI data was used (a $6\,\mathrm{mm}^3$ resolution was used here). The tissue conductivities were selected according to the literature [4].

We computed the lead field from 32 electrode locations (digitized from a real EEG recording) on this particular subject which we co-registered to the head model and used the 33^{rd} electrode near the vertex (Cz) as a reference.

Lead Field Computation: The reciprocity theorem states that the lead field of a given electrode pair is the same as the current pattern generated in the underlying conductor by feeding a unit current through the electrodes. Therefore, we were able to apply the FDTD method to calculate induced current densities using XFDTD software (REMCOM Co.). For dramatical reduction of computational time, simulations at target frequency $f = 20\,\mathrm{Hz}$ were initially performed at a higher frequency $f' = 20\,\mathrm{MHz}$ and then scaled, $J(f) = (f/f')J(f')$, according to the frequency scaling technique [3].

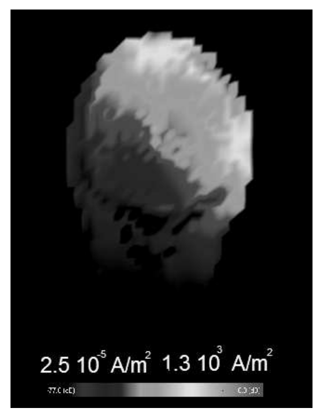

Figure 2: Induced current densities computed after connecting Cz and T8 positions with a current source of 1 A.

RESULTS-CONCLUSIONS: The comparison of the results from the FDTD computation with those given by a three-compartment boundary-element model showed that the lead field distributions are qualitatively similar. The computation of the lead field for one electrode pair took about 80 minutes on a 2-processor desktop computer (Intel XEON 2.8 GHz, 2 GB RAM).

FDTD can incorporate an arbitrary conductivity distribution and anisotropy without the need of complex meshing techniques typically needed in the finite-element and BEM approaches.

REFERENCES

1. Wolters, C. H., et al., *Inverse Problems*, Institute of Physics Publishing, Vol. 20, 1099–1116, 2004.
2. Oostendorp, T. F., et al., *IEEE Trans. on Biomed. Eng.*, Vol. 36, No. 3, 382–391, 1989.
3. Moerloose, J., et al., *Radio Science*, Vol. 32, No. 2, 329–341, 1997.
4. Gabriel, C., Brooks Air Force Technical Report AL/OE-TR-1996-0037.

Support Vector Machine Classification of Unexploded Ordnance Based on EMI Spheroidal Scattering Mode Coefficients

B. J. Zhang
Massachusetts Institute of Technology, USA

K. O'Neill
Dartmouth College, USA

T. M. Grzegorczyk and J. A. Kong
Massachusetts Institute of Technology, USA

This project developed discrimination techniques that might be applied to distinguish unexploded ordnance (UXO) from large clutter pieces using their frequency domain UWB electromagnetic induction (EMI) response measurements. We use a forward scattering model for spheroids to represent UXO because they are typically elongated bodies of revolution. Our forward model describes the EMI response of objects in terms of spheroidal excitation and scattering modes. The coefficients of the scattering modes have been shown to be unique for a given scattering response. Therefore, we use the coefficients of the spheroidal scattering modes as inputs into a support vector machine (SVM), a binary classification algorithm based on statistical learning. We train the SVM by presenting it with the scattering coefficients of objects in known classes. Then, new objects with unknown class can be correctly classified by a trained SVM through analysis of their spheroidal scattering mode coefficients. Previous studies have shown that this approach to classification of similar objects on the basis of object elongation and magnetic permeability is achievable with a high degree of accuracy. Our current study focuses on scatterer volume because the amount of metal present is a key discriminant for field personnel. At the same time, scattering strength (EMI "cross section") depends markedly on type of metal or object shape, as well as volume. Therefore we generated the spheroidal mode coefficients for a population of single spheroids with random shapes, volumes, and metallic composition. Spheroids greater than a certain volume limit were identified as large while the rest were labeled as small. One collection of spheroids was used to train SVM while an independent set was used to validate the accuracy of the SVM classification. Notably, the magnitude of the scattered fields and corresponding scattering coefficients was largely unrelated to object size; nevertheless, the SVM classification in terms of volume for these synthetic objects was shown to be highly accurate. Furthermore, since UXO are often heterogeneous objects, we also generated the spheroidal coefficients from objects composed of two adjacent spheroids of random shape and volume and differing composition. We likewise trained and tested our SVM and were again able to produce predominantly correct classifications.

Environmental Effects on UWB Electromagnetic Induction Inversion Techniques and Forward Modeling of Unexploded Ordnance

B. J. Zhang
Massachusetts Institute of Technology, USA

K. O'Neill
Dartmouth College, USA

T. M. Grzegorczyk and J. A. Kong
Massachusetts Institute of Technology, USA

This project seeks to understand the effect of environmental factors on electromagnetic induction (EMI) measurements of unexploded ordnance (UXO) and the associated inversion techniques applied on the noisy measurements. The environmental factors include clutter, since UXO sites are highly contaminated with metallic clutter, and ground effects, because soil may be slightly permeable.

EMI measurements were taken of UXO overlaid by a surface dispersion of small metallic clutter pieces. Inversion was done to identify the UXO based on those noisy measurements. This was accomplished by optimizing the match between measured and modeled scattered magnetic fields, using a new generation of fast but accurate forward models. We used differential evolution (DE) to find the optimal match. Inversion is successful when the closest match originates from the correct UXO type out of the library of possible UXO types. For UXO obscured by clutter, it was shown that the inversion was successful for measurements which had signal-to-noise ratios up to 2.5 dB. Generally, a DE population size of at least 50 members and over 100 generations were necessary to achieve successful inversion from noisy measurements.

Furthermore, measurements were also taken of UXO buried in soil. Through analytical approximations of spheres embedded in permeable half-spaces, it was found that for the range of realistic soil permeabilities, all halfspace effects are negligible except for a magnitude offset in the real part of the measured frequency domain EMI signal. We incorporated this offset effect in our forward models and did optimization inversion on the measurements. The inversion was successful for UXO buried at shallow depths.

Lastly, clutter can be approximated as directional dipoles and their combined effect can be incorporated into our forward models along with the soil offset effect. Synthetic data was generated using this forward model. Our optimization inversion was successful using this synthetic data with 20 spheres randomly dispersed over an area of 0.7 by 0.7 meters. Furthermore, this improved forward model allows for Monte Carlo-type simulations to help understand the statistics of clutter noise and investigate ways of suppressing or filtering out that noise in measurements. Further research is also needed to enhance the robustness of our inversion techniques to overcome the environmental effects.

Analysis of Uniplanar Resonator Using a Wave Concept Iterative Method W.C.I.P.

N. Sboui, **A. Gharsallah**, **and A. Gharbi**
Faculté des Sciences de Tunis, Tunisia

H. Baudrand
ENSEEHIT, France

A global modeling of uniplanar resonator is presented. The analysis is achieved by using an iterative method based on the wave concept W.C.I.P.. Two techniques of excitations are used to initialize the iterative process. The analysis procedure is described, and S parameters show good agreement with published data. This approach is successfully applied to many problems for microwave and high speed integrated circuit CAD software.

The KMD_EMS System in Chinese Continuous Casting

J. Li and Z. Q. Lai
Hunan Kemeid Mechanicsyco Ltd, China

J. H. Li and G. Q. Xie
GL Geophysical Laboratory, USA

The KMD electromagnetic stirrer (KM_EMS) has widely applications in the Chinese continuous casting industrial. We installed KMD_EMS for the continuous casting in almost 80% steel plant in the China. In this paper, we present our KMD_EMS's applications in China. Recent, we used GLGEO_AGILD EMS modeling to simulate the magnetic filed distribution in our KMD_EMS stirring in the continuous casting. According the GLGEO_AGILD EMS simulation, we improve our KMD design and obtain more high quality stirring function and can reduce the cost for our stirring product. Many simulations show that GLGEO_AGILD is accurate and fast. The magnetic field movie by GLGEO_AGILD clearly shows that the rotational steel flow is driven by magnetic filed. There are MEMS, SEMS, and FEMS installed in the strand. The AGILD can be used for associate simulation of the magnetic field caused by the multiple stirrings that will be important real time tool to monitor the steel and metal continuous casting processes. In the near future, we will use new GLGEO_AGILD EMS modeling to improve my real time control system and increase the efficiency of our KMD_EMS. The GLGEO_AGILD EMS modeling is new Advanced Global Integral and Local Differential electromagnetic stirring software that is mode and patented by GL GEOPHYSICAL Laboratory [1, 2]. The GLGEO_AGILD EMS modeling challenges to FEM, FD, and Born like EM modeling for magnetic field in EMS. The GLGEO_AGILD EMS modeling has excellent advantages over FEM, FD, and Born like modeling.

REFERENCES

1. Xie, G. Q., J. H. Li, and F. Xie, "New global and local electromagnetic field modeling and inversion," *PIERS 2005*, Hangzhou, China, 2005.
2. Xie, G. Q., J. H. Li, and F. Xie, "Advanced GILD EM modeling and inversion," *Proceeding of PIERS 2005*, Hangzhou, China, 105–109, 2005.

A New Formulation for Scattering by Impedant 3D Bodies

B. Collard[1], **B. Fares**[2], **and B. Souny**[1]

[1]Ecole nationale de l'Aviation Civile, France
[2]Centre Européen de Recherche et de Formation Avancée pour le Calcul Scientifique, France

A new integral equation formulation is introduced for solving, in the frequency domain, the problem of electromagnetic scattering by an impedant (IBC) or perfect electric/magnetic (PEC/PMC) 3D body of arbitrary shape. It is based firstly, on a special application of the equivalence principle where the 0-field exterior domain is filled with another impedant medium and, secondly, on the widely used PMCHW (Poggio, Miller, Chang, Harrington and Wu) formulation which forces field continuity through the scatterer surface. Unlike other IBC formulations such as, this one also applies to PEC/PMC. Furthermore, in this last case, it appears to stabilize the numerical scheme in the vicinity of eigen frequencies. We will provide proofs and conditions of the wellposedness of the problem for impedant as well as for PEC/PMC bodies.

Session 3A6
Extended/Unconventionl Electromagnetic Theory, EHD/EMHD, and Electrobiology

Chasmas Including Magnetic Effects

D. K. Callebaut
University of Antwerp, Belgium

A. H. Khater
University of Beni-Suef, Egypt

In a plasma one has by definition quasi-neutrality over distances of the order of the Debye length. In some situations one has no quasi-neutrality over many times the Debye length. E.g., in certain discharges or in the multipactor regime occurring in the cavities of linear accelerators. Such a non-quasi-neutral plasma or charged plasma has been called chasma. We studied previously fairly simple chasmas [1–3] using an integro-differential equation and using the partial differential equations [4], where we obtained the so called 'chasma frequency', playing a role in the steady state and in the stability. Now we extend the latter analysis by considering the Maxwell equations from the start, i.e., including the magnetic terms. Two geometrical situations are considered: electron and ion velocities perpendicular to the 'electrodes' or not. We had derived [4] previously expressions for all steady state quantities without taking into account the magnetic effects. With these (but not yet an external magnetic field) we recover the same situation, however with the additional condition that the electron and ion currents neutralize each other. Perturbation yields instability except in special cases, as was the case in the non-magnetic situation.

REFERENCES

1. Callebaut, D. K. and G. K. Knuyt, "Ion density in ionizing beams. 1.," *Plasma Phys. Contr. Fusion*, Vol. 20, No. 6, 511–524, 1978.
2. Knuyt, G. K. and D. K. Callebaut, "Ion density in ionizing beams. 2. Applications," *Plasma Phys. Contr. Fusion*, Vol. 20, No. 6, 525–544, 1978.
3. Callebaut, D. K. and G. K. Knuyt, "Chasmas in the laboratory and in space," *Relation between Laboratory an Space Plasmas*, (Ed. H. Kikuchi), 207–231, Reidel Publ. Co, Dordrecht, The Netherlands, 1981.
4. Callebaut, D. K., G. K. Karugila, and A. K. Khater, "Chasma Perturbations," *Proc. PIERS 2005*, Hangzhou, China, 720–723, August 22–26 2005.

Generation of Solar Magnetic Fields Using a Quadripolar Seed Field

D. K. Callebaut
University of Antwerp, Belgium

The exact solution for the kinematic dynamo problem in spherical coordinates (r, θ, φ)

$$\partial_t H = curl(v \times H), \tag{1}$$

$$\nabla \cdot H = 0, \tag{2}$$

is given in Ref. [1]. Here H is the magnetic field and v is the azimuthal velocity, which is supposed to be an arbitrary function of r and θ only. Using a bipolar seed field yielded a qualitative agreement with the sunspot butterfly diagram and the polar faculae butterfly diagram. Here we investigate the case that a quadripolar seed field resides in the Sun (maybe in the whole convective zone or rather only in the tachocline at the bottom of the convective zone) as some observations [2] reveal a quadripolar contribution to some surface phenomena. A combination of a bipolar and a quadripolar field yields better agreement. The separation between the sunspot region and the polar faculae, although both are generated by the same mechanism, is manifest: the region where the radial variation of the angular frequency of the rotation vanishes.

REFERENCES

1. Callebaut, D. K., "Exact solution of simple kinematic dynamo," *Solar Phys.*, submitted.
2. Makarov, V. I., A. G. Tlatov, and D. K. Callebaut, "Increase of the magnetic flux from polar zones of the sun in the last 120 years," *Solar Phys.*, Vol. 206, No. 2, 383–399, 2002.

Higher Order Fourier Analysis for Multiple Species Plasma

D. K. Callebaut
University of Antwerp, Belgium

G. K. Karugila
Sokoine University of Agriculture, Tanzania

A. H. Khater
University of Beni-Suef, Egypt

The nonlinear Fourier method of Callebaut consists in concentrating on the family of higher order terms of a single Fourier term of the linearized analysis [1–4]. Thus we have obtained the higher order terms of plasma perturbations, gravitational ones, etc. In the simplest case of cold plasma this resulted in obtaining an analytical expression for the higher order terms. This allowed to investigate the convergence of the series, which in this case is e^{-1} of the equilibrium density. For the cases without an analytical expression we developed a numerical-graphical method to obtain the convergence limit. Near this limit the total amplitude of the wave becomes very large. The convergence limit decreases with increasing pressure.

Several first order perturbations of moderate amplitude may easily occur together in nature in a small interval of time. Each separately leads to a family of higher order terms which may total somewhat larger amplitudes. However, all the nonlinear combination of all first order perturbations may lead for a certain phase to a very large and even a non-convergent result. (A kind of bunching, concentration of the energy in a small interval, occurs.) This may explain sudden outbursts which occur in nature (e.g., in solar flares, CMEs, bright points, etc.) and in the laboratory. Inducing several moderate perturbations in a quiet plasma (e.g., a Q-machine) may allow experimental verification of the theoretical convergence limit. Plasmas with heavy negatively charged ions (fullerenes attach electrons) and positive ions may be suitable for this as their frequencies are much lower than for ordinary plasmas. However, a snag is that some electrons do not attach, resulting in a three species plasma. We develop the higher order analysis for this plasma.

REFERENCES

1. Callebaut, D. K., "Lineaire en niet-lineaire perturbaties in hydro-, magneto- en gravitodynamica," *Journal of the Mathematical Society of Belgium-Simon Stevin*, Vol. 45, 1–315, Ghent, 1972.
2. Callebaut, D. K. and G. K. Karugila, "Nonlinear fourier analysis for unmagnetized plasma waves," *Physica Scripta*, Vol. 68, No. 1, 7–21, 2003.
3. Callebaut, D. K. and G. K. Karugila, "Nonlinear fourier analysis for unmagnetized multi-species plasma waves," *Canadian Journal of Physics*, Submitted.
4. Callebaut D. K., G. K. Karugila, and H. Kikuchi, "Nonlinear stability of a gravitating medium with cosmological constant," *Kuwait J. Sci. Eng.*, in press.
5. Callebaut, D. K. and G. K. Karugila, "Nonlinear fourier approach yielding high fields in ball lightning," *Eighth International symposium on Ball Lightning (ISBL04)*, 3rd-6th August 2004, National Central University (NCU), Chung-Li, Taiwan, 38–43, 2004.
6. Callebaut, D. K. and N. L. Tsintsadze, "Linear and nonlinear interaction of electromagnetic waves with weakly ionized magnetized plasmas," *Physica Scripta*, Vol. 52, No. 5, 565–571, 1995.
7. Callebaut, D. K. and N. L. Tsintsadze, "Heating of plasma by Alfvén waves envelope," *Physica Scripta*, Vol. 50, No. 3, 283–289, 1994.

Significance of Electric Quadrupole in Laboratory, Atmospheric, and Space Electricity — Helicity and Vortex Generation, Particle Acceleration, and Electric Discharges

H. Kikuchi
Institute for Environmental Electromagnetics, Japan

An electric quadrupole can be constructed by four metallic spheres or a pair of dipoles above a metallic plane by positive and negative voltage application, forming an electrically neutral point or an electric cusp and an electric mirror.

A dust particle placed in a cusp region formed by a quadrupole is led to entirely different two consequences, depending upon whether the background gas pressure is below or beyond the gas breakdown threshold, though electric field merging to the particle occurs for both cases, suddenly causing very high local electric fields around the particle, almost zero to infinity. For the former case, the particle goes to helical motion, accompanying acceleration-deceleration and reflecting back at a mirror point or further running beyond the mirror point. So that the quadrupole can become a source-origin of helicity or vortex generation purely electrically. For the latter case, a sequence of processes occurs, namely surface discharge and ionization around the particle, being followed by EHD shocks, critical ionization, streamer and leader elongation, discharge channel formation towards each pole, and eventual main discharge or return stroke as a result of dust-related electric reconnection followed by critical ionization [1].

Consequently, electric cusp-mirror and reconnection model described above offers a unified view of dust dynamics and discharge-ionization and is thought to be useful for our basic understanding of those phenomena.

It should be noted that direct observational evidence of electric cusp-reconnection model has been obtained from a statistical survey by field experiments accidentally during winter thunderstorms (1985–89) in a costal region of the Sea of Japan, indicating that natural cloud-to-ground strokes occur most likely in a cusp region on the ground with an initially low electric field where a sudden change of low to very high electric field, almost zero to infinity, could occur, while such a catastrophe never happens in other areas of initially higher electric fields (pp. 91–93 in [1]). In addition, rocket- and tower-triggered lightning experiments indicate indirect evidence of this model (pp. 86–91 in [1])We are now planning direct laboratory evidence of this model by using a "universal electric-cusp type plasma reactor" (pp. 93–94 in [1]).

REFERENCES

1. Kikuchi, H., *Electrohydrodynamics in Dusty and Dirty Plasmas*, Kluwer Academic Publishers, Dordrecht/The Netherlands, 2001.

Accuracy of Air Ion Field Measurement

T. Vojtek, T. Skoupil, P. Fiala, and K. Bartušek
Brno University of Technology, Czech Republic

An analysis of the electric state of air shows the presence of various ion sorts. The therapeutic effect of negative high-mobility ions of proper concentration is known. This positive effect was observed in caves that are used for speleotherapy. This article presents the capability of methods for measuring ion concentration and for ion spectral analysis.

Air ion concentration and composition belong to the frequently monitored parameters of the atmosphere [1]. Their influence on living organisms has been the subject of intensive studies. Earlier research has demonstrated the positive influence of light negative ions and air cleanness on human health. The Department of Electrotechnology of Brno University of Technology and the Institute of Scientific Instruments of the Academy of Sciences of the Czech Republic are involved in the research of ion field in office and living spaces. The objective is to increase the concentration of light air ions in these spaces. Another task is to set up a simulated therapy room, with conditions similar to speleotherapy caves. It sets the requirements for accurate measurement of ion field with good repeatability. The article deals with the design of gerdien tube and peripheral measuring devices. An optimal design is important for eliminating the inaccuracy of ion concentration measurement.

REFERENCES

1. Israë, H., *Atmosphärische elektrizität*, Akademische Verlagsgesellschaft Leipzig, 1957.

Experimental Verification of Active Traveling Wave Antenna

T. Obata[1], **R. Miyazaki**[1], **and H. Kikuchi**[2]

[1]Gunma National College of Technology, Japan
[2]Institute for Environmental Electromagnetics, Japan

Experimental verification in the principle of a parametric amplifying traveling-wave antenna proposed by Kikuchi [1] is tried. Long ago Carson [2] and also Pollaczek [3] developed a theory in regard to wave propagation along a wire above a dissipative ground. The Carson-Pollaczek theory, however, is restricted to a low frequency range, because of neglecting displacement currents in the air and in the ground and also no effects of the dielectric constant of the ground on equivalent circuit parameters. Kikuchi [4] developed a new theory overcoming these defects in Carson-Pollaczek theory. The new theory showed that attenuation characteristics possess a maximum and a minimum, and this was demonstrated by field experiments. The theory predicted fast waves between the maximum attenuation frequency and the minimum attenuation frequency, too. However, experimental verification of the fast waves is insufficient still now, except for a preliminary experiment by Iwai [5]. After that Kikuchi [6] extended the theory in distributed passive parameter lines so as to cover distributed active parameter lines with dissipative-ground return exposed to an electromagnetic environment. He showed that wave propagation along a wire above a dissipative ground exposed to an external electromagnetic field could be reduced to an active dissipative distributed parameter line with active source elements and passive circuit parameters. This new theory in active dissipative distributed lines predicted a new effect of parametric amplification of the induced line wave by an incident sky wave due to strong coupling or resonance between both waves. This is achieved by making the phase velocity of the induced wave nearly equal to the front velocity of the sky wave along the wire under some conditions. The authors try to verify the fast wave characteristic and the parametric amplification effect by an experiment.

REFERENCES

1. Kikuchi, H., United States Patent, Patent No. 5469179, 1995.
2. Carson, J. R., *Bell. Syst. Tech. J.*, Vol. 5, 539, 1926.
3. Pollaczek, F., *Elek. Nachr. Tech.*, Vol. 3, 339, 1926.
4. Kikuchi, H., *Electrotech. J. Japan*, Vol. 2, 73, 1956.
5. Iwai, T, unpublished work, 1999.
6. Kikuchi, H., *Proc. 7^{th} Int. Wroclaw EMC Symp.*, edited by D. J. Bem et al., 153, Wroclaw Tech. Univ. Press, Wroclaw, 1984.

Some Analogy between Negative Shunt Conductance in a Distributed Parameter Line Equivalent to Parametrically Amplifying Traveling-wave Antenna and Negative Resistance in an Equivalent Lumped Circuit of Esaki Diode

H. Kikuchi
Institute for Environmental Electromagnetics, Japan

Structure of parametrically amplifying traveling-wave antenna is a wire above a semiconducting or lossy dielectric base-plate [1] and its eigen-mode becomes a fast wave for a certain high frequency range where the shunt conductance of its equivalent distributed parameter line becomes negative [2]. This new result of identity of a negative shunt conductance and a fast wave-mode is most remarkable and is a necessary condition for the present antenna to operate.

On the other hand, the Esaki diode is characterized by a negative resistance of an equivalent lumped circuit and plays a significant role as a semiconductor device based on quantum-mechanical tunnel effects as is well known [3].

An induced wave current of the present antenna is a fast wave. Therefore, when it is illuminated by an incident plane wave and its front velocity along the line is adjusted to be equal to the phase velocity of the induced line wave, parametrical amplification of the induced wave current along the line could be expected as a result of synchronization of both waves, thus the part of incident wave energy being transferred to the induced wave. In this way, the present antenna holds a high gain and a high directivity.

At low frequencies, however, the shunt conductance becomes positive, virtually being reduced to the conventional Beverage antenna. This corresponds to a positive resistance in the diffusion-dominant region in the Esaki diode.

Comparison of the present antenna and the Esaki diode is made illustratively in terms of voltage-current characteristics and their causing effects and mechanisms: attenuation and phase characteristics for the present antenna and energy-level diagram for the Esaki diode.

REFERENCES

1. Kikuchi, H., "Parametrically amplifying traveling-wave antenna," UK Patent 2276985, 1996; US Patent 5469179, 1995; French Patent 9404020, 1997; Japanese Patent 2636164, 1997; German Patent 4411720, 2004.
2. Kikuchi, H., "Active distributed parameter lines with ground return," *Proc. 7th Int. EMC Wroclaw Symp.*, 153–162, Wroclaw Technical University Press, Wroclaw/Poland, 1984.
3. Esaki, L., *Phys. Rev.*, Vol. 109, 603, 1958.

Session 3A7
Computational Electromagnetics

A Fast Algorithm for Computing Band Gaps of Three-dimensional Photonic Crystals

C.-C. Chang
Research Center for Applied Mechanics, Academia Sinica, Taiwan

R.-L. Chern
National Taiwan University, Taiwan

C.-C. Chang
Research Center for Applied Mechanics, Academia Sinica, Taiwan

In this talk, we present a finite difference formulation for efficiently computing band structures of three-dimensional photonic crystals. First of all, we will show how to correctly discretize the double-curl equation for the magnetic field so that the transversality condition is exactly satisfied in the discrete sense. The first few branches of nontrivial eigenfrequencies that determine the major full band gaps of photonic crystals are computed by interlacing an inverse method with conjugate gradient projection and full multigrid acceleration. The presently developed method is applied to compute band structures of photonic crystals with modified simple cubic lattice, tetragonal square spiral structure (direct and inverse structures), and diamond structure with sp3-like configuration. The computed results for the modified simple cubic and square spiral structures are in close agreement with those obtained by previous authors. Moreover, the sp3-like configuration made of silicon and air is reported to have a large band gap which is larger than the largest reported elsewhere in the literature.

Numerical Simulation of Nonlinear and Parametric Oscillations in a Semiconductor Resonator Structure

G. S. Makeeva[1], **O. A. Golovanov**[2], **and M. Pardavi-Horvath**[3]

[1]Penza State University, Russia
[2]Penza Military Institute of Artillery, Russia
[3]The George Washington University, USA

The rigorous mathematical modeling of nonlinear oscillations in microwave strip-slot resonator structure (RS) loaded with the distributed Gunn diode with planar geometry is based on the solution of the three-dimensional diffraction boundary problem, formulated rigorously, taking into account the full Maxwell's equations with the nonlinear equation of transport carriers in semiconductor. The computational algorithm is based on the decompositional approach of nonlinear autonomous multimode blocs using the transverse and longitudinal components of weekly-nonlinear wave fields. For computing of the scattering matrix of the strip-slot resonator and the taped section in RS the second decomposition was made.

Using our numerical approach to determine the branching points of the solution of nonlinear Maxwell's equations, the transition region from the stationary regime of the nonlinear semiconductor device behavior (i.e., stable parametric amplification and frequency multiplication) into the generation (the onset of self-oscillations), caused by the instability process in the distributed Gunn diode, was simulated.

The results of numerical calculations of parametric amplification coefficient of signal wave, depending on the value of the biasing electric field (the frequency of pumping wave, i.e., the domain in the transit-time mode) was obtained taking into account variations in the electron concentration in the active layer of the semiconductor. The computer analysis of the magnitudes at the first and second time harmonics of self-excited oscillations, depending on the distance between strips, was performed infinitesimally close to the bifurcation points. The optimum parameters and the size of the planar Gunn diode for the efficiency of frequency multiplication and parametric amplification were determined, considering the constrained geometries of strip-slot RS.

Study of a Simple Geometry Illuminating Convergence Issues in the Method of Auxiliary Sources

G. Fikioris
National Technical University, Greece

The Method of Auxiliary Sources (MAS) is often applied to problems involving a closed, smooth, perfect conductor (PEC), illuminated by an external source: One seeks to approximately satisfy the boundary conditions on the PEC surface using a large number of fictitious sources located inside the surface. Once these sources are determined, one can calculate quantities such as the PEC surface current, or the (total) field. It is natural to understand MAS "convergence" as convergence of the field thus determined to the true field as the number of fictitious sources increases indefinitely. It is known that convergence has to do with the singularities of the true field when extended to the region inside the PEC surface.

Recent papers (e.g., [1, 2]) apply MAS to the case where the aforementioned scatterer is an infinitely long circular cylinder. For this simple special geometry, for which much can be done analytically, the results helps one understand various aspects of MAS and can be used to investigate the accuracy of MAS.

The present paper revisits the infinitely long circular cylinder, but focuses on the issue of convergence. For certain external illuminations and auxiliary-source configurations, we show that an alternative (to the above) concept of "convergence" — namely, convergence of the MAS sources themselves — can also be useful. Although convergence is often unambiguous, there exist cases where the scattered field converges while the MAS sources diverge. Using simple manipulations, we develop conditions — related to the aforementioned singularities of the true field — for this phenomenon to occur. We show that our detailed analytical results (which are possible because of the simplicity of our geometry) provide insight into MAS in general. We point out many similarities between our results and recent studies on the application of numerical methods to Hallen's and Pocklington's equations with the approximate kernel [3].

REFERENCES

1. Larsen, N. V. and O. Breinbjerg, *J. of Electromagn. Waves and Appl.*, Vol. 18, 745–761, 2004.
2. Anastassiu, H. T., D. G. Lymperopoulos, and D. I. Kaklamani, *IEEE Trans. Antennas Propagat.*, Vol. 52, 1541–1547, 2004.
3. Fikioris, G. and T. T. Wu, *IEEE Trans. Antennas Propagat.*, Vo. 49, 383–392, 2001.

A Parallel Computer Implementation of Fast Low-rank QR Approximation of the Biot-savart Law

D. White, B. Fasenfest, and M. Stowell
Lawrence Livermore National Laboratory, USA

The computation of magnetic fields from a prescribed electric current is a common problem in magnetic design and analysis. One approach is to form the problem as a Partial Differential Equation (PDE) for the unknown field with the prescribed electric current as the source term. Regardless of the particular PDE formulation, a large volumetric mesh must be employed, and some boundary condition must be applied on the outer boundary of the mesh. In contrast to the PDE approach, the Biot-Savart law can be employed to directly compute the magnetic field due to the prescribed current [1]. The advantage of the Biot-Savart law approach is that a full volume mesh is not required, and no boundary conditions need be applied. The disadvantage of the Biot-Savart approach is the computational cost, if there are $O(N)$ current samples and $O(M)$ magnetic field observation points the cost is $O(N^*M)$.

In this paper we present a low-rank QR method for evaluating the discrete Biot-Savart law on parallel computers. It is assumed that the known current density and the unknown magnetic field are both expressed in a finite element expansion, and we wish to compute the degrees-of-freedom (DOF) in the basis function expansion of the magnetic field. The matrix that maps the current DOF to the field DOF is full, but if the spatial domain is properly partitioned the matrix can be written as a block matrix, with blocks representing distant interactions being low rank and having a compressed QR representation. Our approach is similar to the low-rank QR approach used in boundary element methods [2, 3], although rather than using an octree, our highest-level partitioning is based on space filling curves and evenly distribute the matrix blocks across the multiple processors for parallel load balancing. While the matrix partitioning is determined by the number of processors, the rank of each block (i.e., the compression) is determined by the specific geometry and is computed dynamically. In this paper we provide the algorithmic details and present computational results for large-scale (100's of processors) computations.

REFERENCES

1. Jackson, J. D., *Classical Electrodynamics*, Wiley, 1975.
2. Kapur, S. and D. Long, "IES3: Efficient electrostatic and electromagnetics solution," *IEEE Comp. Sci. and Eng.*, Vol. 5, No. 4, 60–67, 1998.
3. Gope, D. and V. Jandhyala, "PILOT: A fast algorithm for enhanced 3D parasitic capacitance extraction," *Micro. Opt. Tech. Lett.*, Vol. 41, No. 3, 169–173, 2004.

Complex Coordinate Transformation as a Radiation Condition in Modal Methods

G. Granet, J. P. Plumey, and K. Edee
LASMEA UMR 6602 du CNRS, France

Modal methods and mode matching techniques are well established methods to solve wave guide and scattering problems. Such methods lead to an eigenvalue problem that is transformed into a numerical matrix eigenvalue problem by the method of moments. At this step, the boundary conditions that the field of the physical problem have to satisfy are included in the chosen expansion basis. For instance we chose periodic functions with a pseudo periodic coefficient to represent the field in grating problems or sine function to represent a field that should be zero on some boundary.

When considering problems in which radiation occurs (for instance leaky waves or discontinuities) we face a dilemma: on one hand we would wish to obtain the correct solution and properly takes into account the radiation boundary condition, on the other hand we would like to go on using the numerical tools that we have already developed and optimised. Some ten years ago, those who were using the finite difference time domain method faced also a similar problem. An elegant and efficient solution was then proposed by Berenger [1] who has introduced the concept of the so called perfect matched layers (PML).

Derudder et al. [2] showed that PML could also be very useful in modal methods. Since the pioneer work of Berenger many alternatives have been developed, one of which is the co-ordinate stretching introduced by Chew et al. [3]. We also adopt this point of view that can be easily combined with our own parametric approach [4]. We thus obtain efficient numerical tools able to analyse most guided wave problems including those with surface waves like plasmons. Furthermore, the conjunction of periodic functions and stretched co-ordinates also allows to derive a fast converging series expansion for the Green's function of layered media.

In this presentation, we shall describe from the operator point of view the implementation of the stretched co-ordinates as a radiation condition in any co-ordinate system. We will also discuss the accuracy limits of the proposed approach as a function of the various stretching parameters. Many examples will be given including radiation by structures that support plasmons and radiation by sources embedded in layered media with corrugated interfaces.

REFERENCES

1. Berenger, J. P., "A perfectly matched layer for the absorption of electromagnetic waves," *J. Comput. Phys.*, Vol. 114, 185–200, 1994.
2. Derudder, H., F. Olyslager, and D. De Zutter, "An efficient series expansion for the 2-D Green's function of a microstrip substrate using perfectly matched layers," *IEEE Microwave Guided Wave Lett.*, Vol. 9, No. 12, 505–507, 1999.
3. Chew, W. C. and W. H. Weedon, "A 3-D perfectly matched medium from modified Maxwel's equations with stretched coordinates," *Microwave Opt. Technol. Lett.*, Vol. 7, No. 13, 599–604, 1994.
4. Granet, G., "Reformulation of the lamellar grating problem through the concept of adaptive spatial resolution," *Journal of Optical Society of America A*, Vol. 16, No. 10, 2510–2516, 1999.

Full Wave Analysis of RF Signal Attenuation in a Lossy Rough Surface Cave Using a High Order Time Domain Vector Finite Element Method

J. Pingenot
University of Washington, USA

R. Rieben and D. White
Lawrence Livermore National Laboratory, USA

D. Dudley
University of Arizona, USA

We present a computational study of signal propagation and attenuation of a 200 MHz planar loop antenna in a cave environment. The cave is modeled as a straight and lossy random rough wall. To simulate a broad frequency band, the full wave Maxwell equations are solved directly in the time domain via a high order vector finite element discretization using the massively parallel CEM code EMSolve. The numerical technique is first verified against theoretical results for a planar loop antenna in a smooth lossy cave. The simulation is then performed for a series of random rough surface meshes in order to generate statistical data for the propagation and attenuation properties of the antenna in a cave environment. Results for the power spectral density and phase of the electric field vector components for the planar loop antenna are presented and discussed.

Direct and Accurate FDTD Modeling of Dispersive Media Using a Fourth-order Rational Conductivity Function

C. Rappaport and M. Jalalinia
Northeastern University, USA

To analyze lossy, frequency dependent media over a wide RF bandwidth with FDTD, it is important to capture the wave velocity and attenuation with a simple, efficient model. Using a single pole rational function of the Z-transform variable ($Z = e^{jw\Delta t}$) to model media conductivity along with constant real dielectric constant, it is possible to generate a supplemental discretized time domain equation which closely matches measured values across more than a decade of frequency. The agreement between measured and modeled propagation constant and decay rate for more than 50 materials are often to within 5%. This formulation avoids memory-intensive convolution operations and is at least as accurate as Debye models.

In the FDTD formulation, with electric field sampled at integer time steps $\overline{E}^n$, and magnetic field sampled at half-integer steps $\overline{H}^{n-\frac{1}{2}}$, Ampere's Law presents a difficulty with the current term, which is computed using electric field but which must be available at the magnetic field time instant. This is accomplished by choosing an average current value between adjacent time steps $\overline{J}^{n-\frac{1}{2}} = \frac{\sigma}{2}(\overline{E}^n + \overline{E}^{n-1})$. The central finite differences used in FDTD are second order accurate, while the averaging over adjacent time steps is only first order accurate. A more precise solution is available using the Z-transform formulation of Ampere's Law:

$$\nabla \times \overline{H}(Z) = \frac{1 - Z^{-1}}{\Delta t} \in \overline{E}(Z) + Z^{-\frac{1}{2}}\sigma(Z)\overline{E}(Z) \tag{1}$$

with the understanding that $\overline{E}(Z)$ and $\overline{H}(Z)$ transform to integer and half-integer time samples. The Z-transformed current $\overline{J}(Z) = \sigma(Z)\overline{E}(Z)$, but only when the current values are sampled at the same time instances as the electric field. To keep the time sample alignment of current in synchronism with magnetic field, the last term on the right hand side of Eq. 1 transforms to $\overline{J}^{n-\frac{1}{2}}$. Keeping the finite difference equation form of the constitutive relation relating shifted current to electric field, the new rational function representation of conductivity is:

$$Z^{-\frac{1}{2}}\sigma(Z) = \frac{b_0 + b_1 Z^{-1} + b_2 Z^{-2} + b_3 Z^{-3}}{1 + a_1 Z^{-1}} \tag{2}$$

With this choice, the entire right hand side of Eq. 1 remains a rational function of integer powers of Z, and thus it can be readily converted to finite difference form. The additional term $b_3 Z^{-3}$ in Eq. 2 becomes necessary to ensure three point fitting, with proper curvature, of the conductivity function to measured data. The real part of conductivity, based on Eq. 2, is:

$$Re\{\sigma(Z)\} = \frac{(b_0 + b_1 + a_1(b_1 + b_2))\cos\omega\Delta t/2 + (b_2 + a_1(b_0 + b_3))\cos 3\omega\Delta t/2 + b_3\cos 5\omega\Delta t/2}{1 + 2a_1\cos\omega\Delta t + a_1^2} \tag{3}$$

with five parameters b_0, b_1, b_2, and b_3 to eb determined from matching to measured data. The parameter a_1 is adjusted to satisfy special von Neumann stability conditions requiring that all zeros of the stability equation be within the unit circle for a particular grid spacing interval.

*This work is supported by CenSSIS, the Center for Subsurface Sensing and Imaging Systems under the ERC Program of the NSF (Award number EEC-9986821)

A Matlab-based Virtual Propagation Tool: Surface Wave Mixed-path Calculator

L. Sevgi and Ç. Uluişik
Doğuş University, Turkey

Surface wave high frequency radars (HFSWR) have a great potential for integrated maritime surveillance systems (IMSS), both as primary and complementary sensors. Countries with wide-coastal regions such as USA, Canada, France, Germany, Italy, Brazil, Turkey, Sri Lanka, China, India, etc., have already deployed or completed the designs of such systems for their economic exclusive zones (EEZ) [1, 2]. One major problem in such designs is the prediction of surface wave propagation which determines the total power budget. The propagation scenarios differ quite a lot from region to region. For example, engineers of the IMSS on the East Coast of Canada need to know maximum monitoring range for a given transmitter power. On the other hand, the problem of Turkey in the West Coast is to find out extra multi-mixed path propagation loss because of the existence of many different scaled islands in the region.

At HF frequencies, ground wave propagation is dominated by the surface wave. As long as the transmitter and receiver are close to surface direct and ground reflected waves cancel each other and only surface wave can propagate. The Earth's surface electrical parameters are important in reaching longer ranges. Sea surface is a good conductor, but ground is a poor conductor at these frequencies. A challenging problem is to predict surface wave path loss variations over mixed paths, such as sea-land or sea-land-sea transitions. A sharp decrease occurs in signal strength along sea-land transition and the signal recovers itself beyond the island, known as the Millington (recovery) effect.

We have introduced a few propagation packages for the calculation of surface wave propagation effects [3–5], where analytical ray and mode models (i. e., Norton and Wait formulations) are hybridized to extend their ranges of validity, accuracy, rate of convergence, etc., depending on such problem parameters as operational frequencies, source/observer locations and the physical propagation environment. These hybrid packages sue standard atmosphere over smooth spherical Earth assumption and can be best used from a few hundred kHz up to 40–50 MHz.

In this study, we have developed and designed a new Matlab-based, user-friendly virtual propagation tool (VPT) that can be used for multi-mixed path surface wave path loss calculations. The user may design a propagation scenario by just using the computer mouse, specify all other input parameters, and produce path loss vs. range plots. The effects of multi-mixed paths, electrical parameters of each propagation section, as well as the frequency can be observed and extra path losses can be predicted. The VPT can be used both for design and training purposes.

REFERENCES

1. Sevgi, L., A. M. Ponsford, and H. C. Chan, "An Integrated maritime surveillance system based on surface wave HF radars, Part I-Theoretical background and numerical simulations," *IEEE Antennas and Propagation Magazine*, Vol. 43, No. 4, 28–43, August 2001.
2. Ponsford, A. M., L. Sevgi, and H. C. Chan, "An integrated maritime surveillance system based on surface wave HF radars, Part II-Operational status and system performance," *IEEE Antennas and Propagation Magazine*, Vol. 43., No. 5, 52–63, October 2001.
3. Sevgi, L., and L. B. Felsen, "A new algorithm for ground wave Propagation Based on a Hybrid Ray-Mode Approach," *Int. J. of numerical modeling*, Vol. 11, No. 2, 87–103, March 1998.
4. Sevgi, L., F. Akleman, and L. B. Felsen, "Ground wave propagation modeling: problem-matched analytical formulations and direct numerical techniques," *IEEE Antennas and Propagation Magazine*, Vol. 44, No. 1, 55–75, February 2002.
5. Sevgi, L., Ç. Uluişik, and F. Akleman, "A matlab-based two-dimensional parabolic equation radiowave propagation package," *IEEE Antennas and Propagation Magazine*, 2005.

Implementation of Arbitrarily Oriented Wires in 3D-TLM Method

B. Larbi, J. L. Dubard, and C. Pichot
University of Nice-Sophia Antipolis/CNRS, France

The Transmission Line Matrix method is a well known time domain numerical tool suitable to the analysis of complex structures in a wide frequency range. In 3D-TLM mesh, the six components of the electromagnetic field are located at the center of the cell. This allows accurate modelling of boundaries between different media. In addition, the use of a variable mesh allows the study of complex antenna including fine details with reasonable computation time and memory storage.

However, the simulation of VLF antennas is difficult to perform since such structures are very large (several hundred meters) and contain a multitude of arbitrarily-oriented-thin-conductors (diameters of several millimeters). Furthermore, a reliable analysis of VLF antenna needs also to consider the soil, the finite ground plane and the surrounding infrastructures. With such constraints, the use of a non uniform mesh cannot avoid prohibitive computation time and memory storage. Then, it is necessary to implement an arbitrarily-oriented-thin-wires model in the 3D-TLM method for this kind of electromagnetic analysis.

The model used in this work allows arbitrarily located and oriented wires with respect to the Cartesian grid. The Maxwell equations are discretized by a finite differential approximation on a hexahedral mesh. The wires are described by two equations which symmetrically associate the electrical field and the current along the wire. Those equations are coupled using the TLM scheme in the same way as done in the FDTD method by Edelvik [1]. The performance of the arbitrarily-oriented-thin-wire model in TLM is evaluated for a dipole when comparing theory and the FDTD method. Simulation results for a VLF T-Antenna are provided and compared with measurements and analytical models.

REFERENCES

1. Edelvik, F., "A new technique for accurate and stable modeling of arbitrarily oriented thin wires in the FDTD method," *IEEE Transactions on Electromagnetic Compatibility*, Vol. 45, No. 2, 416–423, May 2003.

An Efficient Band Diagonal Preconditioner for Electromagnetic Integral Equations Using Wavelet Packet Bases

A. Geranmayeh
Amirkabir University of Technology, Iran

Iterative methods are commonly used to solve large scale moment matrix equations resulting from electromagnetic integral equations. The computational cost of iterative solutions is proportional to the moment matrix-vector multiplication operation and the number of iterations required for a convergent solution [1]. The wavelet (packet) basis functions have been deployed to reduce the computational complexity and memory requirement of dense matrix-vector multiplications operation [2]. The total solution time, however, remains dependent on the number of iterations required to achieve an accurate solution. In case the moment matrix is not well conditioned, an approximate-inverse preconditioning matrix is desired to accelerate the convergence rate of the iterative solution [1].

The use of conventional basis functions results in a dense matrix equation, making it difficult to find an effective approximate-inverse preconditioner. In order to find an appropriate preconditioner more easily, one can transform the moment equation to multiresolution wavelet domain so as to make the transformed moment matrix sparse and diagonal dominant [3, 4]. In most previous studies, the approximate-inverse preconditioner have been designed and constructed in the space domain from a block-diagonal approximation of the sparsified moment matrix [3–5]. The significant elements of the transformed moment matrix, however, are located along the near-diagonal positions, as most offdiagonal entries are negligible due to the vanishing moments of bases in wavelet domain [2]. As a result, a more efficient preconditioner can be constructed that consists of only the near-diagonal terms of the transformed matrix.

This paper proposes a band diagonal approximate inverse matrix preconditioning to overcome the complexity and memory bottlenecks in direct computing the inverse of the original matrix in designing the commonly used preconditioners. Additionally, in order to minimize computational cost and memory requirements in preconditioning operation, the multiplication of the preconditioner and the transformed matrix is carried out in sparse scheme [1]. An electrically large gull-shaped piecewise linear antenna excited by a center-fed voltage is analyzed to investigate the computation efficiency of the proposed method. The governing thin-wire electric field integral equation [2] is solved by the wavelet-based moment method to evaluate the current distribution over the antenna. Numerical results show that the iteration numbers for solving the transformed moment matrix equation preconditioned in wavelet domain by the proposed band diagonal matrix are smaller than those preconditioned by the block-diagonal equivalent one designed in space domain [4].

REFERENCES

1. Press, W. H., S. A. Teukolsky, W. T. Vetterling, and B. P. Flannery, *Numerical Recipes in Fortran: the Art of Scientific Computing*, 2nd ed., Cambridge Univ. Press, Cambridge, 1992.
2. Pan, G. W., *Wavelets in Electromagnetics and Device Modeling*, John Wiley, 2003.
3. Deng, H. and H. Ling, "An efficient wavelet preconditioner for iterative solution of threedimensional electromagnetic integral equations," *IEEE Trans. Antennas Propagat.*, Vol. 51, No. 3, 654–660, 2003.
4. —, "An efficient preconditioner for electromagnetic integral equations using predefined wavelet packet basis," *IEEE Trans. Antennas Propagat.*, Vol. 50, No. 11, 1633–1640, 2002.
5. Canning, F. X. and K. Rogovin, "A universal matrix solver for integral-equation-based problems," *IEEE Antennas Propagat. Mag.*, Vol. 45, No. 1, 19–26, 2003.

Session 3P1
Recent Advances in Optical Trapping and Binding

Comparison of Methods for the Calculation of Radiation Pressure on Dielectric and Magnetic Particles

B. A. Kemp, T. M. Grzegorczyk, and J. A. Kong
Massachusetts Institute of Technology, USA

The Maxwell stress tensor [1] and distributed Lorentz force [2, 3] are applied to calculate the time-average radiation pressure on two-dimensional (2D) dielectric and magnetic particles due to incident plane waves. We show that the two methods give identical results for the total force on a lossless medium. We use the Mie theory to calculate the fields scattered from an infinite circular cylinder used to represent a 2D particle, hence there is no restriction on the size of the particle considered. The results are verified using full-wave simulation results from the commercial software CST Microwave Studio ®.

The momentum conservation theorem is derived from the Lorentz force law where the charges and currents are represented by field quantities via the Maxwell equations. Using the momentum conservation theorem, the force on a lossless material body is described by the divergence of the Maxwell stress tensor and is calculated by the integration of the stress tensor on any surface which completely encloses the material body. Thus, the radiation pressure on a three dimensional (3D) object is calculated from a surface integral with knowledge of the total fields external to the object.

The distributed Lorentz force is applied to bound currents due to the polarization of a medium and to bound charges at the material boundary due to discontinuous $\hat{n} \cdot \epsilon_0 \bar{E}$ and $\hat{n} \cdot \mu_0 \bar{H}$, where $\hat{n}$ is the surface normal unit vector and ϵ_0 and μ_0 are the background permittivity and permeability. Contributions from magnetic current densities throughout a material body and magnetic charge densities at the surface are added to the standard Lorentz force on bound electric currents and charges to model the volume force density and the surface force density, respectively. The radiation pressure on a 3D object is determined by the combination of a volume integral with knowledge of fields and polarization inside the medium and a surface integral with contributions from fields on both sides of the boundary.

The results of the force calculation on 2D circular particles demonstrate that the two methods give equivalent results. The distributed Lorentz force can be applied to obtain the force density distribution throughout the medium, whereas the Maxwell stress tensor only provides the total bulk force on the particle. However, the Maxwell stress tensor reduces the surface integral to a line integral for the force on a 2D particle. Since the choice of force calculation method is independent of field calculation, either method can be extended to include multiple particles through the Foldy-Lax multiple scattering equations and to more complex geometries via numerical simulation. These computational abilities allow us to model the optical binding forces of multiple particles submitted to multiple incidences.

REFERENCES

1. Kong, J. A., *Electromagnetic Wave Theory* (EMW, 2000), ISBN 0-9668143-9-8, 2000.
2. Mansuripur, M., "Radiation pressure and the linear momentum of the electromagnetic field," *Optice Express*, Vol. 12, 5375–5401, 2004.
3. Zakharian, A. R., M. Mansuripur, and J. V. Moloney, "Radiation pressure and the distribution of electromagnetic force in a dielectric media," *Optics Express*, Vol. 13, 2321–2336, 2005.

Optical Binding of Small Particles

J. Ng[1], **Z. F. Lin**[1,2], **P. Sheng**[1], **and C. T. Chan**[1]

[1]The Hong Kong University of Science and Technology, China
[2]Fudan University, China

Light-trapping is generally associated with the phenomenon that small particles are driven toward the intensity maxima of a carefully sculpted laser beam. We show, through rigorous calculations, that in addition to the intensity-driven light-trapping due to gradient forces, a long-ranged optical binding force that can also induce stability in a cluster of small particles, even when the incident intensity is homogeneous. Under intense laser illumination (e.g., $10^6\,\mathrm{W/cm^2}$), such optical binding force can dominate over other interactions and bind dielectric microspheres into stable structures that behave like "molecules" which has well defined geometries and vibrational modes. Such photonic clusters can exhibit a multiplicity of static and drifting equilibrium configurations, with some having remarkable geometries such as a quasicrystal-like arrangement. Owing to the nonconservative nature of the system, the photonic clusters exhibit exotic dynamics, and the equilibrium configurations can correspond with either stable or a type of quasi-stable states in which the cluster maintains an average shape, with individual particles executing periodic motion in the presence of frictional dissipation. Photonic clusters consist of Rayleigh particles are also investigated. In contrast to microparticle-cluster which exhibits nonconservative dynamics, the interaction of Rayleigh particles is essentially conservative when the incident wave is a standing wave.

We also consider the light-induced stability of extended system and an interesting stable one-dimensional lattice is found and analyzed. Through analyzing its characteristic vibration modes, we observe, in addition to phonon-like lattice vibrations which are spatially extended, spatially localized modes. The localized modes can be attributed to the extraordinarily long-ranged optical binding force and the underlining principle suggests that similar type of mode is expected for other optically structure that are extended in size.

We also consider another type of inter-particle optical force that is driven by resonance. We found that the tuning of the incident light's frequency to the morphology-dependent resonances of a cluster of high-Q microspheres induces a strong, resonant optical force between the spheres. In contrast to the long range optical binding force described previous, this resonant optical force is very short ranged. The resonant force can be enhanced by orders of magnitude so that it dominates other interactions at modest incident intensity (e.g., $10^4\,\mathrm{W/cm^2}$).

Advanced Studies in Optical Binding

K. Dholakia[1,2], **N. K. Metzger**[1], **and E. M. Wright**[2,1]

[1]University of St Andrews, UK

[2]The University of Arizona, USA

Optical forces arise due to the light matter interaction. These forces have had impact right from the single atom level through Bose-Einstein condensates up to biological cells and colloidal matter. Light-matter interactions may be used to dictate the organization and manipulation of colloidal and biological matter at the microscopic level. An inhomogeneous optical field permits dielectric spheres of higher refractive index than their surrounding medium to be trapped in three dimensions in the field maxima primarily through the dipole interaction [1]. This allows physicists, chemists and biologists to explore a range of fundamental phenomena. From a physics perspective this includes thermally activated escape from a potential well, studies of optical angular momentum, stochastic resonance and various studies of colloidal behaviour in external potentials. From a biological perspective optical trapping has revolutionised our understanding of molecular motors.

Non-zero order light patterns and various families of propagating light fields are of significant interest across numerous branches of the sciences. If one goes beyond a standard Gaussian beam one may look at examples such as Hermite-Gaussian, Laguerre-Gaussian and Bessel light modes. These latter two modes possess cylindrical symmetry and have been of interest for studies of optical angular momentum, optical vortices, micromanipulation and for novel beam characteristics (e.g., studies of the Poynting vector and their reconstruction). Other extended two and three dimensional light patterns too have become of widespread interest: in the realm of optical micromanipulation they may create extended potential energy landscapes that may allow novel studies of extended colloidal systems and interactions therein.

Deformation of the light pattern by the very interaction of the particle with the imposed light field is a relevant issue for three dimensional structures which might be created using these techniques. The light matter interaction may lead to "optical binding". Such "optical binding" is radically different from conventional predefined trapping alluded to above: Here the very interaction between an object and its nearest neighbors creates a self consistent and homogeneous solution that allows an optical geometry to, in principle, create a large scale colloidal array. This topic has come again to the fore: work over a decade ago shows this effect in studies of Burns, Golovechenko and Fournier [2]. The St Andrews group have looked at new forms of optical binding in both counter-propagating and vertical geometries [3]. The key is that the interparticle spacing here is, unlike the earlier form of optical binding, of the order of microns and indeed the stronger interaction between the particles is key to creating the new forms of bound matter currently under study in our group. Interesting behaviour such as bistability may be observed.

In this talk I will discuss recent work on optical trapping in extended light patterns and primarily concentrate on the latest data in the area of optical binding which is proving a rich and surprising area in this field.

REFERENCES

1. Neuman, K. and S. Block, *Rev. Sci. Instrum.*, Vol. 758, 2787, 2004, D. Grier, *Nature*, Vol. 424, 810, 2003; K. Dholakia, G. Spalding, and M. MacDonald, *Physics World*, Vol. 15, 31, Oct. 2002.
2. Burns, M. M., J.-M. Fournier, and J. A. Golovchenko, *Phys. Rev. Lett.*, Vol. 63, 1233, 1989; M. M. Burns, J.-M. Fournier, and J. A. Golovchenko, *Science*, Vol. 249, 749, 1990.
3. Tatarkova, S. A., A. E. Carruthers, and K. Dholakia, *Phys. Rev. Lett.*, Vol. 89, 283901, 2002; D. McGloin, A. E. Carruthers, K. Dholakia, and E. M. Wright, *Phys. Rev. E*, Vol. 69, 021403, 2004; V. Garcés-Chávez, D. Roskey, M. D. Summers, H. Melville, D. McGloin, E. M. Wright, and K. Dholakia, *Appl. Phys. Lett.*, Vol. 85, 4001, 2004.

Simulating the Optical Force and Torque on Metallic Nano-particles

C. Rockstuhl
Friedrich Schiller University Jena, Germany

In this paper we analyze force and torque induced by optical fields on single and coupled silver nano-particles as a function of the wavelength. The geometry of the nano-particles is either a cylindrical one with circular or elliptical cross section or a spherical one.

The most prominent property of those metallic nano-particles is the excitation of the small particle surface plasmon polaritons at well-defined wavelength for which the dielectric constant of the materials takes appropriate values. The resonant oscillation of the free electrons with the frequency of the illuminating wave field causes a tremendous enhancement of the near-field amplitude and the scattering cross section. Such an enhanced scattering might find application in a modified version of a scattering type scanning near-field optical microscope, in which a nano-particle trapped by an optical beam is scanned shortly above the surface of a sample or in a photonic force microscope [1].

For trapping such a particle, all forces acting on it have to be equilibrated. The main forces are the scattering and the gradient force, whereby the first one is proportional to the intensity and the square of the polarizability and it points towards the propagation direction of the laser beam, whereas the latter one is proportional to the gradient of the intensity and the polarizability. If the gradient force is sufficiently strong for compensating the scattering force, the particle is trapped in a position shortly after the waist of a laser beam that has a Gaussian amplitude distribution in the transversal coordinate. For spatial positions deviating from that equilibrium position, the particle is linearly accelerated due to a non-zero net force. In addition to that linear acceleration, non-spherical particles are rotationally accelerated due to a torque and they will align themselves within the wave-field.

In this paper we use the Multiple Mulitipole Method [2] and Mie Theory [3] for a rigorous computation of the wavelength dependent force and torque acting on metallic nano-particles. The observed behavior is physically explained using arguments based on the dipole approximation. It will be shown that different interaction regimes with respect to the plasmon wavelength of the particle exist and specific behavior appears in the different regimes due to a different sign of the polarizability. The conditions for a stable trapping of the particles will be elucidated and the stability of the particles is estimated by comparing the optical force with the Brownian force.

REFERENCES

1. Rohrbach, A., E. L. Florin, and E. H. K. Stelzer, "Photonic force microscopy: simulation of principles and applications," *Proc. SPIE*, Vol. 4431, 75, 2001.
2. Hafner, C., "Post-Modern electromagnetics," *John Wihley* & *Sons*, 1999.
3. Barton, J. P., D. R. Alexander, and S. A. Schaub, "Theoretical determination of net radiation force and torque for a spherical particle illuminated by a focused laser beam," *J. Appl. Phys.*, Vol. 66, 4594, 1989.

Trapping of Microscopic Particles in Specially Designed Optical Fields

S. Bernet and M. Ritsch-Marte
Medical University of Innsbruck, Austria

We report and discuss a few milestones — and side-tracks — reached on our way to ever increasing control over the manipulation of microscopic objects.

Fiber-optical traps, for instance, are ideally suited to investigate the subtle interplay between the light field and the particle positions, which spontaneously leads to a *self-organized* linear array of trapped particles with a spacing which is mainly determined by the particle size. A self-consistent model, valid for particle sizes below the wavelength, was able to predict our experimental findings very well.

If one seeks to predefine the trapping arrangement rather than deal with a self-organized pattern, one may use holographic optical tweezers to create complex light distributions for optical micromanipulation. We show how holographically projected images can be optimized using a setup in the Fresnel regime (intermediate field) instead of the typically used Fourier regime (far-field). Special laser modes like Laguerre-Gaussian beams (doughnut modes) or arbitrary superpositions of such modes can be generated with a high purity, with appealing effects on trapped particles: For example, the size of optical tweezers created by a doughnut mode can be utilized for size-selective trapping of micro-particles.

One may also use static light fields for producing a continuous flow of micro-particles, e.g., an all-optical micro-pump which is driven by orbital angular momentum transfer from the laser modes to the particles. Such optical micro-devices can be locally integrated in an active or passive particle sorting system wherever one needs to generate a flow.

Tailored arrangements of these functional optical fields may be used to create automated microscopic tools for the assembly of microstructures, for the sorting of biological samples, or for the manipulation of selected components within intact biological samples. We report our recent developments approaching these goals.

Polarization Effects in Optically Bound Particle Arrays

C. D. Mellor
University of Oxford, UK

C. D. Bain
Durham University, UK

We have recently reported the formation of optically bound arrays of sub-micron polystyrene particles in the evanescent wave of two counterpropagating laser beams incident at the silica-water interface above the critical angle for total internal reflection([1, 2]). In this talk, we will describe some of the effects of the polarisation of the incident lasers on the packing of the arrays. Under the experimental conditions, the amplitude of the incident field is nearly identical for the two polarisations, but the field is in the surface plane for s-polarised light and almost perpendicular to the surface plane for p-polarised light. The case of orthogonally polarised laser beams has also been explored.

A number of different packing motifs are observed, including centred rectangular and several types of pseudohexagonal arrays that are distinguished by their orientation and periodicity of the lattice. With p-polarised light we have also observed missing row structures, such as that shown in the figure below, in which every third interference fringe is unoccupied. The fringe separation (400 nm) is indicated; the particle diameter is 520 nm. A variety of packing defects are observed, including lattice vacancies and twin planes (such as that shown with an arrow in the figure below). Defects heal at different rates for different polarisations. More than one form of packing can sometimes be observed under the same polarisation conditions, suggesting the presence of multiple minima in the many-body potential energy surface.

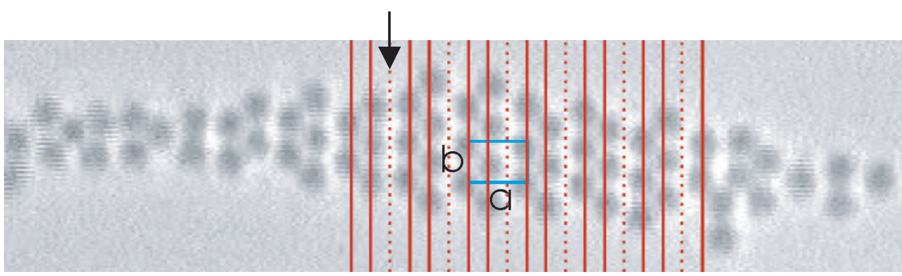

REFERENCES

1. Mellor, C. D. and C. D. Bain, *Optical Trapping and Optical Micromanipulation II.*
2. Dholakia, K. and G. C. Spalding, *Proc. SPIE*, Vol. 5930, 352, Eds., 2005.

Optical Binding in Air

M. Guillon
Université de Provence, France

Optical binding between micron-sized oil droplets in air has recently been observed. The experimental setup, consisting in two vertical, counter propagating and diverging laser beams, builds up a three dimensional trap. The cloud of oil droplets, enclosed in a glass cell, progressively fills in the trap where droplets interact one with another. Scattered intensity is observed on a video camera. Interactions involve optical, electrostatic, radiometric and capillary forces. Orders of magnitude are discussed.

Chains up to four droplets have been observed, the most stable structure being the doublet and not the single drop. In air, viscosity being one thousand times smaller than in water, mean free path of spheres in the range of the micron is much bigger. That is why mean residence times in metastable states are of the magnitude of a few seconds and that brownian motion quickly drives the trapped droplets in the very minimum of potential energy: the doublet structure. Two stable states have also been obtained for the doublet. Observation of interference indicates that oil droplets are phase-locked onto each other every $\lambda/2$.

The spaying technique we use, gives droplets smaller than the micron in radius. This is the intermediate case of the Mie range between the small and large wavelength cases. Those new experimental results exhibit the role of the short and long range interactions in optical binding. They are then theoretically discussed both in the ray model and in the Rayleigh approximation, and compared with previous works on optical binding in water. Moreover, in our case, the index difference is much bigger. It implies stronger scattered intensities, bigger interaction forces with light and therefore, bigger binding forces.

Optical Waveguide Manipulation of Micro- and Nano-spheres

J. S. Wilkinson[1], **O. G. Hellesø**[2], **J. P. Hole**[1], **and K. Grujic**[2]

[1]University of Southampton, UK
[2]University of Tromsø, Norway

Optical tweezers are well-established as a tool for non-contact, non-destructive handling of biological materials [1] and of inorganic nanospheres attached to biological molecules [2]. Recently, interest has grown in optical manipulation at surfaces [3] potentially as part of the toolbox of the "lab-on-a-chip". In particular, advances have been made in trapping and propulsion of metallic and dielectric micro- and nano-particles in the evanescent fields of optical waveguides [4, 5], which may form part of a planar microsystem into which optical detection and spectroscopy of separated species could also be integrated. Optical waveguides embedded in surfaces represent a powerful means of controlling the distribution of optical intensity and intensity gradient at such surfaces, for particle control.

In this paper, the design of optical waveguides and waveguide devices for trapping, propulsion and sorting of gold nanospheres and latex microspheres [6, 7] will be described and recent experimental results presented and compared with theoretical models. The implications of these results for some proposed applications in the biosciences will be discussed.

REFERENCES

1. Ashkin, A., J. M. Dziedic, and T. Yamane, "Optical trapping and manipulation of single cells using infrared laser beams," *Nature*, Vol. 330, 769, 1987.
2. Arai, Y., R. Yasuda, K. Akashi, Y. Harada, H. Miyata, K. Kinosita, and H. Itoh, "Tying a molecular knot with optical tweezers," *Nature*, Vol. 399, 446, 1999.
3. Kawata, S. and T. Sugiura, "Movement of micrometer-sized particles in the evanescent field of a laser beam," *Optics Letters*, Vol. 17, 772, 1992.
4. Kawata, S. and T. Tani, "Optically driven mie particles in an evanescent field along a channeled waveguide," *Optics Letters*, Vol. 211, 768, 1996.
5. Ng, L. N., M. N. Zervas, J. S. Wilkinson, and B. J. Luff, "Manipulation of colloidal gold nanoparticles in the evanescent field of a channel waveguide," *Applied Physics Letters*, Vol. 76, 1993, 2000.
6. Grujic, K., O. G. Hellesø, J. P. Hole, and J. S. Wilkinson, "Sorting of polystyrene microspheres using a Y-branched optical waveguide," *Optics Express*, Vol. 13, 1, 2005.
7. Hole, J. P., J. S. Wilkinson, K. Grujic, and O. G. Hellesø, "Velocity distribution of gold nanoparticles trapped on an optical waveguide," *Optics Express*, Vol. 13, 3896, 2005.

Towards Efficient Modelling of Optical Micromanipulation of Complex Structures

T. A. Nieminen, **V. L. Y. Loke**, **A. M. Brańczyk**, **N. R. Heckenberg**
and H. Rubinsztein-Dunlop
The University of Queensland, Australia

Optical tweezers have seen deployment in a wide range of applications in biology, soft materials, microassembly, and other fields. As well as being used for the trapping and manipulation of a wide range of natural and artificial objects, optically trapped probes are used to measure forces on the order of piconewtons. Compared with this diverse range of experimental applications, theory and accurate computational modelling of optical tweezers has received much less attention and has remained relatively undeveloped, especially for non-spherical particles and non-Gaussian beams. This is unfortunate, especially when we consider the growing fields of controlled rotation of complex microparticles — prototype optically-driven micromachines — and fully three-dimensional manipulation using complex optical fields, where the application of theory and modelling provide insight into the physics, and allow engineering and optimisation.

Since optical forces and torques result from the transfer of momentum and angular momentum from the trapping beam to the particle via scattering, the theory and computational modelling of optical tweezers is, in essence, the theory and computational modelling of the scattering of light or electromagnetic radiation. There are, however, complications that prevent simple direct application of typical light-scattering codes. The first, but not necessarily the most important, is that optical tweezers makes use of a highly focussed laser beam, while most existing scattering codes assume plane wave illumination. Perhaps more fundamental is the need for a large number of repeated calculations to characterise an optical trap — even for an axisymmetric (but nonspherical) particle trapped in a circularly polarised Gaussian beam, we already have four degrees of freedom. Clearly, this places strong demands on computational efficiency.

We review our progress towards efficient computational modelling of optical tweezers, including the trapping and manipulation of nonspherical particles. Our approach has been to use the T-matrix method in order to exploit (a) its efficiency for repeated calculations for the same scatterer, (b) its ability to model trapping of nonspherical particles, and (c) the simple calculation of optical forces and torques that result from the formalism. We show how this can be used to calculate optical forces and torques on nonspherical particles, with close agreement with experimentally observed forces and torques. This also illuminates the fundamental principles behind the transfer of electromagnetic momentum and angular momentum. Of particular interest is the dependence of the transfer of spin and orbital angular momentum on particle shape and the structure of the trapping beam.

However, most implementations of the T-matrix method are restricted to simple geometries, which are likely to be inadequate for the representation of prospective optically-driven micromachines. Solutions include both the use of multiple-scattering methods and the "hybridisation" of the T-matrix method with computational methods that are well-suited to arbitrary geometries and inhomogeneous and anisotropic structures, such as the finite-difference frequency-domain method and the discrete dipole approximation/coupled dipole method. We describe the implementation of such hybrid T-matrix methods.

A further important consideration is that optical micromachines, while complex, are likely to possess a high degree of symmetry; this can be exploited to reduce computation times by orders of magnitude. We demonstrate the effectiveness of this approach by modelling the optical trapping and rotation of a cube. The two principal symmetries of such shapes — mirror symmetry and discrete rotational symmetry about the normal to the mirror symmetry plane — are exactly the symmetries that typify the ideal optically-driven rotor.

Optical Microfluidics

J.-P. Delville[1], **R. Wunenburger**[1], **and C. Baroud**[2]

[1]Université Bordeaux, France
[2]LadHyX, France

The development of applications based on microfluidic technology is still hindered by the lack of robust fundamental building blocks that constitute any fluidic system: pumps, valves and mixers for instance. Yet, these building blocks run into the limits of miniaturization and most of the designs used in human-scale flows are either impractical or completely inapplicable to micron-scale flows. On the other hand, while large scale flows are rather insensitive to small leaks, miniaturized fluidic devices become increasingly sensitive to such imperfections. This problem is made worse by the difficulty of micron-scale fabrication, especially when moving parts are involved. An attractive route is optical actuation because light fields are non invasive and dynamically reconfigurable, and solutions have been proposed through the use of optical tweezers to manipulate small particles in flows. By controlling the position and rotation of many particles independently, pumps, valves and particle sorters have been demonstrated in microfluidic channels. The extension of these techniques to multiphase flows is nevertheless difficult because colloidal particles interact with fluid-fluid interfaces.

Here, we propose two types of optical forcing to drive microfluidic two-phase flows or, conversely to answer the requirements enumerated above, namely to block, merge, divide or sort individual droplets flowing in a microchannel. First, we investigate the effect of the optical radiation pressure on fluid interfaces and analyze microfluidic flow regimes in laser-induced jetting, either droplet dripping or continuous transport in laser-sustained liquid columns (Fig. 1). Then, we investigate a dissipative coupling consisting in heating locally an interface between two immiscible fluids to produce thermocapillary stresses along this interface. This effect, known as the optical Marangoni effect, is implemented in adequate microchannel geometry to devise fundamental building blocks for two-phase flows in microfluidic devices (Fig. 2). This allows the creation of contactless optical actuators such as mixers, valves, droplet sorters and switch, droplet dividers or droplet mergers.

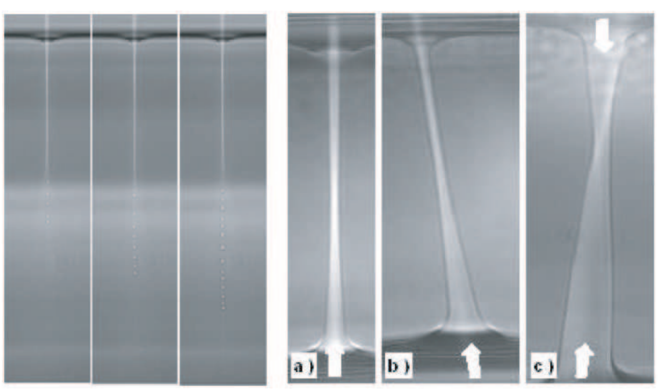

Figure 1: Microfluidic flows driven by the optical radiation pressure, (1) Dynamics of droplet emission during laser-induced jetting (1 fps); (2) Different sort of liquid columns (liquid optical fibres) induced and stabilized by radiation pressure largely beyond the Rayleigh-Plateau instability onset.

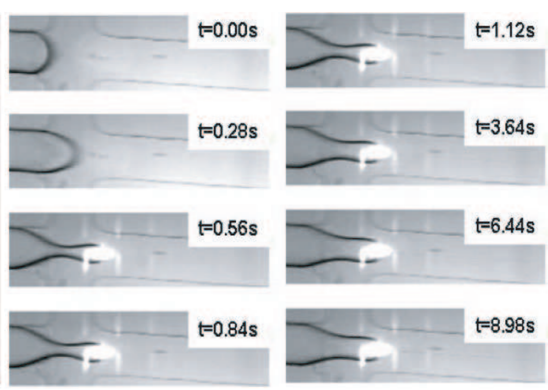

Figure 2: Optical actuation of a water flow in a microchannel, Implementation of an optical valve: the laser pins the interface for several seconds by thermocapillary stresses, producing larger drops of calibrated volume without changing flow rates.

Light-mediated Particle Interactions in a Laser Trap

G. L. Lippi, **S. Barland**, **M. Colombet**, **J. Farmer**, **and R. Kaiser**
Institut Non Linéaire de Nice, France

J.-M. Fournier
Swiss Federal Institute of Technology, Switzerland

Optical manipulation of small objects has been the focus of attention for over three decades and has brought about a revolution in our techical capabilities and in our understanding of the electromagnetic forces acting on different materials ranging from atoms, to dielectric and conductive particles all the way to biological samples. The implications of these developments are so far-ranging that even now we do not foresee their full capabilities.

At first, much of the attention was focussed on the direct forces that are exerted directly on the object by the laser beam used for its control. Recent developments in trapping multiple objects and downscaling the trap's size (and the objects' size as well) open up new questions as to the mutual interactions which take place among the trapped elements. Indeed, when one single coherent beam is used for holding together the sample, the light scattered by each element contributes to the global scattered field which influences all particles. Experimental evidence has already shown that when a sufficiently large number of objects is trapped, the trapping field cannot be considered independently of the scattered components and that the trap is the result of the global superposition of all fields.

We will discuss different aspects of the interaction of multiple particles trapped by a common coherent field. Pairs of spheres [1, 2] and multiplets [3, 4] are known to bind together maintaining preferential distances dictated by the interaction between the scattered and the trapping field. Multiple spheres form structures which depend on the symmetries imposed on the problem.

A such one-dimensional arrangement can be obtained either through the interference of two beams [2] or through a strongly elliptical trap. For this trap geometry the effects of fluctuations are strongly modified in the two directions (parallel and perpendicular to the trapping field). In addition, in the elliptical trap configuration the interaction strength is not constant and can thereby influence the trapping characteristics.

In a two-dimensional arrangements where preferential sites are imposed by the trapping beam [2] the particles mostly sit at the pre-chosen positions but present residual fluctuation-induced motion which is reminiscent of transport problemes. If instead the trap is smooth, states may be found where the particles move quite freely, followed, as the trap power is increased, by "viscous" motion as in a fluid, and terminating in "rigid" structures.

Additional optical interactions may also be induced by cell surfaces, whereby the effectiveness of these contributions depends on the size of the particles, the light polarisation, and in general by the systems parameters. Size considerations will be discussed for downscaling to very small objects.

REFERENCES

1. Burns, M. M., J. M. Fournier, and J. A. Golovchenko, *Phys. Rev. Lett.*, Vol. 63, 1233, 1989.
2. Burns, M. M., J. M. Fournier, and J. A. Golovchenko, *Science*, Vol. 249, 749, 1990.
3. Tartarkova, S. A., A. E. Carruthers, and K. Dholakia, *Phys. Rev. Lett.*, Vol. 89, 283901, 2002.
4. Singer, W., M. Frick, S. Bernet, and M. R. Marte, *J. Opt. Soc. Am.*, Vol. B 20, 1568, 2003.

Non-lorentzian Electromagnetic Resonances

V. A. Markel
University of Pennsylvania, USA

In quantum mechanics, scattering amplitude exhibits resonance behavior if the energy of scattered particles is close to the energy of one of the quasi-stationary states, if such quasi-stationary states exist. For potentials which decay fast enough at infinity, the resonance cross sections, as functions of energy, can be accurately approximated by Lorentzians. A similar phenomenon can be found in electromagnetic scattering. Consider scattering of monochromatic waves with the frequency ω by a homogeneous non-magnetic scatterer of arbitrary shape characterized by the dielectric function $\epsilon(\omega)$. We can define an electromagnetic eigenstate as a solution to $\int_V \hat{G}_0(\omega;\mathbf{r},\mathbf{r}')\mathbf{P}_n(\omega;\mathbf{r}')d^3r' = \xi_n(\omega)\mathbf{P}_n(\omega;\mathbf{r})$. Here V is the volume occupied by the scattering material, $\hat{G}_0(\omega;\mathbf{r},\mathbf{r}')$ is the frequency-domain, dyadic free-space Green's function for the Maxwell's equation which gives electric field at the point $\mathbf{r}$ due to a point dipole oscillating at frequency ω at the point $\mathbf{r}'$, $\mathbf{P}_n(\omega;\mathbf{r})$ is the n-th polarization eigenstate and $\xi_n(\omega)$ is the corresponding eigenvalue (generally, complex). The extinction cross section can be written as a sum over the eigenmodes, i.e., $\sigma_e = \sum_n f_n(\omega)/[z(\omega) - \xi_n(\omega)]$, where $f_n(\omega)$ is the generalized oscillator strength for the n-the eigenmode which has no singularities in the complex plane as a function of ω and $z(\omega)$ is the spectral variable defined by $z(\omega) = (4\pi/3)[\epsilon(\omega) + 2]/[\epsilon(\omega) - 1]$ [1]. Electromagnetic resonances take place when the denominator in the above equation is in some sense small. However, the imaginary part of the denominator can not vanish due to energy conservation considerations. Therefore, we define resonance frequencies ω_n as solutions to $\mathrm{Re}[z(\omega_n)-\xi_n(\omega_n)] = 0$. If ω is close to one of the resonance frequencies ω_n, and if $\xi_n(\omega)$ and $f_n(\omega)$ change slowly in the vicinity of ω_n, one can make the quasi-particle pole approximation and write $\sigma_e \approx [f_n(\omega_n)/z'(\omega_n)]/[\omega - \omega_n + i\gamma_n]$, where $\gamma_n = \mathrm{Im}[z(\omega_n) - \xi(\omega_n)]/z'(\omega_n)$ and prime denotes differentiation. This resonance has the typical Lorentzian structure with the lifetime $\tau_n = 1/\gamma_n$ which is determined by the sum of Ohmic ($\mathrm{Im}[z(\omega_n)]$) and radiative ($-\mathrm{Im}[\xi(\omega_n)]$) losses.

In scatterers which are small compared to the external wavelength, the quasi-particle pole approximation is, typically, quite accurate. This is due to the fact that, within the quasistatics, the real parts of $\xi_n(\omega)$ are ω-independent an satisfy $-8\pi/3 < \mathrm{Re}\xi_n < 4\pi/3$ [2]. In extended systems these statements are, generally, not valid. In particular, in a long periodic chain of nanospheres, real parts of eigenvalues ξ_n diverge logarithmically near certain frequencies which are determined from the synchronism condition [3]. This divergence leads to electromagnetic resonances which are essentially non-Lorentzian. In particular, their width is determined not by relaxation but by the range of frequencies in which the equation $\mathrm{Re}[z(\omega) - \xi_n(\omega)] = 0$ is approximately satisfied. It was shown that these resonances are super-exponentially narrow with the width being proportional to the factor $\exp[-C(h/a)^3]$, where C is a numerical constant of the order of unity, h is the period of the chain and a is the nanosphere radius [4]. The divergence of eigenvalues can also lead to narrow spectral holes which were already reported in [3]. Recent advances in nanofabrication have reinvigorated interest in one-dimensional chains of nanoparticles. A dramatic narrowing of spectral lines and unusual properties electromagnetic resonances were found numerically in chains of large but finite length in [5]. The origin and properties of these resonances in infinite chains were discussed theoretically in [4]. Theoretical treatment of finite chains was recently given in [6].

REFERENCES

1. Markel, V. A. and E. Y. Poliakov, *Phil. Mag.*, Vol. 76, 895, 1997.
2. Markel, V. A., V. N. Pustovit, S. V. Karpov, A. V. Obuschenko, V. S. Gerasimov, and I. L. Isaev, *Phys. Rev. B*, Vol. 70, 054202, 2004.
3. Markel, V. A., *J. Mod. Opt.*, Vol. 40, 2281, 1993.
4. Markel, V. A., *J. Phys. B*, Vol. 38, L115, 2005.
5. Zou, S., N. Janel, and G. C. Schatz, *J. Chem. Phys.*, Vol. 120, 10871, 2004.
6. Citrin, D. S., *Nano Letters*, Vol. 5, 985, 2005.

Exact Calculations of Optical Forces and Optical Binding in Single and Multiple Beam Optical Traps

O. Moine and B. Stout
Université Paul Cézanne Aix-Marseille III et Université de Provence, France

We present essentially exact multi-pole multi-scattering techniques for carrying out optical force calculations in a wide variety of optical trapping situations involving either isolated particles or collections of simultaneously trapped particles.

We illustrate that our exact techniques [1] can quite readily be applied to a variety of trapping situations and particle types for which popular approximate techniques (Rayleigh, geometric optics, Born approx. etc.) are either inapplicable or exceedingly difficult to carry out.

In particular, we highlight the use of our techniques to investigate the intriguing optical binding and optical "crystallization" observed in multiple-beam interferential optical traps [2–4].

We also rapidly illustrate applications of our techniques to the widely employed single-beam optical traps known as optical tweezers. In particular, we discuss the techniques which we have developed in order to model the extremely tightly focused beams which are essential to standard optical tweezers.

REFERENCES

1. Moine, O. and B. Stout, "Optical force calculations in arbitrary beams by use of the vector addition theorem," *JOSA B*, Vol. 22, No. 8, 1620–1631, 2005.
2. Burns, M., J. M. Fournier, and J. A. Golovchenko, "Optical Matter: crystallization and binding in intense optical fields," *Science*, Vol. 249, 713–828, 1990.
3. Burns, M. M, J. M. Fournier, and J. A Golovchenko, "Optical binding," *Phys. Rev. Lett.*, Vol. 63, 1233–1236, 1989.
4. "Optical binding between dielectric particles," *Opt. Express*, Vol. 12, No. 12, 2746–2753, 2004.

Shaping Electromagnetic Fields for Optical Trapping and Binding

J.-M. Fournier, **P. Jacquot**, **J. Rohner**, **and R.-P. Salathé**
Imaging and Applied Optics Institute, Switzerland

Optical traps can be built simply from constructive and destructive interference of two or more coherent light beams. For example, interference of several identical plane waves distributed with an n-fold symmetry lead to periodic or aperiodic arrays of traps [1]. Figure 1 displays such a set of traps. Interference between an intense electromagnetic field impinging on mesoscopic particles and fields scattered by such particles generate ensembles of self distributed traps [2]. This leads to assemblies of the type of the one shown in Figure 2. Other kinds of interference made with two or more beams presenting a variety of complex amplitude distributions lead to atypical intensity landscapes presenting endless configuration possibilities for trap potentials [3]. The design of various trap shapes can then be manipulated at will through such interference, in order to control trap strength or also to command optical forces which channel polarizable dielectric particles. Besides, one can simply take advantage of free space wave propagation to form interference by illuminating a diffractive pattern with a plane wave or with a spherical wave.

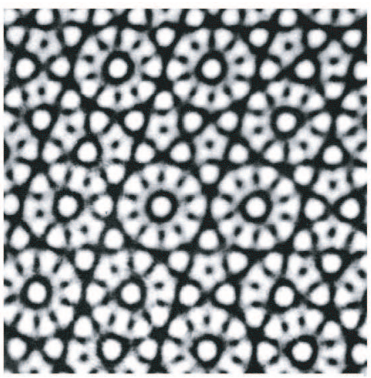

Figure 1: Five-fold symmetry array of optical traps.

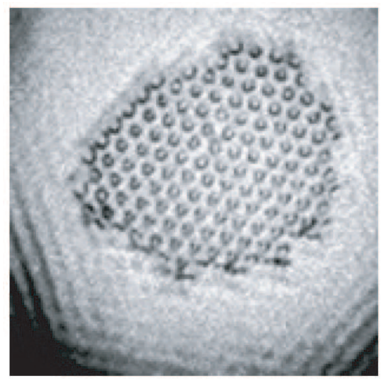

Figure 2: Dielectric particles assembled with gradient and binding forces.

The scope of this paper is to review and discuss several uncommon optical trap designs, such as those using Talbot imaging, a periodic diffractive structure, speckle patterns, or multiple beam interference. Experimental results emphasize the capability of the Talbot effect to generate three-dimensional optical lattices with the advantage of creating stiff traps with strong gradient forces. Several schemes of self-organization representing interesting means for trapping will also be described and discussed.

Mechanisms involved in those trapping procedures do not require the use of bulky high numerical aperture optics and are under test to produce new regimes of optical trapping. Most of the investigated designs account for the possibility of creating large arrays of traps.

REFERENCES

1. Burns, M. M., J.-M. Fournier, and J. A. Golovchenko, "Optical matter, crystallization and binding in intense optical fields," *Science*, Vol. 249, 749–754, 1990.
2. Burns, M. M., J.-M. Fournier, and J. A. Golovchenko, "Optical binding," *Phys. Rev. Lett.*, Vol. 63, 1233–1236, 1989.
3. Fournier, J.-M., J. Rohner, P. Jacquot, R. Johann, S. Mias, and R. P. Salathé, "Assembling mesoscopic particles by various optical fields," *Trapping and Optical Micromanipulation II, SPIE Proc.*, Vol. 5514, 2005.

Theory and Modeling of Optical Forces within a Collection of Mie Scatterers

T. M. Grzegorczyk, **B. A. Kemp**, **and J. A. Kong**
Massachusetts Institute of Technology, USA

Optical binding and trapping have been experimentally verified on dielectric particles by various groups [1–4, to name only a few]. The corresponding theoretical analysis, however, still needs to be developed beyond the simple approximations of Rayleigh scattering or couple of Mie particles. In this work, we present an exact method to compute the optical forces within a system of multiple Mie particles. For the sake of simplicity, the particles are taken to be lossless dielectric cylinders, which is not a severe limitation per se since apart from the depolarization effects, most of the phenomena observed in two-dimensions can be generalized to three-dimensions.

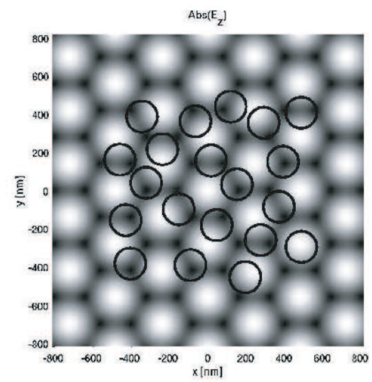

Figure 1: Initial positions of 20 particles in an interference field.

The optical forces are computed from the Maxwell stress tensor, which therefore requires the knowledge of the scattered field from the collection of particles. The latter is computed from the Mie theory for cylinders and the Foldy-Lax multiple scattering equations, which take into account all the interactions between the particles. Hence, apart from the assumption of real permittivity, the method does not make any approximation on the size of the particles or their number in the collection.

In order to conform to the experimental setup, the system of particles is excited by three incident beams, forming an hexagonal interference pattern. For the sake of illustration, we present results for a collection of 20 particles initially randomly positioned in the interference field, like shown in Fig. 1. The forces on each particle is computed and their positions are updated accordingly. At the next time step, the forces are computed anew with the new positions, and the process is reiterated until convergence has been obtained, shown in Fig. 2. It can be seen that for the particle size considered, a gradient force is exerted on the particle which tends to align them with the high eld intensity regions. However, binding forces between the particles tend to disrupt this regular pattern and it is seen that the nal positions of some particles (typically toward the edge of the collection) is shifted from the expected positions. We believe that it is the rst time that this phenomenon, known in experimental situations, is shown by an analytical modeling.

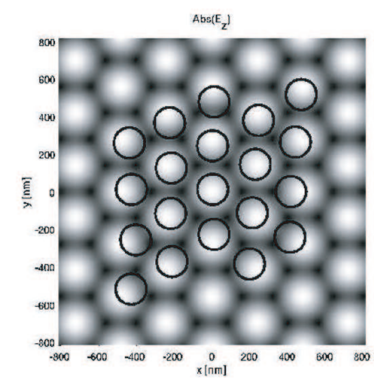

Figure 2: Final positions of 20 particles due to optical forces.

REFERENCES

1. Ashkin, A., "Acceleration and trapping of particles by radiation pressure," *Phys. Rev. Lett.*, Vol. 24, 156–159, 20 January 1970.
2. Burns, M. M., J.-M. Fournier, and J. A. Golovchenko, "Optical binding," *Phys. Rev. Lett.*, Vol. 63, No. 12, 1233–1236, 1989.
3. Zemánek, P., A. Jonáš, L. Šrámek, and M. Liška, "Optical trapping of nanoparticles and microparticles by a gaussian standing wave," *Optics Letters*, Vol. 24, 1448–1450, 1 November 1999.
4. Fournier, J.-M., J. Rohner, P. Jacquot, R. Johann, S. Mias, and R. Salathé, "Assembling mesoscopic particles by various optical schemes," *Proceedings of SPIE*, 2005.

Session 3P2
Advanced Methods for Light Scattering Analysis in Nanotechnology and Biophotonics

Numerical Comparison of Light Scattering Results by Particles in Free Space Obtained by Discrete Dipole Approximation and Volume Integral Equation Methods

V. I. Ivakhnenko
ADE Corporation, USA

Rigorous numerical methods are applied widely for light scattering modeling by nanoparticles located in different media. The most flexible methods that allow simulate arbitrary shaped particles and to take into account permittivity distribution inside the particle and its anisotropy properties as well are Discrete Dipole Approximation (DDA) [1] and Volume Integral Equation (VIE) [2] methods. Both methods look rather similar: they are based on numerical solution of Electric field integral equation for unknown function inside the volume of scatter; the conditions at infinity are taken into account analytically; fast Fourier transform (FFT) technique is utilized in numerical solution of linear equation system in order to accelerate matrix-vector multiplications. Nevertheless, DDA method allows accurate calculations of electromagnetic scattering from targets with "size parameters" $2\pi a/\lambda < 15$ provided the refractive index m is not large compared to unity ($| m-1 |< 1$) where as VIE method area of application is significantly wider. This is illustrated at Fig. 1 where the elements of Jone's matrix for the light scattering by spherical particle calculated by DDA and VIE codes are compared to Mie theory. It is important to underline that the same mesh was used in calculations for DDA and VIE methods.

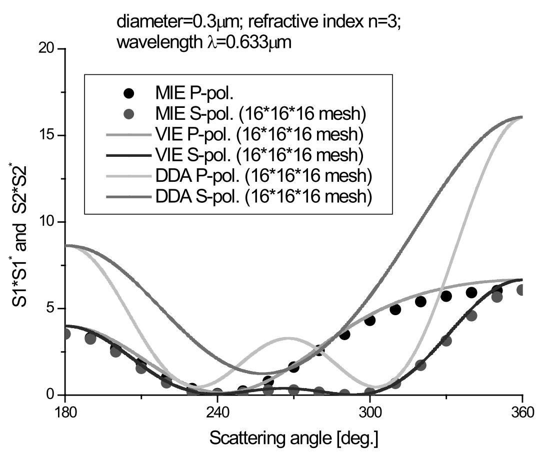

Figure 1.

Analysis of DDA and VIE matrixes structure allows explain why DDA provides rather accurate results for the small values of refractive index but failed for high values.

*Author would like to acknowledge support of this work by ADE Corporation, Westwood, MA, USA.

REFERENCES

1. Draine, B. T. and P. J. Flatau, *J. Opt. Soc. Am. A,* Vol. 11, 1491–1499, 1994.
2. Eremin, Y. and V. Vakhnenko, *JQSRT*, Vol. 60, 475–482, 1998.

Analysis of Evanescent Waves Scattering by a Single Particle in Total Internal Reflection Microscopy

E. Eremina[1], **T. Wriedt**[1], **and L. Helden**[2]

[1]University of Bremen, Germany
[2]University of Stuttgart, Germany

Since its invention in the mid of eighties Total Internal Reflection Microscopy (TIRM) has proven to be an effective technique to measure weak interactions between spherical colloidal particles and surfaces with a resolution of a few femtonewton. It is a single particle evanescent light scattering technique. In an experimental setup a laser beam is coupled into a prism and hits the glass-water interface with an angle slightly above the critical angle of total internal reflection. This generates an evanescent field near the interface that decays in the lower refractive index medium (water) with a characteristic penetration depth which depends on the angle of incidence. A colloidal particle that is dispersed in the medium will scatter light from the evanescent wave if it is in the vicinity of the surface. By registering a scattered intensity it is possible to deduce the particle-substrate distance. Compared to other methods for measure particle wall interactions like the surface force apparatus or the atomic force microscopy where a colloidal particle is attached to the tip, TIRM is the most sensitive technique because thermal fluctuations which limit the other methods in their resolution are exploited to determine the interaction potential. This way forces in the order of a few femtonewton can be detected. TIRM has proven to be a valuable tool for the precise measurement of weak colloidal interactions as double layer forces, van der Waals forces, magnetic interactions and depletion forces. Review on TIRM can be found for example in [1].

To compare experimental results with results of mathematical modeling an effective method is needed. For this purpose the Discrete Sources Method (DSM) has been chosen. The DSM is a well-known method for light scattering analysis, which has recently been applied for evanescent wave scattering [2]. In frame of DSM the scattering problem includes Maxwell equations, infinity conditions and transmission conditions at the interface and boundary conditions at an obstacle surface. An approximate solution of the scattering problem is constructed as a finite linear combination of discrete sources deposited in a domain inside a scatterer with certain amplitudes. The constructed approximate solution satisfies all the terms of the original scattering problem except the boundary conditions at an obstacle surface. At the last stage the amplitudes of the discrete sources are defined from the boundary conditions at the surface of the scatterer following the generalized point-matching technique. Additionally, the DSM gives opportunity to control the accurateness of obtained results by surface residual calculating.

Numerical results obtained on the base of the DSM will be shown in the presentation. Comparison with experimental results which demonstrates a good congruence between theory and measurements will be presented.

*Authors would like to acknowledge financial support of this work by Deutsche Forschungsgemeinschaft (DFG).

REFERENCES

1. Bike, S. G., "Measuring colloidal forces using evanescent wave scattering," *Current Opinion in Colloid & Interface Science*, Vol. 5, 144–150, 2005.
2. Eremin, Y. and T. Wriedt, "Large dielectric particle in an evanescent wave field near a plane surface," *Opt. Comm.*, Vol. 214, 39–45, 2002.

T-matrix Simulation of Plasmon Resonances of Particles on or near a Surface

N. Riefler and T. Wriedt
University of Bremen, Germany

Surface plasmons of small noble metal spheres can be detected as resonance peaks in the measured light scattering spectra. The surface plasmon resonance frequency from a nonspherical particle or from a particle aggregate is different compared with a single spherical particle. With that effect, measuring techniques which use white light as illumination are capable to differ between aggregated particles and a single particle because of their different color. Even when a bio receptor molecule attached to a gold or silver sphere detects a biomolecular counterpart, the resonance frequency changes.

This application shows the significance of using surface plasmons to act as a detector in nano technology [2]. To improve the measuring techniques, it seems to be worthwile to know which combination of materials deliver best results. Therefore, we investigate the differences between gold and silver substrates on the resonance spectra of silver and gold particles near those different surfaces. The geometrical surface thickness are assumed to be greater than the Born/Wolf condition for thick films.

Another problem is the validity of approximation models and to what extend they may be used. For a particle on a perfectly conducting surface, we found identical spectra compared to a system consisting of two spheres. However, the spectra are different if we calculate a particle on a glass or on a noble metal surface. These differences indicate that approximations with a mirror particle together with using cluster simulation programs are not valid in detail. We have observed that even qualitative statements fail. The same holds for studies where conventional light scattering programs based on Mie-theory or T-matrix theory are applied regardless of the influence of the nearby surface [1]. These authors use their results for qualitative statements.

Instead of these approximation models, we want to present a T-matrix method to calculate the scattering response of a particle on or near a surface. On the basis of the nullfield method with discrete sources [3], a computer code is established to simulate some of the problems mentioned above. The scattering problem is a multiple particle problem and the solution method is the separation of variables technique.

Up to now we can calculate spheres as well as spheroids, cylinders and rounded oblate cylinders on or near a surface having arbitrary refractive index.

REFERENCES

1. Wei, Q.-H., K.-H. Su, S. Durant, and X. Zhang, "Plasmon resonance of finite one-dimensional Au nanoparticle chains," *Nano Lett.*, Vol. 4, 1067–1071, 2004.
2. Natan, M. J. and L. A. Lyon, "Surface plasmon resonance biosensing with colloidal Au amplification," *Metal Nanoparticles. Synthesis, Characterization and Applications*, Marcel Dekker, 183–205, 2002.
3. Wriedt, T. and A. Doicu, "Light Scattering from a particle on or near a surface," *Phys. Rev. B*, Vol. 152, 376–384, 1998.

Mean-field Theory of Light Scattering by Naturally Rough Surfaces

V. V. Lopushenko
Moscow State University, Russia

Scattering from rough surfaces is a subject of interest in many diverse research areas, such as optics, spectroscopy, remote sensing, sonar detection, radar imaging. The two classical and widely used methods to study scattering from two-dimensional rough surfaces are the Rayleigh or small-perturbation method (SPM) and the Kirchhoff or physical optics approxi-mation (KA) [1, 2]. The former is valid for small heights and slopes, and the latter is valid for high frequencies and large radii of curvature. In these regions of the surface parameters the two methods give useful results, but they do not overlap except those surfaces that have small and smooth roughness [3].

Therefore, strong interest persists to develop new analytical approaches to obtain better solu-tions in a domain where the accuracy of neither the KA nor the SPM is guaranteed. This makes alternative methods such as the mean-field theory (MFT) interesting since it may bridge the gap between the SPM and the KA. The MFT has been introduced quite recently [4, 5] and has not been systematically tested in the 2D case in scattering from substantially rough surfaces having root-mean square (RMS) height comparable with wavelength of the incident radiation. In this paper the MFT is applied to calculate incoherent scattering from 2D rough natural surfaces with power-law spectra, which are typical for fractal or ocean-like surfaces. An important fact to note is that the RMS/wavelength ratio is not assumed to be a small parameter, that is why both electric field and Green's tensor involved to the integral equation for scattered intensity are calculated numerically as solutions of the reference problem characterized by averaged refractive index.

To study a validity domain of the presented approach, some computer simulations have been made for the surfaces with ocean-like spectrum. The RMS heights of the considered surfaces were well beyond the usual SPM domain. The numerical comparison between the presented modification of the MFT and other approaches [3] show surprisingly good agreement in scattering diagrams plotted in the main incidence plane for both polarization cases.

REFERENCES

1. Beckmann, P. and A. Spizzichino, "The scattering of electromagnetic waves from rough surfaces," Macmillan, New York, 1963.
2. Voronovich, A. G., "Wave scattering from rough surface," 2nd edn, Springer, Berlin, 1998.
3. Soriano, G., C. A. Gu'erin, and M. Saillard, "Scattering by two-dimensional rough surfaces: comparison between the method of moments, Kirchhoff and small-slope approximations," *Waves Random Media*, Vol. 12, 63–83, 2002.
4. Sentenac, A. and J. J. Greffet., "Mean-field theory of light scattering by one-dimensional rough surfaces," *J. Opt. Soc. Am. A*, Vol. 15, No. 2, 528–532, 1998.
5. Lopushenko, V. V., "Calculation of Scattering from Microroughness of Filmed Wafers," *Proc. of the 4st Conference on Electromagnetic and Light Scattering by Nonspherical Particals: Theory and Applications*, 231–238, Vigo, Spain, September 20–21, 1999.

Rigorous Model for Gold Nanorods Spectra Examination Based on Discrete Sources Method

Y. A. Eremin
Moscow Lomonosov State University, Russia

Gold nanorods have received much attention in recent years due to their special electronic and optical properties. For example, the sensitivity of the plasmon resonance frequency toward the refractive index of the surroundings makes them suitable candidates for biological sensing applications [1]. For these applications gold nanorods of diameter from 15 nm up to 90 nm and having a variety of aspect ratios (length/diameter) from 2 to 12 are usually employed. They demonstrate an existence of several resonance peaks in the field of evanescent waves. The necessity to predict the positions and value of the frequency resonances requires to built computer model enables to perform a rigorous analysis of the scattering spectra. A lot of efforts have been spent developing rigorous models to examine light scattering from a nanorod deposited in a vicinity of a plane interface. Nevertheless the most approaches used so far do not account completely the interaction between field scattered by nanorod and the interface surface.

The model used here is based on asymmetrical version of the Discrete Sources Method (DSM) [2]. This technique constructs the scattered field everywhere outside a local obstacle as a finite linear combination of the fields resulting from electric dipoles distributed over an auxiliary surface located inside the obstacle. The Green Tensor of a half-space is incorporated to fit the transmission conditions enforced at the plane interface. Then the scattered field analytically satisfies transmission conditions at the interface, thus accounting for all interactions between particle and interface automatically. Internal field is represented on the basis of regular functions, which fit Maxwell's equations. So, the DSM solution constructed satisfies Maxwell's equations everywhere outside medium discontinuities, required infinity conditions and transmission conditions at the plane interface. Then the unknown DS sources amplitudes are to be determined from boundary conditions enforced at the surface of the local obstacle only.

It has been found that more stable results can be obtained by using pseudo-solution of an over-determined system of linear equations obtained by following the generalised point-matching technique. Select a set of matching points on the particle homogeneously covering the surface. Then distribute homogeneously DS over the auxiliary surface. In each DS point we choose three independent electric dipoles, which originate the scattered field. Then the linear system to be used for determining of the DS amplitudes is derived from matching the boundary conditions at the set of matching points. This procedure leads to an over-determined matrix and the DS amplitudes are evaluated by a pseudo-inversion technique [3]. The numerical scheme allows to consider all incidences and both polarization P and S at once. DSM computer model controls convergence and stability of the result obtained by a posterior evaluation of the surface residual. In the presentation computer simulating results associated with an influence of nanorod aspect ratio, orientation and exciting field polarization on the scattering spectra will be presented.

*Author would like to acknowledge support of this work by ADE Corporation, Westwood, MA, USA and Russian Foundation for Basic Research.

REFERENCES

1. Zhu, J., et al., "Shape dependent resonance light scattering properties of gold nanorods," *Materials Science and Engineering B*, Vol. 121, 199–203, 2005.
2. Eremin, Y. A., J. C. Stover, and N. V. Grishina, "Discrete sources method for light scattering analysis from 3D asymmetrical features on a substrate," *J. Quant. Spectrosc. Radiat. Transfer.*, Vol. 70, 421–431, 2001.
3. Grishina, N. V., Y. A. Eremin, and A. G. Sveshnikov, "Analysis of evanescent waves transformation based on Discrete Sources Method," *J. Commun. Techn. Electron.*, Vol. 49, 117–124, 2004.

Local Biosensor Operation Analysis Based on Discrete Sources Method Model

N. V. Grishina and Y. A. Eremin
Moscow Lomonosov State University, Russia

Interest in electromagnetic wave scattering by nanoshells has increased rapidly within the past years. Nanoshells represent a new type of nanoparticles composed of a dielectric core coated with a thin noble metallic shell. Such particles are of great interest in different applications due to their scattering behavior and ability to demonstrate plasmon resonance response in the visible range of optical spectrum. It has been found that the resonance frequency of a nanoshell depends on its properties: material, size, shape, shell thickness and etc. Varying those parameters enables to shift the resonance peak to a required frequency domain, in particular to the "transparent window" for biological tissue. Nanoshells used for biomedical applications are often called local biosensors [1]. The principle of a local biosensor operation is based on the evanescent waves transformation near water-glass interface. The light scattered by nanoshell is detected by objective lens. Even a small changing of the refractive index in the vicinity of the particle, caused by presence of irrelevant substances, leads to a shift of the resonance peak position. So, from detection of its position one can get information about refractive index of an ambient media in the vicinity of the sensor and detect its deviation from the known refractive index of ambient water [1].

During the last years a lot of effort has been spent developing rigorous model to predict light scattering from nanoshell deposited near a plane interface. Nevertheless the most approaches used so far do not account completely the interaction between nanoshell and interface. The model presented here is based on the Discrete Sources Method (DSM) [2, 3]. This technique constructs the scattered field everywhere outside an axial-symmetric layered particle as a finite linear combination of the fields resulting from multipoles distributed over the axis of symmetry inside the particle. The Green Tensor of a layered substrate is employed to account for the complete interaction of the particle with a stratified interface analytically [2]. The solution for the scattered field satisfies Maxwell's equations and required conditions at infinity. Then the unknown discrete sources amplitudes are determined from transmission conditions enforced at the layers of the particle [3].

DSM numerical scheme is based on axial symmetry of the scattering geometry (particle-interface). Exciting evanescent wave impinging the particle from prism surface is resolve in Fourier series with respect to the azimuth angle. This leads to the reducing surface approximation to a set of one dimensional approximating problems enforced at the layers profiles. To fit the transmission conditions we use generalized point-matching technique. Multipoles amplitudes are determined as pseudo-solutions over-determined systems of the linear equations. The DSM scheme enables to consider all incident angles and both polarization P and S at once. The DSM computer model controls convergence and stability of the results by a posterior evaluation of the surface residual at the particle layers. In the presentation computer simulating results relating to the biosensor synthesis, operation and sensitivity to a local changing of environment will be presented.

*Authors would like to acknowledge support of this work by ADE Corporation, Westwood, MA, USA and Russian Foundation for Basic Research.

REFERENCES

1. Raschke, G., et al., "Gold nanoshells improve single nanoparticles molecular sensors," *Nanoletters*, Vol. 4, 1853–1857, 2004.
2. Grishina, N. V., Y .A. Eremin, and A. G. Sveshnikov, "Analysis of evanescent waves transformation based on discrete sources method," *J. Commun. Techn. Electron.*, Vol. 49, 117–124, 2004.
3. Grishina, N. V., Y. A. Eremin, and A. G. Sveshnikov, "Analysis of the scattering properties of oxide particles at a layered substrate," *Physics Bulletin*, Vol. 54, No. 2, Moscow University, 2000.

Magnetic Nanostructure Hysteresis Loop Calculation for Modified Thin Film Multi-layer by Ion Irradiation

D. Bajalan
Vienna University of Technology, Austria

The fluence of ion irradiation on polycrystalline thin films affects both anisotropy and spontaneous magnetisation M_s. The dependence of coercivity and initial susceptibility on M_s is predicted by a hysteresis model considering the balance of energy with good qualitative agreement.

Magnetic nanostructures have become a centre of great interest in the scientific community and in industry as the core technologies behind magnetic recording devices [1]. Demands for the continuous increase in the data storage density bring the challenge to overcome physical limits for currently used magnetic recording media [2, 3]. Small changes in the way a thin film is produced often give rise to large changes in some of the magnetic properties of the thin film. This is best understood by observing how the microstructure of the film changes with processing and then correlating the microstructure directly with the properties of the thin film [4]. The behaviour of magnetic nanoparticles has fascinated materials scientists for decades. And the magnetic properties of an ultra thin multilayer can be patterned by controlled ion beam irradiation. There are fundamental limits due to the atomic nature of matter which may impose ultimate physical bounds to nanofabrication and miniaturization. Over the past several decades, amorphous and more recently nano-crystalline materials have been investigated for applications in magnetic devices. The benefit found in the nano-crystalline alloys stem from their chemical and structural variations on a nano-scale which are important for optimizing magnetic recording devices. The anisotropy energy ku is essential for evaluation of the thermal stability condition on a given bit. For the three irradiated samples ($A1$, $A2$, $A3$), k_u were calculated (Equation 1).

$$k_u = \frac{H_k \mu_0 M_s}{2} \tag{1}$$

REFERENCES

1. MacMathuna, D., "Surface studies of nanomagnetic systems," A Thesis Submitted to the University of Dublin, Trinity College,Physics Department, Vol. 3, 2002.
2. Solzi, M., M. Ghidini, and G. Asti, *Magnetic Nanostructures*, Vol. 4, 123, 2002.
3. Lapicki, A., K. Kang, and T. Suzuki, *IEEE Trans. Magn.*, Vol. 38, 589, 2002.
4. Laughlin, D. E. and B. Lu, Seagate Research Center, Materials Science and Engineering Department and Data Storage Systems Center, Carnegie Mellon University, Pittsburgh, Vol. 2, 2001.

Energetical Model Interpretation of Thermal Stability by Changing Direction of the Magnetization of Nano Magnetic Structure

D. Bajalan
Vienna University of Technology, Austria

The nonlinear dependence of magnetization on direction of the applied magnetic field and history is described by statistical domain behavior using phenomenological adaptive parameters (like: $g\,[1]$, $h\,[A/m]$, $k\,[J/m^3]$, and q that are related to anisotropy, saturation field, static hysteresis loss, and pinning site density) [1]. The loop simulation data could be used also as parameters for thermal stability [2] equation to calculate the relaxation time of the stored information on any magnetic nano particles (dots) of patterned magnetic media. Magnetic nano particle thermal stability calculation is essential for development of patterned ultra high magnetic storage media. The use of reliable model (like: Energetic Model (EM) in the predication of non linear ferromagnetic materials properties [1, 3, 4], wich may depend also on direction and history of magnetization) is very important. EM simulation of hysteresis opens a very big opportunities to calculate values of parameters which we then use directly for interpretation of the stability condition of stored information on a nano magnetic structure. The main idea behind that is to change the direction of the applied field H and then see the stability conditions on a a given nano bit volume [2]. The value of the f_{BS} depends strongly on K_u and the volume of the nano structure which holds the stored magnetic information (a what so-called nano bit or nano dot).

REFERENCES

1. Hauser, H., *J. Appl. Phys.*, Vol. 96, 2753, 2004.
2. Sun, L., Y. Hao, C. L. Chien, and P. C. Searson, *IBM J. Res. Develop.*, Vol. 49, 79, 2005.
3. Bajalan, D., H. Hauser, and P. L. Fulmek, *Physica B*, Vol. 343, 384, 2004.
4. Hauser, H., D. Bajalan and P. L. Fulmek, *Progress in Electromagnetic Research Symposium*, (March 28 to 31), Pisa, Italy, 2004, *Extended paper (ISBN 88 8492 268 2)*, 667, 2004.

Innovation Use of Nano Technology in Magnetic Storage Devices and Nano Computers

D. Bajalan
Vienna University of Technology, Austria

J. A. Aziz
University Sains, Malaysia

Nano-technology will increase its influence in electrical engineering and electrical materials strongly [1]. New and light magnetic devices will be invented to make life in the 21^{st} century more functional and the researchers have to gain more knowledge of quantum effects within nano-meter body size [1, 2]. Our understanding of interatomic and electrostatic interactions have now reached a point where we can quite comfortably explain the macroscopic properties of matter, based on quantum mechanics and electrostatic interactions between electrons and ionic nuclei in the material. The fundamental equations of Maxwell will continues playing its large influence in nano magnetic devices ($\nabla \cdot \mathbf{E} = \frac{\rho}{\varepsilon}$, $\nabla \cdot \mathbf{B} = 0$, $\nabla \times \mathbf{E} = \frac{\partial \mathbf{B}}{\partial \tau}$, $\nabla \times \mathbf{B} = \mu_0 \mathbf{J} + \frac{\mu_0 \varepsilon \partial \mathbf{E}}{\partial \tau}$). Nano-technology is providing a critical bridge between the physical sciences and engineering, on the one hand, and modern molecular biology on the other. Materials scientists, for example, are learning the principles of the nanoscale world by studying the behavior of biomolecules and biomolecular assemblies. In the case of magnetic devices, which are the subject of this work, there will be continued development in nano magnetic structures.Nano magnetic structures are becoming one of the trends in developing the magnetic devices like magnetic recording, storage, and other electronic devices. The industry of magnetic data storage systems will profit from the nano-magnetic structures to produce ultra high density recording media at lower prices. Nano-technology enables new design concepts and opportunities for the information industry . The computer industry will benefit largely from the size change in magnetic structures, which are used in technologies of hard disk drives (HDDs) or magnetic random access memories (MRAMs), and other hardware of computer systems parts. The cost per data bit will decrease year by year. The bit price decrease will give larger chances to store data onto magnetic recording media. With the advent of thin films and lithography techniques it is now possible to prepare nano-structured objects with a well controlled geometry, and the ability of modern lithography to produce arbitrary nano-scaled images on a given substrate [3].

REFERENCES

1. Bajalan, D., H. Hauser, and P. L. Fulmek, *Physica B*, Vol. 343, 384, 2004.
2. Bajalan, D., H. Hauser, and P. L. Fulmek, *4th Int. Symposium on HMM*, University of Salamanca, Vol. 8, 78, 2003.
3. Hauser, H., D. Bajalan, and P. L. Fulmek, *Progress in Electromagnetic Research Symposium*, (March 28 to 31), Pisa, Italy, 2004, *Extended paper (ISBN 88 8492 268 2)*, Vol. 667, 2004.

Thin Nanoporous Films with a Honeycomb Structure: Internal Fields, Spectral and Scattering Properties

A. N. Ponyavina and R. A. Dynich
National Academy of Sciences of Belarus, Belarus

N. V. Gaponenko and G. K. Malyarevich
Belarusian State University of Informatics and Radioelectronics, Belarus

Nanoporous thin films with a honeycomb structure fabricated at aluminum electrochemical anodization are now of a great interest because of their unique ability to light spectral and angular selection [1, 2]. Utilizing a self-organized matrix of porous anodic alumina (PAA) is considered to be very promising for applications in microelectronics, magnetic recording, formation of nanotubes, etc. [3]. An attractive optical application of the PAA is connected with imbedding of the luminescent centers, for example ions or semiconductor nanocrystalls [4]. Strong transformation of luminescence spectra and angular distribution of light passed through the PAA are due to multiple scattering, local field enhancements into pores and density of states effects caused by a 2 D photon-crystal structure of the PAA.

New opportunities for these effects controlling may arise when pores are infiltrated with colloidal solutions of noble metallic nanoparticles (MNP). The related joint photonic–electronic confinement becomes possible to manifest at the spectral range of the MNP surface plasmon resonances. In order to determine the most favorable conditions we have developed a calculation method and made numerical simulations of internal fields, spectral and scattering properties in dependence on the PAA and MNP structural parameters.

The PAA films were considered as a high-ordered array of finite circular cylinders, parallel to each other and oriented perpendicularly to a planar substrate. Previously [1] we have developed a model of light propagation through the correlated cylinders ensemble that based on the statistical theory of multiple wave scattering considering single cylinder scattering with the use of the volume integral equation formalism [5]. Now we propose the modification of this scheme applied to the PAA infiltrated with colloidal solutions of the MNP.

Using this approach we have analyzed the PAA transmission spectra and field distribution into the pores at different pore sizes and materials embedded under condition of incident light directed along a pore axis. We have found a strong shift of the PAA transmission spectra short-wavelength cut-off boundary with a pore size enlarging. Theoretical results have shown a good agreement with experimental data. We have also established a possibility to increase the steepness of the cut-off boundary and to create a band type of the PAA transmission spectra by the MNP embedding. The transmission spectra modification is found to be accompanied by strong changing of the local internal field picture and scattering properties.

*The work was supported by the International Scientific Technical Center, Grant #B-276-2.

REFERENCES

1. Vereshchagin, V. G., R. A. Dynich, and A. N. Ponyavina, *Opt. Spectrosc.*, Vol. 87, 116–121, 1999.
2. Lutich, A. A. and I. S. Molchan, *Physics, Chemistry and Application of Nanostructure (Nanomeeting-2003)*, Editors Borisenko, V. E., S. V. Gaponenko, and V. S. Gurin, 256–259, 2003.
3. Thompson, G. E. and G. C. Wood, *Nature*, Vol. 290, 231, 1981.
4. Gaponenko, N. V., I. S. Molchan, A. A. Lutich, and S. V. Gaponenko, *Solid State Phen*, Vol. 97–98, 251–258, 2004.
5. Goodman J. J., B. T. Draine, and P. J. Flatau, *Opt.Letters.*, Vol. 16, 1198–1200, 1991.

Fast Computation of Diffraction by Finite-size Multilayered Arrays of Cylinders

Y.-J. Zhang and E.-P. Li
Institute of High Performance Computing, Singapore

Scattering by gratings or arrays of cylinders has been extensively studied for many years in the areas of remote sensing and optics. Scattering matrix method (SMM), also called T-matrix method, is the most popular method used for the calculation of multiple scattering among all the cylinders. SMM utilizes the T-matrix to describe the scattering property of each single cylinder and the addition theorems of cylindrical harmonics to take account of mutual couplings. So it is viewed as a kind of semianalytical method. Recently, many authors found new applications of scattering matrix method on the simulation of finite size photonic crystal devices. Scattering matrix method is much faster than those purely numerical methods such as finite difference time domain (FDTD) or finite element method (FEM). However, its computational complexity is still $O(N^2)$. This prohibits its further applications in large size devices, where N stands for the total harmonics numbers used to expand the fields for all cylinders.

In this paper, a novel algorithm, named as fast multipole accelerated scattering matrix method (FMA-SMM), is proposed to speed up the solution of SMM. Fast matrix method (FMM) has already been used to solve the integral equations of 2D scattering problems. The principal formula is the integration expression of zero-order Hankel function over the range of polar angle. It can be named as the fast multipole expression of zero-order Hankel function. Since Higher order, instead of only zero-order, Hankel functions are often involved in SMM, FMM could not be used directly. Fortunately, we derived the general fast multipole expressions for any order Hankel functions by using the lowering and rising operators of cylindrical harmonics. Through numerical investigations, we found that the higher order Hankel functions requires larger group size to reach specific error criterion. This has not been pointed out before since only zero-order Hankel function was investigated in previous publications. This new finding is especially important in successful implementation of the algorithm. The general expressions derived convert the dense coupling matrix in SMM into the combination of sparse matrices, namely aggregation matrix, translation matrix and disaggregation matrix. Thus results in a lower computational complexity of $O(N^{1.5})$ when iterative method is used to solve the final equations. The details of implementation will be presented to guarantee the accuracy of the algorithm. The accuracy and efficiency of FMA-SMM are verified by several numerical examples. A large array with more than 2,000 dielectric rods is analyzed to show the advantage of this novel fast algorithm.

A Numerical Method for the Analysis of Electromagnetic Scattering by Three Dimensional Magnetodielectric Body

A. G. Dmitrenko and T. N. Pastuhova
Tomsk State University, Russia

It is of considerable interest for researchers to study scattering of radio waves by a homogeneous 3 D magnetodielectric body. This interest arises from the need to solve a number of important problems in radar, meteorology, biology and atmospherical optic (see for example [1]).

Today, the different methods for the analysis of considered problem are existing. These methods base on differential forms of Maxwell's equations or integral relations of electromagnetic theory. But computer codes realized these methods are extraordinary in expenses of computer resources, especially for nonaxisymmetric scatterers.

In the last years, the method of discrete sources named in West as generalized multipole technique was applied to solving problems of electromagnetic wave scattering by bodies of different physical nature [2]. In particular, in [2] (Chapter 8) the version of discrete sources method for analysis of electromagnetic scattering by arbitrary shaped magnetodielectric body was proposed. In this version a system of discrete sources in the form of pair electric dipoles was used. These dipoles were located inside and outside magnetodielectric body on auxiliary surfaces homothetic to the surface of the body and oriented tangentially to them.

In the planning report the generalized variant of [2] will be proposed. The generalization consist of addition pair tangentially oriented magnetic dipoles in each point of electric dipoles location. The mathematical formulation of the variant and briefly description of capabilities of the developed software package will be done. The advantages of using of combined (electric and magnetic dipoles) system of discrete sources will be discussed. Some results illustrated the influence of nonaxisymmetry of body on bistatic cross section will be reported.

REFERENCES

1. Havemann, S. and A. J. Baran, *J. Quant. Spectrosc. Radiat. Transfer*, Vol. 70, 139, 2001.
2. *Generalized Multipole Techniques for Electromagnetic and Light Scattering* (Ed. by T. Wriedt), Amsterdam, Elsevier Science, 1999.

Rough Surface Characterization by Profilometer at Spatial Frequencies Appropriate for Light Scattering Predictions

J. C. Stover
The Scatter Works, Inc., USA

A study has been underway to provide a better scattering model for front surface reflectors that are optically rough. Scatter from optically smooth surfaces (mirrors) is well related to surface roughness by using Rayleigh-Rice vector perturbation theory. This expression relates the bidirectional reflectance distribution function (BRDF) to the surface power spectral density (PSD) for given set of scattering parameters (incident angle, wavelength and polarization). There is a one to one relationship and either quantity can be found if the other is measured. Thus for optically smooth surfaces the perturbation relationship could be checked by changing the scattering parameters. This resulted in different BRDF expressions, but for smooth, clean front surface reflectors the same PSD was found. Unfortunately the situation is not so easy for optically rough surfaces.

Since the one to one relationship between BRDF and PSD no longer exists for rough surfaces several different PSDs can produce the same BRDF. This makes calculation of the PSD from the BRDF impossible, and it becomes necessary to characterize the surface PSD with a profilometer. This raises a couple of problems. First, profilometers report 1-D PSDs. That is, they consider spatial frequencies propagating only in the direction of the scan, but BRDF is related to 2-D PSDs, which contain frequencies propagating on the surface in all directions. Secondly, most profilometers have a high frequency cutoff of about $0.1\,\mu\mathrm{m}^{-1}$. For visible light this corresponds to light scattered into a three degree cone about the specular beam. The rest of the scattering hemisphere cannot be predicted from profilometer generated PSDs, and thus these PSDs cannot be used to check the rough surface scattering model.

This presentation discusses the issues associated with solving these two problems. The 1-D to 2-D problem is solved by working with isotropic surfaces where a conversion expression can be used. The high frequency cutoff issue is more difficult. To solve this, a correction transfer function has to be found for the profilometer. This is developed by measuring a 2-D optically smooth surface and relating the profilometer PSD to that found using the perturbation expression. This is then applied to the measured PSDs of the rougher surfaces. A serious concern is the assumption of linearity (in profilometer response) that may not be true for the rougher surfaces; however, at least early modeling results seem close enough that this may not be an issue.

Of equal importance to the rough surface scattering modeling that this work will facilitate is the issue of specifying optics for low scatter with profilometer measurements. Although used throughout the optics industry, it is simply an indicator — not metrology.

Extended Discrete Sources Method Model for Extremal Scatterers

D. E. Sukhanov
Moscow Lomonosov State University, Russia

Light scattering analysis used in nanotechnology and biophotonics has been a subject of interest in last decades. This is primarily due to the variety of practical applications it is encountered in, for example, aerosol analysis, investigation of air pollution, radio wave propagation in the presence of atmospheric hydrometers, weather radar problems, analysis of contaminating particles on the surface of silicon wafers, remote sensing, etc. Special attention has been paid to extremely shaped particle light scattering problems. Methods being implemented to solve such problems are usually expensive in computer resources, especially if the size of the scattering object relative to the wavelength of the incident radiation is big. Another problem arises if scattering body is asymmetrical. In this case one has to implement more sophisticated methods than he might have been able to use in case of axis-symmetrical obstacle. So advanced methods are constantly developed to solve these both problems mentioned above. We introduce here a new approach which allows one to reach these goals.

Light scattering by extremely shaped local obstacle is considered here. The model used here is based on symmetrical version of the Discrete Sources Method (DSM) [1]. This technique constructs the scattered field everywhere outside a local obstacle as a finite linear combination of the fields resulting from electric and magnetic multipoles distributed over an auxiliary segment of the obstacle's axis of revolution inside the obstacle. Then the scattered field analytically satisfies transmission conditions at the obstacle's surface. Internal field is represented on the basis of regular functions, which fit Maxwell's equations [2]. So, the DSM solution constructed satisfies Maxwell's equations everywhere outside the obstacle, required infinity conditions and transmission conditions at the obstacle's surface. Then the unknown DS sources amplitudes are to be determined from boundary conditions enforced at the surface of the local obstacle.

It has been found that more stable results can be obtained by using pseudo-solution of an over-determined system of linear equations obtained by following the generalised point-matching technique. Select a set of matching points on the particle homogeneously covering the surface. Then distribute homogeneously DS over the auxiliary segment of scatterer's axis of revolution. In each DS point we choose three independent electric multipoles and three independent magnetic mutipoles, which originate the scattered field. Then the linear system to be used for determining of the DS amplitudes is derived from matching the boundary conditions at the set of matching points. This procedure leads to an over-determined matrix and the DS amplitudes are evaluated by a pseudo-inversion technique [3]. The numerical scheme allows one to consider all incidences and both polarization P and S at once. DSM computer model controls convergence and stability of the result obtained by a posterior evaluation of the surface residual. In the presentation computer simulating results associated with an influence of obstacle's aspect ratio, orientation and exciting field polarization on the scattering spectra will be presented.

*Authors would like to acknowledge support of this work by the Russian Foundation for Basic Research.

REFERENCES

1. Eremin, Y. and A. G. Sveshnikov, "Discrete sources method in electromagnetic scattering problems," *Electromagnetics*, Vol. 13, 1–22, 1993.
2. Eremin, Y., "Complete system of functions for the study of boundary value problems in mathematical physics," *Sov. Phys. Dokl.*, Vol. 32, No. 8, 635–637, 1987.
3. Doicu, A., Y. Eremin, and T. Wriedt, "Acoustic and electromagnetic scattering analysis using discrete sources," Academic Press, New York, 2000.

Session 3P3
Devices and Circuits

Application of Finite Network Theory to the Transient Process of Electromagnetic Forming

T. Richter[1], **A. Farschtschi**[1], **and H.-J. Roscher**[2]

[1]Chemnitz University of Technology, Germany
[2]Fraunhofer Institute IWU, Germany

The aim of the authors is the calculation of an example problem of electromagnetic forming (EMF) using the finite network theory (FNM). Our example consists of an rectangular single-loop coil made of copper in front of an aliminum plate. The external network consists of an external inductance, an external resistor and a capacitor connected to the rectangular coil. The external network provides an additional single loop electric network to the problem called main loop. The discharging of the capacitor in the main loop results in a transient process which is calculated by finite network theory (FNM).

FNM discretises the conductive volumes of the coil and the aluminum workpiece into resistor elements with self and mutual inductances. By the use of mutual inductances the generation of eddy currents in the work piece is automatically included. FNM results is an inductive coupled electric network and its 1st order system of differential equations which is formulated in terms of the mesh current method. The authors suggest that FNM is the prefered method for the described kind of problem:

1. Since FNM excludes non-conductive media (e.g., air) from the calculation this method results in a relatively small system of 1st order differential equations compared to the degrees of freedom of standard FEM packages such as ANSYS.

2. The inductive coupled electric network of FNM allows the use of standard methods to cal- culate the transient process. In our case of low-resistivity conductors with strong inductive coupling the explicit Euler-Cauchy method is applicable.

To confirm our hypothesis a comparison is made between ANSYS and the finite network method. The same discretisation of the coil and the workpiece were used. The main costs of FNM consist of the matrix generation of the electric network and the calculation of the Cholesky decomposition of the symmetric inductance matrix. ANSYS provides for transient calculations of electromagnetic-circuit coupled fields only a direct standard direct solver whereas the application of the Euler-Cauchy method in FNM is very cheep. In addition, the degrees of freedom of the ANSYS implementation is about 3 times larger compared to FNM.

The calculated example with an 31-point transient results in an about 35 times higher com- puting time of the ANSYS package. The eddy current distribution of both methods is in good agreement indication the well-done implemention of the example problem in both program systems.

Tensor Harmonic-balance Analysis of Forced Microwave and Millimeter-wave Circuits

O. P. Paixão and H. E. Hernández-Figueroa
Universidade Estadual de Campinas, Brazil

A novel harmonic balance (HB) simulation [1, 2] framework based on recently developed tensor method for sparse nonlinear equations [3, 4] is presented. This new method bases each iteration on a local, quadratic model where the quadratic term is represented by a rank one tensor object. Like standard Newton's methods, tensor methods are general purpose methods intended especially for problems where the jacobian matrix at the solution is singular or ill-conditioned. In the context of forced HB simulation, this situation may be found in the solution of nonlinear circuits operating near a turning point.

The complexity of forming, storing and solving the tensor model is little compared to the solution of the local linear model required by Newton's methods. The tensor term is selected so that the model interpolates a small number of residuals in the recent history of iterates. The solution of the tensor model leads to an unconstrained optimization problem with dimension equals to the number of iterates used in the interpolation. For an interpolation using one past iterate the optimization reduces to a one-variable problem that can be straightforwardly solved in a closed form. Moreover, numerical experiments have shown that using additional iterates in the interpolation produce only a marginal improvement in the computation performance of the tensor method.

In our implementation of a global tensor method, we utilized a novel curvilinear linesearch technique [5] as globalization strategy. This technique has enticing properties and obviates the need to separately compute an extra linesearch in the Newton direction, as previously required by tensor methods.

To improve the computation performance of the tensor method on weakly nonlinear problems we propose the use of simplified tensor iterations where the jacobian matrix is kept constant. If the jacobian matrix is computed only once, we can develop an extension of the linear-centric modeling approach to HB simulation [6]. This extended ("quadratic-centric") modeling approach uses approximated second-order information and therefore, it is expected to perform better than the conventional approach. The basics of the new approach is illustrated for a simple diode circuit.

Finally, the robustness and computation performance of the proposed tensor-oriented HB simulation tool is verified for a different classes of microwave and millimeter-wave circuits, they are: GaAs MESFET power amplifier, HEMT travelling-wave switch and InP HBT downconverter. Indeed, several numerical results from single-tone (distortion) and two-tone (mixing and intermodulation) analysis are performed in these circuits. These benchmark results clearly shows superior power-handling capabilities and lower execution time our proposed simulator when compared with standard Newton-based HB simulators.

REFERENCES

1. Kundert, K. S. and A. Sangiovanni-Vincentelli, "Simulation of nonlinear circuits in the frequency domain," *IEEE Trans. Computer-Aided Design*, Vol. 5, No. 4, 521–535, Oct. 1986.
2. Rizzoli, V., et al., "State-of-the-art harmonic-balance simulation of forced nonlinear microwave circuits by the piecewise technique," *IEEE Trans. Microwave Theory Tech.*, Vol. 40, No. 1, 12–28, Jan. 1992.
3. Schnabel, R. B. and P. D. Frank, "Tensor methods for nonlinear equations," *SIAM J. Numer. Anal.*, Vol. 21, No. 5, 815–843, Oct. 1984.
4. Bouaricha, A. and R. B. Schnabel, *Tensor Methods for Large, Sparse Systems of Nonlinear Equations*, Tech. Report MCS-P473-1094, Mathematics and Computer Science Division, Argonne National Laboratory, Argonne, IL, USA, 1994.
5. Bader, B. W. and R. B. Schnabel, "Curvilinear linesearch for tensor methods," *SIAM J. Sci. Comput.*, Vol. 25, No. 2, 604–622, 2003.
6. Li, P. and L. Pileggi, "A linear-centric modeling approach to harmonic balance analysis," *Design and Automation in Europe 2002*, 634-639.

Split-Torus Configuration of the Toroidal/Helical Electron-Orbits for High-Power-Microwave Amplifiers

R. A. Speciale
Research and Development Inc., USA

A new, innovative geometry was introduced at PIERS 2004 [1], for the electron trajectories of High-Power Microwave sources, in the form of closed, multi-turn Toroidal/Helical orbits. That new electron trajectory geometry provides many technical advantages, such as a very compact implementation of multi-beam HPM klystrons, elimination of the high-voltage pulsed-source and of the beam-dump, possibility of beam-stacking injection and of beam re-acceleration. The originally introduced geometry of closed, multi-turn Toroidal/Helical orbits introduced in Reference [1] is shown in Fig. 1, with 9 turns shown in blue and 120 electron-bunches shown in red.

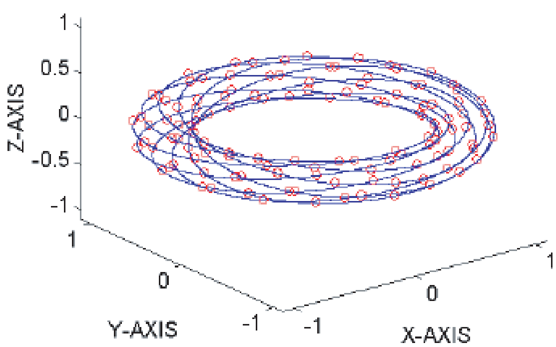

Figure 1: Toroidal/Helical orbits with 120 bunches.

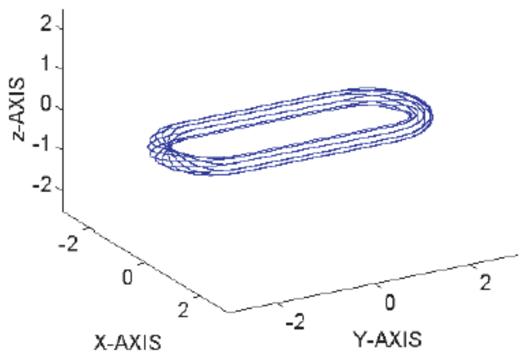

Figure 2: Spli-torus Toroidal/Helical orbit.

An alternate configuration of the closed, multi-turn Toroidal/Helical orbits has now been developed, that provides the possibility of inserting two straight orbit-sections, between the two 180° torus-arcs. That new orbitgeometry provides the possibility of inserting many of the required insertion-devices, such as accelerating and power-extraction microwave-cavities, strong-focusing quadrupole magnetic-lenses, a beam-injection and a beamextraction channels, along the two straight orbit-sections, rather than within the two twisting 180° torus-arcs. The new electron trajectory geometry was obtained by modifying the parametric equations of the original orbit-geometry as required to make both the orbit-curvature and torsion zero along one torus diameter, fom 0° to 180° azimuth.

REFERENCES

1. Speciale, R. A., "High power microwave amplifiers with Toroidal/Helical orbits," *PIERS 2004*, Pisa, Italy.

Exact Expressions of the Orbit-Curvature and Curvature-Radius of the Toroidal/Helical Orbits

R. A. Speciale
Research and Development Inc., USA

The new innovative concept of High Power Microwave (HPM) Amplifier recently introduced [1], combines Multi-Beam Klystron (MBK) and Electron Storage-Ring (ESR) technologies, by using closed, multi-turn Toroidal/Helical electron-orbits. A closed-form expression has now been obtained for the multi-turn electron-orbit *curvature* and *curvature-radius*, as function of the azimuth-angle φ, and *wrapping-angle* θ. The expression is:

$$\kappa(\varphi) = \frac{\sqrt{\frac{1}{8n^2}\left[k_0 + k_1 \cos\left(\frac{n-1}{n}\varphi\right) + k_2 \cos\left(2\frac{n-1}{n}\varphi\right) + k_3 \cos\left(3\frac{n-1}{n}\varphi\right) + k_4 \cos\left(4\frac{n-1}{n}\varphi\right)\right]}}{\left[\sqrt{(1 + c\cos\theta)^2 + c^2\left(\frac{n-1}{n}\right)^2}\right]^3} \tag{1}$$

where the five K_i coefficients are functions of the torus aspect-ratio c and of the number of turns n:

$$k_0 = \frac{1}{8n^6}\left\{8n^6 + 4c^2n^2\{1+2(n-1)n[2+3(n-1)n]\} + c^4(n-1)^2\left\{8+n\{n[57+10n(2n-5)]\}\right\}\right\} \tag{2}$$

$$k_1 = \frac{1}{2n^4}c\left\{3c^2(n-1)^2(1+2(n-1)n) + 2n^2[1+n(3n-2)]\right\} \tag{3}$$

$$k_2 = \frac{1}{2n^4}c^2\left\{\{2n[2+n(2n-3)]-1\} + (n-1)^2[2+n(3n-4)]\right\} \tag{4}$$

$$k_3 = \frac{1}{2n^4}c^3(n-1)^2[1+2n(n-1)] \tag{5}$$

$$k_4 = \frac{1}{8n^4}c^4(n-1)^2(2n-1) \tag{6}$$

while the electron-orbit curvature-radius ρ is quite obviously expressed by $\rho(\theta) = \dfrac{1}{\kappa(\theta)}$, and is a periodic function of the *wrapping-angle* θ, for $0 \le \theta \le n2\pi$, with period $0 \le \theta \le 2\pi$:

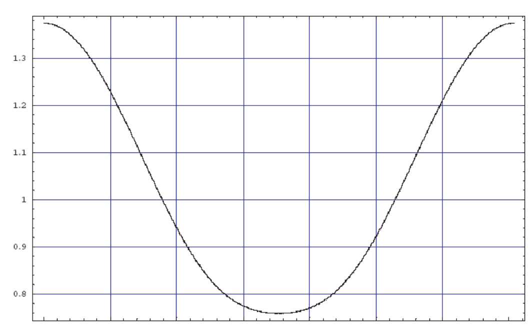

The given exact expression of the electron-orbit *curvature-radius* ρ provides the possibility of computing the required intensity of the beam-steering dipole-fields, that must have orbit-torsion-dependent orientations.

REFERENCES

1. Speciale, R. A., "High power microwave amplifiers with Toroidal/Helical orbits," PIERS 2004, Pisa, Italy.

Dual-band/broadband Circular Polarizers Designed with Cascaded Dielectric Septum Loadings

T.-Y. Huang, Y.-C. Yu, and R.-B. Wu
National Taiwan University, Taiwan

A simple method is presented in this paper for realizing a dielectric septum-loaded type circular polarizer with either dual-band or a single broadband response. Two dielectric septum sections with different dielectric constants and lengths that introduce various phase delay to E_x and E_y polarizations in the same frequency range are cascaded orthogonally (Fig. 1) to obtain a dual-band response, as shown in Fig. 2(a). A single wideband response can also be achieved (Fig. 2(b)) if these two dielectric septum sections are cascaded in parallel instead. Simulations in Ansoft HFSS show that flatter phase response and wider bandwidth can be obtained by the proposed polarizer comparing to single section ones, moreover, a dual-band response can only be achieved with a two-section design. Taking advantage of dielectric septum-loaded type circular polarizers, the fabrication error or inaccurate dielectric constants can easily be compensated by adjusting the lengths of dielectric septum sections.

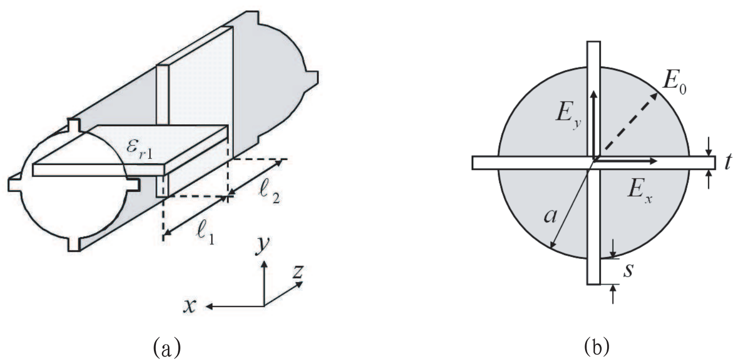

Figure 1: Circular waveguides with two orthogonally cascaded dielectric septum loadings, (a) Three-dimensional view, (b) Front view.

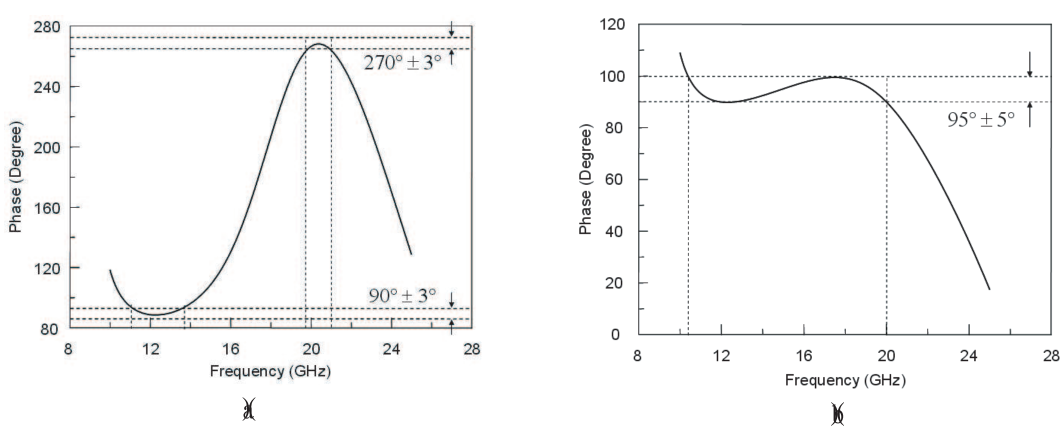

Figure 2: Polarizers with (a) dual-band and (b) a single broadband responses.

Mode Transformer between TEM Mode to 1^{st} Higher Mode in Tri-plate Strip Transmission Line

F. Kuroki and K. Miyamoto
Kure National College of Technology, Japan

Printed transmission lines, such as a microstrip transmission line and a coplanar waveguide, are preferable for applications in centimeter-frequencies. They are commonly used in millimeter-wave regions to realize cost-effective front-ends due to good mass-productivity. The printed transmission lines, however, suffer from considerable transmission loss. To reduce such transmission loss, a higher order mode of microstrip transmission line has been studied, but unfortunately, such a mode easily emits unwanted radiation at curved sections and discontinuities.

To realize a low-loss printed transmission line at millimeter-wave frequencies, we developed the first higher mode in a tri-plate strip transmission line. This transmission line, termed higher mode tri-plate strip transmission line (HS line) in this paper, consists of metal strips inserted in a below cutoff parallel plate waveguide as shown in Fig. 1. A basic reactance component such as a slot was investigated to apply to a matching circuit and a suppressor of the lowest mode, which is the TEM mode in the tri-plate strip transmission line. To apply the HS line to some printed strip transmission lines, a mode transformer between the HS line and the tri-plate strip transmission line with only TEM mode propagation was developed. The field distribution of the HS mode in the cross-sectional plane resembles that of the TE_{10} mode in the hollow rectangular metal waveguide, while that of the tri-plate strip transmission line is similar to the coaxial line mode, that is the TEM mode. With this in mind, a mode transformer between the HS line and the tri-plate strip transmission line could be constructed by making a right-angle corner as shown in Fig. 2. To reduce the reflection from the mode transformer, the corner edge was trimmed off. No TEM mode propagation in the HS line is guaranteed by using the TEM mode suppressor consisting of three slots. Fig. 3 shows the measured VSWR from the mode transformer as circles. A flat VSWR performance measured to be 1.6 on average was obtained. To perform perfect matching at 32 GHz, a matching slot was sited behind the TEM mode suppressor as shown in Fig. 2. The VSWR of the mode transformer with the matching slot is plotted in Fig. 3 as dots. It is obvious that there is no reflection, though the center frequency was shifted to 100 MHz. Fig. 4 shows the measured transmission loss versus frequency in the back-to-back structure of two mode transformers, where, to obtain a flat frequency response, the matching slots were not installed. The transmission loss was measured to be less than 0.6 dB in the frequency range from 31 GHz to 33 GHz.

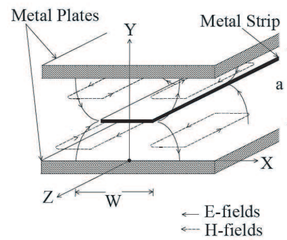

Figure 1: Rough sketch of field distribution of the first higher in tri-plate strip transmission line.

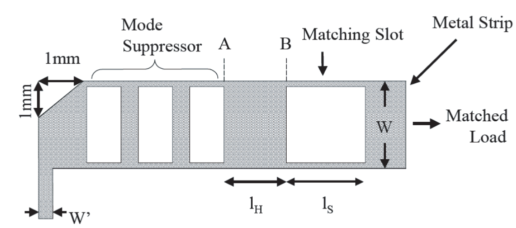

Figure 2: Mode transformer between HS mode and TEM mode.

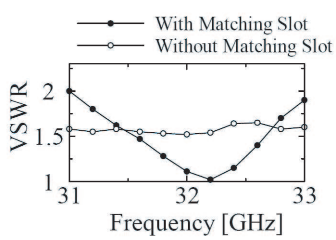

Figure 3: Measured VSWR of mode transformer between HS mode and TEM mode.

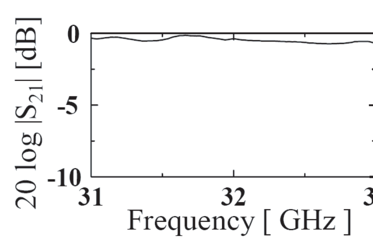

Figure 4: Measured transmission loss versus frequency in back-to-back structure.

High-Accuracy Approximation to the Integrated Length of Toroidal/Helical Orbits

R. A. Speciale
Research and Development Inc., USA

The new innovative concept of High Power Microwave (HPM) Amplifier recently introduced [1], combines Multi-Beam Klystron (MBK) and Electron Storage-Ring (ESR) technologies, by using closed, multi-turn Toroidal/Helical electron-orbits. The original paper [1] gives an exact, closed-form expression of the multi-turn electron-orbit length, as function of the azimuth-angle $\boldsymbol{\varphi}$ around the torus-axis, and of the *wrapping-angle* $\boldsymbol{\theta}$. That expression shows a daunting degree of complexity, by including all three Elliptic Integrals of the first kind $\boldsymbol{E}$, of the second kind $\boldsymbol{F}$, and of the third kind $\boldsymbol{\Pi}$. A high-accuracy approximation has now been developed, that attains much faster numerical computation. It was obtained by expanding the orbit-length rate-of-increase $\boldsymbol{ds/d\varphi}$ (*the speed !*) in powers of the torus aspect-ratio $\boldsymbol{c = r\ /\ R}$, and by integrating the expansion term-by-term. The resulting orbitlength approximate expression includes the five terms:

$$s(\varphi) = h_1\theta + h_2\sin\theta + h_3\sin 2\theta + h_4\sin 3\theta + h_5\sin 4\theta \tag{1}$$

where the *wrapping-angle* $\boldsymbol{\theta}$ depends from azimuth through the linear, rational relation $\boldsymbol{\theta=[(n-1)/n]\varphi}$, and the five h_i coefficients are functions of the torus aspect-ratio c and of the number of turns $\boldsymbol{n}$:

$$h_1 = R\left\{1+\frac{1}{2}\left(\frac{n-1}{n}\right)^2 c^2 + \frac{1}{4}\left(\frac{n-1}{n}\right)^2\left[1-\frac{1}{2}\left(\frac{n-1}{n}\right)^2\right]c^4 - \frac{1}{16}\left(\frac{n-1}{n}\right)^2\left[2\left(\frac{n-1}{n}\right)^4 - 3\frac{(2n-1)^2}{n^4}\right]c^6\right\} \tag{2}$$

$$h_2 = R\left[1-\frac{1}{2}\left(\frac{n-1}{n}\right)^2 c^2 - \frac{3}{8n^2}\left(\frac{n-1}{n}\right)^2(2n-1)c^4\right]c \tag{3}$$

$$h_3 = R\frac{1}{16n^2}\left(\frac{n-1}{n}\right)^2\left[(2-c^2)n^2+3c^2(2n-1)\right]c^4 \tag{4}$$

$$h_4 = -R\frac{1}{24}\left(\frac{n-1}{n}\right)^2 c^5 \tag{5}$$

$$h_5 = R\frac{1}{64}\left(\frac{n-1}{n}\right)^2 c^6 \tag{6}$$

Preliminary numerical computations using $\boldsymbol{n= 9}$ and $\boldsymbol{c= 0.2}$ have shown the residual error of the approximation to be in the order of $\pm \boldsymbol{2}\cdot\boldsymbol{10^{-6}}$, with a single oscillation period for $\boldsymbol{0 \le \theta \le 2\pi}$. The residual error appears to be periodic a function of the *wrapping-angle* $\boldsymbol{\theta}$, for $\boldsymbol{0 \le \theta \le n2\pi}$. While the orbit-length exact expression given in [1] shows a periodic discontinuity jump of -6.3836527 at $\boldsymbol{\theta}$-values that are odd-multiples of $\boldsymbol{\pi}$, the approximation given in (1) is completely continuous, and monotonic across the whole $\boldsymbol{0 \le \theta \le n2\pi}$ range, and its computational speed is quite conveniently substantially higher, thus providing the possibility of determining the electron orbitalperiod, around either a single-turn or an $\boldsymbol{n}$-turn helical orbit. Quite obviously, higher accuracy could be attained by using a higher-order expansion of the orbit-length rate-of-increase.

REFERENCES

1. Speciale, R. A., "High power microwave amplifiers with toroidal/helical orbits," *PIERS 2004*, Pisa, Italy.

Multilevel Modified Nodal/Multiport State-space Approach for Frequency-domain Simulation of Large-scale Nonlinear RF and Microwave Circuits

O. P. Paixão and H. E. Hernández-Figueroa
Universidade Estadual de Campinas, Brazil

A multilevel approach for frequency-domain simulation of large-scale nonlinear RF and microwave circuits, including the presence of noise and thermal effects, is presented. In this approach, the circuit to be simulated is firstly decomposed into hierarchically interconnected supernetworks represented by a nodal equation [1]. Then, for each supernetwork we apply a piecewise network decomposition that separates it into linear and nonlinear subnetworks [2]. The nonlinear subnetwork encompasses all nonlinear devices (e.g., FETs and HBTs) in the supernetwork and it is formulated by an extended multiport state-space analysis (MSSA) [3]. While the embedding linear subnetwork is formulated using the classical modified nodal analysis (MNA) [4].

The advantages of using the extended MSSA instead of MNA for formulating the nonlinear subtnetwork is twofold: (i) it uses one single variable to represent a nonlinear function controlling voltage and, (ii) it naturally separates the nonlinear (controlled sources) equations from the other set of linear equations, namely differential (lumped memory elements), difference (distributed and delay elements) and additional (controlled sources) equations. Nevertheless, the MNA is a very powerful technique for formulating the linear subnetwork. It is well conditioned and structured and, it can be efficiently solved via LU factorization combined with sparse matrix computations. The MSSA uses a simple table-based methodology in order to generate the nonlinear subnetwork equations. It worth pointing out, that a very small matrix inversion is required for eliminating the linear (differential, difference and additional) equations and associated linear state-variables.

Our state-space approach is more efficient than the widely used parametric state-space approach [5], since the later approach may lead to a non-square system of equations and may involve high-order derivatives of nonlinear state-variables. These high-order derivatives leads to cumbersome expressions for the computation of nonlinear functions sensitivities with respect to the state-variables.

Finally, we describe the application of the above theory to the following RF and microwave circuit problems: nonlinear steady-state analysis via harmonic balance [5], large-signal conversion signal and noise analysis, and small-signal multiport hybrid signal and noise correlation matrix analysis [6]. New formulae for conversion from multiport hybrid parameters to multiport scattering parameter representation, and vice-versa, are included. Finally, we present frequency-domain simulation results for GaAs MESFET microwave power amplifier and InP HBT millimeter-wave downconverter. These results, obtained by our in-house software, validate the theory presented herein.

REFERENCES

1. Zhang, X., R. H. Byrd, and R. B. Schnabel, "Parallel methods for solving nonlinear block bordered systems of equations," *SIAM J. Sci. Stat. Comput.*, Vol. 13, No. 4, 841–859, July 1992.
2. Nakhla, M. S. and J. Vlach, "A piecewise harmonic balance technique for determination of periodic response of nonlinear systems," *IEEE Trans. Circuits Syst.*, Vol. 23, No. 2, 85–91, Feb. 1976.
3. Sobhy, M. I., E. A. Hosny, and M. A. Nassef, "Multiport approach for the analysis of microwave nonlinear networks," *Int. J. Num. Modelling: Electronic Net., Dev. Fields*, Vol. 6, 67–81, 1993.
4. Ho, C., A. E. Ruehli, and P. A. Brennan, "The modified nodal approach to network analysis," *IEEE Trans. Circuits Syst.*, Vol. 22, No. 6, 504–509, June 1975.
5. Rizzoli, V., et al., "State-of-the-art harmonic balance simulation of forced nonlinear microwave circuits by the piecewise technique," *IEEE Trans. Microwave Theory Tech.*, Vol. 40, No. 1, 12–28, Jan. 1992.
6. Russer, P. and S. Müller, "Noise analysis of linear microwave circuits," *Int. J. Num. Modelling: Electronic Net., Dev. Fields*, Vol. 3, 287–316, 1990.

Low Cost 60 GHz Gb/s Radio Development

S. Pinel, **C.-H. Lee**, **S. Sarkar**, **B. Perumana**
S. Padvanama, **R. Mukhopadhyay**, **and J. Laskar**
Georgia Institute of Technology, USA

The recent advances of CMOS and SiGe process technologies have now made the design of low-cost highly integrated millimeter-wave radios possible in Silicon. In combination with an optimum organic Liquid Crystal Polymer packaging approach, this represents a unique opportunity to develop Gb/s radio that could address the increasing demand in term of data rate throughput of the emerging broadband wireless communication systems. In this paper we discuss the circuit and module challenges that will enable a successful deployment of 60 GHz gigabits wireless systems.

Session 3P4
Subsurface Imaging through Inverse Scattering Approaches: From Biomedical Applications to UXO Detection

Beam Manipulation of a Monopole Antenna

C. J. Fox, **P. M. Meaney**, **L. Potwin**, **and K. D. Paulsen**
Dartmouth College, USA

We are currently in the process of optimizing our microwave tomographic imaging system for the detection of breast cancer. One area targeted in our optimization efforts is the antenna design. In both tomographic and radar based imaging approaches a broad frequency band is desired. Higher imaging frequencies offer many advantages in the field of breast cancer detection, particularly in improved resolution [1]. A broad target antenna bandwidth of 500 MHz to 3 GHz allows us to analyze the most realistic maximum operating frequency in the actual clinical setting. Broadband capability is especially important for our image reconstruction algorithm which involves the use of a variance stabilizing transformation. This process requires simultaneous analysis of both the signal's magnitude and phase. The phase component poses significant challenges because of its wrapping characteristics and the broadband data is particularly useful in the unwrapping process [2].

There are two ways to generate broadband antennas. One technique involves making the antennas physically large, such as for spiral antennas. Alternatively, the antennas can be resistively loaded. Unfortunately, resistively loading an antenna reduces its efficiency dramatically [3]. Our current clinical system uses 16 monopole antennas submerged in a lossy coupling liquid. We have addressed the loss of antenna efficiency by creating a tomographic system with a large dynamic range and a small target zone. Antennas used in breast cancer imaging systems need to be small as well as operate over a broad frequency range. The resistively loaded coaxial monopole easily satisfies the tight space requirements of breast imaging and has a sufficiently broad frequency range. Additionally, the monopole antenna's beam pattern is isotropic in the dorsal imaging plane.

Even though the beam pattern is isotropic in the imaging plane the orthogonal distribution of the beam is not necessarily centered. Measurements show that the beam narrows and steers upward with increasing frequency. The upward steering of the beam leads to an increase in signal coupling to surface modes which create unwanted multi-path signals. We have undertaken a thorough analysis of this behavior and discussed a strategy for extending the use of these antennas to the full frequency range. We will show a summary of this analysis and an optimized antenna design. We will also show images at higher frequencies made possible by our design optimizations.

*This work was supported by NIH/NCI grant # R01 CA80139.

REFERENCES

1. Fear, E. C., S. C. Hagness, P. M. Meaney, M. Okoniewski, and M. A. Stuchly, "Enhancing breast tumor detection with nearfield imaging," *IEEE Microwave Mag.*, Vol. 3, No. 1, 48–56, Mar. 2002.
2. Meaney, P. M., Q. Fang, M. W. Fanning, T. Raynolds, P. Robbie, and K. D. Paulsen, "Microwave imaging using the adjoint method: facilitating advances in software and hardware development," *2nd International Conference on Electromagnetic Near-Field Characterization and Imaging*, Barcelona, Spain, 67–71, June, 2005.
3. Yin, X., E. C. Fear, and R. H. Johnston, "Compact antenna for radar-based breast cancer detection," *IEEE Trans. on Antennas and Propagation*, Vol. 53, No. 8, 2374–2380, August 2005.

Iterative Reconstruction of Dielectric Rough Surface Profiles through a Single Illumination

I. Akduman[1], **R. Kress**[2], **and A. Yapar**[1]

[1]Istanbul Technical University, Turkey
[2]University of Goettingen, Germany

Imaging of an inaccessible rough surface constitutes an important class of problems in inverse scattering theory due to the large domain of applications such as microwave remote sensing, underground imaging, optical system measurements, underwater acoustics, non-destructive testing etc. In these kinds of problems one tries to recover the location and shape, as well as the surface characteristics of an unknown surface through scattered field measurements in a certain domain. The surface to be reconstructed may be either a perfectly conduction one or a dielectric interface separating two-dielectric media. As far as we know several exact and numerical techniques have been developed for perfectly conducting surfaces, where most of these inversion schemes are concerned with the reconstruction of surfaces with small perturbations. On the other hand reconstruction of a rough dielectric interface is of importance in the practical applications since most of the boundaries in nature are surfaces separating dielectric mediums. Recently little progress has been done for solving this challenging problem [1–3].

In this paper, we give a new, simple and fast method to determine the location and shape of a rough surface separating two lossy dielectric half-spaces. For the sake of simplicity, we consider surfaces having a variation in one direction. The reconstruction is achieved via a single illumination of a plane wave at a fixed frequency and the reflected field measurements are performed on a line parallel to the mean surface. In the method presented here the lossy half-space above the surface is first separated into two parts by a certain plane, and then the scattered field in the upper region above this plane is expressed in terms of a Fourier transform while it is expanded into a Taylor series in the lower part. Similar representation is used for the scattered field in the half-space below the surface. The use of the continuity conditions of the total field and its derivative on the unknown surface allows the reduction of the problem to the solution of a coupled system of equations containing a spectral coefficient for the scattered field and the surface function as unknowns. The coupled system is solved iteratively starting from an initial guess of the surface function, i.e.: for a given initial estimate of the surface profile one of the equations which is linear and ill-posed is solved for the spectral coefficient of the scattered field through Tikhonov regularization. Then one inserts this solution in the other equation which is non-linear and linearize it in the Newton sense and so on. Since the solution is sensitive to the errors in data, a regularization in the least square sense is applied in the Newton iteration scheme. The method yields satisfactory reconstructions for slightly varying surface profiles.

REFERENCES

1. Stankova, M., J. Burov, and M. Burova, "Computer reconstruction of a periodic surface by means of the scattered and transmitted acoustic fields," *Measurements Sci. and Tech.*, Vol. 12, 1330–1335, 2001.
2. Galdi, V., J. Pavlovich, W. C. Karl, D. A. Castanon, and L. B. Felsen, "Moderately rough dielectric interface profile reconsruction via short-pulse quasi-ray Gaussian beams," *IEEE Trans. Antennas and Propagation*, Vol. 51, No. 3, 672–677, 2003.
3. El-Shenawee, M. and E. L. Miller, "Multiple-incidence and multifrequency for profile reconstruction of of random rough surfaces using the 3-D electromagnetic fast multipole model," *IEEE Trans. Geoscience and Remote Sensing*, Vol. 42, No. 11, 2499–2510, November 2004.

The Semi-analytic Mode Matching (SAMM) Algorithm for Fast Computation of Scattered Near Fields from a Variety of Dielectric Targets Buried in Lossy Soil Excited by Underground Borehole Dipole Sources

A. W. Morgenthaler and C. Rappaport
Northeastern University, USA

The 3D semi-analytic mode matching (SAMM) algorithm is used to determine the near field scattering of dipole sources from a variety of 2D or 3D underground targets with complex dielectric constants, extending previous work with uniform plane wave sources. The dipole sources may be located above ground, useful for modeling forward GPR scattering of buried targets like landmines, or below ground which is more useful for simulating cross borehole tomography used to locate and identify pollution pools or for general geophysical sensing.

Scattering is described by moderately low-order superpositions of 2D cylindrical modes or 3D spherical modes, each originating from user-specified coordinate scattering centers (CSCs). The CSCs are chosen where scattering appears to originate, including within the target (multiple CSCs may be required if the target deviates substantially from a quasi-spherical shape), at the source image, and at the above-ground images which model backscatter from the lossy ground surface into the ground region. The mode coecients are found numerically by least-squares fitting all boundary conditions at discrete points along the relevant air-ground and ground-target interfaces. The optimal distribution of fitting points along these interfaces is also discussed. For a favorable choice of CSCs and a careful selection of fitting points, the SAMM algorithm converges with increasing mode number, giving rise to accurate scattering fields in a time 2-3 orders of magnitude faster than FDFD simulations. SAMM can thus be used as a forward model for inverse scattering algorithms, giving them the ability to find buried objects quickly.

*This work is supported by CenSSIS, the Center for Subsurface Sensing and Imaging Systems under the ERC Program of the NSF (Award number EEC-9986821).

Recent Advances on the Use of Kernel-based Learning-by-examples Techniques for Electromagnetic Subsurface Sensing

M. Benedetti, M. Donelli, D. Franceschini, A. Rosani, A. Boni, and A. Massa
University of Trento, Italy

To return areas contaminated with unexploded ordnance (UXO) and anti-tank/anti-personnel landmines to a civilian use, the ordnances should be obviously removed. Such a process is time-expensive and involves complex acquisition procedures. Several solutions have been proposed based on various methodological approaches, which consider different sensor modalities such as ground-sensors or synthetic aperture radars. These techniques are aimed at achieving the following goals: (a) correctly localizing a large number of dangerous targets; (b) reducing the false-alarm rate; (c) reducing the time devoted to the detection process. In such a framework, electromagnetic approaches based on learning-from-samples (LFS) techniques [1] have been proposed for the on-line (after the training phase performed off-line) detection of subsurface objects. The detection process is recast as a regression problem where the unknowns (i.e., geometric and dielectric characteristics of the target) are evaluated from the data (i.e., the value of the scattered field) by approximating the data-unknowns relation through an off-line data fitting process (training). LFS regression-based approaches demonstrated their effectiveness in dealing with detection processes where a limited number of unknowns (i.e., single object) is considered. However, because of the complexity of the underlying architecture, some difficulties occur when a larger number of unknowns (i.e., multiple objects) is taken into account. From a structural point-of-view, the regression technique does not permit one to simultaneously identify multiple positions. As a consequence, LFS regression-based approaches turn out to be very effective for the detection of a single (or few organized in a single cluster of objects) buried object. It should be pointed out that the identification of free-areas and an estimate of the concentration of subsurface objects might be enough in several situations. Then, the goal could be moved from the "*object detection*" to the "*definition of a risk map*" [2]. Consequently, a classification approach, instead of a regression one, should be employed. In this contribution, the classification approach based on a LFS technique preliminary presented in [3] for an on-line sub-surface sensing is analysed and compared to state-of-the-art classification approaches. Starting from the knowledge of the scattered field values collected above the surface, the method is aimed at defining a risk map of the domain under test. By considering a SVM-based classifier, the proposed method estimates the a-posteriori probability of the presence of subsurface dangerous objects. The advantages of the use of such an instance-based classification method can be summarized as follows: (a) no *a-priori* knowledge about the system that generated the data is required; (b) simplicity and reliability of the resolution algorithm; (c) possibility of designing optimal classifier based on the theory by *Vapnik and Chervonenkis*; (d) easy implementation in hardware for real-time applications.

REFERENCES

1. Bermani, E., A. Boni, S. Caorsi, and A. Massa, "An innovative real-time technique for buried object detection," *IEEE Trans. on Geoscience and Remote Sensing.*, Vol. 41, 927–931, Apr. 2003.
2. Caorsi, S., E. Bermani, A. Boni, M. Conci, M. Donelli, and A. Massa, "Learning-by-examples strategies for sub-surface imaging: from regression to classification approach," *PIERS2003*, USA, 118, Oct. 2003.
3. Caorsi, S., E. Bermani, A. Boni, M. Donelli, and A. Massa, "On the effectiveness of kernel-based learning-by-examples techniques for electromagnetic subsurface sensing," *PIERS2004*, Italy, S3.02, Mar. 2004.

Application of Spheroidal Mode Approach to the Detection and Discrimination of Buried Objects

X. D. Chen[1], **K. O'Neill**[2], **T. M. Grzegorczyk**[3], **and J. A. Kong**[3]

[1]National University of Singapore, Singapore
[2]ERDC Cold Regions Research and Engineering Laboratory, USA
[3]Massachusetts Institute of Technology, USA

The detection and removal of buried unexploded ordnance (UXO) is an important environmental problem, made very expensive and challenging by the high false alarm rate. Among the techniques for detecting UXOs, electromagnetic induction (EMI) is promising and has been widely explored. In the magneto-quasistatic (MQS) regime, both the primary and the secondary magnetic fields are irrotational and can be expressed in terms of the gradient of a scalar potential governed by the Laplace equation. In this work, both the primary and the secondary magnetic fields are expressed as linear superpositions of basic modes in the spheroidal coordinate system. Spheroidal modes are chosen because the spheroidal coordinate system can be made to conform to the general shape of an object of interest, whether flattened or elongated, and many of our objects of interest are bodies of revolution. Due to the orthogonality and the completeness of the spheroidal basic modes, the scattering coefficients, in response to unitary magnitude of the primary mode excitation, are uniquely determined. They are characteristics of the object and can then be treated as discriminators in pattern matching and classification. The scattering coefficients are retrieved from the knowledge of the secondary fields, where both the synthetic and measurement data are used. The ill-conditioning issue is dealt with by mode truncation and Tikhonov regularization technique. Stored in a library, the scattering coefficients can produce fast forward models for use in pattern matching. Also they can be used to train a support vector machine (SVM) to sort objects into generic classes, such as elongated or not, permeable or not. The success of the retrieval from both synthetic and measurement data shows the promise of the spheroidal mode approach in the detection and classification of buried objects.

Subsurface Estimation of the Geometry and Electromagnetic Properties of Buried Anomaly and Half-space Background with Unknown Rough Boundary

R. Firoozabadi, E. L. Miller, C. Rappaport, and A. W. Morgenthaler
Northeastern University, USA

A new inverse method is developed to recover the geometric structure and electromagnetic contrast of an anomaly buried in a half-space defined by a rough, unknown boundary. Spline curves are used to model both the shape of the object as well as the profile of the boundary. The problem is then cast as one of determining a relatively small number of control points for these curves along with the complex permittivities of the anomaly and the background medium. The direct relationship between the control points and the boundary points and nonlinear relationship between the geometry and resulting scattered field defined by Maxwell's equations enable us to restore these parameters with a high degree of accuracy even when the data are corrupted by noise.

The physical forward model employed in the inversion algorithm is the Semi-Analytic Mode Matching method (SAMM) which is a fast and efficient method to calculate the scattered near-fields from a buried lossy homogenous object in the lossy homogenous background and is defined in terms of the modal expansions enforcing the boundary conditions at the boundaries of different media. SAMM is of low computational complexity compared to other methods and highly accurate in the region of interest.

The Levenberg-Marquardt method is used as a nonlinear least-squares minimization algorithm to optimize the unknown parameters including the control points and complex permittivities. In the talk accompanying this abstract we provide details concerning the manner in which the SAMM model allows us to compute closed form expressions for the sensitivity of the scattered fields with respect to both the geometric and contrast parameters. Numerical results will be provided to verify the capability of the proposed algorithm.

REFERENCES

1. Morgenthaler, A. W. and C. M. Rappaport, "Scattering from dielectric objects buried beneath randomly rough ground: Validating the semi-analytic mode matching algorithm with 2-D FDFD," *IEEE Trans. Geoscience and Remote Sensing*, Vol. 39, 2421–2428, November 2001.
2. Firoozabadi, R., E. L. Miller, C. M. Rappaport, and A. W. Morgenthaler, "New inverse method for simultaneous reconstruction of object buried beneath rough ground and the ground surface structure using SAMM forward model," *IS&T/SPIE 17th Annual Symposium on Electronic Imaging: Science and Technology*, 382–393, San Jose, CA, 16–20 January 2005.

The Adjoint-field Method for Reconstructing Breast Cancer Tumors of Irregular Shape

M. El-Shenawee[1], O. Dorn[2], and M. Moscoso[2]

[1]University of Arkansas, USA
[2]Universidad Carlos III de Madrid, Spain

In this work we combine the method of moments for 3D electromagnetic propagation and the adjoint field method for shape reconstruction for the problem of breast tumor detection using microwaves. The method of moments forward solver is used to calculate the scattered fields at several receivers surrounding the tumor. Moreover, the total fields are calculated everywhere in the considered domain including the interface of the tumor. The mismatch between calculated and synthetically measured fields is then used as new sources at all receiver locations and is back-propagated towards the tumor by just solving another forward problem with the method of moments code. The gradient is calculated as the product of the forward and adjoint fields at the best guess of the tumor interface in order to extract a new search direction. The location of each surface node is then updated individually based on these new gradient values in the normal direction of the surface. Using this technique, the forward solver will be used only twice, regardless of the shape of the tumor; once for solving the forward problem and once for the adjoint problem. This process is repeated iteratively until the mismatch in the data is minimized according to some criterion.

In our previous work, the irregular shape of a malignant tumor was modeled using a spherical harmonics representation, which leads to smooth reconstructions. However, sometimes it is desirable to be able to recover more irregular shapes, which cannot be achieved efficiently by the spherical harmonics method. Therefore, we will use in this work a more general representation directly given by the discretization mesh of the method of moments. Doing so, we need to find an efficient way for calculating shape gradients. Instead of using the often employed perturbative method for this purpose, we will use an adjoint field method which is more efficient in this situation.

In our numerical experiments, the background medium is assumed to be homogeneous and lossy. The embedded tumors are assumed to be shape-like with constant dielectric parameters inside. The contrast in these dielectric parameters between tumors and background medium is assumed to be high, which is typical for breast tumors. We will present several numerical results in 3D based on the proposed technique using multiple transmitting sources/receivers at multiple microwave frequencies.

Nonlinear Inversion of Multi-frequency Microwave Fresnel Data Using the Multiplicative Regularized Contrast Source Inversion

A. Abubakar and T. M. Habashy
Schlumberger-Doll Research, USA

P. M. van den Berg
Delft University, The Netherlands

Image reconstruction is a complex nonlinear inverse problem in microwave tomography because both the material parameters and the field distributions in the investigation domain are unknown. If the unknown objects have small contrasts, a linearization procedure such as the Born approximation can be used to estimate the internal field distribution so that images can be obtained within a short amount of processing time. Furthermore, the so-called iterative Born method, has been used to reconstruct objects with intermediate contrasts. However, more complicated algorithms are needed to reconstruct objects with high contrasts. The Gauss-Newton method, also known as the Newton-Kantorovich method or the distorted Born method, has been successfully applied to the imaging of twodimensional objects with high-contrast. However, the main bottleneck of this Newton-type approach, which is especially discouraging in three-dimensional problems, is the need to compute multiple forward solutions to construct the sensitivity matrix. Another type of iterative methods, that avoid solving the full forward problem in each iterative step, is introduced in the so-called Modified Gradient (MG) method. In this MG method the material contrast and the fields are updated simultaneously in each iterative step using the Conjugate Gradient (CG) directions. It was shown that by updating the contrast sources (the product of the material contrast with the fields) and the material contrast, one could arrive at a simpler algorithm than the MG method while maintaining its robustness and accuracy. This method is known as the Contrast Source Inversion (CSI) method. This CSI method has also been augmented with a weighted L2-norm regularizer (a variant of the total variation regularization) in order to enhance its resolution. Although the addition of the regularizer to the cost function has a positive effect on the quality of the reconstruction for both 'blocky' and smooth objects, a drawback is the presence of an artificial weighting parameter in the cost function, which can only be determined through considerable numerical experimentation and a priori information of the desired reconstruction images. To alleviate this drawback, it was suggested to include the regularizer as a multiplicative constraint. In this multiplicative regularizer, the un-regularized cost function becomes the weighting parameter of the regularizer. This multiplicative-type regularization seems to handle noisy as well as limited data in a robust manner. We named this method as the Multiplicative Regularized CSI method (MR-CSI).

In this work we apply the MR-CSI algorithm to invert multi-frequency data measured by the Institute Fresnel, Marseille, France, from cylindrical inhomogeneous objects, both for TM (electric field in the vertical axis) and TE (electric filed in the tranverse plane) electromagnetic excitations. We perform simultaneous multi-frequency inversion without using any *a priori* information on the type of the unknown objects (whether it is metallic or dielectric). In all cases we reconstruct both the conductivity and the permittivity of the unknown objects. Positivity of the permittivity and the conductivity are the only *a priori* information which we enforce. The inversion results show that the MR-CSI method successfully performs 'blind' inversion of these Fresnel data set.

Reconstruction of 3-D Dielectric Objects from Experimental Data in the Time Domain

T. Takenaka, T. Tanaka, and H. Zhou
Nagasaki University, Japan

Many nonlinear inversion techniques have been proposed for imaging high-contrast objects both in the frequency domain and in the time domain. Since the use of a broad-band pulse allows a large amount of information about unknown scattering objects than a single frequency scattering data, we have proposed a time-domain inverse scattering imaging technique, the forward-backward time-stepping (FBTS) method, to reconstruct the electrical parameter (the permittivity and conductivity) profiles of the scattering objects. We have also shown its effectiveness in several numerical simulations for inhomogeneous anisotropic as well as isotropic objects in the previous works.

This paper reports the 3-D reconstruction of the relative permittivity profile of an unknown object from the experimental data in the time domain. Eight antenna elements are placed equally spaced in a measurement circle. One of the antenna elements are used as a transmitting antenna and emits a pulsed wave. The scattered wave by the object is collected by the rest of them. Instead of using a pulse generator, we use a vector network analyzer which generates a stepped-frequency signal. The time domain representation of the scattering data is attained via the inverse Fourier Transform. All the transmission response $S_{ji}(j \neq i)$ between the ith transmitting antenna and the jth receiving antenna $(i,\, j = 1,\, 2\, \ldots,\, 8)$ are measured. Then, we change the transmitter point to the next antenna point and repeat the same measurement until all the antenna positions are used as a transmitter point. Next we move the measurement circle in the vertical direction and continue the measurement in the same way. We change the height of the measurement circle twice, so that we get 168 scattered field data. These data S_{ji} are multiplied by the spectrum of an incident pulse. Then taking the inverse Fourier transform of the resultant spectrum, we get the time domain scattering data to apply the FBTS method to the reconstruction of the relative permittivity profile of the unknown object. The FBTS method was tested on the experimental data from a wooden hollow cylinder. The 3-D shape and the relative permittivity profile of the cylinder were successfully obtained.

Session 3P5
Electromagnetic Modeling and Inversion and Applications 3

New Stochastic AGLID EM Modeling and Inversion

J. H. Li, G. Q. Xie, and F. Xie
GL Geophysical Laboratory, USA

The AGILD modeling and inversion have been published in PIERS2005 in Hangzhou [1] A new 2.5D AGILD and new GL modeling and inversion are published in PIERS2006 in Cambridge of USA [2]. In this paper, we present a stochastic AGILD EM modeling and inversion algorithms. We proposed strip stochastic magnetic field differential integral equations for zero order assemble mean magnetic field in [1], cross covariance of magnetic field and conductivity, covariant of the magnetic field, and second order assemble mean magnetic field on the boundary strip and center strip Ω_S with coordinate poles in cylindrical and spherical coordinate system. $FMI1(C_{H(\sigma+i\omega\varepsilon)}, C_{(\sigma+i\omega\varepsilon)}, H_0) = 0$, $FMI2(C_H, C_{H(\sigma+i\omega\varepsilon)}, H_0) = 0$, $FMI3 = 0$, where $FMI1 = 0$ is strip differential integral equation of the cross covariance $C_{H(\sigma+i\omega\varepsilon)}$, the equation $FMI2 = 0$ is strip differential integral equation of the covariance C_H , the equation $FMI3 = 0$ is strip differential integral equation of the second order assemble mean magnetic field $\langle H_2 \rangle$. These new strip stochastic moments magnetic field differential integral equations are employed on the boundary strip domain. In the cylindrical and spherical coordinate system, these differential integral equations should be solved on the small center sub domain with pole $\rho = 0$ or north pole $\theta = 0$ and south $\theta = \pi$. In the remainder internal domain, we use stochastic moments magnetic field Galerkin FEM equations. We coupled these equations to construct new 3D and 2.5D stochastic AGILD EM modeling algorithms. We decomposed the increment of the assemble mean of the conductivity and permittivity, $\delta\langle\sigma + i\omega\varepsilon\rangle$ as $\delta\langle\sigma + i\omega\varepsilon\rangle = \delta\langle\sigma + i\omega\varepsilon\rangle_0 + \delta\langle\sigma + i\omega\varepsilon\rangle_2$ We drive the new strip stochastic conductivity and permittivity increment moment differential integral equation on the boundary strip sub domain, $PMI0 = 0$, $PMI1 = 0$, $PMI2 = 0$, and $PMI3 = 0$. These parameter integral equation are described in [3] in detail. We used the conductivity and permittivity stochastic increment differential integral equations on the boundary strip domain ***SI*** and conductivity and permittivity stochastic increment Galerkin equation [4] in remainder sub domain ***SII*** to construct the stochastic AGILD inversion. In the cylindrical and spherical coordinate system, the ***SI*** should be contained the poles. The new stochastic AGILD modeling and inversion have widely applications in the geophysical and Earthquake exploration, MT, MAIL, VEMP, EM stirring in steel and metal continuous casting, weather radar imaging, medical MRI and X-ray imaging, and environmental engineering, nanometer material and material sciences in rectangle coordinate, cylindrical, and spherical coordinate system [1–4].

REFERENCES

1. Xie, G. Q., J. H. Li, and F. Xie, "Advanced GILD EM modeling and inversion," *Proceeding of PIERS2005*, Hangzhou, China, 105–109, 2005.
2. Xie, G. Q., J. H. Li, and F. Xie, "New GL method and its advantages for resolving historical difficulties," to be presented in PIERS2006 in Cambridge, 2005.
3. Li, J. H., G. Q. Xie, and F. Xie, "Stochastic AGILD EM modeling and inversion," Report of GLGEO, GLP05005, Its copyright and patent belong to the authors in GL Geophysical Laboratory, 2005.
4. Xie, G. Q., J. H. Li, and C.-C. Lin, "SGILD EM modeling and inversion in geophysics and nanophysics using magnetic field equations," *Three-Dimensional Electromagnetic Methods in Geochemistry and Geophysics*, Vol. 35, 103–213, 2002.

Advancements in Microwave Tomography of Strong Scatterers

R. Pierri[1], **G. Leone**[2], **and R. Solimene**[2]

[1]Seconda Università di Napoli, Italy
[2]Università Mediterranea di Reggio Calabria, Italy

The inverse scattering problem of reconstructing strong scatterers, especially metallic ones, from scattered field measured data, is one of the most important issues in microwave imaging applications.

This contribution deals with such a problem in the framework of a two-dimensional and scalar geometry and with the possible scatterers embedded in a homogenous and lossless medium. In particular, we consider both the cases of "large" objects (i.e., scatterers whose cross-section is much larger than the wavelength) and of "thin" objects (i.e., scatterers with their cross-section much smaller than the wavelength).

For large scatterers, the Kirchhoff or Physical Optics (PO) approximation is exploited, whereas unknown scatterers shape, is represented as the support of a single-layer distribution. This allows the problem be formulated as the inversion of a linear operator we tackle by means of its Truncated Singular Value Decomposition (TSVD) [1]. As well known, the PO approximation requires that the objects are non-convex, exhibit a "smooth" surface and are not interacting. Hence, it is worthy of investigating to what extent the model error, arising by objects not meeting the above requirements, affects the linear inversion scheme. In this paper we perform this investigation for three test cases. First, with the aim of pointing out the role of the radius of curvature, we consider a circular cylinder with radius smaller than the working wavelength. Second, two interacting circular cylinders are considered. Finally, a non-convex scatterer is addressed [2].

For 'thin' scatterers, we set a linear scattering model neglecting the mutual interactions between them and consider only the leading term of the low-frequency approximation of the scattered field. Furthermore, a distributional representation of the unknown is again fruitfully introduced. However since, in this case, the unknowns are the positions of the scatterers, we represent them as the support of a linear combination of Dirac pulses. Accordingly, the inversion can be still performed by a TSVD scheme. We assess the performance of this inversion scheme against the model error due to neglecting the mutual interactions [3].

As a final point, for both above cases, a thresholding procedure aiming at mitigating spurious artefacts appearing in the reconstruction owing to regularization and noise, is proposed [4].

REFERENCES

1. Liseno, A. and R. Pierri, "Imaging perfectly conducting objects as support of induced currents: kirchhoff approximation and frequency diversity," *J. Opt. Soc. Am. A*, Vol. 19, No. 7, 1308–1319, July 2002.
2. Pierri, R., A. Liseno, R. Solimene, and F. Soldovieri, "Beyond physical optics SVD shape reconstruction of metallic cylinders," in print on *IEEE Trans. Antennas and Propagation*.
3. Pierri, R., R. Solimene, A. Liseno, and J. Romano, "Linear distribution imaging of thin metallic cylinders under mutual scattering," *IEEE Trans. Antennas and Propagation*, Vol. 53, No. 9, 3019–3029, Sep. 2005.
4. Solimene, R., A. Liseno, and R. Pierri, "A spatially varying threshold for imaging thin metallic cylinders," submitted.

Acceleration of the 3D FDTD Algorithm in Fixed-point Arithmetic Using Reconfigurable Hardware

W. Chen, M. Leeser, and C. Rappaport
Northeastern University, USA

Modelling electromagnetic behavior has become a requirement in key electrical engineering technologies such as cellular phones, mobile computing, lasers and photonic circuits. The Finite-Difference Time-Domain (FDTD) method, which provides a direct, time domain solution to Maxwell's Equations in differential form with relatively good accuracy and flexibility, has become a powerful method for solving a wide variety of different electromagnetics problems. The FDTD method was not widely used until the past decade when computing resources improved. Even today, the computational cost is still too high for real-time application of the FDTD method.

Much effort has been spent on software acceleration research and people have used supercomputers or parallel computer arrays to calculate the FDTD algorithm in software. However, real-time application of the FDTD algorithm needs much faster speed as well as smaller size. Although Application Specific Integrated Circuits (ASICs) provide the speed, designers hesitate to apply the FDTD algorithm to ASICs due to the high cost. Recently, as high capacity Field-Programmable Gate Arrays (FPGAs) have emerged, researchers have become interested in reconfigurable hardware implementations of the FDTD algorithm for faster calculation and real-time applications.

We present the first fixed-point 3D FDTD FPGA accelerator, which supports a wide range of materials including dispersive media. By analyzing the performance of fixed-point arithmetic in both soil-based media and human tissue media, we choose the right fixed-point representation to minimize the relative error between fixed-point and floating point results to less than 0.5%. The FPGA accelerator supports the UPML absorbing boundary conditions which have better performance in dispersive soil and human tissue media than PML boundary conditions. Finally, the FPGA design implements and supports three FDTD applications including the Ground Penetrating Radar buried object detection model, the microwave breast cancer detection model and the spiral antenna model. Based on these three applications, our FPGA design can support a wide range of FDTD applications.

Implementation of the FDTD in hardware greatly increases its computational speed. The speedup is due to three major factors: custom memory interface design, pipelining and parallelism. The FDTD method is a data intensive algorithm; the bottleneck of the hardware design is its memory interface. With the limited bandwidth between FPGA and data memories, a carefully designed custom memory interface will fully utilize the memory bandwidth and greatly improve the design performance. Also, by considering the tradeoff between speedup and chip areas, we implement as much pipeline and parallelism as possible to speed up the design.

The 3D FDTD design is implemented on an AnnapolisWildStar^{TM}-II Pro/PCI FPGA board which represents the leading technology in FPGA COTS (commercial off-the-shelf) hardware. The performance results of the software and hardware implementations are shown in Fig. 1. The hardware design running at 90 MHz on the FPGA chip is 25 times faster than fixed-point software running on a 3.0 GHz PC.

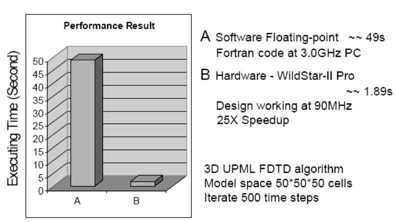

3D FDTD Hardware Implementation Performance

	Software in FORTRAN	Hardware Design All Cells as Center Cells	Hardware Design All Cell as UPML Boundary Conditions Cells	Hardware Design Combined Center and UPML region Preliminary Test
Seconds	49	1.59	2.985	1.89
MNodes/s	1.27	39.31	20.93	33.07
Speedup	1	30.9	16.5	25.9

Figure 1: Performance results—softwares vs. FPGA hardware.

There are two Xilinx Virtex-II Pro FPGAs on our FPGA board. In the near future, our research will focus on a dual-FPGA parallel implementation of the FDTD algorithm which is expected to double the speedup.

Geometric Optics and Electromagnetic Models for Cylindrical Obstacles

D. Trappeniers, **R. G. Gonzàlez**, **E. van Lil**, **and A. van de Capelle**
K. U. Leuven, Belgium

A software prediction tool called EPICS (Enhanced Propagation for Indoor Communications Systems) was developed at the ESAT-TELEMIC division of the K. U. Leuven in two versions: a Geometric Optics (GO) version and a Physical Optics (PO) version. However, like many other three-dimensional software, this can only determine the signal in an environment that can be decomposed into (ir) regular hexahedral obstacles (with 6 sides like rectangular blocks, cubes, etc.) or (complex) combinations of them. Although most of the real life environment can be approximated by these hexahedral obstacles, this might lead to some artefacts like periodic radar cross section variations, the need for multiple diffractions to calculate the signal behind a cylindrical obstacle, or reflections that are ignored (e. g., because the approximated side plane is positioned so that a reflection on that plane can not reach the receiver) is existing. To calculate the signal more accurately for those cases, we need to implement curved obstacles into EPICS. In a first step to achieve this goal, the introduction of cylindrical obstacles is investigated.

In this paper, the general strategy is discussed. The first step is to determine the different intermediate (i. e., penetration, reflection and diffraction) points on the ray between transmitter and receiver. Efficient computational routines have been written and tested for this purpose, mostly solving the problem first in two dimensions (projected in a plane perpendicular to the axis of the cylinder) and then transforming this solution to the three-dimensional problem. Once these intermediate points have been found, one can start with the computation of the electromagnetic field.

In the case of a penetration, the intermediate point(s) can be found very easily (crossing point(s) of a line and a circle) and the electromagnetic computations don't differ from the computations with hexahedral obstacles. For the reflection by a non perfectly conducting surface, the plane wave Fresnel reflection coefficients can be used. Also the finite thickness of the cylindrical walls can be taken into account, using internal (multiple) reflections, if the losses are high or the reflection coefficient of the wall is not to large.

For the diffractions, the two-dimensional geometric problem that needs to be solved to find the diffraction points is the determination of the tangent line to a circle (both from transmitter and receiver). Note that both can have two tangent lines, and one might have to match the two corresponding diffraction points. In this case, the electromagnetic computations for the vertical (i. e., field component parallel with the axis of the cylinder) and horizontal polarisation are done separately. An important issue in these computations is the convergence of the series used for the calculation of the field.

The reflection points on a cylindrical wall can not be found as easily as in the previous two cases. In general, an iterative process is required. This implies that the search for a good starting value is an important issue. Therefore some efficient computer programs were written to find firstly a good starting value of the Newton-Raphson iteration. As for the electromagnetic computations, one has to take into account that the caustics are transformed after the reflections and thus another amplitude factor has to be taken into account.

Although the described routines are not (yet) a part of the EPICS software, new routines based on Geometric Optics (GO) have been written and tested (in matlab) to predict penetration, reflection and diffraction of electromagnetic fields around cylindrical obstacles. This will be used to compute the effects of a curved airport terminal on an Instrument Landing System (ILS).

3D and 2.5D AGLID EMS Stirring Modeling in the Cylindrical Coordinate System

G. Q. Xie, J. H. Li, J. Li, and F. Xie
GL Geophysical Laboratory, USA

In paper [1, 2], we proposed a new 2.5 D boundary strip magnetic field differential integral equations for EM field on the boundary strip and center strip with coordinate poles in cylindrical coordinate system that is denoted by Ω_S. In this paper, we proposed a 2.5 D AGILD EM stirring modeling algorithms and software. In the cylindrical coordinate system, the electromagnetic (EM) filed is vector function of the r, θ, and z. However, the electrical conductivity is only depended on radial coordinate r and vertical coordinate z. Upon substituting the Fourier serious of the magnetic field into the strip differential integral equation on boundary strip with pole $\rho = 0$ sub domain SI and Galerking equation in the internal sub domain SII [1], we construct 2.5 D AGILD electromagnetic stirring modeling in cylindrical coordinate system for the steel and metal continuous casting. It is well-known that there is u/ρ^2 term in the magnetic field MAXWELL differential equation in the cylindrical coordinate system, The pole $\rho = 0$ is strong coordinate singularity in the cylindrical coordinate system. The coordinate singularity is difficult in the EM stirring modeling by using FEM and FD methods. Our new 2.5 AGILD EMS modeling method resolved the difficulties. There is no any coordinate singularity in our 2.5 D EM differential integral equation. Because the conductivity in air is zero but it is 10^5 around in the steel, how does one set boundary condition on $\rho = 0$ for current, electric field, and magnetic field that is other difficult. Our AGILDEMS overcome this difficult. Based on our 2.5 D AGILD EMS algorithm, we developed the new 2.5 D AGILD-EMS modeling software. Many applications show that the 2.5 D AGILD-EMS software is a powerful tool for design of the EM stirring and real time control monitor in the steel and metal continuous casting.

The AGILD K-ε flow modeling and software are developing for continuous casting in GL Geophysical Laboratory [3, 4].

REFERENCES

1. Li, J. H., G. Q. Xie, and F. Xie, "New stochastic AGLID EM modeling and inversion," to be Presented in PIERS 2006 in Cambridge of USA, 2005.
2. Xie, G. Q., J. H. Li, and F. Xie, "2.5 D AGLID EM modeling and inversion," to be presented in PIERS 2006 in Cambridge of USA, 2005.
3. Li, J. H., G. Q. Xie, and F. Xie, *AGILD K-ε Flow Modeling, Report of GLGEO, GLP05006*, Its copyright and patent belong to the authors in GL Geophysical Laboratory, 2005.
4. Xie, G. Q., J. H. Li, and F. Xie, "GL method resolved spherical coordinate singularities and some historical difficulties," to be presented in PIERS 2006 in Cambridge of USA, 2005.

Time-domain Source-model Technique Analysis of Two-dimensional Electromagnetic Scattering Problems

A. Ludwig and Y. Leviatan
Technion - Israel Institute of Technology, Israel

Time-domain integral equation solvers for analyzing transient scattering phenomena continue to be a subject of considerable interest in the computational electromagnetics community. In this paper, we study a somewhat different time-domain integral-equation solution. Instead of using a standard surface formulation, we present a mesh-free formulation for the solution of the electromagnetic scattering problem of a two-dimensional metallic cylinder illuminated by a TM (transverse magnetic) plane wave pulse. In the proposed solution, we adapt the frequency-domain source model technique, which has been found to be efficient and versatile computational tool for analysis of time-harmonic wave scattering problems, to allow direct time-domain analysis of transient scattering problems. In this solution, the scatterer is replaced with a discrete set of spatially impulsive filamentary sources, each carrying longitudinally-uniform but time-dependent electric currents that are subsequently expanded in terms of pulse functions of yet-to-be-determined amplitudes. The filamentary sources are located on a mathematical surface interior to the cylinder surface. They are assumed to radiate in an unbounded free-space and their fields, which are known analytically, span the transient scattered field in the region exterior to the cylinder. The source amplitudes are determined by requiring that the boundary condition for the total tangential electric field be satisfied at a suitably chosen set of time instances and at a selected set of testing points on the boundary of the cylinder. The effect of solution method parameters, such as the spatial density and temporal discretization of the fictitious sources, on the accuracy and stability of the results is studied. A spatio-temporal discretization criterion for an explicit formulation of the time-domain source-model solution is presented to allow the use of a simple marching-on-in-time algorithm. The modification of this algorithm to treat an implicit formulation of the time-domain source-model solution is discussed, and the advantages of such a formulation are outlined. Finally, the use of a combined-source formulation and its effect on the resulting stability is studied.

New 2.5D/3D AGILD Geophysical EM Multiple Cross Holes' Imaging

J. Li[1], **M. Oristaglio**[2], **F. Xie**[1], **and G. Xie**[1]

[1]GL Geophysical Laboratory, USA
[2]Schlumberger-Doll Research, USA

Seismic wave, acoustic wave and electromagnetic (EM) field inversion are used for geophysical subsurface imaging. Because there is electric conductivity in the Earth underground, the diffusion EM field with infinite velocity causes the EM inversion more ill posed than seismic and acoustic inversion. The optimizing data configuration, suitable frequency band, and vanishing boundary error, translating coordinate singularity in forward modeling, and combining strong regularizing and weak regularizing etc. approaches will be benefit for EM inversion. In this paper, we propose a "new 2.5D/3D AGILD geophysical EM multiple cross holes' imaging" algorithm. We choose the three, four, and five cross holes data configuration. Based on the AGILD EM modeling and inversion in Piers 2005 in Hangzhou [1] and 3D and 2.5D AGILD EMS modeling in the cylindrical system in Piers 2006 in Cambridge [2], we present the 3D EM modeling and multiple 2D conductivity inversion using the multiple cross holes data. In existing 2.5D algorithm, the conductivity and EM parameters are supposed to be independent on the variable θ and only 2D inversion is processed. Therefore, the existing 2.5 D algorithm can only make rough imaging for whole cylinder subsurface. By using a variable weight average strategy, our new 2.5D inversion can be used to do multiple 2D conductivity inversions using the multiple cross holes data. In the other hand, there is strong coordinate singularity $1/\rho^2$ at $\rho = 0$ in exiting FD and FEM EM modeling in the cylindrical coordinate that is a historical difficulty. Our 2.5D AGILD geophysical EM multiple cross holes' imaging algorithms overcome this difficulty because the strip magnetic field differential integral equation has no coordinate singularity at $\rho = 0$. We use 3D strip magnetic field differential integral equation in the boundary pole strip domain with pole $\rho = 0$ and use magnetic field Garlekin equation in the remainder domain to construct 3D AGILD magnetic and EM field modeling to obtain the model data. Using statistics geology average strategy, we make the 2, 3, 4, or 5 multiple cross holes' 2D AGILD EM inversions. Our new AGILD multiple cross holes' imaging will be useful for geophysical exploration, oil exploration, Earthquake exploration, geophysical engineering, environment characteristic monitoring, nondestructive testing, medical imaging, and material and nano sciences etc sciences and engineering.

REFERENCES

1. Li, J. and G. Xie, "A cubic-hole finite element for 3D resistivity modeling," "Three-dimensional electromagnetics," edited by Michael Oristaglio, *Geophysical Developments*, No. 7, 591–599, 2000.
2. Li, J., G. Xie, and F. Xie, "New stochastic AGLID EM modeling and inversion," to be presented in *PIERS 2006 in Cambridge of USA*, 2005.
3. Xie, G., J. Li, and F. Xie, "New global and local electromagnetic field (GL) modeling and inversion," *proceeding of PIERS2005 in Hangzhou*, 68, 2005.
4. Xie, G., J. Li, and F. Xie, "Advanced GILD EM modeling and inversion," *Proc. PIERS*, Hangzhou, 105.
5. Xie, G., F. Xie, and J. Li, "New GL method and its advantages for resolving historical difficulties," to be presented in *PIERS 2006 in Cambridge of USA*, 2006.
6. Xie, G., J. Li, and F. Xie, "2.5D AGLID EM modeling and inversion," to be presented in *PIERS 2006 in Cambridge of USA*, 2006.
7. Xie, G., F. Xie, and J. Li, "New GL and GILD superconductor electromagnetic modeling," *Proceeding of PIERS2005 in Hangzhou*, 187, 2005.

Session 3P6
Novel Mathematical Methods

Far-field RCS Prediction from Measured Near-field Data over Ground Plane

Y. Inasawa, **S. Kuroda**, **S. Morita**, **H. Nishikawa**, **N. Yoneda**, **and S. Makino**
Mitsubishi Electric Corporation, Japan

The far-field Radar Cross Section (RCS) measurement of the actual target requires a long measurement range, which can be realized in the outdoor site. One of the problems in outdoor measurement is the difficulty to avoid the effect of ground bounce because the difference between direct and ground-reflected path length is very small. Some measurement sites realize the outdoor RCS measurement in a few kilometer range by the exploitation of the ground bounce. The shorter measurement range may be preferable especially in Japan.

In this paper we evaluate the far-field RCS prediction technique from near-field RCS data measured over the ground plane in order to find out the possibility of the measurement range reduction. We present the results of the far-field RCS prediction from near-field data including the ground bounce. The near-field data is measured on the metal ground plane in an anechoic chamber, not on the actual ground plane because the fundamental characteristics of ground bounce would be evident. The predicted far-field RCS agrees well with the computed far-field RCS for the measurement model with large dimension in horizontal direction. Whereas the small prediction error for the measurement model with large vertical dimension is observed. The applicable scope of the far-field RCS prediction technique over the ground plane is resolved.

Estimation of Buried Pipes Diameter and Position by Ground Penetrating Radar Scans

G. Borgioli, P. Falorni, L. Capineri, B. Morini, and S. Matucci
Università di Firenze, Italy

C. G. Windsor
116, New Road, East Hagbourne, OX11 9LD, UK

The interest of this study is concerned to the problem of determining the position and size of buried pipes by using remote sensing methods like ultra-wide-band radar, which can measure the round trip time (time of flight ToF) of a pulsed wave by an antenna placed just above the surface (y_i). In this study we consider the physical approximation that the diffracted field from the pipe can be received over a wide angle range of antenna positions and so the time of flight information can be measured for several incident field angles. It is common to find in practice pipes that are buried at about one meter under a road with size that is comparable to few radar wavelengths and for them the simple point like scatterer approximation for the time of flight equation doesn't approximate well the experimental data. The aim of this work is to study the feasibility of robust solving methods for the hyperbolic equation of the time of flight, which contains in the most general case four unknown: pipe radius (R), position (lateral y_0, depth z_0), and propagation velocity (v). A mathematical solution of the system of non linear equations is presented. The derived solution has the advantage to be linear for the solution of a new set of unknown ($\psi = Rv$, $\sigma = v^2$ and y_0). Only the solution for z_0 remains non linear. From the numerical point of view the solution of the linear system is straightforward and the sensitivity to measurements errors superimposed to y_i and ToF has been carried out. The application of the solving method to simulated data for defined values of sampling time and noise has shown the difficulties of accurate estimation of pipes diameter while the lateral position y_0 and velocity have been well approximated by the centroid of the distribution of the solutions. Numerical methods for solving this problem are discussed and data are presented on simulated and experimental data. The accurate estimation of the four unknowns together is important not only for devising advanced non destructive testing methods but also for providing information about the soil velocity distribution that can be exploited by inversion methods in the time domain (linear SAR).

The Parallelization of a 2D Floating Random-walk Algorithm for the Solution of the Nonlinear Poisson-boltzmann Equation

K. Chatterjee
Massachusetts Institute of Technology, USA

J. Poggie
Wright-Patterson Air Force Base, USA

This paper presents the parallelization of a two-dimensional floating random walk (FRW) algorithm for the solution of the nonlinear Poisson-Boltzmann (NPB) equation. Historically, the FRW method has not been applied to the solution of the NPB equation and other important nonlinear equations. This can be attributed to the absence of analytical expressions for volumetric Green's functions. Previous studies [1] using the FRW method have examined only the linearized Poisson-Boltzmann equation. Approximate volumetric Green's functions have been derived with the help of perturbation theory, and these expressions have been incorporated within the FRW framework. A unique advantage of this algorithm is that it requires no discretization of either the volume or the surface of the problem domains. Furthermore, each random walk is independent, so that the computational procedure is highly parallelizable. In our previous work [2, 3], we have presented preliminary results for our newly developed one- and two-dimensional FRW algorithm. We now present the results of the parallelization of the two-dimensional algorithm, with its finite-difference based validation. The solution of the NPB equation has many interesting applications, including the modeling of plasma discharges, semiconductor device modeling and the modeling of biomolecular structures and dynamics.

*Support for Dr. K. Chatterjee was provided under a National Research Council Summer Faculty Fellowship at the Air Force Research Laboratory, Wright-Patterson Air Force Base. Additional support was provided by the Air Force Office of Scientific Research, under grants monitored by Dr. J. Schmisseur and Dr. F. Fahroo. We would like to acknowledge valuable discussions with Dr. M. D. White and Dr. D. V. Gaitonde.

REFERENCES

1. Co, H. and M. Mascagni, "Efficient modified 'walk on spheres' algorithm for the linearized poisson-boltzmann equation," *App. Phys. Lett.*, Vol. 78, No. 6, 787–789, 2001.
2. Chatterjee, K. and J. Poggie, "A meshless stochastic algorithm for the solution of the nonlinear Poisson-Boltzmann equation in the context of discharge modeling: 1D analytical benchmark," *AIAA Paper 2005-5339 in Proceedings of the* 17^{th} *AIAA Computational Fluid Dynamics Conference*, Toronto, Ontario, Canada, 6–9, June, 2005.
3. Chatterjee, K. and J. Poggie, "A two-dimensional floating random walk algorithm for the numerical solution of the nonlinear Poisson-Boltzmann equation: Application to the modeling of plasma sheaths," *Proceedings of the* 3^{rd} *MIT Conference on Computational Fluid and Solid Mechanics*, 1058–1061, Cambridge, MA, June 14–17, 2005. Elsevier: Oxford, UK, 2005.

Reduction of FDTD Simulation Time with Modal Methods

D. A. Gorodetsky and P. A. Wilsey
University of Cincinnati, USA

FDTD is a popular scheme that simulates electromagnetic wave propagation in the time domain. We show how to reduce the lengthy simulation times with eigenmodal decomposition. Let the vector $\mathbf{Q}(n)$ denote the state of the electric and magnetic field on a portion of the FDTD grid, called a module [1]. The state transition matrix $\mathbf{A}(n-i)$ produces the state at time n from the state at time i. If the module's inputs are combined in $\mathbf{X}(n)$, of size $I \times 1$, then $\mathbf{Y}(n)$, the output vector of size $O \times 1$, is given as: $\mathbf{Y}(n) = [\mathbf{CA}(n)\mathbf{B}] \otimes \mathbf{X}(n)$, where $\otimes$ represents convolution, and the term in the brackets is the impulse response of the module. Due to the properties of convolution, the computing time grows with every step [1]. In the TLM method each entry of the impulse response can be written as a superposition of the eigenvalues of the state transition matrix [2]. Instead of requiring the storage of the entire history of the inputs, this method requires storage of N matrices, where N is the total number of points in the module. Due to the nature of the algorithm, many eigenmodes can be discarded, replacing N by P. This method takes a constant time for every time step, with the number of multiplications required for the computation proportional to $I \times O \times P$ *(or IOP)*. Our alternative method involves decomposing the input vector $\mathbf{X}(n)$ into a sum of eigenvectors of $\mathbf{A}$. It reduces the total number of multiplications per step to be proportional to OP. A running sum is kept for each eigenvector and convolution now involves only multiplying each running sum by its eigenvalue.

The expression of the inputs in terms of eigenvectors requires a solution of P equations in P unknowns for every iteration. If an interface module is used, then it has a small number of points and P is decreased. The burden of decomposing the inputs into eigenvectors now rests on the interface module. Afterwards, a change of basis can be done to convert the inputs from the interface module's basis to the core module's one or between any two adjacent modules. Every eigenvector of the foreign basis can be expressed as a superposition of the eigenvectors of the local basis by finding the conversion matrix. Multiplication of the conversion matrix by the input vector consisting of the coefficients in the foreign basis will produce the coefficients to express the input vector in terms of the local basis. With this method, any number of core modules can be connected in cascade such that only one interface module is used.

A parallel plate waveguide structure was simulated at 10 GHz. The advantage of over an earlier approach [1] is that the storage of the history of the impulse responses (IOT) is no longer required. The only storage required is that of the P eigenvectors (NP), P eigenvalues, and P coefficients. Another improvement is that the storage of the inputs (IT) is replaced by the much smaller storage of the P coefficients. In regards to the approach published in [2], the storage requirement is improved from $\sim IOP$ to $\sim OP$, analogous to the improvement in multiplications per time step. The significance of this result is that the FDTD computation will take less time, depending on the size of the module. The number of eigenmodes (P) can be reduced further by exploring the limitations imposed by the Nyquist criterion and dispersion errors. The methods discussed in this paper can be extended to a majority of other RF simulation scenarios such as antennas.

REFERENCES

1. Gorodetsky, D. A. and P. A. Wilsey, "A matrix approach to FDTD computations," *IEEE MWS-CAS*, 2005.
2. Chen, Z., "Analytic johns matrix and its application in tlm diakoptics," *IEEE MTT-S Digest*, Vol. 2, 777–780, 1995.

Approximate Decomposition for the Solution of Boundary Value Problems for Elliptic Systems Arising in Mathematical Models of Layered Structures

Y. Shestopalov and N. Kotik
Karlstad University, Sweden

Development of the solution techniques for elliptic equations is a classical field of application of mathematical methods in electromagnetics [1]. It is well-known that the processes which take place in planar layered elastic bodies may be described similarly by elliptic systems, in particular by the Lamé equations, equipped with different types of boundary conditions. The boundary-contact problems (BCPs) [2] describing stresses in thin multi-layered elastic sheets constitute here a particular family. The aim of this study is to present an alternative approach to the solution of boundary value problems (BVPs) for elliptic systems arising in mathematical models of layered structures, particularly, of BCPs. We develop mathematical and numerical methods [3] to obtain acoustic and elastic fields in thin multi-layered structures, including strain-stress fields in an elastomeric sheet that simulates planar cliché-contact surfaces in flexographic printing.

The main idea of simplifying the general BCP statements is to consider auxiliary problems for a 'shifted' Laplacian in long rectangles and to reduce them to a sequence of iterative problems such that each of them can be solved (explicitly) by the Fourier method. The solution sequence is then constructed with the help of a contracting transfer operator evaluated explicitly using a rather general family of boundary 'hat' functions (that simulate surface stresses) for which the resulting Fourier-series solutions converge sufficiently fast. This approach constitutes the essence of *the method of approximate decomposition* (MAD) developed in this study. The method facilitates considerably both the analytic and approximate solutions to BCPs and can be generalized to more complicated mixed BVPs for semilinear partial differential operators.

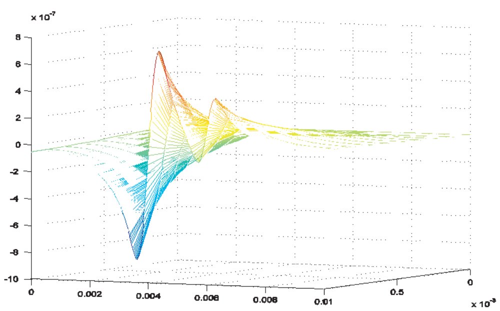

Figure 1: Displacement u_1 in longitudinal direction.

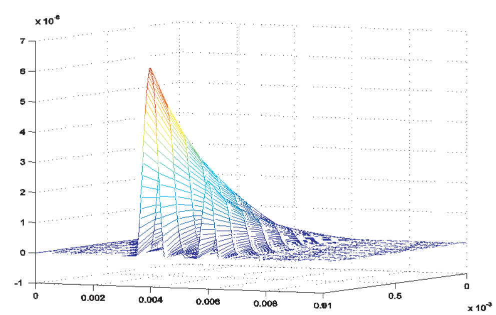

Figure 2: Displacement u_2 in transverse direction.

Figures show examples of longitudinal and transverse displacements in a thin elastic band under the influence of surface stresses (weak loads) through openings in the upper plane, calculated by MAD.

REFERENCES

1. Shestopalov, Y., E. Chernokozhin, and Y. Smirnov, *Logarithmic Integral Equations in Electromagnetics*, VSP Int. Science Publishers, Utrecht, Boston, Köln, Tokyo, 2000.
2. Vorovich, I., et al., *Non-Classical Mixed Boundary Value Problems in Elasticity Theory*, Nauka, Moscow, 1974.
3. Shestopalov, Y. and N. Kotik, "Analysis of mixed boundary value problems for a system of elliptic equations in the layer associated with boundary-contact problems of elasticity," *Proc. Days on Diffraction Int. Seminar*, St Petersburg, Russia, June 28–July 1, 71, 2005.

Generation of Diverse Time-series Data though Monitoring a Death-multiple Immigration Population Model

J. O. Matthews, K. I. Hopcraft, and E. Jakeman
University of Nottingham, UK

Discrete population models have been employed in combination with random walk techniques to model successfully non-Gaussian clutter occurring in coherent imaging systems [e.g., 1, 2]. The method models the coherent returns from an ensemble of scatterers as a random walk comprising a fluctuating number of steps. Non-Gaussian limiting distributions obtain when the stochastic process describing the discrete distribution is subject to clustering. In particular, a simple mathematical paradigm for turbulence is the birth-death-immigration process, where turbulent eddies nucleate (immigration), are shed (birth) and dissipate (death). The equilibrium distribution is then of the negative binomial class, this being the discrete analogue of continuous gamma-distributed fluctuations, and the clutter is then K-distributed [2]. Here we discuss the properties of a death-multiple immigration model [3], which allows for pairs, triplets, $\ldots n$-tuplets to enter the population, and which has the useful property of enabling a very wide class of equilibrium distributions to be constructed, including the negative-binomial class and distributions with scale free-characteristics. Allowing "individuals" to leave the population creates a series of events in time [4], whose characteristics can be tailored to exhibit a wide range of behaviours, together with correlation properties including non-Poissonian processes and fractals. The utility to model non-Gaussian fractal processes using the technique will be discussed [5], together with the wider implications for the generation of time series.

REFERENCES

1. Jakeman, E. and P. N. Pusey, "A model for non-rayleigh sea echo," *IEEE Trans. Antennas and Propagation*, Vol. 24, 807–814, 1976.
2. Jakeman, E., "On the statistics of K-distributed noise," *J. Phys. A: Math. Gen*, Vol. 13, 31–38, 1980.
3. Matthews, J. O., K. I. Hopcraft, and E. Jakeman, "Generation and monitoring of discrete stable random processes using multiple immigration population models," *J. Phys. A: Math. Gen*, Vol. 36, 11585–11603, 2003.
4. Jakeman, E., K. I. Hopcraft, and J. O. Matthews, "Distinguishing population processes by external monitoring," *Proc. Roy. Soc. Lond. A*, Vol. 459, 623–639, 2003.
5. Jakeman, E., K. I. Hopcraft, and J. O. Matthews, "Fluctuations in a coupled population model," *J. Phys. A: Math. Gen*, Vol. 38, 6447–6461, 2005.

Implementation of the PML in the CIP Method

Y. Ando and M. Hayakawa
The University of Electro-communications, Japan

The constrained interpolation profile (CIP) method, a numerical solver for multiphase problems, can be applied to electromagnetic problems. The method is based on the upwind scheme for the finite difference method, but the variables to be calculated are not only the values of the electromagnetic fields, but also the spatial derivatives. Those variables are used to interpolate the profiles between the grids by means of cubic polynomials, and to calculate them at the next time step with good precision.

Invoking the directional splitting in the Maxwells equations allows us to treat electromagnetic fields as two one-way waves in each direction, and to reduce them into advection equations. For example, in $\pm x$-direction of a 2-dimensional problem with $\frac{\partial}{\partial z} = 0$, the equations in free-space are given by

$$\frac{\partial f^{\pm}(r,t)}{\partial t} \pm c\frac{\partial f^{\pm}(r,t)}{\partial x} = 0, \quad \frac{\partial g^{\pm}(r,t)}{\partial t} \pm c\frac{\partial g^{\pm}(r,t)}{\partial x} = 0, \tag{1}$$

where $f^{\pm}(r,t) = \sqrt{\epsilon}E_z \mp \sqrt{\mu}H_y$, $g^{\pm} = \frac{\partial f^{\pm}}{\partial x}$, and c is the velocity. The reduced equations can be solved by using CIP method.

The CIP method has an absorbing boundary condition (ABC) as good as the 1st Mur's ABC in its nature. But, it is necessary to develop the ABC with better performance if required. In this study, we examine the perfect matched layer (PML) in the CIP scheme.

The application is straightforward, but some considerations are necessary in the computation because the implementation yields non-advective terms:

$$\frac{\partial f^{\pm}(r,t)}{\partial t} \pm c\frac{\partial f^{\pm}(r,t)}{\partial x} = -s(x)f^{\pm}(r,t), \quad \frac{\partial g^{\pm}(r,t)}{\partial t} \pm c\frac{\partial g^{\pm}(r,t)}{\partial x} = -\frac{\partial\{s(x)f^{\pm}(r,t)\}}{\partial x}, \tag{2}$$

where $s(x)$ is the normalized conductivity of the PML. One of the solution is obtained by dividing the equations into advection phase:

$$\frac{\partial f^{\pm}(r,t)}{\partial t} \pm c\frac{\partial f^{\pm}(r,t)}{\partial x} = 0, \quad \frac{\partial g^{\pm}(r,t)}{\partial t} \pm c\frac{\partial g^{\pm}(r,t)}{\partial x} = 0, \tag{3}$$

and then, non-advection phase

$$\frac{\partial f^{\pm}(r,t)}{\partial t} = -s(x)f^{\pm}(r,t), \quad \frac{\partial g^{\pm}(r,t)}{\partial t} = -\frac{\partial\{s(x)f^{\pm}(r,t)\}}{\partial x} = -\frac{ds(x)}{dx}f^{\pm}(r,t) - s(x)g^{\pm}(r,t). \tag{4}$$

Let $f^{\pm,*}$ denote the results of advection phase. The first equation can be evaluated analytically:

$$f^{\pm,n+1} = f^{\pm,*} \cdot e^{-s(x)\Delta t}, \tag{5}$$

where $f^{\pm,n+1}$ stands for the value at the next times step. The evaluation of the second equation in Eq. (4) can be performed numerically:

$$g^{\pm,n+1} = g^{\pm,*} - \Delta t\{-\frac{ds(x)}{dx}f^{\pm,*} - s(x)g^{\pm,*}\}. \tag{6}$$

The successful formulation of the PML in the CIP method enables us to absorb the outgoing waves as much as required by increasing the layers. The numerical experiments show the good performance of the present formulation.

Some Elliptic Traveling Wave Solutions to the Novikov-Veselov Equation

J. Nickel[1], **V. S. Serov**[2], **and H. W. Schürmann**[1]

[1]University of Osnabrück, Germany
[2]University of Oulu, Finland

The Novikov-Veselov equation (NVE$[\psi(x, y, t)] = 0$) [1] is a generalization of the celebrated Korteweg-de Vries equation (KdVE) [2]. An approach is proposed to obtain some exact explicit solutions in terms of elliptic functions to the NVE. An expansion ansatz $\psi \to g = \sum_{j=0}^{2} a_j f^j$ [3] is used to reduce the NVE to the ordinary differential equation $(f')^2 = R(f)$, where $R(f)$ is a fourth degree polynomial in f [4]. The well-known solutions of this differential equation are expressed in terms of Weierstrass' elliptic function $\wp$ and lead to periodic and solitary-wave-like solutions ("elliptic solutions").

Subject to certain conditions containing the parameters of the NVE and of the ansatz $\psi \to g$ the periodic solutions can be used as start solutions to apply the (linear) superposition principle proposed by Khare and Sukhatme [5]. By means of this principle it is possible to enlarge the solution set of periodic solutions.

It is known that a 2-soliton solution of the KdVE can be obtained by using Hirota's method [6]. Starting with a solitary solution of the NVE obtained with the method described above a similar procedure leads to a 2-soliton solution of the NVE.

REFERENCES

1. Veselov, A. P. and S. P. Novikov, "Finite-gap two-dimensional Schrödinger operators. Explicit formulas and evolution equations," *Dokl. Akad. Nauk SSSR*, Vol. 279, 20–24, 1984.
2. Hu, X.-B., "Nonlinear superposition formula of the Novikov-veselov equation," *J. Phys. A: Math. Gen.*, Vol. 27, 1331–1338, 1994.
3. Fan, E., "Uniformly constructing a series of explicit exact solutions to nonlinear equations in mathematical physics," *Chaos, Solitons and Fractals*, Vol. 16, 819–839, 2003.
4. Schürmann, H. W. and V. S. Serov, "Traveling wave solutions of a generalized modified Kadomtsev-petviashvili equation," *J. Math. Phys.*, Vol. 45, 2181–2187, 2004.
5. Cooper, F., A. Khare, and U. Sukhatme, "Periodic solutions of nonlinear equations obtained by linear superposition," *J. Phys. A: Math. Gen.*, Vol. 35, 10085–10100, 2002.
6. Drazin, P. G. and R. S. Johnson, *Solitons: An Introduction*, Cambridge University Press, Cambridge, 102–109, 1996.

Source Representations of the Debye Potentials in Spherical Coordinates

M. J. Lahart
U.S. Army Research Laboratory, USA

In a widely cited paper [1], Bouwkamp and Casimir derived the relationship between the Debye scalar potentials and their charge and current sources. They did this by computing the electric and magnetic fields associated with each of the potentials and using Maxwell's equations to compute the charge and current sources. Their derivation specified that the scalar potentials could only by defined outside a sphere that contained all of the charge and current sources. Nisbet [2] challenged the need for this restriction and claimed that the Debye potentials could be defined everywhere, including regions that contained charge and current sources.

This presentation examines the need to define the Debye potentials only in regions where the charge and current sources are zero. Some possible definitions of scalar potentials in terms of magnetic and electric vector potentials will be examined. It will be shown that, to be consistent with Maxwell's equations, some definitions require that the scalar potentials obey the wave equation, while others require that only the components of the gradients of the potentials in two orthogonal directions obey the wave equation. In spherical coordinate systems, only the latter type of definition is possible; potentials that obey the wave equation cannot be defined, but potentials whose gradient components in the θ and ϕ directions can be. By expressing the Debye potentials in terms of the magnetic and electric vector potentials and examining the consistency of the expressions with Maxwell's equations, it will be shown that one of the potentials can be defined in regions that contain charges and currents and the other cannot.

For comparison, it will be shown that scalar potentials that obey the wave equation can be defined in rectangular coordinates. Because of this, a pair of potentials can be defined in regions where charge and current sources are present. An example will be given by expressing fields in a waveguide in terms of scalar potentials and their charge and current sources.

REFERENCES

1. Bouwkamp, C. J. and H. B. G. Casimir, "On multipole expansions in the theory of electromagnetic radiation," *Physica (Utrecht)*, Vol. 20, 539–554, 1954.
2. Nisbet, A., "Source representations for Debye's electromagnetic potentials," *Physica(Utrecht)*, Vol. 21, 799–802, 1955.

On the Stability of the Electromagnetic Field in Inhomogeneous Anisotropic Media With Dispersion

N. V. Budko
Delft University of Technology, The Netherlands

A. B. Samokhin
Moscow University of Radioengineering and Electronics, Russia

From the electromagnetic point of view various meta-materials, optical crystals, geophysical formations, ice, magnetized plasma, etc., can be described as inhomogeneous anisotropic media with dispersion. The interaction of the electromagnetic field with such media can be studied by different analytical and numerical methods. When a three-dimensional object is of finite extent and is situated in free space, then the method of choice is the Volume Integral Equation (VIE) method, sometimes referred to as the Domain Integral Equation method (mathematical literature) and the Discrete Dipole Approximation (physics).

In contrast to the one- and two-dimensional cases, where existence of the solution to the scattering problem is a trivial question, in the three-dimensional case solution exists under certain conditions related to the physical properties of the medium in question. Note that the sufficient uniqueness conditions are basically the same for all cases. Previously we have shown that the singular integral operator of the VIE has an essential continuous spectrum, which is given explicitly in terms of the constitutive parameters of an inhomogeneous object. Now we shall extend this result to anisotropic media with dispersion. We shall also prove that in the quasi-static case the discrete eigenvalues are contained within the complex envelope of the continuous spectrum.

For anisotropic media with dispersion, especially for magnetized plasma, the question of considerable interest is the stability of such a medium. Within the commonly adopted approach, based on the differential form of the Maxwell's equations and Lorentz or Vlasov's equations of motion, very little can be said about the stability of *inhomogeneous* objects of finite extent, whereas the VIE formulation is perfectly suited for this task. Instead of analyzing the stability of the medium itself we propose to analyze the stability of the electromagnetic field in a given medium. Due to self-consistency of the problem the two approaches are in fact identical. Thus, we shall discuss the stability of the field in several practical cases ranging from optical crystals to plasma.

Scattering of Electromagnetic Waves by Inhomogeneous Dielectric Gratings Loaded with Perfectly Conducting Strips

T. Yamasaki, T. Ujiie, and T. Hinata
Nihon University, Japan

The scattering and guiding problems of inhomogeneous dielectric gratings have been of considerable interest such as optical fiber gratings, photonic bandgap crystals, frequency selective devices, and other applications by the development of manufacturing technology of optical devices. Recently, many analytical and numerical methods which are applicable to the arbitrarily dielectric gratings have been proposed. However, most theoretical and numerical studies have considered the periodic structures in which the material forming grating was either metallic or dielectric.

In this paper, we proposed a new method for the scattering of electromagnetic waves by inhomogeneous dielectric gratings loaded with perfectly conducting strips using the combination of improved Fourier series expansion method and point matching method.

In the inhomogeneous dielectric region $S_2(0 < x < d)$, the permittivity profile $\varepsilon_2(x, z)$ is generally not separable with respect to the x and z variables. Main process of our methods are as follows: (1) The inhomogeneous layer is approximated by an assembly of M stratified layers of modulated index profile with step size $d_\Delta(\triangleq d/M$. (2) Taking each layer as a modulated dielectric grating, the electromagnetic fields are expanded appropriately by a finite Fourier series. (3)In the perfectly conducting strip and gap regions at C and $\bar{C}$ for the boundary, the electromagnetic fields are matched on both sides using point matching method(3) Finally, all stratified layers include the metallic regions are matched using appropriate boundary conditions to get the inhomogeneous dielectric gratings loaded with perfectly conducting strips.

Numerical results are given for the transmitted scattered characteristics for the case of incident angle both TM and TE waves.

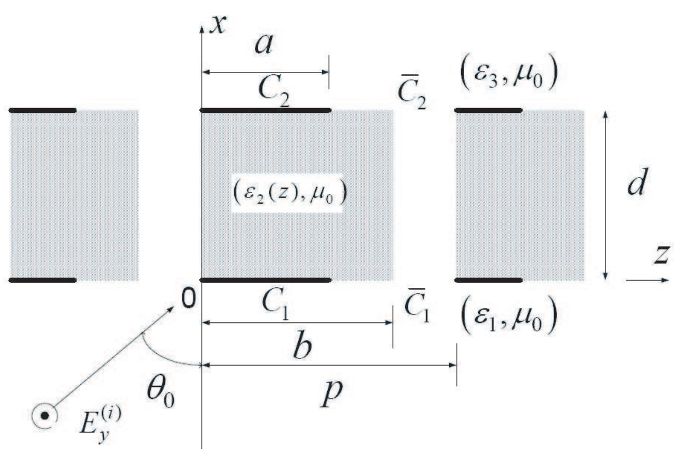

Figure 1: Structure of inhomogeneous dielectric gratings loaded with perfectly conducting strips.

Effects of the Resonant Scattering of Intensive Fields by Weakly Nonlinear Dielectric Layer

V. Yatsyk
Nat. Acad. of Sci. of Ukraine, Ukraine

The transverse inhomogeneous, isotropic, nonmagnetic, linearly polarized, weakly nonlinear (a Kerr-like dielectric nonlinearity) dielectric layer is considered. The algorithms for the solution of nonlinear diffraction problems (with use of approaches developed in [1–3]) and the results of a numerical analysis of the diffraction problem of a plane wave on the weakly nonlinear object with positive and negative value of the susceptibility are shown. The effects: non-uniform shift of resonant frequency of the diffraction characteristics of a weakly nonlinear dielectric layer; itself the channeling of a field to a semicolon increase of the angle of the transparency of the nonlinear layer when growth of intensity of the field (at positive value of the susceptibility); de-channeling of a field (at negative value of the susceptibility) are found out. These effects are connected to resonant properties of a nonlinear dielectric layer and caused by increase at positive value of the susceptibility or reduction at negative value of the susceptibility of a variation of dielectric permeability of a layer (its nonlinear components) when increase of intensity of a field of excitation of researched nonlinear object, see [4, 5].

The principal fields where the results of our numerical analysis are applicable are as follows: the investigation of wave self-influence processes; the analysis of amplitude-phase dispersion of eigen oscillation-wave fields in the nonlinear objects, see [6]; extending the description of evolutionary processes near to critical points of the amplitude-phase dispersion of nonlinear structure; new tools for energy selecting, transmitting, and remembering devices; etc.

REFERENCES

1. Akhmediev, N. N. and A. Ankiewicz, *Solitons*, Fizmatlit, Moscow, 2003.
2. Yariv, A. and P. Yeh, *Optical Waves in Crystals*, Mir, Moscow, 1987.
3. Shestopalov, V. P. and Y. K. Sirenko, *Dynamic Theory of Gratings*, Naukova Dumka, Kiev, 1989.
4. Yatsyk, V. V., "The numerical simulations and resonant scattering of intensive electromagnetic fields of waves by dielectric layer with Kerr-like nonlinearity," *E-print: Computational Physics*, http://arxiv.org/pdf/physics/0412109, No. 12, 1–11, 2004.
5. Yatsyk, V. V., "Effects of resonant scattering of the intensive fields by nonlinear layer," 2005 Workshop on Fundamental Physics of Ferroelectrics (Ferro2005), http://www.mri.psu.edu/conferences/ferro2005, Williamsburg, Virginia, USA, 83–84, Feb. 6–9 2005.
6. Yatsyk, V. V., "Diffraction problem and amplitudes-phases dispersion of eigen fields of a nonlinear dielectric layer," *E-print: Computational Physics, Optics*, http://arxiv.org/pdf/physics/0503089, No. 3, 1–13, 2005.

Theoretical Analysis of Convergence of Rao-Wilton-Glisson Method and Subhierarchal Parallel Algorithm for Solving Electric Field Integral Equation

Y. G. Smirnov
Penza State University, Russia

We consider three-dimensional problem of the electromagnetic wave diffraction by bounded and perfectly conducting screen of arbitrary shape in free space. The problem is reduced to the electric field integral equation (EFIE) [1]. We use very popular Rao-Wilton-Glisson (RWG) method for solving this problem. We have proved theorem of convergence in special Sobolev spaces and obtaind estimation of the rate of convergence for RWG method.

The main difficulties in RWG method are very large time of calculations of matrix elements with sufficiently high accuracy and occurrence of large and dense matrices in systems of linear algebraic equations obtained after discretization of the problem.

If one uses RWG method for the problem discretization, the matrix elements may be calculated independently. A natural way to calculate the matrix elements is utilization of parallel computations using supercomputers or clusters. Note in addition that the structure of matrices is not arbitrary: in the diffraction problems. We have the so-called structured matrices with $O(n)$ different elements, where n denotes the matrix dimension.

We have created and elaborated efficient solvers for several types of diffraction problems on the basis of subhierarchal algorithms of parallel computations [2].

*This study is carried out under the support of the Russian Foundation for Basic Research, grant no 03-07-90274.

REFERENCES

1. Ilyinsky, A. S. and Y. G. Smirnov, *Electromagnetic Wave Diffraction by Conducting Screens*, VSP Int. Science Publishers, Utrecht, the Netherlands, 1998.
2. Medvedik, M. Y. and Y. G. Smirnov, "Subhierarchal parallel computational algorithm and convergence of Galerkin Method in electromagnetic diffraction problem on plane screen," Izvestiya Vyzov, Povolzsky Region, Estestvennye Nauki, ü 5, 3–19, 2004 (in Russian).

Session 3P7
Modeling and Inverse Problems

Modeling of EBG Structures Using the Transmission Matrix Method

K. Bharath, **E. Engin**, **T. Yoshitaka**, **and M. Swaminathan**
Georgia Institute of Technology, USA

Electromagnetic Band Gap (EBG) structures have been employed in noise suppression schemes for mixed signal applications [1]. The design and modeling of these structures typically requires the use of full-wave solvers to characterize their frequency response. However, this can be computationally expensive. In order to reduce the analysis time, the use of a model based simulation tool such as the Transmission Matrix Method (TMM) [2] has been suggested. TMM subsections a given structure into square 'unit cells' and develops an equivalent RLGC netlist. Modeling large plane like structures using this technique has been shown to be very accurate. However, for structures such as the Alternating Impedance (AI) EBG, it was found that simulation results from TMM showed discrepancies from measurement. This was attributed to the Fringe and Gap effects. Thus, accurate simulation of the AI EBG requires the inclusion of these effects into TMM.

The fringe effect can be modeled by adding a fringe capacitor, C_f, and a fringe inductance, L_f, to unit cells that lie along an edge. The fringe elements, C_f and L_f, are calculated by employing empirical formulas for microstrip structures. The Gap effect is modeled as a gap capacitance, Cg, which is added to nodes that lie on either side of an edge. Cg is extracted from the 2D field solver Ansoft Maxwell.

The model to hardware correlation, with and without inclusion of Fringe and Gap Capacitance is shown in Fig. 1. It is seen that the inclusion of Fringe and Gap effects leads to accurate prediction of bandwidth and isolation levels.

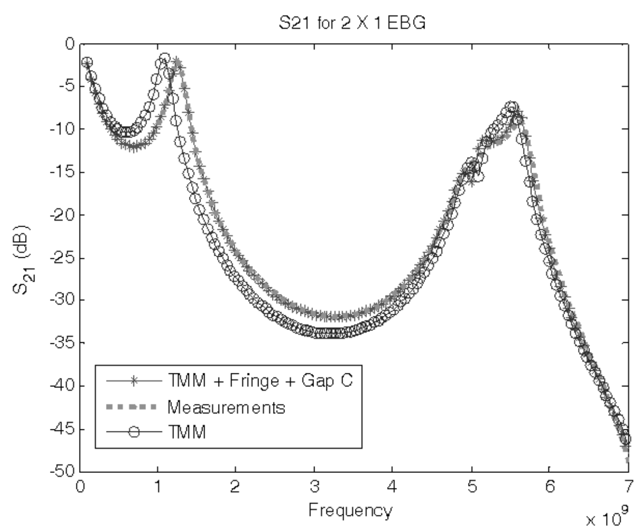

Figure 1: Model to hardware correlation.

The fringe effect is especially pronounced when there are narrow connections between two plane patches. The gap effect becomes important as two separated patches get closer. Hence, both these effects become important to analyze an EBG structure. With a simple extension of TMM to include fringe and gap effects, such complicated structures can be analyzed very efficiently and accurately.

REFERENCES

1. Choi, J., V. Govind, and M. Swaminathan, "A novel electromagnetic bandgap (EBG) structure for mixed-signal system applications," *Proc. of IEEE Radio and Wireless Conference*, 243–246, September 2004.
2. Kim, J.-H. and M. Swaminathan, "Modeling of irregular shaped power distribution planes using transmission matrix method," *IEEE Trans. on Adv. Packag.*, Vol. 24, 334–346, August 2001.

Bloch Mode Modelling of the Scattering of Plane Waves and Fano Resonances for a Photonic Crystal Slab

L. C. Botten, M. A. Byrne, A. A. Asatryan, and N. A. Nicorovici
University of Technology, Australia

R. C. Mcphedran
University of Sydney, Australia

Photonic crystals (PC) are amongst the most active research topics in contemporary photonics, with PC slabs prominent amongst the range of structures that are under investigation. In these, the confinement of light occurs via two mechanisms—two-dimensional band gap confinement in the transverse direction, and total internal reflection vertically.

Our interest in these structures arises from the recent observation that Fano resonances, originally discovered in the field of particle physics, are observable in photonic systems. Recent work by Fan, which involved FDTD simulation and a phenomenological approximation of the scattering matrix, showed that the transmission spectrum of the slab could be constructed from a sequence of Lorentzian resonances (with poles in the complex frequency plane) superimposed on the transmittance curve of the unpatterned slab, which acts as a Fabry-Perot (FP) interferometer.

In this paper, we outline a new formulation for the diffraction of a plane wave by a PC slab and show how we may discover the origin of the Fano resonances directly from the the modes of the structure. The technique, based on a multipole-scattering matrix formulation and closely mirroring the geometry of the structure leads to a countably infinite set of modes with propagation constants β_j in the direction of the axis of the cylinders. Only a finite number are propagating (i.e., with β_j real), while the remainder are evanescent and attenuate as they propagate through the slab. We characterize the diffraction at each of the upper and lower planar interfaces of the structure using matrix generalizations of Fresnel "coefficients". Four such matrices are required: T_{12} and R_{12} which are respectively the transmission and reflection matrices for plane wave incidence from air onto a photonic crystal slab of semi-infinite thickness, and T_{21} and R_{21} which are the corresponding matrices for modes incident in the direction of free space from within the slab. These Fresnel matrices closely resemble their familiar scalar forms with, for example, $R_{21} = (Z_2 + J^H Z_1 J)^{-1}(Z_2 - J^H Z_1 J)$. In this expression, Z_1 and Z_2 are respectively the (diagonal) impedance matrices for the free space and slab Bloch modes, with $J^H Z_1 J$ representing the impedance of free space as "seen" by the PC modes.

Finally, we compute the reflection and transmission ($\boldsymbol{T}$) matrices for the PC slab, from which the reflectance and transmittance is calculated. Here, $\boldsymbol{T} = \boldsymbol{T}_{21}\ \boldsymbol{P}(\boldsymbol{I} - \boldsymbol{R}_{21}\boldsymbol{P}\mathbf{R}_{21}\mathbf{P})^{-1}\boldsymbol{T}_{12}$ (where $\boldsymbol{P} = \mathrm{diag} e^{\beta_j h}$), which closely resembles the Airy formulae for a FP interferometer. The symmetric and anti-symmetric slab modes derive from the solutions of $\det(\boldsymbol{I} \mp \boldsymbol{R}_{21}\boldsymbol{P}) = 0$, the solutions of which lie in the complex plane since the modes are lossy. Finally, we characterize the Fano resonances directly in terms of the resonant behaviour of common pairs of PC modes.

Methods for Mitigating the Effect of Split Reference Planes on High Speed Digital System Interfaces

H. Pan[1], **H.-Y. Chao**[2], **and C. Pan**[1]

[1]Intel Corporation, USA
[2]National Chiao Tung University, Taiwan

In the past few decades, microprocessor operating frequency has increased from a few megahertz to multi gigahertz. Board-level high speed digital interfaces, such as system bus, system memory, and system I/O, that carry information between microprocessor, memory controller, I/O controller, and other components, however, have been operating at a lower frequency. This is in part because transmission line and other higher order electromagnetic effects can dominate board-level interconnect designs due to electrically significant interconnect sizes. Yet, due to the ever increasing demand for more bandwidth, operating frequencies of these board-level high speed interfaces have also been doubling in roughly two-year cycles. Parallel high speed interfaces such as Front-Side Bus (FSB) and Double Data Rate-III (DDR-3) SDRAM, for example, are fast approaching 1 GT/s, where significant frequency content can extend well into multi-GHz. In the mean time, PCI Express-like serial differential high speed interfaces, already operating at speeds over 1 GT/s, are designed into new cross-chip interconnects such as the Direct Media Interface (DMI). Routing a system with such a large number of high speed digital buses while insuring signal integrity, EMI compatibility, and ESD susceptibility, is a challenge.

While on-board interconnects are operating at much higher frequencies, the cost of the overall computing system has been decreasing. Computer manufacturers are therefore continuously looking for ways to lower the production cost. In a mobile computing system, where size is a main constraint and expensive high layer count printed circuit board (PCB) technology has been used to control routing congestion, using cheaper technologies with a smaller number of routing layers is an attractive mean of controlling manufacturing cost. On the other hand, routing on a severely size-constrained mobile platform with a smaller number of routing layers can inadvertently expose wide high speed digital interfaces to non-ideal conditions such as reference plane gaps produced by various power islands. Multi-GHz operation of these high speed signals also means that the traditional mitigation method of adding bypass capacitors across the reference gaps is becoming ineffective. In this paper, we will explore a number of other methods that can be used in conjunction with bypass capacitors to mitigate the effect of these reference plane gaps on signal quality, as well as system EMI and ESD.

Multipath Reduction of GPS Measures through Heuristic Techniques of Compensation

V. Barrile, M. Cacciola, and F. Cotroneo
Univ. Mediterranea, Italy

One of the limitations in retrievable accuracy for differential GPS measurements is due to multipath error when GPS signal is reflected by surfaces around antenna. Improvements during antenna planning phase can be made in order to reduce multipath phenomenon. Classic techniques of multipath error minimization are well known in scientific literature, but they often involve an axcessive computation time or a high number of calculations. By using heuristic techniques (Artificial Intelligence), instead, it is possible to reduce the multipath interference in surveys of GPS data with applicatively acceptable elapsed times.

In this work, the planning criteria and the experimental results retrieved by a high multipath-rejection GPS antenna are described.

Accurate Analysis of Practical Diffraction Gratings

H. A. Kalhor and M. R. Zunoubi
State University of New York, USA

Diffraction gratings have been used in many applications including spectroscopy for many years. Many ingenious approximate, analytical, and numerical techniques have been devised and used for their analysis. However, most of the proposed techniques used idealized models. The structures have been considered infinitely periodic, perfectly conducting and without groove shape imperfections. Attempts have been made to incorporate some imperfections such as finite conductivity and groove shape errors in the idealized models with some success [1–4]. Theoretical and measurement results, however, did not agree in many cases and certain anomalous behavior could not be explained. More recently, a method based on impedance boundary conditions has been proposed to analyze finite planar and curved frequency selective surfaces [5].

Recent developments of new and powerful numerical methods have empowered researchers to study the effects of these imperfections more accurately, and revisiting these classical problems seems in order.

The object of this presentation is to study the performance of practical gratings with all their associated imperfections accurately. A few numerical techniques will be employed and compared and contrasted. The behavior of reflection diffraction gratings of practical interest such as echelette sinusoidal, and lamellar as well as transmission gratings made of wire grids, conducting cylinders, and conducting bars will be studied. Comparison with experimental results will be made where possible.

REFERENCES

1. Kalhor, H. A. and A. R. Neureuther, "Effects of conductivity, groove shape, and physical phenomena on the design of diffraction grating," *J. Opt. Soc. Am.*, Vol. 63, No. 11, 1412–1418, 1973.
2. Christodoulou, C. and J. Kauffman, "On the electromagnetic scattering from infinite rectangular grids with finite conductivity," *IEEE Trans. Antennas Propag.*, Vol. 34, No. 2, 144–154, Feb. 1986.
3. Abboud, T. and H. Ammari, "Diffraction at a curved grating: approximation by an infinite plane grating," *J. Math. Anal. and App.*, Vol. 202, 1076–1100, 1996.
4. Whites, K. W. and R. Mittra, "An equivalent boundary-condition model for lossy planar periodic structures at low frequency," *IEEE Trans. Antennas Propag.*, Vol. 44, No. 12, 1617–1629, Dec. 1996.
5. Stupfel, B. and Y. Pion, "Impedance boundary conditions for finite planar and curved frequency selective surfaces," *IEEE Trans. Antennas Propag.*, Vol. 53, No. 4, 1415–1425, April 2005.

Spectrum Properties of Partially Coherent Modified Bessel-Gauss Beams by a Lens with Aperture

X. R. Lin
Fuzhou University, China

Q. S. Wang
FuJian Dragon Enterprises Co., Ltd, China

C. Y. Peng
Putian University, China

Starting from the propagation equation of partially coherent light, the spectral shift and spectral switch of partially coherent modified Bessel-Gauss beams passing through a lens with aperture are studied. Numerical results show that the on-axis spectrum in the near zone is different from the spectrum of the source, and the on-axis spectrum in the near zone is split into multi-peaks. It is also found that the spectral shift shows a gradual change. However, when z_f approaches a critical value, a rapid spectral transition occurs. The effect is called spectral switch. For example, when the parameters for calculation are the central frequency of the spectrum $\omega_0 = 3.2 * 10^{15} s^{-1}$, effective coherence length on the source plane $\sigma_0 = 0.6 * 10^{15} s^{-1}$, Fresnel number of beam $N_w = 1$, the spectral degree of coherence $\xi = 0.5$, and truncation parameter $\delta = 0.3$. For the axial spectrum at $z_f = 0.0105$, the relative spectral shift is bigger than zero, and the blue shift occurs. The two major peaks reach the same height at the critical point $z_f = 0.0111$, and the subordinate peaks separately at the both sides of major peaks also reach the same height. This means that the spectral shift is transformed from the blue shift to the red shift, and the spectral switch occurs at this point. With the increase of z_f, the red shift decreases. When z_f equals 0.0127, the spectral shift equals 0. When z_f equals 0.0148, the spectral switch occurs again. The distance between the major peaks when z_f equals 0.0127 is larger than that when z_f equals 0.0111. Numerical results also show that the spectral switch positions and the spectral switch performance of partially coherent modified Bessel-Gauss beams depend on the spectral degree of coherence, Fresnel number of beam and truncation parameter. The number of spectral switch increases with the increase of the Fresnel number of beam, and decreases with the increase of the spectral degree of coherence.

Generalized Lorenz-Mie Theory for the Arbitrarily Oriented Shaped Beam Scattering by a Spheroid

F. Xu[1,2], K. F. Ren[2], and X. S. Cai[1]

[1]University of Shanghai for Science and Technology, China
[2]Université et INSA de Rouen, France

Light scattering by a spheroid was firstly studied by S. Asano, et al., [1]. It was extended to the case of arbitrary shaped beam scattering by J.P. Barton [2], who described the incident field through "surface integrals". Within the framework of generalized Lorenz-Mie theory (GLMT) [3], on-axis and off-axis Gaussian beam scattering by a spheroid was also studied by Han, et al., [4, 5].

In the present paper, the scattering of a shaped beam with arbitrary orientation relative to a spheroidal particle is developed within the framework of GLMT, i. e., the arbitrarily oriented incident beam is firstly expressed by the beam shape coefficients (BSC) in spherical coordinates. Then the BSC is transformed to the spheroidal coordinates, thanks to the relationship between the spherical wave vectors ($\mathbf{m}_{mn}$, $\mathbf{n}_{mn}$) [6] and the spheroidal ones ($\mathbf{M}_{mn}$, $\mathbf{N}_{mn}$) [7].

But we found that for BSC evaluation by the localization approximation is no longer valid for the oblique incidence. So the quadrature method is applied instead. Besides, for the sake of consistence with Lorenz-Mie theory, time dependence of $\exp(i\omega t)$ is used, instead of $\exp(-i\omega t)$ in GLMT. The relationship of the BSC in two different time conventions are carefully examined and a simple relationship is found.

Finally, numerical results of the scattered intensity in far field are presented. They are found coincident with those in the cases of both oblique plane wave incidence on a spheroid [1] and shaped beam incidence on a sphere [3].

REFERENCES

1. Asano, S. and G. Yamamoto, "Light scattering by a spheroidal particle," *Appl. Opt.*, Vol. 14, 29–49, 1975.
2. Barton, J. P., "Internal and near-surface electromagnetic fields for a spheroidal particle with arbitrary illumination," *Appl. Opt.*, Vol. 34, 5542–5551, 1995.
3. Gouesbet, G., B. Maheu, and G. Gréhan, "Light scattering from a sphere arbitrarily located in a Gaussian beam, using a Bromwich formulation," *J. Opt. Soc. Am. A*, Vol. 5, 1427–1443, 1988.
4. Han, Y. P. and Z. Wu, "Scattering of a spheroidal particle illuminated by a Gaussian beam," *Appl. Opt.*, Vol. 40, 2501–2509, 2001.
5. Han, Y. P., G. Gréhan, and G. Gouesbet, "Generalized Lorenz-Mie theory for a spheroidal particle with off-axis Gaussian-beam illumination," *Appl. Opt.*, Vol. 42, 6621–6629, 2003.
6. Stratton, J. A., *Electromagnetic Theory*, McGraw-Hill, NewYork, 1941.
7. Flammer, C. and U. Press, *Spheroidal Wave Functions*, Stanford, Calif., 1957.

The Radiated Emission Approach to Specific Emitter Identification

J. Dudczyk and M. Wnuk
Military University of Technology, Poland

The modern ESM/ELINT systems should be able to recognise emitters on the basis of the set of pulse measurements in order to provide surveillance, tracking and platform identification. One of the most principal functions of the ESM system is gathering basic information from entire electromagnetic spectrum and analysing communication and non-communication emitter's characteristics such as their technical parameters, operating role and main tasks. In this analysis there are of special importance methods of data acquisition. The methods of Specific Emiter Identification (SEI) are based on the Measurement and Signature Intelligence (MASINT). Non-intentional emission (calls–radiated emisssion) is a source of knowledge about the analysed emitter. Such information is crucial during the process of emitter identification. The results of classification and identification are presented on a display in a form of tabular or grapfical options.

This paper provides an overview of the methods of radiated emission measurement, for example: Open Area Test Site (OATS), full and semi anechoic chambers, Transverse Electromagnetic Cell (M. L. Crawford Cell–TEM) and Gigahertz Transverse Electromagnetic Cell (GTEM), which may be used to identify radar's equipment.

This paper presents selected aspects of radiated emission acquisiton (in a specially prepared procedure), analysis of their parameters, features extraction using "special linear transformation". According to the presented method of transformation, the "measured function $K(f_n)$" is determined. The function $K(f_n)$ is used to extract radiated emission features, which modify structure of Extended Vector Parameters (EVP). At the end of the procedure, radar emitter source identification is performed. During the process of emitter identification distance functions (Euclidean, Mahalanobis, Hamming) are applied. The process of recognition is connected with the data base, which is an important element in the modern electronic intelligence system. Dinstinctive features extraction from radiated emission is used for special "radar signature" description in the data base.

Taking all above into consideration, applying the radiated emission to the specific emitter identification is an essential element in formation of the examined system. The capability of an ESM/ELINT system to correctly identify detectable radar emissions in a dense environment is key to their application in modern commmand, communication and control system. The problem of radiated emission is essential with respect to Electro-Magnetic Compatibility (EMC).

Backscattering from Rectangular Plates Illuminated at Grazing Incidence

R. A. Ross
17A Phillips Drive, Westford, MA, 01886, USA

A formula is presented for predicting monostatic scattering from rectangular plates at grazing incidence with vertical polarization. The formula uses the Geometrical Theory of Diffraction to describe returns from the front and rear of the plate. The contribution from the rear edge is associated with a new form of double diffraction. Predictions are compared with numerical results from the Method of Moments for objects between 2 and 18 wavelengths in extent. When predicting the characteristic oscillation in RCS of rectangular plates as a function of width, accuracy increases with increase in the height of the plate. When plates are both short and wide, theory underestimates the RCS of peaks.

Optimized Satellite System-like Data Fitting on a Spherical Shell

J. Sanchez-Mondragon[1], **B. Wolf**[2], **M. Tecpoyotl-Torres**[3]
J. Escobedo-Alatorre[3], **and M. Torres-Cisneros**[4]

[1]Instituto Nacional de Astrofísica, Mexico
[2]Centro de Ciencias Físicas, Mexico
[3]Universidad Autónoma del Estado de Morelos, Mexico
[4]Facultad de Ingeniería Mecánica, México

The measurement of irradiance on a spherical shell is a common in different fields that goes from geological, biological and many others. Accuracy depends of a judicious use of the sampling, and the last is often defined by technical limitations due to the available infrastructure in each field. Such is the case of the so called planetary array, described as a set of satellite like trajectories on the spherical shell. Both, the data acquisition and the ideal data base, in this case spherical harmonics, may be optimized. The measured points are distributed over maximal circles obtained from the equator, and each other are related by the corresponding rotations. Each circle has 2L+1 equidistant points (the first one and the last one coincides), and the field on the sphere is adjusted by the determination of the harmonic coefficients, as an optimization problem, with Nc equation systems of 2L+1 simultaneous equations for $(L+1)^2$ variables.

Session 3P8a
Microwave Related Phenomena in Superconductors

Experimental Studies on the Macroscopic Anisotropy of High Temperature Superconductor YBaCuO

H. H. Song, J. Zheng, X. Z. Wang, S. Y. Wang, and J. S. Wang
Southwest Jiaotong University, China

O. de Haas and C. Beyer
IFW Dresden, Germany

To investigate the anisotropy of magnetization critical current density of high temperature superconductor (HTS) YBCO, two kinds of experiments were designed. First the current distributions were obtained from the trapped fields of a cubic bulk (#1) with $10.0 \times 10.0 \times 10.0\,\mathrm{mm}^3$ in size at 77 K. Nextly two small samples were employed using vibration sample magnetometer system. Their size are $4.9 \times 1.1 \times 0.4\,\mathrm{mm}^3$ (#2) and $1.0 \times 3.9 \times 0.8\,\mathrm{mm}^3$ (#3) along the a, b and c axis respectively. It was found that the anisotropy ratios of critical current density in both cases are about 3.5 independent of the applied field at 77 K. While the field is kept constant at 1.0 T, the ratio increases as the temperature decreasing from 85 K to 20 K. Moreover, when the anisotropy ratio into account in the HTS computation modeling, the calculated levitation forces between superconductor and magnet agree with the experimental ones.

*This work is supported by the National High Technology Research and Development Program of China (2002AA3063 61) and National Natural Science Foundation in China (50377036). The authors would like to thank all the people who have contributed to this work.

Interaction between Abrikosov and Josephson Vortices Induced by Microwave Magnetic Field and External Magnetic Field in Bi2212 Crystal: Vortex Dynamics under Crossing Field

T. Endo[1,2], **A. K. Sarkar**[1], **H. Zhu**[1]
K.-I. Nakanishi[1], **A. Nishio**[1], **M. Okada**[1], **and K. Endo**[2]

[1]Mie University, Japan
[2]National Institute of AIST, Japan

Reentrant phase (RP) was proposed by Fisher and Nelson for strong two dimensional high Tc superconductors. Due to less interaction between 2D pancake vortices at low fields, there is Liquid-RP just above Meissner phase under Solid mixed phase. It is very difficult to detect this RP experimentally because it is quite narrow. The vortex phase is concerning to mobility of vortex, then we tried to detect this RP employing modulated microwave absorption (MA) technique utilizing induced vortex dynamics due to high-frequency modulation field. The MA vs field (H) spectrum for H//c shows only a sharp first peak: P1 arising from Meissner state at low field at well low temperatures (T). At some higher T, it shows a Dip just above P1 and following Broad peak: Pb. The Dip and Pb arise from the Liquid-RP and Solid phase, respectively. At much higher T, the Dip and Pb disappear because it approaches to critical temperature. From these results of MA vs T, we can obtain RP experimentally. It exhibits a narrow entrance of RP which is strictly similar to the theoretically proposed RP.

Microewave power (Pm) dependence of MA was obtained for H//c at low T. The Dip and Pb appear at higher Pm and they shift to low field with increasing Pm. Their sharp drops in rather low Pm region are explained by sample temperature rise. However, their gradual drops in much higher Pm region is interpreted by vortex interaction between Abrikosov Votex induced by the applied field (AVa) and Josephson Vortex induced by microwave magnetic field (JVw). AVa is pinned by JVw at the higher Pm then the upper Solid phase boundary extends to higher field.

MA spectra were measured for Crossing field configuration (H//45ì). With increasing Pm, the Dip is extremely enhanced and Pb is shifted to higher fields. JVw decouples 2D pancake vortices then melting is promoted at the low field. While at the higher fields, AVa is pinned by the applied field-induced Josephson vortices (JVa) and JVw, then the upper Solid-Liquid boundary is shifted up.

Calculation of the Field Distributions of Superconducting Strips by Conformal Mapping

Y. Mawatari
National Institute of Advanced Industrial Science and Technology, Japan

We present magnetic-field and current distributions in superconducting strips calculated by using the conformal mapping technique. The thickness of the superconducting strips (i.e., tapes or films) is much smaller than the width, and the strips are infinitely long along the z axis. The field distributions in the xy plane are described by the complex fields $\mathcal{H}(\zeta) = H_y(x, y) + iH_x(x, y)$ that are analytic functions of $\zeta = x + iy$, and the expressions of $\mathcal{H}(\zeta)$ are derived from the conformal mapping.

We consider superconducting strips exposed to a uniform applied magnetic field H_0 and/or a transport current I_0, where H_0 and I_0 are fixed after slow increase from zero. When superconducting strips are exposed to H_0 that is smaller than the penetration field H_s, the strips are in the ideal Meissner state and the magnetic flux does not penetrate into the stirps. For $H_0 > H_s$, on the other hand, the magnetic flux penetrates into the strips: the magnetic flux stays near the center of the ideal superconducting strips without bulk pinning, or the magnetic flux penetrates only near the superconducting strips with bulk pinning. We show field distributions for various arrangements of multiple superconducting strips; i.e., coplanar strips, stacked strips, radially arranged strips, etc.

Electromagnetism of the Rings of Saturn: The Role of Levitation Force and "Negative Pressure" for the Superconducting Origin of the Thin Radially Streched Structure of the Edges of Gaps and Braid Structure of the *F* Ring

V. V. Tchernyi
General Physics Institute, Russian Academy of Sciences, Russia

Presented in the paper model is a direct continuation of the paper by J. K. Maxwell (1859), he deduced that rings consist of particles. Unfortunitely, for his time the was no knowledge about superconductivity (1911) and force of magnetic levitation (1933). Superconductivity of ice and high temperature superconductivity was discovered just in 1986. Importance of the force of magnetic levitation and magnetic "negative pressure" was introduced into space physics for the first time in [1–3] for explanation and mathematical approval of origin of the rings, and organic molecules propagation in between stars. In the disc of rings paricles will be located on such a Kepler orbit, where there is a balance of the three acting forces: gravitational, centrifugal and force of levitation. On another hand, paricles will be holding on the duistance from the planet by the "negative pressure", which is created by the force of magnetic levitation, and directed from the planet, backward to the force of gravity. At the end of its movement within protoplanetary cloud particles will be allocated within Roche zone. It is also following that the plane of the rings is localizing within magnetic equator of the Saturn which is not exactly coincides with its geographical equator. So, it is necessary to measure this small angle gap by the space probe. The movements of the particles driving by centrifugal force within the rings around the planet will be affected by gravitational and levitation forces. Force of levitation is proportional to the gradient of the magnetic field of the planet. The gradient is stronger on the distance closer to the planet. Radial displacements of the particles within the rings, dependce of the balance of gravitational force and force of levitation force. As a result of action of the three forces particles are participating in a helical movements within the rings. Period of the helic is becoming to be bigger with arising distance from the planet. Particles even could move out of the ring, but then the pressure from the bigger magnetic flow in between the rings will push them back to the ring. These displacements is difficult to regester within the structure of the ringlets by the space probe, but obviously dispacements are well observed at the edges of the gaps, how it is happened with the help of Cassini-Huygens observation of the thin radially stretched structure of the edges for the Encke and Keeler gaps. It is clear that the magnitude of displacements will be bigger on inner edges of the gaps. Far from the planet, near by the ring F, levitation force becomes to have less influence, and period of helical movemetns is very much extended. As a result, obsever see it like a braid or strand structures. On the distance from the planet, bihind the ring F, influence of the force of levitation becomes to be negligible, and there is no formation of the rings structure. Certainly, presented picture will be affected by perturbations produced by a satellites on a circular orbits, by fluctuations of the magnetic field of the planet, by plasma phenomena and collisions of the particles, etc.

REFERENCES

1. Tchernyi, V. V. and A. Y. Pospelov, "Possible electromagnetic nature of the Saturn's rings: superconductivity and magnetic levitation," *Progress In Electromagnetic Research (PIER)*, Vol. 52, 277–299, (http://emacademy.org/ pier & jemwa), 2005.
2. Tchernyi, V. V. and E. V. Chensky, "Electromagnetic background for possible magnetic levitation of the superconducting rings of Saturn," *JEMWA*, Vol. 19, No. 17, 987–995, 2005.

Magnetic Field Penetration into Granular Superconductors

B. M. Vladimirovich, T. V. Victorovich, and M. P. Viktorovich
General Physics Institute, Russian Academy of Sciences, Russia

Multiple josephson medium is now the established model of high-temperature supercinductors (HTSC). Josephson medium is generated by a lot of small superconductive grains with weak links (josephson junctions) between them. This model permits to make a qualitative descriptions of some processes in HTSC. Thus, in paper [1] magnetic field penetration into granular superconductor is described which occurs in the form of magnetic vortices. Such vortices are called "supervortices" in [1]. Neither analytic nor numerical study of "hypervortices" are not realized at present time.

In present paper the multiple josephson medium is averaged on the volume containing a lot of grains and, at the same time, large enough to consider magnetic field to be permanent in it. Averaging provides to material equation coupling the current density $\vec{j}$ with magnetic field vector potential $\vec{A}$:

$$\vec{j} = -\frac{\vec{A}}{A}\alpha M(A) - \beta\dot{\vec{A}} - \gamma\ddot{\vec{A}}$$

where α, β and γ are some coefficients depending on medium macroscopic parameters. Dependence $M(A)$ determines by the size-distribution low of the grains and looks approach identical for different media.

Stationary solutions with radial symmetry of equation obtained are analyzed. Magnetic flux containing in such solutions is shown by numerical modeling to be divisible by $2\Phi_0$, where Φ_0–magnetic flux quanta.

Whole energy of the medium described is investigated as the sum of magnetic field energy and the josephson junction energy. Calculation of the solution obtained whole energy permits to plot the graph of its dependence on amount of magnetic flux quanta containing in these solutions. These graphs are monotone for each size-distribution low considered and this fact allows to conclude that solutions are the most energetically benefit containing two magnetic flux quanta.

Thus, magnetic field penetration into multiple josephson medium must take place in the form of vortices as it was shown in [1]. In contrast to type II superconductors and distributed josephson junctions, however, vortices described must contain two quanta of magnetic flux. This result is unexpected, nevertheless, it was point to possibility of multiquantum magnetic formations sooner in [2], and this appearance took place also in complicated josephson structures.

REFERENCES

1. Sonin, E. B., *JETP Letters*, Vol. 47, No. 8, 415, 1988.
2. Belodedov, M. V., *PHYEM'05 Proc.*, 297.

Session 3P8b
Media

Lithium Ferrites for Phase Shifter

F. Q. Yuan
Southwest Jiaotong University, China

The dramatic development of satellite television has attracted people's profound attention on the receipt of satellite television programs by motion carriers such as trains and long distance buses. Meanwhile, to develop the remote education system in our nation so that the border areas can receive satellite television programs, we have conducted research on flat plate phase array antenna system of autotrack synchronous communication satellite. However, the development of this system is dependent greatly on the quality and materials of component. Therefore, we have conducted deep discussion on materials of phase shifter.

Using standard ceramic technique on pure oxide: ZNO, TiO_2, SnO_2, Fe_2O_3 and carbonate Li_2CO_3 as raw materials, we prepared the $Li_{0.5(1-y)}Zn_yFe_{2.5(1-0.2y)}O_4$ Lithium ferrites (with $y = 0$, 0.1, 0.16, 0.25, 0.28) and Kuband Ferrite phase shifter materials $Li_{0.625}Zn_{0.1}Ti_{0.25}Sn_{0.1}Fe_{1.925}O_4$. Flowing-oxygen begins at 800°C to 900°C and the pressure of wet pressing is about 9.8×10^{11} Pa. The temperature of flowing-oxygen sintering is from 850°C to 1050°C and some beneficial materials: Bi_2O_3, NiO, Co_2O_3 and $MnCO_3$ are added.

Through the analysis of the X-ray diffraction, it is shown that all generating materials are monophasic Lithium ferrites. The test results of $Li_{0.625}Zn_{0.1}Ti_{0.25}Sn_{0.1}Fe_{1.925}O_4$ ferrite at 300 K are tabulated in Table 1. Figure 1 shows the relation between specific saturation magnetization of $Li_{0.625}Zn_{0.1}Ti_{0.25}$ $Sn_{0.1}Fe_{1.925}O_4$ and temperature. Figure 2 gives the relation between saturation magnetization of $Li_{0.5(1-y)}Zn_yFe_{2.5(1-0.2y)}O_4$ and substituent y.

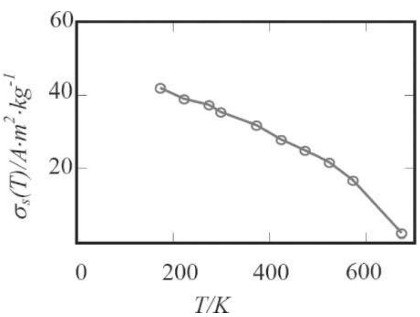

Figure 1: Relation between specific saturation magnetization σ_s and temperature T.

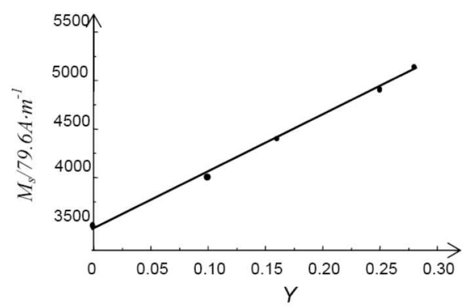

Figure 2: Relation between magnetization M_s and substituent y.

Table 1: Test results of $Li_{0.625}Zn_{0.1}Ti_{0.25}Sn_{0.1}Fe_{1.925}O_4$ ferrite at 300 K.

Sample	g	R_r	H_c	ρ	ε'	$tg\delta_\varepsilon$	M_s	ΔH	T_c
$Li_{0.625}Zn_{0.1}Ti_{0.25}Sn_{0.1}Fe_{1.925}O_4$	2.0	0.9	0.7	4.5	16.2	4.2	2060	285	678

It is shown from above analysis that magnetic dipole moment of ferrite $Li_{0.5(1-y)}Zn_yFe_{2.5-0.2y}O_4$ is equal to the magnetic dipole moment difference of Fe^{3+} on B sites and Fe^{3+} on A sites, which is to say, the number of Bohr magnetons per unit molecular formula in $(Zn_yFe_{1-0.5y})$ $[Li_{0.5(1-y)}Fe_{1.5}]O_4$ ferrite is $n_B = 1.5-1+0.5y = 0.5(1+y)$, an increase in y will increase n_B, therefore, saturation magnetization increase linearly with the increase of substituent y. However, the saturation magnetization is decreased when y is increased to such an extent that the super-exchange interactions of Fe^{3+} on A and B sites become weak owing to excessive concentration of nonmagnetic Zn^{2+} ions, leading to a incline of Fe^{3+} magnetic dipole moment and a partial spinflip.

*This work was supported by National Science Foundation of P. R. China. Grant No. 60371017.

A Novel Thin Microwave Absorber Based on the Concept of Equivalent Transformation Method of Material Constant

Y. Kotsuka and K. Shimodaira
Tokai University, Japan

The authors have thus far proposed the effective methods of changing and improving the matching characteristics of a single magnetic EM wave absorber [1–3]. These methods based on not by adjusting the processing conditions to produce a new magnetic material such as ferrite, but by applying static magnetic fields to a magnetic absorber, by adjusting the geometrical shape of it, and by attaching conductive patterns to the surface of absorbers etc. We have called these methods "Equivalent Transformation Method of Material Constant (ETMMC)" [4]. To change the matching frequency characteristic toward higher frequency regions from the original one, small holes are punched out in a magnetic absorber [2]. Secondly, to shift the matching frequency characteristic toward low frequency regions, conductive patterns are attached periodically to the surface of a ferrite absorber [3, 4].

In this paper, a thin and light weight EM-wave absorber is newly proposed. It becomes possible to merge both the competing characteristics by means of punching out small holes in the magnetic absorber and by attaching periodical conductive patterns to the surface of it as shown in Fig. 1. The question is what kinds of matching frequency characteristic are obtained by combining both the competing characteristics of changing the matching frequency toward high or low frequency regions. The detailed matching characteristics of the present absorber are investigated based on FDTD analysis. The matching mechanism is clarified from input admittance chart viewpoints. Consequently, a new thin and light weight microwave absorber can be realized with the thickness of 2.0 mm at the frequency from 2.45 GHz to above 6 GHz and light weight due to small holes occupying 55% of the area to carbonyl absorber.

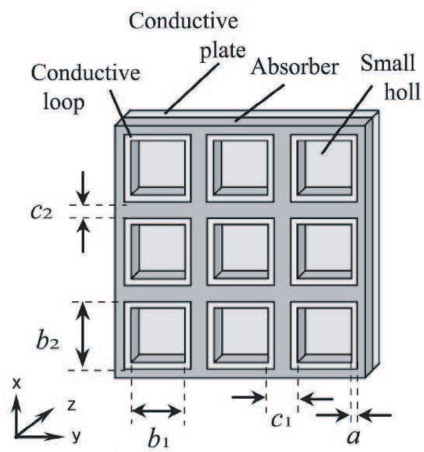

Figure 1: Fundamental construction of present absorber.

REFERENCES

1. Kotsuka, Y., et al., "Fundamental investigation on a weakly magnetized absorber," *IEEE Trans. EMC*, Vol. 42, No. 2, 116–124, May 2000.
2. Amano, M. and Y. Kotsuka, "A method of effective use of ferrite for microwave absorber," *IEEE Trans. MTT*, Vol. 51, No. 1, 238-245, Jan. 2003.
3. Amano, M. and Y. Kotsuka, "A novel microwave absorber with surface-printed conductive line patterns," *IEEE MTT-S Int. Microwave Symp. Dig.*, 1193–1196, Jun. 2002.
4. Kotsuka, Y., "EM-wave absorbers based on equivalent transformation method of material," *Constant, Proc. of the 2004 IEICE Society Conference*, BS-1-1, S-1-S2, Sep. 2004.

A Study of RF Absorber for Anechoic Chambers Used in the Frequency Range for Power Line Communication System

K. Shimada and K. Ishizuka
Riken Eletech Corporation, Japan

M. Tokuda
Musashi Institute of Technology, Japan

Typical semi anechoic chambers lined ferrite tiles are used for 3 m EMI testing over 30 MHz. In this paper, we discuss the measured reflection characteristics of ferrite absorber and the calculated CSA performance of an anechoic chamber in the frequency range from 1 MHz to 30 MHz for Power Line Communication (PLC) system.

We evaluated the characteristics of conventional Ni-Zn-Cu ferrite tile which is used for an anechoic chamber. It is well known that a air gap between ferrite tiles makes larger the reflection coefficient. The square coaxial line which has two ports was used to measure the reflection coefficient, permittivity and permeability of ferrite tiles including the effect by air gaps. The chart in Fig. 1 shows the reflection coefficient of the ferrite tiles from 1 MHz to 30 MHz. The performance of the ferrite tiles below 30 MHz is not sufficient, and it is improved to use the over lap tiles.

We calculated the CSA performance for an conventional 3 m testing semi anechoic chamber by ray tracing method. The chamber dimension was 6 m width $\times$ 9 m length $\times$ 5.5 m heigh. The calculation was performed in the case of only ferrite tiles and using over lap tiles. In the caluculation, test distance was 3 m, transmitting and receiving height was each 1.5 m and 1.0 m. The 80 MHz tuned dipole antennas were adopted for transmitting and reciving antenna from 1 MHz to 30 MHz. Fig. 2 shows the calculated CSA at horizontal polarization for the semi anechoic chamber. A large peak at 21 MHz by resonance is find out from the chart, and it is reduced by using over lap tile.

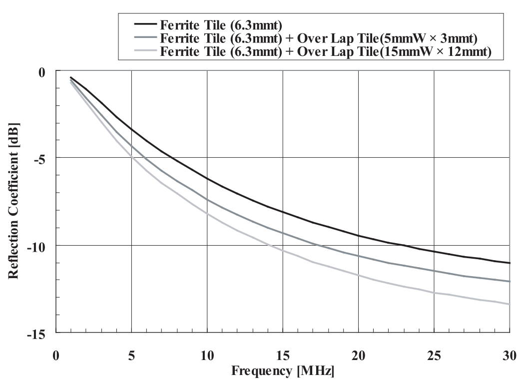

Figure 1: Measured reflection coefficients.

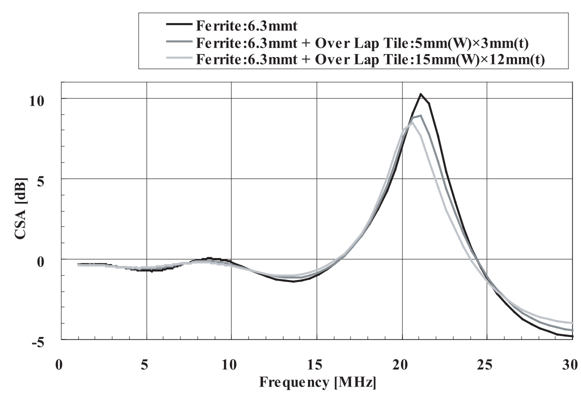

Figure 2: Calculated CSA deviation at horizontal polarization.

REFERENCES

1. Takeya, S. and K. Shimada, "New measurement of RF absorber characteristics by large coaxial air line," *IEEE International Symposium on EMC*, 1993.
2. Watanabe, Y., M. Shiegenaga, and M. Tokuda, "Electromagnetic field near power line for a power line communication system," *International Symposium on EMC Sendai*, 2004.
3. Kawabata, M., Y. Ishida, and K. Shimada, "Comparison of site attenuation analysis results between FDTD and ray-tracing method using compact anechoic chamber," *IEICE Trans.*, Vol. E88-B, No. 8, August 2005.

Effective Medium Theory for Finite Size Aggregates

C. A. Guérin[1,2], **A. Sentenac**[1,2], **and P. Mallet**[2]

[1]Université Paul-Cézanne, France
[2]ONERA-CERT/Institut Fresnel, France

We propose an effective medium theory for random aggregates of small spherical particles which accounts for the finite size of the embedding volume. The technique is based on the identification of the successive orders of the Born series within a finite volume for the coherent field and the effective field. Although the convergence of the Born series requires a finite volume, the effective constants which are derived through this identification are shown to admit a large scale limit. With this approach we recover successively, and in a simple manner, some classical homogenization formulas: the Maxwell-Garnett (MG) mixing rule, the Effective Field Approximation, and a correction to the Quasi-crystalline Approximation (QCA) which takes into account the finiteness of the medium. The last formula will be referred to as Finite-Size Quasi-crystalline Approximation (FS-QCA). In the light of this approach, we re-examine the validity of the MG mixing rule. We show that in certain configurations MG can be accurate even at high density of scatterers or in presence of strong multiple scattering, and we give numerical evidence for this. We then discuss QCA and FS-QCA and their relationship to MG. We show that FS-QCA coincides with the usual low-frequency QCA in the limit of large volumes, while bringing substantial improvements when the dimension of the embedding medium is of the order of the probing wavelength. An application to composite spheres is proposed.

One-dimensional Modeling of Plasma-electrode Pockels Cell Driven by One-pulse Process

X. J. Zhou[1], W. Q. Guo[1,2], X. J. Zhang[2], Z. Sui[2], and D. S. Wu[2]

[1]University of Electronic Science and Technology of China, China
[2]China Academy of Engineering Physics, China

Plasma-Electrode Pockels Cells (PEPC) are used as large-aperture optical switch in laser drivers for inertial-confinement fusion. Plasma electrodes are produced by high discharge current, while a high voltage pulse is applied across a thin KDP crystal plate through plasma, which is produced by discharge in the gas-filled cells. Gaseous ionization rises over the entire transverse section of the cells, and forms highly conductive and transparent plasma charge sheaths on the surfaces of the KDP crystal plate. In the working of PEPC in one pulse process without prior ionization of gas, the discharge plasma evolution process is time dependent. In this paper, we will present a one-dimensional modeling of processes of gaseous discharge and charging on the surfaces of KDP crystal in PEPC. Our modal is based on a simplified set of fluid equations, which is electron motion and ion motion governed by the equations of continuity and momentum conservation. The electric field distribution in the discharge cell is obtained by Poisson equation. This modeling gives the time-dependent discharge current and charging characteristics on the KDP crystal.

High Dielectric Constant Samarium Doped Barium Titanate Microwave Ceramics

D. Kaur, S. B. Narang, and K. S. Thind
Guru Nanak Dev University, India

Microwave dielectrics in ceramic form have been exploited in a variety of applications ranging from communication devices to the military satellite services. These advanced ceramics have revolutionized RF and Microwave technology. During the past decade, new material compositions developed to suit the stringent requirements for microwave resonators, filters, units of various UHF devices, substrate elements and IC packaging applications. The major advantages of microwave ceramics include the high dielectric constant (ε') and low tangent loss ($\tan\delta$) for stimulating the miniaturization and selectivity of components. The high technology dielectrics with new ideas and designs will be the basis for continuing usage of microwave ceramics in the third generation of Wireless and Telecommunication. This presentation addresses some results of investigations of the dielectric properties and the structure of ceramics based on the $BaO - Sm_2O_3 - TiO_2$ ternary system with dielectric constant greater than 70 and tangent loss less than 0.009. Samples of various compounds with appropriate forms were obtained by the solid-state double sintering synthesis or by chemical co precipitation from salt solutions. The composition x was varied based on $Ba_{6-3x}Sm_{8+2x}Ti_{18}O_{54}$ molecular formula, which has been an extensively used microwave ceramic material. The dielectric properties have been observed as a function of the composition, especially the dielectric constant (ε') and tangent loss ($\tan\delta$) changed non-linearly. The dielectric dispersion has been observed at high frequencies. It has been investigated that the dispersion is basically due to the fact that beyond a certain frequency of the applied electric field the particle exchange does not follow the alternating field.

Author Index